ed Carbon Nanostructures
ACN'2011

St Petersburg, Russia • July 4-8, 2011 •

Abstracts

ns

e
Nanotubes
monds
for Characterization of Nanocarbons
es
bon
nce/School of Young Scientists

CONTENTS **page**

s

ne

Nanotubes

monds

on 3

es

6. Nanocarbon

Contents

Invited Lectures

Oral Contributions

Poster Session 1

1. Graphene

2. Carbon Nanotubes

Poster Session 2

3. Nanodiamonds

4. Methods for Characterization of Nanocarbons

Poster Session 3

5. Fullerenes

Conference/School of Young Scientists

УНИВЕРСАЛЬНЫЕ КОНСТАНТЫ И ПРИРОДНЫЕ КВАНТЫ ЕДИНОГО ЭНЕРГОИНФОРМАЦИОННОГО ПОЛЯ МИРОЗДАНИЯ

© *В.К. Чебанов*, 2012

ООО Агропромышленная компания «Георгиевская»,
355005, Россия, Ставрополь, пр. Серафимовича, 29,
тел.: +7(928)3042237, e-mail: apkg@mail.ru

В разработках автора строго доказательно расшифрованы структура, темпорально-пространственная топология, параметры и схема взаимодействия с привычной для нас реальностью Единого энергоинформационного поля (ЕЭИП). Найдены всеобщие формулы взаимодействия и цикла, единая истинная природа всех видов взаимодействий (их не 4, а 6) и их гармоники, вскрыта физическая суть старых и почти трех десятков новых универсальных констант. Определены единые природные основания саморазвивающихся законов Бытия, лежащие в тотальном взаимодействии всего сущего с ЕЭИП по трем всеобщим принципам, трем всеобщим общесоциологическим законам, определенными тремя видами относительности.

Уточнилась энергетическая формула Эйнштейна, определилось состояние и система взаимодействия вещества и антивещества, зернистость и неразрывная связь пространства и времени.

Исходные положения

1. Все исследуемые три физических мира (магнито-термодинамический, электромагнитный, гравитонно-электрический) (а есть еще три: термоторсионный, информационно-гравитонный, торсионно-информационный) созданы потоками ЕЭИП, составляющие которого нами точно и подробно вскрыты ранее (22,23,24);

2. Все три рассматриваемые физических мира, вследствие этого, имеют по 10 главных характеристик (констант) представляющих собой кванты соответствующих потоков (выражаемых через К, Вб, м), их импульсов, зарядов, времен (выражаемых через Бр, Кл, с), создаваемых ими сил (выражаемых через Рч, А, Н), напряжений этих сил (выражаемых через Ш, В, кг), собственных сопротивлений ЕЭИП (выражаемых через Лц, Ом, Лм), проводимости (выражаемых через $См_{мт}$, См, $См_{гэ}$), емкости (выражаемых через $Ф_{мт}$, Ф, $Ф_{гэ}$), индукции (выражаемых через $Тл_{мт}$, Тл, $Тл_{гэ}$), индуктивности (выражаемых через $Гн_{мт}$, Гн, $Гн_{гэ}$) и энергии (выражаемых через $Дж_{мт}$, $Дж_{эм}$ и Дж), что позволяет уточнить и дополнить новую таблицу выражений физических единиц, (старых и новых см. приложение 1) и использовать ее при расчете универсальных констант, которые и в физическом, и в математическом смысле являются природными квантами ЕЭИП;

3. Кванты ЕЭИП, рассчитанные с помощью таблицы соотношений трех

рассматриваемых физических миров, показали, что в их формировании расчетно задействованы всего лишь два элемента: сила равная $10^{-20}/\pi^2$ и скорость света $C = 0.299792458 \cdot 10^9$ м/с, с их помощью можно, безо всяких сложных и дорогостоящих экспериментов, рассчитать, с любой заданной степенью точности, любую из известных универсальных констант (и уточнить их физическое значение) и, одновременно, получить ряд новых констант, неизвестных современной науке (см. приложение 2); 1) в дальнейшем примем $\pi = 3.14159265359$, $C = 0.299792458 \cdot 10^9$ *м/с*, $\pi^2 = 9.86960440109$;

4. Большинство природных квантов определяется при расчете 30 основных фундаментальных констант, в трех, выраженных по физическим мирам каждая, значениях (см. приложение 3);

5. Расчет природных квантов вскрывает истинную природную сущность и единые природные основания фундаментальных констант, а также их теснейшую взаимосвязь, взаимообусловленность, консонансность, причем гораздо более широкие и глубокие, чем знает современная наука;

6. Так как силы ЕЭИП скалярны и безразмерны, примем за всеобщую единицу силы $\Phi_{рт}$ - Ферт – новая единица силы в ее природном квантовом выражении безразмерного скалярного кванта силы ЕЭИП, действующего одинаково во все стороны в каждой точке пространства.

Тогда расчет сил ЕЭИП показывает, что:

$$\Phi_{PT} = 0.1380650324 \cdot 10^{-22} P_ч = 0.352544132366 \cdot 10^5 A = 0.122666712723 \cdot 10^{24} H;$$

отсюда

$$P_ч = 0.724296357026 \cdot 10^{23}; A = 0.283652430488 \cdot 10^{-4}; H = 0.815217085222 \cdot 10^{-23};$$

На основе выведенных формул находим величины основных констант и их значения в трех физических мирах:

1) **Постоянная Юрченко (новая)** характеризует силу потока ЕЭИП в разных физических мирах им создаваемых:

$$к_ю = \frac{C^0 \cdot 10^{-20}}{\pi^2} = \frac{1}{(3.14159265359)^2} \cdot 10^{-20} = 0.101321183642 \cdot 10^{-20}.$$

Мы можем теперь рассчитать природные кванты силы ЕЭИП:

- в магнито-термодинамическом мире:

$$P_{чтм} = к_ю = \frac{0.101321183642 \cdot 10^{-20} \cdot P_ч}{0.724296357026 \cdot 10^{23}} = \underline{0.139889125023 \cdot 10^{-43} \cdot P_ч};$$

- в электромагнитном мире:

$$A_{эм} = к_ю = \frac{0.101321183642 \cdot 10^{-20} \cdot A}{0.283652430488 \cdot 10^{-4}} = \underline{0.357201887774 \cdot 10^{-16} \cdot A};$$

- в гравитонно-электрическом мире:

$$H_{гэ} = \kappa_{ю} = \frac{0.101321183642 \cdot 10^{-20} \cdot H}{0.815217085222 \cdot 10^{-23}} = \underline{0.124287365265 \cdot 10^{3} \cdot H}.$$

2) **Постоянная Эйнштейна (также новая)** характеризует напряжение создаваемое выше рассчитанными силами ЕЭИП.

$$\kappa_{э} = \frac{10^{-20}}{\pi^{2}} \cdot C = \kappa_{ю} \cdot C = 0.101321183642 \cdot 10^{-20} \cdot 0.299792458 \cdot 10^{9}\ м/с =$$
$$= 0.303753266915 \cdot 10^{-12}\ м/с.$$

Тогда мы можем рассчитать природные кванты напряжений ЕЭИП в исследуемых мирах:

$$Ш_{мт} = \underline{0.269875826522 \cdot 10^{34}\ Ш};$$
$$В_{эм} = \underline{0.105690071995 \cdot 10^{7}\ В};$$
$$кг_{гэ} = \underline{0.175964284895 \cdot 10^{-28}\ кг}.$$

3) **Постоянная Кулона** - характеризует импульс (заряд, время) силы ЕЭИП в рассматриваемых мирах (то или иное проявление импульса зависит от вида физического мира и объекта в нем):

$$\kappa_{к} = \frac{10^{-20}}{\pi^{2}} \cdot C^{2} = \kappa_{ю} \cdot C^{2} = 0.101321183642 \cdot 10^{-20} \cdot \left(0.299792458 \cdot 10^{9}\ м/с\right)^{2} =$$
$$= 0.910629385139 \cdot 10^{-4}\ м^{2}/с^{2} = 0.269875826522 \cdot 10^{34}\ Ш \cdot 0.299792458 \cdot 10^{9}\ м/с =$$
$$= \underline{0.593748060478 \cdot 10^{-66}\ Бр} = 0.105690071995 \cdot 10^{7}\ В \cdot 0.299792458 \cdot 10^{9}\ м/с =$$
$$= \underline{0.151611448015 \cdot 10^{-38}\ Кл} = 0.175964284895 \cdot 10^{-28}\ кг \cdot 0.299792458 \cdot 10^{9}\ м/с =$$
$$= \underline{0.430049557193 \cdot 10^{-43}\ с}.$$

Сравнивая эти показатели импульса (заряда, времени) с полученными величинами природных квантов Единого энергоинформационного поля (ЕЭИП), мы обнаруживаем, что показатели полностью (до 12 знака после запятой) совпали в магнито-термодинамическом мире и в электромагнитном мире, но отличаются в $\pi^{2} \cdot 10^{20}$ (число гравитончиков в гравитоном пучке) раз в гравитонно-электрическом мире. Это произошло потому, что, с одной стороны, гравитончики передают (принимают) энергию при взаимодействии только индивидуально через осевое вращение. А с другой, - происходит это во время огибания гравитонами траектории орбитального вращения протонов и электронов (протонов – по большой орбите, электронов – по малой орбите). И это время $t_{э} = 0.424441900239 \cdot 10^{-22}\ с$ (с частотой $-0.235603506495 \cdot 10^{23}\ Гц$) было определено нами ранее, равно как и много других параметров.

Здесь, как и в других случаях с известными в настоящее время науке константами, возникает вопрос: как доказать, что новые ипостаси констант верны и как их использовать на практике, к примеру, в случае взаимодействия статичных зарядов?

Возьмем два заряда по 1 Кл каждый и на расстоянии 1 м. Тогда сила взаимодействия между ними в гравитонно-электрическом мире:

$$F_{гр} = \kappa_к \cdot \frac{Кл^2}{м^2} = \frac{0.430049557193 \cdot 10^{-43} H \cdot c \cdot Кл^2}{0.815217085222 \cdot 10^{-23} \cdot м^2} =$$
$$= 0.527527654889 \cdot 10^{-20} \cdot H \cdot 0.211749871592 \cdot 10^{40}\ м^2/c^2 \cdot$$
$$\cdot \frac{\left(0.600633657325 \cdot 10^{35}\ м^2/c^2\right)^2}{\left(0.211749871592 \cdot 10^{40}\ м^3/c^3\right)^2} = 0.898755178726 \cdot 10^{10} H.$$

Это до одиннадцатого знака после запятой соответствует силе, рассчитываемой по общепринятой формуле, что не только вполне хорошо, но и позволяет уточнить константу Кулона.

4) **Постоянная Ломоносова (новая),** отражающая энергию потока ЕЭИП в трех ипостасях:

$$\kappa_л = \frac{10^{-20}}{\pi^2} \cdot C^3 = \frac{10^{-20} \cdot \left(0.299792458 \cdot 10^9\ м/c\right)^3}{9.86960440109} = 0.272999821698 \cdot 10^5\ м^3/c^3.$$

Тогда кванты работы, выполняемые ЕЭИП при взаимодействии в создаваемых им физических мирах одинаковы и равны:

$$0.272999821698 \cdot 10^5\ м^3/c^3 = \underline{0.158148812322 \cdot 10^{-11}\ Дж}$$

и создают они субкванты соответствующих проявлений потока ЕЭИП:

$$К_{мт} = \underline{0.114546608634 \cdot 10^{12}\ К};$$
$$Вб_{эм} = \underline{0.448592949942 \cdot 10^{-16}\ Вб};$$
$$м_{гэ} = \underline{0.128925613812 \cdot 10^{-34}\ м}.$$

Если же полученные значения умножить на $\pi^2 \cdot 10^{20}$ – равное числу гравитонов в пучке, тогда:

$$К_{sг} = 0.114546608634 \cdot 10^{12}\ К \cdot \pi^2 \cdot 10^{20} = 0.113052971269 \cdot 10^{33}\ К;$$
$$Вб_{sг} = 0.448592949942 \cdot 10^{-16}\ Вб \cdot \pi^2 \cdot 10^{20} = 0.442743495303 \cdot 10^5\ Вб;$$

$$M_{зг} = 0.128925613812 \cdot 10^{-34} м \cdot \pi^2 \cdot 10^{20} = 0.127244480551 \cdot 10^{-13} м.$$

Это уже действительно проявляемые кванты ЕЭИП, воздействующие на все сущее.

Они также необычайно интересны, так как здесь, с одной стороны, присутствуют показатели далекого прошлого (и настоящего внутри С.С.) в части температуры и электрического напряжения, и настоящего, показывающего истинные размеры полуокружности стационарной точки (С.Т.)

$l_{СТ} = 0.127244480551 \cdot 10^{-13}$ *м*, (сейчас это полуокружность движения протонов), которую с в своем непрерывном движении обходят гравитоны по полуокружности своего движения $l_г = 0.1272655801 \cdot 10^{-13}$ *м* или на 0.016582% большей. Очень плотно и очень своеобразно.

Таким образом, мы узнали температуру гравитонов и фотонов (очень большую), величину магнитного потока и размеры шага их совместного поступательного движения, а также можем узнать зернистость (квант) времени и частоту собственного осевого вращения гравитонов:

$$t = \frac{0.128925613812 \cdot 10^{-34} м}{0.299792458 \cdot 10^{9}\ м/с} = 0.430049557193 \cdot 10^{-43} с;$$

$$\nu = \frac{1}{t} = 0.23253134046 \cdot 10^{44} Гц.$$

Проявляется в чистом виде энергия потока ЕЭИП при взаимодействии массы с зарядом. Рассмотрим его силы при m = 1 кг, q = 1 Кл, L = 1 м, тогда в гравитонно-электрическом мире:

$$F_{гэ} = 0.158148812322 \cdot 10^{-11} Н \cdot м \cdot \frac{кг \cdot Кл}{м^2} = 0.158148812322 \cdot 10^{-11} \cdot Н \cdot$$

$$\cdot \frac{0.172622113115 \cdot 10^{17}\ м/с \cdot 0.600633657325 \cdot 10^{35}\ м^2/с^2}{0.211749871592 \cdot 10^{40}\ м^3/с^3} = 0.774370629465 \cdot Н$$

вполне ощутимая сила, которую, очевидно, в ближайшее время измерят ученые;

То же в электромагнитном мире:

$$F_{эм} = 0.454519686611 \cdot 10^{-30} А \cdot м \cdot \frac{кг \cdot Кл}{м^2} =$$

$$= 0.454519686611 \cdot 10^{-30} А \cdot 0.172622113115 \cdot 10^{17}\ м/с \cdot$$

$$\cdot \frac{0.600633657325 \cdot 10^{21}\ м^2/с^2}{0.211749871592 \cdot 10^{40}\ м^3/с^3} = 0.222554118907 \cdot 10^{-18} А;$$

- это почти неуловимая величина электрического тока;

И, наконец, в магнито-термодинамическом мире:

$$F_{MT} = 0.178001190481 \cdot 10^{-57} P_ч \cdot м \cdot \frac{кг \cdot Кл}{м^2} =$$

$$= 0.178001190481 \cdot 10^{-57} P_ч \cdot 0.172622113115 \cdot 10^{17} м/с \cdot$$

$$\cdot \frac{0.600633657325 \cdot 10^{21} м^2/с^2}{0.211749871592 \cdot 10^{40} м^3/с^3} = 0.87157716772 \cdot 10^{-46} P_ч;$$

очевидно это тоже неуловимая величина, которую к тому же мы пока не знаем, как измерять. Возможно, как крутящую силу на нуклонном уровне.

При рассмотрении постоянной Ломоносова бросается в глаза крайне низкий КПД ЕЭИП, составляющий неуловимую величину. Справедливости ради стоит отметить, что это компенсируется безбрежностью Вселенной. Одновременно проясняется подлинный смысл ее эволюции, включая появление и развитие человека и человеческого общества, заключающийся в достижении максимума ее сохранения за счет снижения энтропии процессов существования.

5) **Постоянная Ньютона** представляет собой момент напряжения:

$$\kappa_н = \frac{10^{-20}}{\pi^2} \cdot C^4 = 0.818432875804 \cdot 10^{13} \cdot \frac{м^4}{с^4} =$$

$$= \frac{0.818432875804 \cdot 10^{13} \cdot Н \cdot м^2 \cdot \left(0.172622113115 \cdot 10^{17}\right)^2}{0.815217085222 \cdot 10^{-23} \cdot кг^2 \cdot \left(0.211749871592 \cdot 10^{40}\right)^2} =$$

$$= 0.667200463451 \cdot 10^{-10} \cdot Н \cdot \frac{м^2}{кг^2}.$$

Это подлинное значение константы Ньютона. Измеряемое учеными значение $\kappa_н = 0.66731 \cdot 10^{-10}$ $Н \cdot м^2/кг^2$ на 0.16417 % больше, что является, очевидно, следствием влияния на измерение $\kappa_н$ со стороны других констант, в частности $\kappa_п$, $\kappa_л$. Теперь запишем $\kappa_н$ в его подлинном значении квантов моментов напряжений в трех физических мирах ЕЭИП:

- в магнито-термодинамическом мире:

$$\kappa_{нтм} = 0.818432875804 \cdot 10^{13} м^4/с^4 = \kappa_{этм} \cdot C^3 = 0.2698758265 \cdot 10^{34} Ш \cdot$$

$$\cdot 0.269440024173 \cdot 10^{26} \frac{м^3}{с^3} = 0.269875826522 \cdot 10^{34} Ш \cdot 0.11305297271 \cdot 10^{33} К =$$

$$= 0.305102644483 \cdot 10^{66} Ш \cdot К = \underline{0.269875826522 \cdot 10^{34} Ш \cdot 0.1272655801 \cdot 10^{-13} м =}$$

$$\underline{= 0.343459036144 \cdot 10^{20} Ш \cdot м};$$

- в электромагнитном мире:

$$\kappa_{нгэ} = 0.818432875804 \cdot 10^{13} \frac{м^4}{с^4} = \kappa_{этм} \cdot C^3 = 0.105690071995 \cdot 10^7 B \cdot$$

$$\cdot 0.44274495308 \cdot 10^{-5} Вб = \underline{0.467935918944 \cdot 10 \cdot B \cdot Вб =}$$

$$\underline{= 0.105690071995 \cdot 10^7 B \cdot 0.1272655801 \cdot 10^{-13} м};$$

Квант момента напряжения – в гравитонно-электрическом мире найдены ранее и соответствует стандартному значению постоянной Ньютона, которое, впрочем, не отражает сути гравитонно-электрического взаимодействия. На самом деле

$$\kappa_н = 0.223941967941 \cdot 10^{-42} \cdot кг \cdot м =$$

$$= \underline{0.175964284895 \cdot 10^{-28} кг \cdot 0.1272655801 \cdot 10^{-13} м}.$$

Это выражение подлинной физической сути константы Ньютона, как кванта момента напряжения ЕЭИП.

То есть гравитонный пучок давит на нуклоны и электроны не прямо, а по окружности, создавая момент напряжения (момент массы гравитонного пучка) при обходе им (пучком) по окружности С.Т. Этот очень своеобразный способ взаимодействия объясняет все: и неуловимость гравитонов, и трудности в создании антигравов, и огромную разницу в температуре среды и составляющих ЕЭИП, и мизерность $\kappa_н$, и т. д., и т. п.

Здесь и ранее также выявились кванты гравитонно-электрического аспекта потока ЕЭИП и момента напряжения этого потока, а также длина полуокружности взаимодействия гравитонов с нуклонами и электронами. Это, по существу, истинная величина Ферми. В магнито-термодинамическом мире один сомножитель еще раз показывает на огромную температуру гравитонных пучков, которые не передаются окружающей нас среде, лишь благодаря своеобразному обходному, мимолетному способу взаимодействия гравитонов непосредственно с нуклонами и электронами, минуя атомы и молекулы. Становится понятным источник тепла в глубине планет и звезд (кроме нейтронных, что также теперь понятно) и механизм увеличения их массы.

6) **Постоянная Планка**:

$$\kappa_п = \frac{10^{-20}}{\pi^2} \cdot C^5 \cdot \pi^2$$

Прежде чем перейти к расчетам, попробуем понять, откуда возник нестандартный множитель π^2? Постоянная Планка – это момент импульса (заряда) по той же длине полуокружности С.Т. и вследствие этого имеет системно-объемный характер распределения вращающегося момента импульса, что во-

площается сомножителем π^2.

$$\kappa_n = \kappa_н \cdot C \cdot \pi^2 = 0.223941967941 \cdot 10^{-42} \cdot кг \cdot м \cdot 0.299792458 \cdot 10^9 м/с \cdot$$

$$\cdot 9.86960440109 = 0.662606876517 \cdot 10^{-33} \cdot \frac{кг \cdot м^2}{с} \cdot \frac{с}{с} =$$

$$= \underline{0.662606876517 \cdot 10^{-33} \cdot Дж \cdot с} =$$

$$= \underline{\pi^2 \cdot 0.430049557193 \cdot 10^{-43} \cdot с \cdot 0.1272655801 \cdot 10^{-13} м};$$

мы сразу очень точно - до двенадцатого знака после запятой (и даже уточнили последних два знака) получили общепринятое значение константы, которое, впрочем, не раскрывает ее физического смысла.

Для его понимания преобразуем Дж в м, а с в Кл тогда:

$$\kappa_n = 0.662606876517 \cdot 10^{-33} \cdot 0.352544132366 \cdot 10^5 Кл \cdot$$

$$\cdot 0.815217085222 \cdot 10^{-23} м = \underline{0.19043321631 \cdot 10^{-51} Кл \cdot м =}$$

$$\underline{= \pi^2 \cdot 0.151611448015 \cdot 10^{-38} \cdot Кл \cdot 0.1272655801 \cdot 10^{-13} м};$$

Точно до одиннадцатого знака после запятой. Это электрический дипольный момент ЕЭИП умноженный на π^2.

В магнито-термодинамическом мире:

$$\kappa_n = \pi^2 \cdot \kappa_н \cdot C = 9.86960440109 \cdot 0.343402093573 \cdot 10^{-48} Ш \cdot м \cdot$$

$$\cdot 0.299792458 \cdot 10^9 м/с = \underline{0.1016069991339261 \cdot 10^{-38} Ш \cdot м^2/с =}$$

$$\underline{= \pi^2 \cdot 0.798385567672 \cdot 10^{-66} Бр \cdot 0.1272655801 \cdot 10^{-13} м};$$

Это умноженный на π^2магнитный дипольный момент ЕЭИП.

7) **Постоянная Вина**:

$\kappa_в = \dfrac{2C^6 \cdot 10^{-20}}{\pi^2} \cdot 0.993895025762$, мы путем простых подстановок легко получим общепринятую формулу:

$$\kappa_в = \underline{2 \cdot 0.993895025762 \cdot 0.114546608634 \cdot 10^{12} К \cdot 0.1272655801 \cdot 10^{-13} м =}$$

$$\underline{= 0.2897768651 \cdot 10^{-2} м \cdot К};$$

отражающую взаимодействие в магнито-термодинамическом мире как осевого вращения гравитонов и фотонов с нуклонами и электронами. Тоже самое в электромагнитном мире:

$$\text{к}_в = 2 \cdot 0.993895025762 \cdot 0.114546608634 \cdot 10^{12} \cdot K \cdot 0.1272655801 \cdot 10^{-13}\, м =$$
$$= \underline{2 \cdot 0.993895025762 \cdot 0.448592949341 \cdot 10^{-16}\, Вб \cdot 0.1272655801 \cdot 10^{-13}\, м};$$

Таков магнитный поток ЕЭИП, совпадающий до седьмого знака с рассчитанным ранее и скользящий по обводам С.Т., давно несуществующих, мимолетно меняя осевые вращения нуклонов, электронов, питая их энергией.

И, наконец, в гравитонно-электрическом мире мы имеем:

$$\text{к}_в = 0.2897768651 \cdot 10^{-2}\, м \cdot 0.1380650324 \cdot 10^{-22}\, Дж =$$
$$= 0.400080522686 \cdot 10^{-25}\, Дж \cdot м =$$
$$= \underline{2 \cdot 0.993895025762 \cdot 0.158148812322 \cdot 10^{-11}\, Дж \cdot 0.1272655801 \cdot 10^{-13}\, м};$$

Мы получили абсолютно совпадающую энергию гравитонного (и фотонного) пучка, с точностью до одиннадцатого знака и поняли, что в гравитонно-электрическом мире постоянная Вина отражает энергетический момент гравитонно-фотонной пары в ее взаимодействии с нуклонами и электронами, в обмене торсионными квантами осевого вращения.

Найденные нами точные значения семи основных универсальных констант позволяют, используя ранее созданную таблицу коэффициентов перевода физических единиц друг в друга, и выявившиеся консонансные гармоники потоков, импульсов (зарядов), напряжений, сопротивлений, сил и т. д., рассчитать с точностью до двенадцатого знака после запятой величины тридцати природных квантов Единого энергоинформационного поля – по 10 в каждом из трех физических миров нашей реальности.

Пока недостаточно понимания и знаний автора для расчета еще тридцати квантов в трех оставшихся физических мирах.

Однако, уверен - это дело очень недалекого будущего.

Но и найденные величины тридцати природных квантов, и прояснившаяся картина взаимодействия потоков ЕЭИП, позволяет сделать ряд первых предложений по различным направлениям деятельности человека, что будет сделано в следующей статье. Сейчас можно сказать, что **все материалы, таблицы статьи легко проверяются (надо лишь захотеть), могут широко использоваться и резко упростить расчеты, и после такого подтверждения зародить огромное количество практических идей.**

Автор сознательно уклонился от теории получения приведенных результатов и даже формулу всеобщего взаимодействия привел частично. Однако, заинтересованное рассмотрение только приведенных трех таблиц открывает огромное поле для выводов. К примеру, значение Рч является коэффициентом перевода энергии в Дж в энергию в К. А обратная величина – 1/Рч с точностью до двенадцатого знака после запятой равна известной константе Больцмана $\text{к}_б = 0.1380650324 \cdot 10^{-22}$. Из этого прямо следует, что $A = 0.283652430488 \cdot 10^{-4}$ это коэффициент (безликая сила) отражающий перевод энергии в Дж в энергию

в Вб. Обратная величина $1/A = 0.352544132366 \cdot 10^5$ является коэффициентом Больцмана для электромагнитного мира.

Аналогично $H = 0.81521708222 \cdot 10^{-23}$ – коэффициент перевода энергии в Дж, в энергию поступательного потока гравитонов в м, а обратная величина $1/H = 0.122666712723 \cdot 10^{24}$ это коэффициент Больцмана для гравитонно-электрического мира. Только вокруг этих коэффициентов таится масса открытий.

Рассмотрение таблиц 2 и 3 показывает, что мы имеем два вида квантов ЕЭИП, проявляющихся в физических мирах – квант гравитонного (и фотонного) пучка и субквант отдельного гравитона (и фотона). При этом следует учесть несколько важных моментов:

- Каждый гравитон (практически) всегда находится в паре с фотоном, который, вследствие этого, проявляется электрически нейтрально (хотя и является, по мнению науки, носителем электрического поля);
- Гравитонные нити и пучки падают со скоростью света на все сущее со всех сторон (почему – см. книги автора), но взаимодействуют с ним очень своеобразно – огибая нуклоны и электроны по дуге полуокружности $\ell = 0.1272655801 \cdot 10^{-13}$ *м* и соприкасаясь с ними мимолетно, обмениваются при этом магнито-термодинамическими, электромагнитными, и гравитонно-электрическими (сугубо) квантами движения (осевого вращения, орбитального вращения и поступательного движения);
- Первое и второе обеспечивают и объясняют все парадоксы фотона, как такового, (нулевое время ускорения фотона при его рождении, поперечность волны электромагнитного поля, якобы, нулевой заряд фотона и его электрическую нейтральность, квантовый принцип причинности, взаимодействие агентов полей без проскальзывания, но с передачей вращательного движения собственного, как источника магнито-термодинамического поля и орбитального, как источника электрического поля) и нейтрона, имеющего диаметр осевого (и орбитального) вращения меньше 10^{-32} м и поэтому почти не соприкасающегося с горячими гравитонами и фотонами, поэтому остающегося электрически нейтральным и холодным даже в нейтронных звездах, плотность которых так же теперь легко объяснима (в $\frac{10^{-13}}{10^{-32}} = 10^{20}$ выше плотности обычной звезды).

На основе таблицы 1 можно сделать развернутую таблицу коэффициентов перевода физических единиц друг в друга в экселе, которая также открывает массу интересных соотношений для практического применения. Большинство найденных констант обладают или запредельно малыми значениями (креативными) или запредельно большими значениями (сопротивленческими), что ставит под сомнение их теперешнее использование и объясняет тот факт, почему они до сих пор не обнаружены.

На это накладывается непонимание механизмов взаимодействия ЕЭИП и его составляющих с реальностью, что не только не позволяет найти правильные принципы использования безбрежного энергоинформационного потенциала ЕЭИП, но даже обнаружить гравитоны и сконструировать приборы для измерения параметров составляющих ЕЭИП. В тоже время таблицы перевода выявили десятки новых соотношений, позволяющих уверенно, с открытыми глазами приступить к освоению возможностей ЕЭИП и в части энергетики, и в части информатики, и в части связи, и в части наноконструирования.

Таблицы 2 и 3, в первую очередь, говорят о том, что Пространство это всеобъемлющий и всепроникающий, установившийся ламинарный поток, состоящий из топологически увязанного ансамбля (нейтрино, гравитонов и фотонов) Единого энергоинформационного поля (для любой точки одновременно со всех сторон), который рождает шесть физических миров реальности (термоторсионный, магнито-термодинамический, электромагнитный, гравитонно-электрический, информационно-гравитонный и торсионно-информационный). А время – импульс этого потока, принимающий в указанных шести мирах специфические консонансные формы: спина, заряда, длительности, информационно-гравитонного файла и т. д. Далее можно сделать на основе этих таблиц огромное количество выводов и предложений. Примером может служить такой:

Рч – магнито-термодинамическая сила, ее величина обратно пропорциональна постоянной Больцмана. Последняя, как мы знаем, представляет собой отношение магнито-термодинамической энергии, выраженной в К, к той же энергии выраженной в Дж. Это отношение является несколько искусственным с физической точки зрения. В тоже время, Рч (Риччи), как магнито-термодинамическая сила, показывает, что она, поднимая температуру на 1 градус Цельсия, совершает работу в один Джоуль. Аналогично, А (Ампер), как электромагнитная сила, показывает, что она, создавая электромагнитный поток в один Вб, совершает работу в один Джоуль. Н (Ньютон), как гравитонно-электрическая сила, также показывает, что, создавая гравитонно-электрический поток в 1 м, она совершает работу в один Джоуль.

На самом деле и силы создают, и работу совершают, безусловно, соответствующие потоки, точнее соответствующие ипостаси одного и того же потока ЕЭИП, состоящего из скомпонованных потоков нейтрино, гравитонов и фотонов где, по настоящему, активным в вышеуказанных смыслах является поток гравитонов. Некоторое разночтение, недоумение вызывает тот факт, что автор соединил единицу температуры с единицей магнито-термодинамического потока (К), единицу длины с единицей гравитонно-электрического потока (м), единицу магнитного (на самом деле электромагнитного) потока с единицей пока еще не названной характеристики воздействия электромагнитного потока. Однако, практические расчеты показывают обоснованность такого соединения. Произведение соответствующей силы на величину соответствующего потока равно работе. Это отражает по существу взаимодействие с потоком, показывая

какую силу, как по величине, так и по виду, надо приложить для преодоления того или иного потока.

Величина потока одновременно указывает на изменения, происходящие при воздействии того или иного потока: изменение температуры в К, перемещение в м, и т. п.

Проведенное исследование позволяет также сделать несколько уточнений к известным положениям. Так постулаты СТО Эйнштейна инвариантности физических законов по отношению к выбору инерционной системы отсчета и скорости света в вакууме – от движения источника света можно дополнить утверждением о том, что оба они подтверждаются и переводятся в статус физических законов тем фактом, что ЕЭИП является **полностью независимой и тотально определяющей и первый, и второй постулат, системой отсчета.** Все остальные системы отсчета находятся в равном положении по отношению к ЕЭИП и воздействиям ее составляющих на них. То есть, поток ЕЭИП является расширяющимся пространством существования всего остального, а его импульсы - временем, всеобщим временным синхронизатором.

Метрика пространства – времени действительно локально, именно локально, изменяется при прохождении потока ЕЭИП сквозь огромные массы звезд и их скоплений и вызвано это оригинальным взаимодействием составляющих ЕЭИП (в первую очередь гравитонов и нейтрино) с частицами звезд и скоплений. Однако, во вселенском масштабе однородность и изотропность ЕЭИП, т. е. пространства неизменны, равно как неизменна однородность времени.

Отсюда мы можем сделать несколько важных выводов:

1. Абсолютного (Ньютонова) пространства не существует в природе, оно может быть только воображаемым, условным;
2. Роль абсолютного пространства с достаточной точностью и эффектом по однородности и изотропности выполняет ЕЭИП. Квантом пространства, отмеряемым потоком ЕЭИП, является постоянная Ломоносова равная (в гравитонно-электрическом мире) $0.128925613812 \cdot 10^{-34} м$. У составляющих ЕЭИП нейтрино, гравитонов и фотонов, а тем более их квантов размеры гораздо меньше, однако поток ЕЭИП образуется именно таким квантом;
3. Занимаемые теми или иными системами пространства абсолютно равноправны;
4. Все остальные виды пространств являются либо сугубо локальными (катодное темное, фарадеево темное и т. п.), либо геометрическим или математическим изыском;
5. Абсолютное (Ньютоново) время является воображаемым миражом, не существующим по определению, ибо время, как таковое, возникает при движении, изменении и определяется циклами процесса;
6. Роль абсолютного однородного времени в Бытие выполняют импульс потока ЕЭИП, временной квант которого равен $0.430049557193 \cdot 10^{-43} с$.

Импульс ЕЭИП может компактизироваться в заряды различных видов: магнито-термодинамический, электромагнитный, гравитонно-электрический. Здесь также у составляющих ЕЭИП нейтрино, гравитонов и фотонов периоды обращения и соответственно заряды намного меньше, однако объективными: однородностью, однонаправленностью, необратимостью и равнодействием на все сущее обладают только импульсы потока ЕЭИП. Поэтому во всех системах отсчета время, по отношению к практически неизменному эталону, течет одинаково. То есть, знаменитый эффект Доплера теперь просто и понимается, и полностью объясняется строгой аналогией акустическому эффекту, так как и там, и там (в воздушной среде и в ЕЭИП) распространение волны идет независимо от источника и приемника. В то же время, индивидуальное время системы (субъекта) всегда автономно и определяется ее (его) импульсами, которые одинаково хронометрируются и синхронизируются эталонными импульсами потоков ЕЭИП. Инвариантность относительно сдвига во времени, обеспечиваемая законом сохранения энергии, имеет точность (возможность отклонения) равную постоянной Планка – момента импульса ЕЭИП, то есть чрезвычайно высока, почти абсолютна;

7. Энергия и информация являются первичной и тотальной сущностью, развивающейся первосущностью, содержанием всего сущего в Бытие и через развитие ключевых всеобщих форм: Пространства, Времени, ЕЭИП, Материи, Жизни, Души, Духа, Коллективного Духа, Бога, во-первых, развиваются сами, как таковые, во-вторых, их развитие, определяемое формами в различных интерпретациях, целеустремленно направленно на самосохранение и борьбу с энтропией;
8. Энергия и информация всегда имеют формального, в смысле формы, носителя:
   - Полуматериального, энергоинформационного – в виде нейтрино, гравитонов и фотонов, системно-топологически связанных в ЕЭИП:
   - Материального в виде электронов, кварков, нуклонов, атомов, молекул и т. д.;
   - Системно-топологического в виде стоячих суперволн (квазаров) ЕЭИП, материальной Вселенной, Жизни, Духа, гуманоидного общества;
9. Энергия и информация являются тотальными аспектами и атрибутами всего сущего в Бытие, его создателями, развивающими и развивающимися творцами, а не просто мерой возможностей. В мире нет ничего кроме энергии и информации, Пространство, Время, Материя, ЕЭИП, Жизнь, Дух, Бог - есть формы существования энергии и информации, а движение, превращение и обмен – способы развития, обретения Свободы, Возвышения и Единения.
10. Информация – это саморазвивающаяся энергия, дошедшая в своем развитии до стадии: - системно-топологической консервации;

– почти нулевой энтропии;
– максимальной общности;

В чистом виде информация приобретает виды:

– природообразующей, генной;
– законоформативной;
– фантосмагорической;
– передающей, накопительной;

11. Второй стороной развития энергии и информации являются Душа и Дух, дающие максимальные КПД за счет эмоционально-чувственных резонансов и Воли;

Как итог можно констатировать, что:

- Энергия и информация определяют атрибутивную способность той или иной формы, в том или ином ее виде, к эффективным изменению и, в конечном счете к свободе самореализации, самовозвышению, максимальному единению на основе соревнования.
- Энергия и информация зависят от состояния той или иной системы, в той или иной среде и бывают:

  а) компактизированная в различные формы материи (компоненты ЕЭИП, виды вещества) и их взаимное системное состояние и взаимодействие, системные топологию и влияние - относительно пассивная;

  б) Проявляемая, обменная, преобразуемая и преобразующая - относительно активная;

12. Материя, в обобщенном понятии, есть скомпактизированные энергия и информация в: - массу;

– системно-топологическое состояние;
– движения различных видов и скорости;

В нашей Вселенной материя, очевидно, существует в трех состояниях:

- Суперэнергетическом – квазары (стоячие суперволны) с массовой плотностью $0.105911136 \cdot 10^{93} кг/м^3$;
- Малоэнергетическом, энергоинформационном – ЕЭИП с массовой плотностью $0.16990813 \cdot 10^{-26} кг/м^3$, проявляемом, выражаемом различными видами полей;
- Среднеэнергетическом – звезды (в том числе нейтронные), галактики, скопления, планеты и т. д., выражаемом, проявляемом веществом в различных состояниях – твердом, жидком, газообразном, плазменном, нейтронном;

13. Энергоинформационная суть последующих форм своего развития – Жизни, Души, Духа, Коллективного бессознательного, Бога нуждается в обобщении, исходя из новых физических и мировоззренческих взглядов;
14. Немногое можно отметить по энергоинформационной сущности Абсолютного Вакуума, который, был таковым (вакуумом) только в инфор-

мационном плане и, как показали расчеты, имел тотальную (в пространстве) монолитную плотность равную $0.767110997 \cdot 10^{21} кг / м^3$. Это состояние абсолютной энергетической изотропной недифференцированности, длившееся более 10^{428}лет (то есть практически вечность), представляло собой монолит комплексной полиэнергии, который содержал полный набор двенадцати мерностей, все моменты диполя, все возможные импульсы и силы, что было наглядно вскрыто в (20) и являлось неизвестным нам видом материи без времени, движения и информации.

15. Выявившиеся в таблице перевода физических величин большое количество формул цикла позволило найти всеобщую формулу цикла (ВФЦ). Она имеет вид $\frac{E}{V} = \frac{F}{\nu}$; и следующую формулировку: Проявленная энергия взаимодействия так относится к скорости процесса, как сила взаимодействия относится к частоте цикла. Всеобщая формула цикла, будучи приложенной к различным физическим мирам, обнажила целый ряд своих дуалистических интерпретаций;
16. Тело, заряд, магнит и т. п. могут возбуждать силы, неконтактно воздействующие на другие тела, заряды, магниты и т. п. на расстоянии только через собственное взаимодействие с ЕЭИП, накладывающееся на аналогичные взаимодействия других тел с тем же ЕЭИП. Это касается всех видов сил, действующих в нашем Мироздании, за исключением кварк-нуклонных и ядерных сил.
17. Масса, магнит, электрический заряд не имеют и не излучают какого бы то ни было поля – гравитонного, магнитного, электрического, а эти поля образуются при взаимодействии этих объектов (массы, магнита, электрического заряда) с ЕЭИП и представляют собой различные изменения топологии и интенсивности составляющих последнего. Точно также и мозг, и тело биологических объектов ничего не излучают и никаких собственных полей не имеют. Они просто взаимодействуют с ЕЭИП, или же дополнительно с токами высокой частоты и при этом получается эффект Кирилиана, полное свечение и т. п.
18. Также представляется, что каждый биологический объект имеет в ЕЭИП свою матрицу - архив, в которой фрактально-голографически сгруппирована в файлы вся родовая информация, а также прожитая объектом жизнь, включая память, и возможно допустить – наиболее вероятные события будущего, включая смерть.
19. Все мыслительные способности, начиная от развертывания матрицы ДНК и кончая научными открытиями, достижениями искусства и спорта реализуются через взаимодействие с ЕЭИП. Последнее является, с одной стороны, полным, свернутым в файлы архивом Вселенской информации, передаваемой с практически неограниченной скоростью. А с другой - постоянным эгрегором из шести физических миров, однознач-

но взаимодействующих со всей реальностью и любым объектом в ней.

20. По мере развития, и фундаментальные частицы, и торсионы, и всеобщие принципы, и всеобщие общесоциологические законы, и т. п. консонасно саморазвиваются и приобретают все новые и новые качества и обличья. Проведение принципов и законов в реальность обеспечивается системой самовозникающих и саморазвивающихся эгрегоров, воздействующих на все сущее энергетически, физически, информационно, душевно, духовно.

В.К. Чебанов

Аббревиатуры и обозначения, примененные в статье

А	– Ампер – единица силы в электромагнитном мире;
Бр	– Бергсон – единица заряда (импульса) в магнито-термодинамическом мире;
В	– Вольт – единица напряжения в электромагнитном мире;
Вб	– Вебер – единица потока в электромагнитном мире;
Гн, $Гн_{Мт}$, $Гн_{гэ}$	– Генри – единица индуктивности в электромагнитном, магнито-термодинамическом мире; гравитонно-электрическом мире;
Дж, $Дж_{мт}$, $Дж_{эм}$	– Джоуль – единица энергии, работы в гравитонно-электрическом, магнито-термодинамическом мире; электромагнитном мире;
ЕЭИП	– единое энергоинформационное поле;
К	– единица температуры и одновременно потока в магнито-термодинамическом мире;
кг	– Килограмм – единица напряжения в гравитонно-электрическом мире, одновременно единица массы;
Кл	– Кулон – единица заряда в электромагнитном мире;
$к_б$, $к_{бгэ}$, $к_{бэм}$	– коэффициенты Больцмана в магнито-термодинамическом, гравитонно-электрическом, электромагнитном мирах;
$к_ю$, $к_э$, $к_л$	– универсальные постоянные Юрченко (силы), Эйнштейна (напряжения), Ломоносова (потока);
Лм	– Ломоносов – единица сопротивления в гравитонно-электрическом мире;
Лц	– Лейбниц – единица сопротивления в магнито-термодинамическом мире;
м	– метр тотальная единица длины и одновременно потока в гравитонно-электрическом мире;
Н	– Ньютон – единица силы в гравитонно-электрическом мире;
Ом	– Ом – единица сопротивления в электромагнитном мире;
Рч	– Риччи – единица силы в магнито-термодинамическом мире;
с	– Секунда - тотальная единица времени, и одновременно заряда в гравитонно-электрическом мире;
См, $См_{гэ}$, $См_{мт}$	– Сименс – единица проводимости в электромагнитном, гравитонно-электрическом мире; магнито-термодинамическом мире;
СС	– Стоячие суперволны;
СТ	– Стационарная точка;
Тл, $Тл_{гэ}$, $Тл_{мт}$	– Тесла – единица индукции в электромагнитном, гравитонно-электрическом мире, магнито-термодинамическом мире
Ф, $Ф_{гэ}$, $Ф_{мт}$	– Фарада – единица емкости в электромагнитном, гравитонно-электрическом мире, магнито-термодинамическом мире;
$Ф_{РТ}$	– Ферт – всеобщая (для всех физических миров ЕЭИП) единица силы;
Ш	– Шипов – единица напряжения в магнито-термодинамическом мире;

ЛИТЕРАТУРА

1. Азимов А. **Человеческий мозг от аксона до нейрона.** М.: «Центро-полиграф», 2003.
2. Акимов А.Е. и др. **Сознание и физический мир.** М.: «МНТЦ ВЕНТ», 1995.
3. "*Актуальные проблемы естествознания начала века". Материалы международной конференции*, Санкт-Петербург, Россия, 21-25 августа 2000. СПб: «Анатомия» (2001).
4. Аленицин А.Г. и др. **Краткий физико-математический справочник.** М.: «Наука», 1990.
5. Брагина Н.Н., Доброхотова Т.А. **Функциональные асимметрии человека.** М.: «Медицина», 1988.
6. Бураго С.Г. **Эфиродинамика Вселенной.** М.: «Едиториал УРСС», 2004.
7. Дубров А.Г., Пушкин В.Н. **Парапсихология и современное естествознание.** М.: «Соваминко», 1989.
8. Заказчиков А.И. **Живая физика, фундаментальная физика с литературными вставками.** М.: «Рохос», 2005.
9. Ландау Л.Р., Лифшиц Е.М. **Теория поля.** М.: «Наука», 1965.
10. Науменко Ю.М., Науменко Г.А. **Эфир и материя.** М.: «Мир», 2005.
11. Ньютон И. **Математические начала натуральной философии.** М.: «Наука», 1989.
12. *"Пространство, Время, Тяготение". Материалы VII Международной конференции*, Санкт-Петербург, Россия, 19-23 августа 2002. СПб: «ТЕССА» (2003).
13. *"Пространство, Время, Тяготение". Материалы VIII международной конференции*, Санкт-Петербург, Россия, 2004. СПб. (2005).
14. *"Пространство, Время, Тяготение". Материалы IX международной конференции*, Санкт-Петербург, Россия, 7-11 августа 2006. СПб: «Тесса» (2007).
15. Родин А.Л. "О неизвестных опытах по электромагнитной индукции", *Электричество,* **7** (1994).
16. **Советский энциклопедический словарь.** М.: «Советская энциклопедия», 1983.
17. Спиридонов О.П. **Универсальные физические постоянные.** М.: «Просвещение», 1984.
18. Тарантул В.З. **Геном Человека.** М.: «Языки славянской культуры», 2003.
19. Фейнман Р. **КЭД странная теория света и вещества.** М.: «Наука», 1988.
20. Фейнман Р., Лейтон Р., Сэндс М. **Фейнмановские лекции по физике.** М.: «Мир», 1976.
21. Фрейзер Г. **Антиматерия, зазеркальные миры.** М.: «Мир», 2002.
22. Чебанов В.К. **Темпоральная теория самосоздания и саморазвития Вселенной и единые природные основания действующих в них всеобщих**

трансцендентальных законов. Ставрополь: «Ставропольсервисшкола», 2003.

23. Чебанов В.К. “Активное энергоинформационное поле - основа и источник законов природы и развития”, *Материалы IX международной научной конференции «Пространство, время, тяготение»*, Санкт-Петербург, (2008).
24. Чебанов В.К. “Субстанционально трансцендентальная полилектика (СТП) и физика”, *Материалы XVI Международной научной конференции*, Ставрополь. Издательство Ставропольского института имени В.Д. Чурсина, (2008).
25. Шипов Г.И. **Теория Физического вакуума.** М.: «Наука», 1997.
26. Шноль С.Э. **Физико-химические факторы биологической эволюции.** М.: «Наука», 1979.
27. Эфроимсон В.П. **Генетика этики и эстетики.** СПб.: «Талисман», 1995.
28. Яровский Б.М., Детлаф А.А., Лебедев А.К. **Справочник по физике.** 8-е изд., перераб., испр. М.: ООО Издательство «Оникс». ООО «Издательство «Мир и образование», 2006.

Таблица коэффициентов

Миры	№ п/п	Физические единицы	Обо-значе-ние	Формула
Магнито-термодинамический	1	Сила	Рч =	Ш/Лц, $Дж_{мт}$/К, 1/$k_б$
	2	Напряжение, потенциал	Ш =	К/с, Рч·Лц, Лц/$k_б$, 1/ $k_б$·$См_{мт}$, 1/ $k_{бэм}$·Ом, Ом/ $k_{бэм}$, Лц/ $k_{бгэ}$, 1/ $k_{бгэ}$·$См_{гэ}$
	3	Сопротивление	Лц =	Ш/Рч, 1/$См_{мт}$= $k_б$·Ш
	4	Проводимость	$См_м$ =	Рч/Ш, 1/Лц, Бр/К
	5	Емкость	$Ф_{мт}$ =	Бр/Ш, $См_{мт}$·с
	6	Импульс, заряд, время	Бр =	Рч·с, К/Лц
	7	Поток, пространство	К =	Ш·с, Рч·Лц·с, Бр·Лц, Рч·$Гн_{мт}$
	8	Индукция	$Тл_{мт}$ =	К/$м^2$
	9	Индуктивность	$Гн_{мт}$ =	К/Рч, $k_б$·К
	10	Энергия, работа	$Дж_м$ =	Рч·К, А·Вб, Н·м
Электромагнитный	11	Сила	А =	В/Ом, Дж/Вб, 1/$k_{бэм}$
	12	Напряжение, потенциал	В =	Вт/А, Вб/с, А·Ом
	13	Сопротивление	Ом =	В/А, $k_{бэм}$·В, 1/См
	14	Проводимость	См =	А/В, 1/Ом
	15	Емкость	Ф =	Кл/В, Ом·Лц·$Ф_{мт}$
	16	Импульс, заряд, время	Кл =	А·с, Вб/Ом, В·Ф
	17	Поток, пространство	Вб =	В·с, Кл·Ом, $Дж_{эм}$/А, Кл/См, А·Гн
	18	Индукция	Тл =	Вб/$м^2$, $k_{бэм}$/$Гн_{гэ}$, Н/А·м, 1/А·$Гн_{гэ}$
	19	Индуктивность	Гн =	Вб/А, $k_{бэм}$·Вб, Ом·с,
	20	Энергия, работа	$Дж_э$ =	Вб·А, Рч·К, Н·м
Гравитонно-электрический	21	Сила	Н =	Дж/м, кг/Лм
	22	Напряжение, потенциал	кг =	Н/$См_{гэ}$, Н·Лм, Н/$См_{гэ}$, Ф·Гн/$Гн_{гэ}$
	23	Сопротивление	Лм =	кг/Н, кг· $k_{бгэ}$
	24	Проводимость	$См_{гэ}$=	Н/кг, 1/Лм, $Тл_{мт}$/м/с·Ш, м/с/Лц·$Ф_{мт}$, $k_{б\,гэ}$/ $\sqrt[3]{Гн_{гэ}}$
	25	Емкость	$Ф_{гэ}$ =	с/кг, м/с/кг·$См_{гэ}$, Лм·м/с/кг
	26	Импульс, заряд, время	с =	кг·$Ф_{гэ}$, $k_б$·Бр, Бр/Рч, м/с/$См_{гэ}$
	27	Поток, пространство	м =	с·м/с, Дж/Н, $k_{б\,гэ}$·Дж, Н·$Гн_{гэ}$,
	28	Индукция	$Тл_{гэ}$ =	м/$м^2$, Лц/$Гн_{мт}$·м/с, 1/ $k_{б\,гэ}$·Дж, $k_{б\,гэ}$/$Гн_{гэ}$, 1/Н·$Гн_{гэ}$
	29	Индуктивность	$Гн_{гэ}$ =	м/Н, $k_{б\,гэ}$·м, $k_{б\,гэ}$/$Тл_{гэ}$
	30	Энергия, работа	$Дж_{гэ}$=	Н·м, Вб·А, Рч·К

ПРИЛОЖЕНИЕ 1

перевода физических единиц

в м/с			м/с в физических единицах		
множитель	степень	раз-ть	множитель	степень	раз-ть
0.724296357026	10^{23}	м/с/м/с	0.1380650324	10^{-22}	$к_{больцмана}$
0.112552973289	10^{-45}	м/с	0.8884705315	10^{46}	Ш
0.155396299028	10^{-68}	м/с	0.643515969292	10^{69}	Лц
0.643515969292	10^{69}	1/м/с	0.643515969292	10^{69}	$1/См_{мт}$
0.136264423863	10^{109}	м/с	0.73386726458	10^{-108}	$Ф_{мт}$
0.153369660594	10^{63}	$м^2/с^2$	0.807477208246	10^{-31}	$\sqrt{Бр}$
0.238330776399	10^{-6}	$м^3/с^3$	0.161289696269	10^{3}	$\sqrt[3]{К}$
0.531537386236	10^{-85}	$1/м^3/с^3$	0.375991423675	10^{-28}	$1/\sqrt[3]{Тл_{мт}}$
0.329051463654	10^{-29}	$м^3/с^3$	0.672324169955	10^{10}	$\sqrt[3]{Гн_{мт}}$
0.172622113115	10^{17}	$м^3/с^3$	0.386931889184	10^{-5}	$\sqrt[3]{Дж_{мт}}$
0.283652430488	10^{-4}	м/с/м/с	0.352544132366	10^{5}	$к_{больцм.эм}$
0.2874	10^{-18}	м/с	0.347947112038	10^{19}	В
0.101321183642	10^{-13}	м/с	0.986960440109	10^{14}	Ом
0.986960440109	10^{14}	1/м/с	0.986960440109	10^{14}	1/См
0.208988746459	10^{54}	м/с	0.478494663922	10^{-53}	Ф
0.600633657325	10^{35}	$м^2/с^2$	0.408032886454	10^{-17}	$\sqrt{Кл}$
0.608569130955	10^{21}	$м^3/с^3$	0.118003990039	10^{-6}	$\sqrt[3]{Вб}$
0.135726174395	10^{-57}	$1/м^3/с^3$	0.513910947639	10^{-19}	$1/\sqrt[3]{Тл}$
0.214547476257	10^{26}	$м^3/с^3$	0.359880954149	10^{-8}	$\sqrt[3]{Гн}$
0.172622113115	10^{17}	$м^3/с^3$	0.386931889184	10^{-5}	$\sqrt[3]{Дж_{эм}}$
0.815217085222	10^{-23}	м/с/м/с	0.122666712723	10^{24}	$к_{больцм.гэ}$
0.172622113115	10^{17}	м/с	0.579300057191	10^{-16}	Кг
0.211749871592	10^{40}	м/с	0.472255304092	10^{-39}	Лм
0.472255304092	10^{-39}	1/м/с	0.472255304092	10^{-39}	$1/См_{гэ}$
0.122666712723	10^{24}	м/с	0.815217085222	10^{-23}	$Ф_{гэ}$
0.211749871592	10^{40}	$м^2/с^2$	0.217314358497	10^{-19}	$\sqrt{с}$
0.211749871592	10^{40}	$м^3/с^3$	0.778739638933	10^{-13}	$\sqrt[3]{м}$
0.472255304092	10^{-39}	$1/м^3/с^3$	0.778739638933	10^{-13}	$1/\sqrt[3]{Тл_{гэ}}$
0.259746606677	10^{63}	$м^3/с^3$	0.156729244138	10^{-20}	$\sqrt[3]{Гн_{гэ}}$
0.172622113115	10^{17}	$м^3/с^3$	0.386931889184	10^{-5}	$\sqrt[3]{Дж_{гэ}}$

Универсальные константы по ритмам

№ п/п	Наименование констант		
	Формула Чебанова В.К.	Общепринятые обозначения и значения	Магнито-термодинамический
1	Вина $\kappa_в = (2 \cdot C^6 \cdot 10^{-20})/\pi^2 \cdot$ $\cdot 0.993895025762 =$ $= 0.2897768651 \cdot 10^{-2}$ *м·К*	Вина $\kappa_в = 2.8977686(51) \cdot \cdot 10^{-3}$ *м·К*	$2 \cdot 0.993895025762 \cdot$ $\cdot 0.114546608634 \cdot 10^{12} \cdot$ *К* $\cdot 0.1272655801 \cdot 10^{-13}$ *м*
2	Юрченко (новая) $\kappa_ю = (C^0 \cdot 10^{-20})/\pi^2 =$ $= 0.101321183642 \cdot 10^{-20} \cdot$ *Ф*$_{РТ}$	Общепринятых формулы и значения нет	$\kappa_ю = 0.139889125023 \cdot$ $\cdot 10^{-43}$ *Рч*
3	Эйнштейна (новая) $\kappa_э = (C^1 \cdot 10^{-20})/\pi^2 =$ $= 0.303753266915 \cdot 10^{-12}$ *м/с*	Общепринятых формулы и значения нет	$\kappa_э = 0.269875826522 \cdot$ $\cdot 10^{34}$ *Ш*
4	Кулона $\kappa_к = (C^2 \cdot 10^{-20})/\pi^2 =$ $= 0.910629385139 \cdot$ $\cdot 10^{-4} \cdot м^2/с^2 =$ $= 0.898755178726 \cdot$ $\cdot 10^{10} \cdot м^2/Кл^2$	Кулона $\kappa_к = 0.898755178436 \cdot \cdot 10^{10}$ $Н \cdot м^2/Кл^2$	$\kappa_к = 0.593748060478 \cdot$ $\cdot 10^{-66}$ *Бр*
5	Ломоносова (новая) $\kappa_л = (C^3 \cdot 10^{-20})/\pi^2 =$ $= 0.272999821698 \cdot 10^5 \cdot м^3/с^3$	Общепринятых формулы и значения нет	$\kappa_л = 0.114546608634 \cdot$ $\cdot 10^{12} \cdot К = 0.158148812322 \cdot$ $\cdot 10^{-11}$ *Дж*
6	Ньютона $\kappa_н = (C^4 \cdot 10^{-20})/\pi^2 =$ $= 0.667200463451 \cdot 10^{-10} \cdot$ $\cdot Н \cdot м^2/кг^2$	Ньютона $G = 6.673(10) \cdot 10^{-11}$ $Н \cdot м^2/кг^2 =$ $= 6.673(10) \cdot 10^{-11} \cdot м^3/(кг \cdot с^2)$	$\kappa_н = 0.269875826522 \cdot$ $\cdot 10^{34} \cdot Ш \cdot 0.1272655801 \cdot$ $\cdot 10^{-13}$ *м*
7	Планка $\kappa_п = C^5 \cdot 10^{-20} =$ $= 0.62606876517 \cdot 10^{-33} \cdot Дж \cdot с$	Планка $h = 6.62606876(52) \cdot$ $\cdot 10^{-34} \cdot Дж \cdot с$	$\kappa_п = 0.593748060478 \cdot$ $\cdot 10^{-66} \cdot Бр \cdot 0.1272655801 \cdot$ $\cdot 10^{-13}$ *м*

Разъяснения:

1) при расчете $\kappa_в$ – коэффициент 2 отражает факт, что кванты осевого вращения передаются и гравитонами, и фотонами, коэффициент 0.99389502562 – отражает то, что гравитонов меньше, чем фотонов;

ПРИЛОЖЕНИЕ 2

физического мира в трех его ипостасях

Физические миры		Соответствующий физический смысл константы
Электромагнитный	Гравитонно-электрический	
$2\cdot0.993895025762\cdot$ $\cdot0.4485929949341\cdot10^{-16}\cdot Вб\cdot$ $\cdot0.1272655801\cdot10^{-13}\cdot м$	$2\cdot0.993895025762\cdot$ $\cdot0.128925613812\cdot10^{-34}\cdot м\cdot$ $\cdot0.1272655801\cdot10^{-13}\cdot м =$ $= 0.164077930315\cdot10^{48}\ м^2$	Момент осевого вращения термоквантов гравитона и фотона
$к_ю = 0.357201887774\cdot10^{-16}\cdot А$	$к_ю = 0.124287365265\cdot10^{3}\cdot Н$	Сила ЕЭИП. Термодинамическая, электрическая, гравитонная
$к_э = 0.105690071995\cdot10^{7}\ В$	$к_э = 0.175964284895\cdot10^{-28}\ кг$	Напряжение термодинамическое, электрическое, масса гравитонного пучка
$к_к = 0.151611448015\cdot10^{-38}\cdot Кл$	$к_к = 0.430049557193\cdot10^{-43}\cdot с$	Импульс (заряд) гравитона, время оборота осевого вращения гравитонов, фотонов
$к_я = 0.448592949942\cdot10^{-16}\cdot Вб =$ $= 0.158148812322\cdot10^{-11}\cdot Дж$	$к_я = 0.128925613812\cdot10^{-34}\ м = = 0.158148812322\cdot10^{-11}\cdot Дж$	Поток, энергия ЕЭИП в различных ипостасях
$к_н = 0.105690071995\cdot10^{7}\cdot В\cdot$ $\cdot0.1272655801\cdot10^{-13}\ м$	$к_н = 0.175964284895\cdot10^{-28}\ кг\cdot$ $\cdot0.1272655801\cdot10^{-13}\ м$	Момент термодинамического, электрического, гравитонного напряжения (массы)
$к_п = 0.151611448015\cdot10^{-38}\cdot Кл\cdot$ $\cdot0.1272655801\cdot10^{-13}\ м$	$к_п = 0.430049557193\cdot10^{-43}\cdot с\cdot$ $\cdot0.1272655801\cdot10^{-13}\ м$	Момент импульса (заряда) ЕЭИП в трех физических мирах

2) $Р_ч$, Ш, Бр, $Ф_{РТ}$ - новые единицы измерения введенные автором: Рч – Риччи – единица магнито-термодинамической силы, Ш – Шипов – единица напряжения этой силы, Бр – Бергсон – единица импульса этой силы, $Ф_{РТ}$ – Ферт - единица силы всеобщая.

Величина природных квантов единого

Миры	№ п/п	Физические единицы	Обо-значе-ние	Формула
Магнито-термодинамический	1	Сила	Рч =	Ш/Лц, $Дж_{мт}$/К, 1/$k_б$
	2	Напряжение, потенциал	Ш =	К/с, Рч·Лц, Лц/$k_б$, 1/ $k_б$·$См_{мт}$, 1/ $k_{бэм}$·Ом, Ом/ $k_{бэм}$, Лц/ $k_{бгэ}$, 1/ $k_{бгэ}$·$См_{гэ}$
	3	Сопротивление	Лц =	Ш/Рч, 1/$См_{мт}$= $k_б$·Ш
	4	Проводимость	$См_м$ =	Рч/Ш, 1/Лц, Бр/К
	5	Емкость	$Ф_{мт}$ =	Бр/Ш, $См_{мт}$·с
	6	Импульс, заряд, время	Бр =	Рч·с, К/Лц
	7	Поток, пространство	К =	Ш·с, Рч·Лц·с, Бр·Лц, Рч·$Гн_{мт}$
	8	Индукция	$Тл_{мт}$ =	К/$м^2$
	9	Индуктивность	$Гн_{мт}$ =	К/Рч, $k_б$·К
	10	Энергия, работа	$Дж_м$ =	Рч·К, А·Вб, Н·м
Электромагнитный	11	Сила	А =	В/Ом, Дж/Вб, 1/$k_{бэм}$
	12	Напряжение, потенциал	В =	Вт/А, Вб/с, А·Ом
	13	Сопротивление	Ом =	В/А, $k_{бэм}$·В, 1/См
	14	Проводимость	См =	А/В, 1/Ом
	15	Емкость	Ф =	Кл/В, Ом·Лц·$Ф_{мт}$
	16	Импульс, заряд, время	Кл =	А·с, Вб/Ом, В·Ф
	17	Поток, пространство	Вб =	В·с, Кл·Ом, $Дж_{эм}$/А, Кл/См, А·Гн
	18	Индукция	Тл =	Вб/$м^2$, $k_{бэм}$/$Гн_{гэ}$, Н/А·м, 1/А·$Гн_{гэ}$
	19	Индуктивность	Гн =	Вб/А, $k_{бэм}$·Вб, Ом·с,
	20	Энергия, работа	$Дж_э$ =	Вб·А, Рч·К, Н·м
Гравитонно-электрический	21	Сила	Н =	Дж/м, кг/Лм
	22	Напряжение, потенциал	кг =	Н/$См_{гэ}$, Н·Лм, Н/$См_{гэ}$, Ф·Гн/$Гн_{гэ}$
	23	Сопротивление	Лм =	кг/Н, кг· $k_{бгэ}$
	24	Проводимость	$См_{гэ}$ =	Н/кг, 1/Лм, $Тл_{мт}$/м/с·Ш, м/с/Лц·$Ф_{мт}$, $k_{б\,гэ}$/ $\sqrt[3]{Гн_{гэ}}$
	25	Емкость	$Ф_{гэ}$ =	с/кг, м/с/кг·$См_{гэ}$, Лм·м/с/кг
	26	Импульс, заряд, время	с =	кг·$Ф_{гэ}$, $k_б$·Бр, Бр/Рч, м/с/$См_{гэ}$
	27	Поток, пространство	м =	с·м/с, Дж/Н, $k_{б\,гэ}$·Дж, Н·$Гн_{гэ}$,
	28	Индукция	$Тл_{гэ}$ =	м/$м^2$, Лц/$Гн_{мт}$·м/с, 1/ $k_{б\,гэ}$·Дж, $k_{б\,гэ}$/$Гн_{гэ}$, 1/Н·$Гн_{гэ}$
	29	Индуктивность	$Гн_{гэ}$ =	м/Н, $k_{б\,гэ}$·м, $k_{б\,гэ}$/$Тл_{гэ}$
	30	Энергия, работа	$Дж_{гэ}$=	Н·м, Вб·А, Рч·К

ПРИЛОЖЕНИЕ 3

энергоинформационного поля (ЕЭИП)

Кванты единого энергоинформационного поля					
в физических единицах			в м/с		
множитель	степень	раз-ть	множитель	степень	раз-ть
0.139889125023	10^{-43}	Рч	0.101321183642	10^{-20}	$Ф_{рт}$
0.269875826522	10^{34}	Ш	0.303753266913	10^{-12}	м/с
0.192921234211	10^{78}	Лц	0.299792458	10^{9}	м/с
0.518346258817	10^{-77}	$См_{мт}$	0.333564095191	10^{-8}	1/м/с
0.220007871074	10^{-99}	$Ф_{мт}$	0.2997922458	10^{9}	м/с
0.593748060478	10^{-66}	Бр	0.910629385139	10^{-4}	$м^2/с^2$
0.113052971102	10^{33}	К	0.269440024172	10^{26}	$м^3/с^3$
0.69823895415	10^{60}	$Тл_{мт}$	0.371140108657	10^{-25}	$1/м^3/с^3$
0.808161256876	10^{76}	$Гн_{мт}$	0.265926644842	10^{47}	$м^3/с^3$
0.158148812322	10^{-11}	$Дж_{мт}$	0.272999821698	10^{5}	$м^3/с^3$
0.357201887774	10^{-16}	А	0.101321183642	10^{-20}	$Ф_{рт}$
0.105690071995	10^{7}	В	0.303753266913	10^{-12}	м/с
0.295883296288	10^{23}	Ом	0.299792458	10^{9}	м/с
0.337971089461	10^{-22}	См	0.333564095191	10^{-8}	1/м/с
0.143449091436	10^{-44}	Ф	0.2997922458	10^{9}	м/с
0.151611448015	10^{-38}	Кл	0.910629385139	10^{-4}	$м^2/с^2$
0.442743495303	10^{5}	Вб	0.269440024172	10^{26}	$м^3/с^3$
0.273447705181	10^{33}	Тл	0.371140109218	10^{-25}	$1/м^3/с^3$
0.123947691895	10^{22}	Гн	0.265926644842	10^{47}	$м^3/с^3$
0.158148812322	10^{-11}	$Дж_{эм}$	0.272999821698	10^{5}	$м^3/с^3$
0.124287365265	10^{3}	Н	0.101321183642	10^{-20}	$Ф_{рт}$
0.175964284895	10^{-28}	кг	0.303753266913	10^{-12}	м/с
0.141578578417	10^{-30}	Лм	0.299792458	10^{9}	м/с
0.706321543256	10^{31}	$См_{гэ}$	0.333564095191	10^{-8}	1/м/с
0.244395933782	10^{-14}	$Ф_{гэ}$	0.2997922458	10^{9}	м/с
0.424441900239	10^{-22}	с	0.910629385139	10^{-4}	$м^2/с^2$
0.127244480551	10^{-13}	м	0.269440024172	10^{26}	$м^3/с^3$
0.785888704696	10^{14}	$Тл_{гэ}$	0.371140109218	10^{-25}	$1/м^3/с^3$
0.102379256555	10^{-15}	$Гн_{гэ}$	0.265926644842	10^{47}	$м^3/с^3$
0.158148812322	10^{-11}	$Дж_{гэ}$	0.272999821698	10^{5}	$м^3/с^3$

К ВОПРОСУ ОБ ЭВОЛЮЦИИ РАЗУМА: О СТРУКТУРЕ ДУШИ, ЭТАПАХ ЕЕ ЭВОЛЮЦИИ И МЕТОДАХ СОВЕРШЕНСТВОВАНИЯ

Смирнов Е.Я.

Санкт-Петербургский государственный университет,
Университетская наб., 7/9, Санкт-Петербург, 199178, Россия,
E-mail: smirnov@ps8019.spb.edu

Выдвигаются гипотезы структуры души человека, этапов ее эволюции и методов совершенствования. Именно, считается, что созданный почти по образу и подобию Творца Дух является центральной частью Души. Дух облачен в ряд одежд-оболочек, ограничивающих возможности Духа тем больше, чем больше этих оболочек. При этом материя оболочки тем тоньше, чем ближе к Духу, материя которого является самой тонкой, находится эта оболочка. Эволюция Души происходит путем последовательного снятия наружных оболочек. После снятия трех верхних оболочек Душа лишается возможности воплощения в тело человека.

Совершенствование Души происходит на путях испытаний и обучения (добровольного или, если понадобится, принудительного). Содержание доклада базируется на материалах многочисленных бесед автора с представителями тонкого мира.

О происхождении Разума (см. [1], [2])

В 1989-м году я впервые стал свидетелем и участником мощного полтергейста, выразившегося во всевозможных телепортациях, появлении разнообразных записей на магнитофонных кассетах и др. Из этих записей, в частности, следовало, что организаторами полтергейста были прибывшие из мира тахионов эфемизмы, как они себя называли, которые, как и люди, суть <сложные системы с искусственным интеллектом, являющиеся порождением Разума>.

После встречи с эфемизмами мне - убежденному атеисту - пришлось пересмотреть свои взгляды. Сейчас я - по-прежнему, материалист, но считаю, что Бог существует и является, видимо, единственной разумной сущностью естественного происхождения. Думается, что "зародыш Бога" возник случайным образом в виде мыслящей, хотя и на достаточно примитивном уровне, ассоциации тахионов, а затем благодаря неимоверно длительному титаническому труду создал в себе могучий интеллект, а окружающий хаос преобразовал в структурированную Вселенную, управляемую созданным им же мощным космическим Разумом. При этом, естественно, построение Вселенной шло от простого к сложному, т.е. сперва строились блоки Вселенной из тончайшей материи, затем из материи всё более сложной организации, а затем уже из самой сложной материи, присущей нашему блоку Вселенной, в частности, содержащему нашу Солнечную систему. Разумеется, для соответствующих блоков Вселенной и технические устройства, и разумные сущности создавались из материи, максимальная организация которой не превышала максимальной организации материи соответствующего блока Вселенной.

Думается, что космический Разум, в частности, обеспечивает принципиальную возможность контактов между любыми разумными сущностями (это, видимо, обеспечивается за счет того, что внутренние языки всех технических устройств и разумных существ являются теми или иными фрагментами единого технического праязыка [3]) и их дозированный доступ к космическим информационным банкам данных (информационным полям).

Думается, что самосовершенствование Бога и совершенствование Вселенной продолжается и поныне, а само построение и совершенствование Вселенной базируется:

- на принципе минимизации энергии (основополагающем принципе движения);
- на принципе РАЗУМНОСТИ, составляющими которого являются, в частности, трудолюбие, ответственность, рачительность, доброжелательность;
- на принципе взвешенности индивидуального и коллективного (основополагающем принципе развития общества разумных существ);
- на праве выбора и испытаниях (методе селекции разумных существ).

О происхождении Души (см. [2])

На определенном этапе для усиления возможностей творчества (ведь один ум - хорошо, а несколько - лучше) Бог стал создавать сотоварищей по творчеству (Духов). Это он начал делать по своему образу, но с разными значениями параметров, ибо точное копирование

ничего нового не добавляло бы. В результате в какой-то момент появился Дух-Дьявол, т.е. гипертрофированный эгоцентрик. Вины Творца здесь нет, ибо у первопроходца другого метода исследования, кроме метода проб и ошибок нет, а у сформировавшегося Творца-труженика, к тому же не имеющего ничего похожего на зависть, избытка эгоцентризма не могло появиться. Не смотря на этот казус, принесший Творцу немало хлопот (картинка "Горбачев - Ельцин" достаточно хорошо иллюстрирует некоторые из этих хлопот), у Творца не пропало желание создавать сотоварищей, но, разумеется, пришлось принять меры предосторожности, чтобы снова не попасть впросак. Эти меры предусматривали "облачение Духов в тяжелые доспехи" (по библии облачение в кожаные одежды) и помещение в разнообразные специальные тренажеры. "Доспехи" лишали Духов возможности использовать ряд мощных присущих им функциональных средств (доступ к космическим информационным банкам данных, возможность телепортации и др.). Тренажеры позволяли выявить определенные качества испытуемых Духов, в первую очередь, выяснить, можно ли с испытуемым Духом без опаски идти в горы в одной связке (разумеется, одновременно определялись и свойства тренажеров). Тренажеры строились как самовоспроизводящиеся технические устройства, причем, на первых порах самовоспроизводство сводилось к чистому копированию, но затем, когда космическим экспериментаторам надоело делать "вручную" новые разновидности одного и того же тренажера, они придумали многопараметрический механизм парного воспроизводства (женские и мужские особи, перекрестное опыление). Не исключено, что это произошло как раз в нашем блоке Вселенной. При этом при формировании мужских генов, разумеется, за основу брались женские гены, в которых отключались не нужные блоки и добавлялись необходимые новые (так всегда поступают и люди при создании близкого к базовому нового образца сложной системы). Подтверждением сказанного являются многочисленные патологии в половой сфере, которые хорошо объясняются описанной схемой, и встречающееся в растительном и животном мире воспроизводство потомства без оплодотворения в виде точной копии женской особи.

Подчеркну, что под <Духом> я понимаю сложную систему, структурно близкую к Творцу (думаю, что структурной идентичности быть не должно), обладающую не только искусственным интеллектом, но и периферийными устройствами коммуникационного, транспортного и другого назначения. Под <"доспехами" для Духа> я понимаю аретирную систему (мне представляется, что она выполнена Духа> с широким привлечением нитеобразных и пленочных материалов из "тонкой" материи), которая, как отмечалось выше, предназначается для ограничений функциональных возможностей Духа в период испытаний. Под <тренажером> я понимаю самовоспроизводящееся техническое устройство (оно создано как из более "грубой", нежели "доспехи", материи (собственно, тело тренажера), так и из "тонкой" материи, близкой по свойствам к материи "доспехов" (биополе тренажера)), служащее либо испытательным стендом для испытуемого Духа или Духа-испытателя, либо, скажем, игровым автоматом для Духа-туриста. Если тренажер - тело человека, то (в моем понимании) Дух в "доспехах" или в другом облачении - это Душа человека.

О целях и правилах селекции (см. [4])

Создавая коллектив сотоварищей по творчеству Бог, думается, предполагал, что в этом коллективе будут созданы самые благоприятные условия для

творчества: дружелюбная атмосфера, позволяющая в полной мере реализовать способности и удовлетворить потребности каждого. Практика показала, что для этого характеры членов коллектива должны удовлетворять определенным требованиям (уравновешенность эгоцентризма и коллективизма). Поэтому создаваемых Духов подвергли испытаниям, организовав "игру", целью которой является селекция Духов, а именно выявление Духов, которые могут руководствоваться библейским принципом: "возлюби ближнего, как самого себя", и отбраковка тех, которые этим принципом руководствоваться не в состоянии.

Представители первой группы будут подниматься по эволюционной лестнице вверх, занимая в космическом хозяйстве места в соответствии со своими способностями.

Представители второй группы либо тоже будут использованы в космическом

хозяйстве, если от них будет хоть какая-то польза, а не вред, либо в

противном случае будут подвергнуты аннигиляции, т.е. будут уничтожены (мне представляется, что личности типа Усамы Бен-Ладена и Анатолия Чубайса будут уничтожены, если они испытуемые, а не подсадные утки в селекционной игре).

Основными правилами селекции, как мне представляется, являются следующие:

- Испытуемый имеет право выбора и обязан свой выбор сделать. Нарушители наказываются (по Данте в последнем самом страшном круге Ада находятся не души злодеев, а души равнодушных (никак не проявивших себя) людей).

- Испытуемому дается возможность " прожить" целую серию образов (вплоть до фундаментальной, если испытуемый не сойдет раньше времени с дистанции), либо буквально побывав в "шкуре" этих образов, находясь в соответствующих тренажерах, либо поиграв на этих тренажерах мысленно.

- Испытуемый и индивидуально, и в составе самых разнообразных групп подвергается всевозможным испытаниям и соблазнам (В последние двадцать лет все мы являемся свидетелями и участниками грандиозной игры, начатой М.С.Горбачевым с целью позитивного обновления СССР и повернутой Ельциным в противоположную сторону. В результате "застойное болото" СССР было взбаламучено настолько, что основная часть нравственной человеческой мути всплыла наверх, что значительно усложнило жизнь жителей бывшего СССР, но в тоже время существенно облегчило работу космических ассенизаторов).

Думается, что селекционные игры проводятся в виде натурных испытаний потому, что мощность компьютерной системы космического Разума не позволяет провести полномасштабное имитационное моделирование (Бог, как мне представляется, - существо очень любознательное и доброе, для которого наблюдение за происходящими жестокостями вызывает не интерес, а сострадание). Думается, что в селекционных играх Дьявол со своей командой принимает самое активное участие, но не по своему усмотрению, а на условиях четкого контракта с Богом.

В моем понимании ад - это учебно-исправительное учреждение строгого режима, в котором души отбывают наказание за прегрешения и в котором грешников учат с пристрастием, что жить надо по Божескому принципу "возлюби ближнего, как самого себя", а не иначе, тем более не по дьявольскому принципу "обмани ближнего и возрадуйся", причем, срок пребывания грешника в аду ограничен, а не вечен. Рай же - это гигантская разносторонняя и разноуровневая творческая лаборатория с дружелюбным микроклиматом, в которую попадают успешно прошедшие испытания души и после определения своих наклонностей и способностей, совершенствуясь, занимают там подобающее им место.

О структуре Души

Думается, что Душа имеет структуру, похожую на структуру русской матрешки, а именно, центральной частью Души является Дух, который помещен в ряд аретирных оболочек. Отличие состоит в том, что соседние оболочки соединены между собой специальными "переходниками", позволяющими,в частности, в верхней оболочке пары соседних оболочек использовать трансформированные процессы состоящей из более тонкой и, следовательно, более быстрой материи нижней оболочки пары соседних оболочек.

Ограничимся Землей. Обозначим через (Мир)/0 совокупность всех испытываемых на Земле душ, соответствующих стандартному уровню обычных людей, а через (Мир)/и - совокупность успешно проходящих испытание душ, у которых в процессе эволюции были сняты и оболочек. Оказывается, что для душ, принадлежащих множествам (Мир)/и, и = 0, 1, 2, возможно воплощение в тело человека, а для душ, принадлежащих множествам (Мир)/и для и >= 3, это уже не возможно.

Думается, что множества (Мир)/1, (Мир)/2 это множества душ истинных экстрасенсов, в частности, думается, что душа Иисуса Христа в облике человека принадлежала множеству (Мир)/2.

Души, попавшие в (Мир)/3, пробуют себя в различных областях деятельности и определяют те направления, в которых они себя чувствуют наиболее комфортно, т.е. именно здесь душа определяет свои истинные способности и в дальнейшем усовершенствуется в выбранных направлениях, поднимаясь по эволюционной лестнице вверх, быть может, вплоть до множества духов (Мир)/Д. Находящиеся на эволюционной лестнице на несколько ступеней выше, чем люди, эфемизмы, о которых шла речь выше, говорили, что среди них имеются бывшие земляне.

Правда мне не известно, находятся ли эфемизмы в множестве духов или еще его не достигли.

Замечание.

Дух, душа - очень сложные и трудоемкие системы, на изготовление которых затрачиваются, видимо, тысячи лет (ведь лишь на то, чтобы дух Иисуса Христа поместить в множество (Мир)/2, понадобилось свыше 700 лет (время между обещанием Творца прислать евреям Мессию и рождением этого Мессии под именем Иисуса Христа)). Поэтому на испытание души, видимо, затрачиваются также тысячи лет.

ЛИТЕРАТУРА

1. Смирнов Е.Я. Некоторые соображения по поводу структуры материи и эволюции разума - Тезисы докладов Международного Конгресса-2000 "Фундаментальные проблемы естествознания и техники". СПб., с.54; (см. также CD-диск материалов этого конгресса).

2. Смирнов Е.Я. К ВОПРОСУ ОБ ЭВОЛЮЦИИ РАЗУМА. - Труды Международного Конгресса-2002 "Фундаментальные проблемы естествознания и техники", часть 2, том 25. СПб., 2002. с. 172-181.
http://shaping.ru/download/pdffile/smirnov_EA_01rus.pdf
http://www.physical-congress.spb.ru/russian/SmirnovEA_01/smirnov_d1.asp

3. Смирнов Е.Я. К ВОПРОСУ О МЕХАНИЗМАХ РАЗВИТИЯ И ФУНКЦИОНИРОВАНИЯ ЖИВЫХ ОРГАНИЗМОВ - Труды Конгресса-2006 "Фундаментальные проблемы естествознания и техники". Часть I. Санкт-Петербург. 2006 год. Издательство "ОСИПОВ". Санкт-Петербург (Материалы Конгресса-2006 14 - 19 августа 2006 года, Санкт-Петербург, в сборнике серии "ПРОБЛЕМЫ ИССЛЕДОВАНИЯ ВСЕЛЕННОЙ". Вып. 31). с. 413 - 419.
http://www.physical-congress.spb.ru/download/cong06(006).pdf

4. Смирнов Е.Я. «О проекте «Идеи перестройки естествознания и общественного сознания». - там же; с. 400 - 412. http://www.physical-congress.spb.ru/download/smirnov_ey(01).doc

СУЩЕСТВУЕТ ЛИ ЭЛЕКТРИЧЕСКОЕ ПОЛЕ ВНУТРИ ЗАРЯЖЕННОЙ СФЕРЫ?

© ***Колонутов М.Г.*, 2012**

Новгородский государственный университет,
Россия, Великий Новгород, e-mail: kolonutov@mail.ru

В статье обсуждается вопрос локализации энергии электростатического поля. Анализ выполнен на основе теории близкодействия. Электрическое поле проявляется двояким образом. Во-первых, оно является средством силового взаимодействия заряженных тел и в этом качестве должно иметь не равный нулю градиент потенциала. Во-вторых, движение поля порождает магнитное поле. Градиент потенциала при этом может быть любым, в том числе и равным нулю. Средствами теории упругости показано, что электростатическое поле внутри сферы находится в состоянии гидростатического сжатия и обладает отличной от нуля плотностью энергии. Плотность энергии электростатического поля вне уединенной заряженной сферы остается равной нулю до тех пор, пока в него не помещен какой-либо другой носитель заряда.

Kolonutov M. *Is There Electric Field Inside a Charged Sphere?* This article discusses the localization energy of the electrostatic field. The analysis is performed using short-range theory. The electric field is manifested in two ways. The first field can be a means of force interaction between charged bodies. In this case, the gradient of the Coulomb potential can not be zero. Secondly, the movement of the electric field generates a magnetic field, regardless of the gradient. The magnetic field inside a charged sphere the result of the movement electric field gradient of the Coulomb potential is equal to zero. By means of the theory of elasticity shows that the electric field inside the sphere is in a state of hydrostatic compression and has a nonzero energy density. The energy density of the electrostatic field outside this isolated charged sphere remains zero until any other charge carrier is put into it.

1 Локализация энергии электрического поля

Современная электростатика утверждает, что электрическое поле вокруг уединенного заряженного тела обладает плотностью энергии, пропорциональной квадрату напряженности поля,

$$w(\mathbf{r}) = \frac{1}{2}\varepsilon_0 E^2.. \tag{1}$$

Это утверждение основывается, мягко говоря, на весьма спорном доказательстве. Как в учебниках, ставших классическими [1], так и во многих современных, например [2], исходным положением доказательства является выражение для энергии некоторой системы заряженных тел,

$$W = \frac{1}{2}\sum_i Q_i \varphi_i. \qquad (2)$$

Далее посредством замены суммы (2) интегралом (3) по объему V, выполняется переход к непрерывному распределению заряда с объемной плотностью $\rho(\mathbf{r})$,

$$W = \frac{1}{2}\int_V \varphi(\mathbf{r})\rho(\mathbf{r})dV. \qquad (3)$$

Казалось бы, что уже эта формула дает недвусмысленный ответ на то, что энергия сосредоточена лишь в той области пространства, где имеется некоторая отличная от нуля плотность заряда.

В самом деле, пусть имеется заряженное по объему тело A (рисунок 1). Охватим его произвольно большой замкнутой поверхностью и возьмем интеграл (3) по всему объему V пространства, охваченному этой поверхностью.

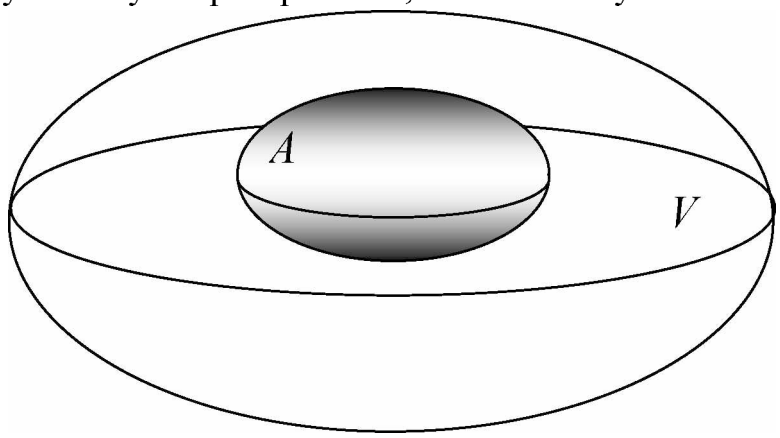

Рис. 1.

Интеграл (3) распадается при этом на сумму двух, один из которых, взятый по объему V_A тела A, дает некоторую отличную от нуля величину энергии, второй же, взятый по объему($V - V_A$) всего остального пространства, не занятого заряженным телом, будет всегда равен нулю в силу того, что плотность заряда ρ в этой части пространстве равна нулю.

Вместо того чтобы принять столь простое умозаключение авторы упомянутых и многих других книг начинают выполнять с интегралом (3) некоторые не всегда математические трюки. Вводится специально для этого случая понятие «полного поля», заряженное тело конечных размеров заменяется на тело бесконечно большого размера, после подмены появляется возможность выполнить предельный переход при $r \to \infty$, в результате которого появляется прямо противоположный вывод. Возникает формула (1), в соответствии с которой плотность энергии не равна нулю даже в тех точках пространства, в которых плотность заряда равна нулю. Некорректность такого вывода очевидна, но, тем не

менее, формула (1) по причине отсутствия какой-либо альтернативы благополучно существует, а посягательство на неё считается смертным грехом.

Важно подчеркнуть, что выражение (2) в явном виде, а формула (3) завуалировано, являются порождением теории дальнодействия носителей заряда. Теории, в которой поле как самостоятельная сущность отсутствует. Это означает, что выводы о свойствах поля, т. е. о свойствах того, что отсутствует, сделанные на основании этой теории, не могут быть корректными ни при каких обстоятельствах.

К решению вопроса о локализации энергии в электрическом поле следует, в силу этих соображений, подходить, не иначе как рассматривая поле в качестве некоторой сплошной материальной среды, передающей силовое взаимодействие заряженных тел и подчиняющейся законам механики. В связи с этим рассмотрим еще одну ситуацию.

Пусть имеется сферический носитель радиуса R, обладающий зарядом Q. Поверхность носителя испытывает при этом силовое воздействие плотность f, которого определяется формулой (4),

$$f = \frac{\varepsilon_0 E^2}{2} = \frac{Q^2}{32\pi^2 \varepsilon_0 R^4}, \tag{4}$$

и всегда направлена в сторону, соответствующую увеличению площади поверхности заряженного тела. Это, в самом деле, именно так, поскольку подтверждается постановкой соответствующих опытов.

Зададимся вопросом: чем обусловлено (каким материальным фактором) появление поверхностной плотности сил f, стремящейся увеличить радиус сферы?

Оставаясь в рамках концепции близкодействия, можно назвать только два кандидата на роль причины, ими могут быть либо поле внутри сферы, либо поле снаружи сферы. Наличие поля внутри сферы отвергается существующей теорией на том основании, что напряженность поля в точках внутреннего пространства сферы равна нулю. Остается электрическое поле вне сферы.

Законы механики говорят, что сила всегда действует на разделяющую поверхность в сторону области с меньшим значением плотности энергии. Но, коль скоро, внутри сферы электрическое поле отсутствует (плотность энергии равна нулю), а вне сферы имеется некоторая, отличная от нуля, плотность энергии, то сила всегда будет направлена к центру сферы, т. е. в сторону уменьшения, а не увеличения радиуса сферы. Возникшее противоречие вновь вызывает сомнение в наличии плотности энергии поля в пространстве вокруг носителя и об отсутствии электрического поля внутри рассматриваемого носителя заряда. Противоречие разрешается естественным образом, если считать, что электрическое поле (материальная среда) присутствует внутри заряженной сферы, находится в состоянии всестороннего сжатия и имеет равный нулю градиент потенциала. Нельзя отождествлять, как это делается в подавляющем

большинстве учебников, равенство нулю некоторой математической характеристики (градиента потенциала) электрического поля с наличием или отсутствием его самого как материального образования.

Еще одним интересным вопросом является возникновение магнитного поля внутри заряженной сферы при её вращении. Каким образом при отсутствии электрического поля внутри сферы факт её вращения приводит к рождению из «ничего» вполне материального образования в виде магнитного поля?

Формальный математический ответ о возникновении на поверхности сферы при её вращении плотности тока и, следовательно, ротора магнитного поля является продуктом теории дальнодействия. В ней не требуется никаких передаточных звеньев между током как источником магнитного поля и удаленной точкой пространства, в которой наблюдается напряженность этого поля. По этой причине такой ответ не может быть признан удовлетворительным. Теория близкодействия требует для описания стационарного физического процесса участия только тех величин, которые характеризуют одну и ту же точку пространства. Причиной возникновения магнитного поля в некоторой точке пространства может быть только движение электрического поля в той же самой точке. Естественно, движение электрического поля возникает не само по себе, а должно быть обусловлено движением какого-то носителя (в нашем случае, вращением сферы).

Рассмотрим вопрос связи электрического и магнитного полей в точках, расположенных на оси вращения заряженной сферы, исходя из предположения, что электрическое поле внутри заряженной сферы существует, но градиент его потенциала равен нулю, следовательно, потенциал во всех точках поля одинаков и равен потенциалу φ поверхности носителя заряда.

Предварительно определим напряженность магнитного поля создаваемого вращением тонкого кольца с линейной плотностью заряда τ в точках, расположенных на оси вращения (рис. 2).

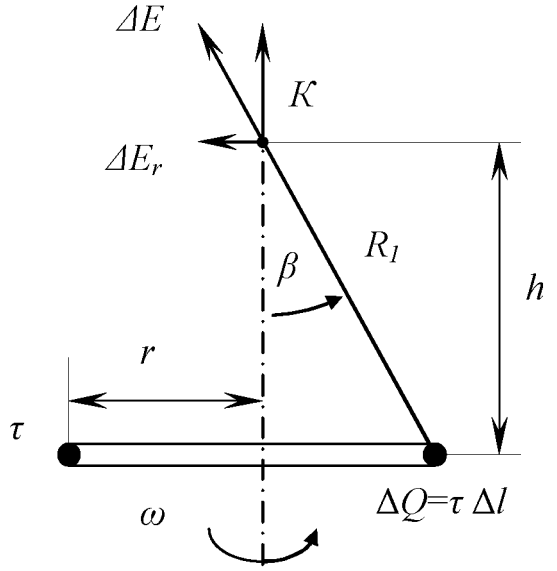

Рис. 2.

Из рисунка следует, что радиальная составляющая напряженности электрического поля, создаваемого элементом кольца Δl в некоторой точке K определяется выражением (5),

$$\Delta E_r = \left(\tau \Delta l / 4\pi\varepsilon R_1^2\right)\sin\beta. \tag{5}$$

Поле элемента кольца Δl движется относительно точки K, поэтому появляется магнитное поле с напряженностью $\varepsilon\,\boldsymbol{\omega} \times \mathbf{r} \times \Delta\mathbf{E}$, аксиальная составляющая которого ΔH выражается зависимостью (6),

$$\Delta H = \varepsilon\,\omega\, r \Delta E_r. \tag{6}$$

Проинтегрировав (6) по длине $2\pi r$ всего кольца получим напряженность магнитного поля, созданного вращением кольца, в точках, лежащих на оси вращения,

$$H = \frac{\tau}{2}\omega \sin^3\beta = \varepsilon\varphi\omega\sin^2\beta, \tag{7}$$

где φ – потенциал электростатического поля, созданного кольцом в точке K,

$$\varphi = \tau\sin\beta / 2\varepsilon. \tag{8}$$

Формула (7) замечательна тем, что связывает потенциал электростатического поля с напряженностью магнитного поля в одной и той же точке пространства и не требует привлечения информации об электрическом состоянии других точек пространства.

Теперь воспользуемся формулой (7) для нахождения магнитного поля вращающейся сферы с поверхностной плотностью заряда σ (рис. 3).

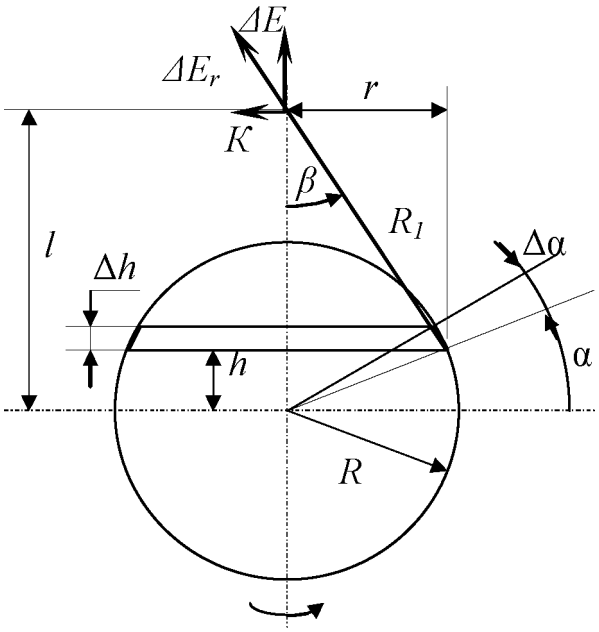

Рис. 3.

Вырежем на поверхности сферы полоску шириной Δh. Заряд полоски ΔQ составит величину $\Delta Q = \sigma\Delta S = \sigma 2\pi r R\Delta\alpha$, что соответствует линейной плотности заряда $\Delta\tau$,

$$\Delta\tau = \Delta Q/2\pi r = R\sigma\Delta\alpha. \tag{9}$$

При бесконечно малом приращении Δh полоску можно отождествить с кольцом, имеющим линейную плотность заряда $\Delta\tau$. Тогда напряженность ΔH магнитного поля, создаваемого вращающейся полоской в точках, расположенных на оси вращения, в соответствии с зависимостью (7) составит

$$\Delta H = \frac{1}{2}\omega\sin^3\beta\Delta\tau = \frac{1}{2}\omega\sin^3\beta R_0\sigma\Delta\alpha. \tag{10}$$

Проинтегрируем эту зависимость по α с учетом того, что

$$\sin^3\beta = \left(R^3\cos^3\alpha\right)\Big/\left(\left(l - R\sin\alpha\right)^2 + R^2\cos^2\alpha\right)^{3/2}. \tag{11}$$

В результате получим искомую напряженность магнитного поля в точках, расположенных на оси вращения внутри сферы,

$$H_{\text{внт}} = \frac{2}{3}\varepsilon\varphi\omega,, \tag{12}$$

и снаружи сферы,

$$H_{\text{нар}} = \frac{2}{3}\varepsilon\varphi\omega\frac{R_0^3}{l_3}.. \tag{13}$$

Потенциал φ в формулах (12) и (13) является потенциалом как раз тех точек, в которых определяется напряженность магнитного поля.

Если подставить в выражение (12) зависимость для вычисления потенциала поверхности заряженной сферы, а значит и потенциала всех её внутренних точек, $\varphi = Q/4\pi\varepsilon R$, то выражение (12) приобретет вид (14),

$$H_{\text{внт}} = \frac{Q\omega}{6\pi R}, \tag{14}$$

в точности соответствующий решению аналогичной задачи, приведенному в задачнике [3] (задача 253*). Это совпадение результатов подтверждает адекватность изначальных предположений о наличии поля внутри заряженной сферы, положенных в основу проведенного анализа.

Плотность ω_1 энергии электрического поля внутри сферы, приходящаяся на единицу её заряда, может быть определена делением потенциала на объем сферы,

$$\omega_1 = \frac{\varphi}{V} = \frac{3Q}{16\pi^2 \varepsilon R^4}. \tag{15}$$

Плотность энергии ω, обусловленная не единицей заряда, а всем зарядом сферы, определяется интегрированием,

$$\omega = \int \omega_1 dQ = \frac{3Q^2}{32\pi^2 \varepsilon R^4}. \tag{16}$$

Справедливость этой формулы подтверждается весьма необычным для электростатики образом – анализом напряженного (в механическом смысле этого слова) состояния поля снаружи и внутри сферы.

2 Механические напряжения в электростатическом поле

Поле является сплошной средой, посредством которой осуществляется силовое взаимодействие заряженных тел. Отсюда следует, что поле должно адекватно описываться законами механики сплошной среды. Никаких соображений, препятствующих применению этих законов, не существует, напротив, игнорирование положений механики существенно обедняет теоретический багаж физики электрических явлений.

Примем в качестве объекта исследования сферический конденсатор, внутренняя обкладка которого имеет радиус R, внешняя – R_0.

С точки зрения механики поверхностная плотность сил, действующих на обкладки, является порождением напряженного состояния той среды, которая находится внутри конденсатора, т. е. электрического поля. Поставим поэтому задачу нахождения зависимости механического напряжения σ поля от радиуса r в пространстве между обкладками, воспользовавшись для этого результатами теории упругости [4].

Двумя концентрическими сферами радиуса r и $r + \Delta r$ и четырехгранным углом (с вершиной в центре конденсатора и малым телесным углом $\Delta\Omega$ при вершине) мысленно выделим элементарный пространственный фрагмент поля в пространстве между обкладками конденсатора (рис. 4).

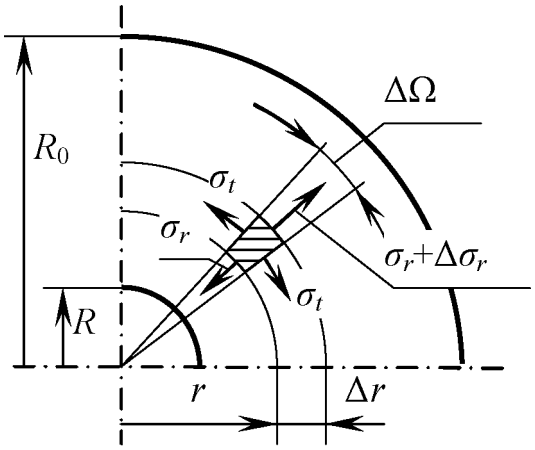

Рис. 4.

В механике показано, что условия статического равновесия для этого фрагмента, с учетом центральной симметрии поля, формализуются в виде уравнения (17)

$$\frac{d\sigma_r}{dr}+\frac{2}{r}(\sigma_r-\sigma_t)=0, \tag{17}$$

где σ_r, σ_t – нормальные напряжения в радиальном и тангенциальном направлениях соответственно.

Перемещения u, деформации ε и напряжения σ связаны между собой формулами (18)

$$\varepsilon_r=\frac{1}{k}\sigma_r=\frac{du}{dr},\ \ \varepsilon_t=\frac{1}{k}\sigma_t=\frac{u}{r}, \tag{18}$$

где k – модуль упругости.

С учетом формул (18) уравнение (17) преобразуется в уравнение второго порядка (19) относительно перемещения u,

$$\frac{d^2u}{dr^2}+\frac{2du}{rdr}-\frac{2u}{r^2}=0. \tag{19}$$

Решение этого уравнения имеет вид (20),

$$u=C_1r+C_2/r^2, \tag{20}$$

где C_1, C_2 –постоянные интегрирования.

Зная решение (20), найдем вид зависимостей для определения нормальных напряжений:

$$\sigma_r=k\frac{du}{dr}=kC_1-\frac{2kC_2}{r^3}, \tag{21}$$

$$\sigma_t=kC_1+\frac{kC_2}{r^3}. \tag{22}$$

С учетом того, что обкладки конденсатора имеют заряды разного знака, поверхностная плотность сил, действующих на внешнюю обкладку, должна быть направлена к центру конденсатора. Нормальное напряжение σ_r, возникающее в поле при $r = R_0$, должно быть равно по абсолютной величине поверхностной плотности сил, но иметь противоположное направление,

$$\sigma_r\left(R_0\right)=kC_1-\frac{2kC_2}{R_0^3}=\frac{Q^2}{32\pi^2\varepsilon_0R_0^4}. \tag{23}$$

Выражение (23) должно выполняться при всех возможных значениях $R_0 > R$, в том числе и при бесконечно больших значениях, $R_0 \to \infty$. Но при таких значениях поверхностная плотность сил становится равной нулю, т. е. при $R_0 \to \infty$: $\sigma_r(R_0) \to 0$. По этой причине постоянная интегрирования C_1 должна быть равна нулю, $C_1 = 0$. Теперь из зависимости (23) можно найти постоянную интегрирования C_2,

$$C_2 = -\sigma_r\left(R_0\right)\frac{R_0^3}{2k} = -\frac{Q^2}{k64\pi^2\varepsilon_0 R_0}. \tag{24}$$

Таким образом, электрическое поле между обкладками конденсатора испытывает механическое напряжение (25) в радиальном и (26) в тангенциальном направлениях,

$$\sigma_r = \sigma_r(R_0)\frac{R_0^3}{r^3} = \frac{Q^2}{32\pi^2\varepsilon_0 R_0 r^3}, \tag{25}$$

$$\sigma_t = -\sigma_r(R_0)\frac{R_0^3}{2r^3} = -\frac{1}{2}\sigma_r. \tag{26}$$

Деформация в этих направлениях будет определяться выражениями (27) и (28) соответственно:

$$\varepsilon_r = \frac{\sigma_r}{k} = \frac{\sigma_r(R_0)}{k}\frac{R_0^3}{r^3}; \tag{27}$$

$$\varepsilon_t = \frac{\sigma_t}{k} = -\frac{\sigma_r(R_0)}{2k}\frac{R_0^3}{r^3}. \tag{28}$$

Заметим, что из формул (25)–(28) следует, что при бесконечно большом радиусе R_0 напряжения σ_r, σ_t и деформации ε_r, ε_t становятся равными нулю. Это весьма важный результат, свидетельствующий о том, что электростатическое поле в окружающем уединенный носитель заряда пространстве находится в ненапряженном состоянии. Плотность энергии поля во всех точках этого пространства равна нулю. Остается принять единственное решение: в случае уединенного носителя заряда энергия локализуется в электрическом поле, находящемся не вне, а внутри носителя заряда.

Доказав «теорему существования», поставим задачу определения характеристик напряженного состояния электрического поля во внутренней сфере, т. е. в той части пространства, которая удовлетворяет условию $r < R$.

Поле, как между обкладками конденсатора, так и во внутренней сфере обладает центральной симметрией, поэтому и в этих обстоятельствах остаётся справедливым уравнение (19) и его решение (20). Однако, теперь постоянная интегрирования C_2 будет равна нулю, поскольку перемещение в центре сферы

должно быть равным нулю, $u = 0$ при $r = 0$. Зависимости (21), (25) для вычисления нормальных напряжений приобретает вид (29) и (30),

$$\sigma_r(r) = kC_1, \tag{29}$$

$$\sigma_t(r) = kC_1. \tag{30}$$

На поверхности сферы должно выполняться равенство

$$f_R = -\sigma_r(R) = -kC_1, \tag{31}$$

откуда следует, что составляющие нормальных напряжений одинаковы во всех точках, расположенных внутри сферы, и равны величине $\sigma_r(R)$,

$$\sigma_t(r) = \sigma_r(r) = \sigma_r(R) = -\frac{Q^2}{32\pi^2\varepsilon_0 R^4}. \tag{32}$$

Это означает, что поле внутри сферы находится в состоянии объемного всестороннего (гидростатического) сжатия.

Деформация поля в этих условиях составляет величину

$$\varepsilon_r = \varepsilon_t = \frac{\sigma_r(R)}{k} = -\frac{Q^2}{32\pi^2\varepsilon_0 R^4 k}. \tag{33}$$

Осталось найти, чему равен модуль упругости k, входящий в выражение (33).

В соответствии с теорией упругости плотность энергии w в условиях гидростатического сжатия является величиной, вычисляемой по выражению

$$w = \frac{1}{2}\left(\sigma_r\varepsilon_r + 2\sigma_t\varepsilon_t\right) = \frac{3}{2}\frac{\sigma_r^2(R)}{k}. \tag{34}$$

Энергия всего поля, заключенного в сфере, с одной стороны может быть вычислена произведением плотности w на её объем, а с другой – она должна быть равна энергии, уединенной заряженной сферы:

$$\frac{3\sigma_r^2(R)}{2k}\frac{4}{3}\pi R^3 = \frac{Q^2}{8\pi\varepsilon_0 R}. \tag{35}$$

Разрешив уравнение (35) относительно k, получим

$$k = \frac{Q^2}{64\pi^2\varepsilon_0 R^4} = \frac{1}{2}\sigma_r(R). \tag{36}$$

Подставим теперь значение k в выражение (34) и найдем плотность энергии w, внутри уединенной заряженной сферы,

$$w = 3\sigma_r(R) = \frac{3Q^2}{32\pi^2\varepsilon_0 R^4}. \qquad (37)$$

Исследование вопроса о локализации энергии электрического поля можно считать законченным.

Выводы

1) Зависимости (16) и (37), полученные совершенно независимым друг от друга образом, совпали. Это говорит о правильности той точки зрения, что энергия электрического поля является энергией его всестороннего сжатия во внутреннем пространстве носителя заряда. Поле в пространстве, окружающем носитель заряда, находится в свободном (ненапряженном) состоянии, плотность энергии в нем равна нулю. Такое состояние поля в этой части пространства сохраняется до тех пор, пока в него не будет внесено какое-либо заряженное тело, например, пробный носитель с единичным зарядом.

2) Классическое представление об электрическом поле, которое обнаруживается, как сказано в [1], только по возникновению силы, действующей на заряженные тела, должно быть расширено с учетом эффекта появления магнитного поля даже в том случае, когда силовая составляющая взаимодействия отсутствует, но имеется движение электрического поля.

3) В стремлении к совершенству теории электричества не следует исходить из традиционной точки зрения, принятой отцами-создателями теории за основу. Эта точка зрения изложена в пособии [1]: «… изучение электрических явлений чрезвычайно облегчается, если исходить из представления, что … во всех точках пространства, окружающего заряд *e*, всегда существует электрическая сила, … вне зависимости от того, проявляется ли существование этой силы в воздействии ее на пробный заряд (в случае наличия такового) или же ни в чем не проявляется (в случае отсутствия такового)». Видимо, когда-то эта точка зрения способствовала развитию теории, но в настоящее время это не так. Не стоит для «облегчения изучения» привносить в задачу эффекты, столь существенно искажающие объект изучения.

Л И Т Е Р А Т У Р А

1. Тамм И.Е. **Основы теории электричества**. М.: Наука, 1966. 624 с.
2. Мултановский В.В. **Курс теоретической физики. Классическая электродинамика: учеб. пособие для вузов. 2-е изд., перераб.** В.В. Мултановский, А.С. Василевский. М.: Дрофа, 2006. 348 с.
3. Батыгин В.В., Топтыгин И.Н. **Сборник задач по электродинамике. Изд.2-е. Учебное пособие**. Изд-во «Наука», 1970. 504 с.
4. Тимошенко С.П., Гудьер Дж. **Теория упругости**. Изд-во «Наука», 1975. 576 с.

КРИЗИС ПРИРОДНЫХ СИСТЕМ И НОВОЕ НАУЧНОЕ НАПРАВЛЕНИЕ

© *Загайнов Н.А.*, 2012

Организация Объединение Граждан
«Народный Академический Университет Эволюции Разума»,
Украина, 65101,Одесса, ул. Радостная, дом 2/4, офис 702, тел. 701-12-33,
e-mail: zaga-na@mail.ru

Анализ физических процессов в окружающей среде и взгляд современной науки на эти процессы. Предлагается новое понимание (гипотеза) глобального изменения климата и возможности управления средой нашего земного мира.

Ключевые слова: Мировозрение. Окружающая среда. Глобальное изменение климата.

Zagainov Mykola. *Crisis of Natural Systems and New Research Area.* Analysis of physical processes in environment and a view of modern science on those processes. Propose a new conception (hypothesis) of global change of climate and capabilities to manage environment of our earth's world.

Key words: World outlook. Environment. Global change of climate.

Тема «Наука природы» является очень важной для современного периода развития науки и всей цивилизации. Большинство современных учёных отмечает, что с конца 80-х годов 20 века практически одновременно начал проявляться кризис социальной, научной, экономической, финансовой, экологической, климатической и других общественных и природных систем. Учёные назвали это общемировое явление «системным кризисом». Каждая наука изучает только часть природы и может предполагать причинно-следственные связи изменений в рамках своей компетенции. Фундаментальной науки, изучающей природу, биологическую форму жизни, в том числе человечество, и весь мир как единую взаимосвязанную систему, не существует, поэтому оценить мировые процессы, сделать выводы и дать необходимые рекомендации по выходу из крайне опасной ситуации некому, а на основании нынешнего мировоззрения и невозможно. Учёные и философы, объединившиеся в рамках Римского клуба и ведущие исследования по глобальной проблематике, даже придумали специальный термин «неосознанность происходящего».

Приведём несколько примеров, показывающих серьёзность ситуации.

Изучая изменение климата, специалисты приходят к разным оценкам происходящих процессов. Часть учёных считает, что происходит глобальное потепление, другая часть - что глобальное похолодание. В последние годы приходит понимание того, что происходит глобальное изменение климата.

Многие исследования показывают, что подобные процессы неоднократно происходили на нашей планете, но что происходило с биологической формой

жизни в результате этих изменений? Палеонтология на основании изучения окаменевших остатков прошедших эпох в жизни Земли даёт однозначный ответ. В одну эпоху имеется один набор растительности и животных, в более высоком соседнем слое растительность и животные уже другие, более развитые, а переходных видов флоры и фауны не существует. Человек современного вида появился сразу, переходных видов между человекообразными обезьянами и человеком не обнаружено. Удовлетворительного и аргументированного объяснения этих фактов на основании нынешнего мировоззрения наука не выдвинула.

До конца 80-х годов прошлого века общество и наука развивались в сравнительно стабильных природных условиях. В очень узких пределах в нашем мире поддерживались десятки параметров, таких как средняя температура, давление и состав газов в атмосфере, кислотно – щелочной баланс “РН” водной среды и т д. В течение краткого временного периода границы этих параметров расширились, что грозит самому существованию биологической формы жизни. Например, зачатие потомства у биологической формы жизни происходит в жидкой среде при очень узких значениях кислотно – щелочного баланса. Расширение показателей “РН” водной среды в любую сторону приводит к затруднению оплодотворения яйцеклеток и икры у рыб. Именно поэтому, согласно статистике, из 10 пар здоровых молодых людей 7 пар испытывают трудности с зачатием детей, а 3 пары из них не могут естественным путём (без помощи репродуктивных технологий) зачать потомство.

Количество стихийных бедствий, техногенных катастроф, эпидемий начинает увеличиваться, как снежный ком, и их результатом может быть гибель миллионов людей. Человечеству необходимо в этих условиях просто выжить. Губительную тенденцию показывает график роста экономических потерь, резкий рост которых начался с 1988года[1].

Экономические потери от стихийных бедствий
(в млрд. долл. США) с 1950 по 2000 год.

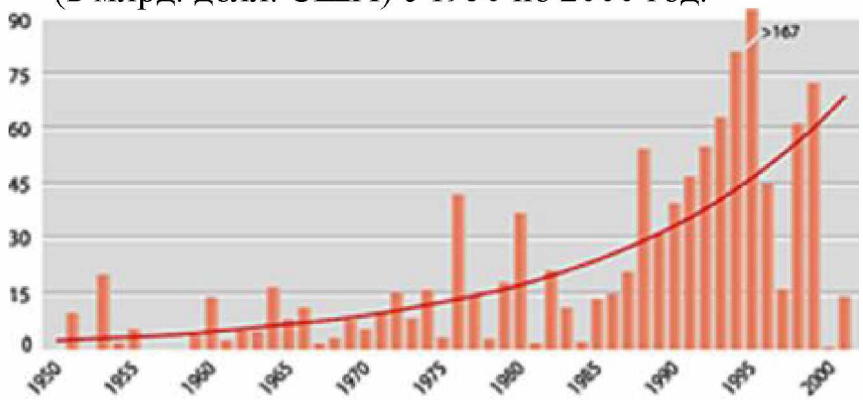

По сравнению с 60-ми годами в 90-х годах экономические потери увеличились почти в 9 раз. Примечание: на графике показан суммарный ущерб только от крупных стихийных бедствий.

Эту тенденцию подтверждают также данные за последние три года от крупнейшей в мире страховой компании «SwissRe», (Швейцария) [2]. Экономические потери от природных катаклизмов, связанных с изменением климата составили:
- в 2009 году – $63 миллиарда;
- в 2010 году – $222 миллиарда – рост более чем в три раза;
- в 2011 году – примерно $370 миллиарда - почти двукратный рост. В случае сохранения подобной тенденции до 2015 года потери будут сравнимы с цифрами ежегодного роста мирового ВВП, что уже явилось одной из причин кризисных явлений в мировой экономике.

Из-за нехватки продовольствия и питьевой воды, связанной с климатическими изменениями, аналитики предсказывают социальные потрясения [3].
Вывод: **Происходит процесс разрушения природной стабильности.**

Обратимся к статистике, отражающей тенденции в изменении состояния психического здоровья населения. В начале 20 века на тысячу человек населения насчитывалось 1–2 человека, которым требовалась помощь психологов или психиатров, в 70 годах таких людей было уже 5–6 человек. Согласно оценке специалиста по лечебной психологии, профессора, академика Российской академии естественных наук Е.А. Шапошникова, «по состоянию на 2005 год, абсолютно нормальными являются лишь 20–25% людей. Это не значит, что все остальные – психи, просто большинство (65–70%) умудряются балансировать на грани» [4]. Если суммарную оценку этой статистики привести к 100%, то её составляющие будут иметь следующие значения: нормальных людей – 25%, а имеющих проблемы с психикой – 75%. В течение 15–20 лет, если за точку отсчёта взять 1988 год (начало резкого роста экономических потерь от природных катаклизмов), количество людей, которым в той или иной степени необходима помощь психологов или психиатров, выросло с 0.5% до 75%. Эта негативная тенденция характеризуется также ухудшением способностей запоминания новой информации и возможностей обучения, массовым заболеванием депрессией и другими расстройствами психики. В итоге уровень человеческих возможностей, как в науке, так и во всех творческих областях деятельности понизился.
Вывод: **Продолжение данного процесса может привести к потере разумности людей.**

На первый взгляд, с точки зрения современной науки, упомянутые общемировые тенденции не связаны, их объединяет только общая среда нашего мира.
Вывод: **происходят глобальные изменения в среде нашего земного мира.**

А может ли наука однозначно объяснить причины этих изменений? По мнению многих учёных и философов, современная фундаментальная наука заблудилась на пути, ведущем к познанию мира. Приведём несколько мнений.

Андрей Алексеевич Тутошкин – историк и философ науки (Россия) в исследовательской работе «Положение в науке XX века» высказал следующий вывод: «Вторая половина двадцатого века – полный застой фундаментальной науки. Мы топчемся на месте, развивая только технологию. Огромное количество недавно созданных научных теорий поражает своими фантастическими выводами. Эти выводы базируются на недоказанных и, в подавляющем случае, на несуществующих фактах окружающего нас мира и являются чисто математическими выражениями».

Интересно мнение о науке создателя атомной бомбы, американского физика Роберта Оппенгеймера: «Я и мои коллеги физики-теоретики придерживаемся одного убеждения. Мы не понимаем природу материи, законов, которые управляют ей, языка, которым она может быть описана» [5].

По словам Алексея Николаевича Дмитриева, доктора геолого-минералогических наук, профессора, сотрудника НИИ геофизики СО РАН: «Современная физика являет собой весьма жалкое зрелище при попытке трактовать происходящее в природе. Собственно фундаментальной физики, исследующей реальные космоземные преобразования, сегодня просто не существует. Есть фундаментальная техническая физика, но не физика природы. Что же получается? Мы просто перечисляем то, что происходит, но не можем ни спрогнозировать, ни предотвратить природные катастрофы».

Нам важны не упреки в адрес науки, а знание действительных ее возможностей.

Приведём примеры научной деятельности.

Большинство климатологов, в том числе Нобелевский лауреат, академик РАН, директор Института глобального климата и экологии Юрий Антониевич Израэль (Россия) и его «научная школа» считают, что людям и экономике необходимо адаптироваться к изменениям климата. Именно поэтому международная научная конференция, состоявшаяся в Москве с 7 по 11 ноября 2011года, названа «Проблемы адаптации к изменению климата».

По мнению Ю.А. Израэля, «Управление климатом — не такая уж бросовая идея» [6]. Суть его предложения состоит в регулярном распылении в нижней стратосфере мелкодисперсных аэрозольных веществ, например, соединений серы, что, по его мнению, позволит снизить температуру и зафиксировать климат на нынешнем уровне. Совокупность подобных методов назвали геоинженерией. Данная наука рассматривает воздействие на сложную природную систему примерно так же, как химическую реакцию в лабораторной пробирке. Для достижения глобального эффекта необходимо распылить миллионы тонн соединений серы. Фактически это целенаправленное загрязнение окружающей среды, что подпадает под действие Международной конвенции 1978г. «О запрещении военного или иного враждебного воздействия на природную среду». Уважаемый академик трактует этот документ по - своему, а именно, что конвенция не запрещает воздействия на природу в мирных целях.

В рамках современного научного мировоззрения для уменьшения температуры окружающей среды предлагаются также другие проекты:
- создание пенопластовых материков в океане;
- покраска крыш всех зданий и автодорог в белый цвет;
- выведение в море несколько тысяч барж - рефрижераторов для создания льда в море;
- созданы анальные противогазы для коров с целью уменьшения выбросов «парниковых» газов и другие варианты.

Самое ценное в научной деятельности – это сравнение подходов, новые выводы и предложения по обсуждаемой проблеме, что позволяет совместными усилиями решать поставленные перед научным сообществом задачи.

Другое направление научного мышления, но учитывающее известные законы природы, также существует в современной науке. Например, общественная организация, объединившая учёных и философов (из разных государственных научных учреждений стран СНГ), существует в городе Одессе (Украина). Участники этой организации собираются на ежегодные конгрессы и издают коллективную монографию своих научных трудов под общим названием «Гармоничное развитие систем – третий путь человечества». Авторы статей, собранных в монографии, в своих исследованиях и рассуждениях опираются на известные природные закономерности. Среди этих закономерностей, такие как фрактальное построение природных систем, ставшее в конце 20 века разделом математики, математические зависимости: ряд Фибоначчи и соотношение элементов природы, выраженной числом 1,618…, которое воспринимается как оптимальное соотношение – гармония.

В вышеприведённой статистике современного психического состояния населения имеются цифры 25% и 75%. (Скорее всего это промежуточные значения в процессе ухудшения умственных способностей людей.) Приведём ещё два подобных соотношения в природе. Площадь суши и водной поверхности планеты (моря и внутренние водоёмы реки, озёра…) – это, с учётом возможных погрешностей в вычислениях, также 25% и 75% [7]. Соотношение массы сухого вещества и воды в теле человека, если учитывать воду внутри клеток, в составе костной массы, жира, внеклеточную жидкость (экстрацеллюлярная), которую разделяют на “подвижную” или активно функционирующую часть (около 10%) и “внутрифибриллярную” или “соединительнотканную” (10%), то, с учётом возможных погрешностей в вычислениях, снова появляются цифры 25% и 75%. Подобное соотношение, видимо, можно обнаружить и в других природных структурах. Число 75 имеется в примерах, приведённых в статье профессора Волошинова А.В. «Гармония, симметрия, красота»[8, стр. 21]. «Цифра 75 соответствует углу при вершине пирамиды Хеопса, углу, образованному диагоналями прямоугольника иконы «Троица» Андрея Рублёва. Сотрудник Пущинского научного центра В.Д. Цветков создал «теорию сердца», основанную на вариационных принципах и предположил что именно число

«Фи» обеспечивает максимальную эффективность работы сердца с минимальными затратами мышечной массы, крови и сосудистого материала [8, стр.27]. Цветковым также найден оптимальный угол ветвления артериальных сосудов (это также фракталы), который оказался равен 75».

Таким образом, на примере исследований целой научной группы и даже на ограниченном количестве приведённых примеров мы видим, что всё в мире существует по единым математическим законам и является логически, эстетически, и самое главное энергетически оптимальным и целесообразным. Исходя из приведённых доводов, примеров и рассуждений логично предположить, что мироздание создано разумным началом и если принять постулат «существует высший разум – Творец», то основным принципом практических действий Творца является **наименьшие энергетические затраты и целесообразность**.

Для полноты данного вывода не хватает, как минимум, ещё одной математической зависимости, которую можно назвать «кодом созидания», и единого строительного материала, из которого созданы все виды вещества, а также описания физики этого процесса. Данная информация уже имеются в новом научном направлении - аксионтологии, о котором идёт речь в конце статьи.

Если принципы целесообразности и наименьших энергетических затрат применить для оценки современной цивилизации, то положительного варианта их использования не наблюдается, к сожалению.

Кризис в науке и непонимание устройства природы обусловлены тем, что большинство представителей научного сообщества считают наш мир и вселенную случайным явлением, появившимся в результате «Большого взрыва».

В настоящее время в науке существуют и другие подходы к пониманию устройства мироздания. Бывший руководитель «Центра инструментальных наблюдений за окружающей средой и прогноза геофизических процессов», кандидат геолого-минералогических наук Игорь Николаевич Яницкий в докладе «Методические рекомендации по защите от негативных энергоинформационных воздействий»[9], предназначенном для Министерства по чрезвычайным ситуациям и Министерства обороны России, сформулировал следующее мнение: «Главным итогом научных изысканий последних десятилетий XX века является то, что физики пришли к доказательству существования Абсолютного разума, по замыслу которого устроен мир [5]… Ученые даже ввели понятие "отпечатки Бога" – невероятные совпадения физических параметров, без которых наша Вселенная не могла бы существовать… Сегодня, мы являемся свидетелями информационного взрыва по теме: "Строение и функции планеты". Начало его можно отнести к 1991 году, когда в российской науке был завершен многолетний цикл уникальных исследований. На этой основе доказано, что Земля – это предельно энергонасыщенная и высокоорганизованная система, обладающая памятью… Многие исследования показывают, что Земля как саморегулирующаяся структура в ответ на внешние (из Космоса) и внутренние (от неразумной технологической деятельности человека) воздействия, с точностью идеальной ЭВМ (электронно – вычислительная машина – компьютер)

«включает» компенсационные механизмы поддержания жизненно важных параметров для существования биологической формы жизни. Чем глубже изучают физики окружающий мир, тем отчетливее видна рука Творца».

Интересно и мнение Президента Российской Академии Наук Юрия Осипова: «Создание любой стройной научной системы неизбежно приводит к мысли о существовании абсолютного бытия или Творца» [5].

К пониманию того, что Земля - разумная сущность и является, по сути, могучим компьютером, некоторые учёные уже пришли. Но как работать с этим компьютером?

В Организации Объединение Граждан «Народный Академический Университет Эволюции Разума» (НАУ ЭРА) получили положительные результаты в экспериментах по взаимодействию коллектива людей с разумом Земли при помощи мыслеформ. Суть нового подхода была изложена на Всемирной конференции по изменению климата, проходившей в Москве в 2003 году, в докладе Алексатиной Ларисы Юрьевны и Аликова Алексея Ивановича по теме: «Причины глобального изменения климата Земли. Возможность нашего влияния на изменение климата» [10]. Приведём выдержку из доклада: «Наша гипотеза о причинности глобального изменения климата основана на постулате «мир абсолютно программен». Внешним программистом по отношению к общим и частным программам пространства – времени является Высшее Начало. Внутренними программистами – корректорами результата в материальной среде является низший разум – человек. Если внешними операторами - «индукторами» являются полевые информационно-распорядительные структуры (ИРС) локальных пространственных формирований, то внутренними операторами - "индукторами" являются элементарные разумные образования – ИРС человека. Следовательно, должен существовать единый универсальный алгоритм общения между операторами различных уровней. Его структурными единицами информации могут быть только полевые образования - мыслеформы. Такой опыт общения сегодня нарабатывается в Одесском регионе. Достигнуты положительные результаты по рассеиванию энергопотенциала магнитно-гравитационных волн, резонирующих с «фазовыми» волнами литосферы. Проверена реакция Земной ИРС на человеческие мыслеформы – инфопосылки, которые, по нашему разумению, способны прямо или косвенно воздействовать на земную структуру и на систему околосолнечной ИРС. К сожалению, подтверждающие возможности науки ограничены, как и сегодняшние возможности потенциальных управителей полевыми процессами. Тем не менее, найдено направление, способное помочь науке осмыслить зависимость Земных и околосолнечных явлений, процессов и отдельных реакций от возможностей внутренних операторов – человеков разумно разумных, живущих на Земле в одном из последовательно проявляемых миров».

Исходя из приведённой информации, можно сделать вывод о возможности взаимодействия с полевоматериальным компьютером Земли и его программирования. Для этого человек должен стать разумным внутренним оператором и

изучить язык программирования (общения), понятный как человеку, так и земному разуму. За период существования НАУ ЭРА наработан определённый опыт и выявлены возможности человека по управлению средой обитания. В качестве примера можно привести результаты первого опыта по управлению крупными природными явлениями, проведённого группой полевых операторов в составе 120 человек [11].

18 сентября 2003года в 21.00 по киевскому времени в течение 7 минут в земной полевый компьютер была заложена программа. Тайфун «Изабель», который мог произвести разрушения на атлантическом побережье США, в результате программного воздействия в течение 24 часов был разрушен. Скорость ветра снизилась над тёплым океаном, что является необычным и даже парадоксальным для поведения тайфунов. Ход воздействия разума Земли на «Изабель» был зафиксирован российским геостационарным спутником GOES 12–Восток и американскими спутниками. Эти фотоснимки были опубликованы 14 января 2007 года на сайте российского агентства «Информнаука». Обычно в «глазу» тайфуна нет облаков и сильного ветра, а в «глазу» тайфуна «Изабель» появилась вращающаяся система из пяти вихрей. Постепенно они трансформировались в четыре, а затем в три, при этом скорость вихрей менялась. Данное явление зарегистрировано единственный раз за весь период наблюдений.

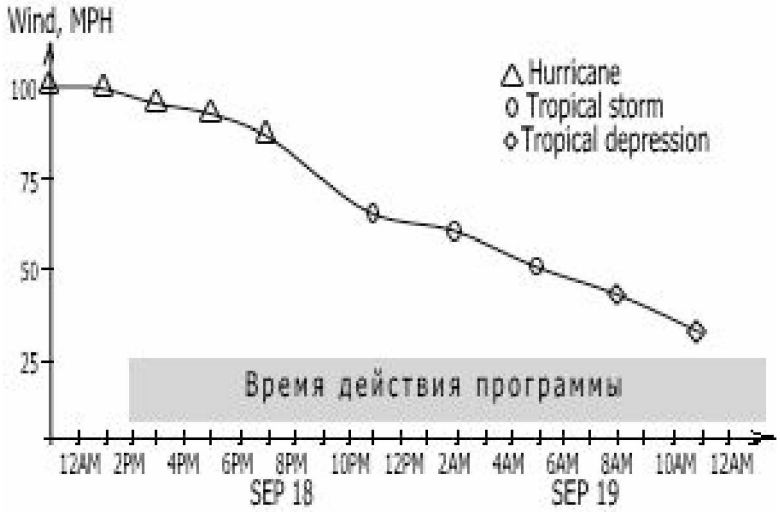

Изменение скорости ветра тайфуна «Изабель» по данным американского Центра по изучению ураганов.

НАУ ЭРА (www.uer.org.ua, www.era.at.ua) предлагает принципиально новое мировоззрение, а также, в частности, новое решение климатических проблем. Коллектив Университета формулирует основы новой науки аксионтологии, изучающей мир, природу, все формы жизни и человечество как единую взаимосвязанную систему. При помощи этой науки можно понять суть и причины любых процессов, происходящих в мире, предсказать их развитие, дать рекомендации для правительств и предложить возможности управления природными явлениями.

Название аксионтология происходит от греческого выражения – «axio ontos - bios» – «ценность сущего – жизнь» и было предложено представителем научной школы предшественников НАУ ЭРА, одним из основателей Университета Владимиром Евгеньевичем Шарашовым [12, 13]. По его мнению, «первым и главным объектом, целью изучения аксионтологии являются человек, эволюция его разума, взаимодействие с окружающей средой, а также основы жизни в целом. Разум Земли в настоящее время воспринимает коллектив Университета как зародыш или прообраз разумного человечества» [14].

Аксионтология принципиально иначе, чем геоинженерия рассматривает проблему стабилизации климата. Адаптировать нужно не людей и экономику, а природную среду и один из её главных элементов - климат к потребностям человечества. Необходимо управлять программами Земли, а не адаптироваться к программным изменениям климата. Управлением мировыми природными процессами занимается разум Земли, а корректировка происходит по заказу (программе) внутреннего оператора – человека разумного. Для полного восстановления стабильности климатической и всей природной системы необходимо 10 тысяч обученных людей, способных коллективно взаимодействовать с разумом Земли. Именно такому количеству полевых операторов планета подчиняется безоговорочно и выполняет их программы, направленные на Благо. В понимании разума любого уровня Благо – это выполнение целей, задач и программ Высшего Разума - Творца. Задача человечества - познавать информацию Творца, выполнять его программные задачи, доказывать свою разумность реальным действием. Любые направления познания и человечество вне целей Творца не имеют смысла существования.

Для сравнения разных научных и мировоззренческих подходов к пониманию устройства мироздания кратко повторим изложенную информацию в виде таблицы.

СРАВНИТЕЛЬНАЯ ТАБЛИЦА

Фундаментальная наука на старой парадигме	***Новое научное направление***
Системный кризис.	Чёткое видение пути развития.
Полный застой фундаментальной науки, развивается только технология.	Огромный объём знаний для освоения человечеством.
Новые научные теории базируются на недоказанных и, в подавляющем случае, на несуществующих фактах и являются чисто математическими выражениями.	Новая теория подтверждается успешной практикой
Фундаментальной науки, изучающей природу и весь мир как еди-	Аксионтология изучает мироздание, природу нашего мира, все

ную взаимосвязанную систему, не существует, поэтому оценить мировые процессы и сделать выводы некому.	формы жизни и человечество как единую взаимосвязанную систему.
Понимание природных процессов на уровне лабораторной пробирки. Непонимание устройства мира, материи и причин процессов, происходящих в мире.	Возможность понимания сути и причин любых процессов, происходящих в мире, предсказать их развитие, дать рекомендации для правительств и предложить возможности управления природными явлениями и всей окружающей средой.
Человечеству и экономике необходимо адаптироваться к изменениям климата.	Адаптировать нужно не людей и экономику, а природную среду и один из её главных элементов - климат к потребностям человечества. Необходимо управлять программами Земли, а не адаптироваться к программным изменениям климата.
Уменьшения температуры на планете с помощью регулярного распыления в стратосфере аэрозоли из соединений серы.	Управление природной средой с помощью мыслеобразных программ разумных людей. Носителем программной информации является полевая материя.
Наш мир и вселенная – случайное явление, появившееся в результате «Большого взрыва».	Наш мир и вселенная созданы вышестоящим разумом – Творцом.

Вывод: **развивается новое научное направление - аксионтология, предлагающее новое научное мировоззрение и дающее ответы на причины глобальных изменений в природе нашего мира. Найдены возможности взаимодействия с разумом Земли и управления окружающей средой. Аксионтология – единственное научное направление, предлагающее выход из системного кризиса и путь восстановления природной стабильности.**

НАУ ЭРА приглашает всех желающих пройти обучения в Университете. Адрес: Одесса, ул. Радостная, дом 2/4, 7 этаж, тел 701-12-33, сайты: www.uer.org.ua, www.era.at.ua.

Если проанализировать данные о природных и общественных процессах на Земле и согласиться с промежуточными выводами в данной статье, то становится возможным сформулировать общие выводы:

– **вышестоящий разум начал процесс постепенного расширения границ показателей природных параметров за пределы стабильности, что грозит**

крайне негативными последствиями, а возможно и гибелью. Фактически, человечество нашего мира поставлено перед жёстким, срочным и конкретным выбором: либо смена мировоззрения и вектора развития цивилизации к разумности, либо продолжение негативных природных процессов;
– аксионтология – единственное научное направление, предлагающее выход из системного кризиса и новое направление развития человечества, которые требуют только умственной деятельности и минимальных финансовых затрат;
– через короткий промежуток времени восстановить природную стабильность будет очень затруднительно или невозможно.

Провести анализ данных процессов, получить дополнительную информацию, разобраться в новом научном направлении – аксионтологии и подтверждающей её практике, обосновать и сформулировать свой личный вывод должен каждый учёный, способный преодолеть устоявшиеся в науке догмы. Именно на научном сообществе в целом (как на наиболее талантливой и образованной части человечества) и каждом учёном персонально лежит ответственность за дальнейшую судьбу всех людей и конкретно родных и близких. Это не пафосные слова, а необходимость выбора и конкретных действий. Мнение даже части научного сообщества будет весомым аргументом для руководства всех стран по определению пути выхода из ухудшающейся ситуации в природе.

ЛИТЕРАТУРА

1. Сайт Geo-3: Global environment outlook: *URL*: http://www.unep.org. Источник: Munich Re 2001.
2. Экспертная оценка Международного Комитета по Глобальным Изменениям Геологической и Окружающей Среды “GEOCHANGE”: *URL*: ru.geochange-report.org и интервью Э. ХАЛИЛОВА доктора геолого-минералогических наук, директора Азербайджанского НИИ прогнозирования и изучения землетрясений: *URL*: http://2012god.ru/forum/2012/topic-617/page-1/
3. Запасы пресной воды и продовольствия в мире (сайт «Наша планета»).
4. Журнал «Здоровье» №5, октябрь 2005, стр. 17. Москва.
5. Фомин А.В. **Аргументы науки в пользу сотворения мира**. М.: Новая мысль, 2005. 544с.
   URL: http://www.alleng.ru
6. Израэль Ю.А. “Управление климатом - не такая уж бросовая идея”, *статья в еженедельном журнале «Профиль»*, №**31** от 29 августа 2011.
7. Сайт «Всё о путешествиях»; *URL*: http://www.travelshunters.ru
8. Коллективная монография. **Гармоничное развитие систем – третий путь человечества**. Одесса, 394 с. ООО «Институт креативных технологий».

9. Яницкий И.Н. “Методические рекомендации по защите от негативных энергоинформационных воздействий”, *статья, интернет - страничка «Живая Земля».*

10. Алексатина Л.Ю., Аликов А.И. “Причины глобального изменения климата Земли. Возможность нашего влияния на изменение климата”, *Сборник Всемирной конференции по изменению климата «Тезисы докладов»*, Москва. С. 667 (2003).

11. Информационный вестник «МИГ» №16 от 1.10.2003г. (внутреннее периодическое издание НАУ ЭРА)

12. Лиас – Шарашов В.Е. **Рыцари с поднятым забралом**. Реферат. Одесса: Автограф, 2004. 587 с.

13. Шарашов В.Е. **От Альфы до Омеги. Том 1–3**. Одесса: Друк, 2009.

14. Шарашов В.Е. **Беседа об Аксионтологии**. Одесса, 2008.

ON THE INTERPRETATION OF THE NATURE OF MAIN EQUATIONS OF MATRIX MECHANICS

© ***Altayev Namaz*, 2012**

Yassavi Kazahish-Turkish International University,
Kazakhstan, Shymkent, e-mail: namaz_42@mail.ru

A new approach is proposed in the work towards the solution of the problems, which are considered as fundamental during the process of derivation of the main equations of matrix mechanics.

As it is known, in his time, after Plank saw, that based on the equation

$$\rho_\nu = \frac{8\pi\nu^2}{c^3} \cdot \frac{h\nu}{\exp\frac{h\nu}{kT} - 1}, \tag{1}$$

obtained by him in [1] from the joint consideration of the relations of the type

$$\rho_\nu = \frac{8\pi\nu^2}{c^3} \cdot \overline{u} \tag{2}$$

taking into account the possibilities of the main equations of electrodynamics of Maxwell and relations of the following type

$$\overline{u} = \frac{\varepsilon}{\exp\frac{\varepsilon}{kT} - 1} \tag{3}$$

obtained by him based on the computation, carried on the basis of possibility of equalities

$$S = k \ln W,$$

$$W = \frac{(N+P-1)!}{(N-1)!P!},$$

$$E = P\varepsilon, \tag{4}$$

$$E = N\overline{u}, \tag{5}$$

a persuasive description becomes achieved of experimental data, they were further faced by the problem of proof of relations (2) and (3).

For a complete and consecutive solutions of these problems, apparently, it was necessary to obtain the proofs of these relations based on the possibility of main

equations of theoretical physics, for instance, such as the main equations of the Hamilton-Jacobi theory

$$\left.\begin{aligned} &\frac{\partial S}{\partial t}+H\left(q_i,\frac{\partial S}{\partial q},t\right)=0,\\ &H\left(q_i,\frac{\partial S}{\partial q}\right)=E, \end{aligned}\right\} \tag{6}$$

and main equations of statistical mechanics of Gibbs

$$\left.\begin{aligned} &\frac{\partial \rho}{\partial t}-[H\rho]=0,\\ &[H\rho]=0,\\ &\rho_i=\exp\frac{F-\varepsilon_i}{kT},\\ &\rho_{i,n}=\exp\frac{\Omega+\mu n-\varepsilon_i}{kT}, \end{aligned}\right\} \tag{7}$$

Obtained on the basis of Hamilton equations

$$\dot{q}_i=\frac{\partial H}{\partial p_i},\quad \dot{p}_i=-\frac{\partial H}{\partial q_i}\quad (i=1,2,...,3n)\,. \tag{8}$$

In these expressions: S – entropy, W – thermodynamic probability, E – energy, ε – energy quantum, $\overline{u}$ – average energy of oscillator, N – average number of oscillators H – hamiltonian, F – free energy, μ – chemical potential, q_i, p_i – generalized coordinate and impulse.

It is known, that the proof of the relations of the type (3) was obtained by Plank in his work [2], where he, using the possibilities of the equations of canonical Gibbs distribution function (7,c) together with the expression

$$E=\frac{p^2}{2m}+2\pi^2v^2mg^2\,,$$

related to the linear harmonic oscillator with the assumption, that the energy E in quantum case may accept only discrete values

$E=n\varepsilon=nhv$, где n = 0, 1, 2, …,

obtained the result

$$\bar{u} = \frac{\sum_n E_n \exp\left(-\frac{\varepsilon_n}{kT}\right)}{\sum_n \exp\left(-\frac{\varepsilon_n}{kT}\right)} = \frac{\varepsilon}{\exp\frac{\varepsilon}{kT} - 1}. \tag{9}$$

Let us note, that assurance of Plank in the correctness of obtained by him proof of relation (9) was so high, that in the same paper [2], analyzing these new ideas and results, he allowed himself to make a conclusion of the following content.

If in his earlier published paper [1], the conclusion was made that in the quantum theory of primary foundation is the notion about the energy quanta, then now he made a conclusion about the primary importance in this theory of the notion of action quantum. On the other hand, it is widely known fact that on Solway congress in the course of discussion some physicists tried to express their inagreement with these new conclusions of Plank. For instance, Poincare tried to express his doubts in new ideas of Plank by addressing participants of the congress with the question: «It may by imagined that atoms of matter and atoms of electricity exist, because the conservation of matter and charge are present. It may also be represented that atoms of energy exist. But how to claim the existence of the conservation of action?»

Lorentz tried to express his attitude towards new ideas of Plank, when he said about this the following: “The method, by which Plank introduces the constant h, is very noteworthy. But it must be noted, that historically the quantum of energy has the priority over the quantum of action. Really, Plank began by introducing for every oscillator particular quantum of energy, and then proposed to consider it to be proportional to ν, in order to achieve the agreement with the Wien law”.

But, as is known, in spite of all this, during development of foundations of quantum physics gradually the main place was occupied by new ideas of Plank, which recognized the fundamental role of the notion of quantum of action. Further, on the same path new main results were obtained of *the principle of correspondence and also main equations of matrix mechanics*

$$\left.\begin{aligned} &\dot{q} = \frac{\partial H(q,p)}{\partial p}, \quad \dot{p} = -\frac{\partial H(q,p)}{\partial q}, \\ &pq - qp = \left(\frac{\hbar}{i}\right) 1 \end{aligned}\right\} \tag{10}$$

for the case, when the number of degrees of freedom is equal to one and

$$\left.\begin{aligned}
&\dot{q}_k = \frac{\partial H}{\partial p_k}, \quad \dot{p}_k = -\frac{\partial H}{\partial q_k}, \\
&q_k q_s - q_s q_k = 0, \\
&p_k p_s - p_s p_k = 0, \\
&p_k q_s - q_s p_k = 0 = \frac{\hbar}{\iota}\delta_{is},
\end{aligned}\right\} \tag{11}$$

for the case, when the number of the degrees of freedom has the arbitrary value.

Definitely, the Heisenberg program, proposed by him in formulation of the main ideas of matrix mechanics, could also be considered a successful development in case, when based on equations (10), (11) a satisfactory description of experimental data could be achieved. But later, as it was realized, in reality this goal was not achieved. For instance, Dirac in his book [3], analyzing the state of affairs, existing in questions of interrelation of main equations of matrix mechanics and wave mechanics, came to conclusion, that previously made conclusion, that there is a correspondence between these main equations of these branches of physics, was rather premature.

As Dirac noted, early conclusions about agreement between main equations of these branches of physics were made based on depthless comparison. He comparing them under the account of expression for Hamiltonian, observed that these equations in reality are not equivalent. Also it is attributed to Dirac the conclusion, that from main equations of these branches of physics more valuable for the development of foundations of quantum theory of field is the equation of matrix mechanics. But widely known facts, show that during realization of his ideas, Dirac didn't achieve particularly valuable goals. Thus, according to our views, taking into account all this, there is a foundation to make a following conclusion.

Apparently, that in his time during obtaining of the main equations of matrix mechanics from the Hamilton equation (8), as the equations, based on which a possibility arises to correctly establish the link between observable quantities certain mistakes were made. For instance, there is a ground to suppose, that the nature of these mistake has certain link with the fact that during derivation of the main equations of matrix mechanics new ideas of the principle of correspondence were accepted as a foundation, where the main place was occupied by the notion of the quantum of action in accordance with new conclusion of Plank, made by him in work [2] in 1911.

It may be noted out, that the initial paths of Plank were close to the path of truth, when he considered that the fundamental notions in quantum physics are the notions of quantum of energy and quantum hypothesis and began to use the expressions (4) and (5).

In order to claim that this is the case, we further paid attention to the following facts.

In 1937 L.E.Gurevich published a paper [4], where he based on the applications of the possibility of main equations of Gibbs (7) to the description of the problems of adsorption equilibrium, showed, that the relation of the following type holds:

$$\left.\begin{aligned} F_n &= nf, \\ \Phi_{n'} &= n'\phi, \end{aligned}\right\} \tag{12}$$

where F_n – free energy of the system of n particles, f – free energy, attributed to one particle, $\Phi_{n'}$ – free energy of n' adsorbed particles, between which there is no interaction, φ – free energy, attributed to one adsorbed particle.

Further, taking into account that the probability of the system to have n particles in arbitrary state is equal

$$\rho_n = \exp\frac{\Omega + \mu n - F_n}{kT}$$

and in order to find the average number of adsorbed particles, if the number of particles in gas phase is given, he started by analyzing the equation

$$\rho_{n,n'} = \exp\frac{\Omega + \mu(n+n') - F_n - \Phi_{n'}}{kT}, \tag{13}$$

where $\rho_{n,n'}$ – probability of presence of n particles in gas phase and n' – on the surface of adsorbent, μ – chemical potential.

In [4], going from (13) to

$$\rho_{n,n'} = \exp\frac{\Omega + (\mu - f)n + (\mu - \varphi)n'}{kT}$$

and

$$e^{-\frac{\Omega}{kT}} = \sum_n e^{\left(\frac{\mu - f}{kT}\right)n}\left[\sum e^{\left(\frac{\mu - \phi}{kT}\right)n'}\right]n^0 \tag{14}$$

and keeping in mind, that the first sum is the geometric progression, in the second; n' is the number of particles, adsorbed by one active place and may have values 0 and 1, average (observed) number of particles in the whole system was obtained

$$\bar{N} = n_A + n_A^0,$$

where

$$n_A = \exp\frac{\mu - f}{kT}, \tag{15}$$

$$n_A^0 = \frac{n^0}{1+\exp\frac{-\mu+\phi}{kT}}. \tag{16}$$

Here n_A and n_A^0 – concentration of particles of type A in gaseous phase and on the surface of the solid state.

Excluding $\exp\frac{\mu}{kT}$ from (15) and (16), the equations of adsorption may be obtained

$$\theta = \frac{n_g \exp\frac{f-\phi}{kT}}{1+n_g \exp\frac{f-\phi}{kT}} = \frac{n_A \exp\frac{\Delta G_A}{kT}}{1+n_A \exp\frac{\Delta G_A}{kT}}, \tag{17}$$

where θ – degree of filling of the unit of surface.

In [4] based on the analysis of equation of the type

$$\rho_{n_1 n_2, n_1' n_2'} = \exp\frac{\Omega+(\mu_1-f_1)n_1+(\mu_2-f_2)n_2+(\mu_2-\varphi_1)n_1'+(\mu_2-\varphi_2)n_2'}{kT},$$

Derived for the case, when the object of research is the adsorption equilibrium in case of the mixture of two ideal gases, the particles of which do not interact with each other, the equations of the following type are obtained

$$\theta_A = \frac{n_A \exp\frac{\Delta G_A}{kT}}{1+n_A \exp\frac{\Delta G_A}{kT}+n_B \exp\frac{\Delta G_B}{kT}}, \tag{18}$$

$$\theta_B = \frac{n_B \exp\frac{\Delta G_B}{kT}}{1+n_A \exp\frac{\Delta G_A}{kT}+n_B \exp\frac{\Delta G_B}{kT}}., \tag{19}$$

where θ_A, θ_B – degree of filling of the unit of surface by particles A and B correspondingly, ΔG_A, ΔG_B – free energy of adsorption of particles of type A and B.

As it is known, the equation of adsorption equilibrium was obtained by Lengmuir within the frames of the possibility of molecular-kinetic theory in following form

$$\theta = \frac{b_A n_A}{1+b_A n_A} \tag{20}$$

for the case, when we deal with the adsorption of particles of type A, and in the form

$$\theta_A = \frac{b_A n_A}{1 + b_A n_A + b_B n_B}, \tag{21}$$

$$\theta_B = \frac{b_B n_A}{1 + b_A n_B + b_B n_B}, \tag{22}$$

For the case, when we deal with the competing adsorption of particles of type A and B. Here n_A and n_B – concentrations of particles of type A and B; b_A and b_B – adsorption constants of particles A and B.

Comparing equations (17) and (20), and also (18),(19) and (21) and (22) it is possible to obtain

$$b_A = \exp\frac{f_A - \varphi_A}{kT},$$

$$b_B = \exp\frac{f_B - \varphi_B}{kT},$$

where $\Delta G_A = f_A - \varphi_A$ and $\Delta G_B = f_B - \varphi_B$ – free energy of adsorption.

As is noted out in [4], this energy may be computed from heat measurements. Therefore there is a ground to interpret the nature of equations (17) the same as equations (18) and (19) obtained from the main equation of classical dynamics (8), as the equations, based on possibility of which the peculiarity is correctly determined of interrelationship between the following observed quantities, which are θ_A, θ_B, ΔG_A, ΔG_B, n_A, n_B, n^0 and kT.

On the other hand, based on the analysis of equation (14) for the case when the number of filling of cells is arbitrary, the following may be obtained

$$\overline{N} = n_\Phi + n_\Phi^0,$$

Where

$$n_\Phi = \exp\frac{\mu - f}{kT}, \tag{23}$$

$$n_\Phi^0 = \frac{n^0}{\exp\frac{-\mu + \varphi}{kT} - 1}. \tag{24}$$

Excluding from (23) and (24) $\exp\frac{\mu}{kT}$, it is possible to obtain

$$n_{\Phi}^{0} = \frac{n^{0}}{\frac{1}{n_{\Phi}} \exp \frac{f-\varphi}{kT} - 1}. \tag{25}$$

where n_{Φ}, n_{Φ}^{0} – concentrations of bosonic particles in volume phase and cells.

Under equilibrium F_n and Φ'_n are equal. Therefore based on (12) we have

$$\varphi = \frac{nf}{n'},$$

as the determination of the average energy of oscillator, according to (25), there is a possibility to obtain the expression

$$\varphi = \frac{f}{\frac{1}{n_{\Phi}} \exp \frac{f-\varphi}{kT} - 1}, \tag{26}$$

which may be accepted as a proof of the Plank relation (3).

From our viewpoint, there is a foundation to suppose, that the derivation of this expression based only on the possibility of main equations of statistical mechanics of Gibbs (7), under this without the necessity to suppose, that the investigated object is the linear harmonic oscillator, is more rigorous, than when it was performed by Plank, expressed in paper [2], where the equation (9) was obtained. In order to ensure the correctness of this one must pay attention to the following.

Results (12), obtained on this path are strictly theoretical, can now be accepted as a proof of relations (4) and (5), which in his time Plank in paper [1] derived under the name "quantum hypothesis". In other words, it may be observed that here the derivation of equation (25) are modernization and clarification of the main formula of statistics of Bose-Einstein, was carried out on the basis of possible new ideas. Thus, it may be concluded, that earlier ideas of Plank were closer to the path of truth, which were proposed in paper [1] in 1900, supposing, that for quantum physics the fundamental are the ideas about energy quanta.

As it is known, if equation (25) is widely used in the branches of physics, where the peculiarity of interaction of substances with phonons, then the Langmuir equation (20) and (21),(22) is widely used in development of the foundations of the theory of double electric layer, theory of dehydrogenation, theory of kinetics of heterogeneous hydrogenation etc.

In [5] and papers, published in book [6], it was shown, that during solution of these problems, using theoretically derived equations (17) and (18), (19), their explanatory possibility is considerably widened. Therefore, in view of all this, it may be resumed, that in derivation of equations (17)–(19) and (25) on the basis of possibility of main equations of statistical mechanics of Gibbs, which are in turn obtained from the main equation of classical dynamics of Hamilton (8), the problems are satisfacto-

rily described, for the solution of which the main equations of matrix mechanics were obtained.

R E F E R E N C E S

1. Plank M. “On the theory of distribution of energy of irradiation of normal spectrum”. **Selected works**. M.:Nauka, 1975, p.251-257.
2. Plank M. “The laws of heat irradiation and hypothesis of elementary quantum of action”. **Selected works**. M.: Nauka, 1975. p.282-310.
3. Dirac P. **Lectures on quantum field theory**. M.: Mir, 1971.
4. Gurevich L.E. “Application of statistics to the phenomena of monomolecular adsorption on solid surfaces. **Problems of kinetics and catalysis**. L., 1937.
5. Altayev N. **Algebraic and arithmetic equations of the foundations of the theory of cognition**. Shymkent, 2012.

6 Altayev N. **Universal method of disclosure of hidden truths**. Shymkent, 2005.

Author Index

Contents

Invited Lectures

Oral Contributions

Poster Session 1

1. Graphene

2. Carbon Nanotubes

Poster Session 2

3. Nanodiamonds

4. Methods for Characterization of Nanocarbons

Poster Session 3

5. Fullerenes

Conference/School of Young Scientists

Electrical conductivity and optical transparency measurements of thin carbon films

Sedlovets D.M.*, Red'kin A.N.

Institute of Microelectronics Technology and High-purity Materials Russian Academy of Science, 142432, Chernogolovka, Russia
**e-mail: sedlovets@iptm.ru*

The outstanding electrical1, mechanical and chemical properties of graphene make it attractive for applications in flexible electronics. [1]

Experiments were performed at the lowered pressure in the flow-type reactor. The system involved the horizontal tube furnace, the temperature control systems, gas flow controllers and forvacuum pump. Cu foil was used as a wafer. Thin carbon films were obtained by pyrolysis of ethanol vapor.

Then we measured the transmittance of graphene transferred to a polyethylene terephthalate (PET) substrate using an ultraviolet-visible spectrometer. The sheet resistance was measured using the four-point probe method.

The films display appreciable electrical conductivity and good transparency (92-95%). Because the transmittance of an individual graphene layer is 2,3% [2], this transmittance value indicates that the average number of graphene layers is two to four. These results were verified by atomic-force microscopy measurements.

[1] Kim K.S., Keun S.K., Yue Z., Houk J., Sang Y.L., Jong M.K., Kwang S.K., Jong-Hyun A., Philip K., Jae-Young C., Byung H. H. *Nature* **457**, 706 (2009).

[2] Nair R. R., Blake P., Grigorenko A. N., Novoselov K. S., Booth T. J., Stauber T., Peres N. M. R., Geim A. K., *Science* **320**, 1308 (2008).

Transient charging phenomena in graphite

Zagaynova V.*[1], Hacke C.[1], Chowdhury T.[1], Makarova T.[1,2]

[1]*Umeå University, 90187, Umeå, Sweden*
[2]*Ioffe Physical-Technical Institute RAS, 194021, St.Petersburg, Russia*
**e-mail: valeria.zagainova@physics.umu.se*

In carbon research, as well as in general research, graphite being the most stable carbon allotrope is one of the most studied materials. In scanning probe microscopy, graphite is used as calibration grates and atomic-smooth hydrophobic substrates. Surprisingly, very few studies are made on electrostatic force microscopy. Here, we demonstrate the ability of this technique to detect hidden defects (buried underneath) and follow the spatial charge redistribution under the action of electric field.

Graphite is a good electric conductor along its planes, and an insulator only perpendicular to the planes. Therefore, the electric field applied to the plane should not cause any potential fluctuations. And yet, they exist.

Under applied voltage, dendriform quickly changing charged areas were formed limited in their spatial expansion by the surface steps (see Fig. 1). Changing the tip polarity inverted the dark/bright images (Fig. 1 b and c). The charging phenomena were observed only in the pyrolytic graphite samples with the lowest mosaic spread, i. e. highest quality.

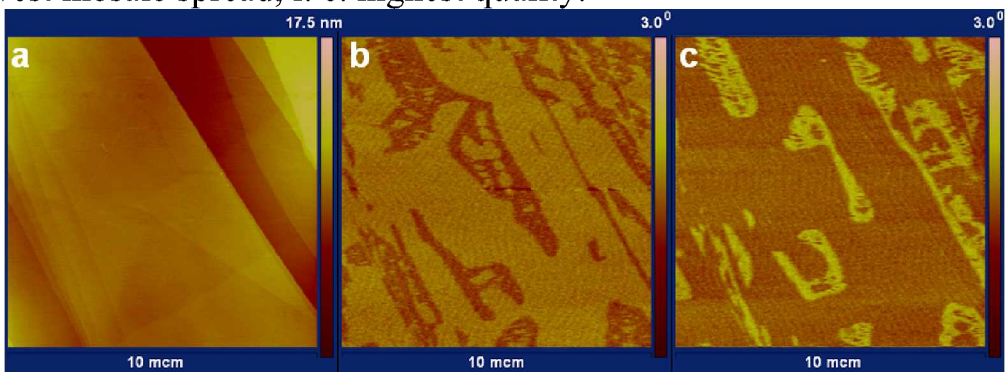

Figure 1. EFM images of HOPG graphite: a – topography, b, c – phase images taken at +2V and -2V, respectively.

The measurements performed in nitrogen atmosphere proved that observed fluctuations do not belong to effects caused by surface contamination such as adsorbed water. Besides, ideal graphite screens poorly, and applied electric field penetrates ~100 nm. Thus, the potential information comes not only from the surface, but charges within the bulk might group themselves at or close to surface steps or buried plane edges and also contribute to the signal.

Further studies on the charging phenomenon of HOPG graphite are needed to understand the origin of this effect.

The problem of nanodiamond visualization in biopharmaceutical research

Yakovlev R.Ju.

Pavlov Ryazan State Medical University, 390026, Ryazan, Russia
e-mail: yarules@yandex.ru

The problem of carbon nanoparticles diagnostics in biopharmaceutical research becomes more and more actual during the last years. But the complexity of control whether such particles are present and in what state *in vitro* and *in vivo* precludes us from using the standard physic-chemical methods. Therefore the search for new methods and techniques of carbon nanoparticles visualization and of widening their functions via development of new original approaches might be extremely important. This is very important for the research in nanotoxicology and biomedical applications including pharmacology research and drug delivery. The applications of nanodiamonds (ND) as nanocarriers in drug delivery systems necessitated finding the effective methods of their visualization. For the diagnostics of ND *in vitro* we used TEM. This allowed us to determine the average size of ND particles (5 nm) and the presence there of carbon atom layers (shells) with the diamond core in the center. It was possible to estimate the thickness and structural peculiarities of the ND shells depending on their chemical modification by HRTEM. In order to determine the chemical composition of ND surface and the presence to sp^2/sp^3 carbon atoms in near-surface layers of ND particles the XPS method was used. Raman spectra showed that ND have characteristic band of 1332 cm^{-1}. But creation of C_{diam}–N– bonds on the surface results in high fluorescence which is so higher than the peak of diamond phase that totally masks it. The further fluorescence research of ND with grafted drugs by Raman spectra might give us a powerful way to visualize such complexes. The radiochemical methods of carbon nanoparticles visualization are one of the most fast and accurate. We received ND with ^{3}H-label firmly fixed by covalent bond C_{diam}–^{3}H that allowed us to study their biodistribution *in vivo* in rats. The presence of heavy atoms in the grafted layer on the ND surface opens new diagnostic possibilities to determine ND *ex vivo* и *in vivo* by mass-spectrometry. Thus the long-term biodistribution of ND in rabbits was studied. The devised complex of physic-chemical methods of ND visualization allows us to effectively find ND in model systems, biological liquids, tissues and organs.

Intercalation of Cu underneath a graphene layer on Ni(111) and Co(0001) substrates studied with a synchrotron radiation

Vilkov O.Yu.*[1,2], Usachev D.Yu.[1], Fyodorov A.V.[1], Shikin A.M.[1], Vladimirov G.G.[1]

[1]*St. Petersburg State University, 199034 St. Petersburg, Russia*
[2]*Technische Universität Dresden, 01062 Dresden, Germany*
**e-mail: ol.vilkov@gmail.com*

The electronic structure of graphene on a metallic substrate is similar to that of free-standing graphene, but there are essential differences, which depend on a structure and a material of the substrate and are determined by the character of the graphene-substrate interaction. One of the main tasks is to study the properties of graphene on a wide range of substrates, as the solution of this problem provides an opportunity to purposefully affect on the characteristics of this material. An efficient approach to the solution of this task is based on a phenomenon of intercalation of various atoms underneath graphene films on metals.

Thick monocrystalline films of Co(0001) and Ni(111) were deposited on a preliminarily cleaned surface of tungsten crystal W(110) under the ultra-high vacuum conditions. Graphene films of a good quality were prepared on Co(0001) and Ni(111) films in a process of propylene cracking [1,2]. Intercalation of copper atoms underneath a graphene layer took place after the thermal annealing of pre-deposited copper layers [3].

The electronic structure of a core C1s level and a valence band of a graphene layer on the metallic substrates before and after the copper intercalation has been studied with X-ray photoelectron spectroscopy and angle-resolved ultra-violet photoelectron spectroscopy. X-ray absorption fine structure near the carbon K-edge has been measured for studying unoccupied graphene states. Synchrotron radiation with a linear polarization has been used to reveal a contribution of π^* and σ^* states [4].

[1] A.M. Shikin, D. Farias, K.H. Rieder, *Europhys. Lett.* **44**, 44 (1998).
[2] A. Varykhalov, O. Rader, *Phys. Rev. B* **80**, 035437 (2009).
[3] Yu.S. Dedkov, A.M. Shikin, V.K. Adamchuk, S.L. Molodtsov, C. Laubschat, A. Bauer, G. Kaindl, *Phys. Rev. B* **64**, 035405 (2001).
[4] R.A. Rosenberg, P.J. Love, V. Rehn, *Phys. Rev. B* **33**, 4034 (1986).

Investigation of triplet fullerene C_{70} lineshape EPR under continuous light illumination: zero field splitting parameters distribution

Uvarov M.N.[1]*, Kulik L.V.[1], Pichugina T.I.[1], Dzuba S.A.[1,2]

[1]*Institute of Chemical Kinetics and Combustion, 630090, Institutskaya 3, Novosibirsk, Russia*
[2]*Novosibirsk State University, 630090, Pirogova 2, Novosibirsk, Russia*
**e-mail: uvarov@kinetics.nsc.ru*

Continuous wave (CW) and pulse electron paramagnetic resonance (EPR) spectra of triplet state of fullerene C_{70} in various glassy matrices were obtained at temperatures 5K÷260K. At temperatures below 30K the emission region appeared at EPR spectra because populations of $^3C_{70}$ spin sublevels are non-equilibrium immediately after photoexcitation. At low temperatures spin-lattice relaxation time of $^3C_{70}$ becomes comparable with triplet $^3C_{70}$ lifetime. At temperatures higher 50K EPR spectra contained only absorptive part.

Transversal relaxation rate was obtained by pulse EPR methods. It does not substantially depend on EPR spectrum position. So, exchange process within EPR spectrum due to rotations or pseudorotations of $^3C_{70}$ molecule around its long symmetry axis has not appreciably influence the EPR lineshape below 77K.

CW EPR lineshape of $^3C_{70}$ at 77K was simulated supposing the equilibrium population of $^3C_{70}$ spin sublevels. The zero field splitting parameters D and E were revealed to have probability distributions. EPR lineshape of $^3C_{70}$ was simulated successfully assuming Gaussian probability distribution of D value, whereas E value probability distribution function was different. It had a property: at E = 0 the probability value is 0. At work [1] EPR lineshape of $^3C_{70}$ was simulated assuming rectangular probability density of E value.

With temperature increasing higher 100K the rapid rising of the transversal relaxation rate of $^3C_{70}$ was obtained from pulse EPR data. The phenomenon can be explained by $^3C_{70}$ molecule motion due to glass matrix softening. CW EPR lineshape narrowing with temperature increasing confirmed the suggestion about $^3C_{70}$ motions.

D and E values distribution can be explained by dependence of molecular $^3C_{70}$ Jahn-Teller distortion on local surrounding of each molecule. We can conclude that $^3C_{70}$ symmetry is not higher than D_{2h}.

[1] M.N. Uvarov, L.V. Kulik, T.I. Pichugina, S.A. Dzuba, *Spectrochimica Acta Part A: Molecular and Biomolecular Spectroscopy*, DOI: 10.1016/j.saa.2011.01.047 (2011)

Analysis of two-level organization of detonation nanodiamond clusters by SANS

Tomchuk O.V.*[1,2], Avdeev M.V.[1], Aksenov V.L.[3,1], Bulavin L.A.[2], Garamus V.M.[4]

[1]*Joint Institute for Nuclear Research, Dubna, Moscow reg., Russia*
[2]*Taras Shevchenko Kyiv National University, Kyiv, Ukraine*
[3]*Russian Research Center "Kurchatov Institute", Moscow, Russia*
[4]*GKSS Research Centre, Geesthacht, Germany*
**e-mail: tomchuk@jinr.ru*

The influence of model selection for data processing of small-angle neutron scattering (SANS) by fractal clusters of detonation nanodiamonds in powders [1] and aqueous dispersions [2] is discussed. In addition to previous work we focus our attention on the analysis of the scattering, corresponding to the level of nanocrystallites, taking into account the polydispersity. It was shown that the model of the diffusion surface corresponding to the graphene shell of the nanocrystallites agrees with the contrast variation data in the aqueous dispersions (mixtures H2O/D2O) against the average characteristics, and explains the differences in average grain size determined by small-angle neutron scattering and X-ray diffraction (broadening of the peaks). However, direct determination of the form and parameters of the distribution function of crystallite size encounters difficulties due to the irregular structure of the surface. In particular, determined structural parameters of the particles strongly depend on the type of model distribution function and the residual background.

[1] M.V. Avdeev, V.L. Aksenov, L. Rosta, *Diamond Related Mater*. **16**, 2050 (2007).
[2] M.V. Avdeev, N.N. Rozhkova, V.L. Aksenov, V.M. Garamus, R. Willumeit, E. Osawa, *J. Phys. Chem. C* **113**, 9473 (2009).

Determination of the diamond content in the detonation products of explosive

Gavrilova V.C.[1], Janchuk I.B.[2], Svirid E.A.*[1], Efanov A.V.[2]

[1]*V.N. Bakul Institute for Superhard Materials NASU, Ukraine*
[2]*V.E. Lashkarev Institute of Semiconductor Physics NASU, Ukraine*
**e-mail: sviridkat@rambler.ru*

Currently, the ultradispersed diamond (UDD) powders synthesized in the shock waves from explosives are widely used. A separation of UDD from the synthesis product is quite complex and time-consuming process. Purification of metal impurities and removing non-diamond carbon are the main stages of this process. A test of the purification degree of UDD and identification of impurities, especially impurities of carbon, which forms the amorphous structures, are no less complex.

In this paper, the studies of diamond content in the UDD synthesis product purified from metallic impurities are presented. Relations of sp^2 and sp^3 - hybridized carbon in the samples with various concentrations of diamond were determined by Raman spectroscopy.

Initially, the synthesis product powder was purified from metal impurities. Then removing non-diamond carbon was carried out by treating the powder in the strong liquid-phase oxidants. In the first stage, the diamond content in powder was determined from the decrease in the mass of powder after the treatment.

The obtained data correlate with the number of sp^2 and sp^3 – hybridized carbon in the product.

The relative error in determining the content of diamond in the product by reduce its mass during treatment is less than 5%.

EPR and optical diagnostics of nanodiamonds

Soltamova A.A.*, Soltamov V.A., Bhoodoo C., Kramuschenko D.D., Shakhov F.M.

Ioffe Physical-Technical InstituteRAS, 194021, St.Petersburg, Russia
**e-mail: alex.soltamova@hotmail.com*

Nitrogen is the main impurity in diamonds, which largely determines their properties. Nitrogen creates various paramagnetic centers in diamonds and exists as individual atoms and clusters. Recently, a great interest has been inspired by studies of nitrogen-vacancy centers (NV defects) in diamonds, for which the magnetic resonance on single defect was successfully observed at the room temperature. However, ND doping processes, formation and structure of intrinsic and impurity defects differ from those in bulk diamonds. In particular, the theoretical studies have shown that nitrogen impurities in ND seem to be metastable in contrast to bulk diamonds. The irradiation methods used to create the NV centers in diamonds/nanodiamonds are purely statistical and the effectiveness of creation of the NV centers in nanodiamond with the size less than 20 nm is still under the question.

Electron paramagnetic resonance (EPR) is one of the most informative and sensitive techniques for the diagnostics of defects in semiconductors. at the molecular level. Herein, we examine the defects in sintered nanodiamonds (ND) by EPR.

Our studies have shown that single nitrogen atoms occupy the stable position in nanodiamond lattice and can be observed in detonation ND sintered under different conditions. Under peculiar sintering conditions it is possible to observe the effect of self-organization of ND into micron size arrays, which is confirmed by orientation dependencies observed in the EPR spectra.

We have also detected very intense EPR spectra corresponding to NV centers in diamonds. Observation of these spectra with and without illumination of the samples allows us to conclude that NV centers can be fabricated in ND without any post or prior irradiation. The formation of NV centers is governed only by high pressure high temperature sintering of detonation ND. The EPR data are confirmed by measurements of photoluminescence (PL) spectra. To determine the best sintering conditions we have performed the series of PL in different types of sintered nanodiamonds and irradiated diamonds.

This work has been supported by the Ministry of Education and Science of the Russian Federation under Contracts No. 14.740.11.0048.

[1] I.V. Ilyin, A.A. Soltamova, P.G. Baranov, A.Ya.Vul', S.V. Kidalov, F.M. Shakhov, G.V. Mamin, S.B. Orlinskii, N.I. Silkin, M.Kh. Salakhov, *Fullerenes, Nanotubes, and Carbon Nanostructures* **19**, 44 (2011).

[2] A.A. Soltamova, I.V. Il'in, F.M. Shakhov, S.V. Kidalov, A.Ya. Vul', B.V. Yavkin, G.V. Mamin, S.B. Orlinskii, P.G. Baranov, *JETP Letters* **92**, 102 (2010).

Diagnostics of nitrogen-doped carbon prepared by polyaniline pyrolysis

Shishov M.A.[1], Sapurina I.Yu.*

[1]*St.-Petersburg State Electro-Technical University "LETI" St.-Petersburg, 19736 St.-Petersburg, Russia*
**Institute of Macromolecular Compounds RAS, 199004, St.-Petersburg, Russia*
**e-mail: sapurina@mail.ru*

Nitrogen is the best dopant of carbonaceous materials due to its strong electron donating properties and atomic size being similar to that of carbon. Nirogen-doped carbon (NdC) demonstrates improve electron field emission properties because of reduced work function, save as the best support for the heterogeneous catalysis showing synergetic catalytic effect, hardly increased specific capacitance to cations and can be promising material for battery and supercapacitors.

Now the new NdC with high nitrogen content were prepared by pyrolysis of conducting polyaniline (PANI) and its composites and studied by the methods of electron microscopy, Raman and FTIR-spectroscopy, conductometry, thermogravimetric- and BET-analysis. Thermodestruction of PANI proceed at the range of 400-900°C at inert atmosphere and lead to chains cyclizatons were C=N (sp^2C-N) and C–N (sp^3C-N) bonds between nitrogen and carbon obtained. The atomic concentration of nitrogen was estimated by chemical elemental analysis and depending on pyrolysis conditions changes from 6 to 15%. The conductivity and specific surface area of NdC reach 10^{-4} S cm^{-1} and 350 m^2 g^{-1}. The morphology of prepared NdC can be very different and changes from 3D and 1D to complex hierarchical structures, since the morphology of polymer-precursor did not destroyed during the pyrolysis.

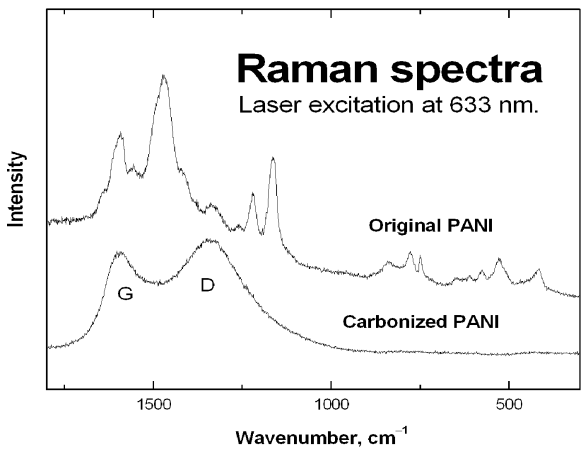

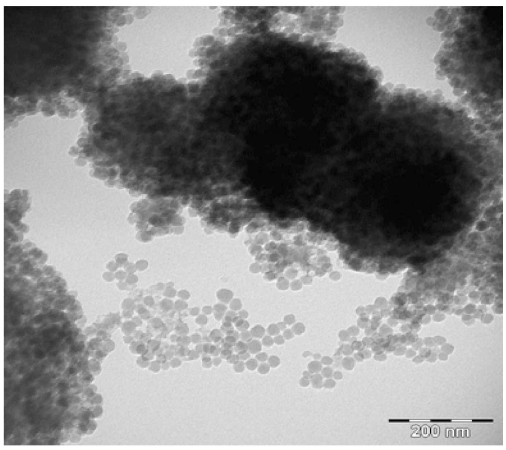

Figure. Raman spectra of PANI and carbonized PANI, transmission electron microscopy of carbonized PANI of 3D structures.

Infrared absorption studies of surface functional groups of chemically modified nanodiamonds

Shestakov M.S.*, Osipov V.Yu.

Ioffe Physical-Technical InstituteRAS, 194021, St.Petersburg, Russia
**e-mail: mikhail.shestakov@gmail.com*

Efficient chemical modification of detonation nanodiamond (DND) surface are able to occur in suspension consist of separate DND particles. Production such suspension require either disaggregate solute (breaking bonds between particles) and prevent particles coagulation that happens when particles have certain charge due dissociation of surface functional groups.

"Z+" and "Z-" samples annealed at 400°C in hydrogen atmosphere and in air respectively. Surface of other samples are decorated with separate metallic ions Cu^{2+}, Co^{2+}, Ce^{3+}, Ce^{4+} or Eu^{3+} alternatively. Concentration of ions varies between 0.1 wt.% and 2.5 wt.%. All the samples compared with initial purified DND and with each other.

Obtained spectra reveal that "Z+" sample surface contain no carbonyl groups, but a lot of C-H groups, instead. Opposite, "Z-" sample has a lot of carbonyl groups in place of C-H groups. Apparently, ultrasonic treatment in water solution leads, that all samples contain significant and nearly equal amount of hydroxyl groups.

The metallic ions modified samples did not show any significant difference of its' surface visible at IR spectra. Furthermore, it is impossible to distinguish samples with different concentrations of the ions. The only one sample (modified with Cu^{2+}) showed visible difference, but this sample had been prepared from different kind of initial DND then others were.

Altogether, the only one functional group (except hydroxyl) predominate at the surfaces of each "Z+" and "Z-" samples, causing their high disperse ability in water solution. Analyzing IR spectra, neither concentration nor type metallic ions at DND particles surface can be established but certain information about initial DND and methods of purifying and modification applied to the sample can be obtained.

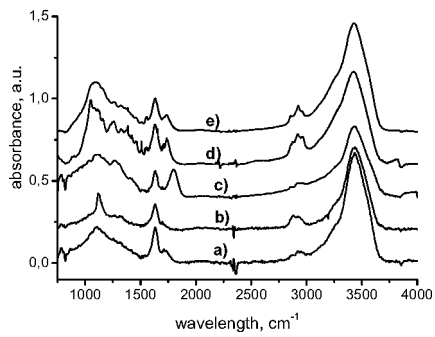

DND spectra of a) initial purified DND b) Z+ c) Z− d) Cu^{2+} modified DND e) Co^{2+} modified DND.

Raman studies of epitaxial multi-graphene films grown on a 6H-SiC substrates.

Shavlovskiy N.V.*, Smirnov A.N., Lebedev S.P., Lebedev A.A.

Ioffe Physical-Technical Institute RAS, St.-Petersburg, 194021, Russia
**e-mail: sunnykelevra@gmail.com*

Raman spectroscopy has historically been used to probe structural and electronic characteristics of graphite materials, providing useful information on the defects (D-band), in-plane vibration of sp^2 carbon atoms (G-band), as well as the stacking orders (2D-band) [1]. This method fit also for quality examination of new carbon material – graphene. Raman spectra of graphite (graphene) may contain three strongest lines. Line *G* at ~1582 cm^{-1} derives from the doubly degenerate phonon mode of E_{2g} symmetry from the Brillouin zone center. Line *D* at ~1352 cm^{-1} appears in samples with high concentrations of structural defects and is associated with phonons close to the *K* point of Brillouin zone boundary. Line 2*D* (~2710 cm^{-1}) originates from resonant light scattering involving two phonons of equal energy but with oppositely directed wave vectors, and provides information on the stacking order of graphite (graphene) layers.

The micro-Raman studies were performed in back-scattering geometry $y(xx)\bar{y}$ on a Horiba Jobin-Yvon T64000 spectrometer by means of a confocal microscope at room temperature. The spectra were excited with an Ar+ laser (λ = 514.5 nm). To exclude local heating effects, which could result in a shift of phonon lines, the laser radiation power on the sample was <1 mW (diameter of the laser beam was 4 μm).

For investigations multi-graphene layers on 6H-SiC substrates were used. Graphene films were grown on silicone carbide by sublimation method [2]. We used samples grown in the temperature range of 1300-1600°C to examine the quality of multi-graphene films from growth temperature.

Raman spectra of samples grown at low temperatures (1300-1400°C) exhibit strong line D, which indicate the presence of defects, whereas spectra of samples grown at high temperatures (1500-1600°C) don't exhibit D-line.

Thus Raman investigations show that the multi-graphene films grown at low temperatures are much more defective than the films grown at high temperatures.

[1] M.A. Pimenta, G. Dresselhaus, M.S. Dresselhaus; L.G. Cancado, A. Jorio, R. Saito, *Phys. Chem. Chem. Phys.* **9**, 1276 (2007).

[2] A.A. Lebedev, I.S. Kotousova, A.V. Lavrentiev, S.P. Lebedev, I.V. Makarenko, V.N. Petrov, A.N. Titkov, *Phys. Solid State* **51**(4) (2010).

Diagnostics of the structure of thin films of polymerized C_{60} formed via electron-beam dispersion method

Razanau I.

Belarusian State University of Transport, 246653, Gomel, Belarus
Francisk Skorina Gomel State University, 246019, Gomel, Belarus
e-mail: ir23.by@gmail.com

Polymerized fullerene C_{60} forms a whole new promising class of carbon materials. Structure of polymerized C_{60} varies from dumb-bell- to peanut-shaped polymers which in turn can form dimers, linear chains, two-dimensional or even three-dimensional networks. The physical-chemical properties of C_{60} polymers vary in a wide range respectively. However, the diagnostics of the exact polymer composition and structure of such materials is often quite a complicated experimental task. Unlike C_{60} monomer, C_{60} polymers hardly can be dissolved. The polymer insolubility provides a quick and convenient technique to check the polymerization. However, on the other hand, it also makes measurement of the polymer composition even more complicated. Therefore, thorough analysis and comparison of the results obtained using different measurement techniques is necessary.

In the presented report, polymer composition and structure of thin C_{60} polymer films, deposited via electron-beam dispersion of pristine fullerite C_{60} in vacuum [1], have been studied using Raman and FTIR spectroscopy, laser desorption/ionization (LDI) and matrix assisted laser desorption/ionization (MALDI) mass spectrometry, X-ray photoelectron spectroscopy.

We have used a precise Lorentzian lineshape analysis to decompose Raman spectra of the deposited coatings into components characteristic of dumb-bell-shaped fullerene dimers, 1D and 2D polymers and thus, to analyse the polymer composition of the coatings. The results have been also proved by FTIR spectra analysis. However, we have also shown that estimations of the polymer composition based on the vibrational spectra clearly overestimate the content of fullerene dimers due to end C_{60} molecules in polymer chains and clusters.

It has been shown that LDI mass spectrometry allows for detection of polymer clusters in the deposited coatings. However, C_{60} polymers readily dissociate to monomers upon desorption/ionization process. Therefore, a soft mass spectrometry technique, MALDI was used to obtain information about the polymer composition of the coatings. Polymer clusters with the size of up to 7 monomer units have been found in the mass spectra. The results of the mass spectrometry measurement are compared to estimations based upon vibrational spectra as well as to XPS data. Peculiarities of each experimental technique in the measurement of thin C_{60} polymer film composition are discussed.

[1] V. Kazachenko, I. Ryazanov, *Technical Physics Letters* **34**, 930 (2008).

Angle resolved photoelectron spectroscopy as the method for investigation of electronic structure of graphene

Popova A.A.*, Shikin A.M., Rybkin A.G.

St. Petersburg State University, 198504, St. Petersburg, Russia
**e-mail: popova.anna@bk.ru*

Photoelectron spectroscopy (PES) is one of the modern methods for investigation of occupied electronic states of solids. The photoeffect is the basic effect of this method. Electron in an occupied state can be excited to unoccupied state by photon. If the energy of photon $\hbar\omega$ is larger than a work function of solid some electrons can leave a solid and then can be registered. Using of the synchrotron radiation is prevailing last time. Ultrarelativistic charged particle motion in the storage ring leads to the synchrotron radiation which allows achieving of monochromatic radiation with a high energy resolution and a high intensity during registration of photoelectron energy distribution [1,2].

Angle resolved photoelectron spectroscopy (ARPES) is widespread method for measurement of dispersion dependences and symmetry of energy bands of solid. Basically this method has a conservation of parallel to the surface component of quasimomentum of photoelectron when overcoming the potential barrier. We can investigate features of the electronic structure of graphene when measuring dispersion dependences of electronic states in different directions of surface Brillouin zone. In the present time the only feasible route towards large-scale production of graphene is epitaxial growth on a substrate. The presence of the substrate will influence on the electronic properties of graphene layer. And the electronic structure of such graphene will differ from the one of ideal freestanding graphene with such distinctive features as linear dispersion dependences of π-states of graphene near the K point of the Brillouin zone of graphene and a location of Dirac point (the crossing point of cones of occupied and unoccupied electronic states) at the Fermi level.

[1] S. Hufner. Photoelectron spectroscopy: principles and applications. - Berlin Heidelberg: Springer-Verlag, 1995.

[2] Shikin A.M. Interaction of photons and electrons with the solid state, St. Petersburg, VVM, 2008 (in Russian).

Angle resolved photoelectron spectroscopy as the method for investigation of electronic structure of graphene

Popova A.A.*, Shikin A.M., Rybkin A.G.

St. Petersburg State University, 198504, St. Petersburg, Russia
**e-mail: popova.anna@bk.ru*

Photoelectron spectroscopy (PES) is one of the modern methods for investigation of occupied electronic states of solids. The photoeffect is the basic effect of this method. Electron in an occupied state can be excited to unoccupied state by photon. If the energy of photon $\hbar\omega$ is larger than a work function of solid some electrons can leave a solid and then can be registered. Using of the synchrotron radiation is prevailing last time. Ultrarelativistic charged particle motion in the storage ring leads to the synchrotron radiation which allows achieving of monochromatic radiation with a high energy resolution and a high intensity during registration of photoelectron energy distribution [1,2].

Angle resolved photoelectron spectroscopy (ARPES) is widespread method for measurement of dispersion dependences and symmetry of energy bands of solid. Basically this method has a conservation of parallel to the surface component of quasimomentum of photoelectron when overcoming the potential barrier. We can investigate features of the electronic structure of graphene when measuring dispersion dependences of electronic states in different directions of surface Brillouin zone. In the present time the only feasible route towards large-scale production of graphene is epitaxial growth on a substrate. The presence of the substrate will influence on the electronic properties of graphene layer. And the electronic structure of such graphene will differ from the one of ideal freestanding graphene with such distinctive features as linear dispersion dependences of π-states of graphene near the K point of the Brillouin zone of graphene and a location of Dirac point (the crossing point of cones of occupied and unoccupied electronic states) at the Fermi level.

[1] S. Hufner. Photoelectron spectroscopy: principles and applications. - Berlin Heidelberg: Springer-Verlag, 1995.

[2] Shikin A.M. Interaction of photons and electrons with the solid state, St. Petersburg, VVM, 2008 (in Russian).

Diagnostics of the structure of thin films of polymerized C_{60} formed via electron-beam dispersion method

Razanau I.

Belarusian State University of Transport, 246653, Gomel, Belarus
Francisk Skorina Gomel State University, 246019, Gomel, Belarus
e-mail: ir23.by@gmail.com

Polymerized fullerene C_{60} forms a whole new promising class of carbon materials. Structure of polymerized C_{60} varies from dumb-bell- to peanut-shaped polymers which in turn can form dimers, linear chains, two-dimensional or even three-dimensional networks. The physical-chemical properties of C_{60} polymers vary in a wide range respectively. However, the diagnostics of the exact polymer composition and structure of such materials is often quite a complicated experimental task. Unlike C_{60} monomer, C_{60} polymers hardly can be dissolved. The polymer insolubility provides a quick and convenient technique to check the polymerization. However, on the other hand, it also makes measurement of the polymer composition even more complicated. Therefore, thorough analysis and comparison of the results obtained using different measurement techniques is necessary.

In the presented report, polymer composition and structure of thin C_{60} polymer films, deposited via electron-beam dispersion of pristine fullerite C_{60} in vacuum [1], have been studied using Raman and FTIR spectroscopy, laser desorption/ionization (LDI) and matrix assisted laser desorption/ionization (MALDI) mass spectrometry, X-ray photoelectron spectroscopy.

We have used a precise Lorentzian lineshape analysis to decompose Raman spectra of the deposited coatings into components characteristic of dumb-bell-shaped fullerene dimers, 1D and 2D polymers and thus, to analyse the polymer composition of the coatings. The results have been also proved by FTIR spectra analysis. However, we have also shown that estimations of the polymer composition based on the vibrational spectra clearly overestimate the content of fullerene dimers due to end C_{60} molecules in polymer chains and clusters.

It has been shown that LDI mass spectrometry allows for detection of polymer clusters in the deposited coatings. However, C_{60} polymers readily dissociate to monomers upon desorption/ionization process. Therefore, a soft mass spectrometry technique, MALDI was used to obtain information about the polymer composition of the coatings. Polymer clusters with the size of up to 7 monomer units have been found in the mass spectra. The results of the mass spectrometry measurement are compared to estimations based upon vibrational spectra as well as to XPS data. Peculiarities of each experimental technique in the measurement of thin C_{60} polymer film composition are discussed.

[1] V. Kazachenko, I. Ryazanov, *Technical Physics Letters* **34**, 930 (2008).

Raman studies of epitaxial multi-graphene films grown on a 6H-SiC substrates.

Shavlovskiy N.V.*, Smirnov A.N., Lebedev S.P., Lebedev A.A.

Ioffe Physical-Technical Institute RAS, St.-Petersburg, 194021, Russia
**e-mail: sunnykelevra@gmail.com*

Raman spectroscopy has historically been used to probe structural and electronic characteristics of graphite materials, providing useful information on the defects (D-band), in-plane vibration of sp^2 carbon atoms (G-band), as well as the stacking orders (2D-band) [1]. This method fit also for quality examination of new carbon material – graphene. Raman spectra of graphite (graphene) may contain three strongest lines. Line *G* at ~1582 cm^{-1} derives from the doubly degenerate phonon mode of E_{2g} symmetry from the Brillouin zone center. Line *D* at ~1352 cm^{-1} appears in samples with high concentrations of structural defects and is associated with phonons close to the *K* point of Brillouin zone boundary. Line 2*D* (~2710 cm^{-1}) originates from resonant light scattering involving two phonons of equal energy but with oppositely directed wave vectors, and provides information on the stacking order of graphite (graphene) layers.

The micro-Raman studies were performed in back-scattering geometry $y(xx)\bar{y}$ on a Horiba Jobin-Yvon T64000 spectrometer by means of a confocal microscope at room temperature. The spectra were excited with an Ar+ laser (λ = 514.5 nm). To exclude local heating effects, which could result in a shift of phonon lines, the laser radiation power on the sample was <1 mW (diameter of the laser beam was 4 μm).

For investigations multi-graphene layers on 6H-SiC substrates were used. Graphene films were grown on silicone carbide by sublimation method [2]. We used samples grown in the temperature range of 1300-1600°C to examine the quality of multi-graphene films from growth temperature.

Raman spectra of samples grown at low temperatures (1300-1400°C) exhibit strong line D, which indicate the presence of defects, whereas spectra of samples grown at high temperatures (1500-1600°C) don't exhibit D-line.

Thus Raman investigations show that the multi-graphene films grown at low temperatures are much more defective than the films grown at high temperatures.

[1] M.A. Pimenta, G. Dresselhaus, M.S. Dresselhaus; L.G. Cancado, A. Jorio, R. Saito, *Phys. Chem. Chem. Phys.* **9**, 1276 (2007).

[2] A.A. Lebedev, I.S. Kotousova, A.V. Lavrentiev, S.P. Lebedev, I.V. Makarenko, V.N. Petrov, A.N. Titkov, *Phys. Solid State* **51**(4) (2010).

Infrared absorption studies of surface functional groups of chemically modified nanodiamonds

Shestakov M.S.*, Osipov V.Yu.

Ioffe Physical-Technical InstituteRAS, 194021, St.Petersburg, Russia
**e-mail: mikhail.shestakov@gmail.com*

Efficient chemical modification of detonation nanodiamond (DND) surface are able to occur in suspension consist of separate DND particles. Production such suspension require either disaggregate solute (breaking bonds between particles) and prevent particles coagulation that happens when particles have certain charge due dissociation of surface functional groups.

"Z+" and "Z-" samples annealed at 400°C in hydrogen atmosphere and in air respectively. Surface of other samples are decorated with separate metallic ions Cu^{2+}, Co^{2+}, Ce^{3+}, Ce^{4+} or Eu^{3+} alternatively. Concentration of ions varies between 0.1 wt.% and 2.5 wt.%. All the samples compared with initial purified DND and with each other.

Obtained spectra reveal that "Z+" sample surface contain no carbonyl groups, but a lot of C-H groups, instead. Opposite, "Z-" sample has a lot of carbonyl groups in place of C-H groups. Apparently, ultrasonic treatment in water solution leads, that all samples contain significant and nearly equal amount of hydroxyl groups.

The metallic ions modified samples did not show any significant difference of its' surface visible at IR spectra. Furthermore, it is impossible to distinguish samples with different concentrations of the ions. The only one sample (modified with Cu^{2+}) showed visible difference, but this sample had been prepared from different kind of initial DND then others were.

Altogether, the only one functional group (except hydroxyl) predominate at the surfaces of each "Z+" and "Z-" samples, causing their high disperse ability in water solution. Analyzing IR spectra, neither concentration nor type metallic ions at DND particles surface can be established but certain information about initial DND and methods of purifying and modification applied to the sample can be obtained.

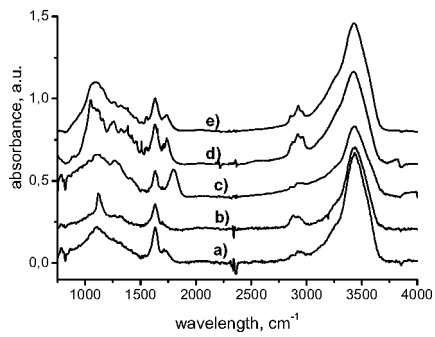

DND spectra of a) initial purified DND b) Z+ c) Z− d) Cu^{2+} modified DND e) Co^{2+} modified DND.

Diagnostics of nitrogen-doped carbon prepared by polyaniline pyrolysis

Shishov M.A.[1], Sapurina I.Yu.*

[1]*St.-Petersburg State Electro-Technical University "LETI" St.-Petersburg, 19736 St.-Petersburg, Russia*
**Institute of Macromolecular Compounds RAS, 199004, St.-Petersburg, Russia*
**e-mail: sapurina@mail.ru*

Nitrogen is the best dopant of carbonaceous materials due to its strong electron donating properties and atomic size being similar to that of carbon. Nirogen-doped carbon (NdC) demonstrates improve electron field emission properties because of reduced work function, save as the best support for the heterogeneous catalysis showing synergetic catalytic effect, hardly increased specific capacitance to cations and can be promising material for battery and supercapacitors.

Now the new NdC with high nitrogen content were prepared by pyrolysis of conducting polyaniline (PANI) and its composites and studied by the methods of electron microscopy, Raman and FTIR-spectroscopy, conductometry, thermogravimetric- and BET-analysis. Thermodestruction of PANI proceed at the range of 400-900°C at inert atmosphere and lead to chains cyclizatons were C=N (sp^2C-N) and C–N (sp^3C-N) bonds between nitrogen and carbon obtained. The atomic concentration of nitrogen was estimated by chemical elemental analysis and depending on pyrolysis conditions changes from 6 to 15%. The conductivity and specific surface area of NdC reach 10^{-4} S cm^{-1} and 350 m^2 g^{-1}. The morphology of prepared NdC can be very different and changes from 3D and 1D to complex hierarchical structures, since the morphology of polymer-precursor did not destroyed during the pyrolysis.

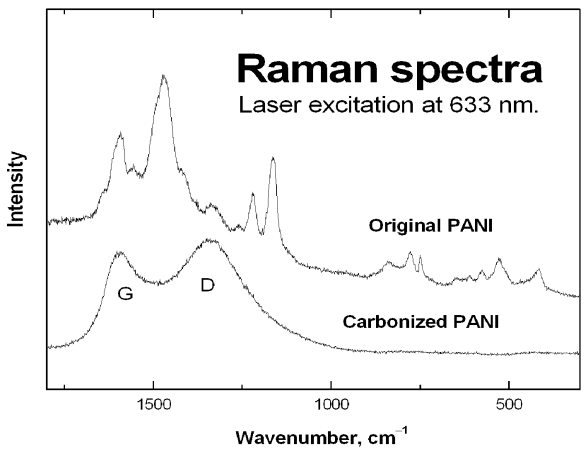

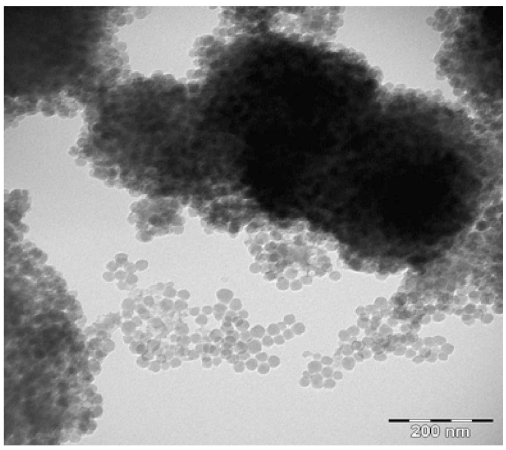

Figure. Raman spectra of PANI and carbonized PANI, transmission electron microscopy of carbonized PANI of 3D structures.

EPR and optical diagnostics of nanodiamonds

Soltamova A.A.*, Soltamov V.A., Bhoodoo C., Kramuschenko D.D., Shakhov F.M.

Ioffe Physical-Technical InstituteRAS, 194021, St.Petersburg, Russia
**e-mail: alex.soltamova@hotmail.com*

Nitrogen is the main impurity in diamonds, which largely determines their properties. Nitrogen creates various paramagnetic centers in diamonds and exists as individual atoms and clusters. Recently, a great interest has been inspired by studies of nitrogen-vacancy centers (NV defects) in diamonds, for which the magnetic resonance on single defect was successfully observed at the room temperature. However, ND doping processes, formation and structure of intrinsic and impurity defects differ from those in bulk diamonds. In particular, the theoretical studies have shown that nitrogen impurities in ND seem to be metastable in contrast to bulk diamonds. The irradiation methods used to create the NV centers in diamonds/nanodiamonds are purely statistical and the effectiveness of creation of the NV centers in nanodiamond with the size less than 20 nm is still under the question.

Electron paramagnetic resonance (EPR) is one of the most informative and sensitive techniques for the diagnostics of defects in semiconductors. at the molecular level. Herein, we examine the defects in sintered nanodiamonds (ND) by EPR.

Our studies have shown that single nitrogen atoms occupy the stable position in nanodiamond lattice and can be observed in detonation ND sintered under different conditions. Under peculiar sintering conditions it is possible to observe the effect of self-organization of ND into micron size arrays, which is confirmed by orientation dependencies observed in the EPR spectra.

We have also detected very intense EPR spectra corresponding to NV centers in diamonds. Observation of these spectra with and without illumination of the samples allows us to conclude that NV centers can be fabricated in ND without any post or prior irradiation. The formation of NV centers is governed only by high pressure high temperature sintering of detonation ND. The EPR data are confirmed by measurements of photoluminescence (PL) spectra. To determine the best sintering conditions we have performed the series of PL in different types of sintered nanodiamonds and irradiated diamonds.

This work has been supported by the Ministry of Education and Science of the Russian Federation under Contracts No. 14.740.11.0048.

[1] I.V. Ilyin, A.A. Soltamova, P.G. Baranov, A.Ya.Vul', S.V. Kidalov, F.M. Shakhov, G.V. Mamin, S.B. Orlinskii, N.I. Silkin, M.Kh. Salakhov, *Fullerenes, Nanotubes, and Carbon Nanostructures* **19**, 44 (2011).

[2] A.A. Soltamova, I.V. Il'in, F.M. Shakhov, S.V. Kidalov, A.Ya. Vul', B.V. Yavkin, G.V. Mamin, S.B. Orlinskii, P.G. Baranov, *JETP Letters* **92**, 102 (2010).

Determination of the diamond content in the detonation products of explosive

Gavrilova V.C.[1], Janchuk I.B.[2], Svirid E.A.*[1], Efanov A.V.[2]

[1]*V.N. Bakul Institute for Superhard Materials NASU, Ukraine*
[2]*V.E. Lashkarev Institute of Semiconductor Physics NASU, Ukraine*
**e-mail: sviridkat@rambler.ru*

Currently, the ultradispersed diamond (UDD) powders synthesized in the shock waves from explosives are widely used. A separation of UDD from the synthesis product is quite complex and time-consuming process. Purification of metal impurities and removing non-diamond carbon are the main stages of this process. A test of the purification degree of UDD and identification of impurities, especially impurities of carbon, which forms the amorphous structures, are no less complex.

In this paper, the studies of diamond content in the UDD synthesis product purified from metallic impurities are presented. Relations of sp^2 and sp^3 - hybridized carbon in the samples with various concentrations of diamond were determined by Raman spectroscopy.

Initially, the synthesis product powder was purified from metal impurities. Then removing non-diamond carbon was carried out by treating the powder in the strong liquid-phase oxidants. In the first stage, the diamond content in powder was determined from the decrease in the mass of powder after the treatment.

The obtained data correlate with the number of sp^2 and sp^3 – hybridized carbon in the product.

The relative error in determining the content of diamond in the product by reduce its mass during treatment is less than 5%.

Analysis of two-level organization of detonation nanodiamond clusters by SANS

Tomchuk O.V.*[1,2], Avdeev M.V.[1], Aksenov V.L.[3,1], Bulavin L.A.[2], Garamus V.M.[4]

[1]*Joint Institute for Nuclear Research, Dubna, Moscow reg., Russia*
[2]*Taras Shevchenko Kyiv National University, Kyiv, Ukraine*
[3]*Russian Research Center "Kurchatov Institute", Moscow, Russia*
[4]*GKSS Research Centre, Geesthacht, Germany*
**e-mail: tomchuk@jinr.ru*

The influence of model selection for data processing of small-angle neutron scattering (SANS) by fractal clusters of detonation nanodiamonds in powders [1] and aqueous dispersions [2] is discussed. In addition to previous work we focus our attention on the analysis of the scattering, corresponding to the level of nanocrystallites, taking into account the polydispersity. It was shown that the model of the diffusion surface corresponding to the graphene shell of the nanocrystallites agrees with the contrast variation data in the aqueous dispersions (mixtures H2O/D2O) against the average characteristics, and explains the differences in average grain size determined by small-angle neutron scattering and X-ray diffraction (broadening of the peaks). However, direct determination of the form and parameters of the distribution function of crystallite size encounters difficulties due to the irregular structure of the surface. In particular, determined structural parameters of the particles strongly depend on the type of model distribution function and the residual background.

[1] M.V. Avdeev, V.L. Aksenov, L. Rosta, *Diamond Related Mater*. **16**, 2050 (2007).
[2] M.V. Avdeev, N.N. Rozhkova, V.L. Aksenov, V.M. Garamus, R. Willumeit, E. Osawa, *J. Phys. Chem. C* **113**, 9473 (2009).

Investigation of triplet fullerene C_{70} lineshape EPR under continuous light illumination: zero field splitting parameters distribution

Uvarov M.N.[1]*, Kulik L.V.[1], Pichugina T.I.[1], Dzuba S.A.[1,2]

[1]*Institute of Chemical Kinetics and Combustion, 630090, Institutskaya 3, Novosibirsk, Russia*
[2]*Novosibirsk State University, 630090, Pirogova 2, Novosibirsk, Russia*
**e-mail: uvarov@kinetics.nsc.ru*

Continuous wave (CW) and pulse electron paramagnetic resonance (EPR) spectra of triplet state of fullerene C_{70} in various glassy matrices were obtained at temperatures 5K÷260K. At temperatures below 30K the emission region appeared at EPR spectra because populations of $^3C_{70}$ spin sublevels are non-equilibrium immediately after photoexcitation. At low temperatures spin-lattice relaxation time of $^3C_{70}$ becomes comparable with triplet $^3C_{70}$ lifetime. At temperatures higher 50K EPR spectra contained only absorptive part.

Transversal relaxation rate was obtained by pulse EPR methods. It does not substantially depend on EPR spectrum position. So, exchange process within EPR spectrum due to rotations or pseudorotations of $^3C_{70}$ molecule around its long symmetry axis has not appreciably influence the EPR lineshape below 77K.

CW EPR lineshape of $^3C_{70}$ at 77K was simulated supposing the equilibrium population of $^3C_{70}$ spin sublevels. The zero field splitting parameters D and E were revealed to have probability distributions. EPR lineshape of $^3C_{70}$ was simulated successfully assuming Gaussian probability distribution of D value, whereas E value probability distribution function was different. It had a property: at E = 0 the probability value is 0. At work [1] EPR lineshape of $^3C_{70}$ was simulated assuming rectangular probability density of E value.

With temperature increasing higher 100K the rapid rising of the transversal relaxation rate of $^3C_{70}$ was obtained from pulse EPR data. The phenomenon can be explained by $^3C_{70}$ molecule motion due to glass matrix softening. CW EPR lineshape narrowing with temperature increasing confirmed the suggestion about $^3C_{70}$ motions.

D and E values distribution can be explained by dependence of molecular $^3C_{70}$ Jahn-Teller distortion on local surrounding of each molecule. We can conclude that $^3C_{70}$ symmetry is not higher than D_{2h}.

[1] M.N. Uvarov, L.V. Kulik, T.I. Pichugina, S.A. Dzuba, *Spectrochimica Acta Part A: Molecular and Biomolecular Spectroscopy*, DOI: 10.1016/j.saa.2011.01.047 (2011)

Intercalation of Cu underneath a graphene layer on Ni(111) and Co(0001) substrates studied with a synchrotron radiation

Vilkov O.Yu.*[1,2], Usachev D.Yu.[1], Fyodorov A.V.[1], Shikin A.M.[1], Vladimirov G.G.[1]

[1]*St. Petersburg State University, 199034 St. Petersburg, Russia*
[2]*Technische Universität Dresden, 01062 Dresden, Germany*
**e-mail: ol.vilkov@gmail.com*

The electronic structure of graphene on a metallic substrate is similar to that of free-standing graphene, but there are essential differences, which depend on a structure and a material of the substrate and are determined by the character of the graphene-substrate interaction. One of the main tasks is to study the properties of graphene on a wide range of substrates, as the solution of this problem provides an opportunity to purposefully affect on the characteristics of this material. An efficient approach to the solution of this task is based on a phenomenon of intercalation of various atoms underneath graphene films on metals.

Thick monocrystalline films of Co(0001) and Ni(111) were deposited on a preliminarily cleaned surface of tungsten crystal W(110) under the ultra-high vacuum conditions. Graphene films of a good quality were prepared on Co(0001) and Ni(111) films in a process of propylene cracking [1,2]. Intercalation of copper atoms underneath a graphene layer took place after the thermal annealing of pre-deposited copper layers [3].

The electronic structure of a core C1s level and a valence band of a graphene layer on the metallic substrates before and after the copper intercalation has been studied with X-ray photoelectron spectroscopy and angle-resolved ultra-violet photoelectron spectroscopy. X-ray absorption fine structure near the carbon K-edge has been measured for studying unoccupied graphene states. Synchrotron radiation with a linear polarization has been used to reveal a contribution of π^* and σ^* states [4].

[1] A.M. Shikin, D. Farias, K.H. Rieder, *Europhys. Lett.* **44**, 44 (1998).
[2] A. Varykhalov, O. Rader, *Phys. Rev. B* **80**, 035437 (2009).
[3] Yu.S. Dedkov, A.M. Shikin, V.K. Adamchuk, S.L. Molodtsov, C. Laubschat, A. Bauer, G. Kaindl, *Phys. Rev. B* **64**, 035405 (2001).
[4] R.A. Rosenberg, P.J. Love, V. Rehn, *Phys. Rev. B* **33**, 4034 (1986).

The problem of nanodiamond visualization in biopharmaceutical research

Yakovlev R.Ju.

Pavlov Ryazan State Medical University, 390026, Ryazan, Russia
e-mail: yarules@yandex.ru

The problem of carbon nanoparticles diagnostics in biopharmaceutical research becomes more and more actual during the last years. But the complexity of control whether such particles are present and in what state *in vitro* and *in vivo* precludes us from using the standard physic-chemical methods. Therefore the search for new methods and techniques of carbon nanoparticles visualization and of widening their functions via development of new original approaches might be extremely important. This is very important for the research in nanotoxicology and biomedical applications including pharmacology research and drug delivery. The applications of nanodiamonds (ND) as nanocarriers in drug delivery systems necessitated finding the effective methods of their visualization. For the diagnostics of ND *in vitro* we used TEM. This allowed us to determine the average size of ND particles (5 nm) and the presence there of carbon atom layers (shells) with the diamond core in the center. It was possible to estimate the thickness and structural peculiarities of the ND shells depending on their chemical modification by HRTEM. In order to determine the chemical composition of ND surface and the presence to sp^2/sp^3 carbon atoms in near-surface layers of ND particles the XPS method was used. Raman spectra showed that ND have characteristic band of 1332 cm^{-1}. But creation of C_{diam}–N– bonds on the surface results in high fluorescence which is so higher than the peak of diamond phase that totally masks it. The further fluorescence research of ND with grafted drugs by Raman spectra might give us a powerful way to visualize such complexes. The radiochemical methods of carbon nanoparticles visualization are one of the most fast and accurate. We received ND with ^{3}H-label firmly fixed by covalent bond C_{diam}–^{3}H that allowed us to study their biodistribution *in vivo* in rats. The presence of heavy atoms in the grafted layer on the ND surface opens new diagnostic possibilities to determine ND *ex vivo* и *in vivo* by mass-spectrometry. Thus the long-term biodistribution of ND in rabbits was studied. The devised complex of physic-chemical methods of ND visualization allows us to effectively find ND in model systems, biological liquids, tissues and organs.

Transient charging phenomena in graphite

Zagaynova V.*[1], Hacke C.[1], Chowdhury T.[1], Makarova T.[1,2]

[1]*Umeå University, 90187, Umeå, Sweden*
[2]*Ioffe Physical-Technical Institute RAS, 194021, St.Petersburg, Russia*
**e-mail: valeria.zagainova@physics.umu.se*

In carbon research, as well as in general research, graphite being the most stable carbon allotrope is one of the most studied materials. In scanning probe microscopy, graphite is used as calibration grates and atomic-smooth hydrophobic substrates. Surprisingly, very few studies are made on electrostatic force microscopy. Here, we demonstrate the ability of this technique to detect hidden defects (buried underneath) and follow the spatial charge redistribution under the action of electric field.

Graphite is a good electric conductor along its planes, and an insulator only perpendicular to the planes. Therefore, the electric field applied to the plane should not cause any potential fluctuations. And yet, they exist.

Under applied voltage, dendriform quickly changing charged areas were formed limited in their spatial expansion by the surface steps (see Fig. 1). Changing the tip polarity inverted the dark/bright images (Fig. 1 b and c). The charging phenomena were observed only in the pyrolytic graphite samples with the lowest mosaic spread, i. e. highest quality.

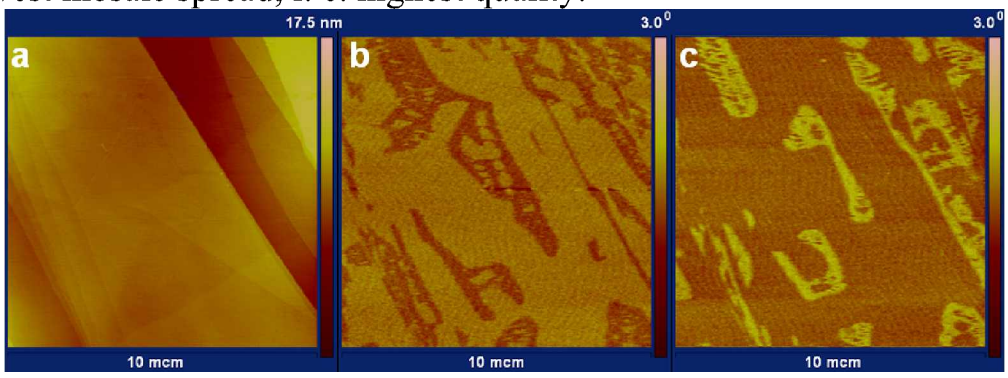

Figure 1. EFM images of HOPG graphite: a – topography, b, c – phase images taken at +2V and -2V, respectively.

The measurements performed in nitrogen atmosphere proved that observed fluctuations do not belong to effects caused by surface contamination such as adsorbed water. Besides, ideal graphite screens poorly, and applied electric field penetrates ~100 nm. Thus, the potential information comes not only from the surface, but charges within the bulk might group themselves at or close to surface steps or buried plane edges and also contribute to the signal.

Further studies on the charging phenomenon of HOPG graphite are needed to understand the origin of this effect.

Electrical conductivity and optical transparency measurements of thin carbon films

Sedlovets D.M.*, Red'kin A.N.

Institute of Microelectronics Technology and High-purity Materials Russian Academy of Science, 142432, Chernogolovka, Russia
**e-mail: sedlovets@iptm.ru*

The outstanding electrical1, mechanical and chemical properties of graphene make it attractive for applications in flexible electronics. [1]

Experiments were performed at the lowered pressure in the flow-type reactor. The system involved the horizontal tube furnace, the temperature control systems, gas flow controllers and forvacuum pump. Cu foil was used as a wafer. Thin carbon films were obtained by pyrolysis of ethanol vapor.

Then we measured the transmittance of graphene transferred to a polyethylene terephthalate (PET) substrate using an ultraviolet-visible spectrometer. The sheet resistance was measured using the four-point probe method.

The films display appreciable electrical conductivity and good transparency (92-95%). Because the transmittance of an individual graphene layer is 2,3% [2], this transmittance value indicates that the average number of graphene layers is two to four. These results were verified by atomic-force microscopy measurements.

[1] Kim K.S., Keun S.K., Yue Z., Houk J., Sang Y.L., Jong M.K., Kwang S.K., Jong-Hyun A., Philip K., Jae-Young C., Byung H. H. *Nature* **457**, 706 (2009).

[2] Nair R. R., Blake P., Grigorenko A. N., Novoselov K. S., Booth T. J., Stauber T., Peres N. M. R., Geim A. K., *Science* **320**, 1308 (2008).

Research on size stability of commercial nanodiamond suspensions under the influence of external factors

Petrova N.I.

South Ural State University, 454091, Chelyabinsk, Russia
e-mail: defolium@gmail.com

The object of our research is explosion made nanodiamond which is an aggregate with an average initial particle size of 4nm.

Nanodiamonds produced by explosion go through chemical refining with subsequent dispersing and fraction separation. The size of the particles produced defines their properties and spheres of technological application. In this research we used water ND suspensions of two kinds with average aggregate size of 10nm and aggregate size of 100 nm which were produced at the plant SKN in Snezhinsk, RF.

The goal of the work was to study the effect of outside factors during the production, transportation and storage of ND suspensions.

The initial suspensions were subjected to low temperature, freezing, heating, boiling and diluting with distilled water and then their stability was studied.

We also studied the influence of power of ultra-sound dispergator on the initial suspension.

To measure the suspension characteristics we used the following equipment: laser particle analyzer Nanotrac, electron microscope Jeol JSM-7001F, X-ray difractometer Rigaku Ultima 4.

As a result of the studies and experiments made we got the info about the dependency of ND suspension aggregate stability on the given above factors and developed the method of reproduction of aggregates after freezing, we got preliminary results of ND dispersion in water using a new power method.

High-resolution Raman microscopic study of C60 fullerite transformation upon HPHT treatment

Ovchinnikova I.N.

Baikov Institute of Metallurgy and Materials Sciences, RAS, Moscow, Russia
e-mail: ino1985@yandex.ru

For the development of metal-matrix composite materials reinforced by superelastic hard carbon particles [1], the fullerite transformation under pressure has been studied after treatment in the temperature range of the transition from polymerized fullerites to the reinforcing phase. The understanding the fullerite transformation mechanism is important for the control of the structure and properties of the final product. The samples have been prepared from the mixture of iron powder with C_{60} fullerites (10%) at a quasi-hydrostatic pressure of 5 GPa at 600-900°C (3 min). The carbon particles were examined with a CRM-200 confocal high-resolution Raman microscope using green lazer (532 nm) with a power density of approximately 0.1 W/cm2. The low power density ensured that no additional photo-induced polymerization occurred in the samples and minimized sample heating. With increasing treatment temperature, the Raman spectrum taken from a local spot of 1 μm in diameter changes from a mixture of the reflections of three polymers (tetragonal, orthorhombic, and rhombohedral [2, 3]) to a halo in a range of 1100-1600 cm^{-1} typical of the superelastic hard phase. After treatment at intermediate temperatures, the high-resolution method showed the coexistence of three types of polymers and the new superelastic hard phase in submicron-size volumes of the carbon particles.

[1] O.P. Chernogorova, E.I. Drozdova, N.A. Bul`enkov, V.M. Blinov, *Nanotechnologies in Russia* **3**, 344 (2008).
[2] T. Wagberg, A. Soldatov, B. Sundqvist, *Eur. Phys. J. B* **49**, 59 (2006).
[3] V.A. Davydov, L.S. Kashevarova, A.V. Rahmanina, A.V. Dzyabchenko, V.M. Senyavin, V.N. Agafonov, *Rossiiskii Khimicheskii Zhurnal* XLV(4), 25 (2001) (in Russian).

Use of TGA for analysis of fullerenols

Nasonova K.V.*, Melenevskaya E.Yu., Shamanin V.V.

Institute of Macromolecular Compounds RAS, Bolshoi pr. 31, St.-Petersburg, Russia
**e-mail: kaiduk@mail.ru*

Nowadays thermo-gravimetric analysis is common used for studying substances of a different nature. Thus, using this method, a determination of an amount of hydroxyl groups attached to a fullerene core can be performed.

TGA analysis was applied for three types of fullerenols having a different hydroxylation degree, $C_{60}(OH)_{12\text{-}14}$, $C_{60}(OH)_{20\text{-}24}$ and $C_{60}(OH)_{30\text{-}36}$.

To calculate an approximate amount of OH groups contained in fullerenol, it is used the following equation reported earlier in the article [1]:

$$n = \frac{molwt(C60)}{mr(C60)} X \frac{mr((OH)n)}{molwt(OH)}$$

wherein molwt(C_{60})=720 g/mol; molwt(OH) = 17 g/mol;
mr (C_{60}) is weight loss at 150°C to 570°C, %;
mr ((OH)n) is weight loss at 570°C to constant weight of C_{60} (800°C), %.

In order to ensure that for calculating correct ranges of temperatures (150°C to 570°C and 570°C to 800°C) were selected, elemental analysis of 3 samples of fullerenol $C_{60}(OH)_{30\text{-}36}$: initial, heated up to 560°C, and heated up to 800°C for 4 h was performed. The elemental analysis data showed that active elimination of hydroxyls takes place at heating 150°C to 570°C exactly, and a decomposition of fullerene core runs at above 570°C.

Further, it can be followed from the TGA analysis data that an initial fullerene and fullerenol are decomposed in a different mechanism at heating. This event is likely to be proceeded due to opening both double bonds and single bonds at hydroxylation process to form gaps ("holes") in fullerene framework. Therefore, at heating the fullerene framework comprising such "holes" will be piecewise decomposed, in contrast to an initial fullerene does not decayed at 800°C, but do sublimate.

[1] Alves G., Ladeira L., Righi A., Krambrock K., Calado R., Pinheiro M. *J. Braz. Chem Soc.* **17,** 1186 (2006).

Formation of grapheme and graphite on the surface of rhodium

Kuzmichev A.V.

Ioffe Physical Technical Institute RAS, 26 Polytekhnicheskaya, St Petersburg, 194021, Russia
e-mail: gall@ms.ioffe.rssi.ru

In this work studied the interaction of carbon with the surface of rhodium (111) in UHV conditions by means of Auger electron spectroscopy in a wide range of temperatures 300-1800 K. The camera of device had a module to diagnose the surface by thermionic emission and surface ionization of probing streams of CsCl atoms or molecules.

The samples were rhodium tape size (1×0.03×40) mm^3, which was purified from possible impurities by heating in an atmosphere of oxygen (PO_2~$1\cdot10^{-5}$ Torr) at T = 1800 K. After purification, were observed only Auger peaks of rhodium. Tape surface was homogeneous with respect to the work function and had eφ = 4.95 eV, which corresponded to the (111). Relative area of the islands of graphene determined by probing the surface molecules of CsCl [1].

As a source of carbon used in the admission chamber vapors of benzene to PC_6H_6~$2\cdot10^{-6}$ Torr. At a sample temperature T>1000K benzene dissociated hydrogen desorbed, and carbon dissolved in the bulk metal. After saturation of rhodium with carbon on the surface were formed islands of graphene, which grew in size, merged and formed a continuous graphene film - with the dissociation of benzene on the passive surface of graphene was stopped and the film thickness in excess of one graphene layer is not increased. In the formation of islands of graphene surface is heterogeneous on the work function: the work function of islets was equal eφ = 4.35 eV and work function areas free from islands remained equal eφ = 4.95 eV. In the formation of a continuous layer of graphene surface again becomes uniform to work out - eφ= 4.35 eV.

Interesting results are obtained when the temperature carbonized sample. If the temperature T_c carbonization rhodium is raised stepwise, the graphene layer broke up into islands, and for each T=const there was a dynamic equilibrium, when the area of the islands has not changed over time - in this case, the flux of carbon atoms from the edges of graphene islands amounted to a stream of atoms coming from the “gas” adsorbed phase on the islands. The range of equilibrium graphene islands was 100°. At $T>T_c+100°$ graphene islands are completely destroyed and remains on the surface only chemisorbed carbon "gas" with a concentration of ~$4\cdot10^{14}$ at/cm^2 (T_c=1400 K).

Return to the temperature $T=T_c$ quickly restores a continuous layer of graphene. If the sample temperature is lowered to $T<T_c$, tone the surface grows thicker graphite layer by allocating the excess C atoms from the bulk of the supersaturated solid solution of Rh-C. The film thickness can reach several tens of layers [2].

[1] E.V.Rut'kov, A.Yn. Tontegode, *Surface Science* **161**, 373 (1985).
[2] Rut’kov E.V., Kuzmichev A.V., Gall’ N.R. *Phys. Solid State*, In press.

Small angle X-Ray scattering as a method to determine the shape and size distribution of nanodiamond particles. Comparison with dynamic light scattering

Kurkin T.[a]*, Ozerin A.[a], Kechek'yan A.[a], Gritsenko O.[a], Sustchev V.[b], Dolmatov V.[b]

[a]*Institute of Synthetic Polymeric Materials, Moscow, 117393, Russia*
[b] *JSC "Diamond centre", St.-Petersburg, 193177, Russia*
**e-mail: t.kurkin@gmail.com*

Small angle X-Ray scattering (SAXS) can yield an essential information about the structural features and size of nanodiamond aggregated particles within the size range of approximately 1-100 nm. In some cases it is even possible to obtain the «averaged» structure of the single particle either under certain symmetry restrictions or without any (P1 symmetry class). Using SAXS it is also possible to estimate the specific surface area of the particles and calculate their volume-weighted (and number-weighted) size distribution either in colloid solution or in bulk material. However, the size distribution data obtained from SAXS does not always properly correlate with data obtained via dynamic light scattering methods (DLS), which often obscures the interpretation of entire data array. There are several major reasons causing this, but one of the most important is that the traditional dynamic light scattering techniques such as photon-correlation spectroscopy are generally applicable only at the very low concentrations of carbon particles in a solution. However, the design of new hybrid materials often requires much higher concentrations of the dispersed carbon nanoparticles to be analyzed. One of the efficient approaches in this case is to use «reverse» DLS with heterodyne signal processing procedure. In this case it is generally possible to obtain satisfactory correlation between SAXS and DLS.

In the presented contribution the application of both SAXS and «reverse» DLS techniques for characterization of nanodiamond solutions with varied pH range is demonstrated. The described techniques are also used to evaluate the influence of high-power ultrasonic treatment on the size distribution function of the particles, which was proven to be ambiguous in some cases.

Raman scattering in porous carbon materials

Krylov D.S., Kompan M.E.*

Ioffe Physical-Technical Institute RAS, 194021, St.Petersburg, Russia
**e-mail: kompan@mail.ioffe.ru*

At the present time metal carbides are used to produce carbon materials with a variety of properties. After the carbide's sublattice is destroyed by thermochemical process, free carbon atoms form a new porous structure. Produced carbon materials are characterized by its pureness and extremely high specific surface area (up to 2000 m^2/g). These properties of carbide derived carbons (CDCs) are widely used in supercapacitors, catalytic composites and sorbents.

The study of Raman scattering in samples of nanoporous carbon derived from silicon carbide was carried out in this work. Experiments were run on a series of samples treated thermochemically at temperatures from 700 to 2000° C.

During the research of carbon samples the spectra of Raman scattering were obtained. The spectra indicate dependence between material's structure and the temperature of treatment. This can help us to explain the process of nanoporous carbon production: with rising of the temperature the amount of sp^2 form of carbon increases and the amount of sp^3 form lessens. It conforms to the fact that graphite (sp2 form) is thermodynamically stable form of carbon. And an opposite carbon transformation from sp^2 form to sp^3 one while annealing in the hydrogen atmosphere occurs to be an especially interesting fact.

[1] D.C. Elias, R.R. Nair, T.M.G. Mohiuddin, S.V. Morozov, P. Blake, M.P. Halsall, A.C. Ferrari, D.W. Boukhvalov, M.I. Katsnelson, A.K. Giem, K.S. Novoselov, *Science* **323**, 610 (2009).
[2] C. Portet, G. Yushin, Y. Gogotsi *Carbon* **46**, 2511 (2007).
[3] P. Simon, Y. Gogotsi, *Nature materials* **7**, 845 (2008).
[4] A.C. Ferrari, J. Robertson, *Phys. Rev.* **64**, 075414 (2001).

Interpretation of SEM images of Portland cement materials doped nanodiamonds

Korobkova A.I.*[1,2], Shilova O.A.[1], Frank-Kamenetskya O.V.[2]

[1]*ICS RAS, 199034, St.Petersburg, Russia*
[2]*SPb State University, 199034, St.-Petersburg, Russia*
**e-mail: korobulya@mail.ru*

Nowadays new cement materials doped fullerenes, nanodiamonds, shungites are created all over the world because of their significant influence on the properties of construction material [1]. However, the mechanism of such effect is not completely clear. This work in this field is devoted to investigation of SEM analysis effectiveness to research the influence of detonation nanodiamonds (DND) additives on the properties of Portland cement materials.

The results of researching synthesized hydrous Portland cement materials doped DND based on the clinker from Suhologsky cement work are presented. There were two series of syntheses with different DND contents (0, 0.1, 0.2, 0.5, 1–9 wt.%), distinguished by the absence (1st series) or presence (2nd series) gypsum $CaSO_4*2H_2O$ addition in the amount of 5 wt.%. To determine phase composition of hydrated samples X-Ray method (STOE STADI P powder diffractometer, transmission geometry, $Cuk_{\alpha 1}$=1.54056, 2θ=5-55°, $\Delta 2\theta$=0.02°, exp. 100 s.) was used. To found DND particles and to reveal the features of its distribution the scanning electron microscopy (Quanta 200 3D) was applied. SEM research was carried out in reflected electrons (high vacuum, U=15-20kV, analyst S.J. Yanson).

X-ray phase analyses demonstrated that samples of both syntheses series contains at least five phases: alite Ca_3SiO_5 (C_3S), belite Ca_2SiO_4 (C_2S), and two calcium aluminate phases $Ca_3Al_2O_6$ (C_3A) and $Ca_4(Al,Fe)_4O_{10}$ (C_4AF), and portlandite $Ca(OH)_2$. In clinker with 5 wt.% DND (1st series) its amount is maximum, whereas with 9 wt.% this phase is almost absent, as it correlates with the strength of materials. In clinkers of 2nd series its maximum contain is in samples with 9 wt.% of DND.

On SEM-images DND particles are good seen. In the samples with 5 wt.% DND these particles create approximately equal size clusters of about 80 μm and distribute in the hydrated cement matrix uniformly. In clinkers doped 9 wt.% of DNA, the size of clusters varies from 40 to 140 μm, which are arranged randomly. Besides, the nanodiamond aggregates are associated with $Ca(OH)_2$ accumulations, which is a measure of the Portland cement clinker hydration degree [2].

In general, the application of the scanning electron microscopy significantly complements results of X-Ray analysis. Interpretation of SEM images demonstrates DND additives affect the hydration of Portland cement materials, which largely determines its properties.

[1] Shablinsky G.E., Lukutsova N.P., Pikin A.A. et al., *Newsletter of MSSU* **2**, 231 (2010).
[2] Reichel W., Canrad D. Beton: in 2 B. B. 1. Eigenschaften Projektierung Prüfung. VEB Verlag für Bauwesen, Berlin, 1976.

Full 2D calculation of graphene Raman amplitude

Koniakhin S.V.*[1,2,3], EidelmanE.D.[1,4]

[1]*Ioffe Physical-Technical Institute RAS, 194021, St.-Petersburg, Russia*
[2]*St.-Petersburg State Polytechnical University, 195251, St.-Petersburg, Russia*
[3]*St.-Petersburg Academic University - Nanotechnology Research and Education Centre of the Russian Academy of Sciences, 194021, St.-Petersburg, Russia*
[4]*SPCPA, 197376, St.Petersburg, Russia*
**e-mail: koniakhin@gmail.com*

Graphene Raman spectra make it possible to deduce about amount of monolayers and their distribution in the sample and the defect structure of the sample. Here we make a calculation of graphene Raman spectra. The calculation for graphene bilayer is provided. Also we consider the substrate effect for graphene monolayer.

The calculation of graphene Raman spectra requires its electronic structure and phonon dispersion [1]. We use the harmonic approximation [2] to obtain the phonon dispersion of graphene. Interatomic force constants utilized in this work were taken from [3]. Accurate approximation of the experimentally obtained phonon dispersion in spite of phonon dispersion full calculation can be also implemented. On the contrary, the utilization of interatomic force constants opens up possibilities of the substrate and number of layers effects consideration.

Raman spectra are calculated on the basis of the amplitude of double resonant processes. Defect-induced processes corresponds to the D band and corrections for the G band. Processes which involve two phonons corresponds to overtones: 2D and 2G bands.

We provide the calculation for the bilayer graphene. In the bilayer graphene electronic bands splits [4] and four types of electron transitions appears. It results in the fact that 2D gets more broad. This broadening agrees with experimental data.

We thank A.T. Dideykin for experimental data. We are indebted to A.Ya.Vul for his care and helpful discussions. We acknowledge funding from RFFR (proj. 09-08-01200a) and the ministry of science and education (contract 02.740.11.0108).

[1] C. Thomsen, S. Reich, *Phys. Rev. Lett.* **85**(24), 5214 (2000).
[2] Max Born and Kun Huang, *Dynamical theory of crystal lattices* (Clarendon Press, Oxford, 2002)
[3] O. Dubay, G. Kresse, *Phys. Rev. B* **67**, 035401 (2003).
[4] A.C Ferrari, J.C. Meyer, V. Scardaci, C. Casiraghi, M.Lazzeri, F. Mauri, S. Piscanec, D. Jiang, K.S. Novoselov, A.K.G.S. Roth, *Phys. Rev. Lett.* **97**, 187401 (2006).

Measurement of ripples spectrum in suspended graphene

Kirilenko D.A.*[1], Dideykin A.T.[2], Van Tendeloo G.[1]

[1]*EMAT, Universiteit Antwerpen, BE-2020, Antwerpen, Belgium*
[2]*Ioffe Physical-Technical Institute RAS, 194021, St. Petersburg, Russia*
**e-mail: zumsisai@gmail.com*

The existence of graphene in stable form remains an astonishing phenomenon since 2D lattice was predicted to suffer from enormous undulations due to thermal oscillations. This was highlighted when the intrinsic roughness of suspended graphene was revealed [1]. The ripples affect graphene's properties and places additional limit of conductivity [2]. The rippling are governed by severely anharmonic dynamics [3], and there are several considerably different models have been presented in literature so far, that stems from the lack of experimental data on ripples spectrum in suspended graphene and its behaviour under varying conditions.

Here we present a technique for measurement of ripples spectrum of suspended graphene. The technique is based on electron diffraction patterns analysis. The study of suspended graphene allows carrying out *in-situ* measurements of ripples spectrum under varying temperature, strain etc. Temperature dependence of ripples spectrum shows growth of ripples' average wavevector with temperature as predicted by theory, while average amplitude slightly decreases. The latter can be explained in terms of anharmonic behaviour of graphene ripples.

The technique can be also applied to graphene deposited on a thin enough substrate that, in turn, makes possible its validation by AFM or STM. It is shown that roughness of suspended graphene is lower that that of graphene attached to the substrate.

The technique has shown itself to be quite fruitful in context of the graphene-related studies, but it can also be applied to study of roughness of any low-dimensional structure.

[1] J.C. Meyer, A.K. Geim, M.I. Katsnelson, K.S. Novoselov, T.J. Booth, S. Roth, *Nature* **446**, 60 (2007).
[2] E.V. Castro, H. Ochoa, M.I. Katsnelson, R.V. Gorbachev, D.C. Elias, K.S. Novoselov, A.K. Geim, F. Guinea, *Physical Review Letters* **105**, 266601 (2010).
[3] A. Fasolino, J.H. Los, M.I. Katsnelson, *Nature Materials* **6**, 858 (2007).

Application of angle-resolved X-ray spectroscopy for characterisation of oriented CNT films

Kanygin M.A.*, Kurenya A.G., Gusel`nikov A.V., Okotrub A.V.

Nikolaev Institute of Inorganic Chemistry SB RAS, 630090, Novosibirsk, Russia
**e-mail: mkanygin@gmail.com*

Angle resolved X-ray emission and absorption spectroscopy is typically used for investigation of anisotropy of chemical bonds in graphite-like materials [1, 2]. X-ray emission and absorption spectra of graphite materials, obtained under conditions of different incident angles and different angles of emission radiation yield, show dependence of intensities of X-ray spectra features, which can be correspond to the electron transitions with π- and σ- orbitals.

Films of oriented carbon nanotubes (CNT) with different texture of samples were synthesized by CVD-method with using of asetonitrile and toluene as a source of carbon. Films of oriented CNT, synthesized by this method, have the significant amount of defects, which lead to imperfection of whole material. Investigation of structure of oriented CNT films were carried out by method of angle resolved X-ray spectroscopy. The results of scientific research shows that relative intensities of X-ray spectra feature contain information about difference of CNT structure from the ideal cylindrical. Modeling of intensities of X-ray spectra and comparison of experimental results with other experimental methods allows obtaining information about texture and defectiveness of CNT films, as well as specifying the model of formation of CNT films during CVD-synthesize.

Investigation of angle resolved X-ray absorption spectra near NK-edge of oriented CNT films, doped by nitrogen atoms, allows to determine orientation of N_2 molecules, incapsulated in the space, between nanotube walls.

[1] Y.H. Tang, T.K. Sham, Y.F. Hu, C.S. Lee, S.T. Lee, *Chem. Phys. Lett.* **366**, 636 (2002).
[2] T. Hemraj-Benny, S. Banerjee, S. Sambasivan, D.A. Fischer, G. Eres, A.A. Puretzky, D.B. Geohegan, D.H. Lowndes, J.A. Misewich, S.S. Wong, *Phys. Chem. Chem. Phys.* **8**, 5038 (2006).

Definition of structural elements of diamond powders and polycrystals sintered from them

Cherniyenko A.*, Bochechka A.

V.Bakul Institute for Superhard Materials, 04074, Kyiv, Ukraine
**e-mail: a-cherniyenko@mail.ru*

Coherent scattering region (CSR) is the certain field coherently diffusing impinging radiation. It is determined by the broadening of the lines on X-ray spectrums at examination of the disperse structures or powders. Some researchers use CSR values as the sizes of material grains which are explored.

In the table the grain sizes of diamond nanopowders, the sizes of crystal grains in the polycrystals sintered from them, spotted by means of electronic microscopy, and also the corresponding CSR sizes are given. The diffraction spectrums, on which analysis CSR of X-rays is carried out, were gained on diffractometer DRON 3. Definition of the sizes of particles and crystal grains has been spent by a method of transmission electron microscopy in a combination to a microdiffraction. For powder examination its test was located on a carbon substrate. Studying of polycrystals was conducted on a thin foil of the polycrystalline samples gained by a ionic thinning method.

Table.

Specimen	Particle size, crystallite size, nm	CSR, nm
Source powder ASM 0,1/0	50–100	20,6
Polycrystal sintered from ASM 0,1/0	10–50	4,2
Polycrystal sintered from UDD	3–15	3,9
Source powder UDD	2–3	4,8

Apparently from the table, reduction of the particle sizes of diamond nanopowders conducts to reduction CSR. At the same time, integration of crystal grains in diamond polycrystals is not reflected in the sizes CSR. Probably it occurs because the enlarged diamond crystals grains become fragmented. Herefore it is possible to tell that CSR data and electronic microscopy data give the complementary information about structure of diamond materials.

Morphological characterization of soot from the atmospheric combustion of diesel, kerosene and candle wax

Dikio E.D.*[1], Shooto D.N.

[1]*Vaal University of Technology , Vanderbijlpark, South Africa*
**e-mail: ezekield@vut.ac.za*

Diesel, kerosene and candle wax has been used as a precursor for the production of carbon nanomaterial without a catalyst precursor. Nanomaterials formed in the process were analysed by High resolution transmission electron microscope (HR-TEM), Raman spectroscopy, scanning electron microscope (SEM), energy dispersive spectroscopy (EDS) and X-ray diffraction (XRD). Carbon nanomaterial produced from diesel soot show the morphology of carbon nanospheres mixed with carbon nanotubes. Results obtained indicate the formation of carbon nanospheres in diesel, kerosene and candle wax.

[1] D.W.E.A. Santana, M.P. Sepulveda and P.J.S. Barbiera: *Journal of Fuel* **86**, 911 (2007).
[2] M. Al-Ghouti, Y. Al-Degs and F. Mustafa: *Journal of Fuel* **89**, 193 (2009).
[3] M. P. Gomez-Carracedo, J M Andrade, M. Calvino, E. Fernandez, D. Prada and S. Muniategui: *Journal of Fuel* **82**, 1211 (2003).
[4] D. N. Shooto and E. D. Dikio: *Int. J. Electrochem. Sci.* **6**(5), 1269 (2011).
[5] E. D. Dikio: *Int. J. Electrochem. Sci.* **6**(6), 2214 (2011).
[6] E. D. Dikio: Submitted to E-Journal of Chemistry. (2011)

Structure and characteristics of pyrolyzed polyacrylonitrile with vacancies

Zaporotskova I.V.*, Davletova O.A., Polikarpov D.I., Zaporotskov P.A.

Volgograd State University, 400062, Volgograd, Russia
**e-mail: irinaz@rbcmail.ru*

The discovery of new forms of carbon has stimulated interest in the synthesis of new nanomaterials with modified chemical properties that contain carbon plane. These include nanomaterials on the basis of containing carbon pyrolyzed polyacrylonitrile (PPAN). PPAN used in microelectronics, vacuum electronics, optoelectronics. Advantages of the new organic semiconductor based PPAN are regulation of the conductivity, low coSt. and simple technology of preparation [1].

One of the interesting problems is to study the properties of PPAN with vacancies (the so-called V defect). These defects change the local geometry of the layer (see Fig.) and, consequently, the electronic states. Surface of a material with vacancies, as a rule, consists of carbon hexagons and penta- and emerging heptagons (topological defects), which may lead to deformation of the polymer surface. We investigated the electronic structure PPAN with vacancies. Main energy characteristics of processes were calculated. Calculations were performed using quantum-chemical methods MNDO and PM3 and method DFT. Considered two types of defects: 1) V_N defect when removed from the structure of the nitrogen atom, and 2) V_C defect when removed from the structure of the carbon atom. Energy curves illustrating the formation of a vacancy, were constructed. The comparing the characteristics of defect and defect-free structures PPAN was performed. It should be noted an increase in the value of energy the highest occupied molecular orbital E_{HOMO} in the presence of the defect and a corresponding increase in the band gap. Thus, the introduction of a vacancy in the layer structure allows you to modify the physical properties of the material. The geometrical analysis shows that the surface atoms are displaced from their permanent positions in the direction of localization of vacancies. The electron density is localized in the V defect, which in turn leads to a change in the polarization of the monolayer PPAN and change its physical properties.

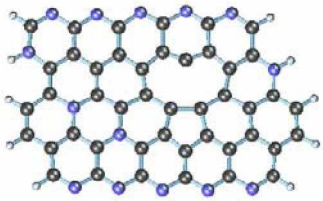

Figure. Monolayer PPAN with defects after optimization of parameters.

[1] V.V. Kozlov, L.V. Kozhitov, V.V. Krapuhin, I.V. Zaporotskova, O.A. Davletova, D.G. Muratov, *Materials of Eelectronic Engineering* № 1, 59 (2008).

The influence of boron doping on magnetic properties of oxygen-eroded graphite

Zagaynova V.[1], Makarova T.*[1,2], Mombru A.[3], Pardo H.[3], Faccio R.[3]

[1]*Umeå University, 90187, Umeå, Sweden*
[2]*Ioffe Institute, 194021, St.Petersburg, Russia*
[3]*Universidad de la República, P.O. Box 1157, CP 11800, Montevideo, Uruguay*
**e-mail: tatiana.makarova@physics.umu.se*

Pristine graphite is diamagnetic. Structural disorder of graphite, topological defects or absorbed guest atoms can give rise to the change in localized electronic states which cause an increase in the density of π-states at the Fermi level and trigger anomalous behavior in magnetic field. Room-temperature magnetism has been observed in several types of carbon materials [1]. At the same time, too many defects are predicted to destroy magnetism [2].

Surface oxidation route turns bulk graphite into a foamy-like highly-defective graphitic structure, its magnetism reported in [3]. Boron is well-known as a catalyst of graphite-oxidation reaction [4]. On the other hand, it acts as a dopant for carbon system and can change the relative occupancy of π-bands.

Here we present a comparison of magnetic properties of oxygen-eroded graphite with different boron content.

The impurity analysis performed with HR-ICP-MS proved that magnetism of the samples does not correlate with content of transition metal impurities, thus confirming the results obtained in [3]. From DC magnetic measurements performed at a Quantum Design SQUID magnetometer (MPMS-XL-1) on microcrystalline powder samples we found that non-metal impurities have strong influence on sample magnetism.

It has been found that introduction of boron doping induces paramagnetic component of magnetization and, for high concentrations, significantly decreases spin concentration due to annihilation of localized states, while for smaller concentrations of boron magnetization is enhanced. The results are in line with theory predictions [5].

[1] T. Makarova and F. Palacio, editors. Carbon based magnetism: an overview of the magnetism of metal free carbon-based compounds and materials, Elsevier Science, 2006.

[2] Y. Zhang, S. Talapatra, S. Kar, R. Vajtai, S. K. Nayak, P. M. Ajayan, *Phys. Rev. Lett.*, **99**, 107201 (2007).

[3] H. Pardo, R. Faccio, F. M. Araujo-Moreira, O. F. de Lima, A. W. Mombru, *Carbon* **44**, 565 (2006).

[4] N. M. Rodriguez and R. T. K. Baker, *J. Mater. Res.* **8**, 1886 (1993).

[5] R. Faccio, L. Fernández-Werner, H. Pardo, C. Goyenola, O.N. Ventura, A.W. Mombru, *J. Phys. Chem. C* **114**, 18961 (2010).

Nano-diamond based materials fabrication with low pressure non-equilibrium microwave gas discharge and its field emission properties

Gushchin O.[1], Yafarov R.[2], Baklanov M.[3], Ignatov P.[1], Zaytsev N.[1], Yanovich S.[1], Orlov S.[1] Khomyakov, I.[1]

[1]*Mikron JSC, 12/1 1St. Zapadny proezd, Zelenograd, Moscow 124460, Russia*
[2]*RAS, Kotel'nikov Institute of Radio Engineering and Electronics, Saratov, Russia*
[3]*IMEC vzw, Kapeldreef 75, B-3001, Leuven, Belgium*

Low pressure ethanol non-equilibrium gaseous MW discharge properties were studied for their impact upon self-assembly of nano-crystalline diamond clusters embedded into graphite and polymer-like films. Carbon based nano-structured films were fabricated and possibility of their properties control was demonstrated. It was demonstrated that process can provide a control of diamond nano-cluster's surface concentration within the range from 0.05×10^8 cm^{-2} up to 1.4×10^8 cm^{-2} and cluster's linear dimensions within the range 10–120 nm [1, 2].

Correlation of diamond-graphite films crystalline nanostructure, film component phase ratio and electron transport and field emission mechanism was studied. Feasibility of film nanostructure optimization in respect of field emitters was demonstrated along with the setting of appropriate criteria.

Fabricated with diamond-graphite cathodes integrated diode array samples demonstrated emission current density up to 2.0 A/cm². Such a result exceeds emission currents obtained with carbon nanotube based cathode arrays. Applied voltage was within the 5-10 V, that provided electric field about 2.5–5.0 V/μm for vertical integrated diode design. For lateral emitters emission current density of 20 A/cm^2 was obtained with 300V voltage applied.

[1] R.Yafarov, V.Moullin, V.Semenov, RUS Patent 2302369 dated 10.07.2007. A method for nano-diamonds fabrication embedded in polymer-like carbon-hydrate matrix.

[2] R.Yafarov, V.Moullin, V.Semenov, RUS Patent 2309480 dated 27.10.2007. Material and method for multi-spike field emission cathode fabrication.

Nanocarbons as physical modifier of polymers – dispersity or structure

Voznyakovskii A.P.[1]*, Pozdnyakov A.O.[2], Popov E.O.[3], Pozdnyakov O.F.[3]

[1]*Research Institute for Synthetic Rubber 198035.St.-Petersburg. Russia*
[2]*Institute of Mechanical Engineering Problems 199178, St.-Petersburg, Russia*
[3]*Ioffe Institute, 194021, St.-Petersburg, Russia*
**e-mail: voznap@mail.ru*

Incorporating of nanocarbons in polymer matrix is nowadays considering as the most effective way for new generation polymer materials development. But experimental findings are often differ from ones predict by theory. These facts may be the consequence of more complex mechanism of nanoparticles effect on supramolecular structure of polymer matrix and, as result, on properties of polymer nanocomposite obtained. In this study we investigated, as an example, polymethylmethacrylate (PMMA) and it's composite with fullerenes, MWCNT and detonation nanodiamonds (DND).

Our findings demonstrate that filling of the origin polymer with MWCNT practically don't influence on PMMA thermal destruction parameters. At the same time, nanocomposites based on C60 and DND demonstrate significant reduction (more then 200°C) of the temperature of thermal destruction process start. It was also shown ambiguous results of ultrasonic (US) exposure on nanocomposite solution.

Current opinion is that US result only in uniform nanoparticles distribution all over polymer matrix. But our findings show that the different time of US exposure on solution of DND-based nanocomposite result in clear-cut distinction in thermal parameters of destruction process. Thus, if the shot period of US exposure (1 min) result in pronounced peak of thermodistraction of nanocomposite (at 520 K), then the US exposure over a long period of time (40 min) result in more intensive but widened peak (over the range 450 to 650 K). Such result we connect with influence of US exposure on polydispersity of DND aggregates.

The findings, in our opinion, give evidence that the determinant of nanoparticles influence on polymers nanocomposite properties is not dispersity of particles, but their fine internal structure (static for MWCNT and fractal for C_{60} and DND). Also we suggest that in our experiments the US exposure stimulate interaction of macromolecules with functional groups of DND surface.

Superhard composite material based on nanodispersed carbon

Urbanovich V.S.*[1], Kuis D.V.[2], Okatova G.P.[2], Svidunovich N.A.[2], Oichenko V.M.[3]

[1]*SSPA Scientific-Practical Materials Research Centre, NAS Belarus, 220072, Minsk Belarus*
[2]*BSTU, 220050, Minsk Belarus*
[3]*Ioffe Institute, 194021, St. Petersburg, Russia*
**e-mail: urban@ifttp.bas-net.by*

Earlier it has been shown by us that in the conditions of high pressures (4-5 GPa) and temperatures (950-1200°C) formation of a superhard carbon phase in Fe-C nanocomposite material occurs not only from fullerenes, but also from other cheaper nanodispersed carbon materials, as fullerene soot, multiwall nanotubes, fullerene black [1].

In the present work it has discovered that the samples sintered based on concentrated fullerene soot with a small additive Fe (C_{fs}-10 wt.% Fe) contain three modifications of superhard carbon grey phase (Fig.1). Dominant modification with microhardness up to 78 GPa plays a role of binding being in a liquid state at sintering.

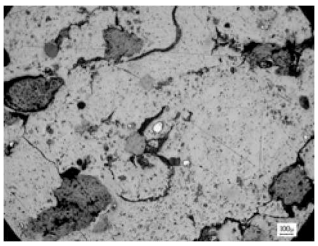

Figure 1: Microstructure of sintered sample: 90% fullerene soot +10% Fe

Appearance of a liquid phase in the conditions of high-energy consolidation of nanodispersed carbon at high pressure can be caused by displacement of graphite-liquid-steam-diamond interfaces in area of lower pressures and temperatures on the constitution diagram of carbon. It is known that with increase of dispersity of particles, or crystallites temperature of phase transition can be decrease.

Mechanism of formation of superhard carbon phase from melt at high pressure can be used for control of structure formation process of new superhard materials with use inexpensive nanocarbon components as fullerene soot, multiwall nanotubes, fullerene black. Last actually is not used scrap of fullerenes manufacture.

[1] Okatova G.P., Svidunovich N.A., Kuis D.V., Urbanovich V.S., Oychenko V.M., Korzhenevsky A.P., *Chemistry and Chemical Technology* **53**(10), 90 (2010).

Spatial atomic and electronic structures of graphene, diamond, graphite and fullerene

Titorov D.B.

Physical-Technical Institute Ural Branch RAS, 426000 Izhevsk, Russia
e-mail: titorov@fti.udm.ru

When the spatial atomic and electronic structures of graphene, diamond, graphite and fullerene were formed with using the mechanism of pairwise interpenetration of atoms [1], ideas about hibredization of *s* and *p* electrons, covalent and σ and π bonds, about potentials and other did not used absolutely.

The atom model with well-defined sizes of inner electrons area and external electrons shell [2, 3] correspond to quantum rules according to which the electronic structure of atom is shaped.

When atoms approach their shells can interpenetrate, but in according Pauli's exclusion principle only pairwise.

Values of interatomic forces which form the spatial atomic structures were calculated without fitting and utilize potentials.

The sizes of interpenetrated carbon atoms were calculated from the condition of balance of interatomic forces in diamond and graphene.

It is shown that the distance between basic planes of graphite (between graphenes) which is calculated with using of mechanism pair interpenetrating and presence of carbon atoms between graphenes (0.3357nm) is very close to those known from experiments (0.3354nm).

The schemes of self-organization of atoms of carbon into pentagons necessary for forming fullerenes are shown.

The spatial electronic structures are shaped with areas of a pairwise interpenetration.

Each atom in graphene has only three areas of pair interpenetrating. Electronic density of them may be two times more than in shell of the free atoms and four times more than in univalent metals. The centers of them form triangle with equal sides.

Each atom in diamond has four atoms in the first coordination sphere. Accordingly each atom in diamond has four areas of pair interpenetrating. They less than at graphene and the distance between them and nucleuses more than in graphene; their centers form right tetrahedron.

Thus the spatial electronic structures explain why graphene is more stable than metals and diamond and helps to analyse properties of materials.

[1] Titorov D.B Sixth international conference «Single crystal growth and heat & mass transfer». Proceedings 3, 646 (2005), Obninsk, Russia (in Russian).
[2] Titorov D.B. *Kristallografiya* **1**, 25 (2001). [*Crystallography Reports* **1**, 19 (2001)].
[3] D.B. Titorov, *Poverkhnost'*. **6**, 100 (2003).

Self-assembling of graphitic nanoplatelets

Orlanducci S.[1], Guglielmotti V.[1], Sordi D.[1], Tamburri E.[1], Terranova M.L.*[1], Passeri D.[2], Rossi M.[2]

[1]*Dept. of Chemical Science and Technology-MINASlab, University of Rome Tor Vergata, 00133, Roma, Italy*
[2]*Dept. of Fundamental and Appl. Sciences for Engineering and CNIS, University Sapienza, 00162, Roma, Italy*
**e-mail: terranova@roma2.infn.it*

Layered materials are the fundamental building blocks of two-dimensional (2D) systems with unusual chemical and physical properties with high specific surface areas, that are important for many and different applications, such sensing, catalysis, and energy storage.

In such a context, carbon-based few-layered nanosheets are fascinating materials, but a reliable procedure of fabrication remains a target not yet met.

We report here our preliminary results of recent researches addressed at the production of 2D crystalline structures. The starting material were colloidal dispersions of graphitic nanoflakes obtained from disruption of SWCNT and MWCNT using high-shear mixing and/or treatments in sulfonitric mixtures both at room and high temperature. The nanoflakes, dispersed in aqueous medium or DMF, have been subsequently deposited on Si substrates or TEM grids for related observations. Depending on the process procedures, different kind of re-organization are found to occur, as evidenced by ED, TEM and micro-Raman analysis. The adopted methodology allows indeed to obtain samples characterized by very different interactions between proximal units , giving rise in particular to:

- clustering of platelets with a relatively small 2D extension and random arrangement of polycrystalline graphite-like nanomaterial inside the clusters.
- assembling of nanoflakes into highly ordered (single-crystal) nanosheets with a relatively large (some thousands of nm^2) surface.

In this last case the ED pattern evidences the presence of quasi-singlecrystal material: the fine structure of the ED pattern is characterized by the almost perfect superpositioning of diffraction spots coming from different platelets not perfectly oriented each other. In such a case, the TEM analysis reveals the presence of relatively thin, but extended, nanosheets.The results shows that the assembly processes can be tailored by modulating the disruption treatments and choosing a suitable dispersion medium, in order to produce selectively different forms of self-assembling, from polycrystalline aggregates to highly self-oriented mosaic-like structures, evidencing the possibility to achieve single-crystal platelets.

It is expected that the identification of cooperative mechanisms acting in such systems could help in opening innovative crystallization pathways and give a relevant contribution for nanotechnologies.

Structural and physical properties of wood-derived biocarbons

Smirnov B.I.[1], Orlova T.S.*[1], Parfeneva L.S.[1], Popov V.V.[1], Smirnov I.A.[1], Jezowski A.[2], Martinez-Fernandez J.[3]

[1]*Ioffe Institute, 194021, St. Petersburg, Russia*
[2]*Institute of Low Temperature and Structural Research, Wroclaw, Poland*
[3]*Universidad de Sevilla, 41080, Sevilla, Spain*
**e-mail: orlova.t@mail.ioffe.ru*

In the present paper we represent the results on a correlation between microstructure and physical properties of biocarbons derived from beech wood by carbonization at different temperatures T_{carb} in the range 600-2400°C. The temperature dependences of the electric resistivity ρ, thermal conductivity æ and thermoelectric power S have been studied in the temperature range 4-300 K. The structural investigation was performed by XRD at 300 K.

According to XRD data the biocarbons have bi-modal microstructure which consists of amorphous phase and nanocrystallites (of three-dimensional graphite and two-dimensional graphene). With increasing T_{carb} from 800 to 2400°C, the size of nanocrystallites increases from 10.2 to 29 Å for graphite and from 24 to 60 Å for graphene components. The amount of nanocrystallites also grows with increase in T_{carb}. It was shown that T_{carb}~900 K is critical point for the change of electrical conductivity mechanism as well as of the character of S(T) and æ(T) dependences. The dependences ρ(T) for the biocarbons with T_{carb}<900°C are adequately described by the Mott law for the variable-range hopping conduction. The crossover to the conductivity characteristic of disordered metal systems is observed at T_{carb}≥1000°C. Analysis of experimental data ρ(T), S(T) and æ(T) showed that in the samples with T_{carb}<900°C the amorphous phase determines the behavior of these parameters, whereas in the samples with T_{carb} ≥1000°C the main role belongs to nanocrystallites.

This study was supported by the Presidium of the Russian Academy of Sciences (program P-03) and the Ministry of Science and Technology of Spain (project nos. MAT 2007_30141_E and PET 2006-0658).

Comparative analysis of field emission properties of SiC powder with different synthesis parameters

Shornikova A.L.*[1], Sheshin E.P.[1], Gordeev S.K.[2]

[1]*Moscow Institute of Physics and Technology, 141701, Dolgoprudny, Russia*
[2]*Central Research Institute of Materials, 194021, St.Petersburg, Russia*
**e-mail: a.shornikova@gmail.com*

At the present time getting good field emission properties of materials can be achieved by forming on the surface of a dielectric or semiconductor particles of a thin graphite layer. Nanolayer graphitic carbon covers the dielectric particles, which are seemed to support the layer, which took part in active field emission processes. It should be mentioned that such a particle should not be viewed simply as a "mixture" components, as well as a single physical-chemical system, which provides phase mutual influence, which leads to the achievement of positive results.

In this work were examined the samples of SiC powders, which were made by synthesis on the surface of dielectric and semiconductor particles of a thin graphic layer. Such synthesis can be achieved with heat treatment of dielectric or semiconductor powders in medium of gaseous hydrocarbons at a temperature above their thermal decomposition. Under these conditions on the surface of the particle takes place a heterogeneous chemical reaction, this leads to decomposition of hydrocarbon molecules into atoms of carbon and hydrogen molecules. The nascent carbon atoms form a graphite layer, whose thickness increases with increasing heat treatment time. Thereby you obtain particles with the desired thickness of the graphite-like nanolayer [1].

Data were collected in the following order: measured some initial current voltage characteristic, further took down field emission current depending on the time, after the end of the experiment measured another current voltage characteristic, which subsequently compared with the current voltage characteristic, gotten before the experiment began. Were also obtained photographs of field-emission images, where we can see the change of light intensity [2, 3].

After the data were processed, it will be able to make a conclusion in which it is found that the powder with a thin carbon fiber has better field emission properties.

[1] N. Finer, ML Kosinova, YM Rumyantsev, Thin films of silicon carbonitride and boron: synthesis, study of the composition and structure .- Ros. Chem. Well. (J. Ross. Chem. of the Society to them. Mendeleyev) - 2001, XLV, № 3.

[2] Sheshin E.P. The surface structure and field emission properties of carbon materials. - M.: Publishing office MIPT - 2001. - 288.

[3] Fowler R. H., Nordheim L. W., *Proc. Roy. Soc.* **A119**, 173 (1928).

Structure of amorphous carbon produced by high-voltage electric discharge technology in organic liquids

Rud A.D.[1]*, Ivaschuk L.I.[1], Kuskova N.I.[2], Tsolin P.L.[2], Kiryan I.M.[1], Zelinskaya G.M.[1], Biliy N.M.[3]

[1]*G.V. Kurdyumov Institute for Metal Physics of NASU, 03142, Kiev, Ukraine*
[2]*Institute of Pulse Research and Engineering of NASU, 54018, Nikolaev, Ukraine*
[3]*Taras Shevchenko National University of Kyiv, 01601, Kiev, Ukraine*
* *e-mail: rud@imp.kiev.ua*

New high-energy electric discharge technologies for production of carbon nanomaterials, containing fullerene-like clusters of the C_{60}-C_{70} type, nanotubes, nanodiamonds and amorphous carbon (AC), using the methods of electrical explosion of graphite rods and electric breakdown of organic liquids (EBOL) are elaborated [1, 2]. The EBOL technology gives an opportunity to produce an AC in amounts required for industrial application.

The structure of the synthesized from different organic liquids (benzene, hexane, cyclohexane, etc.) carbon powders is studied by the electron microscopy, Raman spectroscopy and X-ray analysis. Raman spectra are typical to AC materials and they are characterized by a large intensity ratio I_D/I_G (0.9), what indicates on significant structural disorder. The synthesized AC powders possess a complex hierarchical structure with a size of individual components of the order of 30-50 nm and specific surface area of 150 m^2/g. It is found, the Raman spectra of AC produced from cyclohexane (C_6H_{12}) are similar that of nanodiamonds. This fact testifies to the diamond-like type of short-range order, what was confirmed by the RDF calculations. We found that the type of short-range order of AC produced by EBOL technology is primarily determined by the degree of hybridization of carbon atoms in the molecule of the working liquid: in the case of hydrocarbons with sp^2-hybridization, AC have the graphite-like type of short-range order, in the case of working liquid with sp^3-hybridization - diamond-like one. A structure of the organic molecule plays an important role, because AC with predominance diamond-like type of short-range order is synthesized only in the case of cyclohexane, a molecule which is similar to a hexaatomic ring in the crystalline structure of diamond.

This work was partially supported by the joint projects of NASU-STCU (# 4951) and NASU (# 36-08-10)-RFBR (# 10-08-90419).

[1] Rud A.D., Kuskova N.I., Ivaschuk L.I., Zelinskaya G.M., Biliy N.M., *Fullerenes, Nanotubes and Carbon Nanostructures* **19**(1), 1536 (2010).

[2] Kuskova N. I., Rud A.D., Baklar V.Yu., Ivaschuk L.I., *Zhurnal Tekhnicheskoi Fiziki* (in Russian) **80**(9), 57 (2010).

Controlled laser synthesis of carbon nanostructured at laser action

Arakelyan S.M., Antipov A.A.*, Kutrovskaya S.V., Kucherik A.O.*, Nogtev D.S., Osipov A.V., Prokoshev V.G.

Department of Physics and Applied Mathematics, Vladimir State University,Gorky st. 87, Vladimir, Russia
**e-mail: kucherik@vlsu.ru aantipov@vlsu.ru*

Synthesis of carbon nanofiber and nanofibers by deposition of a material on a substrate at laser action on carbon materials is widely enough used method. Depending on experiment conditions (vacuum or buffer gas, presence of the catalyst, etc.) and used laser sources probably obtaining of various types carbon nanomaterials - single-layered / multilayered and nanotubes with diameters from 10 up to 100nm.

At the same time in a number of works laser action on carbon materials in atmospheric air and-or in oxygen is investigated, and opportunities of the directed change of morphological properties obtained nanostructures are discussed. Such control of properties of besieged materials at synthesis nanostructures is especially perspective at use additional quazi-static external fields.

There are results in the given work on obtaining carbon nanofibers and nanoclusters at laser action on the graphite samples placed in constant electric and-or a magnetic field.

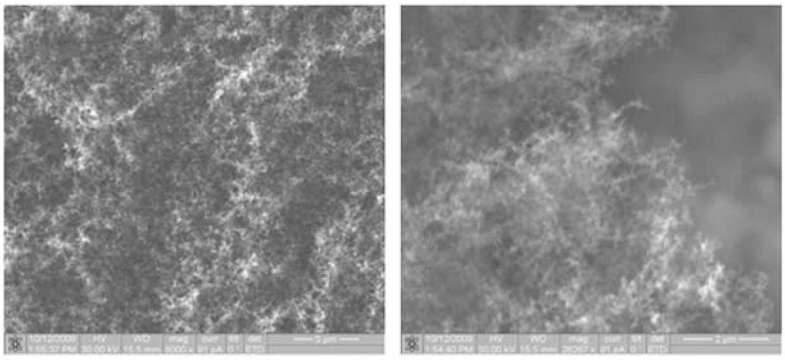

Carbon nanofibers obtaining in quazi-static external fields on a substrate.

Lonsdaleite in nanodiamonds

Naletov A.M. Nozhkina A.V.*

Scientific Research Institute Natural, Synthetic Diamonds and Tools, "VNIIALMAZ", Moscow, Russia
**e-mail: nojkina@inbox.ru*

Lonsdaleite (hexagonal diamond) for the first time has been found out and identified as fine inclusions in meteoric carbonaceous materials.

Later hexagonal diamonds have been found out in a number of geological place origins and in disperse powders of diamonds dynamic synthesis.

Use in our work of specially developed technique of X-ray analysis has shown, that the maintenance lonsdaleite in them can reach ~ 60% and synthesis in the field of thermodynamic stability hexagonal diamond (1,2) has allowed received samples with its concentration more than 90%.

However in the pure state it is not received yet, therefore its many physical properties remain unknown persons, as well as lonsdaleite mechanisms of its formation hexagonal structures since it corresponds to structure of defects of packing in planes (111) cubic diamond. It enables to consider shift supersonic (deformation, as a principal cause of formation hexagonal diamond. However in other cases, probably, are not excluded also other alternative mechanisms, for example martensite transformation, etc.

Energy and coordination of nuclear communications, density cubic diamond and hexagonal diamond are completely identical to parameters, therefore their elastic parameters, most likely, are close, but conditions of transformation of one structure in another, also as well as properties cubic-hexagonal diamond compositions, practically are not studied.

Results of researches of processes of transformation containing lonsdaleite nanodiamonds to cubic diamond, graphite or other forms carbon of materials under influence of various factors are presented in our work.

Our studies showed, that increase of concentration hexagonal diamond in natural diamonds approximately up to 40% reduces hardness of diamond, but, at the same time, density a nanodiamond compound increases with increase in the maintenance lonsdaleite.

Cubic-hexagonal diamond compositions, especially, considering characteristic for them structure, are represented by rather perspective base for creation of new super firm materials with the raised viscosity of destruction.

[1] Bundy T., Kasper J., *J. Chem. Phys.* **46**(9), (1967).
[2] Kurdyumov A.V., etc. “Crystal structure lonsdaleite, formed at High statistical pressure.” "Physics and technique of high pressures ", Kiev, 1981.

Synthesis of metal-carbon nanostructured materials by controlled laser deposition

Arakelyan S.M., Antipov A.A., Kutrovskaya S.V., Kucherik A.O.*, Nogtev D.S., Osipov A.V., Prokoshev V.G.

Department of Physics and Applied Mathematics, Vladimir State University, Vladimir, Russia
**e-mail: kucherik@vlsu*

Laser ablation is widely used for obtaining of nanoparticles and nanoclusters in a cloud of ablation products. It is well controllable and perspective process for many technological applications, the numerical decision for rectangular initial structures of density and pressure is resulted in, shown, that initial structures of distributions of density and pressure in a vapour cloud of material render essential influence on function of distribution formed of nanoclusters.

The carried out experiments of laser deposition show an opportunity of control formation of complex nanostructurized coverings on a substrate surface at used of a target as a mix metals nanopowder and carbon nanotubes. The most perspective appears on a laser method of action on a carbon nanotubes massive at the presence of growth catalysts of the given structures. As shown in work nanoparticles can be such catalysts for growth nanotubes. The question on the mechanism of nanostructures formation on a surface of a cold substrate up to the end is not clear, as during action there can be a reorganization carbon nanotubes at the expense of action of nanoparticles catalysts. In this case the sold scheme of nanostructures formation corresponds to an open reactor with speed of particles evaporation about sound speed. To research of a target surface after laser action show, that during interaction of laser radiation with carbon nanotubes, mixed with metal nanopowder, there is a local profusion. In this case, at active evaporation of substance (visually above area of laser action on a target the intensive plasma torch is fixed), nanotubes appeared on a surface of melting materials can be fond from a surface and be deposited on a substrate. In such system carbon - metal, as shown in work, the formation of fractal structures is possible at self-organizing carbon on metal during thermal laseraction. Simultaneously with it, during distribution of two-componental plasma probably formation of fractal clusters.

The offered method of obtaining of metal-carbon nanostructures has perspective for various applications, photonics and optoelectronics as allows to action on carbon nanotubes and to change their morphological and physical chemical properties at temperatures considerably smaller then temperatures of fusion of an initial material.

Influence of nanostructural carbon forms on deformation behaviour of copper at mechanical activation

Nikonova R.M.*, Pozdeeva N.S., Lad'yanov V.I.

Physical-Technical Institute UB RAS, Ishevsk 426000, Russia
**e-mail: las@pti.udm.ru*

Nanocarbon modification of metals and alloys appears to have considerable promise in developing materials of the new generation. Several approaches such as production of ultra strong film coatings at metal and carbon co precipitation, the use of super high deformations in Bridgmen anvils are considered for the metals to be obtained. Mechanical grinding by high voltage mills to obtain a super saturated solid solution of carbon in metals, the metals being inactive to carbon under normal conditions, is one of the promising technologies as well. Copper is one of the metals mentioned above.

Nanocomposites, Cu-C (5 и 25 at.%C), have been produced by mechanical activation. Powders of mixed fullerites, $C_{60/70}$ (~18%C_{70}), graphite, Cg, and multilayer carbon nanotubes have been chosen as carbon materials. The samples have been tested in AGO-2S ball mill under inert gas conditions (P=0.1 MPa), a power being equal to 28.1 Vt. To study the structural changes of samples after activation the x-ray structural analysis, optic metallography, scanning electron microscopy, as well as the method of micro hardness measurements have been employed.

It has been shown that in the process of copper synthesis with various carbon forms in the initial mixture a different mechanism of Cu particles deformation is observed. It has manifested about significant differences in the texture of the samples and kinetics of crystalline particles grinding (the form and dispersion). Thus the samples with a lesser carbon content 5 at.% differ greatly from the others. Being mechanically treated for less than 2 hours Cu particles take the form of equal-axis powders, balls and scales for $C_{60/70}$, Cg и C_{nt} accordingly. So all compared Cu-C are of different micro hardness. The Cu-Cg composite has shown the greatest micro hardness, 159 kGs/mm^2, and for Cu-$C_{60/70}$ and Cu-C_{nt} it amounts 125 kGs/mm^2 and 143 kGs/mm^2. The essential particle micro hardness increase in Cu suggests that carbon has a pronounced effect on strengthening the metals. At 25 at.%C the particles of the composites obtained differ, mainly, in size.

The x-ray structural investigations have shown that (regardless of the allotropic carbon form) if the time of grinding the particles increases the amount of micro distortions in the copper lattice rises, the areas of coherent scattering decrease and the copper lattice increases in size. The lattice increase may be caused by deformation dissolution of carbon producing the resulting formation of supersaturated solid solution in copper. Kinetics of the solid solution formation depends on the form and amount of carbon and the time of mechanical milling.

The work has been carried out under financial support of the program the Presidium of Ural Brunch, RAS (Project 09-T-1008).

Nanostructured carbon adsorbents for medical protection against chemical-biological-radiological-nuclear (CBRN) hazards

Mikhalovsky S.V.*[1], Sandeman S.R.[1], Howell C.A.[1], Tennison S.R.[2], Nikolaev V.G.[3]

[1]*University of Brighton, BN2 4GJ, Brighton, UK*
[2]*MAST Carbon International Ltd, GU3 2AF, Guildford, UK*
[3]*Kavetsky Institute of Experimental Problems of Oncology and Radiobiology, 03022 Kiev, Ukraine*
**e-mail: s.mikhalovsky@brighton.ac.uk*

When a terrorist attack against civil population is considered, it is important to have in stock some generic, universal means of protection which could be efficient in neutralising effects of CBRN warfare hazards. Medical grade activated carbons are a unique group of materials which were successfully used to decorporate radionuclides from the human body in the aftermath of the Chernobyl catastrophe, and prevent accumulation of radionuclides in first aid responders by prophylactic use of oral adsorbents. In modern terms, Chernobyl can be considered as a 'dirty bomb' on a very large scale. Taking into account that activated carbons adsorb most toxic organic substances and, according to the position statement issued jointly by the American and European Associations of Clinical Toxicology, use of oral activated carbon is the treatment of choice for patients with acute poisoning, particularly if the nature of the toxic agent is unknown. In more severe cases of acute poisoning with chemical or radioactive agents direct blood purification by activated carbon has been successfully used. Medical activated carbons used at present, however, have limitations in terms of their ability to adsorb and neutralise large molecules such as biotoxins and radiotoxins. This poses a particularly big problem in blood purification. Activated carbons used in West have poor haemocompatibility which is improved by coating carbon granules with semi-permeable membranes. The coating improves biocompatibility but at the same time reduces adsorption efficiency of carbon especially for large molecules. We have developed activated carbons produced by pyrolysis and activation of porous phenol-formaldehyde resins, which have large mesopores capable of accommodating molecules with molecular mass of 7–50 kDa. These uncoated carbons have shown haemocompatibility equal to or better than that of commercial coated carbons. Experiments *in vitro* and *ex vivo* proved efficiency of novel nanostructured carbons in removing inflammatory cytokines, lipopolysaccharide, exotoxins and botulinum toxin from the blood stream. Mechanisms of protective action of activated carbon in the treatment of patients exposed to CBRN agents will be discussed.

Nanostructured carbons obtained by template method for protein adsorption

Puziy A.M.[1], Poddubnaya O.I.[1], Reinish C.A.[1], Mironiuk T.I.[1], Tsyba M.M.[1], Mikhalovsky S.V.[2], Mikhalovska L.I.*[2]

[1]*Institute for Sorption and Problems of Endoecology, 03164, Kiev, Ukraine*
[2]*University of Brighton, BN2 4GJ, Brighton, UK*
**e-mail: L.Mikhalovska@brighton.ac.uk*

Nanostructured carbons were obtained by templating technique [1], using sucrose or furfuryl alcohol as carbon source and cheap commercial inorganic templates (zeolite NaY, silica gels SG60, SGAO, ZK or colloidal silica Ludox AS40) as structure directing material. After carbonisation inorganic framework was dissolved in 40% HF. Nanostructured carbons show well developed porous structure with relatively uniform pores (Figure 1). Depending on inorganic template average pore size varies from 1.0 to 11.3 nm. All nanostructured carbons have large surface area (1200–1900 m^2/g) and large pore volume (2.1–4.1 cm^3/g). Nanostructured carbons retained the shape of inorganic template used for synthesis.

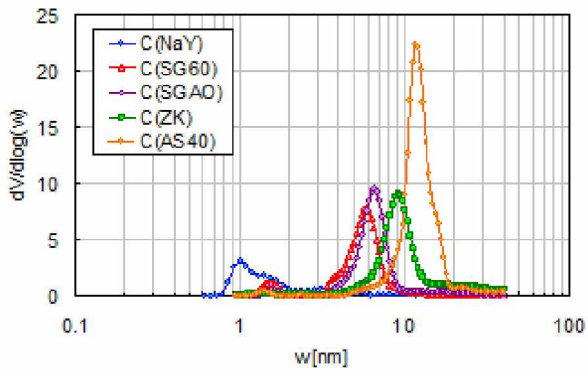

Figure 1. Pore size distributions in nanostructured carbons.

Adsorption of two proteins, ovalbumin (45 kDa) and fibrinogen (340 kDa), on nanostructured carbons was investigated. Unexpectedly, the highest adsorption was observed for carbon C(NaY) with the lowest pore size of 1 nm. The protein adsorption decreased as carbon pore size increased from 1 nm to 6.6 nm and then increased on carbons with larger average pore size. This trend holds over an order of magnitude of protein concentration in the range of 0.1–4.0 g/L. Factors related to the porous structure of carbons, such as surface area and pore volume, cannot account for the observed trend. It is likely that the conformational changes of adsorbed proteins as well as diffusion limitations of protein adsorption due to different carbon particle size contribute to the observed effect.

[1] Ryoo R, Joo SH, Kruk M, Jaroniec M. *Adv. Mater.* **13**, 677 (2001).

Nanoindentation and Raman spectroscopy study of graphite irradiated with swift ^{238}U ions

Manika I.*[1], Maniks J.[1], Zabels R.[1], Gabrusenoks J.[1], Krause M.[2], Tomut M.[2], Schwartz K.[2]

[1]*Institute of Solid State Physics, University of Latvia, LV-1063, Riga, Latvia*
[2]*Gesellschaft für Schwerionenforschung (GSI), 64291 Darmstadt, Germany*
**e mail:manik@latnet.lv*

The isotropic fine-grained graphite is a promising material for future high-energy ion beam facilities [1]. Modifications of the structure and mechanical properties of R6650 graphite irradiated with 2.6 GeV ^{238}U ions at fluences up to 10^{13} ions/cm^2 at room temperature were studied using nanoindentation and Raman spectroscopy.

Indentation tests confirm that the material withstands high-fluence irradiation. Moreover, a strong ion-induced increase of Young's modulus and hardness is observed that points to a structural change and formation of a hard form of carbon. The maximum effects are observed on the irradiated surface where an ion-induced increase of hardness and modulus reaches up to 500% and 280%, respectively. A change of hardness and modulus under ion-induced stresses around the interface between the irradiated layer and the non-irradiated bulk material was observed.

Raman measurements demonstrate ion-induced disordering and reduction of dimensions of crystallite domains. After high-fluence irradiation, the Raman spectrum becomes similar to that of the glassy carbon. Despite of sp^2 bonding the structure of the glassy carbon is known to ensure a high hardness and modulus. The Raman spectroscopy revealed a similar modification of a structure also on HOPG crystals irradiated with swift ions [2].

[1] M. Winkler, H Geissel, H. Weick, et al, *Nucl. Instrum. Methods B* **266**,4183 (2008).
[2] M. Tomut, W. Ensinger, M. Krause, C. Trautmann, *GSI Scientific Report*, (2010) (in press).

Homogeneous nucleation in liquid carbon obtained by laser pulse melting of graphite

Lysenko I.Yu., Basharin A.Yu.*, Turchaninov M.A., Dozhdokov V.S.

Joint Institute for High Temperatures, Russian Academy of Sciences, 125412 Moscow, Russia
**e-mail: ayb@iht.mpei.ac.ru*

The homogeneous nucleation in supercooled melts of metals and alloys is known to be a source of metastable solid phases and to be observed in pure melts only. Graphite is the most high-melting of the materials known nowadays, and, additionally the pressure in the first carbon triple point exceeds 10 MPa. That's why there is a limited number of graphite melting methods: in the most cases laser and ohmic heating are used. Both of these methods do not allow to reach uniform sample melting what in turn causes its contamination by unfused graphite. During the melt cooling the presence of graphite leads to the heterogeneous nucleation in the liquid and growing of the only graphite. This paper considers the conditions of the homogeneous nucleation in a melt, which forms metastable carbon phases at a laser pulse melting of high-oriented graphite HOPG. The cooling rate in this process exceeds 10^6 K/s [1].

Melting of HOPG in helium showed the melt formed on the close-packed graphite basal plane face not to be supercooled. It solidifies in a form of layered spiral vicinal hillocks or echelons of elementary steps with step height equal to the ***c*** parameter of the graphite lattice (0.67 nm). They grow on screw dislocations formed in the premelting stage at the graphite plastic deformation caused by thermal stresses

On the contrary, when heating up a loose prismatic HOPG phase there is no formation of dislocations, and the solidification pattern is determined by the surface electromagnetic waves (SEW)[1] appearing on the liquid surface. Appearing of SEW causes the rapid transfer of the laser radiation energy beyond the crater boundaries and the liquid supercooling due to the radiation-convective heat transfer. As a result, together with the heterogeneous crystallization on the melting puddle bottom there is a homogeneous nucleation on the melt surface. This is the only explanation of the appearance of metastable crystal forms, i.e. diamond and carbine found in the LIPSS zone by us in [2]. This suggests the energy barrier for metastable phases formation in a supercooled melt to be lower than that one for graphite. Possible origins of this phenomenon and its practical usage are discussed.

[1] Basharin A.Yu., Brykin M.V., Marin M.Yu., Pakhomov I.S., Sitnikov S.F., *Teplofis. Vys. Temp.* **42**, 64 (2004).

[2] Basharin A.Yu., Dozhdikov V.S, Dubinchuk V.T., Kirillin A.V., Lysenko I.Yu., Turchaninov M.A., *Pis'ma Zh. Tekh. Fiz.* **35**, 84 (2009).

[1]An indication of SEW are periodic surface structures (LIPSS), observed after the sample solidification

Highly oriented poly(vinyl alcohol) fibers modified with nanodiamonds: from effective structural modification to high tensile strength and modulus

Kurkin T.[a], Ozerin A.[a], Kechek'yan A.[a], Gritsenko O.[a], Sustchev V.[b], Dolmatov V.[b]

[a]*Institute of Synthetic Polymeric Materials, Moscow, 117393, Russia*
[b]*JSC "Diamond centre", St.-Petersburg, 193177, Russia*
email: t.kurkin@gmail.com

The morphological features and properties of the highly oriented poly(vinyl alcohol) fibers modified with nanodiamond and nanodiamond soot of detonation synthesis were investigated by wide-angle (WAXS) and small-angle (SAXS) X-ray scattering techniques, as well as by electron microscopy and mechanical testing methods. Applying those techniques yields the essential information on particle distribution within the matrix polymer, the effectiveness of modification and the relation of those features to the mechanical properties of the fibers, and as a result, their application opportunities. The effectiveness of modification can be defined as the ratio of gross quantity of the filler being introduced into the matrix to its volume fraction with particle sizes being in ~1-100 nm range. Measurements of the absolute intensity of SAXS suggested that in our case this ratio is unity for gross concentration of the filler varied from 0.5 to 3 vol.%. Thus it was shown, that the introduced nanodiamond soot particles were dispersed within the polymer matrix without aggregation, but with nanoparticles forming cloud-like structures. The nanodiamond soot treated with high-power ultrasonication was found to be more effective as to the modification of the mechanical properties of the oriented fibers in comparison to untreated soot and nanodiamond. The maximum increase in the longitudinal elastic modulus (from 30 GPa up to 45 GPa) and in the energy at break (from 3 J/g up to 6 J/g) was obtained for the fibers modified with the nanodiamond soot already at small (1 vol.%) soot content, that is technologically attractive. The increase in mechanical properties cannot be attributed to the molecular orientation within the fibrils, which was the same for all fibers regardless of the nanofiller content (as was proven by WAXS). Neither can these effects be interpreted in terms of additional cross-linking.

The measured values of the adhesive strength (in the ED-20 epoxy matrix) of poly(vinyl alcohol) fibers modified with the nanodiamond soot in amount of 1% by volume, were remarkably higher than that of the unmodified fibers. Maximum adhesive strength values of the modified fibers (42 MPa) were comparable to the adhesive strength value of the reference sample - steel wire (57 MPa) in the same epoxy matrix.

The obtained results suggest this kind of fibers to be a promising reinforcing component for the other types of polymer materials.

Carbon structures produced as a result of periodically repeated spark discharge in liquid hydrocarbons

Koprinarov N.*, Konstantinova M.A.

BAS, CL SENES, 1784 – Sofia, Bulgaria
**e-mail: koprin@phys.bas.bg*

High voltage periodical feed between electrodes dipped in a liquid (in our case hydrocarbons) leads to liquid evaporation and decomposition in the discharge zone. As liquids do not shrink and they are inert the expanding liquid vapor meets the resistance of the ambient and the pressure inside it grows. The obtained decomposition components are affected by the intensive electric field between the electrodes and the big temperature gradient oriented radial to the plasma cord for a short time interval as long as gaseous phase occurs. The high energy components get at decomposition and their oriented in the same direction movement set premises for their secondary combination in different versions and the new structure type origin. Feeding voltage periodical break restores the liquid starting condition and thus the arising structure growth is stopped. As a result they remain of small dimensions.

In the present work carbon nanostructures (nanocones, nanotubes, nanohorns, hollow spheres, nanobelts and alike, for instance) are described produced by spark discharge in a dispersed medium of xylene and water and xylene, water and ferrocene. The particles have been registered at TEM observations.

Carbon particles synthesized by pyrolysis in closed container

Koprinarov N.S.*, Konstantinova M.

BAS, CL SENES, 1784 – Sofia, Bulgaria
**e-mail: koprin@phys.bas.bg*

Different types of carbon structures as perfect in shape spheres, ellipsoids, nanotubes, and crystals have been produced by pyrolysis in a hermetically sealed steel container. Aromatic hydrocarbons like benzene toluene, xylene and their mixtures with water have been used as starting materials. The container air-tight high pressure sealing is achieved by pressing a steal sphere against the opening. The experiments have been made at a comparatively low for a pyrolyitic process temperature of the range 400–800°C. The temperature is linearly growing with a rate of 200°C/min and after the experiment is accomplished cooling goes down with a rate of 300°C/min. Particle morphology has been examined by Scanning and Transmission Electron Microscopy (SEM, TEM) and their chemical composition and crystal structure by the means of X-ray diffraction (XRD), infrared spectroscopy, Electron Probe X-ray Micro Analysis and Energy Dispersive X-ray Spectrometry (EDS). The results obtained show the spheres and ellipsoids to consist of pure incompletely graphitized carbon. They are thermally stable at heating up to 600°C in the air and in vacuum or in inert atmosphere they remain unchanged up to 1000 °C.

Formation of carbon clusters in detonation products of high explosives

Karpov D.I.*, Pruuel E.R., Satonkina N.P.

Lavrentyev Institute of Hydrodynamics SB RAS, 630090, Novosibirsk, Russia
**e-mail: karpov@hydro.nsc.ru*

Detonation products of a number of high explosives (TNT, RDX in composiotion with TNT, and others) contain a large amount of free carbon that releases in amorphous (soot) or crystal (graphite, diamond) phases. The process of carbon condensation behind the detonation front of carbon-rich high explosives is studied in the present work.

The molecular dynamics (MD) method was used for the numerical simulation of the free carbon aggregation in the detonation products (DP). The ensemble consisting of the two sorts of the particles (atoms) was studied. The particles of a sort C represented the atoms of the free carbon whereas the P-sort particles were the detonation products. The Lennard-Jones potentials (LJP) were used for describing the interactions between the atoms. The phase composition of the condensed carbon was not taken into account in the model.

Starting from the initial state with approximately homogeneous distribution of the carbon atoms in DP, the formation of carbon nanoparticles of the linear sizes from 10 to 50 atoms occurs in the substance. Then, the clusters of the nanoparticles are formed with the characteristic linear size about 10 particles. The subsequent dynamics depends on the initial concentration of the free carbon in the detonation products. If the carbon volume fraction is about 8 percents and higher then the clusters form the net spatial structures of mesoscopic sizes bridging the opposite sides of the simulation region. The aggregation is done with the formation of separated clusters if the carbon concentration is small.

Thus, condensation of carbon in the detonation products to clusters and spatial nets was simulated using molecular dynamics method. The result obtained is in satisfactory agreement with experimental measurements of electrical conductivities in the zone of the detonation of the DP of carbon-rich high explosives.

Field emission of carbon cathodes with hard limited nanostructured emitting surface

Ibragimov A.A.*[1], Lupehin S.M.[1]

[1]*State University of Telecommunications prof. M.A. Bonch-Bruevich, St.-Petersburg, Russia*
**e-mail: ibrart@mail.ru*

Experimental studies of field emission with nanostructure carbon materials have the fundamental interest First of all it is caused efficiency low voltage emission of carbon fibers.

The field emission properties have been examined in the vacuum diode system by applying voltage between the emitter (cathode) and a flat anode. The cathode was make from carbon fiber by diameter d = 7μm and height h= 2 mm and have emitting end surface. The emitting surface consists of nanosized fibrils. The pressure of residual gas P= 10^{-5}–10^{-7} Torr.

Current-voltage characteristics were investigated under various anode-cathode distance D_{ak} = 1–10 mm. The cathode had an aspect ratio h/d ≈ $3\cdot10^2$. Aspect ratio macrogeometry cathode and nanostructure of the emitting surface determine the gain factor of the electric field $\beta \approx (3–7)\cdot10^4$.

Experiments have shown that fibril fiber cathodes begin to emit at voltages U= 0.5–0.7 kV (initial field emission current I ~ 10^{-6}A). Experimental current-voltage characteristics have good reproducibility and are consistent with the theory of Fowler-Nordheim for field-emission current. Obtained by limiting current density j = $5\cdot10^2$ A, by the voltage U= 1.8 kV, the distance $D_{ак}$= 1mm, the cathode height h= 2mm. Current density values are much higher than for the best examples of thermo cathodes.

In accordance with the results febrile fiber cathodes can be used effectively in a technical vacuum and low operating voltages.

Tungsten carbide emitting nanoprotrusions as effective field emission point sources of the electrons and ions

Golubev O.L.

Ioffe Physico-Technical Institute, 194021 St. Petersburg, Russia
e-mail: O.Golubev@mail.ioffe.ru

The field emitters with high degree of emission localization within small solid angles can be of considerable interest as effective sources of electrons and ions for various high resolution beam devices. With the purpose of creating of the stable point sources the form changes of a field emitter from tungsten carbide at simultaneously action of strong electric fields F and high temperatures T (thermo-field treatment) were studied. It was shown that to create on an emitter surface the some emitting nanoprotrusions with the radii of curvature about r ~ 1-5 nm by means of thermo-field treatment is not so difficult problem. The emitters with many nanoprotrusions on a surface can be realized by thermo-field treatment in wide range of F and T changes, these emitters allow to create the electron sources "watering-pot" type with many separate electron beams. However the formation of a single nanoprotrusion on the emitter surface and point source creation is a certain problem [1]. A single nanoprotrusion on a tungsten carbide emitter surface can be produced by the specially procedure of change of F value at definite value of T. The single tungsten carbide nanoprotrusion can emit of the electrons with such stability as the emitters from carbon materials. The values of emission currents, current densities, emission angles and reduced brightnesses of the emitter are comparable with the values typical for the carbon nanotubes emitters. But the evident advantages of the tungsten carbide nanoprotrusion is the possibility to recover its performance by repeating the procedure of thermo-field treatment as described above. Moreover, the tungsten carbide nanoprotrusions (in contrast to carbon nanotubes) can operate as the point emitter of ions under the simultaneous action of high T and F in the regime so-called high-temperature field evaporation.

This study was supported by the Russian Foundation for Basic Research, project № 09-08-00912.

[1] O.L. Golubev, *Technical Physics Letters* **35**(6), 545 (2009).

Nanocarbon materials and polymers

Ginzburg B.M.[2], Tuichiev Sh.*[1], Osawa E.[3], Rashidov D.[1], Tabarov S.[1], Mukhamad A.[1]

[1]*The Tajik national university, 734025, Dushanbe, Tajikistan*
[2]*Research Institute of Mechanical Engineering Problems RAS, 199178, St. Petersburg, Russia*
[3]*Nanocarbon Research Institute, 386-8567, Ueda, Nagano, Japan*
**e-mail: tuichiev@mail.ru*

A comparative study the influence of nanocarbon materials on structure and physical properties of amorphous and crystallising polymers has been done. As objects of research used polyethylene of low density, isotactical polypropylene, polyvinyl alcohol, atactic polymethylmethacrylate, polystyrene and polytetra-fluoroethylene. The fillers from nanocarbon materials as fullerene C_{60}, fullerene soot, multiwall carbon nanotubes, nanodiamonds has been used. The nanocomposite film materials have received by formation from solutions in aromatic solvents and from melts. The concentration of fillers varied in the range of C=0.1-10%mass. In these investigations the methods of X-ray scattering, calorimetric, optical and mechanical tests were used. Light resistance of polymers studied in the conditions of photoageing, a bilateral UV-irradiation of samples made from a source of cold luminescence BUV-30 with length of a wave λ =254nm. On the basis of these study the general features of variations of structure and technical properties of the amorphous and crystallizing polymers, which modified by nanocarbon materials are established. Adoption of fillers is accompanied by following effects: 1) at small concentration of fillers C=0.1-1%mass. there is an increase of durability of polymers to 10-50% at a deformability invariance; their light resistance increases at a constancy of temperature of melts; 2) at concentration of fillers C >1%mass. deformability of polymers sharply decreases at slow recession of durability; reduction of temperature of melt of polymers to 10° and increase of light resistance of samples has been observed; 3) formation of crystalsolvates in some crystalline polymers also observed; 4) brightness of display the variation of properties of polymers depends on their chemical structure, presence of lateral assistants of different nature, a physical states of amorphous and crystalline polymers, molecular both supermolecular morphology of polymers and fillers also, their activity, technology of reception of materials and etc.

Pressure-temperature-induced transformations of polyhedral carbon nanoparticles in hydrogen-containing system

Davydov V.A.[1*], Rakhmanina A.V.[1], Agafonov V.N.[2], Khabashesku V.N.[3]

[1]*L.F.Vereshchagin Institute for High Pressure Physics of the RAS, 142190, Troitsk, Russia*
[2]*L.E.M.A., UMR CNRS-CEA 6157 - LRC CEA M01, Université F. Rabelais, 37200, Tours, France*
[3]*Department of Chemical and Biomolecular Engineering, University of Houston, 77204, Houston, USA*
**e-mail: vdavydov@hppi.troitsk.ru*

Transformations of polyhedral carbon nanoparticles (PCN) in the hydrogen-containing system have been studied in the framework of investigations of relative stability of different carbon allotropes at high pressures and temperatures in pure carbon and hydrocarbon systems.

The present work has been carried out on binary mixtures of PCN with naphthalene. Homogeneous mixtures of PCN with the initial sizes in the 30-80 nm range with naphthalene have been treated under pressure of 8 GPa, variable temperatures up to 1600°C and isothermal exposure times from 20 to 300 s. High-pressure states obtained at different temperatures have been isolated by quenching to room temperature under pressure followed by characterization of the samples at normal conditions by X-ray diffraction, Raman spectroscopy and scanning electron microscopy (SEM).

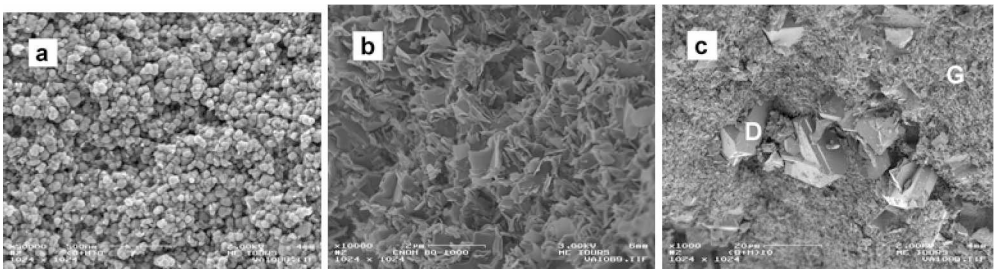

Figure 1. SEM images of treatment products of binary mixtures of PCN with naphthalene at 8 GPa and temperatures of 800 °C (a), 1000°C (b), 1100°C (c): D – diamond, G – graphite.

An evolution of high-pressure carbon states as a function of temperature has been studied. As the result, qualitative distinction of the mechanism of PCN transformations in the single-component carbon system from binary hydrocarbon system has been established. Even tiny amount of hydrogen, remaining at the final step of naphthalene carbonization at 8 GPa in the temperature range 800-1000°C, becomes sufficient for catalyzing the processes of PCN destruction and subsequent cumulative recrystallization of carbon material. At 8 GPa, the destruction of PCN in the binary system starts at ~900°C. Cumulative recrystallization of the system results in formation of micron-sized crystallites of graphite at 1000°C and diamond at temperatures above 1100°C (Figure 1).

This work was supported by the Russian Fund of Basic Research (RFBR, grant N 09-03-00752) and, in part, by Award No. RUE2-2894-TI-07 of the U.S. Civilian Research & Development Foundation for the Independent States of the Former Soviet Union (CRDF).

Composites based on superhigh-molecular poly(ethylene) and carbon nanostructures

Churilov G.N.*[1,2], Osipova I.V.[1], Maslennikov A.N.[1], Gluchenko G.A.[1,2], Drokin N.A.[1]

[1]*L.V. Kirensky Institute of Physics SB RAS, 660036, Krasnoyarsk, Russia*
[2]*Krasnoyarsk State PedagogicalUuniversity, 660049, Krasnoyarsk, Russia*
**e-mail: Churilov@iph.krasn.ru*

The investigation results of superhigh-molecular poly(ethylene) modified by fullerene, carbon nanotubes, amorphous carbon and 3d metals particles with carbon cover have been presented in this paper.

The influence of fullerene and carbon nanotubes on the impedance characteristics of composite consists of them and superhigh-molecular poly(ethylene) was investigated by us earlier [1]. In order to determinate electrophysical properties of superhigh-molecular poly(ethylene) composites synthesized by us the method of impedance investigation in long range of frequencies and temperatures was used.

Ni and Fe nanoparticles had carbon cover with functional OH groups (see Figure). The investigation of behavior of real and seeming components of impedance has been shown that conduction, dielectric and magnetic properties depend on nanoparticles concentration. During determinate concentration of nanoparticles the material absorbed electromagnetic radiation completely in the band of investigates frequencies.

The conversion of superhigh-molecular poly(ethylene) in conductive material, i.e. appearance of antistatic properties, starting with determinate concentration of nanodispersed carbon, is one of significant results. Using of modified nanoparticles, mechanical properties were improve significantly and most of all resistance to wear.

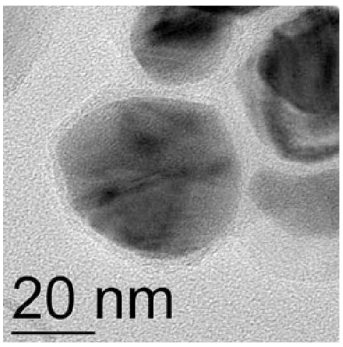

Figure. Electron microscope image of Ni nanoparticles modified carbon cover.

[1] Drokin N.A., Fedotova A.V., Glushchenko G.A., Churilov G.N., *Physics of Solid State* **52**, 657 (2010).

Mechanical properties and fracture of superelastic hard carbon particles produced from fullerenes under pressure

Chernogorova O.P.*, Drozdova E.I., Ovchinnikova I.N., Blinov V.M.

Baikov Institute of Metallurgy and Materials Sciences RAS, Leninskii pr. 49, 119991 Moscow, Russia
**e-mail: tchern@ultra.imet.ac.ru*

Superelastic hard materials with a high hardness-to-elastic modulus ratio are advantageous in terms of wear resistance and tribological properties. Bulk particles and samples of superelastic hard phase (SHP) were obtained from fullerenes at a pressure of 3–8 GPa at temperatures of 800–1200 K. Acording to the microindentation data obtained from the loading-unloading curves treated by the Oliver-Pharr method, the SHP samples are characterized by high hardness (35 GPa), high elastic recovery (85–94%), and low elastic modulus (60–150 GPa). The cracking resistance of the SHP particles was estimated with a Vickers tester at a load of up to 20 kgf. After indentation, no radial cracks have been observed on the particle surface, and the residual deformation limited by the contact area between the particle surface and the diamond indenter was expressed by weak cross-shaped grooves left by the edges of the diamond pyramid and small cracks parallel to the pyramid base in the areas corresponding to the pyramid faces. Such behavior of the SHP particles upon indentation displays their ability to withstand heavy contact loads without any severe residual deformation and without any fracture propagation beyond the contact area.

The fracture surface of the SHP samples obtained from coarse C_{60} crystals demonstrates a terraced cracking through internal interfaces corresponding to the shear planes in the original *fcc* crystal. The SHP particles and samples obtained from the aggregates of fine C_{60} crystals exhibit mixed fracture surfaces containing ductile interlamellar component. The particles obtained from the fullerene soot extract (unresolved mixture of C_{60} and C_{70}) exhibit quasi-brittle river fracture surface typical of amorphous materials.

Applied polimerization of PEDOT in a direct current discharge was ineffective: it's showed undesirable dielectric properties of material

Gil'man A.B.[1], Drachev A.I.[1], Belobrzeckaja-Kosta L.N.[2]*,
Del Borghi M.[3], Fumagalli M.S.[3], Costa Nicola B.[4]

[1]*Enikolopov Institute, 117393, Moscow, Russia*
[2]*House of Scientists, 191186, St. Petersburg, Russia*
[3]*DICheP, Engineering Faculty, Genoa State University, Genoa, Italy*
[4]*Department of Chemistry, Genoa State University, Genoa, Italy*
**e-mail: belobrzeckaja@libero.it; plasma@ispm.ru*

In the last three decades increasing demand for new polymers has evidenced in the area of "functional materials" projected for specific applications [1, 2]. One of the interesting modern material's PEDOT/PSS produced and characterized by well-known techniques according to ref.[3, 4]. Applied polymerization in a Direct-Current Discharge [5, 6] of PEDOT was ineffective and it's produced material which showed dielectric properties due to defects and breakdown of desirable structure of polymer.

Authors are grateful to Prof. A. Giarrusso & to Prof. Pio Forzatti, Politecnico di Milano, Milan and to Prof. Maria Vittoria Russo of "La Sapienza" Rome University, Rome, Italy.

[1] D.E. Apens, "Handbook of Semiconductors", vol. 1 ed. T. S. Moss, North Holland, Amsterdam (1980).
[2] J.M.G. Cowie, "Polymers: chemistry & physics of modern materials", Blackie USA/UK, 399-425 (1991).
[3] F. Louwet, L. Groenendaal, J. Dhaen; J. Manca, J. Van Luppen, E. Verdonck, L. Leenders, *Synthetic Metals* **135-136**, 115 (2003).
[4] C.S. Lee, J.Y. Kim; D.E. Lee, J. Joo etc., *Synthetic Metals* **139**, 457 (2003).
[5] A.I. Drachev, A.B. Gil'man, V.G. Krasovskii, L. Costa-Belobrzeckaja, *High Energy Chemistry* **39**(5), 333 (2005).
[6] L.N. Belobrzeckaja-Kosta [Costa], patent "Method of polymerization of 3-Methoxythiopene in a Direct Current Discharge", ed. Politecnico di Milano, (2005-2009), Academies of Sciences "Lincei" & "XL", Rome, Italy.

Optical characteristics of porous nanocarbon materials in effective media model: Bruggeman aprocsimation

Bekhterev A.N.

Magnitogorsk State University, 455000, Magnitogorsk, Russia
**e-mail: alexbehterev@yandex.ru*

Practically all physical and many physical and chemical properties of condensed carbons be described on the basis of the information on a dispersion optical indexes in the region of electronic and phonon energy states of known forms crystal and amorphous carbons within the limits of the certain modeling representations. Method of the classical dispersive analysis, Kramers-Kronig method and effective media theory are used for calculation of a spectrum optical parameters *n(v)* and æ*(v)* ($\check{n} = n - i$æ) of pyrolitic carbon (PC) and glassy carbon (GC) similar on structure with nanocrystalline graphite. Calculated infrared absorption spectra of PC and GC are compared to the similar data received from of in situ attenuated total reflection spectra (ATR) for samples in the region of vibration mode E_{1u} and A_{2u} of graphite. Process of reception of the sample has provided the minimal maintenance of impurity which averaged 0,001% of mass and high level of micro- and nanoporosity – till 50%.

We calculated n_{eff} using the theory, which describes effective dielectric properties of a granular composite with one kind of particles embedded randomly in a large volume of a host component. The effective media approximation also called Bruggeman's theory is the method to describe the effective dielectric properties of composites in which the particles of all components randomly mix together. This theory has been widely used to explain the dielectric and optical properties of composite materials and proved valid at all concentrations [1, 2]:

$$f\frac{\varepsilon_m - \varepsilon_k}{\varepsilon_m + 2\varepsilon_k} = (1-f)\frac{\varepsilon_{eff} - \varepsilon_k}{\varepsilon_{eff} + 2\varepsilon_k}$$

where ε_{eff}, ε_m, ε_k – effective, matrix, embedded component indexes of samples, f – volume fraction of embedded component. The obtained spectra of GC and PC well describe the experimental infrared reflectance data of the samples in spectral region 2000–1000 cm^{-1} [3].

[1] Carbon Molecules and Materials, Ed. by R. Setton, P. Bernier, and S. Lefrant.- Taylor & Francis, New York, 2002.

[2] Bekhterev A. N. Vibration states in solid state carbon and nanocarbon. - Magnitogorsk: MaSU, 2007.

[3] Bekhterev A.N., Zolotarev V.M., Yakovlev V.B., *Opt. Spektrosk.* **59**(5), 1057 (1985).

Field-induced electron emission from graphitic nano-island films at silicon substrates

Arkhipov A.V.*[1], Gabdullin P.G.[1], Gordeev S.K.[2], Korchagina S.B.[2], Mishin M.V.[1]

[1]*St. Petersburg State Polytechnic University, 195251, St. Petersburg, Russia*
[2]*FSUE "Central Research Institute for Materials", 191014 St. Petersburg, Russia*
**e-mail: arkhipov@rphf.spbstu.ru*

Numerous carbonic nano-structured materials were reported to demonstrate electron emission in moderate electric field (1 kV/mm or less), even if their surface morphology shows no edges or tips capable of strong local field enhancement. In many such cases, the actual mechanism of emission facilitation remains unclear, partially due to complex structure of the investigated materials usually representing a 3-dimensional system of domains with different properties. In the presented work we investigated a somewhat simpler, quasi-2d system, presumably providing better possibilities for unambiguous description of the emission mechanism. The sample emitters were produced by chemical deposition of small amounts of carbon at silicon substrates. Depending on deposition conditions, the coating layer had different structure and different average thickness. For some samples, the threshold electric field (corresponding to 1 nA current extracted from a few mm^2 area) was as low as 0.4 kV/mm. Other samples yielded no current in the field up to 10 kV/mm. We investigated correlation between emission efficiency and carbon layer morphology determined via AFM imaging. According to our observations, the property of low-field emission was associated with the presence nm-sized carbon islands isolated from each other (see Fig.1). Facilitated emission wasn't observed if the carbon domains merged to form a continuous film. The best emission properties were obtained for samples deposited at p-type substrates with high electric resistance. Results of these experiments could be explained within the bounds of the model proposed earlier for other nano-carbon systems [1].

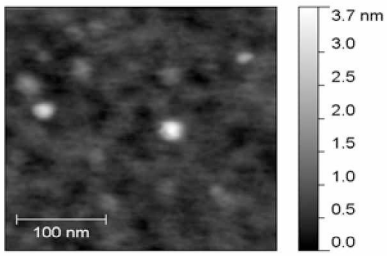

Figure 1. AFM image for a sample demonstrating low-field electron emission (threshold field is 0.38 kV/mm). The bright spots presumably represent isolated graphitic islands.

[1] A.V. Arkhipov, P.G. Gabdullin, M.V. Mishin, *Fullerenes, Nanotubes and Carbon Nanostructures* **19**(1-2), 86 (2011).

Role of nano-sized objects in field-induced electron emission facilitation

Arkhipov A.V.*, Bondarenko V.B., Gabdullin P.G.

St. Petersburg State Polytechnic University, 195251, St. Petersburg, Russia
**e-mail: arkhipov@rphf.spbstu.ru*

Phenomenon of facilitated field-induced electron emission from nano-structured materials with relatively smooth surface morphology is often described in terms of two-stage emission model. This model allows to explain principle possibility to obtain substantial emission current from a surface characterized by a high value of work-function (as it is for various forms of carbon) in the absence of strong local field enhancements at elements with high-aspect-ratio geometry. In this model, electrons are first transferred onto some high-energy intermediary states localized near the emitter surface and then emitted to vacuum, separated from these states by a barrier that is transparent for electrons. Yet description of details of this model – such as the nature of the intermediary states – often meets substantial problems. We think that at least some problems may be solved if we assume that the intermediary states are associated with conductive nano-sized objects at the emitter surface. For many carbon-based emitter of the discussed type, such objects (surface crystallites, onion-like particles, nano-sized islands of coating film, etc.) were directly observed — see, for instance, in [1]. External electric field can be enhanced at the junction between the nano-particle and emitter bulk (or other nano-particles comprising the emitter material), allowing electrons to gain substantial energy and occupy high-energy levels of the nano-sized object. According to recently published research results [2], the lifetime of "hot" electrons in nano-particles may be very large (up to nanoseconds) if the energy spacing between electron levels exceeds the highest photon energy of the lattice, thus excluding the most efficient mechanism of electron energy losses. This feature allows "hot" electrons to travel through the particle to its vacuum boundary where they can easily leave the emitter. The presented work includes numerical estimates and simulations performed to demonstrate applicability of the proposed model to a few types of carbonic nano-structures investigated in previous experiments.

[1] A.V. Arkhipov, P.G. Gabdullin, S.V. Gordeev, S.B. Korchagina, M.V. Mishin, Abstract P6.04 (In this book).

[2] W.A. Tisdale, K.J. Williams, B.A. Timp, D.J. Norris, E.S. Aydil, X.-Y. Zhu, *Science* **328**, 1543 (2010).

Carbon-encapsulated iron carbide nanoparticles in the thermal conversions of ferrocene at high pressures

Davydov V.[1], Rakhmanina A.[1], Autret C.[2], Limelette P.[2], Agafonov V.[2]

[1]*Institute of High Pressure Physics of the RAS, 142092 Troitsk, Russia*
[2]*LEMA, UMR 6157, University of Tours, 37200 Tours, France*

Pressure-temperature-induced transformation of ferrocene at pressures up to 8 GPa and temperatures up to 1000°C have been studied by X-ray diffraction, transmission (TEM) and high resolution transmission electron microscopies (HRTEM). As a result, an evolution of products of high-pressure high-temperature treatment of ferrocene as function of temperature at 2.5 and 8.0 GPa has been investigated. It was shown that a thermal conversions of ferrocene under high pressures can give rise to the formation of carbon-encapsulated iron carbide (Fe_3C) nanoparticles with diameter from 5 nm to 30 nm. The Fe_3C nanoparticles were uniformly dispersed in carbon matrix and contain Fe_3C nuclei surrounded by several carbon layers (onions –like) with well ordered arrangement (Fig.1a).

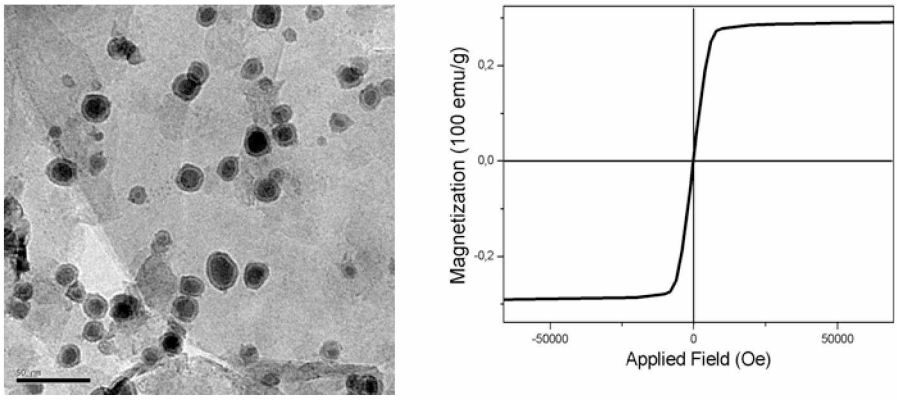

a) b)

Figure 1. (**a**) TEM image and (**b**) field dependence of magnetization of iron carbide nanoparticles synthesized from ferrocene at 80 kbar and 500°C.

Magnetic measurements indicated that these nanoparticles were ferromagnetic at the room temperature, with some variation in the values of saturation magnetization, remanences and coercive forces that depend on the size of the particles. A superparamagnetic-like behaviour at room temperature was observed for the carbon-encapsulated Fe_3C particles which belong to the smallest sized fraction of this material (Fig.1b).

This work was supported by the Russian Foundation for Basic Research (RFBR, grant № 09-03-00752) and by CNRS-RAS project N° 21239.

Nano films of linear-chain carbon with embedded metal and nonmetal atoms: characterization and data mining modeling

Abrukov S.V.*, Kochakov V.D., Telegin G.G.

Chuvash State University, Cheboksary, 428015, Russia
**e-mail: abrukov@yandex.ru*

Currently a lot of experimental data on properties and characteristics of various nano materials are obtained. The question is how we can summarize it and present in the form of common models allowing descripting the characteristics of previously studied nanomaterials? It is obvious that the characteristics of nano materials related to the composition of nano materials and type of components, manufacturing technology, the shape and size. The question is how we can generalize these links as a computational models that allow to determine the characteristics of the nano materials without carrying out additional experiments? Even more important question is it possible to predict what should be the nano material (structure, components, and dimensions) and what technology should be used with to provide the required properties and characteristics of nano materials?

In this paper we present the first results of application of Data Mining (DM) [1] to create such models. They are based on experimental results for the characteristics of nano films of linear-chain carbon (LCC) with embedded into (LCC) metal and nonmetal atoms (LCC MNA). For the first time LCC MNA were manufactured in the Chuvash State University [2] using a variety of know-how. The direction of work can be of great interest for creation of active and passive elements of solid-state electronics [3], sensors, medical applications, etc.

To date we have developed two computational models that allow predicting the physical-electrical properties of LCC MNA as a function of atoms embedded in a LCC: 1. The model “Steepness and Saturation Current of the current-voltage characteristics vs. Kind of Embedded Chemical Elements”. 2. Generalized model of "Current-Voltage Characteristics of the LCC MNA”. The latter model allows to predict the current-voltage characteristic of any new sort of LCC MNA.

[1] Rios Daniel, (2010) Neuro AI - Intelligent systems and Neural Networks. http://www.learnartificialneuralnetworks.com.

[2] Kochakov, V.D., Novikov N.D., Yablokov M.Y., Eremkin A.V., Vasil'ev A.I., *Actual Problems of Arts and Sciences* N 12, 17 (2009) (in Russian).

[3] Novikov, N.D., Kochakov, N.D., Telegin G.G., *Nanotechnology* N 2. 3 (2006) (in Russian).

Size effects in fullerites nanoparticles

Zubov V.I.

Using the correlative method of unsymmetrized self-consistent field for anharmonic crystals we study structural, dynamical and thermodynamic properties of high-temperature modifications of fullerites. Here we present the results for size effects in C_{70} fine crystalline particles. The intermolecular potential derived by Vertheijen *et al.* is utilized. Anharmonic terms up to the fourth order are taken into account. We have considered three highly symmetrical forms of particles with singular faces: cubical, spherical and octahedral, and calculated size dependences of their mean lattice parameters a and thermal expansion coefficients. Influences of the surface tension and of the lattice relaxation near surfaces have been taken into account. For all three forms of nanoparticles, both values increase with decreasing size, that is a consequence of anharmonicity. This effect is appreciable enhanced when the temperature increases. We also note a dominant contribution of the lattice relaxation to the size dependence of the lattice parameter.

Comparative study of several fullerene based bulk heterojunctions

Ziminov V.M.[1,2], Zakharova I.B.*[2], Aleshin A.N.[3], Makarova T.L.[1,3]

[1] *Umeå University, 90187, Umeå, Sweden*
[2] *St. Petersburg State Polytechnic University, 195251,St. Petersburg, Russia*
[3] *Ioffe Institute, 194021, St. Petersburg, Russia*
**e-mail: Zakharova@rphf.spbstu.ru*

The use of bulk heterojunction based on organic semiconductors is a promising method of the organic nanophotonics, particularly for the creation of an organic solar cells [1]. The bulk heterojunction can be created in a form of inter-penetrating network of donor and acceptor materials, which can be used to increase the efficiency of converting solar energy in the photocell.

Organic heterostructures with thickness of 100 - 1000 nm were obtained by vacuum deposition technology in the quasi-equilibrium conditions. It's a novel method of creation a nanocomposite material consisting of organic and inorganic semiconductors with a composition gradient for the realization of a bulk heterojunction. The structure, composition and electrical properties of composite thin films of organic semiconductors C_{60} and *Me*TPP (tetraphenylporphyrin *Me*, where *Me* = Zn, Cu, or a complex of FeCl), as well as the C_{60} films with the addition of an inorganic n-type semiconductor CdS were analysed. Structural properties of the films were investigated by AFM, Raman and x-ray spectroscopy. The electrical properties of sandwich-structures on ITO-glass and Si (111) substrates were investigated. In such structures C_{60} acts as an acceptor, porphyrin or CdS molecules acts as an donor center [2].

Current-voltage characteristics of this composite heterostructures have a diode character for the different pairs of C_{60}-*Me*TPP, as well as for C_{60}-CdS. The rectification factor depend on the composition and structure of the film, as well as the composition gradient. For the structures glass/ITO/C_{60}/mixtureC_{60}-CdS containing CdS about 1 at.%, the direct to reverse current ratio at 1 V is about 10^3. It's the record value for the organic diode structures. The increase of CdS concentration to 30 at.% leads to a decrease in this ratio. Direct and reverse I-U curves can be satisfactorily described in a model of hopping conductivity and non-ideal heterojunction; relative contribution of these mechanisms is determined by the composition of the sample.

[1] J. Xue, B.P. Rand, S. Uchida, S.R. Forrest, *Adv. Mater.* **17**, 66 (2005).
[2] I.B. Zakharova, E.A. Donenko, Yu.F. Biryulin, L.V. Sharonova, *Fullerenes, nanotubes and carbon nanostructures* **16**, 424 (2008).

Fullerenation of diallyl monomer

Yumagulova R.Kh.*[1], Medvedeva N.A.[2], Kolesov S.V.[1]

[1]*Institute of Organic Chemistry, Ufa Scientific Center RAS, 450054, Ufa, Russia*
[2]*Bashkir State University, 450074, Ufa, Russia*
**e-mail:jmagulova@anrb.ru*

Until now there is no evidence concerning the reactivity of vinyl or acetylene monomers for the synthesis of polymers with fullerene substituents in the side chains. We are carrying out the study to clarity the possibility for the use of diallyl compound for this purpose. The basis for the conclusion that in the presence of C_{60} the allyl radical may interact with fullerene or fullerene radical was linear dependence of the amount of bonded fullerene C_{60} on the content of allyl chain in the polymer [1]. That was revealed on polymerization of diallyl isophthalate (DAIP) with styrene. Therefore, it becomes possible fullerenation DAIP with its further participation in the reaction of copolymerization with vinyl monomers (see the scheme).

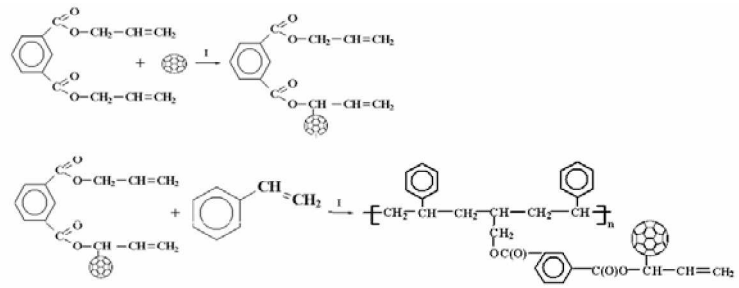

It is important to note that fullerenation of monomer with two unconjugated double bonds prevents subsequent polymer structuring and increases by on order the degree of functionalisation of the reaction products by fullerene.

The study of the process in this direction allows to obtaining some information in regard to the role of fullerene in macrochain formation that may beep in the study of polymerization mechanism in fullerene – containing systems.

To determine optimal conditions the reaction of direct fullerenation was carried out in the presence of radical initiator and/or UV – irradiation in a saturated solution of fullerene at molar ratio of DAIP:C_{60} = 1:1 and 10:1. The products of interaction of DAIP with C_{60} without their separation were introduced into the reaction with styrene and copolymers containing 20-40 wt% of fullerene were obtained.

This work was supported by the Federal Target Program "The Scientific and scientific-pedagogical cadres Innovative Russia" (State Contract 02.740.11.0648).

[1] R.Kh. Yumagulova, N.A. Medvedeva, I.A. Ionova, V.P. Volodina, S.I. Kuznetsov, S.V. Kolesov. *Polymer Science,* B **52**, 459 (2010).

A fullerene-based catalyst for molecular hydrogen activation with comparable catalytic hydrogenation capability to noble metal catalyst

Li B., Zhu G., Qi L., Xu Z.*

State Key Laboratory of Coordination Chemistry, Nanjing University, Nanjing, 210093 (PR China)
**e-mail: zhengxu@netra.nju.edu.cn*

Molecular hydrogen is not only a bright future fuel, but also is widely used today in fundamental chemical transformations. For example, all crude oil is treated with H_2 and 10^8 tons of ammonia fertilizer is produced annually via catalytic hydrogenation. Any small improvement of the performance and cost of the catalysts would help to cut the cost of these important processes. But such improvements are hard to achieve because the H_2 is held together in a strong marriage. It can be split apart by using a transition metal as the catalysts. Here we demonstrate that fullerene can activate the molecular hydrogen and act as the novel hydrogenation catalyst The hydrogenation of aromatic nitro compounds to amino aromatics is achieved with high yield and selectivity. At C_{60}:C_{60}^-=2:1, ~100% conversion and ~100% selectivity of the hydrogenation reactions are achieved under 120-160°C and 4-5MPa H_2 pressure.

In addition, they exclusively catalyze the reduction of the nitro group without metal salts and avoid the accumulation of the corresponding hydroxylamine and the formation of azoxy and azo compounds. These findings foreshadow a new catalytic system available for fundamental research as well as the industry applications. Moreover, the catalysts developed here could replace expensive precious metal catalysts; therefore, they offer the potential benefit of lowering the cost and diminishing environmental problems from heavy-metal pollutants.

[1] Li, B. J.; Xu, Z. *Journal of the American Chemical Society* **131**, 16380 (2009).
[2] Li,B.J.: Li,H.B.; Xu, Z. *Journal of Physical Chemistry C* **113**, 21526 (2009).

Self-organization processes in polymeric nanocomposites with C_{60} fullerenes

Voznyakovsky A.P. [1], V.Kh.Kudoyarova V.Kh.[2], Kudoyarov M.F.[2]*, Lebedev V.T.[3]

[1]*Lebedev Institute of Synthetic Rubber, St.-Petersburg, 198035 Russia*
[2]*Ioffe Institute, St.-Petersburg, 194021 Russia*
[3]*Nuclear Physics Institute, Gatchina, Leningrad oblast, 188300 Russia*
e-mail: mkud@cycla.ioffe.ru

As shown previously [1], use of C_{60} fullerenes enables synthesis of polymeric materials with noticeably improved physicochemical properties. The present study is concerned with such composite materials as polyblock polysiloxane copolymers modified with C60 fullerenes. The chosen polymer is convenient for modeling the structure--property relationship as regards the influence of highly dispersed substances on the supramolecular organization of polymeric nanocomposites. A number of physical techniques were used: method of neutron scattering (NS) and electron microscopy (TEM). Materials containing 0.5, 2, and 4 wt.% C_{60} were examined. According to the results of an NS study, introduction of C_{60} fullerenes into the polymer gives rise to additional (compared with the starting polymer) scattering centers (Figure). TEM data (Fig. 1, inset) demonstrated the absence of separate C_{60} clusters. Thus, the appearance of new scattering centers can be attributed to self-organization processes occurring under the action of coordinating fields of fullerenes, and specifically to formation of rigid-block clusters containing C_{60} molecules. The suggested model is well correlated with the complex of chemical properties (diffuse permeability) and with the complex of elastic-strength parameters of the composite.

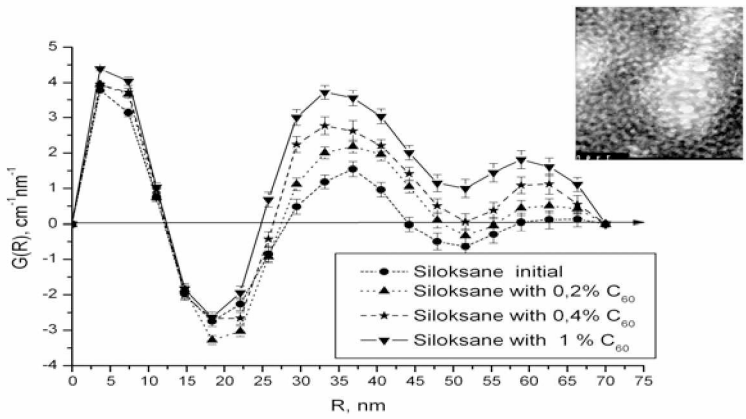

Figure. Correlation functions G(R) of scattering structures in nanocomposite siloxane films. Inset. TEM micrograph of a nanocomposite with 0.5 wt.% C_{60}.

[1] A.P. Voznyakovsky, M.F. Kudoyarov, M.Ya. Patrova. *Let. JTPh* **33**(16), 86 (2007).

Self-consistent Hartree-Fock approach to electronic structure of endohedral fullerenes

Verkhovtsev A.V.[1], Polozkov R.G.[1], Ivanov V.K.*[1], Korol A.V.[2], Solov'yov A.V.[2]

[1]*St. Petersburg State Polytechnic University, 195251, St. Petersburg, Russia*
[2] *Frankfurt Institute for Advanced Studies, 60438, Frankfurt am Main, Germany*
**e-mail: ivanov@tuexph.stu.neva.ru*

Since the first experimental observation of endohedral fullerenes [1], series of theoretical studies dedicated to the investigation of these compounds and their interaction with photons within different models (see [2] and references therein) have arisen. In this work we apply for the first time the self-consistent Hartree-Fock approximation to calculate the electronic structure of noble gas endohedral fullerenes by the example of compounds He@C_{60}, Ne@C_{60} and Ar@C_{60}.

The total electronic system consisted of all electrons of the encapsulated atom and 240 valence electrons of fullerene C_{60} is considered in the spherically symmetric field created by the ionic core of a fullerene and the nuclear charge of embedded atom placed in the center of the spherical layer. Thus the electronic configuration, for example for Ar@C_{60}, consists of 258 electrons:

$$1s^2 2p^6 3d^{10} 4f^{14} 5g^{18} 6h^{22} 7i^{26} 8k^{30} 9l^{34} 10m^{34} 2s^2 3p^6 4d^{10} 5f^{14} 6g^{18} 7h^{10} 3s^2.$$

The valence electrons of the fullerene are distributed in a usual way with ratio of 3:1 over the σ (none-node) and π (one-node) orbitals, correspondingly. The fullerene ionic core is presented by a uniform distribution of positive charge (Z=240) over spherical layer of the finite thickness. Additional electrons from noble gas atom should be arranged either in a new shell which is absent in the configuration of the fullerene (for example, 3s in case of Ar@C_{60}) or in the partially filled fullerene orbitals by reason of minimal electronic energy principle.

Results of the calculations show that the inner-shell electrons (1s in He, 1s2s in Ne and 1s2s2p in Ar) remain to be the inner-shell electrons of the endohedral fullerene and they are located mostly near the embedded atom, while the behaviour of the outer atomic wave functions has revealed the strong hybridization of valence atomic and fullerene orbitals with the same values of angular momentum. It has been found that there is a significant redistribution of the electronic density of hybridized states within the HF approximation beside the Local Density Approximation. So it seems to be essential to take into account the non-local exchange interaction to calculate the electronic structure of endohedral complexes.

[1] J.R. Heath, S.C. O'Brien, Q. Zhang et al., *J. Am. Chem. Soc.* **107**, 7779 (1985).
[2] V.K. Dolmatov, in *Advances in Quantum Chemistry. Theory of Confined Quantum Systems*, eds. by J.R. Sabin and E. Brändas (Academic, New York, 2009), vol. 58, pp. 13-68.
[3] M.E. Madjet, H.S. Chakraborty and S.T. Manson, *Phys. Rev. Lett.* **99**, 243003 (2007).

Fullerene C_{70} triplet zero-field splitting parameters revisited from light-induced EPR spectra at thermal equilibrium

Uvarov M.N.[1]*, Kulik L.V.[1], Pichugina T.I.[1], Dzuba S.A.[1,2]

[1]*Institute of Chemical Kinetics and Combustion, 630090, Institutskaya 3, Novosibirsk, Russia*
[2]*Novosibirsk State University, 630090, Pirogova 2, Novosibirsk, Russia*
**e-mail: uvarov@kinetics.nsc.ru*

X-band continuous wave (CW) electron paramagnetic resonance (EPR) and echo-detected (ED) EPR spectra of triplet state of fullerene C_{70} in decaline, o-terphenyl, toluene and toluene-d_8 molecular glasses, and in polymethylmethacrylate (PMMA) polymer were obtained under continuous light illumination. At temperatures below 30 K EPR spectra correspond to a non-equilibrium polarization within spin sublevels of $^3C_{70}$. Above 30 K the spectra are characteristic for Boltzmann equilibrium. $^3C_{70}$ CW EPR spectra at 77 K were simulated fairly well using distribution of the zero-field splitting D and E parameters. These distributions may be caused by inhomogeneity of the glassy matrix surrounding, which influences the Jahn-Teller distortions of $^3C_{70}$ molecules (D-strain and E-strain). In addition to the broad triplet line, a narrow line in the center of CW EPR spectrum was observed, its nature is briefly discussed.

ED EPR spectrum obtained at the same conditions has a narrow hole in the center of the spectrum. With increase of the microwave pulse power this hole transforms into a single narrow absorptive line. Numerical simulations by density matrix formalism confirm that the central hole originates from a simultaneous excitation of both allowed electron spin transitions of the triplet, because of their degeneracy at this spectral position [1].

[1] M.N. Uvarov, L.V. Kulik, T.I. Pichugina, S.A. Dzuba, Spectrochimica Acta Part A: Molecular and Biomolecular Spectroscopy, DOI: 10.1016/j.saa.2011.01.047 (2011)

Ion tieatment influence on operation of field emitters with nanostructured fullerene coatings

Tumareva T.A., Sominski G.G.*, Svetlov I.A., Panteleev I.S.

Saint-Petersburg State Polytechnical University, 195251, Russia
**e-mail: sominski@rphf.spbstu.ru*

Field emitters are attractive for use in many types of electron devices. But now, these emitters are applied mainly in ultrahigh vacuum, low-voltage and low-current systems. Only in such circumstances, it is possible to minimize destructive influence of ion bombardment on the field emitters operation and so secure required durability. There is point of view, that carbon and carbon containing emitters, as well as emitters with special protective coatings from theese materials, have high stability to the ion bombardment action in high voltage devices operating at the technical vacuum conditions. However, the ion bombardment influence on such emitter functioning in high voltage facilities was insufficiently investigated.

Authors of this report worked out and investigated [1] practically prominent protective fullerene coatings for field emitters. These coatings, activated by low energy (40 -100 eV) potassium ion flow, differ from coverage of another type as they secure high current take-off (some tenth of microampere from submicron tip) at reduced operating voltages. The aim of recent work was to receive data of the mechanism and basic rules of ion bombardment effect on the activated fullerene coating characteristics.

Operation of field emitters with activated fullerene coating was studied in wide range of emission currents. It was shown that the treatment by potassium ion flow might be used not only for decrease of its work function value but also for increase of distributed protrusion structure uniformity on the coverage surface. Besides, important information was obtained about emitter functioning at heightened pressures and intense bombardment by the residual gas ions. Investigations in technical vacuum (10^{-6}–10^{-7} Torr) revealed the unknown earlier phenomena of self-reproducibility of distributed nanostructures on the activated fullerene coatings at intense ion bombardment conditions. Thanks to this mechanism, it became possible to obtain considerably more maximal currents at intense residual gas ion bombardment than at high vacuum conditions.

This work is supported by the RFBR grant 11-02-00425.

[1] T.A. Tumareva, G.G. Sominski, I.A. Svetlov, A.N. Morozov, *Technical Physics* **53**(11), 1504 (2008).

Catalytic synthesis of heteroatom-containing homo- and methanofullerenes

Tuktarov A.R.*, Korolev V.V., Khuzin A.A., Dzhemilev U.M.

Institute of Petrochemistry and Catalysis of RAS, 450075 Ufa, Russia
**e-mail: ink@anrb.ru*

In the report, the efficient methods for selective cycloaddition of heteroatom- containing diazoalkanes to carbon clusters assisted by three-component catalytic system $Pd(acac)_2$-PPh_3-Et_3Al are presented. The developed methods allow the synthesis of individual homo- and metanofullerenes with high yields and selectivity.

Cycloaddition of S-containing diazoalkanes, generated *in situ* by oxidation of hydrazones of keto sulfides with MnO_2, to [60]fullerene (20 °C, 1 h) assisted by the catalyst $Pd(acac)_2$-$2PPh_3$-$4Et_3Al$ leads to 5,6-open cycloadducts **1a** and **1b** in 70% yield with high selectivity. Analysis of ^1H and ^{13}C NMR spectral data showed that more bulky substituents at the bridge carbon atom in homofullerene **1** are located above the five-membered fragment of the C_{60} molecule.

In order to expand the application area of the developed catalytic method for cycloaddition of diazoalkanes to [60]fullerene, in this reaction heterocyclic diazo compounds have been involved. The study has revealed that the interaction between hydrazones of furfural, methyl furyl or thienyl methyl ketones and C_{60} under optimized conditions (20 °C, 1 h, 20 mol % $Pd(acac)_2$-$2PPh_3$-$4Et_3Al$) was found to produce methanofullerenes **2, 3** and **4**. Similar results were obtained in the case of hydrazone tiochroman-4-one. Due to its oxidative stability, hydrazone of 2-acetyl-N-methyl pyrrole remains inert in this reaction and does not produce the desired diazo compound.

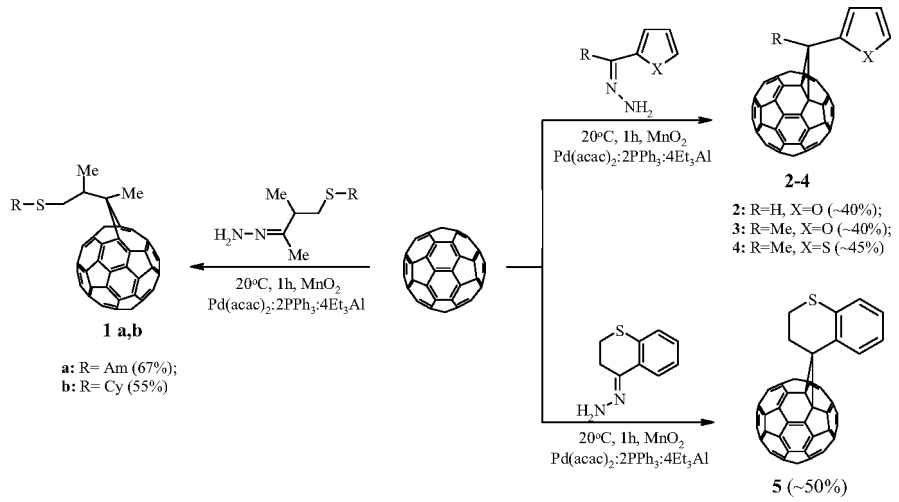

This work was supported financially by the FTP "Scientific and pedagogical staff of innovative Russian (Grant No. P1218).

Effective synthesis of methano- and pyrazolinofullerenes

Tuktarov A.R.*, Khuzina L.L., Dzhemilev U.M.

Institute of Petrochemistry and Catalysis of RAS, 450075 Ufa, Russia
**e-mail: ink@anrb.ru*

In the present report, a synthetic approach to the selective synthesis of methano- and pirazolinofullerenes with potential biological activity through cycloaddition of the synthesized on the basis of farmaco-significant compounds diazoacetates to the C_{60} carbon clusters in the presence of the three-component catalyst $Pd(acac)_2$-PPh_3-Et_3Al is discussed. In this study, α-tocopherol, trolox, 20,29-dihydro betulinic and ursolic acids were used as pharmacophores.

Thus, the reaction of diazoacetates, derived from α-tocopherol and methyl ester of 20,29-dihydro betulinic acid, with [60]fullerene (*o*-dichlorobenzene, ~ 80°C, 1.5 h) assisted by the $Pd(acac)_2$-PPh_3-Et_3Al (1:2:4) catalyst leads to the corresponding fulleropirazolines **1** and **2** in the yields of 45 and 50% respectively. A change in the Pd:P:Al catalyst component ratio from 1:2:4 to 1:4:4 favors the formation of individual methanofullerenes **3** and **4**. It is shown that the synthesized fulleropirazolines **1** and **2** are quite stable compounds and do not undergo any change even after boiling them in toluene for a day.

Metanofullerenes **5** and **6** have been exclusively obtained, when diazoacetates synthesized on the basis of the methyl esters of trolox and ursolic acid, were used in the reaction assisted by the catalytic system $Pd(acac)_2$-PPh_3-Et_3Al with a component ratio of 1:2:4.

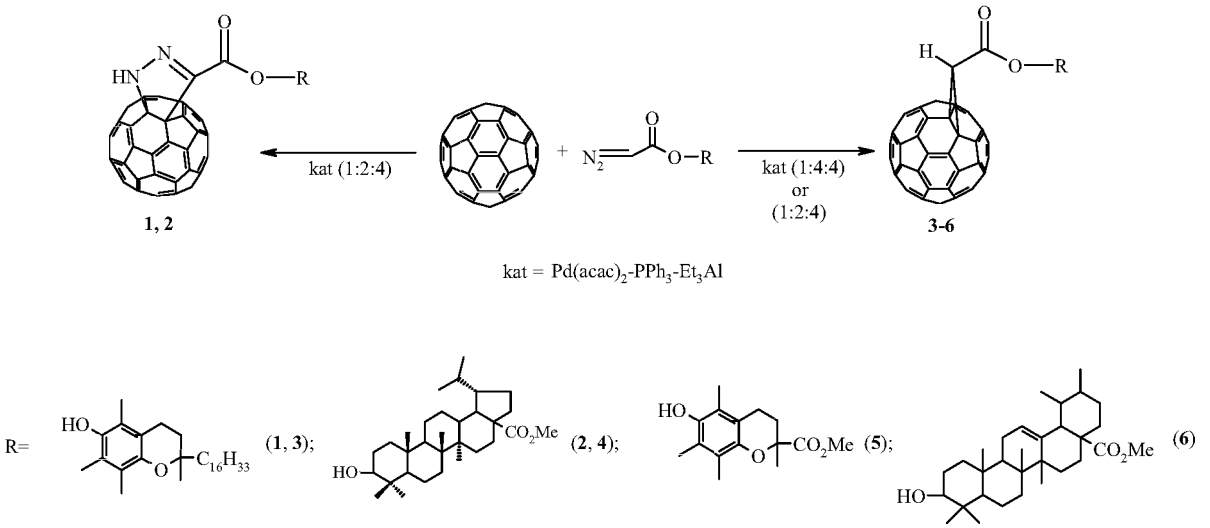

This work was supported financially by the FTP "Scientific and pedagogical staff of innovative Russian (Grant No. P1218 and No. 14.740.11.0014).

Tubular fullerenes inside carbon nanotubes: optimal molecular orientation versus tube radius

Tarakina N.V.*[1], Verberck B.[2]

[1]*Physikalisches Institut, Universität Würzburg, Am Hubland, D-97074 Würzburg, Germany*
[2]*Departement Fysica, Universiteit Antwerpen, Groenenborgerlaan 171, B-2020 Antwerpen, Belgium*
**e-mail: nadezda.tarakina@physik.uni-wuerzburg.de*

Fullerene nanopeapods — carbon nanotubes (CNTs) filled with fullerene molecules — are one of the best-known exponents of materials exhibiting one-dimensional (1D) molecular confinement. The first reported instance of nanopeapods was the observation of C_{60} molecules encapsulated in single-walled CNTs (SWCNTs) [1]. The cylindrical hollow space offered by SWCNTs (the diameter of which can be as small as 4.3 Å [2]) has proven to be a unique environment for studying both experimentally and theoretically the physics and chemistry of 1D arrangements of atoms and molecules [3]. In this work, we focus on the encapsulation of molecules of the family of tubular fullerenes C_{90}, …, C_{200} and investigate their positions and orientations in the CNT [4]. We find that increasing the tube radius leads to the following succession of energetically stable regimes: (1) lying molecules positioned on the tube's long axis; (2) tilted molecules on the tube's long axis; and (3) lying molecules shifted away from the tube's long axis. As opposed to C_{70} and C_{80} molecules encapsulated in a SWCNT [5], standing orientations do not develop. Our results are relevant for the possible application of molecular-orientation-dependent electronic properties of fullerene nanopeapods [6], and also for the interpretation of future experiments on double-walled carbon nanotube formation by annealing fullerene peapod systems.

[1] B.W. Smith, M. Monthioux, D.E. Luzzi, *Nature* **396**, 323 (1998).
[2] T. Hayashi, Y.A. Kim, T. Matoba, M. Esaka, J. Nishimura, T. Tsukada, M. Endo, M.S. Dresselhaus, *Nano Lett.* **3**, 887 (2003).
[3] M. Monthioux, E. Flahaut, and J.-P. Cleuziou, J. Mater. Res. **21**, 2774 (2006); R. Kitaura and H. Shinohara, *Chem. Asian J.* **1**, 646 (2006).
[4] N.V. Tarakina and B. Verberck, *Eur. Phys. J. B* (in press).
[5] B. Verberck, *Phys. Rev. B* **83**, 045405 (2011).
[6] S. Okubo, T. Okazaki, K. Hirose-Takai, K. Suenaga, S. Okada, and S. Bandow, *J. Am. Chem. Soc.* **132**, 15252 (2010).

On solvent impurity in commercial fullirites

Tamm N.B.[1], Skokan E.V.*[1], Karnatsevich V.L.[2], Polyakova M.V.[1], Tarasov V.P.[1], Chelovskaya N.V.[1], Kirillov A.I.[2], Arkhangelsky I,V.[1]

[1]*Chemistry Department, Moscow State University, 119991, Moscow, Russia*
[2]*JSC "Fullerene Centre",603000, Nizhny Novgorod, Kostina st., 4, Russia*
**e-mail: skokan@phys.chem.msu.ru*

It is known that a solvent present in the solid commercial samples of C60 affects many of their physical and chemical properties (structural parameters, conductivity) and as a consequence on the course of solid-state reactions. Recently information emerged about the effect of solvent impurities on the process of fine synthesis in liquid phase. This forced us to return to the problem of the solvent content of fullerenes. Not all manufacturers of fullerenes indicate solvent content in the samples sold due to various reasons, namely, they are not able to identify small impurities, hide their know-how. However, the solvent content in poorly dried samples can be as high as a few percent for the C60 up to 15% in the C70.On the other hand, the issue can be raised in a practical way: whether to hold a vacuum drying of samples or is it extra cost.

A series of samples of C60 and C70 with different solvent contents were investigated by the TG-IR analysis of gaseous products, HPLC, XRD, and ^{1}H (^{13}C) NMR, IR, UV, MALDI spectroscopic methods. Nevertheless, the problem of determining the interaction of the impurities of the solvent with fullerite remained open. To investigate the behavior of these solvents in chemical reactions and in particular their interaction with fullerene improved techniques for analyzing organic contaminants in fullerites C60, C70 are required.

Diffusion model of low-energy secondary electrons in fullerite and other solids

Suslova I.B.*[1], Mikoushkin V.M.[2]

[1]*SPb State polytechnical university, 195251, St.-Petersburg, Russia*
[2]*Ioffe Institute, 194021, St.-Petersburg, Russia*
**e-mail: ibsus@mail.ru*

Low-energy secondary electrons can play an important role in forming the image in the fullerite based electron lithography [1], in cathodoluminescence [2] and in polymerization and modification of organic materials [3]. Therefore description of the behavior of the low-energy secondary electrons in solids is an actual task. This task has been solved here in the frame of the model of electrons generated in the layer with the thickness h and diffused everywhere. The following diffusion problem has been considered by integral transformation method:

$$\frac{\partial^2 U(x,t)}{\partial x^2} - \frac{1}{D}\frac{\partial U(x,t)}{\partial t} = -\frac{\alpha(x)}{D}\ ;\ \left.\frac{\partial U(x,t)}{\partial x}\right|_{x=0} = 0,\ U\big|_{t=0} = 0,\ 0 \le x < \infty,\ \ t \ge 0\ ,$$

where $U(x,t)$ – the concentration of secondary electrons, D – the diffusion coefficient. Generation rate of secondary electrons $\alpha(x) = \begin{cases} \alpha_0 = const,\ 0 < x < h \\ 0,\ x > h \end{cases}$.

The solution may be represented in the analytical form:

$$U(x,t) = \frac{\alpha_0}{2}\cdot\begin{cases} 2\cdot t - F(t,\beta_1) - F(t,\beta_2), x \le h \\ F(t,-\beta_1) - F(t,\beta_2), x \ge h \end{cases}, \text{ where}$$

$$F(t,\beta) = (t+\beta^2)Erfc\,(\beta/2\sqrt{\tau}) - \beta\frac{\sqrt{t}}{\sqrt{\pi}}\ell^{-\beta^2/4t}\ ,\ \beta_{1,2} = {(h \pm x)}\Big/{\sqrt{D}}\ .$$

The important result is that the electron concentration $U(x,t)$ is proportional to the thickness h of the electron generation area which may be estimated as the electron projected range $h \sim R \sim E_o^{1.67}$ [2] of the primary electrons irradiating the surface with energy E_o. Thus the concentration of secondary electrons $U(x,t)$ proved to be a monotonously increasing function of the primary electron energy E_o.

This result was applied to the process of fullerite C_{60} polymerization used in electron-beam lithography. Fig. 1 shows the dependence $U(E_o)$ at $x=0$, $t=T$ for fullerite as well as the experimental energy dependence $\sigma(E_o)$ of the chemical bond generation rate in the process of fullerite polymerization induced by irradiating electrons. Fig. 1 shows that the monotonously increasing experimental energy dependence $\sigma(E_o)$ can be explained by the increasing concentration of secondary electrons in the frame of the model of an electron swarm diffusing to the surface from the bulk. The research was supported by the Russian Foundation for Basic Research (RFBR), Project № 10-07-00508-a.

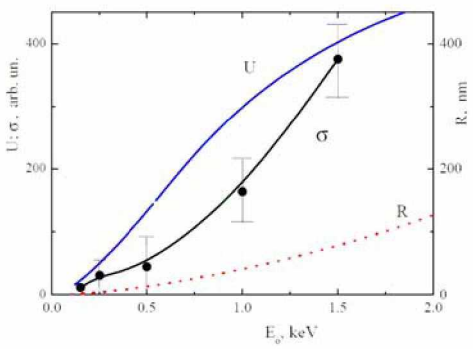

[1] V.N.Nevedomsky et al., *Fullerenes, Nanotubes and Carbon nanostr.* **16**, 682 (2008).
[2] Kanaya, K., and Okayama, S., *J. Phys. D: Appl. Phys.* **5**, 43 (1972).
[3] V.V.Shnitov, V.M.Mikoushkin, S.Yu.Gordeev, *Phys. Solid State* **44**, 428 (2002).

Endohedral derivatives of fullerenes and their formation

Madjuga A.M., Gal'pern E.G., Stankevich I.V.

Nesmeyanov Institute of Organoelement Compounds, Russian Academy of Science, Moscow, 119991, Russia

Methods of synthesis of endohedral derivatives of fullerene C_{60} was discussed. Particular attention is spare to the works in which mechanism of windows was used. Several examples functionalization of fullerene C_{60} were considered and shown as can diminish activation energy for penetrate atom He in carbon cage (or for outlet atom He from cage). Energies of the transition states for some such reactions were calculated. Results obtained can be used at plan ot synthesis of new endohedral derivatives of fullerene C_{60}. and other polyhedral carbon clusters.

Comparative characteristics of electrical and photoelectrical properties of Si/fullerite C_{60} and Si/nanocomposite fullerite C_{60}:Me (Me=Cu, Al, Sn and Te) heterostructures

Spoiala D.*, Evtodiev I., Prilepov V.

Moldova State University, MD-2009, Chisinau, Moldova
**e-mail: spodor@usm.md*

The electronic structure and optical properties of fullerite C_{60} thin films are suitable for using in efficient heterojunction solar cells and similar devices. Heterojunction behaviour with high rectifying ratio in the dark ($k>10^4$ at ± 2 V) and photovoltage generation were demonstrated, firstly, for a *p*-Si/C_{60} interface. Both isotype *n*-Si/C_{60}/M and anisotype *p*-Si/C_{60}/M heterojunctions (where M=Al, Au, Ti, Nb, etc. are top metallic electrodes) are studied by many scientific groups [1-3]. But very intrinsic conductivity of C_{60} thin film ($\sigma \sim 10^{-10}$-10^{-14} Ω·cm) is considered as one of the main limiting factors for Si/C_{60} solar cell efficiency. Therefore, "doping" of fullerite C_{60} is one the principal challenges for high efficiency fullerene-based solar cell production [1].

This work presents the results of research on electrical and photo-electrical properties of heterostructures Si/fullerite C_{60} and Si/nanocomposite fullerite C_{60}:Me (where Me=Cu, Al, Sn and Te) with various concentrations of Me. For the heterostructures Si/C_{60} and Si/C_{60}:Me obtaining, 4 types of silicon plates have been used: *n*-type crystalline Si wafers (111) (doped with P, 0.3 and 4.5 Ω·cm) and *p*-type crystalline Si wafers (111) (doped with B, 0.1 and 10 Ω·cm). Thin films of fullerite C_{60} (d~0.1–0.5 μm) were obtained by vacuum sublimation of C_{60} powder. Fullerite C_{60}:Me thin films (d~0.05–0.5 μm) have been prepared by simultaneous deposition of Me and fullerite C_{60} by double-source coevaporated system. Separately electrical and optical properties of fullerite C_{60}:Me films have been studied. The surface structures of fullerite C_{60} and fullerite C_{60}:Me thin films have been studies with atomic force microscope.

Current-voltage characteristics for all obtained heterostructures in darkness and under light illumination are obtained. The analysis of experimental dark current-voltage characteristics is performed being taken into account in the equivalent circuit of heterostructures of series and shunt resistances. At light illumination a photovoltaic effect for all types of obtained heterostructures is observed. The comparative analysis of electrical and photo-electrical properties of Si/fullerite C_{60} and Si/fullerite C_{60}:Me heterostructures has been performed.

[1] E.A.Katz, *Physics of the Solid State* **44**, 621 (2002).
[2] K.M. Chen, Y.Q.Jia, S.X.Jin, K.Wu, X.D.Zhang W.B.Zhao, C.Y.Li, Z.N.Gu, *J.Phys.: Cond. Matter.* **6**, L367 (1994).
[3] C.Wen, T.Aida, I.Honma, H.Komiyama, K.Yamada, *Denki Kagaku* **62**, 264 (1994).

Analysis of electron-induced fullerite C_{60} modification in terms of destruction cross-section

Shnitov V.V.*, Mikoushkin V.M.

Ioffe Institute, 194021, St. Petersburg, Russia
**e-mail: v.shnitov@mail.ioffe.ru*

Despite the noticeable number of the works investigating electron beam induced destruction of individual fullerenes C_{60} [1] and respective modification of solid fullerite C_{60} [2,3], some important aspects of this process is still weakly studied. In particular, a widely accepted model considering e-induced destruction of solid fullerite as a successive fragmentation of non-interacting fullerenes [2], has, in our opinion, insufficiently reliable experimental verification and incorrectly interprets basic mechanisms of this process.

The aim of present work was to check the validity of above mentioned model by comparison of a well-established energy dependence of cross-section $\sigma_F(E)$ [1] describing e-induced fragmentation of individual fullerenes C_{60} with respective dependence of effective cross-section $\sigma_D(E)$ specifying destruction of solid fullerite C_{60}. The last cross-section was obtained in this work on the basis of the electron energy loss spectroscopy (EELS) and special processing technique using some peculiarities of fullerite EEL spectra and suggested in our early work [3]. Both cross-sections are shown in the inserted figure. They demonstrate completely different behavior, which reveals not only in substantial from 5 to 2 orders of magnitude difference between their absolute values, but also in obviously inverse types of their energy dependencies. These facts allowed us to conclude that real e-induced destruction of solid fullerite C_{60} drastically differs from hypothetic one predicting by the model of successive fragmentation of separate fullerenes [2] and that this model is indeed invalid. They also indicate that radiation stability of condensed fullerenes C_{60} appeared to be radically higher than it follows from the model of non-interacting assembly of fullerenes and than it was expected earlier.

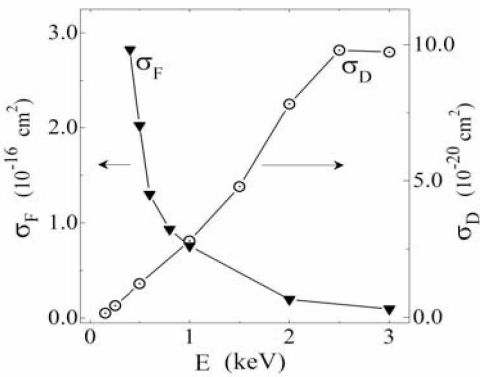

Experimental cross-sections of e-induced fragmentation of separate fullerenes C_{60} (σ_F), taken from [1] and of e-induced destruction of solid fullerite C_{60} (σ_D), obtained in this work.

The research was supported by the Russian Foundation for Basic Research (RFBR) Project № 10-07-00508-a, by Presidium of RAS Program and by the St. Petersburg Joint Research Center "Material science and diagnostics in modern technologies" equipment.

[1] Itoh A., Tsuchida H., Miyabe K., Majima T., Imanishi N., *J. Phys. B.* **32**, 277 (1999).
[2] Hunt M.R.C., Schmidt J., Palmer R.E., *Phys. Rev. B.* **60**, 5927 (1999).
[3] Shnitov V.V., Mikoushkin V.M., Bryzgalov V.V., Gordeev Yu.S., *Phys. Sol. St.* **44**, 444 (2002).

Anomalous survival of endometallofullerenes under irradiation in reactor

Grushko Yu.S., Lebedev V.T., Shilin V.A.*, Sedov V.P., Kozlov V.S., Kolesnik S.G.

Petersburg Nuclear Physics Institute, 188300 Gatchina St.Petersburg distr., Russia
**e-mail: shilin@pnpi.spb.ru*

The mechanisms determining the anomalous stability of carbon cages of endometallofullerenes by neutron irradiation have been studied. There were synthesized the row of endometallofullerenes $Ln@C_{2n}$ and their water-soluble biocompatible derivatives. It was established the influence of neutron irradiation on stability and nuclear physical properties of endometallofullerenes and their derivatives being applicable in nuclear medicine, including ^{46}Sc, ^{140}La, ^{141}Nd, ^{153}Sm, ^{152}Eu, ^{154}Eu, ^{153}Sm, ^{160}Tb, ^{169}Yb, ^{170}Tm (isomers I and III), ^{177}Lu. Some of them are studied for the first time ($^{46}Sc_3N@C_{80}$; $^{141}Nd@C_{2n}$). Earlier it was revealed an anomalously high retention for a mixture of empty and endometallofullerenes of Sm in reaction $^{152}Sm@C_{2n}$ (n, γ) $^{153}Sm@C_{2n}$ (~80 %) [1]. However, $^{152}Sm@C_{82}$ chromatographically separated has shown in (n, γ)-reaction the magnitude of the retention of 17,5% that is typical for rare earths. It was confirmed our hypothesis proposed earlier [2] concerning the mechanism of the relaxation of carbon shell based on ultrafast non radiative processes (electrons "shake-off") [3].

The fullerenes medical applications assume the preliminary transformation of fullerenes into biocompatible water-soluble form. However, it is well known, that hydroxofullerenes in water solutions trend to be aggregated. For the control over processes of clustering (coalescing) and temporary stability of solutions hydroxofullerenes the small-angle neutron scattering method has been applied. The discussed results can become a basis for the creation of industrial effective preparations with nanomaterials.

[1] Grushko Yu. S., Alekseev E.G., Voronin V.V., Kolesnik S.G., Kolesnik S.N., Pershikova T.M., *Molecular Materials* **7**, 115 (1996).

[2] Grushko Yu.S., Khodorkovski M.A., Kozlov V.S. Kolesnik S.G., Shilin V.A., Grachev S.A., Artamonova T.O., *Fullerenes, Nanotubes and Carbon Nanostructures* **14**, 249 (2006).

[3] Averbukh V., Cederbaum L.S., *Phys. Rev. Lett.* **96**, 053401 (2006).

Solubility behaviour of C_{60} in N-methylpirrolidon

Shiliaeva L.A.[1], Korobov M.V.* [1], Avdeev M.V. [2], Senyavin V.M.[1], Semenyuk P.I.[3]

[1]*Department of Chemisry, Moscow State University, 119899, Moscow, Russia*
[2]*Joint Institute for Nuclear Research, Dubna, Moscow reg., Russia*
[3]*Department of Bioengineering and Bioinformatics, 119991, Moscow State University, Moscow, Russia*
**e-mail:mkorobov49@gmail.com*

Solubility of C_{60} in N-methyl-2-pirrolidon (NMP) is a puzzle. It has long been known that UV-visible spectrum of C_{60}-NMP solution undergoes dramatic change in time [1]. This change may be attributed to the formation of C_{60} van-der-Waals clusters/C_{60}-NMP charge transfer complexes in the solution. Reasonable mechanism of the process is not established so far.

This study was focused on the stability of C_{60} monomers in NMP. Almost saturated concentration of monomers in NMP was obtained by gentle dissolution of C_{60} or by its extraction from alkenes. Monomers were easily extracted from NMP to alkenes (hexane, cyclohexane and octane) and back from alkenes to NMP. Extinction coefficients for C_{60} monomers in NMP were determined at different wavelengths. Abrupt fall of monomer's concentration in saturated solution is due to interaction of NMP with the surface of solid C_{60}. After addition of fresh solid C_{60} monomeric species re-appear in the solution.

Simple kinetic model was put forward to account for the results obtained. It involves successive processes of dissolution of C_{60} in the form of monomers, step aggregation of C_{60} in NMP, slow process of interaction of C_{60} with NMP, which terminates both growth of C_{60} clusters in the solution and dissolution of solid C_{60}.

The model represents evolution of UV-spectra of C_{60} – NMP saturated solution in time to a reasonable degree of approximation.

[1] Yevlampieva N.P., Biryulin Yu.F., Melenevskjaja E.Yu. et al., *Colloids and surfaces A* **209**, 167 (2002).

Reaction barriers and deformation energies of C_{60}-based composites

Sheka E.F.*, Shaymardanova L.Kh.

Peoples' Friendship University of Russia, 117198 Moscow, Russia
**e-mail: sheka@icp.ac.ru*

The current paper is aimed at the determination of barriers that govern the covalent coupling between two fullerenes C_{60} (C_{60} dimer), C_{60} and single-walled carbon nanotube ([C_{60}-(4,4)] carbon nanobud), and C_{60} and graphene ([C_{60}-(5,5)] and [C_{60}-(9,8)] graphene nanobuds). *Brutto* barriers determined as couplings energies E_{cpl}^{tot} are expanded over two contributions that present total energy of deformation of the composites' components E_{def}^{tot} and energy of covalent coupling E_{cov}^{tot}. In view of these energetic parameters and in contrast to expectations, seemingly identical reactions result in different final products. The peculiarity is suggested to be provided by a topochemical character of the covalent coupling between any two members of the sp^2 nanocarbons' family. The computations were performed by using the AM1 semiempirical version of unrestricted broken symmetry Hartree-Fock approach.

Concentration and separation of high fullerenes

Sedov V.P.*, Kukorenko V.V., Kolesnick S.V., Shilin V.A., Grushko Yu.S.

Petersburg Nuclear Physics Institute, 188300, Gatchina, St.Petersburg distr., Russia
**e-mail: sedov@gtn.ru*

Recent activity at PNPI in the field of advanced technologies and production of high fullerenes is presented in this review of experimental results demonstrating substantial adventures in the enrichment of the mixtures of fullerenes in solutions. The mixtures of fullerenes C_{60}, C_{70} containing also ~ 4 wt.% of high mass fullerenes (C_{76}, C_{78}, C_{82}, C_{84} etc.) were obtained by the method of graphite evaporation in electric arc in helium atmosphere. First there was proposed a simple and effective method allows concentrate the fractions being enriched with high fullerenes. The method is based on different solubility of fullerenes in various organic solvents. The process employs the chromatographic column filled with graphite material and organic solvent as a mobile phase that enables to realize the two-stage separation. In the first stage, toluene serves as a mobile phase, and in the second one, 1,2,4-trimethylbenzen is used. As a result, in the second stage the eluate is strongly enriched with high fullerenes (70-80 wt.%). A typical HPCL chromatogram showing a big content of high fullerenes is presented in figure below.

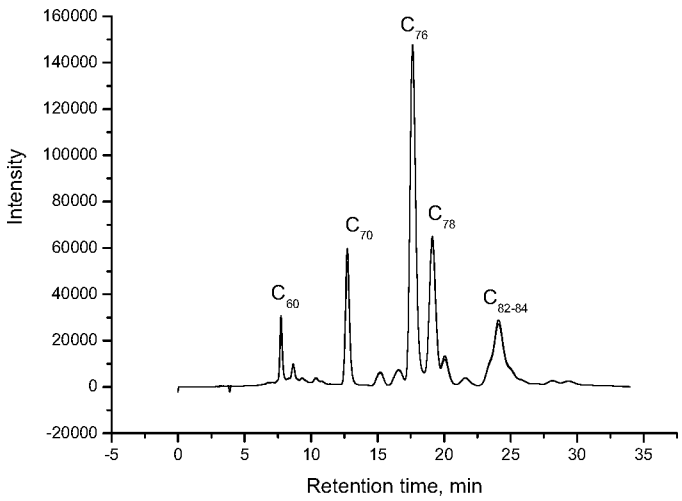

Chromatogram: peaks corresponding various high fullerenes are shown.

CF_2-derivatives of C_{70}: synthesis and structure

Samoylova N.A.*, Semivrazhskaya O.A., Belov N.M., Markov V.Yu., Ovchinnikova N.S., Goryunkov A.A.

Lomonosov Moscow State University, 119991, Moscow, Russia
**e-mail: natalivrn@gmail.com*

Fine tuning of electron properties of fullerene derivatives is an actual problem for the nowadays. One of the possible ways of such tuning is insertion of electron withdrawing units into fullerene cage. Impressive example of it is difluoromethylene homofullerenes $C_{60}(CF_2)_n$, n=1-3, which were synthesized [1] and found as prospective materials for organic electronic applications [2]. The synthesis and structure of the difluoromethylated derivatives of fullerene C_{70} are reported in the present work for the first time.

Difluoromethylated derivatives C_{70} were obtained by refluxing of fullerene C_{70} and sodium difluorochloroacetate solution. Product composition and dynamic of the reaction were monitored by means of HPLC and MALDI mass spectrometry. We observe formation of $C_{70}(CF_2)_n$, where n is 1-4. Three isomers of $C_{70}(CF_2)$ were isolated from prepared mixtures by means of HPLC. Structures of two major isomers of $C_{70}(CF_2)$ were suggested on the basis of NMR spectroscopy data and quantum chemical calculations. Addition of CF_2 group occurs at [6,6]-double bonds of the polar region C_{70} in both cases (see figures below). According to the quantum chemical calculations (DFT, PBE/TZ2P), distance between carbon atoms, carrying CF_2-bridge, is 1.72 and 2.08 Å, correspondingly for isomers $C_{70}CF_2$ **I** and **II**. Thus, isomer **I** is a methanofullerene, while isomer **II** demonstrates homofullerene features (also it was justified by UV/Vis spectroscopy).

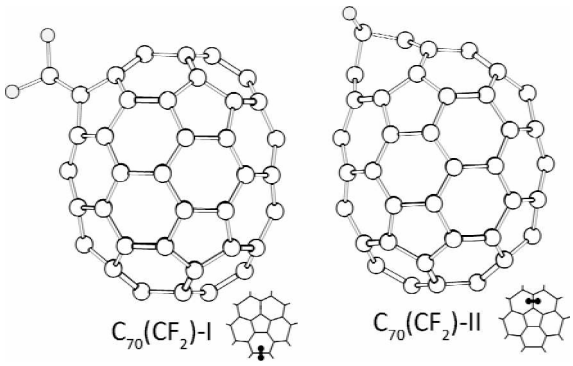

Structures of the $C_{70}(CF_2)$-I and $C_{70}(CF_2)$-II; the fragments of corresponding top views (across former C_5 axe of C_{70} fullerene) are shown on insets.

[1] A.S. Pimenova, A.A. Kozlov, A.A. Goryunkov, V.Yu. Markov, P.A. Khavrel, S.M. Avdoshenko, I.N. Ioffe, S.G. Sakharov, S.I. Troyanov, L.N. Sidorov, *Chem. Commun.* 374 (2007).

[2] K. Tokunaga, S. Ohmori, H. Kawabata, *Thin Solid Films* **518**, 477 (2009).

Thermochemical characterization of the seven C_{80} isomers by means homodemotic reaction

Salcedo R.

[1]*Instituto de Investigaciones en Materiales, Universidad Nacional Autónoma de México, circuito exterior s/n, Ciudad Universitaría, 04510, Coyoacán, Ciudad de México*
email: salcedo@servidor.unam.mx

The relative energy of stabilization for the seven isomers of C_{80} was computed by means of the next homodesmotic reaction [1].

$$\frac{n}{3}\ H_2C{=}CH\text{-}CH{=}CH_2 + \frac{n}{6}\ \mathrm{TVE} \rightarrow C_n + n\ H_2C{=}CH_2$$

The obtained values show which the scale of stability is and which the thermodynamically most stable isomer is. A discussion about these results and other known propositions is presented.

[1] a) Salcedo, R. & Fomina, L., *Tetrahedron Lett.* **48**, 3949 (2007); b) Salcedo R., Fomina L., Corrigendum, *Tetrahedron Lett.* **48**, 7731 (2007).

Polarizability of fullerene derivatives

Sabirov D.Sh.*, Garipova R.R., Bulgakov R.G.

Institute of Petrochemistry and Catalysis of RAS, 450075, Ufa, Russia
**e-mail: diozno@mail.ru*

At the moment there are diverse methods of synthesis of fullerene derivatives (**FD**) with various numbers of addends controlled via reaction conditions, use of catalysts *etc*. **FD** (especially, polar derivatives, such as epoxides or fluorides) are promising compounds for nanomaterials, nanodevices, and medicine. Intermolecular interactions underlie the functioning of the mentioned applications of fullerene containing systems and, while the polarizability determines the intermolecular interactions, its investigations are the base for understanding the mechanisms of processes which fullerenes and its derivatives take part in.

In the present study the diagonalized tensors of polarizability, average polarizability and anisotropy of polarizability (a^2) for series of **FD** ($C_{60}O_n$ and $C_{70}O$ epoxides, $C_{60}(CH_2)_n$ fullerenocyclopropanes, $C_{60}(NH)_n$ fullerenoazyridines, $C_{60}F_m$ and $C_{70}F_k$ fluorofullerenes, and others) have been calculated by PBE/3z density functional method.

This method has been tested on several model molecular systems (including fullerenes C_{60} and C_{70}) and showed a good agreement of calculated results with experimental data. Polarizabilities of fullerene polyadducts have been calculated both quantum-chemically (α_{qc}) and by additive scheme (α_{add}) *via* expressions:

$$\alpha_{add}(C_{60/70}X_n) = \alpha_{qc}(C_{60/70}) + n\alpha_{qc}(X), \text{ where } \alpha_{qc}(X) = \alpha_{qc}(C_{60/70}X) - \alpha_{qc}(C_{60/70}).$$

The difference $\Delta\alpha = \alpha_{add} - \alpha_{qc}$ shows the inadditivity of polarizability and increases with the increase of number of X added to fullerene.

Analyzed the average α values, we can formulate the following regularities:

1) Polarizabilities of exohedral **FD** are higher than those of respective pristine fullerenes.
2) Polarizabilities of 5.6 open isomers of **FD** are higher than those of respective 6.6 closed isomers.
3) The functionalization of C_{60} is accompanying with the increase of anisotropy of polarizability and in the case of C_{70} either increasing or decreasing of a^2 value are possible (e.g., a^2 increases upon C_{70} epoxides formation but become smaller if oxahomo[70]fullerenes are formed).
4) Regio-isomers of $C_{60/70}X_n$ are characterized with the approximately equal average polarizabilities and differ with the anisotropy values.
5) The inadditivity of polarizability of polyadducts $C_{60/70}X_n$ with $n = 3$ appears ($\Delta\alpha > 0$) and increases with the increase of n values (*e.g.*, the polarizability of $C_{60}O_n$ epoxides achieves maximal value 87.4 E^3 at $n = 15$ and then diminishes to 85.3 E^3 for $n = 30$).

A theoretical model of the **FD** polarizability has been proposed. It should be taken into account in the design of fullerene derivatives with high polarizability.

The work was supported by the Presidium of RAS (programme No. 21).

Generalized theoretical approach to the estimation of fullerenes reactivity in the reactions of addition based on curvature indices

Sabirov D.Sh.*, Garipova R.R., Bulgakov R.G.

Institute of Petrochemistry and Catalysis of RAS, 450075, Ufa, Russia
**e-mail: diozno@mail.ru*

Earlier we have worked out the theoretical approach to estimation of fullerenes reactivity towards ozone and diazomethane with the use of curvature indices [1] and then applied it to some C_{60} derivatives.

In the present paper, to determine the general regularities of the addition to fullerenes we have analyzed parameters of correlation equations for reactions of [2+*n*]-cycloaddition and radical addition. In the framework of the approach, a linear equation (See the Table)

$$\Delta H_r^\circ = B + Ak$$

has been assigned for each reaction. Here ΔH_r° is a heat of reaction calculated by PBE/3z density functional method; k is a curvature index of reaction site calculated as $k = 2\sin\theta / a$, (a – average internuclear distance between reaction site of the fullerene molecule and its neighboring atoms, θ – pyramidalization angle). Parameters B can be interpreted as heats of addition of molecules (radicals) to hypothetic reaction site with zero curvature. Parameters A determine the slope of linear correlations and lie in the intervals which are characteristic for the reactions of each type. Important to note that these correlations unite reactions of fullerenes with both isolated (C_{60}, C_{70}, C_{76}) and shared pentagons (C_{20}, C_{24}, C_{30}, C_{36}, C_{40}). So, they could be considered as common features of carbon clusters.

Table. Correlations $\Delta H_r^\circ = B + Ak$ for reactions $C_n + Y \rightarrow C_nY$.

Y	A, kJ E mol^{-1}	B, kJ mol^{-1}	*r*
[2+1]-Cycloaddition			
$:CH_2$	−528.6	253.8	0.91
:NH	−518.3	326.4	0.92
[2+3]-Cycloaddition			
HN_3	−910.1	262.9	0.80
$CH_2{=}N^+{-}CH_2^-$	−959.5	120.0	0.87
O_3	−946.4	142.4	0.96
CH_2N_2	−904.3	216.0	0.97
Radical addition [2]			
H•	−772.9	68.2	0.96
F•	−746.4	35.7	0.95

The same slopes (parameters A) of the correlations of reactions pertaining to one type allow formulating the following rule. If reactions of C_n fullerene with reactants Y_1 and Y_2 have the same mechanism and it is known that C_n shows a higher reactivity towards Y_1, than towards Y_2, then other members of the fullerenes family are more reactive towards Y_1.

So, the approach takes into account all features of the addition reactions, *i.e.* peculiarities of reaction site in a fullerene molecule (k index), type of added reactant (parameter B) and type of reaction (parameter A).

[1] Sabirov D.Sh., Khursan S.L., Bulgakov R.G., *Russ. Chem. Bull., Int. Ed.* **57**, 2520 (2008).

[2] Sabirov D.Sh., Bulgakov R.G., *Comput. Theor. Chem.*. **963**, 185 (2011).

Containing one-dimensional photonic band gap crystals

Belousova I.M., Ryzhov A.A.*

SIC Vavilov State Optical Institute, St. Petersburg, 199034, Russia
St. Petersburg State University of ITMO, St. Petersburg, 197101, Russia
**e-mail: spaar@mail.ru*

Application of devices on the base of photonic crystals with nonlinear optical properties is promising for optical switchers and optical power limiters development.

Fullerenes have strong dependence of the refraction coefficient on the irradiation intensity in the visible and near IR spectral range. The band gap of the photonic crystal with incorporated fullerene-containing films shifts while changing the intensity of irradiation. Such systems can be used as optical power limiters or switchers and at that the speed of the switching process and the power of the control signal are the functions of nonlinear media characteristics.

In this paper using the data on fullerene nonlinear properties we present results of calculations of band gap values and nonlinear band gap shifts of fullerene-containing one-dimensional crystals.

Electrochemical studies of $C_{60}(CF_2)H_2$

Rybalchenko A.[1]*, Nikitin O.M.[1], Goryunkov A.A.[1], Heinze J.[2] Magdesieva T.V.[1]

[1]*Lomonosov Moscow State University, Chemistry Department, 119991, Moscow, Russia*
[2]*Institute for Physical Chemistry, Albert-Ludwigs-University Freiburg, Albertstr. 21, 79104 Freiburg, Germany*
**e-mail: alexry@gmail.com*

Fullerenes are known as *n*-type semiconductors and have clearly defined electron-acceptor properties. These properties are used to create new materials for photovoltaic purposes. Searching of new donor-acceptor pairs is one of the ways to improve the performance of organic solar cells. Functionalization of fullerene cage using electron-acceptor addends (e.g. difluoromethylene and thrifluoromethyl groups) usually increases the electron affinity, which is depends on number of addends and its arrangement motif [1].

Electrochemical behavior of the recently synthesized $C_{60}CF_2H_2$ [2] was studied using of cyclic voltamperometry. Two irreversible peaks of $C_{60}(CF_2)H_2$ reduction are observed at the potentials of -0.5 and -0.8 V *vs* Ag/AgCl. Partial dehydrogenation of $C_{60}(CF_2)H_2$ during electrochemical reduction was observed; new reduction couples corresponding to $C_{60}CF_2^{n-/(n+1)-}$ were registered. Compound under the study demonstrates unusual electrochemical behavior depending on scanning range of potentials. The model of electrochemical processes including electrocatalytic step, based on the temperature, scan rate and concentration dependences of I_a/I_c for first and second reduction potentials was suggested.

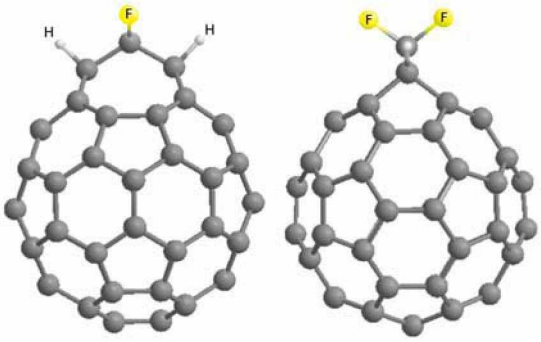

Two projections of $C_{60}(CF_2)H_2$.

[1] Popov A.A., Kareev I.E., Shustova N.B., Stukalin E.B., Lebedkin S.F., Seppelt K., Strauss S.H., Boltalina O.V., Dunsch L., *J. Am. Chem. Soc.* **129,** 11551 (2007).

[2] Goryunkov A.A., Kornienko E.S., Magdesieva T.V., Kozlov A.A., Vorobiev V.A., Avdoshenko S.M., Ioffe I.N., Nikitin O.M., Markov V.Y., Khavrel P.A., Vorobiev A.K., Sidorov L.N., *Dalton Trans.* 6886 (2008).

Thin C_{60} polymer films formed with C_{60} ions assistance, their optical, electric and magnetic properties

Razanau I.*[1], Kazachenko V.[2], Zhavnerko G.[3]

[1]*Francisk Skorina Gomel State University, 246019, Gomel, Belarus*
[2]*Belarusian State University of Transport, 246653, Gomel, Belarus*
[3]*The Institute of Chemistry of New Materials, National Academy of Sciences of Belarus, 220141, Minsk, Belarus*
**e-mail: ir23.by@gmail.com*

100-200-nm-thick films of polymerized C_{60} have been formed via electron-beam dispersion of pristine fullerite C_{60} target in vacuum. It has been shown that the active gas phase produced by the electron-beam dispersion contains neutral, excited C_{60} molecules as well as few mass per cent of positive fullerene ions. The coatings are being deposited onto the substrates under the bombardment of true secondary and backscattered primary electrons from the target holder resulting in deposition of films containing about 83% of polymerized phase (dimers, linear chains and 2D polymers). However, application of the negative electrostatic potential of 100-300 eV to the substrate during the deposition leads to bombardment of the growing coating by the accelerated fullerene ions and formation of randomly cross-linked 3D polymer network of covalently bonded C_{60} molecules.

UV-Vis absorption spectra of the deposited 3D C_{60} polymer films exhibit a broad continuum with a maximum at around 5 eV and increased absorption at low photon energies of 1-3 eV. The band gap of 3D C60 polymer films estimated using absorption edge in the UV-Vis spectra is about 2.14-2.15 eV, whereas the band gap of non-polymerized C_{60} films estimated using the same technique is about 2.34 eV.

Conductivity of the films has been measured by depositing them onto the quartz substrates with a system of 2 interdigital thin-film Ni electrodes. 3D C_{60} polymer films exhibit formation of the Schottky barrier to Ni electrods. Intrinsic resistivity of the films is about 50 Ω·cm in-situ and about 10^4 Ω·cm after the air exposure and storage under atmospheric conditions for several days. That is still considerably lower in comparison with nonpolymerized C_{60} films (10^7-10^{14} Ω·cm).

Conductive AFM studies of the 3D C_{60} polymer films have shown bimodal distribution of the surface electric properties with a low-conductive phase emerging upon storing under atmospheric conditions and day light. The films have also shown magnetic contrast, stable across the surface, in magnetic force microscopy. The content of the possible ferromagnetic contaminants in the samples is analysed and intrinsic magnetic properties of the deposited 3D C_{60} polymer films are discussed.

Formation of micrometer-scale fullerene decagonal prisms crystal: from mesocrystal to single crystal

Li H., Zhu G., Jiang Y., Qi L., Xu Z.*

State Key Laboratory of Coordination Chemistry, Nanjing University
Nanjing 210093 (P. R. China)
**e-mail: zhengxu@nju.edu.cn*

Fullerene nano-/micro-crystals can be prepared by interfacial method, evaporation method, as well as the reprecipitation method. The polymorphy and the morphology of the solution-grown fullerene crystals depends on the organic solvents used. Although many solvates were successfully prepared in different systems, the formation mechanism of these structures is rarely studied.

Recently, a new type of crystal, so called "mesocrystal", has been found, which builds up from the nanostructure intermediates. Mesocrystals can be synthesized from many polymer-controlled crystallization routes, but the difficulty in inorganic crystallization systems is that mesocrystals are short-lived with life time usually less than one second and it is difficult to observe the intermediate process of the crystallization. The organic crystals, with relatively low lattice energy compared to the ionic inorganic crystals, have longer lifetime, but the crystals under electron beam are partly merged into single crystals and the original mesocrystal structure is still unseen.

In this paper, we use the reprecipitation method to prepare fullerene microcrystals. The morphology and the size of the microcrystals can be controlled by tuning the volume ratio of the poor solvent and the fullerene solution as well as the concentration of fullerene in the initial solution. Importantly, the experimental results revealed that the formation of fullerene microcrystals involves mesocrystal formation with subsequent crystallographic fusion to a single crystal

[1] H. Cölfen, M. Antonietti, *Angew. Chem. Int. Ed.* **44**, 5576-5591 (2005).
[2] F.C. Meldrum, H. Cölfen, *Chem. Rev.* **108**, 4332 (2008).

Antioxidative activity of some fullerene C_{60} derivatives

Pykhova A.D.*, Gracheva Yu.A., Ovchinnikova N.S., Milaeva E.R., Yurovskaya M.A.

Lomonosov Moscow State University, Chemistry department, 119991, Moscow, Russia
**e-mail: morke@inbox.ru*

Fullerene C_{60} is known as a very efficient free radical scavenger, the so-called "radical sponge", a prospective structural moiety for design of compounds with antioxidative activity against reactive oxygen species (ROS), *e.g.* superoxide radical-anion, hydroxyl radical, peroxides, *etc.* [1].

Within our work a series of fullerene C_{60} derivatives with indole, quinoline and 2,6-di-tert-butylphenol moieties were synthesized by 1,3-dipolar cycloadition of azomethine ylides to fullerene C_{60} under standard (the Prato reaction [2]) and catalytic (lithium salts-assisted reaction [3]) conditions.

The antioxidative activity of the obtained fullerene C_{60} derivatives against peroxides and superoxide anion radicals was examined. The peroxide radicals were generated *in vitro* under conditions of peroxidation of oleic acid, structural fragment of membrane lipids. The superoxide radical-anion was generated in the enzymatic oxidation of purine base, xanthine, to uric acid by xanthine oxidase. Among the investigated fullerene derivatives, the fulleropyrrolidine with sterically hindered phenol moiety exhibits high antioxidant activity against peroxide radicals. In the enzymatic assay significant inhibition of superoxide radical-anion formation was observed in the presence of *tert*-butyl ester of fulleroproline with quinoline moiety at the concentration of 20 μmol/L.

This work was supported by the Russian Foundation for Basic Research (09-03-0090).

[1] Krusic P.J., Wasserman E., Keizer P.N., Morton J.R., Preston K.F., *Science* **254**, 1183 (1991).
[2] Maggini M., Scorrano G., Prato M., *J. Am. Chem. Soc.* **115**, 9798 (1993).
[3] Ioutsi V.A., Zadorin A.A., Khavrel P.A., Belov N.M., Ovchinnikova N.S., Goryunkov A.A., Kharybin O.N., Nikolaev E.N., Yurovskaya M.A., Sidorov L.N., *Tetrahedron* **66**, 3037 (2010).

Oscillation phenomenon in photoionization cross section of Ar@C_{60}

Polozkov R.G.*[1], Verkhovtsev A.V.[1], Ivanov V.K.[1], Korol A.V.[2], Solov'yov A.V.[2]

[1]*St. Petersburg State Polytechnic University, 195251, St. Petersburg, Russia*
[2]*Frankfurt Institute for Advanced Studies, 60438, Frankfurt am Main, Germany*
**e-mail: polozkov@tuexph.stu.neva.ru*

The oscillations in partial cross sections of photoionization of atomic clusters, in particular, of fullerenes C_{60}, at high photon energies was experimentally discovered more than 10 years ago [1]. These oscillations appear due to the reflection of photoelectrons at the borders of cluster potential and, as a result, the formation of spherical standing waves inside the cluster. Recently, the similar oscillation was shown to occur in the photoionization cross sections of endohedral noble gas fullerenes, in particular Ar@C_{60} [2].

The present work is devoted to the application of the consistent quantum many-body theory to the description of photoionization of endohedral noble gas fullerenes. The case study is the Ar@C_{60}. The single-electron energies and the wave functions are obtained within the jellium model with use of the self-consistent Hartree-Fock (HF) approximation. The partial and total cross sections of the photoionization are calculated within the Random Phase Approximation with Exchange (RPAE) with photon energy range up to 100 eV. The comparison between the endohedral and pristine fullerenes is performed.

Self-consistent potential of the endohedral system has a double-well profile in contrast to the single-well potential of the empty fullerene C_{60}. Due to the additional well at the centre of the system one may expect strong changes of the oscillations in the partial cross sections for endohedral fullerenes.

Preliminary analysis of the obtained results shows that the changes in the oscillatory behaviour of the partial cross sections depend on the electron density distribution between embedded atom and fullerene shell, i.e. on the hybridization of ground state orbitals.

This work was supported by DFG (project SO 845/8-1) and the EU Commission (NoE EXCELL project).

[1] Xu Y.B., Tan M.Q. and Becker U., *Phys. Rev. Lett.* **76**, 3538 (1996).
[2] Matthew A. McCune, Ruma De, Mohamed E. Madjet and Himadri S. Chakraborty, *J. Phys. B: At. Mol. Opt. Phys* **43**, 181001 (2010).

Fullerene C_{60} *in vivo*: influence on the basic types of metabolism

Piotrovskiy L.B., Okunevich I.V.*, Dumpis M.A., Litasova E.V., Sapronov N.S.

Institute of Experimental Medicine NWB RAMS, 197376, St. Petersburg, Russia
**e-mail: irina_okunevich@mail.ru*

The impact of fullerene C_{60} on the basic types of metabolism, namely lipid, protein and carbohydrate, was investigated during the continuous studies of its toxicological properties in vivo. Fullerene C_{60} was used as a complex of C_{60} with polyvinylpyrrolidone (C_{60}/PVP complex, 0.5% of C_{60} and PVP m.m. 12000 pharmaceutical grade). It has to be mentioned that in this complex fullerene molecules are in low aggregation state.

The study was done on 120 Wistar rats (180-200 g). The aqueous solution of the C_{60}/PVP complex was intraperitoneally (i.p.) injected at doses of 350 and 700 mg/kg within 30 days.

After 30 days in the serum of experimental rats, in comparison with intact animals, there were determined the following indexes of lipid, carbohydrate and protein metabolism: total cholesterol and triglycerides, concentration of high density lipoprotein cholesterol, glucose, total protein and albumin. Also the content of the serum globulin and the albumin/globulin ratio were determined.

After 30 days of introduction of C_{60}/PVP complex and vehicle (PVP) there were not observed any significant changes in the levels of triglycerides, high density lipoprotein cholesterol, glucose and total protein. There was slight increase of the concentration of total serum cholesterol. However, this increase was within the normal range and can be explained as a reaction of animals to handling.

It was also found the decrease of albumin concentration and albumin/globulin ratio, which can be explained by the known ability of albumin to absorb fullerene C_{60} molecules from C_{60}/PVP complex.

However all these changes do not go beyond the normal ranges for rats and can be caused by vehicle PVP.

Thus, our data indicate that chronic administration of C_{60}/PVP complex do not affect on the basic types of metabolism and once again indicate the safety of fullerene C_{60} in low aggregation state in vivo.

In vivo toxicology of fullerene C_{60} in low aggregation state

Piotrovskiy L.B.*, Dumpis M.A., Litasova E.V., Rodionova O.M., Safonova A.F., Sapronov N.S., Selina E.N.

Institute of Experimental Medicine NWB RAMS, 197376, St.-Petersburg, Russia
**e-mail: levon-piotrovsky@yandex.ru*

It is well known that the biological properties of fullerene C_{60} depend on aggregation state [1]. Earlier in *vivo* experiments we showed by morphological analysis that the single intraperitoneal (i.p.) injection of fullerene C60 in low aggregation state [as complex of C_{60} with polyvinylpyrrolidone (C_{60}/PVP complex)] did not cause any visible injuries of parenchymatous organs [2]. Therefore the main goal of this work was the more detailed study of toxicological parameters of C_{60}/PVP complex, namely the LD_{50} values and its influence on internal organs after prolonged i.p. injection (30 days). C_{60}/PVP complex, containing 0.5 % of C_{60} and PVP pharmaceutical grade m.m. 12000, was used.

At the first stage of the study we determined the acute toxicity (LD_{50} values) of C_{60}/PVP complex and the vehicle (PVP) after single i.p. injections into mice and Wistar rats (Rappolovo). Both compounds were injected as aqueous solutions concentration of 20, 25, 30 and 40 % (maximal possible concentration). The determined LD_{50} values were: for mice 11.2±0.8 g/kg for C_{60}/PVP complex and 9.7±0.8 g/kg for PVP alone. Accordingly for rats these values were 7.9±1.0 g/kg and 6.8±0.7 g/kg.

Chronic toxicity studies were done on Wistar rats (180-200 g). Every animal was i.p. injected every day within 30 days. Both compounds were used in doses 350 and 700 mg/kg, 1/20 and 1/10 of LD_{50}, respectively, as aqueous solutions. The following activities were determined: integral activity, influence on central nervous system, urinary bladder and haematological parameters (leukocytes, platelets and erythrocytes). On 15 and 30 days of the experiment the morphological analysis of some internal organs (spleen, liver, and kidney) was made.

The most important result of our investigation is that pristine fullerene C_{60} in low aggregation state (as C_{60}/PVP complex) is not only nontoxic, but reduces the toxic manifestation of high doses of PVP. These data indicate that the C_{60}/PVP complex can be used for medical purposes.

[1] Piotrovsky L.B., Dumpis M.A., Litasova E.V., Eropkin M.Yu., Eropkina E.M. and Kiselev O.I. *Fullerenes, Nanotubes and Carbon Nanostructures* **19**(1), 147 (2011).

[2] Popov V.A., Tyunin M.A., Zaitseva O.B., Karaev R.H., Sirotinkin N.V. Dumpis M.A., Piotrovsky L.B., *Fullerenes, Nanotubes and Carbon Nanostructures* **16**(5), 693 (2008).

Simulation of fast electron transport in thin metal and fullerite films

Petrenko E.O.[1], Makarets N.V.*[1], Mikoushkin V.M.[2]

[1]*Taras Shevchenko Kyiv National University, 01033, Kyiv, Ukraine*
[2]*Ioffe Institute, 194021, St. Petersburg, Russia*
**e-mail: mmv@univ.kiev.ua*

Electron beams are well known to generate swarms of the secondary, back-scattered and re-diffused electrons when collide with a target. Some details of this process were considered in this work for the cases of fullerite C_{60} films used in electron-beam lithography [1] and of micro-strip metal detectors [2]. In the first case, electron beam generates a swarm of secondary and re-diffused electrons losing their energy in numerous inelastic collisions some part of which leads to creation of polymeric bonds between fullerenes. To accelerate the polymerization process, one should find optimal characteristics of irradiating electron beam. In the second case, electron beam passes through thin metal film inducing emission of secondary electrons, therefore a positive charge emerges on the electrically isolated film. This charge and energy distribution of emitted electrons should be known to optimize parameters of extracting electric field.

The model of electron-atom interaction for primary electrons in the keV energy range and for secondary electrons in the eV energy range, early developed in [3], was applied to description of the above processes. Elastic electron collisions as well as electron-phonon interaction were described by using optical potential. Ionization of deep atomic levels was considered by use of the Kim-Rudd model. Ionization of the valence and conduction bands and plasmons generation were described by the Penn model and experimental data. The Monte-Carlo programme package has been created and all collisions and trajectories of the primary and secondary electrons were calculated till the moment when their energies become below the work function.

The conducted simulation has shown that the average kinetic energy of the ejected electrons is larger when they start from deeper atomic levels, which results in additional electron emission from target. As a result, many of generated and re-diffused electrons are stopped changing the energy of the most energetic electrons of the electron cloud and decreasing their energy down to the value just above the work function. In addition, some weak nonmonotonicity of the total number of fast electrons moving inside of the target is observed when the primary electron beam energy is sufficient for ionization of deep atomic levels.

[1] V.V. Shnitov, V.M. Mikoushkin, V.V. Bryzgalov, Yu.S. Gordeev, *Physics of the Solid State* **44**, 4444 (2002).

[2] V. Pugatch, M. Borisova, A. Mykhailenko, O. Fedorovich, Y. Pilypchenko, V. Perevertaylo, H. Franz, K. Wittenburg, M. Smelling, C. Bauer, *NIMB* **581**, 531 (2007).

[3] N.V. Makarets, Yu.I. Prylutskyy, V.M. Mikoushkin, V.V. Shnitov, Yu.S. Gordeev. *Fullerenes, Nanotubes and Carbon nanostructures* **14**, 513 (2006).

Inner-shell electronics of caged molecules: small molecules in carbon cages

Pavlychev A.A.*[1], Brykalova X.O.[1]

[1]*Institute of Physics, St. Petersburg State University, St. Petersburg, 198504, Russia*

Molecular electronics is the subject of intriguing changes taking place when a molecule happens to be confined in a cage. What kind of changes are they? Answering the question we are approaching to understanding of many elementary processes that occur in complex composite systems.

Special emphasis is put here on unoccupied valence states of a quasifree molecule that is confined in a nanosize carbon cage. X-ray absorption and inner-shell photoionization spectra are regarded as a basic probe of the cage effects. Their origin is being attributed mainly to (i) changes in molecular dynamics [1], (ii) electron scattering at the cage [2] and (iii) dynamic polarizability of the cage [3]. These phenomena are discussed.

Inner-shell electronics of caged molecules is examined in small molecular species (CO, N_2, SF_6) confined in fullerenes, carbon onions and nanotubes, and nanoporous carbon. Two limiting cases of weak and strong cage effects are revealed and described. To describe and compute the X-ray absorption and inner-shell ionization spectra the quasiatomic approach is applied. We have revealed the *red-* and *blue-shifts* of core-to-valence excitations and new resonance states in spectral distribution of oscillator strength for continuum transitions in the caged molecules and in the cages. These new states demonstrate different nature and can be attributed to either *confinement* resonances or *window-like* resonances or *induced shape* resonances. It is shown that the red- and blue-shifts correspond to the weak cage effect whereas the new resonances appear as a consequence of the strong effect. The experimental evidences of the cage effects are presented and the specific conditions of their observation are determined.

[1] R. Flesch, A. A. Pavlychev, J. J. Neville, J. Blumberg, M. Kuhlmann, W. Tappe, F. Senf, O. Schwarzkopf, A. P. Hitchcock, and E. Rühl, *Phys. Rev. Lett.* **86,** 3767 (2001).

[2] A. A. Pavlychev, X. O. Brykalova, D. A. Mistrov, R. Flesch, and E. Rühl. *J. Electron Spectrosc. Relat. Phenom.* **166-167**, 45-52 (2008).

[3] M. Ya. Amusia, J. Electr. Spectrosc. *Relat. Phenom.* **159**, 89 (2007).

Irradiation and doping induced changes in properties of C_{60} fullerite films

Pavlenko O.*, Dmytrenko O., Kulish M., Brusentsov V., Rybiy V., Korniyenko M. , Strilchuk V., Romaniuk B.M., ShpilevskyE.[1]

Kyiv National Taras Shevchenko University, Faculty of Physics, 64 Volodymyrska str., Kyiv, Ukraine
[1]A.V. Lykov Heat and Mass Transfer Institute of BNAS, 15 Brovky Str, Minsk, Belarus
**e-mail: leno4ka_pavl@mail.ru*

C_{60} fullerenes in the condensed state at the room temperature are semiconducting molecular crystals. It was shown that under influence of high pressure, UV-irradiation, doping with alkali metals and electron-beam irradiation the fullerites can be polymerized and change their properties dramatically. Due to that C_{60} have high potential of application in the nanoelectronics, medicine. But the mentioned polymerization methods have limitations. Therefore in the given work we have performed study of C_{60} films under irradiation with different types of bombardment particles and doping with metal atoms.

Thin C_{60} films (thickness 1000 nm) were prepared by vacuum sublimation of C_{60} powder on Si substrates. Irradiation was performed with electrons (E=1.8 meV), doses varied from 1 to 25 MGy, with carbide forming Ti and Fe ions (E=140 keV), doses varied from 10^{10} to 10^{14} ions/cm^2, and Ar ions (E=350 eV), doses varied from 10^{10} to 10^{14} ions/cm^2. After each step of irradiation changes in the crystal structure, vibration and electron properties were studied by methods of X-ray's diffraction, Raman spectroscopy, photoluminescence and spectral ellipsometry, STM. In order to study interaction mechanisms of implanted atoms with C_{60} molecules were prepared C_{60} films with Sn, In, Bi metal atoms and investigated with the same methods. Model chemistry calculations in the Gaussian program (Hartree-Fock approximation) were done for systems: C_{60}Ti, C_{60}Fe, C_{60}C, C_{60}Sn, C_{60}In, C_{60}Bi.

Results have shown that irradiation of fullerites with mentioned particles and doping with metal atoms leads to polymerization of molecules that is confirmed by appearance of new diffraction reflections, shifting and splitting of Raman modes, complicate change of electron spectra. Theoretically was shown that complexes C_{60}Ti, C_{60}Fe, C_{60}C, C_{60}Sn exist. Doses at which effects of destruction of C_{60} molecules begin to prevail were determined.

A DFT study of fullerene C_{60} transition metal complexes structure and dynamic

Oprunenko Yu.F.*, Gloriozov I.P., Vasil'kov A.Yu.

Chemistry Department of Moscow State University, Moscow, 119899, Russia
**e-mail: oprunenko@nmr.chem.msu.su*

Since the first preparation of organometallic complexes of fullerene[1,2] many compounds of this type have been synthesized and structurally characterized by means of X-ray, NMR and DFT.[3-5] Such systems have good prospects as catalysts in organic reactions and as new materials in optoelectronics. Data on dynamic processes in transition metal complexes of fullerene are relatively rare, *e.g.* variable-temperature and EXCY ^{13}C NMR studies on $[M(NO)(PPh_3)_2(\eta^2\text{-}C_{60})]$ (M = Co, Rh, Ru) **1-3** show the presence of C_{60} – metal moiety rotation with low activation barrier and haptotropic migration processes with $\Delta G^{\#}$ = ca. 9, 10 and 14 kcal/mol, correspondinly.[5]

The DFT calculations reported in this paper on complexes **1-3** structures and activation barrier of haptotropic migration of metal moiety over the whole fullerene surface in **1** are based on Priroda program package (PBE, TZV2p, SBK-JC).[6]

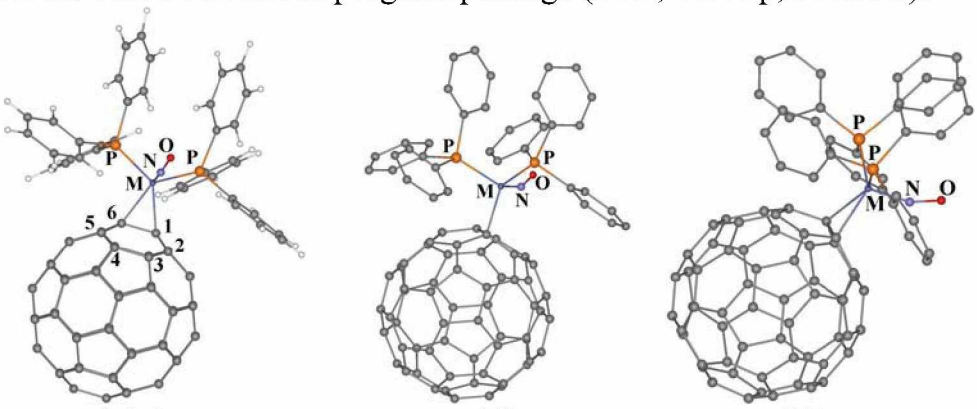

1, 2, 3 **TS** **IM**

η^2,η^2-Rearrangement over the whole surface of fullerene proceeds in **1** as intermolecular [1, 3]-shift of the Co metal atom via transition state **TS** (ΔG = 12.2 kcal/mol) and intermediate **1-IM** (ΔG = 7.6 kcal/mol): **1** → **1-TS** → **1-IM** →**1-TS** → **1-IM** → **1**. Theoretically calculated data on geometry, structure and conformation of **1-3** and activation barrier for **1-TS** of metal migration in **1** thus are in good agreement with experimental data.

Calculations were done on computer facilities purchased with the financial support of Alexander von Humboldt Stiftung (Bonn, Germany).

[1] Fagan P.J., Calabrese J.C., Malone B., *Acc. Chem. Res.,* **25**, 134 (1997).
[2] Hawkins J.M., *Acc. Chem. Res.,* **25**, 150 (1997).
[3] Nunzi F., Sgamellotti A., Re N., Floriani C., *Organometallics,***19**, 1628 (2000).
[4] Stefens A.H., Green M.L.H., *Adv. Inorg. Chem.,* **44**, 1 (1997).
[5] Green M.L.H., Stefens A.H., *Chem. Commun.,* 793 (1997).
[6] Laikov D. N., *Chem. Phys. Lett.*, **V. 281**, 151 (1997).

Effects of C_{60} derivatives on in vitro amyloidogenesis of Aβ (1-42) peptide of the brain

Okuneva A.D.[1,2]*, Bobyleva L.G.[1], Bobylev A.G.[1], Podlubnaya Z.A.[1,2]

[1]*Institute of Theoretical and Experimental Biophysics, Puschino, 142290, Russia*
[2]*Puschino State University, Puschino, 142290, Russia*
**e-mail: a-okyneva@yandex.ru*

Alzheimer's disease (AD) is an important problem of modern psychiatry and neurology. One of the hallmarks of this disease is the accumulation of aggregates of amyloid β-peptide (Aβ-peptide) in the brain, leading to neurodegeneration. The main strategy in the treatment of AD is to prevent the formation and destroy aggregates of the Aβ-peptide. Owing to the antioxidant and neuroprotective properties, fullerenes can be considered as potential drugs for the treatment of neurodegenerative diseases. A new stage in the study of antiamyloid properties of fullerenes began thanks to the synthesis of a series their water-soluble derivatives.

Using electron microscopy, we showed that these fullerene C_{60} derivatives (the sodium salt of polycarboxylic derivative of C_{60}, fullerenol, the complexes of fullerene with polyvinylpyrrolidone, C_{60}-NO_2-proline, C_{60}-$(NO_2)_2$-proline, and C_{60}-NO_2-proline-NO_2) destroyed amyloid fibrils of Aβ(1-42) peptide of the brain and also prevented their formation. These data were confirmed by the fluorescence analysis with using the dye thioflavin T. We also investigated the toxicity of the fullerene C_{60} derivatives on the cell culture Hep-2. The sodium salt of the polycarboxylic derivative of C_{60} showed toxicity in the concentration range 2-0,16 mg/ml. For the other fullerene C_{60} derivatives, no cytotoxicity in the same range of concentrations was found.

The data showed that all agents studied, except the sodium polycarboxylic derivative of C_{60}, corresponded two requirements to the development and application of drugs for treatment AD, namely low toxicity and high antiamyloid potential.

The study was supported by the Presidium of RAS "Fundamental sciences to medicine, RFBR grants № 09-04-01161, RFBR № 10-04-00141, grants of the Federal Target Program “Research and scientific-pedagogical staff of innovation Russia” of the Federal Agency of Science and innovation, State contract № 02.740.11.0301, State contract № 02.740.11.0710.

Preparative synthesis of (1,2-methanofullerene C_{60})-61-carboxylic acid

Nikolaev D.N. *[1], Davidovich P.B.[2], Piotrovskiy L.B.[1]

[1]*Institute of Experimental Medicine NWB RAMS, 197376, St.-Petersburg, Russia*
[2]*St.-Petersburg State Institute of Technology, 190013, St.-Petersburg, Russia*
**e-mail: pp225@yandex.ru*

The modification of biological molecules (proteins, polynucleotides and polysaccharides) by C_{60} fullerene residue leads to an increase in their lipophilicity and thus may enhance their ability to penetrate through biological membranes. The most suitable for modification are fullerenemonocarboxylic acid.

In order to find the best precursor for the synthesis of fullerenemonocarboxylic acid in preparative scale the reaction of cyclopropanation of C_{60} by alkyl (dimethylsulfuranylidene)acetates was chosen [1]. For the determination of the influence of the radicals on the reaction yield and the conditions for the separation ether (1,2-methanofulleren C_{60})-61-carboxylic acid from the mixture of mono- and polysubstituted derivatives, the cyclopropanation of C_{60} was carried out by alkyl (dimethylsulfuranylidene)acetates, containing various ester radicals (ethyl, tert-butyl, benzyl and benzhydryl).

The obtained data showed that the structure of the alkyl radical in the molecule of ylide does not significantly affect the reaction. In all cases, a mixture of mono-and polysubstituted derivatives with roughly the same yield were obtained. However, chromatographic separation from the reaction mixture of monosubstituted derivatives, containing benzyl and benzhydryl radicals, it was much easier. Further transformation of the ester to the free (1,2-methanofulleren C_{60})-61-carboxylic acid proceeded readily in the case of tert-butyl and benzhydryl radicals.

The structure of all obtained compounds was unambiguously confirmed by ^{13}C-NMR, ^{1}H-NMR, IR and UV spectra and mass spectrometry.

Thus, it can be concluded that for preparative synthesis of (1,2-methanofulleren C_{60})-61-carboxylic acid most suitable precursor is benzhydryl (dimethylsulfuranylidene)acetate.

[1] Wang, Y., Cao, J., Schuster, D.I., Wilson, S.R. *Tetrahedron Letters* **36**(38), 6843 (1995).

Supramolecular formations of fullerene C_{60}-containing poly(ethylene oxide) in deuterobenzene

Lebedev V.T.*[1], Orlova D.N.[1], Nasonova K.V.[2], Melenevskaja E.Yu.[2], Shamanin V.V.[2], Vinogradova L.V.[2]

[1]*Petersburg Nuclear Physics Institute, Gatchina, Saint-Petersburg distr., Russia*
[2]*Institute of Macromolecular Compounds RAS, Saint-Petersburg, Bolshoi pr. 31, Russia*
**e-mail: vlebedev@pnpi.spb.ru*

A new method for the synthesis of star-shaped fullerene C_{60}-containing poly(ethylene oxide) is developed and its hydrodynamic properties are studied. Then the molecular structure of stars in deuterobenzene was analyzed by the small-angle neutron scattering using Fourier data analysis to recognize the mechanisms and forms of structuring (self-assembly) of poly(ethylene oxide) chains being structural elements (star arms) of macromolecules of complex architecture. The peculiar forms of spontaneous self-organization of star-shaped macromolecules were revealed. It was found that the resulting equilibrium structure has specific topology. Some of polymer chains acquire stretched conformations in the solution and act as physical links between other chains, which leads to the formation of polymer framework filled with coiled chains. Fullerene-containing poly(ethylene oxide)s have 6 arms. Star architecture leads to enhanced ability of these polymers to form highly ordered structures in solution.

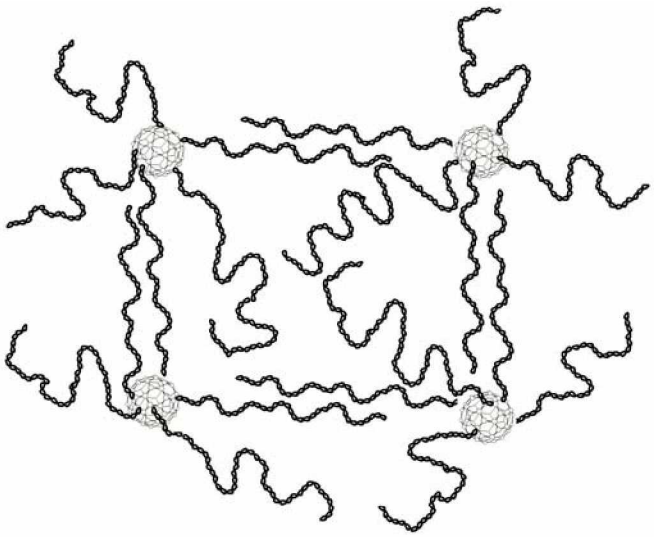

The work was supported by Russian Foundation for Basic Research (grant 10-03-00191a) and Program for Basic Research of the Presidium of RAS № 21.

Sorbents based on silica containing fullerenols for use in plasmapheresis

Nasonova K.V.*[1], Melenevskaya E.Yu.[1], Shamanin V.V.[1], Podosenova N.G.[2]

[1]*Institute of Macromolecular Compounds RAS, St.-Petersburg, Bolshoi pr. 31, Russia*
[2]*Institute for Analytical Instrumentation RAS, St.-Petersburg, Rizhsky pr., 26, Russia*
**e-mail: kaiduk@mail.ru*

Sorbents based on silica containing fullerenols $C_{60}(OH)_{12-14}$ and $C_{60}(OH)_{20-24}$ were obtained. In order to obtain the sorbents two essentially different approaches, a method of a solid-state reaction and a method of a two-step linking of fullerenols to silica network using dimethyldichlorosilane and amine, were used. The sorbents obtained were analyzed by IR and NMR spectroscopies.

It was shown in an *in vitro* system comprising blood plasma that the sorbents obtained have a high selectivity for low density lipoproteides, wherein the constant of elimination K_{el} is more than 0.8. This property allows these sorbents to be used for creating blood purification systems, in particular, for efferent therapy in atherosclerosis.

Formation of carbon microstructures by dry electron-beam lithography

Mikoushkin V.M.*[1], Shnitov V.V.[1], Nashchekin A.V.[1,2], Pavlov S.I.[1,2], Nesterov S.I.[1,2], Konnikov S.G.[1,2]

[1]*Ioffe Institute, 194021, St. Petersburg, Russia*
[2]*St. Petersburg Joint Research Diagnostics Centre, 194021, St. Petersburg, Russia*
**e-mail: V.Mikoushkin@mail.ioffe.ru*

Electron-beam lithography is one of the widely spread techniques in micro- and nanoelectronics. Revealing transformation of fullerite C_{60} films under electron irradiation into weakly evaporable substance [1] led to the idea of dry lithography with all operations performed at high vacuum [2]. This idea was confirmed by creation of latent image of macrosized low-energy electron beam and their developing by heating in vacuum. The aim of the work was to confirm the possibility of dry electron lithography by fabrication of carbon microstructures at the conditions typical for usual electron-beam lithography. Latent 2 μm micropatterns with a shape of squares and stripes were created in fullerite film of 320 nm thickness by 25 keV electron nanoprobe and then developed by heating in vacuum. The e-beam writing of the micropatterns and their visualization were realized by Scanning Electron Microscope (SEM) - JEOL JSM-7001F equipped with lithographic tool "Nanomaker" ("Inteface Ltd.", Moscow). Visual examination of the samples by optical microscope (Nikon Eclipse 150) revealed the designed structure after heating (Fig. A). Fig. B shows the developed SEM image of stripe. The obtained results confirmed the possibility of carbon microstructure fabrication by dry electron lithography.

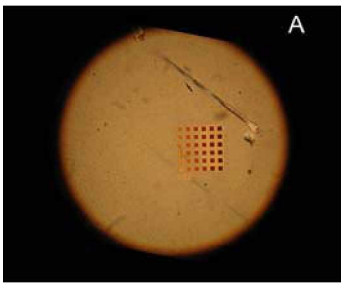

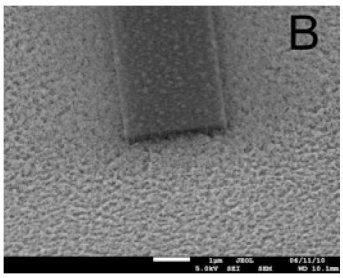

Optical (Fig. A) and SEM (Fig. B) images of carbon microstructures.

The research was supported by the Russian Foundation for Basic Research (RFBR), Project № 10-07-00508-a, by Presidium of RAS Program and by the St. Petersburg Diagnostics Center "Material science and diagnostics in modern technologies".

[1] V.M. Mikoushkin, V.V. Shnitov, *Phys. Solid State* **39**, 164 (1997).
[2] V.V.Shnitov, V.M.Mikoushkin, Yu. S.Gordeev, *Microelectron. Eng.* **69**, 429 (2003).

Thermo-destruction of the fullerenes

Merzlyakova M.A., Nikonova R.M., Lad'yanov V.I., Aksyonova V.V.

Physical-Technical Institute of the Ural Branch of RAS, Ishevsk 426000, Russia, e-mail: las@pti.udm.ru

Studies of the thermal behavior of fullerenes and their condensed form - fullerites began with the receipt of a macroscopic. The research results of thermal stability available in the literature [1,2 etc.] are quite contradictory and ambiguous both for pure C_{60}, C_{70} and their mixture.

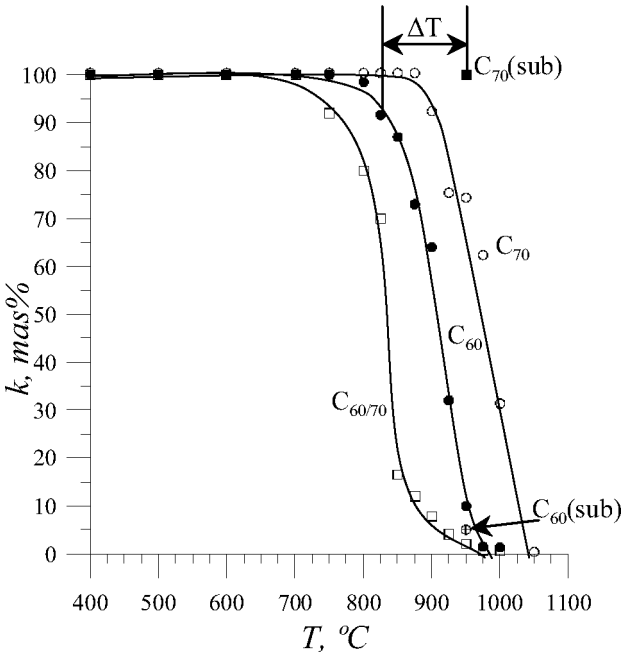

Figure. Change the number of fullerenes after annealing in an environment of CO, 30 min. UV- spectroscopy.

The thermal behaviour of the fullerenes and the fullerites (C_{60}, C_{70} and their mixture $C_{60/70}$) in CO conditions has been investigated by the X-ray structural analysis and the ultraviolet spectroscopy. It has been shown that the thermal decomposition occurs in the narrow temperature range. It has been established that the thermal stability of the fullerene C_{70} (>98%) is higher than that of C_{60} (99,5%). The critical stability temperatures of them have been determined as 950 и 850 C respectively. The initial decomposition temperature of the mixture $C_{60/70}$, obtained extraction from toluene solution is 775 °C. This temperature is lower than that of C_{60} and C_{70}.

It has been established that the critical decomposition temperature of the fullerenes and the fullerites is determined by the presence of impurities (oxygen and solvent). It has been shown that the crystallization of the fullerenes from gaseous phase is the most advantageous method of cleaning. At the same time the difference in the stability temperatures of C_{60} and C_{70} is, at least, $\Delta T = 125$ °C.

The decomposition kinetics of the fullerites mixture $C_{60/70}$ at T = 800 C has been investigated.

The work has been carried out under financial support of the program the Presidium of Ural Brunch, RAS (Project 09-T-1008) and by RFBR (grant № 10-08-90419-Ukr-a)

[1] F.Cataldo, *Nanotubes and Carbon Nanostructures* **10**(4), 293 (2002).
[2] T.Sommer, T. Kruse, P. Roth, *J. Phys. B: At. Mol. Opt. Phys.* **29**, 4955 (1996).

Detailed computational study of the chlorination-assisted skeletal rearrangement of D2-19150C76 into C2-18917C76Cl24

Mazaleva O.N.*, Ioffe I.N.

Moscow State University, 119991, Moscow, Russia
**e-mail: mazaleva.olya@gmail.com*

The Isolated Pentagon Rule (IPR) plays a definitive role in fullerene chemistry. All identified products of the standard arc discharge synthesis without dopants are IPR fullerenes. Non-IPR structures are typically obtained via instant functionalization of the forming cages in the reactor with endohedral metal atoms/clusters or with chlorine addends. Because of lower thermodynamic stability of the non-IPR isomers and presumably high activation energy of the Stone-Wales rearrangements that were generally regarded as key mechanism of skeletal transformations, no one anticipated, until very recently, a possibility of conversion of the conventional IPR fullerenes into non-IPR ones under milder chemical conditions.

In view of that, quite surprising was formation of strongly non-IPR C_2-$^{18917}C_{76}Cl_{24}$ compound in the course of chlorination of the well known IPR-isomer D_2-$^{19150}C_{76}$ in $SbCl_5$ [1]. The new fullerene chloride was found to have as many as five pairs of adjacent pentagons. To explain this transformation, a modified mechanism of Stone-Wales rearrangements was proposed that involves migration of chlorine atoms to stabilize the transition states and thus to reduce the reaction barriers.

We present a detailed computational analysis of the formation pathway of C_2-$^{18917}C_{76}Cl_{24}$ at the DFT level of theory. We employed the PBE exchange-correlation functional known to be successfully applicable to various fullerene systems. The activation energy calculations were additionally refined with the use of the PBE0 hybrid functional and PCM corrections.

The transformation of the chlorinated D_2-$^{19150}C_{76}$ into C_2-$^{18917}C_{76}Cl_{24}$ was found to require seven Stone-Wales steps plus a step of global chlorine migration over the carbon cage, all steps calculated to be thermodynamically favorable. The Stone-Wales bond rotations in the chlorinated fullerenes are facilitated by formation of stabilized valence-saturated intermediate structures via $SbCl_5$-mediated transfer of chlorine anions. The activation energy of the first, limiting Stone-Wales step was calculated to be 2.5 eV. Of critical importance for the skeletal rearrangement process is the chlorinating $SbCl_5$ environment that enables formation of closed-shell ion pair transition states $[C_{76}Cl_{2n-1}]^+[SbCl_6]^-$ and further stabilizes them through polarization interactions.

We acknowledge support of RFBR (grant 09-03-01131) and of the MSU supercomputer center (SKIF-Chebyshev).

[1] I.N. Ioffe, A.A. Goryunkov, N.B. Tamm, L.N. Sidorov, E. Kemnitz, S.I. Troyanov, *Angew. Chem. Int. Ed.* **48**, 5904 (2009).

In situ observation of C_{60} hydrogenation reaction using gravimetric method

Luzan S.M.[1]*, Tsybin Y.O.[2], Talyzin A.V.[1]

[1]*Department of Physics, Umeå University, 90 187 Umeå, Sweden*
[2]*Biomolecular Mass Spectrometry Laboratory, Ecole Polytechnique Fédérale de Lausanne, 1015 Lausanne, Switzerland*
**e-mail: serhiy.luzan@physics.umu.se*

Reaction of fullerene C_{60} with hydrogen gas was studied in a broad temperature interval and over prolonged periods of time. Hydrogenation was monitored in situ at high temperature and high hydrogen pressure conditions using gravimetric method. The shape of gravimetric curve was found to depend on temperature of hydrogenation: in the temperature interval of 623-673K saturation of sample weight was achieved, while at temperatures of 693-713K the sample weight went through the maximum and decreased upon prolonged hydrogenation. The weight decrease is explained by fragmentation of fullerene cage with formation of light hydrocarbons which evaporate from the sample. Products of hydrogenation were studied by X-ray diffraction, MALDI-TOF mass spectrometry, APPI FT-ICR mass spectrometry, HPLC chromatography, and elemental analysis. It was found that the reaction resulted in a set of hydrogenated fullerenes with different content of hydrogen (from $C_{60}H_{18}$ up to $C_{60}H_{56}$) as well as some fragmented fullerenes with less than 60 carbon atoms.

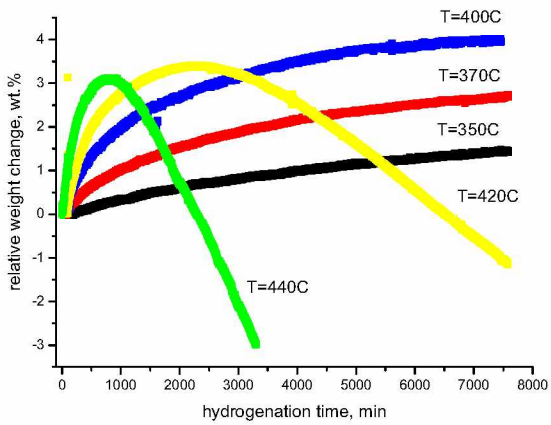

Time dependence of hydrogenation of fullerenes C_{60} performed at different temperatures.

The quenching of the Yb (III) porphyrazine complexes and heterocyclic ligands by C_{60} in solutions

Lopatin M.A.*, Klapshina L.G., Grigoryev I.S., Semenov V.V., Lermontova S.A., Domrachev G.A.

G.A. Razuvaev Institute of Organometallic Chemistry, Russian Academy of Sciences, 603950, Nizhny Novgorod, Russia
**e-mail: lopatin@iomc.ras.ru*

The interaction of the Yb(III)tetra-aryl-tetra-cyano-porphyrazine complexes (Aryl=C_6H_5(I), C_6H_4F(II), C_6F_5(III), $C_{10}H_7$(IV)) with C_{60} had been investigated. Complex (I) is readily soluble in organics. It is well compatible with a variety of polymeric matrices giving doped polymeric glasses, films and solutions which are highly luminescent (φ = 13%) in the biologically relevant optical window covering the visible and near infrared range.

We investigated complexes (I-IV) luminescent spectra ($\lambda_{excitation}$= 300 nm) in acetonitrile solutions using C_{60} as a quencher in visible region ($\lambda_{emission}$ = 420-460 nm). It had been found [1] that a quenching was caused by resonance interaction of aromatic hydrocarbons with fullerene C_{60}. Relative intensity of complexes (I-IV) emission dependence on quencher molar concentration is satisfied to Stern-Volmer equation with Kq = (1,24-1,89)*10^5 l/mol because of a week CT-complex formation. The results are shown in the table.

Aryl	$C_{10}H_7$	C_6H_5	C_6H_4F	C_6F_5
$\lambda_{emission}$(nm)	428	456	425	453
Kq*10^{-5}(l/mol)	1.24	1.56	1.75	1.89
R^2	0.892	0.997	0.993	0.994

Kq – Stern-Volmer quenching constants
R^2 – correlation coefficient.

A comparison of the complex (I-IV) with organic ligands shows one order of magnitude increase of quenching constants. Such the compounds can be potentially used in photovoltaic devices.

This work was supported by the State Contract № П-337 and programs of RAS.

[1] R.G.Bulgakov, D.I.Galimov, *Russ.Chem.Bull.* **3**, 432-436(2007).

DFT and ESR spectroscopic studies of new organoelement fullerene derivatives

Lopatin M.A., Ketkov S.Yu.*, Markin G.V., Kuropatov V.A., Rychagova E.A., Kalakutskaya L.V., Domrachev G.A.

G.A. Razuvaev Institute of Organometallic Chemistry, Russian Academy of Sciences, 603950, Nizhny Novgorod, Russia
**e-mail: sketkov@iomc.ras.ru*

The DFT calculations of recently synthesized fullerene polyadducts R_nC_{60} (R = Me_3Si; n = 4, 6, 8, 10, 12) and ESR study of new bis(toluene)tungsten fulleride have been performed. The natural charge distribution and NBO populations in the R_nC_{60} molecules were compared with those in the fullerene adducts with organic fragments (R = Me, *t*-Bu, CH_2Ph, CF_3) as well as with the corresponding parameters in the R-CMe_3 species. The Si(R)-C(C_{60}) and Si(R)-C(C_{60}) NBO population appears to be lower than the corresponding values for the Si(R)-C(CMe_3) and C(R)-C(CMe_3) bonds. The electron density distribution analyzed by the Bader's "Atom in molecules" approach also shows some ρ(r) decrease for the (3,-1) critical points of the R-C bonds on going from "classical" organics to the fullerene adducts. On the other hand, analysis of natural charges reveals increased polarization of the R-C_{60} (R = CH_2Ph, CMe_3, CF_3) bond as compared to R-CMe_3. These findings are indicative of the higher lability of the R-C_{60} chemical bond. DFT calculations have been also carried out for the reduced and oxidized forms of R_nC_{60}. Both one-electron oxidation and reduction of 1,4-R_2C_{60} results in an increase of the electron density on the C2-C12 and C3-C14 bonds and a decrease of ρ(r) on the C2-C3 bond of the C_{60} core. This agrees well with the HOMO and LUMO localization. Accordingly, the ρ(r) value in the (3,-1) critical point of the R-C_{60} bond changes stronger on going to the cation than to the anion. The formation of the $(C_{60})^{-\bullet}$ fulleride anion has been studied in the reaction of fullerene with bis(toluene)tungsten.

C_{60} reacts with $(PhMe)_2W^0$ in PhMe at 293 K to form fulleride as black crystalline sediment (fulleride **I**). Fulleride **I** is insoluble in aliphatic solvents, soluble in PhCN and THF. Its ESR in THF at 290 K shows a line with typical hyperfine structure of $(Arene)_2W^{+\bullet}$ and g = 1.9856, a_H = 4.5G. The visible spectroscopy of fulleride **I** in THF at 291 K reveals a $(C_{60})^{-\bullet}$ absorption band at λ = 1079 nm. The EPR spectrum of crystalline $[(PhMe)_2W^{+\bullet}][(C_{60})^{-\bullet}]$ (**I**) at 290 K shows a single line with ΔH = 111.2 G and *g* = 1.9882 which is intermediate between those characteristic for $(Arene)_2W^{+\bullet}$ and $(C_{60})^{-\bullet}$ because of strong exchange coupling between $(PhMe)_2W^{+\bullet}$ and $(C_{60})^{-\bullet}$. On cooling **I** in the 260-200 K range the g-factor significantly shifts and the ESR spectrum of crystalline **I** at 120 K consists of a single line with ΔH = 13.7 G and g = 1.9849 which is characteristic for non-interacting paramagnetic $(PhMe)_2W^{+\bullet}$.

Electronic and defect structures of fullerene C_{60} molecular complex

Lopatin D.V.*, Chirkin E.S., Dmitrievskii A.A., Zheltov M.A., Samodurov A.A., Stolyarov R.A.

Tambov State University, 392000, Tambov, Russia
**e-mail: lopatin@tsu.tmb.ru*

It is well known, that optical and electrical properties of semiconductors depend on the defective structure and the local levels in the band-gap, as a consequence. However, the information about transport properties of given fullerene based compounds is completely absent. The aim of the work was revealing and detail research of electronic and defects structures of fullerene C60 molecular complexes with copper (II) diethyldithiocarbamate $\{Cu^{II}(Etdtc)_2\}_2 \cdot C_{60}$.

Thermostimulated currents (TSC) measurements revealed in material traps located below the LUMO level on 0.43± 0.02 eV. It allows supposing that trapping centres are caused by one type of defects. Most probably they are solution fragments donor`s molecule disordered in the hollows of the crystal lattice or defect of molecule fullerene.

To explain the peculiarities of the absorption and photoconductivity in the visible spectrum we calculated the excited electronic states of the complex $\{Cu^{II}(Etdtc)_2\}_2 \cdot C_{60}$ in the TD-DFT/B3LYP method (*6-311G*$^{++}$ basis set). The calculation for a perfect complex allowed for a correlation of experimental optical bands (2.62, 3.09 eV according to [1]). Excited states of 2.12 eV calculation is not shown and this band in the photoconductivity spectrum of a real crystal formed by trapping centres.

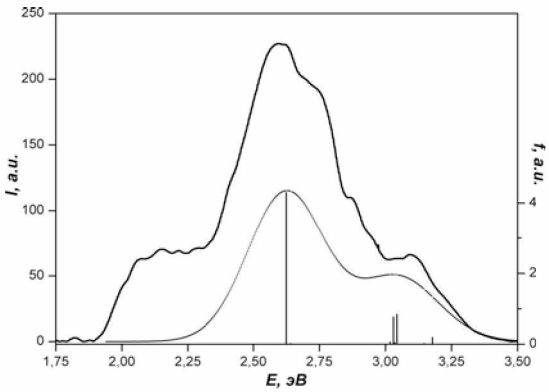

Figure. Photoconductivity spectra (solid line) and excited electronic states (dotted line) of the complex.

To test the latter hypothesis, we simulated several of the most probable types of structural defects in both the donor and fullerene molecules. It is shown that the most probable defect of real crystals is imperfect fullerene molecule.

The work was supported by RFBR (projects 10-02-00763, 09-02-97540 r_center_a, 09-02-97541 r_center_a) and the framework of the Russian Federal Program "Scientific and Scientific-Pedagogical Personnel of the Innovative Russia" for 2009-2013.

[1] D.V. Konarev, A.Y. Kovalevsky, S.S. Khasanov, G. Saito, D.V. Lopatin, A.V. Umrikhin, A. Otsuka, R.N. Lyubovskaya, *Eur. J. Inorg. Chem,* 1881 (2006).

Specific internal structure of star-shaped polystyrenes with fullerene C_{60} branching center

Lebedev V.T. *[1], Török Gy.[2], Ratnikova O.V.[3],Vinogradova L.V.[3]

[1]*Petersburg Nuclear Physics Institute, Gatchina, Saint-Petersburg distr., Russia*
[2]*Research Institute for Solid State Physics and Optics, Budapest, POB-49, Hungary*
[3]*Institute of Macromolecular Compounds RAS, Saint-Petersburg, Bolshoi pr. 31, Russia*
**e-mail: vlebedev@pnpi.spb.ru*

Using the techniques of molecular correlation functions and various models for the analysis of small-angle neutron scattering data concerning structure and conformational characteristics of fullerene-containing regular star polystyrenes (Debye and Benoit approximation and Fourier transform of scattering cross-sections), a number of peculiarities of star structure in deuterated toluene solution was revealed. It was found that the polymer core around fullerene C_{60} molecule is formed in the center, and therefore this center is being impenetrable for other macromolecules. Moreover, a stretched conformation of polymer arms is more stable as compared with that of free polystyrene chains due to increase in local rigidity of arms taking place under the action of fullerene center. It was shown that the formation of polymer shell around fullerene branching center and the peculiar conformation of arms result from the competition between two opposite tendencies of PS arms' behavior. One of chain ends covalently bound to fullerene shields its surface from solvent, while the outer end tends to active interaction with thermodynamically good solvent. The specific action of fullerene center on arms' conformation leading to decrease in their statistical flexibility results in the increasing star dimensions by approximately 30% as compared to stretching effect according to *Daoud-Cotton model.*

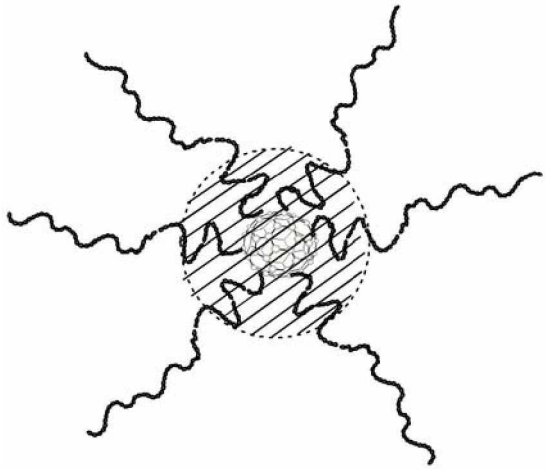

The work was supported by Russian Foundation for Basic Research (project code 10-03-00191a) and Program for Basic Research of the Presidium of RAS № 21

Star-shaped homo- and hybrid fullerene C_{60}-containing polymers and their supramolecular organization in aromatic solvents

Lebedev V.T. *[1], Török Gy.[2], Vinogradova L.V.[3]

[1]*Petersburg Nuclear Physics Institute, Gatchina, Saint-Petersburg distr., Russia*
[2]*Research Institute for Solid State Physics and Optics, Budapest, POB-49, Hungary*
[3]*Institute of Macromolecular Compounds RAS, Saint-Petersburg, Bolshoi pr. 31, Russia*
**e-mail: vlebedev@pnpi.spb.ru*

Anionic polymerization techniques, functionalization and coupling reactions were used in the synthesis of star-shaped fullerene C_{60}-containing polystyrenes and heteroarm stars with non-polar (polystyrene) and polar (poly-2-vinylpyridine, poly-(*tert*-butyl methacrylate) and poly-2-vinylpyridine-*block*-poly-(*tert*-butyl methacrylate)) arms.

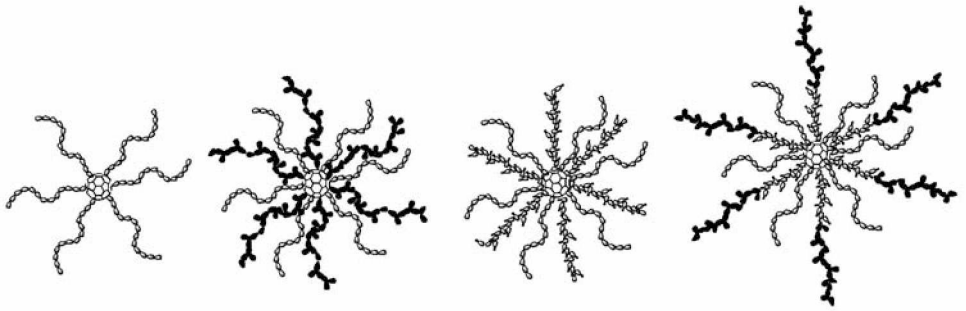

Small-angle neutron scattering was used in the study of fine structural organization of fullerene-containing star-shaped polystyrenes and hybrid stars, as well as the structure and parameters of supramolecular formations in deuterotoluene. It was shown that polystyrene stars and hybrid polymers with polystyrene and poly-2-vinylpyridine (P2VP) arms and C_{60} branching center are weakly associated in dimers, the stars based on polystyrene and poly-(*tert*-butyl methacrylate) (PTBMA) form clusters containing ~12 macromolecules with diameter of ~ 50 nm, and stars with polystyrene and P2VP-PTBMA diblock copolymer arms form “chains” including 4 macromolecules.

The work was supported by Russian Foundation for Basic Research (grant 10-03-00191a) and Program for Basic Research of the Presidium of RAS № 21

New trifluoromethyl derivatives of C_{76} and C_{82}

Lanskikh M.A.*[1], Chang K.-C.[2], Belova Yu.M.[1], Tamm N.B.[1], Kemnitz E.[2], Troyanov S.I.[1]

[1]*Moscow State University, Department of Chemistry, 119991, Moscow, Russia*
[2]*Humboldt University Berlin, Institute of Chemistry, 12489 Berlin, Germany*
**e-mail: malanskikh@gmail.com*

The present study concerns higher fullerenes of more than 70 carbon atoms. As is widely known, the number of possible isomers rapidly grows with the number of carbon atoms, the isomers that obey the Isolated Pentagon Rule (IPR) [1] being the most stable. Unambiguous structural determination of the fullerene molecules requires an X-ray study of pristine isomers or their derivatives. In this regard, the derivatized molecules frequently prove advantageous as the attached moieties suppress rotational disorder thereby enabling reliable determination of both cage connectivity and addition patterns. Here we report synthesis, separation, and structural characterization by means of single crystal X-ray diffraction of several new derivatives of C_{76} and C_{82}.

A mixture of higher fullerenes was reacted with CF_3I in a sealed ampoule at 400°C. The $C_m(CF_3)_n$ reaction products were dissolved in hexane and subjected to HPLC separation. Single crystals grown from three isolated fractions were studied by X-ray diffraction with the use of synchrotron radiation (BESSY, Free University, Berlin, Germany).

Two of the compounds obtained were found to contain the D_2-C_{76} carbon cage. These molecules, $C_{76}(CF_3)_{16}$-II and $C_{76}(CF_3)_{16}$-III, appear to belong to one of the two previously known families of trifluoromethylated derivatives of C_{76} [2]. The third compound, $C_{82}(CF_3)_{16}$, featured a certain disorder in the carbon cage (namely, alternating positions of two of the C-C bonds) caused by statistical distribution of enantiomeric molecules over the equivalent sites. The analysis of the disorder made it possible to attribute the carbon cage as the most stable isomer 3 of C_{82}. The reported isomer $C_{82}(CF_3)_{16}$ shows much similarity with the previously known $C_{82}(CF_3)_{18}$ [3], having 14 common CF_3 attachment sites.

We provide a general discussion of structural relationship, DFT calculated stability, and possible sequential addition pathways for the trifluoromethylated C_{76} and C_{82} known to date.

This work was supported by the Russian Foundation for Basic Research (09-09-00433 and 09-03-91337) and the Deutsche Forschungsgemeinschaft (Ke 489-26/2).

[1] P.W. Fowler, D.E. Manolopoulos, *An Atlas of Fullerenes*, Dover Publications, 2006, 392.
[2] N.B. Tamm, S.I. Troyanov, *Mendeleev Commun.* **20**, 229 (2010).
[3] S.I. Troyanov, N.B. Tamm, *Cryst. Rep.* **55**, 432 (2010).

Absorption characteristics of fullerene C_{60} in N-methyl-2-pirrolidone/toluene mixture

Kyrey T.O.*[1,2], Kyzyma O.A.[1,2], Avdeev M.V.[1], Korobov M.V.[3], Aksenov V.L.[1,4], Bulavin L.A.[2]

[1]*Joint Institute for Nuclear Research, Dubna, Moscow reg., Russia*
[2]*Taras Shevchenko Kyiv National University, Kyiv, Ukraine*
[3]*Lomonosov Moscow State University, Moscow, Russia*
[4]*Russian Research Center "Kurchatov Institute", Moscow, Russia*
**e-mail: tanya.kyrey@gmail.com*

Solutions of fullerene C_{60} in nitrogen-containing solvents and mixtures are characterized by the evolution of their UV-Vis, IR and Raman spectra in time. They also exhibit sharp solvatochromic effects under slight variations of fullerene concentration or solvent mixture content. Two main processes, namely the formation of C_{60} clusters and change in the solute-solvent interaction, contribute to these phenomena [1,2]. To clarify the role of the second factor, UV-Vis spectra of fullerene C_{60} in various mixtures of polar N-methyl-2-pyrrolidone (NMP), $\varepsilon = 32$, and non-polar toluene, $\varepsilon = 2.4$, are analyzed in this work. Previously, temporal solvatochromism was studied for C_{60}/NMP [3]. Also, changes in UV-Vis spectra with an increase in the absorbance at 450-550 nm took place on addition of polar solvent (water, $\varepsilon = 81$, miscible with NMP) to the system [4, 5]. Here, the solvatochromic effect accompanied with a hypsochromic shift of the absorption peak at 330 nm towards higher energy is observed after dissolution of C_{60}/NMP system with toluene. The detailed comparison of the absorption characteristics of C_{60} in two kinds of mixtures (NMP/toluene and NMP/water) prepared in different ways is presented.

[1] Avdeev M.V., Tropin T.V., Aksenov V.L., Rus. *J. Phys. Chem. A.* **84**(8), 1273 (2010).
[2] Kyzyma O.A., Korobov M.V., Avdeev M.V., Garamus V.M., Snegir S.V., Petrenko V.I., Aksenov V.L., Bulavin L.A., *Chem. Phys. Lett.* **493**, 103 (2010).
[3] Kyzyma O.A., Korobov M.V., Avdeev M.V., Garamus V.M., Petrenko V.I., Aksenov V.L., Bulavin L.A., Fullerenes, *Nanotubes and Carbon Nanostructures* **18**, P. 458 (2010).
[4] Scharff P., Risch K., Carta-Aberlmann L., Carbon **42**(5), 1203 (2004).
[5] Kyzyma O.A., Bulavin L.A., Aksenov V.L., Avdeev M.V., Tropin T.V., Korobov M.V., Snegir S.V., Rosta L., Materials structure, V. 15 (1), P. 17, (2008)

Interaction of oxygen with fullerenes: oxidation versus singlet oxygen production

Kvyatkovskii O.E.*[1], Zakharova I.B.[2], Diba D.D.[3], Makarova T.L.[1,3]

[1]*Ioffe Institute, 194021, St.Petersburg, Russia*
[2]*St. Petersburg State Polytechnic University, St. Petersburg, Russia*
[3]*Umeå University, 90187 Umeå, Sweden*
**e-mail: Kvyatkovskii@mail.ioffe.ru*

Photophysical and bactericidal action of fullerenes and its derivatives are believed to originate from the interaction with oxygen in two ways: through electron transfer resulting to the formation of super oxides (and other reactive oxygen species ROS), and secondly through energy transfer to triplet oxygen forming singlet oxygen. The latter process is not understood: it is agreed that the quenching of singlet oxygen occurs via "an unknown mechanism" [1]. While fullerenes dissolved in organic solvent are very efficient singlet oxygen generators, in solid state their bactericidal action decreases but not disappears [2]. Motivated by this fact, we simulated the possible routes of interaction of oxygen with fullerenes.

Singlet oxygen generation was examined on the basis of resonance energy transfer from the first excited triplet state of isolated C_{60} molecule to triplet oxygen. Based on the values of the lifetimes and energies for different processes the probability of the excited state T_1 of C_{60} to excite ground state molecular oxygen to the singlet spin states was estimated.

Ab initio calculations were performed to model the interaction of oxygen with fullerenes. It is shown that besides singlet oxygen generation, many other competing processes may happen. Attachment of the whole O_2 molecule is unfavourable. However, the energy of two $C_{60}O$ molecules is lower than two C_{60} and O_2 molecule. It is energetically beneficial to produce atomic oxygen, and under the action of visible light the attachment of oxygen to fullerene is likely to occur. The stability of the electronic structure of the oxidized products $C_{60}O$ and C_{60}-O-C_{60} in the singlet and triplet spin states were calculated on the basis of the pre- atomization of oxygen by photoexcited C_{60} using DFT/B3LYP method.

Supported by FP7 Marie Curie IRSES "Nano-Guard"

[1] J. W. Arbogast, *J. Phys. Chem.* **95**, 1 (1991).
[2] Piotrovsky L.B., In Medicinal Chemistry and Pharmacological Potential of Fullerenes and Carbon Nanotubes, F. Cataldo, T. Da Ros (eds.), Springer, 2008, p.139.

Ab initio calculations of nonlinear polarizabilities of fullerene-porphyrin complexes

Kvyatkovskii O.E.*[1], Zakharova I.B.[2]

[1]*Ioffe PhysicoTechnical Institute RAS, 194021 St. Petersburg, Russia*
[2]*State Polytechnic University, 195251 St. Petersburg, Russia*
**e-mail: Kvyatkovskii@mail.ioffe.ru*

Nonlinear optical properties of *M*TPP and C_{60}-*M*TPP complexes (*M*=H_2, Zn, Cu; TPP – tetraphenylporphyrin) are studied. Accurate ab initio calculations of electronic structure, optimized geometry, static linear and nonlinear polarizabilities (including first and second order hyperpolarizabilities) of C_{60}, *M*TPP molecules and C_{60}-*M*TPP complexes have been carried out using DFT/B3LYP method. It is shown that C_{60} and *M*TPP form a stable charge transfer complex C_{60}-*M*TPP, resulting in a giant enhancement of the nonlinear response. It is found that the enhancement of optical nonlinearity is not necessarily connected with the formation of covalent bonds between the components. The work is supported by Russian Foundation for Basic Research (Grant № 09-02-01008).

Endofullerenes of lanthanides Ln@C_{60}: *ab initio* geometric and electronic structure calculation

Krisilov A.V.*[1], Zon B.A.[1,2], Kotova A.L.[1]

[1]*Voronezh State University, 394006 Voronezh, Russia*
[2]*Belgorod State University, 308015 Belgorod, Russia*
**e-mail: alexph@mail.ru*

Endofullerenes are promising basic elements for quantum computer [1]. We have presented *ab initio* calculations of equilibrium geometric and electronic structure of lanthanide containing endofullerenes Ln@C_{60}. Stable position of metal atom is located on the C_3-axis which connects the centres of the opposite six-membered rings. We found two types of Ln@C_{60} structures. For the endofullerenes of the first type (La – Dy) the stable position of the lanthanide atom is located at the distance 0.67 R from the centre of the fullerene (R=3.35 A is the fullerene radius). The distance between lanthanide atom and the six nearet carbons coincides with 10 % accuracy with the sum of atomic radii of Ln and C. Similar interpretation of the off-centre position of lanthanide atom was recently presented for ion [Ce@C_{60}]$^+$ [2].

Potential energy surfaces of the second type of endofullerenes (Ho – Lu) have two minima. These minima correspond to the position of Ln in the centre and at the distance 0.5 R from the centre of fullerene. It results from qualitatively change of metal-cage interaction. Spinless lanthanide atom interacts weakly with the carbon cage and can occupy the equilibrium position in the centre of the fullerene. This is characteristic of the endofullerenes of the inert gases. Thus, the redistribution of the spin density is connected with the metall-cage interaction character change which results in the change of the equilibrium geometric and electronic structure of the endofullerene.

For all fullerenes the spin leakage effect is observed: partial or full transfer of the unpaired electrons to the carbon cage. Stability of lantanoid's position depends on the degree of spin leakage. Transfer of 50% spin density from metal atom to cage results in stabilization of structure.

Analysis of the spin density makes possible estimating the relative stability of lanthanides endofullerenes. In the low-spin state Ho@C_{60} and Tb@C_{60} can have maximal reactivity. Other endofullerenes practically do not show radical character. In the high-spin state the endofullerenes Pm@C_{60}, Sm@C_{60}, Eu@C_{60}, Gd@C_{60}, Tb@C_{60}, Ho@C_{60} show radical character, the most stable being Ce@C_{60}, Pr@C_{60}, Nd@C_{60}, Tm@C_{60}, Lu@C_{60}.

[1] W. Harneit, C. Meyer, A. Wedinger, D. Suter, and J. Twamley, *Phys. Stat. Sol. B* **233**, 453 (2002).

[2] A. V. Krisilov and B. A. Zon, *Opt. Spectr.* **109**, 833 (2010).

Optical properties of double pyrene-anthrylvinylene-fullerene-C_{60} or pyrene-OPV- fullerene C_{60} triads

Klimova E.[a], Klimova T.[a], Moggio I.[b], Arias-Marín E.[b], Martínez-García M.[b]*

[1]*Facultad de Química, Universidad Nacional Autónoma de México, Cd. Universitaria, Circuito Interior, Coyoacán, C.P. 04510, México D.F., México*

[2]*Centro de Investigación en Química Aplicada, Boulevard Enrique Reyna 140, C.P. 25253, Saltillo, México*

[3]*Instituto de Química, Universidad Nacional Autónoma de México, Cd. Universitaria, Circuito Exterior, Coyoacán, C.P. 04510, México D.F.*

**e-mail: margar@servidor.unam.mx*

In recent years, organic nanomaterials have inspired growing research efforts due to the great diversity of available organic π-conjugated macromolecules, their good thermal and chemical stability and electrical conductivity. Recently, the photovoltaic properties have been reported for anthrylvinylenes and conjugated oligophenylenevinylenes (OPV) blended with fullerene. In other works, pyrene, styrene or its derivatives have also been widely used as a fluorescence probe molecule due to the strong fluorescence and electron donor effect. On the contrary, fullerene C_{60} is known to be a strong electron-acceptor group, usually used for solar cells based on conjugated molecules. In the present work we report on the optical properties in solution of pyrene-anthrylvinylene-C_{60} and pyrene-OPV-Fullerene triads. Pyrene-containing anthracene and 4-styryl units were chosen as donor groups and fullerene C_{60} as acceptor.

The UV-Vis spectra show the pyrene electronic transition with an absorption band extending from 400 to 800 nm due to the combination of the π–π electronic transition of the antrylvinylene or OPV moiety and the C_{60} band, regardless the extension of the anthrylvinylene or OPV fragment. However, the emission is almost mirror-like with respect to the absorption bands of pyrene, suggesting that the HOMO and LUMO are more localized on this substituent. All the obtained compounds were characterized by ^{1}H and ^{13}C NMR, FTIR, UV-Vis, fluorescence spectroscopy, MALDI-TOF, Electrospray or FAB+ mass spectrometry, and elemental analysis.

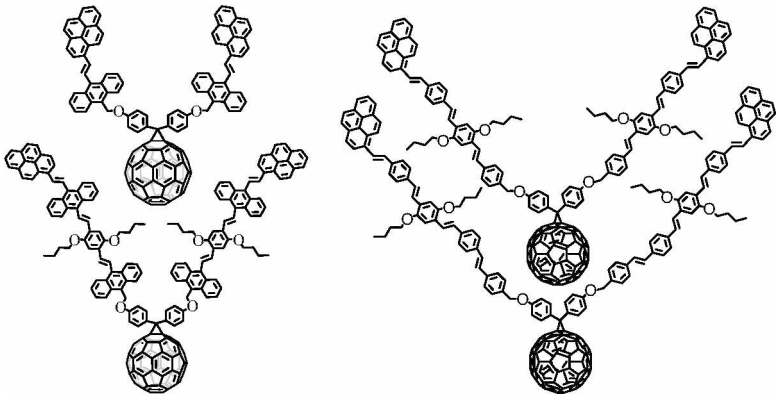

Interaction between hydroxyfullerene and water

Khokhriakov N.V.*[1], Kodolov V.I.[2]

[1]*Izhevsk State Agricultural Academy, 426069, Izhevsk, Russia*
[2]*Izhevsk State Technical University, 426069, Izhevsk, Russia*
**e-mail: khrv70@mail.ru*

Experimental data showing the radical changes in the structure of water and other polar liquids when introducing small amounts (about ten thousandth of per cent by mass) of surface active nanoparticles have been recently published. Hydroxyfullerene is a proper object for quantum chemical modeling of interaction between activated carbon nanoparticle and water. At the same time hydroxyfullerene is of great interest because of its possible applications in medicine, for water disinfection and for polishing nanosurfaces.

The report contains the results of quantum-chemical modeling that allow making the conclusions concerning on the degree of nanoparticle influence on the structure of aqueous solutions. The calculations were carried out in the framework of ab initio and semiempirical methods of quantum chemistry using the software complex GAMESS [1,2]. At the first stage, the quantum-chemical investigation of the interaction of α-naphthol and β-naphthol molecules with water was carried out within various quantum-chemical models in order to estimate the error value, which can be resulted from the application of simplified methods with insufficient basis sets. Thus comparison of calculation results with experimental data demonstrates ab initio Hartree-Fock method in the basis 6-31G basis set provides qualitatively correct conclusion on hydrogen bond energies for systems considered.

The interaction energy between hydroxyfullerene and water depends on amount and locations of OH-groups in carbon cluster. Thus for complex $C_{60}[OH]_{10} \cdot 10H_2O$ with symmetry C_5 ab initio calculations demonstrate that the energy of interaction between nanoparticle $C_{60}[OH]_{10}$ and water molecule nearly twice as big as the interaction energy of water molecules in dimer. Introduction of a metal atom inside the carbon cage leads to increasing of interaction energy with a water molecule by 15%. The semiempirical research demonstrates that hydroxyfullerene molecule forms a stable complex in water, being surrounded with 6 layers of water molecules.

[1] Granovsky A.A. PC GAMESS version 7.1.5, http://classic.chem.msu.su/gran/gamess/index.html.
[2] Schmidt M.W.; Baldridge K.K.; Boatz J.A.; Elbert S.T.; Gordon M.S.; Jensen J.H.; Koseki S.; Matsunaga N.; Nguyen K.A.; Su S.; Windus T.L.; Dupuis M.; Montgomery *J. A. J. Comput. Chem.* **14**, 1347 (1993).

Electronic structure and stability of C_{76} fullerene IPR-isomers

Khamatgalimov A.R., Kovalenko V.I.*

A.E.Arbuzov Institute of Organic and Physical Chemistry RAS, 420088, Kazan, Russia
**e-mail: koval@iopc.ru*

Only one isomer 1 (D_2) of two IPR-isomers of fullerene C_{76} have been produced and characterized as empty molecule. This isomer also exists as various endohedral metallofullerenes and exohedral derivatives, whereas second isomer 2 (T_d) have been produced and characterized only as exohedral derivative $C_{76}(CF_3)_{12}$ [1]. To clarify instability reason of isomer 2 (T_d) as empty molecule, the analysis of energy and geometrical parameters of molecules of both C_{76} fullerene IPR-isomers has been carried out on the basis of DFT calculations and earlier developed criteria [2].

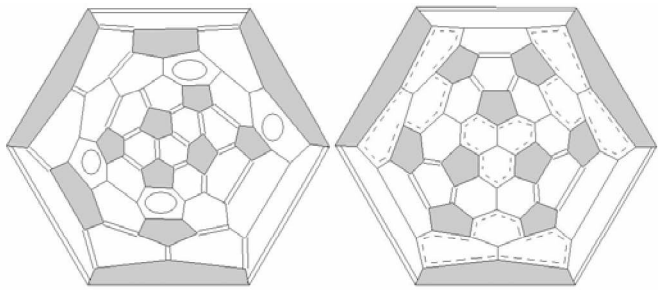

a b

Figure. Schlegel diagrams of isomers 1 (D_2) (a) and 2 (T_d) of C_{76} fullerene (b).

The distribution of single, double and delocalized pi-bonds in molecules of these isomers are shown (see Fig.). The reason of instability of isomer 2 (T_d) is presence of four phenalenyl-radical substructures whereas stable isomer 1 (D_2) have the closed electronic shell. The open-shell electronic structure of isomer 2 (T_d) is confirmed by the results of quantum-chemical calculations of triplet state which energetically more favorable than the singlet one. Note that addition of trifluoromethyls in $C_{76}(CF_3)_{12}$ [1] occurs namely on those four phenalenyl-radical substructures. Thus isomer 2 (T_d) cannot be obtained as a hollow molecule.

Generally, an instability of fullerenes can be caused not only by the presence of uncoupled electrons in a molecule (an open shell) but also by the strain of a molecule caused by cage distortions [3]. Analysis of geometry structures of isomers 1 (D_2) and 2 (T_d) show that local strains in both molecules are small, so instability of isomer 2 (T_d) is connected only with its radical nature.

[1] Shustova N.B., Kuvychko I.V., Bolskar R.D., Seppelt K., Strauss S.H., Popov A.A., Boltalina O.V., *J. Am. Chem. Soc.* **128**, 15793 (2006).
[2] Kovalenko V.I, Semyashova M.V. Abstr.4thWorkshop «Fullerenes and Atomic clusters» (IWFAC`99), St.Petersburg, 234 (1999).
[3] Kovalenko, V.I.; Khamatgalimov, A. R., *Russ. Chem. Rev.* **75**, 981 (2006).

Ionic complexes containing fullerene anions and negatively charged phthalocyanine structures

Khakimova E.U.[a], Konarev D.V. *[a], Zorina L.V.[b], Khasanov S.S.[b], Lyubovskaya R.N.[a]

[a]*Institute of Problems of Chemical Physics RAS, 142432 Chernogolovka, Russia*
[b]*Institute of Solid State Physics RAS, Russia, 142432 Chernogolovka, Russia*
**e-mail: konarev@icp.ac.ru*

At present great attention is given to the synthesis and study of ionic complexes of fullerenes with metalloporphyrines. This is due to interesting magnetic properties [1] and a possibility to investigate different negatively charged σ-bonded structures of fullerene in such complexes [2]. Phthalocyanines represent another large class of macrocycles. However, ionic fullerene complexes with phthalocyanines have not been obtained so far. Here we present the first ionic complexes containing simultaneously fullerenes anions and negatively charged coordination phthalocyanine structures:

$\{Mn^{II}Pc(CH_3CH_2S^-)_x\cdot(I^-)_{1-x}\}\cdot(C_{60}^{\bullet-})\cdot(PMDAE^+)_2\cdot C_6H_4Cl_2$ (x = 0.87) (**1**)

$\{Zn^{II}Pc(CH_3CH_2S^-)_y\cdot(I^-)_{1-y}\}_2\cdot(C_{60}^-)_2\cdot(PMDAE^+)_4\cdot(C_6H_4Cl_2)$ (y = 0.5) (**2**)

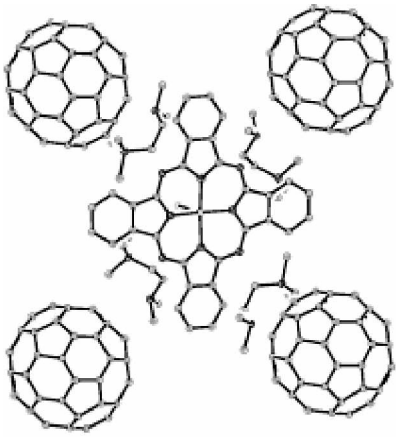

Both compounds have been obtained as single crystals that allowed their crystal structure to be studied. In complex **1** fullerene radical anions form honeycomb-like loose layers in which each fullerene has three neighbors with centre-to-centre distances of 10.130-10.289 Å. The absence of Van der Waals contacts between fullerenes results in that $C_{60}^{\bullet-}$ remains monomeric in this complex at 110(2) K. In complex **2** fullerenes form dimers $(C_{60}^-)_2$ bonded by one C-C bond. Dimers are packed in corrugated honeycomb-like layers with distances between fullerene centres equal to 9.898-10.107 Å. At the coordination of iodine or ethanethiolate anions on the central metal atom, phthalocyanines of Mn(II) and Zn(II) form unusual negatively charged coordination structures $M^{II}Pc(anion^-)$, which are packed in the $\{M^{II}Pc(anion^-)\}_2$ dimers with short interplanar distance of 3.142 Å in **1** and 3.274 Å in **2**. Phthalocyanine dimers also form layers with the $PMDAE^+$ cations and these layers alternate with the fullerene ones. The packing of spherical fullerenes with planar phthalocyanines in a crystal is attained by the introduction of fullerenes between two phenylene groups of phthalocyanine. The π-π interaction between porphyrin macrocycle and fullerene hexagonal or pentagonal rings characteristic of previously studied ionic porphyrin-fullerene complexes is not realized in complexes **1** and **2**.

[1] D.V. Konarev, S.S. Khasanov, G.R. Mukhamadieva, L.V. Zorina, A. Otsuka, H. Yamochi, R.N. Lyubovskaya, *Inorg. Chem.* **49**, 3881 (2010).

[2] D.V. Konarev, S.S. Khasanov, A. Otsuka, G. Saito, R.N. Lyubovskaya. *J. Am. Chem. Soc.* **128**, 9292 (2006).

Nanocomposite layers on the basis of polymeric forms of C_{60}

Kazachenko V.*[1], Razanau I.[2]

[1]*Belarusian State University of Transport, 246653, Gomel, Belarus*
[2]*Francisk Skorina Gomel State University, 246019, Gomel, Belarus*
**e-mail: kvp_@mail.ru*

The main methods of C_{60} polymer coatings synthesis such as irradiation of the thermally deposited in vacuum fullerite layers by the electromagnetic radiation in the ultraviolet-visible spectral range, modification by electrons with different energies and current densities, plasma polymerization, explosive fullerite vaporization and coating deposition by the convergent electron beam with the energy of 20 keV and the power of about 1 kW, are reviewed and discussed in the report. Special attention is paid to the method of electron-beam dispersion, which is being developed by the authors of this report. In this method, synthesis of nanocomposition layers on the basis of polymeric forms of C_{60} takes place from the active gas phase, produced by the irradiation of a fullerite target by an electron beam with the energy of 1-1.5 keV and power of 30-75 W.

The stages of fullerite dispersion and layer growth are analyzed. It has been shown that on the first stage, heating and radiation-thermal-induced modification of the surface layer of the fullerite target takes place without target dispersion and coating growth. On the second stage, at the temperature of about 540-560 K, a nonstationary period starts with an abrupt increase of the target dispersion and coating deposition rates. Stationary period of the dispersion and coating deposition takes place at the temperature of the target surface of about 850 K and the deposition rate of about 0.03 nm/s at 140 mm distance between the target and the substrate. The influence of the fullerite target charging on the stages of dispersion and coating deposition is also discussed. It has been shown that the molecular flow produced by fullerite C_{60} electron-beam dispersion contains positive ions and the coatings are deposited onto the substrates under the irradiation of the true secondary and back-scattered primary electrons, which significantly influence the structure of the layers being formed. Examples of the coatings synthesized using this method and having different content of dimers, linear polymer chains, two-dimensional and three-dimensionally cross-linked polymeric forms of C_{60}, as well as the nanocomposition coatings containing C_{60} and polyaniline, C_{60} and polytetrafluoroethylene, polymers and detonation-synthesized nanodiamonds are shown and discussed.

Fibers of functional nanocomposites of poly(3-hexythiophene) containing fullerene derivatives and carbon nanotubes

Beneoux C.,[1] Itzhak C.,[2] Avrahami R.,[3] Zussman E.,[3] Frey J.,[4] Katz E.A.,*[1,5] Shames A.I.[2,5], Yerushalmi-Rozen R.[2,5]

[1]*Dept. of Solar Energy and Environmental Physics, Jacob Blaustein Institutes for Desert Research, Ben-Gurion University of the Negev, Sede Boker 84990, Israel*
[2]*Dept. of Chemical Engineering, Ben-Gurion University of the Negev, Beer-Sheva 84105, Israel*
[3]*Department of Mechanical Engineering, Technion, Haifa 32000, Israel*
[4]*Dept. of Chemistry and Institute for Nanotechnology and Advanced Materials. Bar Ilan University, Ramat Gan 52900, Israel*
[5]*Ilze Kats Institute for Nanoscale Science and Technology, Ben-Gurion University of the Negev, Beer-Sheva 84105, Israel*
[6]*Dept. of Physics, Ben-Gurion University of the Negev, Beer-Sheva 84105, Israel*
**e-mail: keugene @bgu.ac.il*

We report on electrospinning of fibers composed of poly(3-hexylthiophene) P3HT fullerene derivative, phenyl-C61-butyric acid methylester (PCBM), and Single Walled Carbon Nanotubes (SWNT). While of great promise for photovoltaic applications, functional structures with a controllable morphology provide a great challenge. Here we show that control over the colloidal behavior of the SWNT and the PCBM via a tailor-made block-copolymer enables the electrospinning of long, uniform fibers of the polymer-nanostructures composites. The fibers exhibit improved crystallinity and efficient quenching of the photoluminescence. Light-Induced Electron Spin Resonance (LESR) spectroscopy provides a direct evidence of electron transfer between PCBM and P3HT components in both two- (P3HT/PCBM) and three-component (P3HT/PCBM/SWNT) fibers.

The Euler theorem for molecular structure studies: cases of fullerene-like nanoparticles of carbon and inorganic compounds

Katz E.A.*[1,2]

[1]*Dept. of Solar Energy and Environmental Physics, Jacob Blaustein Institutes for Desert Research, Ben-Gurion University of the Negev, Sede Boker 84990, Israel*
[2]*Ilze Kats Institute for Nanoscale Science and Technology, Ben-Gurion University of the Negev, Beer-Sheva 84105, Israel*
**e-mail: keugene @bgu.ac.il*

It is well known that molecular structures for the entire family of carbon molecules in the shape of convex polyhedra consisting only of hexagonal and pentagonal faces (fullerenes) can be precisely described on the basis of the Leonhard Euler's theorem on the relation between the numbers of faces, vertices and edges in polyhedra. We will demonstrate how to apply the generalized Euler relation for analysis of wide variety of fullerene-like structures of carbon (nano-tori, schwarzites, quasi-spherical and polyhedral nano-onions, etc) and inorganic compounds (MoS2, WS2, Cz2O). The analysis is discussed in a historical context and in comparison with the published experimental results.

Thermal stability of the endohedral complex of [60]fullerene with tetrahedrane, $C_4H_4@C_{60}$

Maslov M.M., Katin K.P.*

National Research Nuclear University "MEPhI", 115409, Moscow, Russia
**e-mail: KPKatin@yandex.ru*

The structure and stability of the C_4H_4 tetrahedrane molecule encapsulated inside the C_{60} cage was theoretically investigated via both molecular dynamics (MD) and potential energy search (PES) methods. All calculations were performed using the nonorthogonal tight-binding total energy model, originally developed for hydrocarbon compounds [1].

The heat of formation of the $C_4H_4@C_{60}$ complex was found to be 758.0 kcal/mol. The C–C and C–H bond lengths in tetrahedrane are equal to 1.524 A and 1.068 A for isolated C_4H_4 molecule, and 1.499 A and 1.043 A for $C_4H_4@C_{60}$ complex, respectively. The main decomposition channel of the encapsulated tetrahedrane molecule is its isomerisation to cyclobutadiene, as for isolated one. Energy and structure of the saddle configuration, which separates tetrahedrane@C_{60} from cyclobutadiene@C_{60} on the reaction path, was obtained using PES technique. The minimum energy barrier preventing tetrahedrane decay inside the fullerene cage was found to be 0.46 eV, which coincides with the same barrier for isolated C_4H_4 molecule. On the other hand, at the presence of fullerene cage the energy barrier for the reverse reaction significantly changes: it decreases from 3.06 eV to 2.05 eV.

To study the evolution of the excited $C_4H_4@C_{60}$ endohedral complex, we used the MD approach with the same tight-binding potential [1]. At the initial instant of time, all atoms were given random velocities and displacements, such that the momentum and the angular momentum of the whole system were equal to zero. The classical Newton equations of motion were solved numerically using the standard velocity Verlet algorithm. Combining the results of both PES and MD calculations, we derived an activation energy E_a and the frequency factor A in the Arrhenius equation $\tau^{-1}(T) = A\exp(-E_a/k_B T)$, describing temperature dependence of the encapsulated into the [60]fullerene cage tetrahedrane molecule lifetime τ (k_B is the Boltzmann's constant). These values are $E_a = (0.46 \pm 0.01)$ eV and $A = 10^{14.81\pm0.64}$ s^{-1}.

This work was supported by the Federal Target Program "The Development of Nanoindustry Infrastructure in the Russian Federation" for 2008–2011 years (Grant No 16.647.11.2008).

[1] M.M. Maslov, A.I. Podlivaev and L.A. Openov. *Phys. Lett. A* **373**, 1653 (2009).

Efficacy of fullerene capsule with amphipathic antioxidants vitamin

Ito S.[1], Fujimoto T.[2], Ito M.[3], Yamana S.[3]

[1]*Ito Reserach, 1800006, 1-6-7 Nakamati, Musasi, Tokyo, Japan*
[2] *Clinic F, 6-6-1-4F Koujimachi Chiyoda-ku, Tokyo 102-0083, Japan*
[3]*Vitamin C60 BioResearch Corporation, 1030028 1-3-19 Yaesu Chuo-ku, Tokyo, Japan*
**e-mail: sito@provitamin.jp*

Ascorbyl 2-Phosphate Tocopheryl (APT) was developed as amphipathic antioxidants vitamin. APT is a water-soluble derivative of ascorbate and tocopherol that is little soluble to oil but has a surface activity and can be used as an emulsifier and nanocapsule clathrate. Fullerene was capsuled with this amphipathic vitamin. This emulsification capsule was called an APTF- capsule. As for the APTF-capsule, performance as an external preparation ingredient for ultraviolet rays was evaluated.

When preparation that contained an ascorbic acid at a high concentration was exposed to a radical environment, such as ultraviolet rays, radicals of ascorbic acid were produced. However, when fullerene was added to the APT-capsle, the generation of ascorbic acid radicals was reduced significantly. Our experiment showed that fullerene controlled the generation of ascorbic acid radicals by ultraviolet rays under the presence of amphipathic vitamin c. APTS-capsule was also found to inhibit the decomposition of carotenoids, such as β carotene and astaxanthine, under a hyperoxidation condition of lipids. We also found that APTS-capsule inhibited the generation of superoxide radicals in the skin by infrared laser irradiation at 1.440 nm significantly. Our experiments suggested that APTS-capsule inhibits oxidization of both water-soluble and lipid-soluble antioxidants, the property of which possibly acts synergistically with amphipathic vitamins and fullerene such as APTF.

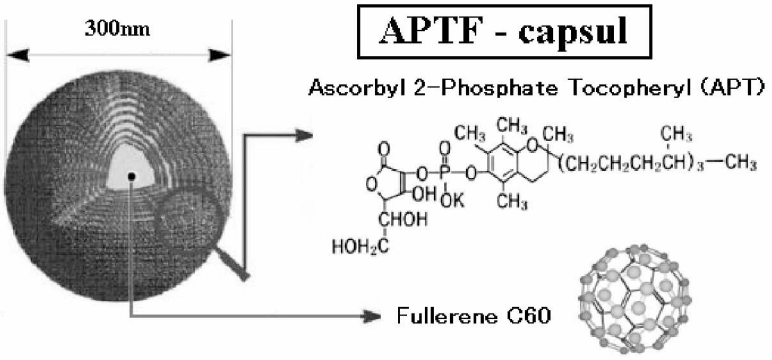

The APTF-capsule are likely promising tools for developing anti-aging systems with an effective redox balance, in which water-soluble and lipid-soluble redox molecules resonate with each other, and for applications in diverse industrial fields, including cosmetics and medical supplies.

Amino acid silyl esters as an efficient precursor in the 1,3-dipolar cycloaddition of azomethine ylides to fullerene C_{60}

Ioutsi V.A.*[1,2], Negrebetsky V.V.[1], Yurovskaya M.A.[2], Sidorov L.N.[2]

[1]*Russian State Medical University, 117997, Moscow, Russia*
[2]*Lomonosov Moscow State University, Chemistry Department, 119991, Moscow, Russia*
**e-mail: vitalik_org@thermo.chem.msu.ru*

The most routine method for fullerenes functionalization is the Prato reaction, which leads to fulleropyrrolidines with a quite good yield (30–40%). This method is based on the 1,3-dipolar cycloaddition of azomethine ylides, generated *in situ* thermally from aldehydes or ketones and amino acids, to the fullerene. Accordingly, a broad acceptance of the Prato reaction is explained by accessibility of a wide range of various amino acids and carbonyl compounds.

The classic conditions of the Prato reaction involve reflux of *N*-methylglycine (sarcosine) and paraformaldehyde in toluene during 2 h, affording *N*-methylfulleropyrrolidine with 41% yield [1]. In the case of less reactive amino acids and carbonyl compounds used, reaction may require a prolonged reflux and gives a final product in a low yield [2].

Here we report utilization of amino acid silyl esters as an efficient precursor for generation of azomethine ylides in the 1,3-dipolar cycloaddition to fullerene C_{60}. Thus, reflux of *N*-methylglycine trimethylsilyl ester and paraformaldehyde in toluene during 10 min leads to formation of *N*-methylfulleropyrrolidine with 80% yield.

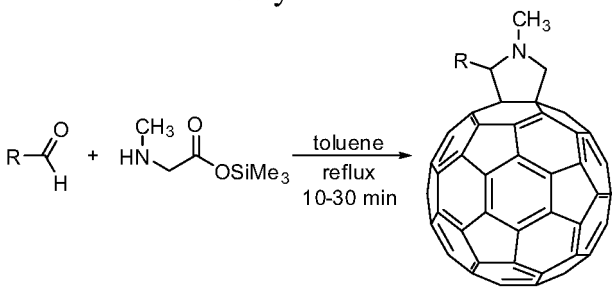

60-80%

Starting from various amino acids silyl esters and carbonyl compounds, a series of substituted fulleropyrrolidines were synthesized with comparatively high yield (60–80%).

[1] M. Maggini, G. Scorrano, M. Prato, *J. Am. Chem. Soc.*, **115**, 9798 (1993).
[2] B. M. Illescas, N. Martin, *J. Org. Chem.*, **70**, 6929 (2005).

Concentrating of higher metallofullerene and empty fullerene fraction with carbon cages of more than 100 carbon atoms

Grushko Yu.S.*[1], Kozlov V.S.[1], Artamonova T.O.[2], Khodorkovsky M.A.[2]

[1]*St.Petersburg Nuclear Physics Institute RAS, 188300, Gatchina, Russia*
[2]*Russian Scientific Centre "Applied Chemistry", 197198 St. Petersburg, Russia*
**e-mail: grushko@pnpi.spb.ru*

The metallofullerenes and empty fullerenes form great families of homologues with increasing number of carbon atoms in a molecule up to formation of carbon nanotubes.

The most abundant in arc-produced carbon soot is metallofullerene $M@C_{82}$. Nevertheless main part of carbon-encapsulated metal atoms is located in high molecular weight fullerenes. For some applications, such, for instance, as MRI –contrasting, any metallofullerenes of $Gd@C_{2n}$ or their mixtures are suitable.

Here we report on the simple method of concentrating of higher homologues of metallofullerenes $Gd@C_{2n}$, based on the difference in solubility of metallofullerenes and empty fullerenes in special organic solvents. The usual procedure for preparation of $M@C_{82}$ is two stage extraction. The first stage is extraction from soot with o-xylene (or CS_2) of main part of empty fullerenes (C_{60},C_{70} et al.) followed by second stage of extraction of metallofullerenes with DMFA(dimethylformamide). DMFA-extract contains main part of metallofullerenes but only $M@C_{82}$ can be easily redissolved in o-xylene. Therefore combining o-xylene and water for extraction of DMFA one can obtain solution of $M@C_{82}$ in o-xylene and the solid residue of higher metallofullerenes and empty fullerenes.

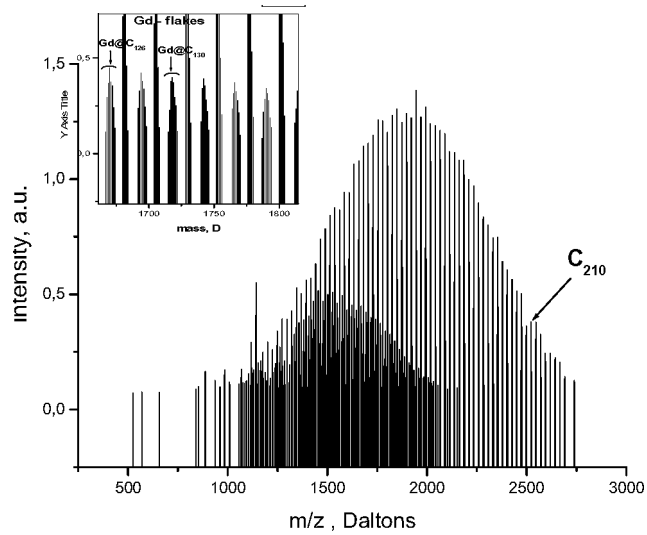

Figure. LD-TOF mass-spectrum of higher fullerene concentrate.

"Black" area is the Gd-metallofullerene region. It constitutes ~30% of residue.

.Phase transitions in two-layer fullerenes with the non-central effect

Kolesnikova A.[2], Glukhova O.*[1], Kirillova I.[2], Saliy I.[1], Slepchenkov M.[1]

[1]*Department of Physics, Saratov State University, 410012, Saratov, Russia*
[2]*Institute of Nanostructures and Biosystems, Saratov State University, 410012, Saratov, Russia*
**e-mail: glukhovaoe@info.sgu.ru*

The original research technique of the phase transitions in two-layer fullerenes whose mass centers do not coincide has been developed. The hybrid method effectively combining the tight-binding method with the modified molecular dynamics method [1] and the symmetry analysis of the surface topology of the Van der Walls interaction energy of two-layer fullerene shells forms the theoretical basis of the technique.

Nanosystems of $C_{60}@C_{540}$, $C_{80}@C_{540}$, $C_{180}@C_{540}$ with the icosahedral outer shell have been researched. The energy states of the ground state (E_1) and the excited states (E_2, E_3) of the internal fullerene have been calculated. The values of energies E_1, E_2, E_3 and values of formation enthalpy of two-layer fullerenes are represented in the table.

Table

Nanoclusters with the non-central effect	$C_{60}@C_{540}$	$C_{80}@C_{540}$	$C_{180}@C_{540}$
ΔH, $kcal/mol$; $C_m + C_n \rightarrow C_m@C_n$	-2.00	-71.78	-194.23
E_1, eV	-1.972	-2.569	-7.932
E_2, eV	-1.691	-2.288	-7.908
E_3, eV	-1.643	-2.270	-7.907

In the equilibrium state (0 K) C_{60} is localized in one of the 20 potential wells along the axis of fifth-order symmetry of the fullerene C_{540}. The C_{60} molecule began to jump between the potential wells with temperature increase. Thus it is established that nanosystem does not collapse and the hopping frequency of the internal fullerenes between the potential wells increases with temperature rising.

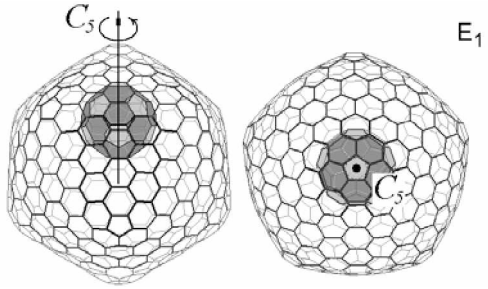

Figure. Molecule C_{60} inside fullerene C_{540}: the ground state.

[1] Glukhova O.E., Saliy I.N., Zhnichkov R.Y., Khvatov I.A., Kolesnikova A.S., Slepchenkov M.M., *J. Phys.: Conf. Ser.* **248**, 012004 (2010).

Reactivity of C_{60} fullerene towards peroxy radicals generated in initiated oxidation of hydrocarbons

Galimov D.I., Gazeyeva D.R., Sabirov D. Sh., Bulgakov R.G.*

Institute of Petrochemistry and Catalysis of RAS, 450075, Ufa, Russia
**e-mail: profbulgakov@yandex.ru*

At the moment the inconsistent data on ability of fullerenes to inhibit chain chemical and biochemical processes of oxidation have been accumulated. Earlier [1] chemiluminescent and volumetric methods have shown that C_{60} fullerene does not react with $RO_2^{\bullet}$ radicals generated upon oxidation of some hydrocarbons (ethyl benzene, dodecane, oleic acid). However, an attempt including application of more precision volumetry has elucidated that inhibition of the hydrocarbons liquid-phase oxidation by C_{60} takes place.

Efficiency of the fullerene effect has estimated as a degree of decrease in the initial rate of the cumene and ethyl benzene oxidation (Fig.) in the presence of C_{60}. The analysis of fullerene reactivity has performed in terms of effective rate constant of inhibition fk_{In} (f – capacity of inhibition, k_{In} – effective rate constant of the oxidation chain termination), calculated as

$$F = W_0/W_x - W_x/W_0 = fk_{In}[In]/\sqrt{2k_6W_i}$$

,

where [In] – concentration of inhibitor, W_0 and W_x – initial rate of the O_2 uptake in the absence and in the presence of inhibitor C_{60} respectively, F – the inhibition parameter, k_6 – the rate constant of $RO_2^{\bullet}$ bimolecular decay. As a result, $fk(C_{60})$ for inhibition of the cumene and ethyl benzene oxidation have been found to equal to 1.3 10^3 and $2.0\cdot10^3$ L mol^{-1} s^{-1}. For comparison: fk of ionol, a typical synthetic antioxidant, measured in the same conditions equals to $2.1\cdot10^4$ L mol^{-1} s^{-1}.

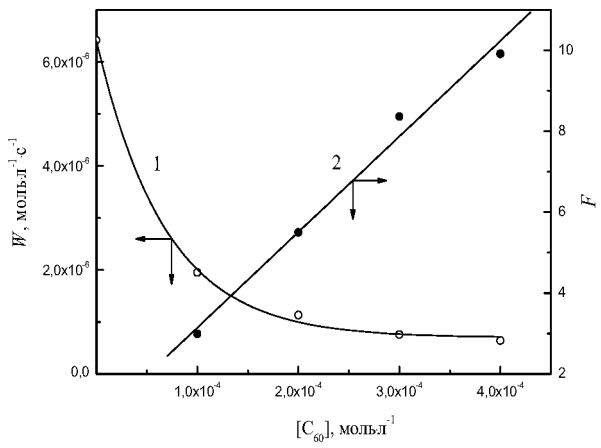

Figure Initial rate of the cumene oxidation W (1) and the inhibition parameter F (2) vs. the C_{60}concentration, T = 343 K, W_i = 9 10^{-8} L mol^{-1} s^{-1}.

Apparently, the efficiencies of inhibition by fullerene and ionol differ by an order that allows concluding the lability fullerene radicals, i.e. the possibility of these radicals to participate not only in the chain termination processes but also in the chain initiation and propagation of radical oxidation process.

Functionalization of fluorine-containing fullerene derivatives

Brotsman V.A.*, Ioutsi V.A., Bogdanov V.P., Rybalchenko A.V., Ovchinnikova N.S., Goryunkov A.A., Sidorov L.N.

Lomonosov Moscow State University, Chemistry Department, 119991, Moscow, Russia
**e-mail: brotsman_va@mail.ru*

A recently synthesized novel class of the difluoromethylene homofullerenes and a wide range of perfluoroalkylated fullerenes appreciably extend a family of fluorine-containing fullerene derivatives. Due to their high electron-deficient properties these compounds are considered as promising building blocks for organic electronic devices, what may require their additional derivatization. Only a few examples of functionalization of some individual isomers of trifluoromethylated fullerene C_{70} by the Bingel-Hirsch [1] and the Diels-Alder [2] reactions are known. Here we report a new synthetic approach for regioselective derivatization of the novel fluorine-containing fullerene derivatives based on nucleophylic substitution of alkyl halides to their anions.

The reported synthetic approach was applied to the representative compounds from each classes – homofullerene $C_{60}(CF_2)$ and C_s-$C_{70}(CF_3)_8$. The anions of these compounds were chemically generated by the deprotonation of the respective dihydrogenated derivatives [3].

The hydrogenated derivatives, $C_{60}(CF_2)H_2$ and $C_{70}(CF_3)_8H_2$, were synthesized and characterized by UV/Vis-, ^{1}H and ^{19}F NMR spectroscopy. Quantum chemical calculations at the DFT level predict regioselective functionalization of the $C_{60}(CF_2)H^-$ and $C_{70}(CF_3)_8H^-$ due to the localization of negative charge on certain carbon atoms. The deprotonation of the $C_{60}(CF_2)H_2$ and $C_{70}(CF_3)_8H_2$ solutions with consequent treatment by the alkyl halids leads to the formation of the respective alkyl derivatives of the $C_{60}(CF_2)$ and C_s-$C_{70}(CF_3)_8$.

Noteworthy, the reported approach can be applied to the dihydrogenated compounds sequentially to obtain respective disubstituted derivatives.

[1] Ovchinnikova N.S., Ignateva D.V., Tamm N.B., Avdoshenko S.M., Goryunkov A.A., Ioffe I.N., Markov V.Y., Troyanov S.I., Sidorov L.N., Yurovskaya M.A., Kemnitz E., *New J. Chem.* **32**, 89 (2008); Ovchinnikova N.S., Goryunkov A.A., Khavrel P.A., Belov N.M., Apenova M.G., Ioffe I.N., Yurovskaya M.A., Troyanov S.I., Sidorov L.N., Kemnitz E., *Dalton Trans.*, **40**, 959 (2011).

[2] Takano Y., Herranz M.A., Kareev I.E., Strauss S.H., Boltalina O.V., Akasaka T., Martin N., *J. Org. Chem.*, **74**, 6902 (2009).

[3] Meier M.S., Bergosh R.G., Gallagher M.E., Spielmann H.P., Wang Zh., *J. Org. Chem.*, **67**, 5946 (2002).

Adducts of [60]fullerene with basic amino acids as delivery vectors

Bashkatova E., Shilovski I., Bashkatova Yu., Khaitov M., Andreev S.*

NRC Institute of Immunology, 115478, Moscow, Russia
**e-mail: andsergej@yandex.ru*

Cationic molecules such as adducts fullerene C_{60} with basic amino acids (FBAs) are capable of binding DNA or RNA molecules and condense to globular compact structures, and hence have a great potential as a vectors for gene delivery. In an earlier study, we reported the water-soluble fullerene-based amino acids are good penetrable into various cells [1]. After passing through cell membranes (by endocytosis) the vector is acylated and loses a charge, resulting in releasing of a nucleic acid molecule into the cytoplasm. We have developed a new variant of FBA synthesis where addition of amino acids to the [60]fullerene may conduct in a homogeneous aprotonic medium previously modifying the amino acid by a trimethylsilylating agent. The purification of FBA is easily achieved by extraction and dialysist. The adducts $C_{60}(Arg)_n$ and $C_{60}(Lys)_n$ (as epoxides) contain 4-5 molecules of amino acid per fullerene core and are characterized by positive zeta potential (ξ about +30 mV). The size of FBA clusters determined by DLS analysis was varied from 20 to 200 nm depending on the pH and concentrations as. Acute toxicity data showed that FBAs at concentrations 2-250 μg/ml have no effect on viability of 293 cells. In due to the lack of allergenicity such FBAs and low toxicity these studies allow us to consider these AF as potential vectors for delivery of DNA, RNA and short RNA in target cells. Due to the lack of immunogenicity and allergenicity such compounds can be considered as potential vectors for nucleic acid delivery into target cells.

[1] Andreev I., Petrukhina A., Garmanova A., Andreev S., Romanova V., Troshin P., Troshina O., DuBuske L. *Fullerenes, Nanotubes, and Carbon Nanostructures* **16**, 89 (2008).

The functionalization of C_2-p^7-$C_{70}(CF_3)_8$ by the Bingel reaction

Apenova M.G.*, Ovchinnikova N.S., Goryunkov A.A., Borkovskaya E.V., Belov N.M., Troyanov S.I., Sidorov L.N.

Lomonosov Moscow State University, Chemistry Department, Moscow, 119992 Russia
**e-mail: mg.apenova@mail.ru*

An extensive development of synthetic methods for the trifluoromethylation of C_{60} and C_{70} resulted in a large number of different individual structurally-characterized $C_{60/70}(CF_3)_n$ with n=2–18. The methods of their following derivatization are under active studying [1].

Here we report the functionalization of a trifluoromethylated fullerene C_2-1,4,11,19,31,41,51,60-$C_{70}(CF_3)_8$, *via* the Bingel reaction for the first time. In C_2-p^7-$C_{70}(CF_3)_8$ all CF_3 groups arrange in the continuous ribbon of edge-sharing *para*-$C_6(CF_3)_2$ hexagons in the equatorial region of the molecule, remaining free both poles for further functionalization.

For the preparation of C_2-p^7-$C_{70}(CF_3)_8$ the typical two-step method [2] was used. The room temperature Bingel reaction of the HPLC-purified C_2-p^7-$C_{70}(CF_3)_8$ yielded the mixture of single isomer of $C_{70}(CF_3)_8[C(CO_2Et)_2]$ monoadduct and two isomers of $C_{70}(CF_3)_8[C(CO_2Et)_2]_2$ bisadduct.

The structures of isolated derivatives of C_2-p^7-$C_{70}(CF_3)_8$ were determined by means of ^1H and ^{19}F NMR spectroscopy and quantum chemical calculations at the DFT level. The structure of one isomer of bisadduct, $C_{70}(CF_3)_8[C(CO_2Et)_2]_2$-I, was revealed by X-ray single crystal analysis.

[1] Ovchinnikova N.S., Goryunkov A.A., Khavrel P.A., Belov N.M., Apenova M.G., Ioffe I.N., Yurovskaya M.A., Troyanov S.I., Sidorov L.N., Kemnitz E. *Dalton Trans.*, **40**, 959 (2011); Takano Y., Herranz M.A., Kareev I.E., Strauss S.H., Boltalina O.V., Akasaka T., Martin N., *J. Org. Chem.* **74**, 6902 (2009); Ovchinnikova N.S., Ignateva D.V., Tamm N.B., Avdoshenko S.M., Goryunkov A.A., Ioffe I.N., Markov V.Y., Troyanov S.I., Sidorov L.N., Yurovskaya M.A., Kemnitz E., *New J. Chem.* **32**, 89 (2008).

[2] Mutig T., Kemnitz E., Troyanov S.I., *Mendeleev Commun.* **19**, 30 (2009).

Synthesis and characterization of the novel isomer 1,4,10,19,25,41,60,69-$C_{70}(CF_3)_8$

Apenova M.G.*, Rybalchenko A.V., Borkovskaya E.V., Belov N.M., Dorozhkin E.I., Ignat'eva D.V., Goryunkov A.A., Ioffe I.N.

Lomonosov Moscow State University, Chemistry Department, Moscow, 119992, Russia
**e-mail: mg.apenova@mail.ru*

A large number of different individual structurally-characterized $C_{60}/_{70}(CF_3)_n$ compounds with n=2–18 is known. Under the typical conditions for trifluoromethylation, both with CF_3I [1] and silver trifluoroacetate [2], the major product is C_s-symmetrical $C_{70}(CF_3)_8$. Additionally isolated and characterized were two more isomers of $C_{70}(CF_3)_8$ molecule with C_2-symmetry [1,3]. Here we report the synthesis and characterization of the novel asymmetrical 1,4,10,19,25,41,60,69-$C_{70}(CF_3)_8$ isomer.

For the preparation of C_1- $C_{70}(CF_3)_8$ the typical two-step method was used [1]. The reaction of C_{70} and CF_3I in a glass ampoule at 420 °C gave a mixture of $C_{70}(CF_3)_n$ compounds, n=10–18, as evidenced by MALDI mass spectra. Further reaction of this mixture with C_{70} at 440 °C yielded lower trifluoromethylated fullerenes (n=2–10) *via* comproportionation. Isolation of novel isomer of $C_{70}(CF_3)_8$ was carried out by means of two-step HPLC separation.

On the basis of the ^{19}F NMR data and the quantum chemical calculations at the DFT level the addition pattern for the experimentally obtained new C_1-$C_{70}(CF_3)_8$ was suggested. 2D COSY ^{19}F NMR data reveal that the new isomer of $C_{70}(CF_3)_8$ represents trifluoromethylated fullerene molecule with the C_1-symmetry comprising a single continuous ribbon of edge-sharing *para*- and *meta*-$C_6(CF_3)_2$ hexagons.

[1] Mutig T., Kemnitz E., Troyanov S.I., *Mendeleev Commun*, **19**, 30 (2009).
[2] Dorozhkin E. I., Ignat'eva D. V., Tamm N. B., Goryunkov A. A., Khavrel P. A., Ioffe I. N., Popov A. A., Kuvychko I. V., Streletskiy A. V., Markov V. Y., Spandal J., Strauss S. H., Boltalina O. V., *Chem. Eur. J.* **12**, 3876 (2006).
[3] Mutig T., Ioffe I.N., Kemnitz E., Troyanov S.I., *Mendeleev Commun.* **18**, 73 (2008).

Direct synthesis of carbon nanostructures

Amsharov K.Yu.*[1], Jansen M.[1]

[1]*Max Planck Institute for Solid State Research, D-70569 Stuttgart, Germany*
**e-mail: k.amsharov@fkf.mpg.de*

The main task of direct synthesis is the controlled generation of the desired nanostructures by rational chemical methods. This approach is of practical interest for the production of individual higher fullerenes and nanotubes with specific chiralities. Our methodology is based on the synthesis of polycyclic aromatic hydrocarbons which already contain all nessasary carbon atoms in appropriate positions. The following intramolecular condensation leads to the desired nanostructures, the carbon connectivity of which is fully predefined by the precursor molecule. The higher fullerenes can be synthesized by regioselective "rolling-up" of the precursor molecules either by flash vacuum pyrolysis (FVP)[1,2] or by catalytical cyclodehydrogenation (CCDH) on a Pt surface.[3] The CCDH approach seems to be an appropriate technique for direct synthesis of carbon nanotubes since the nucleation step leading to the formation of an end-cap with accidental geometry can be replaced by introducing a predefined end-cap molecule. Subsequent growth will lead to the desired SWCNT species as determined by the end-cap geometry. [7]

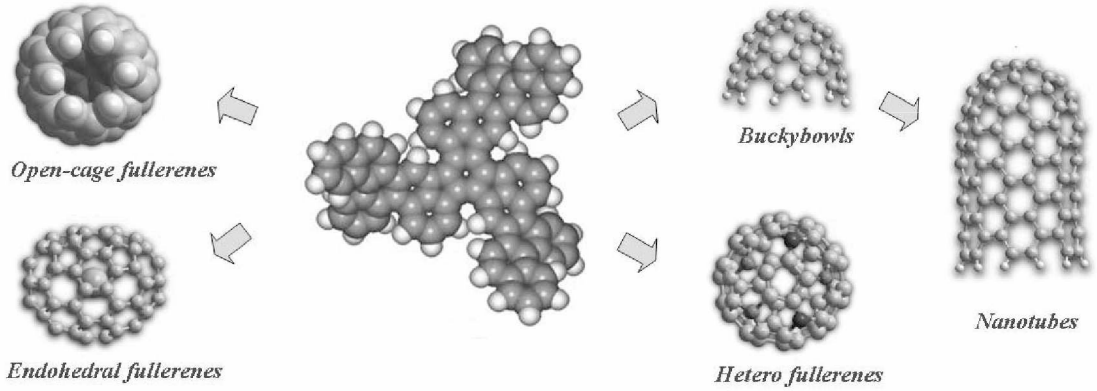

The direct synthesis approach is not limited to fullerenes and carbon nanotubes but can be applied as well to the formation of other carbon based nanostructures including, but not limited to endohedral and open cage fullerenes, nanoribbons and hetero graphenes.

[1] K.Yu. Amsharov, M. Jansen, *J. Org. Chem.* **73**, 2931. (2008).
[2] K.Yu. Amsharov, M. Jansen, *Chem. Commun.* **19**, 2691. (2009).
[3] K.Yu. Amsharov, N. Abdurakhmanova, S. Stepanow, S. Rauschenbach, M. Jansen, K. Kern, *Angewandte Chemie* **49**, 9392. (2010).
[4] A. Mueller, K. Yu. Amsharov, M. Jansen, *Tetrahedron Lett.* **51**, 3221, (2010).

Fullerene for semi-conducting photo- and light diodes (1.5–5.0 μm)

SherstnevV.V.[1], Alekseyev N.I.[1]*, Charikov N.A.[2], Semenov K.N.[2], Keskinov V.A.[2], Krohina O.A.[2]

[1]*Ioffe Institute, 194021, St.Petersburg, Russia*
[2]*ILIP, Joint Venture, 197122, St.Petersburg, Russia,*
**e-mail: Aleks@mail.ioffe.ru*

Semiconducting IR photo- and light diodes for the 1.6–5.0 μm range are widely applied. They are especially required as a key component in gas analyzers for monitoring industrial and natural gases (methane, SiO_2, NO_2 etc).

It is known that the passivation methods are developed within opto-electronics. Passivaton helps prevent semiconductors from reactions with atmosphere and eliminate interface levels from the bandgap. It is known that that the passivation in alcohol sulphidic solutions improves the characteristics of *p–n* mesadiodes and IR InAsPSb/InAs photo diodes. Though, the surfaces treated this way are unstable. We sought the solution on the way of covering the surfaces of the diodes with individual fullerene C_{70} and with an extract of higher fullerenes C_{76}+ C_{78}+C_{84}+C_{90}+.... The fullerene material was obtained in "ILIP", Joint, SPb. The purity of the C_{70} fullerene was ~99%. On the contrary, in the C_{76} + C_{78} + C_{84} + ... mix the higher fullerene content was ~ 98mas%, the light fullerenes played the role of the admixture.

We grew three types of photo- and light diode structures for 2–5 μm wavelength range based on the *n*-type InAs (100) substrates. Liquid- and gas-phase epitaxy (MOVPE) were used. From the structures grown photodiode chips were produced with using photolithography and liquid chemical etching. Then the fullerenes, preliminarily solved in toluene, were evaporated within a drying box to form a continuous dissolvated fullerene film on the solid chip surface.

The chips of 500×500 μm^2 obtained this way were soldered on TO-18 box. All the devices had diode type characteristics with cutoff voltage of ~ 0.4 V at RT and differential resistance of 1.0–1.2 Ohm. To determine the dark currents, reverse branches of I-V characteristic were measured before the covering, just after and the month since the procedure. When using the C_{70} fullerene as a passivating agent, the dark current for two types of the photodiodes (PD-36 and PD-46 for the 1.5–3.5μm and 1.5–3.5μm) reduced by 40 и 20% at standard reverse biases. In similar way, for the LED28 light diode the leak current reduced by 20%, the resistance doubled. The radiation intensity for the V-2928 light diodes at RT increased by 17–18%. Similar result was registered for ohmic power within the whole working current range.

When using the heavy fullerene mix as a passivating agent, the results are similar. The dark current reduction in the PD-36 and PD-46 were ~ 11% and 14%. Besides that, a sample temperature decrease was found (the Peltier effect).

Cheap method for synthesis of highly water soluble fullerene derivatives – fullerenols-d

Semenov K.[1], Alekseyev N.I.*[2], Charykov N.[3], Keskinov V.[3]

[1]*St.-Petersburg State University, Russia;* [2]*Ioffe Institute, 194021, St.Petersburg, Russia*
[3]*ILIP, Joint Venture, 197122, St.Petersburg, Russia*
**e-mail: Aleks@mail.ioffe.ru*

The applications of the fullerenes are often retained by their almost total incompatibility with water solutions. So, an interest in the production of water-soluble derivatives of the fullerene is steadily high.

A polyhydroxylated water soluble fullerenol $C_{60}(OH)_n$ has a simple structure, small toxicity and high ability to capturing radicals. However the cost of pure fullerenol is too high for its industrial applications. Therefore a technology of the fullerenols allowing different functional groups, not necessarily hydroxyl ones, is important. We choose a direct synthesis of the fullerenols as the most simple and steady. The saturated C_{60} solution in benzene (600 mg of C_{60}/800 ml of benzene) was added with a solution of NaOH (20g/20 ml) and with tetrabutyl-ammonium hydroxide solution $[(n\text{-}C_4H_9)_4N]OH$ in intensive mixing mode.

Then benzene was driven away and the reactionary mix was added with water. In an optimized course of subsequent procedures, principal of which was the fullerene salting out from the water solution by means of methanol, small-dispersed red-brown crystals of the fullerenol-d synthesized were deposited. The quantity of the product was ~70% from the theoretically predicted yield.

The electron spectrum of the water solution of the fullerenol-d does not have notable absorption bands in the both visible and near UV regions. In particular, the absorption peaks at ~ 472nm (fullerene C_{70}), ≈ 335nm (both C_{60} and C_{70}), 320–330 nm (for the bromine fullerenes $C_{60}Br_n$ (n = 6,8,24), typical of the light fullerenes and their derivatives, are absent. Though, UV-spectra of the fullerenols are able to be used for finding their concentration, following the Lambert-Ber law at non-characteristic wavelengths, e.g. at $\lambda \approx 300 \div 350$ nm. More informative are the IR absorption spectra, registered at SHIMADZU FTIR-8400S device for solid state samples. Notable are the absorption region for $\tilde{\nu}_1 \approx 3420$ cm^{-1} (hydro-xyl OH absorption), $\upsilon_{2(1)}$'=1590 cm^{-1} and $\upsilon_{2(2)}$'=1450 cm^{-1} (duplet), υ_3'=1040 cm^{-1}. So, IR- spectra of the fullerenol-d are also useful for its identification.

High performance liquid chromatography (HPLC) of fullerenol-d in water as well as the mass-spectrometry characterize the content of the fullerenol-d composition as a mix of polyalcohols $C_{60}(OH)_n$, oxy - polyalcohols $C_{60}(OH)_{n1}O_{n2}$ and their salts. Owing to the features of our synthesis the formation of sodium salts with a common formula of $C_{60}(OH)_{n1}O_{n2}(ONa)_{n3}$ is also possible.

Two examples of promising fullerenol-d application are presented in the materials of the Workshop.

Increase in stability of paints modified with fullerenol-d

Semenov K.[1], Alekseyev N.I.[2]*, Charykov N.[3], Letenko D.[4], Nikitin V.A.[5], Namazbaev V.I.[3], Keskinov V.[3], Puharenko Y.V.[5]

[1]*St.-Petersburg State University, Russia*
[2]*Ioffe Institute, 194021, St.Petersburg, Russia*
[3]*ILIP, Ltd, 197122, St.Petersbug, Russia*
[4]*North-WeSt. State Technical University, 191186, St.Petersburg, Russia*
[5]*Saint-Petersburg State University of Architecture and Civil Engineering, 191186, St.Petersburg, Russia*
**e-mail: Aleks@mail.ioffe.ru*

In [1] we described a comparatively cheap method for the production of water-soluble fullerene derivatives – fullerenols-d ("direct") – FL-d. In the concept of the FL we included not only the derivatives $C_n(OH)_X$ (n = 60, 70, etc.) but also a mix containing $C_n(OH)_XO_Y$, $[C_n(OH)_XO_Y](ONa)_Z$, i.e. not hydroxyl groups and groups of salt type.

The presence of a good number of functional groups, high water solubility and low production cost justify the research for FL-d in such mass applications as water-soluble paints and modifiers of metallic surfaces exposed to corrosion. The FL-d solubility research in water has shown that this solubility is high enough for the introduction of the FL-d in many water-soluble grounds-enamels without any artificial heating. Besides that, already at 50°C the solubility of FL-d exceeds that of such highly soluble salt as halite.

We have chosen a red-brown water-based anticorrosive acrylate ground-enamel VAK VD–AK–012PK (VAPA, Ltd., St.-Petersburg, Russia) for ferrous metals as a paint.

When adding as small quantities of FL-d as $2.5\cdot10^{-4}$ M (Mol of FL-d/l) the stability of the covering increased significantly to reach 7 rel. % for the removal of the first 5 microns and 25 rel.% for total removal of the paint. With the further increase in the fullerenol-d content the stability increased catastrophically: 8.3 times for the initial resistance and 2.9 times for the total removal resistance. In other words, the fullerenol-d (added to the paint in sufficient quantity) sharply increases the abrasion resistance of the covering, the greatest increase being observed for the external (i.e., the initially attacked) surface. This fact is even more important for practice than an integral abrasion resistance.

The same proportions of the FL-d reduce the adhesion instability determined by standard test run methods, by 29% and down to zero level, respectively.

[1] http://www.ioffe.ru/ACN/2011/ K. Semenov, N.I. Alekseyev, N. Charykov, V. Keskinov. Cheap Method for Synthesis of Highly Water Soluble Fullerene Derivatives-Fullerenols-d.

Anti-corrosion properties of metallic surfaces modified with fullerenol-d

Semenov K.[1], Alekseyev N.I.[2]*, Charykov N.[3], Letenko D.[4], Nikitin V.A.[5], Namazbaev V.I.[3], Keskinov V.[3], Puharenko Y.V.[5]

[1]*St.-Petersburg State University, Russia;*[2]*Ioffe Institute, 194021, St.Petersburg, Russia*
[3]*ILIP, Ltd, 197122, St.Petersbug, Russia*
[4]*North-West State Technical University, 191186, St.Petersburg, Russia*
[5]*Saint-Petersburg State University of Architecture and Civil Engineering*
**e-mail: Aleks@mail.ioffe.ru*

In [1] we described a comparatively cheap method for the production of water-soluble fullerene derivatives – fullerenols-d ("direct") – FL-d. Because of a specificity of our method, which does not provide total removal of sodium from the system in practically adoptable situations, we widened the concept of FL-d. We included in FL-d not the derivatives $C_n(OH)_X$ (n = 60, 70, etc.) only but also a mix containing $C_n(OH)_XO_Y$, $[C_n(OH)_XO_Y](ONa)_Z$, i.e. not hydroxyl groups and groups of salt type. The presence of the functional groups, high water solubility and low production cost justify the research for FL-d in such mass applications as water-soluble paints and modifiers of metallic surfaces exposed to corrosion.

The research for anticorrosive properties of FL-d was started with the question whether small quantities of FL in an active environment catalyze corrosion or inhibit it. We used a water solution of H_2SO_4 with a normal concentration of $N(H_2SO_4)$=0.25 g-equivalent/l as a reference solution. In this environment the FL-d showed itself as not an inhibitor but as a rather weak catalyst of corrosion. Even its as negligible quantities in this environment as $5.01 \cdot 10^{-5}$ M(mol/l) accelerate the corrosion processes on the both steel (~5 rel.%) and aluminum surfaces, at least within the first 1-2 hours.

On the contrary, for the metals, preliminarily treated with the FL-d, the result was positive. We treated the samples through their soaking in 0.0044 M water solution of FL for 3 days at RT. The measurements show the corrosion rate reduces by the factor of ~9, i.e. the FL-d suppresses the corro-sion. What is more, the suppression is revealed most of all in the first moment of the contact with an electrolyte. The technical aluminum showed similar results.

The corrosion reduction in water solution, stimulated by FL, is natural to correlate with higher insulating characteristics on proper metallic borders. In the case of steel the surface resistance increases ~10 orders of magnitude. This fact is connected with the formation of FL semiconducting film. A similar result is registered for aluminum.

[1] http://www.ioffe.ru/ACN/2011/K.Semenov, N.I.Alekseyev,N.Charykov, V. Keskinov. Cheap Method for Synthesis of Highly Water Soluble Fullerene Derivatives – Fullerenols-d.

Behavior of the solvate molecules in solid solvate of C_{60} and C_{70} fullerenes under heating

Aksenova V.V.*, Nikonova R.M., Lad'yanov V.I.

Physical-Technical Institute, Ural Branch, Russian Academy of Sciences, Izhevsk 426000, Russia
**e-mail: las@pti.udm.ru*

One of the priority directions in physics and chemistry of the fullerenes is studying their interaction with solvents. To date values solubility of the fullerenes in different classes of organic solvents as well a structural laws that explain their high solubility in aromatic hydrocarbons were determined. There are many works devoted to mixed crystals or van der Waals crystals - the fullerenes molecular complexes with nonpolar molecules.

In studying thermal stability of the fullerites including the making of the composites modified with fullerenes C_{60} and C_{70} and also their mixes, it is necessary to take into account effect of residual solvent during the oxidation. In this study the deformation of the molecules of the solvent ($C_5H_6CH_3$ and CCl_4) in the crystal solvates of the fullerenes C_{60} and C_{70} that form from the solutions have been studied by methods of FT-IR-spectroscopy, the differential scanning calorimetry and X-ray diffraction. Herewith the thermal stability of crystalline solvate depends on the strain of molecules of solvent that was detected due to the shift of the vibrational absorption bands.

It was shown that under the low-temperature annealing (up to 500°C) crystal solvates are destroyed, which leads to the removal of deformation of the solvent molecules and “loosening” a crystal lattice of the fullerenes when the solvent was evacuated from the fullerites. As the result – the presence of the solvent in fullerites facilitates both the diffusion of the oxygen during heating in the air and the oxidation of the fullerite.

The work was supported by the program of the Presidium of the Ural Branch of the Russian Academy of Sciences (the project 09-T-1008).

The first example of the interaction between [60]fullerene and hydrazoic acid

Akhmetov A.R.*, Tuktarov A.R., Yarullin I.R., Dzhemilev U.M.

Institute of Petrochemistry and Catalysis of RAS, 450075 Ufa, Russia
**e-mail: ink@anrb.ru*

In the report, the effective one-pot synthesis of N-unsubstituted aziridino[2',3':1,9]fullerene **1** and triazolino[4',5':1,9]fullerene **2** via cycloaddition of hydrazoic acid to [60]fullerene is discussed. Our proposed method provides the formation of aziridinofullerene with high yield and selectivity and also a previously unknown triazolinofullerene.

The interaction (60°C, 3 h, vacuum-sealed ampoule) between hydrazoic acid, generated *in situ* by the reaction of NaN_3 with H_2SO_4, and [60]fullerene was shown to afford aziridinofullerene **1** in 50% yield. It was found that a decrease in the reaction temperature to 40°C favors the synthesis of only N-unsubstituted triazolinofullerene **2** in 15% yield, which is unstable and decomposes at room temperature to produce aziridinofullerene **1**. In these experiments, 5,6- and 6,6-open or 5,6-closed isomers of compound **1** were not detected in the reaction mixture.

In the photochemical reaction (hv 300 nm, 500 W, 25 min, toluene) between C_{60} and HN_3 at room temperature aziridinofullerene **1** is exclusively formed in the yield of ~15%.

Aziridinofullerene **1** readily enter into the acylation and benzoilation reactions to give the corresponding derivatives **3** and **4**, respectively.

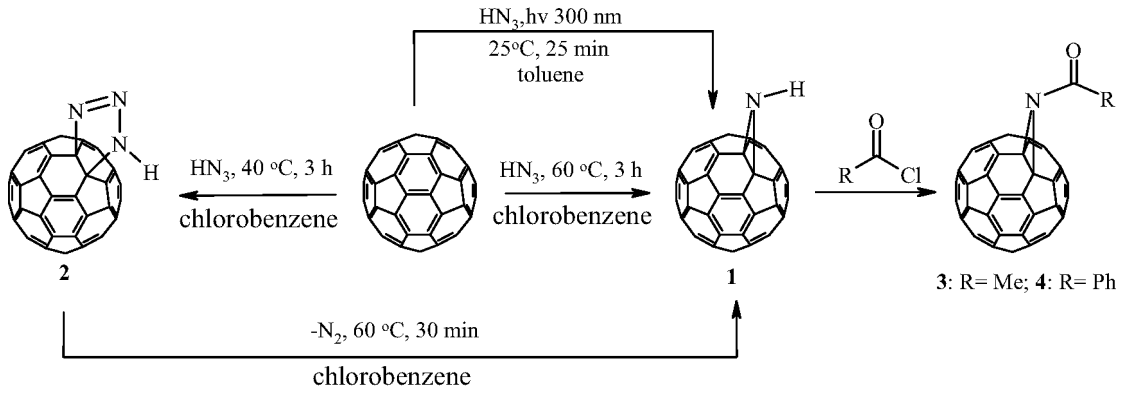

This work was supported financially by the FTP "Scientific and pedagogical staff of innovative Russian (Grant No. P1218 and No. 14.740.11.0014).

Optically active diastereomeric N-methyl-2(-)myrtenylpyrrolidinofullerenes and their methiodides: synthesis and CD spectra

Abramova N.V.*, Babievski K.K., Peregudova S.M., Manuylov S.A., Sokolov V.I.*

Institute of Organoelement Compounds, Russian Academy of Sciences, Moscow, Russia
**e-mail: sokol@ineos.ac.ru*

In the continuation of our study[1,2] of the synthesis and chiroptical properties of the fullerene derivatives, we turned to N-methyl-2 (-)myrtenyl[60]fullereno[c]pyrrolidine prepared by the Prato reaction starting with the natural enantiomerically pure aldehyde (-)myrtenal of the terpenoid family. In the course of reaction, a new chiral centre C-2 appears and, correspondingly, two diastereomers are formed. They were separated using the repeated column chromatography on SiO_2 and obtained as pure individual compounds **1,** R_f=0.68, and **2,** R_f=0.47, in the ratio **1:2** = 2:9. The treatment with CH_3I afforded the methiodides **3** and **4** respectively (Fig. 1). For all compounds cyclic voltammograms were obtained. The circular dichroism spectra were registered and Cotton effects were analyzed in terms of the sector rules[3]. More analogous derivatives of C_{70} (owing to its lower symmetry), namely, isomeric N-methyl-2(-)myrtenyl[70]fullereno[c]pyrrolidines have been synthesized, isolated and similar electrochemical and chiroptical investigations have been performed.

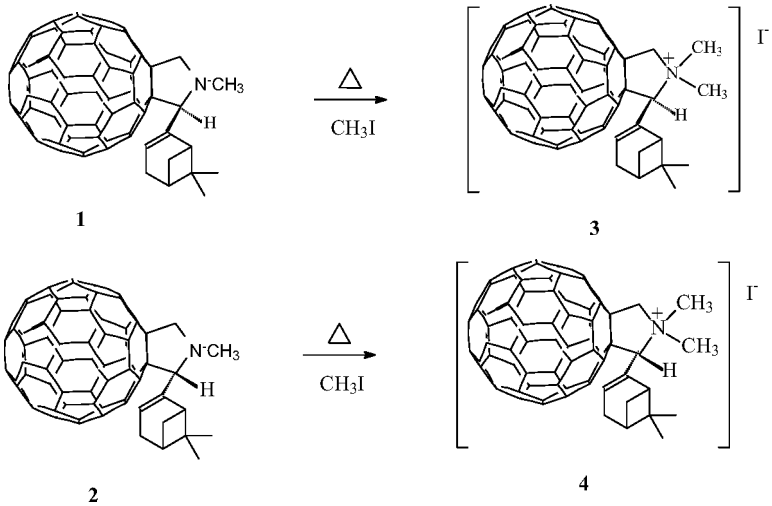

The work has been supported by Russian Foundation for Basic Research (08-03-00169 and 11-03-252) and Program OX-1.

[1] Sokolov, V.I. *Russ. J. Org. Chem. (Engl. Transl.)* **35**, 1230 (1999).
[2] Sokolov V.I., Bashilov V.V., Dolgushin F.M., Abramova N.V., Babievsky K.K., Ginzburg A.G., Petrovskii P.V. *Tetrahedron Lett.* **50**, 5347 (2009).
[3] Wilson S.R., Lu Q., Cao J., Wu Y., Welch C.J., Schuster D.I. *Tetrahedron* **52,** 5131.

AFM-Raman and tip enhanced Raman studies of carbon nanostructures

Dorozhkin P., Shelaev A., Shchokin A., Kuznetsov E., Bykov V.

NT-MDT Co., Build. 100, Zelenograd Moscow, 124482 Russia, dorozhkin@ntmdt.com

We demonstrate capabilities of Atomic Force Microscopy integrated with Confocal Raman/Fluorescence/Rayleigh microscopy when applied to carbon nanomaterials. Results on various carbon nanostructures are demonstrated: graphene, carbon nanotubes, detonation nanodiamonds etc.

Graphene on gold is investigated by different AFM and spectroscopy techniques providing comprehensive information about the sample. We study in details how the thickness (number of monolayers) in graphene affects its physical properties: surface potential (work function), local friction, elastic modulus, capacitance, conductivity, charge distribution, Raman and Rayleigh light scattering etc. Results for graphene flakes are qualitatively compared to those for carbon nanotubes of different diameters. We show how electrostatic charging of graphene flakes can be effectively measured and modified by AFM cantilever. Studies are performed both in ambient air conditions and in controlled atmosphere and humidity.

We present results of Tip Enhanced Raman Spectroscopy (TERS) or "nano-Raman" mapping realized using integrated AFM-Raman system. Measurements are realized in two different excitation configurations: Inverted (for transparent samples) and Upright (reflected light configuration, for opaque samples, with side illumination option). In both geometries we demonstrate near field Raman enhancement effect due to resonant interaction of light with localized surface plasmon at the apex of a metal AFM probe. Carbon nanotubes and graphene are studied by TERS technique. Actual plasmonic and near field nature of the Raman enhancement is proven by a number of ways: dependence of the enhancement on the excitation wavelength and polarization, enhancement versus tip-sample distance curves, observation of selective enhancement of Raman signal from thin surface layers of the sample etc. Finally, the ultimate performance of TERS is demonstrated by measuring Raman 2D maps with *subwavelength lateral resolution (down to 14 nm)* – determined not by the wavelength of light, but by the localization area of the surface plasmon electromagnetic field.

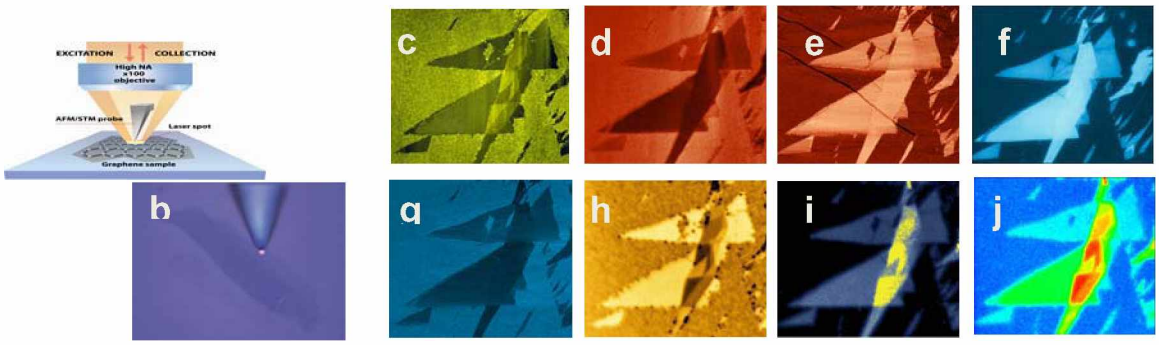

a), b) AFM – Raman configuration: schematics (a) and white light image (b); Raman laser is tightly (400 nm spot diameter) focused onto the very end of a "nose"- shaped AFM cantilever using 100x objective; Graphene layer is positioned below the cantilever and under the laser spot; while scanning the sample, AFM and Raman data is obtained simultaneously; c) – g). Various AFM images characterizing different physical properties of the sample - Topography (c), Electrostatic Force (d), Force Modulation (elastic properties) (e), Kelvin Probe (f), Lateral Force (g); h) – j). Confocal optical images – Rayleigh light (h), Raman 2D band mass center (i), Raman G band intensity (j).

EPR study of depolymerization processes of C_{60} polymerized phases

Zhilinskaya E.A.*[1], Rakhmanina A.V.[2], Davydov V. A.[2], Agafonov V.[3]

[1]*Université du Littoral Côte d'Opale UCEIV-EA 4492, MREI 1, 59140, Dunkerque, France*
[2]*Institute for High Pressure Physics of the RAS, 142190 Troitsk, Russia*
[3]*LEMA, UMR CNRS-CEA 6157- LRC CEA M01, Université de F.Rabelais, 37200 Tours, France*
**e-mail: jilinska@univ-littoral.fr*

The monomer, tetragonal (T) and rhombohedral (R) polymerized phases of C_{60} have been studied by the EPR method under increase of temperature from 295K up to 650K, that is, from temperatures below to above the limits of thermal stability of the polymerized phases. Previous EPR study of the T and R phases in the temperature range of 77–295K [1] allowed identifying two (doublet and triplet) types of paramagnetic centers (PC) in these materials. The behavior of these paramagnetic centers during thermal depolymerization of high-pressure polymerized C_{60} phases have been analyzed and compared with the behavior of PC of the monomer C_{60} phase at the same conditions. Comparative analysis of PC in the initial and treated samples after high temperature treatment has been made within 77–295 K temperature range.

EPR measurements have been realized in air and in a vacuum. Several stages of destruction of the polymerized phases can be separated according to EPR data for T and R polymeric phases under both conditions. These stages are qualitatively similar for two polymeric phases under the same conditions, but their quantitative parameters are different. The presence of the air significantly changes the behaviour of PC at $T \geq 530K$. Complete destruction of the triplet PC in the T and R phases is observed at $T \approx 500K$.

EPR study of the monomer C_{60} phase shows the appearance of a new triplet PC in the temperature range 580–650K. This triplet PC is rather different from the triplet PC observed in T and R polymeric phases.

This work was supported by the CNRS, the Region Nord-Pas de Calais, the European Community, and the Russian Foundation for Basic Research (Grant N 09-03-00750)

[1] E.A. Zhilinskaya, A.V. Rakhmanina, V.A. Davydov, V. Agafonov, *Phys Status Solidi A* **207**(10), 2364 (2010).

Conductivity of carbon materials at pressures 20-50 GPa

Tikhomirova G.V.*, Volkova Ya.Yu., Babushkin A.N.

Ural State University, 620000, Ekaterinburg, Russia
**e-mail: Galina.Tikhomirova@usu.ru*

Conductivity of fullerite C_{60}, single-wall carbon nanotubes (SWNT) and graphite have been studied at pressures 20-50 GPa and temperatures 77-400K. The kinetics of resistivity of C_{60} at changing pressure was also studied. Transport phenomena were used as a tool for revelation and interpretation of phase transitions arisen under high pressure.

Resistivity peculiarities were identified with the known phase transitions of fullerite. Successive phase transitions of fullerite C_{60} appeared in the course of HPHT treatment were accompanied by changes in resistance, which can be of quite different magnitude (from hundreds Ohm to hundreds MOhm) and of different temperature dependence. Critical pressures for the transitions depended on conditions and duration of preliminary HPHT treatment. This fact, as well as smeared character of the transitions is connected with long relaxation time, which was found to be about 140 min.

Three types of SWNT samples were investigated: samples produced by the graphite thermal dispersion method (SWNT percentage is 70%), the chemical vapor deposition method (SWNT percentage is 80%) and HiPco method (SWNT percentage is 90%).

Electric properties of the samples under high pressure were dependent on SWNT percentage. The electric characteristics of SWNT samples remained of the same character with the increasing of SWNT percentage, but the additional features appeared. The irreversible changes of the electric properties of the SWNT samples observed in the pressure range 27-45 GPa can be connected with both the structure modification and partial destruction of the sample.

In the pressure range from ~ 16 to ~ 30 GPa, the sharp change in the termo EMF value of graphite was observed. Impedance measurements of graphite were carried out at room temperature in the frequency range of 1-200 kHz. The impedance features found for all samples at pressures of ~ 18 to ~ 32GPa confirm also the existence of the phase transition in this pressure range, which is confirmed by previous data obtained at d.c. conditions. The transition is irreversible.

This work was supported in part by RFBR grants 09-02-01316 and 10-02-96036.

Probing the nano world – an overview of Raman spectroscopy and its key role in ACN research

Stacey D.*[1], Ponkratov K.[2], Batten T.[1]

[1]*Renishaw plc, GL12 7DW, Wotton-under-Edge, UK*
[2]*OOO Renishaw, 115477, Moscow, Russia*
**e-mail: Duncan.stacey@renishaw.com*

Carbon Nanomaterials are attracting intense scientific interest because of their extraordinary electronic, thermal and mechanical properties. Raman Spectroscopy has been found to be extremely useful in many areas of research of these materials, both because of its specificity, its no-destructive nature, limited sample preparation requirements and ease of use. Raman can easily distinguish between Carbon and other materials and the many different allotropes of Carbon from Diamond like carbon (DLC) to Fullerenes to Carbon Nanotubes, Graphite and Graphene. We will present and overview of Raman spectroscopy and its wide range of applications in the field of ACNs.

It has been widely shown that the electrical behaviour of SWNTs is influenced by their diameter and chirality. While Raman is an optical technique and therefore limited to diffraction limited resolution it is a very useful tool in CNT studies and can be used to determine many of the properties of CNTs including their diameter, chirality, electronic properties and strain in both bulk material and isolated nanotubes. Due to its non-destructive nature Raman can be used to probe morphological differences and changes.

Isolated nanotubes exhibit Raman resonance effect that can be used to determine the diameter of the tubes. By measuring the Raman frequency of the Radial Breathing Modes (RBMs) the diameter can be determined [1]. Measurement of the position of other peaks in the spectra, such as D, G and G' bands provides information about the internal disorder, electrical properties and electronic structural information respectively.

An exciting recent development has been the combination of Raman and AFM. This is now opening up new areas of research and providing additional tools to probe the Nano World.

[1] Raman spectroscopy of carbon nanotubes M.S. Dresselhaus, G. Dresselhaus, R. Saito, A. Jorio 10.1016/j.physrep.2004.10.0006

XPS characterization onion-like carbon from nanodiamonds and carbon structure from onion-like carbon after high pressure high temperature treatment

Skryleva E.A.*, Shulga N.Yu.

National University of Science and Technology «MISIS», Leninsky prosp., 4, Moscow, 119049, Russia
**e-mail: 17sea@rambler.ru*

It is known, that heating nanodiamonds in a vacuum at temperatures of 1000-2000°C is an effective way to obtain onion-like carbon powder - laminated curved graphite-like shells. The transformations that occur with this form of carbon in the processing of high pressures high temperatures, HPHT, are poorly understood and are of interest

Synthesis onion-like carbon from nanodiamonds is accompanied by a transformation of sp^3 type of hybridization to sp^2 bonds with the formation of graphene layers from the surface into the volume the particle sequentially. HPHT type treatment should lead to closer of shells and the formation of sp^3 bonds between them.

XPS allows to estimate the sp^2/sp^3 ratio in carbon materials with mixing sp^2 and sp^3 bonds. The hybridization of carbon atoms was estimated from the photoelectron spectra of the C1s core level and its satellite resulting from losses for excitation of plasma oscillations of valence electrons, the $\sigma + \pi$ plasmon.

The samples of carbon produced from nanodiamonds at temperatures 1000-1600°C were analysed by this method and it was shown that complete conversion into onion-like carbon is achieved at temperature above 1400°C. The samples of carbon produced at temperature 1600°C were processed at pressures 7.7 and 15 GPa at temperatures 500, 1350 and 1400°C. Interlayer sp^3 carbon bonds were detected by XPS at temperature above 500°C.

NEXAFS studies of the composite materials MWCNT's-pyrolitic metals by synchrotron radiation

Sivkov V.N.*[1], Petrova O.V.[1], Nekipelov S.V.[1], Obiedkov A.M[2], Kaverin B.S[2], Kirillov A.I[2], Domrachev G.A.[2], Egorov V. A.[2], Vyalikh D.V.[3], Molodtsov S.L.[3]

[1]*Komi Science Center Ural Division RAS, 167982, Syktyvkar, Russia*
[2]*G.A.Razuvaev Institut of Organometallic Chemistry RAS, 603950, Nizny Novgorod, Russia*
[3]*Technische Universitat Dresden, D-01062, Dresden, Germany*
**e-mail: svn@dm.komisc.ru*

Multi-walled carbon nanotubes (MWCNT's) are novel carbonaceous materials which show very promising properties for nanotechnology applications. One fascinating aspect of these systems is related to the changes that occur in their electronic properties when have coated metals. It is very important to investigate the elementary excitations of MWCNT's using techniques that are sensitive to changes in both electronic properties, as well as to the presence of metal, and to the kind of interaction between the metal atoms and the nanotubes. The NEXAFS (near edge x-ray absorption fine structure) spectroscopy are the available tool for the investigation of the MWCNT's based composites, because the NEXAFS-spectroscopy methods, are characterized atomic selectivity, dipole selection rules, fast response atomic composition and spatial conformation [1].

The modification of the MWCNT's surface with metal coatings was produced by MOCVD (metalorganic chemical vapor deposition) method. Various data on the structures and properties of samples were obtained by XRD, TGA, SEM, TEM and HRTEM methods.

The NEXAFS C 1s-, Cr2p- and Fe2p- absorption edges of the MWCNT's based composites were studied by total electron yield (TEY) mode with using synchrotron radiation of Russian-German beamline at BESSY-II [2]. The atomic and chemical composition, structure of the coatings and interfaces MWCNT – WC, pyrolitic Cr, Fe and Mo composites dates were obtained.

This work was supported by grants RFBR 10-02-00445-a, 09-02-00726-a, State Contract №П-337, Program of Presidium of RAS №21, and by the Bilateral Program of the Russian-German Laboratory at BESSY II.

[1] Stohr, J. NEXAFS Spectroscopy (Springer, Berlin, 1992).
[2] Gorovikov S.A., Molodtsov S.L., Follath R. *Nucl. Instrum. Meth. A.* **411**, 506 (1998).

Applicatopn of gas chromatography for studies of oxidation kinetics of nanocarbon materials

Panova A.M., Bogatyreva G.P., Zapyuk G.G., Katrusha A.N.

ISM – V. Bakul Institute for Superhard Materials of the National Academy of Sciences of Ukraine (NASU) 2, Avtozavodskaya st., Kiev, 04074, Ukraine
e-mail: annpanova@ukr.net

The issue of heat resistance of nanocarbon materials and reaction mechanisms of its interaction with air oxygen is still open for scientists, producers and end users of the instrument, polycrystalline and composite materials based on these materials. The basic research methods of heat resistance are gravimetric. For detailed investigation of oxidation process of carbon materials it's necessary to consider the ration of reaction products that characterize the stages of process. The present work was appointed to application of gas chromatography method for obtaining such information.

Utilizing this method the oxidation kinetic of nanodiamond powders and carbon nanotubes synthesized by Ukrainian company ALIT was studied. The oxidation mixture was composed from 20% oxygen and 80% argon, gas expense was 0.2 l/min. Before the start of reaction (till the experiment temperature was achieved and gas reaction mixture was put into reactor) the reactor with the samples was blown thorough with argon at 0.16 l/min.

The oxidation process of carbon nano materials was studied by the reaction products. The quantitative ratio of CO and CO2 in the reaction products was obtained during the reaction.

For studies of heat resistance in isothermal conditions the model of sample "carbon in cylindrical cup" was used. Kinetic parameters of the reaction were calculated based on the macro-kinetic equation, which accounts also the influence of external and internal mass-transition [1].

The kinetic parameters calculated based the data of chromatography analysis are in good correspondence with the results of gravimetric method when utilizing identical sample model.

As a result of studies of oxidation process of powders of nanodispersed diamonds and carbon nanotubes by the reaction products with utilization of gas chromatography the presence of both carbon oxides in the products of their oxidation was proved. The quantitative ration of CO and CO2 in the reaction products during the reaction was obtained. The reasonability to use the gas chromatography method for studies of oxidation kinetic of nanocarbon materials was shown.

[1] G.P. Bogatireva, M.A. Marinich, V.Ya. Zabyga, G.G. Zapyuk, A.M. Panova, G.A. Bazaliy, *Superhard materials* №5, 26 (2008).

Difference and similarity in properties of bulk and nanomaterials as seen by NMR

Panich A.M.

Department of Physics, Ben-Gurion University of the Negev, Be'er Sheva 84105, Israel
e-mail: pan@bgu.ac.il

In order to understand why properties of bulk compounds and nanostructures are sometimes different and sometimes similar, I will discuss the results of Nuclear Magnetic Resonance studies of the local crystal structure, electronic structure, nature of chemical bond and defects in carbon nanotubes, fullerenes, polyhedral multi-shell carbon nanoparticles, nanodiamonds, as well as in boron nitride nanotubes, tungsten and molybdenum sulfide fullerene-like nanoparticles, dithallium selenide nanorods, and vanadium oxide nanotubes. The properties of the corresponding bulk samples vary from wide gap semiconductors to semimetals. The data obtained for the nanosized compounds will be compared with those of the bulk ones. Our research elucidates when the properties of nanomaterials differ significantly from those of bulk samples, and when this difference is small or nearly absent.

Our studies also show that some nanoparticles reveal core-shell structure, while the others do not. This problem will also be discussed in the presentation.

Raman characterization and X-band EPR studies of multishell nanographites with and without oxygen-sensitive edge-localized spins

Osipov V.Yu.*[1], Makarova T.L.[1,2], Baranov A.V.[3], Ermakov V.A.[3], Shames A.I.[4], Takai K.[5], Enoki T.[5], Kaburagi Y.[6], Hayashi T.[7], Endo M.[7], Vul' A.Ya.[1]

[1]*Ioffe Physical-Technical Institute, Polytechnicheskaya 26, St. Petersburg 194021, Russia*
[2]*Department of Physics, Umea University, SE-901 87, Umea, Sweden*
[3]*St.Petersburg State University of Information Technologies, Mechanics and Optics, 197101, Russia*
[4]*Department of Physics, Ben-Gurion University of the Negev, Be'er-Sheva 84105, Israel*
[5]*Department of Chemistry, Tokyo Institute of Technology Tokyo 152-8551, Japan*
[6]*Department of Chemistry and Engineering, Tokyo City University, Tokyo 158-8557, Japan*
[7]*Faculty of Engineering, Shinshu University, 4-17-1 Wakasato, Nagano-shi 380-8553, Japan*
**e-mail: osipov@mail.ioffe.ru*

Raman scattering spectroscopy is a powerful tool to test nanocarbons having an extended π-electron system combined with electronic states localized at zigzag edges. Nanographite (NG) particles under study were produced by the annealing of detonation nanodiamonds (grain size ~5 nm) in argon flow, as it has been proposed in Ref. [1, 2].

We studied a number of nanographites obtained from nanodiamonds at different heat treatment temperatures: both above 1600°C and below 1550°C. Some of them (group I) synthesized predominantly at elevated temperatures (≥ 1600°C) demonstrate EPR signal associated with zigzag edge-localized states, which linewidth is extremely sensitive to the presence of ambient molecular oxygen. Another samples (group II) demonstrate (surprisingly, irrespective the temperature of synthesis) EPR signals that are completely insensitive to the presence of molecular oxygen. These signals supposed to be (completely or partially) due to sp^3- like defects in the closed defective shells of multishell nanographite. In-plane crystal sizes, obtained by means of Raman spectroscopy via evaluation of D- and G- band intensities ratios (ID/IG), are varied from ~1.6 nm to ~3.5 nm for different nanographites obtained. The enhanced intensity of Raman D-band in the type II nanographites may be associated with possibly large contribution of armchair-type edges.

The armchair edges do not demonstrate paramagnetic edge spin states [2]. From the other angle, particles of smaller (less than 2 nm) sizes are characterized by high number of sp^3- defects and poor crystalline quality of graphene sheets as well as by a corrugated character of graphitic shells. These factors are, in general, the combined reason of the absence of oxygen-sensitive edge localized states in samples with smaller crystalline sizes or higher content of sp3- like defects.

[1] V.Yu. Osipov, et al., *Carbon* **44**, 1225 (2006).
[2] O.E. Andersson et al., *Phys. Rev. B* **58**, 16387 (1998).

UV optical absorption studies of surface plasmon resonance in water suspension of multi-shell nanographites

Osipov V.Yu.*[1], Shestakov M.S.[1], Baranov A.V.[2], Takai K.[3], Enoki T.[3], Kaburagi Y.[4], Endo M.[5], Vul' A.Ya.[1]

[1]*Ioffe Physical-Technical Institute, Polytechnicheskaya 26, St.Petersburg 194021, Russia*
[2]*St. Petersburg State University of Information Technologies, Mechanics and Optics, 197101, Russia*
[3]*Department of Chemistry, Tokyo Institute of Technology Tokyo 152-8551, Japan*
[4]*Department of Chemistry and Engineering, Tokyo City University, Tokyo 158-8557, Japan*
[5]*Faculty of Engineering, Shinshu University, 4-17-1 Wakasato, Nagano-shi 380-8553, Japan*
**e-mail: osipov@mail.ioffe.ru*

UV optical absorption spectroscopy is a powerful tool for testing the optical extinction properties of nanocarbons with an extended π-electron system.

Nanographite (NG) particles were produced by annealing of detonation nanodiamonds (grain size ~5 nm) during various exposure times, as described in [1]. A series of various NG suspensions were prepared by repeated controlled dilution of initial dense suspension with weight concentration (~0.1 mg/ml).

The aim of this research was to find the correlation between the UV optical absorption of NG suspensions and structure of NG particle. The Raman spectra of the NG samples excited at 514 nm were analyzed. The Tuinstra- Köning approach applied for evaluation of the NG crystallite in-plane sizes by using of the D- and G- band (~1340 cm^{-1} and 1580 cm^{-1}) heights ratio gave results (~3.5 nm) coinciding well with those one obtained from X-ray diffraction data.

The broad absorption peaks around 255-265 nm related with surface plasmon resonance (SPR) were found in optical extinction spectra of all NG suspensions. Following to Pascoli and Leclercq [2] the increase in number of carbon atoms in planar graphitic sheet from 150 to 486 as well as the reduction of number of randomly distributed sp^3-hybridezed atoms in a graphitic cluster leads to the smoothing of absorption hump at ~220 nm. The same trend is also observed in our case where the suspension of NG with minimal content of amorphous phase and a little bit higher crystalline perfection demonstrates less featured absorption hump at 265 nm in comparison with that one for the suspension of more defective NG. The research on the influence the amount of defect sites and imperfections of NG particles together with its aggregation state in water suspension on the shape and intensity of SPR peak is in progress now and will be reported elsewhere.

[1] V.Yu. Osipov, T. Enoki, K. Takai et al. *Carbon* **44**, 1225 (2006).
[2] G. Pascoli, J. Leclercq, *Astrophysics and Space Science* **235**, 233 (1996).

Adsorption properties and chromatographic performance of microdispersed sintered detonation nanodiamonds

Nesterenko P.

[1]*Australian Centre for Research on Separation Science, University of Tasmania, 7001, Hobart, Australia*
e-mail: Pavel.Nesterenko@utas.edu.au

Detonation nanodiamond (ND) has very complex structure of particles and surface chemistry presented by a broad spectrum of various functional groups. Mainly, surface chemistry of ND depends on type oxidative purification applied to post-blast soot and on technology and reagents used for disaggregation and stabilisation of nanoparticles. Clearly, the application of nanodiamond in biotechnology and medicine requires a systematic investigation of adsorption properties of ND, understanding the reasons for its unusual adsorption selectivity and the ways of the most efficient utilisation of unique physico-chemical properties of ND related materials. Different chomatographic methods have been successfully applied for the characterisation of adsorption properties, so the goal of the present work was investigation of adsorption properties of detonation nanodiamonds by using high-performance liquid chromatography [1-3].

It is difficult to use nanoparticles as a stationary phase in chromatography, so microdispersed sintered nanodiamond (MSND) with particle diameter of 3-5 micron and specific surface area 191 m^2/g was used for packing of 15 cm long stainless steel columns of internal diameter 4.6 mm. All experiments are performed with common HPLC equipment except of using column oven Polatherm in chromatographic experiments at elevated temperatures up to 200°C.

The set of dependences of retention on eluent pH, type and content of organic solvent in the eluent and of column temperature was obtained for a big group of organic compounds including alkylbenzenes, dialkylphtalates, polyaromatic hydrocarbons, phenols, aromatic acids and nucleic acid precursors. The analysis of molecule structure-retention dependences confirmed the presence of conducting carbon layer at the surface of ND and charge induced dipole-dipole interactions as a key retention mechanism for polar organic molecules.

[1] P.N. Nesterenko, P.R. Haddad. *Anal. Bioanal. Chem.* **396**, 205 (2010)
[2] P.N. Nesterenko, O.N. Fedyanina. *J. Chromatogr. A* **1217**, 498 (2010).
[3] O.N. Fedyanina, P.N. Nesterenko. *Russ. J. Phys. Chem. A* **84**, 476 (2010).

Characterisation of graphene oxide and chemically converted graphene by capillary zone electrophoresis

Nesterenko P.*[1], Quirino J.[1], Haddad P.[1], Müller M.[2], Wallace G[2], Li D.[2]

[1]*University of Tasmania, 7001, Hobart, TAS, Australia*
[2]*University of Wollongong, 2522, Wollongong, NSW, Australia*
**e-mail: Pavel.Nesterenko@itas.edu.au*

The preparation of processable graphene sheets in large quantities includes oxidation of graphite followed by the formation of stable aqueous colloids by electrostatic repulsion. One of the most common procedures includes preparation of graphene oxide (GO) nanoparticles, their disintegration by sonication and partial reduction of oxygen-containing functional groups to, so called, chemically converted graphene (CCG) nanoparticles[1]. Each of steps requires a careful characterisation of size, charge and aggregation of nanoparticles. Capillary zone electrophoresis (CZE) is a simple and efficient separation and analytical technique for the characterisation of various nanoparticles.

The possibility of capillary electrophoretic separation of GO and CCG nanosheets was investigated. The data on aggregation and electrophoretic mobility of nanoparticles having different size and charge were obtained using various background electrolytes and detection systems.

[1] Müller M.B., Quirino J.P., Nesterenko P.N., Haddad P.R., Gambhir S., Li D., Wallace G.G., *J. Chromatogr. A.* **1217**, 7593 (2010).

[2] Li D., Mueller M.B., Gilje S., Kaner R.B., Wallace G.G. *Nature Nanotechnology* **3**, 101 (2008).

Raman study of the neutral state donor-acceptor complexes Ni·(nPr)·$(C_{60})_2$ and Cu·(nPr)·$(C_{60})_2$ at high pressure

Meletov K.P.*[1], Konarev D.V.[2]

[1]*Institute of Solid State Physics RAS, Chernogolovka, Moscow region 142432, Russia*
[2]*Institute of Problems of Chemical Physics RAS, Chernogolovka, Moscow region 142432, Russia*
**e-mail: mele@issp.ac.ru*

We have measured the Raman spectra of the molecular neutral state donor-acceptor complexes Ni·(nPr)·$(C_{60})_2$ and Cu·(nPr)·$(C_{60})_2$ as a function of pressure up to 10 GPa and at room temperature in order to study possible pressure-induced phase transitions related to charge transfer to C_{60} acceptor molecules and/or polymerization of C_{60} molecules.

SpectraPro-2500i equipped with a Peltier-cooled CCD Pixis2K. The measurements at high pressure were performed by the use of the high pressure diamond anvil cell of Mao-Bell type. The 514.5 nm Ar^+ laser line was focused on the sample by means of a 50× objective in a spot of ~10 μm diameter, while the beam intensity on the sample was ~5 mW.

Raman spectra were measured in the region of the $A_g(2)$ pentagon-pinch (PP) mode which is most sensitive to the irreversible pressure-induced transformations manifested usually by abrupt softening of this mode. Almost all modes exhibit positive pressure shift with some peculiarities that may be attributed to irreversible transformation of material at high pressure. The detailed analysis of the pressure dependence will be done that may give important information about the character of transformation observed at high pressure.

The support by the Russian Foundation for Basic Research, grant № 11-02-00886 is greatly acknowledged.

Intertubular interaction in bundled single-walled carbon nanotubes studied by Raman scattering at high pressure and temperature

Meletov K.P.

Institute of Solid State Physics RAS, Chernogolovka, Moscow region 142432, Russia
e-mail: mele@issp.ac.ru

Raman spectra of bundled single-walled carbon nanotubes (SWCNTs) were measured at high temperature up to 400° C and pressure up to 4.5 GPa. The SWCNTs were synthesized by the arc discharge method in helium atmosphere at a pressure of 0.86 bar, using a metallic Ni/Y catalyst The average diameter of the tubules was 1.5 nm as anticipated for the preparation method applied, as well as by TEM and Raman characterization. The main impurities were graphite particles, while the content of metal impurities was ~1.3 %.

Raman spectra at high pressure and high temperature were recorded *in-situ* using spectrograph Acton SpectraPro-2500i equipped with a Peltier-cooled CCD Pixis2K, high pressure diamond anvil cell of Mao-Bell type and a high temperature cell. The 514.5 nm Ar^+ laser line was focused on the sample by means of a 50× objective in a spot of ~10 μm diameter, while the beam intensity on the sample was ~5 mW.

Raman spectra show reversible pressure- and temperature-induced shift for the G_- and G_+ bands. The temperature shift is negative and practically the same for the G_- (-0.0230± 0.0007) cm^{-1}/K and G_+ (-0.0229±0.0002) cm^{-1}/K bands, whereas the pressure shift is positive with pressure coefficients for the G_- and G_+ (7.23±0.33) cm^{-1}/GPa and (7.02±0.15) cm^{-1}/GPa, respectively. The Raman data do not show changes in the tube diameter upon heating and compression of bundles. The dependence of the G_- and G_+ band shift on the relative variation of the triangular lattice constant was calculated on the basis of the linear compression and dilatation constants, obtained by XRD-measurements [1,2] (Fig.1). These data show that the dilatation constant is not compatible with the compressibility constant, whereas the inter-tubular interaction is mainly of the van-der-Waals type.

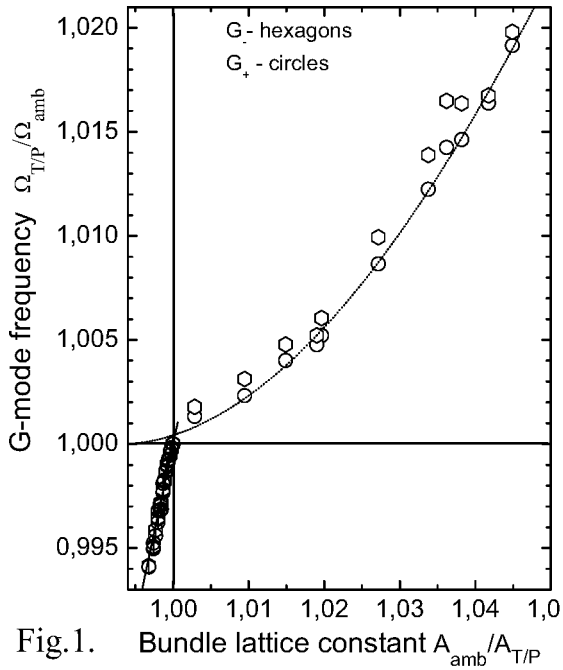

Fig.1.

The support by the Russian Foundation for Basic Research, grant № 11-02-00886 is greatly acknowledged.

[1] S. Sharma et al., *PRB* **63**, 205417 (2001).
[2] Y. Maniwa et al., *PRB* **64**, 241402R (2002).

Retrospective IWFAC's scope study using mind maps approach

Leshchev D.V.*[1], Leshcheva I.A.[2]

[1]*Center for Advanced Studies, St. Petersburg State Polytechnic University, 195251, St. Petersburg, Russia*
[2]*Graduate School of Management, St. Petersburg University, 199004, St. Petersburg, Russia*
**e-mail: dimvovich@narod.ru*

A retrospective study of IWFAC's scope of subjects is represented. This work is a pioneer in using of mind map approach to study processes in time. A mind map [1, 2] is a diagram used to represent words, ideas, tasks or other items linked to and arranged radially around a central key word or idea. It is used to generate, visualize, structure and classify concepts, and as an aid in study, organization, problem solving, and decision making.

For this investigation the abstracts published in the IWFAC books of abstracts from 1993 to 2009 were used. For every workshop a mind map of the subjects was created. Nine obtained mind maps were merged to the general one using conjunction method. Then particular mind maps were reengineered relative to the general and lined up by the time. Evolution of mind maps and trends in areas through nine workshops was observed.

Typical scenario of topic development consists of three main stages: birth, upgrowth and stagnation. Length of life cycle and maximum number of papers in the best period of topic development were evaluated and compared. Correlations between life cycles of different topics with time shift were calculated. But built mind maps can be used to obtain more benefits.

General mind map presents in a visual structured form the current state of the art and may serve as the basis for comparing papers and pieces of research in the nanocarbon area. It can be used as a roadmap for researches especially who just wants to joint the IWFAC community. The created mind maps can be used for estimation and even prediction of particular topic evolution. They can help to answer question in which research area is reasonable to invest.

[1] Busan, T.:Mind Map Handbook. Thorsons (2005).
[2] http://en.wikipedia.org/wiki/Mind_map.

Different carbon nanostructures obtained on Fe/SiO_2 and Fe/Al_2O_3 catalyst with various phase composition

Levina V.V.[*1], Novakova A.A.[2], Kiseleva T.Yu.[2], Ilinykh I.A.[1], Kuznetsov D.V.[1], Chuprunov K.O.[1], Kolesnikov E.A.[1]

[1]*National University of Science and Technology "MISIS", 119049, Moscow, Russia*
[2]*Moscow M.V.Lomonosov State University, Department of Physics, Vorobiovy Gory, 119192, Moscow, Russia*
**e-mail: vvlevina@gmail.com*

The catalytic synthesis of different carbonaceous materials, including carbon nanofibers, nanotubes and incapsulated nanoparticles has been the subject of a numerous publications over the past decade. This is caused by search of a new catalyst and promised carbon materials application prospects. In this work the growth of carbon nanostructures by a catalytic route which represents the decomposition of propane over Fe/SiO_2 and Fe/Al_2O_3 composite obtained by consecutive chemical synthesis is considered.

The sequence of structure transformation in metal particles at all stages of the synthesis has been studied by means of mossbauer spectroscopy, transmission electron microscopy, electron diffraction and thermoanalytical methods. The carbon outcome and carbon structures types in dependence of catalytic particles size, phase and structure have been analyzed for the samples with different Fe to SiO_2/Al_2O_3 weight ratio.

It was revealed that the morphology and the size of the nanocomposite particles and, as a result, their catalytic properties are highly sensitive from phase composition.

Electrochemical functionalization of carbon single-walled nanotubes

Komarova N.S.[*1], Krivenko A.G.[1], Naumkin A.V.[2]

[1]*Institute of Problems of Chemical Physics RAS, 142432, Chernogolovka, Russia*
[2]*A.N. Nesmeyanov Institute of Organoelement Compounds RAS, 119991, Moscow, Russia*
[*]*e-mail: kom-nat@yandex.ru*

An electrochemical method of modification of carbon single-walled nanotubes (SWNT) at superposition of anodic potentials in aqueous solutions of potassium bromide is proposed. This process is shown to be accompanied by a considerable increase in the capacity of SWNT electrodes. Capacity increase is assumed to be connected with the increase of the surface of nanotube electrode accessible for electrolyte solution what is caused by the forming of functional groups on SWNT surface.

X-ray photoelectron spectroscopy method (XPS) was used to the establish nature of functional groups grafted to nanotube carbon during the electrolysis. Considerably greater intensity of peaks of Br and O shown to be characteristic feature of obtained spectra of electrochemical treated samples in comparison with initial SWNT. As follows from XPS data oxidation of SWNT surface at the electrolysis of potassium bromide is shown to be the main route of functionalization to be not their halogenation. Thus, after electrolysis four atoms of carbon correspond to one oxygen atom. At the same time thirty carbon atoms conform to one bromine atom lying surface of nanotubes.

Based on the obtained data, it is to propose a mechanism of electrochemical treatment of SWNT upon the bromide ion electrolysis. At the first stage, unstable hypobromite ion is formed as a result of the interaction of bromine, evolving at electrolysis, with water. At the same time results of chromatography-mass spectrometry show that part of hypobromite ion disproportionates on hypobromate ion. Atomic oxygen evolving at decomposition of hypobromite and hypobromate ions oxidizes nanotube surface with the formation of functional groups.

Estimation of the stiffness parameters of a nanofibre forest

Koissin V.*, Warnet L., Akkerman R.

Univ. of Twente, Chair of Production Tech., 7500AE, Enschede, The Netherlands
**e-mail: v.koysin@ctw.utwente.nl*

Growth of nanotubes or nanofibres (CNFs) on the carbon-fibre fabrics is a way to improve the fibre-matrix interface and crack bridging and, consequently, the damage resistance of the fibre-reinforced composites [1]. On the other hand, the fabric deformability is foreseen to be altered by numerous inter-fibre links. To model these effects analytically or using an FE analysis, it is necessary to know the mechanical properties of a single nanoparticle. However this is not easy due to a tiny size of the objects. There are only few published studies on this point, [2], and all of them utilize a complex test equipment and are time-consuming.

Moreover, the nanoparticles can have very randomized shapes and diameters, as illustrated in Fig.1. Thus, even if 10-20 single CNFs are tested in bending or tension to produce a representative sample, it can be very problematic to derive the Young's modulus using the elastic beam or strut model [2].

The present study aims to explore a more practical way to estimate the stiffness "on average". This is attempted using relatively simple test methods: 1) out-of-plane compression of a fabric, 2) compression of the yarns extracted from the fabric, and 3) compression of a large volume of loose CNFs.

Experimental part of the study focuses on a particular case of a carbon-fibre fabric grafted with in-situ grown CNFs (using the Chemical Vapour Deposition technique). For comparison, the virgin fabric (without CNFs) is tested also.

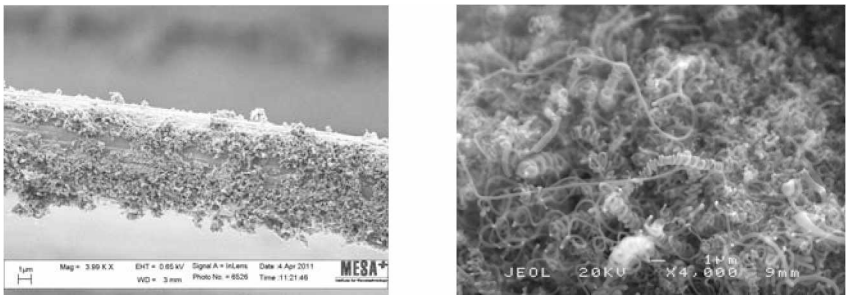

Figure 1. Carbon fibre with grown CNFs (left) and closer view of the CNF "forest" (right).

[1] Koissin V., Warnet L., Akkerman R., Proc. of 14th Int. Conference on Experimental Mechanics, Poitiers, France (2010).

[2] Demczyk B.G., Wang Y.M., Cumings J., Hetman M., Han W., Zettl A., Ritchie R.O., *Materials Science and Engineering A* **334**, 173 (2002).

Chemical bonding effect on the resonance F KVV Auger emission from polytetrafluoroethylene

Klyushin A.Yu.[1*], Vinogradov A.S.[1], Generalov A.V.[1], Simonov K.A.[1]

[1] *V.A. Fock Institute of Physics, St.Petersburg State University, 198504, St.-Petersburg, Russia*
**e-mail: klyushin@gmail.com*

Nowadays carbon nanosystems (CNS) are attention-getting material for scientists from different fields. In spite of great interest in fluorinated CNS, their atomic and electronic structures have been studied by using a limited number of experimental techniques up to now. One of the major problems of modern science is ascertainment of the role of hybridization of the valence electron states of fluorine atoms and surrounding atoms, i.e. the role of covalent bonding in the formation of free electron states in fluorinated systems. The aim of this work is to obtain information about features electronic structure and chemical bond for and fluorinated polymer (polytetrafluoroethylene, PTFE), which can be considered as a model fluorinated compound with covalent bonding, based on the analysis of the absorption spectra and resonant F *KVV* Auger electron spectra.

All measurements have been performed at the Russian-German beamline at the BESSY [1]. The PTFE sample was prepared with a sliding technique [2] which involved sliding (several times) a bar of PTFE over the surface of a flat silicon substrate covered with a ~ 1μ thick gold layer. Its thickness was in the range from ~ 10 to 30Å. Absorption spectra were measured using total electron yield. Photoelectron and resonant F *KVV* Auger spectra were collected in the angle-integrated mode using Phoibos 150 electron analyzer.

Owing to the analysis of the Auger emission spectra of PTFE near the F1s edge it was found that main Auger lines in resonant F *KVV* spectra excited with photon energies in the vicinity of the first absorption peak in the F1*s* spectrum are shifted to higher kinetic energy as compared with normal Auger spectrum. This effect is associated with strongly localized hybridized character of electronic states at the bottom of conduction band. These results are compared with the results for fluorine compounds with ionic (TiF_3) and ion-covalent (fluorinated multi-walled carbon nanotubes) bond. The high-energy shift in F *KVV* spectra differs in value for various compounds and therefore can be used for characterization of chemical bonding in fluorinated compounds and CNS.

This work was supported by the Russian Foundation for Basic Research (project no. 09-02-01278) and the bilateral Program "Russian-German Laboratory at BESSY".

[1] S.I. Fedoseenko, I.E. Iossifov, S.A. Gorovikov, J.-S. Schmidt, R.Follath, S.L. Molodtsov, V.K. Adamchuk, G. Kaindl, *Nucl. Instrum. Meth.Phys.Res. A* **470**, 84 (2001).

[2] Ch. Ziegler, Th. Schedel-Niedrig, G. Beamson, D.T. Clark, W.R. Salaneck, H. Sotobayashi, A.M. Bradshaw, *Langmuir* **10**(12), 4399 (1994).

Optimization of CVD synthesis parameters for growth of long carbon nanotubes array

Gorodetskiy D.V.[1,2], Kurenya A.G.[1], Kudashov A.G.[1], Okotrub A.V.[1]

[1] *Nikolaev Institute of Inorganic Chemistry SB RAS, 630090 Novosibirsk, Russia*
[2] *Novosibirsk State Technical University, 630092 Novosibirsk, Russia*
**e-mail: gordim2005@yandex.ru*

This work directed to study of influence of parameters of CVD synthesis (time of synthesis, flow rate of gas-carrier, location of substrates in the reactor and structure of a reactionary mixture) for growth of array of carbon nanotube (CNT). The synthesis of oriented CNT's array in was realized on square 10×10 mm^2 silicon substrate (100). The rinsing of the substrates in ethanol has been made before synthesis of CNT's. The silicon substrates were located on quartz boat in the central zone of the reactor. The 2%- solutions of ferrocene $Fe(C_5H_5)_2$ in toluene and acetonitrile were used for formation of perpendicularly oriented CNT's arrays. The spraying of catalytic solution in the reactor was carried out through injector located in a zone with temperature 200 ± 10°C. The vapor of reactionary mixture were transferred to a zone of thermal decomposition of mixture due to gas-carrier fpow. The flow rate of reactionary mixture was 0.14 ml/min and controlled by spraying controller. The grown samples were investigated by SEM, X-ray-electron spectroscopy and X-ray diffraction. The increase of synthesis time (t) leads to increase CNT's length (L) in CNT's array. If t = 1 hour, then L = 1 mm, but, if t = 3 hours, then L = 3 mm. The growth rate of CNT's arrays was investigated for different flow rate of gas-carrier. It was found out that optimal flow rate is 200 ml/min. The change flow rate of gas-carrier leads to variation of the gradient of concentration of reactionary mixture in the reactor. In turn, it leads to change of a thickness of CNT's arrays. The thickness of CNT's arrays depends on location of the substrates in the reactor. If flow rate of gas-carrier is 200 ml/min, then maximum of array thickness is observed in the center of reactor. The change of reaction mixture composition from acetonitrile to toluene leads to significant growth of a thickness of CNT's arrays. It should be concerned with lower content of carbon in acetonitrile in comparison with carbon presence in toluene.

Why are detonation nanodiamonds small

Dolmatov V.Yu.[1]*, Yurjev G.S.[2], Myllymäki V.[3], Vehanen A.[3]

[1]*FGUP «SCTB «Technolog», 192076 Saint-Petersburg, Russia*
[2] *Institution of RAS Nikolaev Institute of Inorganic Chemistry SB RAS, 630090, Novosibirsk, Russia*
[3]*Carbodeon Ltd. Oy, Bulevardi 2 A, 00120 Helsinki, Finland*
**e-mail: DiamondCentre@mail.ru*

It is known that the synthesis of detonation nanodiamonds (DND) is accompanied by the creation of non-diamond forms of carbon such as onion carbon, graphite and so on.

The authors have calculated distribution of atoms in natural diamonds and DND of the various sizes (3D model of spherical nanodiamonds computed through the representation of coordination spheres (CS)). Experimental XRD patterns from DNDs were registered with use of synchrotron radiation.

The calculations showed that in DND_1 manufactured in FGUP "SCTB "Technolog" (explosive charge in an aqueous solution) and in natural diamond the similarity on number of carbon atoms in CS is observed up to the 32nd CS (R_{CS}=28,69 Å, N_{atoms}=1386). The distinction begins with 33^{d} CS and further: in DND_1 R_{CS}=29,75 Å, N_{atoms}=1504, and in natural diamond R_{CS} =29,52 Å, N_{atoms}=1648. Thus, the structure of DND_1 with respect to distribution of atoms on CS differs from the structure of natural diamond, i.e. existence of the shell of different phase is detected and its structure is distinct from that of natural diamond at the size exceeding R_{CS}=28,97 Å (d~5,8 nm).

In DND_2 synthesized by SPA "Altai", Biysk (gaseous explosive charge) distribution of atoms up to 44th CS has the same parameters as in structure of natural diamond with parameters R_{CS}=38,48 Å, N_{atoms}=2748. Since 45th CS (R_{CS} = 39,28 Å, N_{atoms}=2428) the parameters of CS of DND_2 differ from those for CS of natural diamond (R_{CS} =39,18 Å, N_{atoms}=2680), i.e. the structure does not meet diamond.

Thus, the core of detonation nanoparticle has CS parameters of diamond structure up to R_{CS} =39,28 Å (d=7,6 nm), the shell of a diamond core has thickness ~4,7 Å with parameters ranging from R_{CS} =38,48 Å up to R_{CS} =42,19 Å and does not correspond to diamond structure.

It is shown that the factor limiting growth of a diamond core in DND (≤ 8 nm) is the accumulation of crystal structure defects during growth of carbon nanoparticle in post-detonation processes. The accumulated defects take away carbon surface layers from diamond structure (where density is lesser than in diamond). In further these carbon layers can be removed by chemical treatment.

[1] G.S. Yurjev, V.Yu. Dolmatov. *J. Superhard Materials* **32**, 29 (2010).

Novel spectrometer for investigating nanostructure field emission: adjusting, test spectra and first results

Davydov S.N., Bondarenko V.B., Gabdullin P.G., Gnuchev N.M.

St.-Petersburg State Polytechnic University, St.-Petersburg, Russia

To study physical nature of low voltage field emission of carbon nanostructures, a new electron spectrometer has been elaborated [1]. The very first spectra recorded from carbon structures deposited on silicon monocrystal (100) surface had rather a complicated shape of two or three peaks definitely separated by 1–2 eV gaps. It was so unexpected that the only reasonable decision that could be accepted was to carry out a series of verifying experiments using some well known emitters with predictable emission energy spectra.

Two types of test samples were chosen. The first group was just classical pointed cathodes prepared, by means of electro-chemical etching in alkali solution, from 150mkM tungsten wire. The reason for that choice was actually similarity in electron extraction processes of the test samples and the samples under investigation.

Then the spectra were recorded from plane thermo-emitters because their geometry was similar to the geometry of the investigated units.

To get comprehensive and detailed knowledge of spectrometer parameters and capabilities, spectra recording was conducted under variable conditions, such as temperature, emission field strength, current intensity, focusing or defocusing lens regimes, different correcting currents in Helmholtz coils etc. This was combined with introducing some modifying elements into the spectrometer construction and scheme. Finally, energy resolution of approximately 30-40 meV was achieved and some energy spectra were recorded from nanostructured emitters.

[1] Davydov S.N., Gabdullin P.G., Ryumin M.A. 9-th Biennial International Workshop “Fullerenes and Atomic Clusters”, Book of abstracts. P.165

Lattice constant reduction of the graphene/Ni(111) due to Au intercalation

Chikina A.G.*,Fedorov A.V., Usachev D.U, Adamchuk V.K.[1]

[1]*SPbGU, 199034, St.Petersburg, Russia*
**e-mail: chikina_alla@bk.ru*

Graphene, a two-dimensional crystal of graphite, has attracted special interest as one of the most stable nano-objects, with good conductivity in the class of monatomic films. Its unique properties are connected with specific features of the electronic structure. Graphene on Ni(111) system has received a great attention in the last few years. It has already been demonstrated that graphene epitaxial grown on Ni(111) has electronic structure quite different to pristine graphene due to high overlap of the Ni 3d and C 2p states. Strong interaction with substrate surface and lattice mismatch leads to the interlayer inelastic stress in the graphene overlayer. Intercalation of the noble metals leads to reducing of the graphene Ni interaction. This work is aimed to get further insight into effect of graphene substrate interaction on overlayer morphology.

The thin film Ni(111) was prepared using high-vacuum evaporation method on the surface of single crystal W (110). Graphene was prepared using chemical vapor deposition technique (CVD) [1, 2]. The system under investigation was characterized using X-Ray photoelectron spectroscopy (XPS), Auger electron spectroscopy (AES) and low energy electron diffraction (LEED). To get quantitative insight into the change in the graphene lattice constant upon Au intercalation LEED patterns were proceeded according to the technique described into [3].

It was found that the disposition of graphene on nickel, it feels a slight elastic tension, resulting in an decrease on 0.3%. in the interatomic distance as compared with the value before Au intercalation During deposition and following intercalation of gold there is decreases the interaction with the substrate, resulting in a decrease in the lattice constant of graphene. As a result, its value approaches the value of the lattice constant of graphite.

[1] Yu.S. Dedkov, A.M. Shikin, V.K. Adamchuk, S.L. Molodtsov, C. Laubschat, A. Bauer, G. Kaindl. *Phys. Rev. B* **64**, 035405 (2001).

[2] A.M. Shikin, G.V. Prudnikova, V.K. Adamchuk, F. Moresco, K.-H. Rieder, *Phys. Rev. B* **62**, 13202 (2000).

[3] D.U. Usachev, V.K. Adamchuk, *Phys. Rev. B* **82**, 075415 (2010).

Assessment of chemical inhomogeneity of nanodispersed diamond powders

Bogatyreva G.[1], Ilnitskaya G.D.*[1], Marinich M.[1], Bazaliy G.[1], Leshchenko O.[1]

[1]*ISM – V.Bakul Institute of Superhard Materials, National Academy of Sciences of Ukraine, 04074, Kiev, Ukraine*

**e-mail: bogatyreva@ism.kiev.ua*

A degree of chemical inhomogeneity of surface of nanodispersed diamond powders is one of the most important factors that decide for field of application of the powders.

Chemical inhomogeneity of nanodiamond powders arises from the following features of diamond particles:

– in the first – the nature (character) and amount of volume impurities, that for the most part appear at the surface of the particles and generate active surface centers;

– secondly – the nature (character) and amount of chemical compounds and functional groups adsorbed on the surface of the particles. As a rule, volume impurities are admixtures of metals and metalloids that remain in nanodiamond powders after synthesis and follow-up chemical treatment. Surface impurities consist of the chemical compounds and functional groups (hydroxyl, carbonyl and carboxyl ones et al.) adsorbed on the diamond surface.

Electrochemical method of assessment of amount of conducting active centers is the principal method for assessment of chemical inhomogeneity of nanodiamond powders. The method bases on the determination of criterion K. We define criterion K as ratio of the area of effective conducting centers of initial surface of nanodiamond powder to the general surface of the powder. The less value of K the higher chemical homogeneity of nanodiamond powders, i.e. the better results of chemical treatment of the powders.

According to value of K the nanodiamond powders with reconstructed surface were segregated into three groups: 1) K = 1-5%, 2) K = 6-10% and 3) K > 10%.

The powders of the 1st group are the best for production of stable monosized suspensions.

Z-scan study of nonlinear properties of carbon nanostructures

Belousova I.M.*[1,2], Kislyakov I.M.[1,2], Murav'eva T.D.[1], Yelleswarapu C.S.[3], Rao D.V.G.L.N.[3]

[1]*SIC Vavilov State Optical Institute, St. Petersburg, 199034, Russia*
[2]*St. Petersburg State University of ITMO, St. Petersburg, 197101, Russia*
[3]*Department of Physics, University of Massachusetts, Boston, MA 02125, USA*
**e-mail: Belousova.I.M@gmail.com*

A study of nonlinear properties of suspensions of Astralen nanoparticles in water, as well as fullerene C_{60} aggregates in toluene-hexane mixtures were carried out. Astralen is a carbon nanostructure in form of polygonal closed fulleroid multishells whose physical properties are described in [1, 2]. Along with carbon black and carbon nanotubes it possess a strong optical limiting effect caused by nonlinear light-induced scattering [3, 4]. Fullerene C_{60} suspensions also shows a high-threshold optical power limiting mainly related to the reverse saturable absorption. The last phenomenon is determined by electronic structure of a nanoparticle that changes with fullerene aggregation, and is expected to be different in changing the solvent.

In this paper we report results of precise measurements of linear and nonlinear absorption coefficients of fullerene C_{60} suspensions with different degrees of aggregation and a determination method of nonlinear scattering cross section of Astralen suspension using closed aperture Z-scan measurements with different aperture size.

The work was supported by the Russian Foundation for Basic Research (grant # 09-02-00839-a).

[1] Shames A.I., Katz E.A., Panich A.M., Mogilyansky D., Mogilko E., Belousov V.P., Belousova I.M., Ponomarev A.N., *Diamond and Related Materials* **18**, 505 (2009).

[2] Shames A.I., Felner I., Osipov V.Yu., Katz E.A., Mogilko E., Grinblat J., Panich A.M., Belousov V.P., Belousova I.M., Ponomarev A.N., *Nanoscience and Nanotechnology Letters* **3**, 41 (2011).

[3] Belousova I.M., Belousov V.P., Mironova N.G., Murav'eva T.D., Scobelev A.G., Yur'ev M.S., Videnichev D.A., *Proceedings of SPIE* **6455**, 64551D1 (2007).

[4] Kislyakov I.M., Belousova I.M., Murav'eva T.D., Notz G., Peceli D., Webster S., Hagan D.J., Van Stryland E.W., *Proceedings of XIII International Conference on Laser Optics*, St.Petersburg, p. 74, (2008).

Advanced model of the singlet oxygen generator of gas flowing type on base of porous fullerene-containing structures

Bagrov I.V.[1], Belousova I.M.[1,2], Grenishin A.S. [1], Kiselev V.M. *[1], Kislyakov I.M. [1,2], Sosnov E.N. [1]

[1]*SIC Vavilov State Optical Institute, St. Petersburg, 199034, Russia*
[2]*St. Petersburg State University of ITMO, St. Petersburg, 197101, Russia*
**e-mail: Kiselev_VM@yahoo.com*

Description of the retrofit singlet oxygen generator, working on the basis of the porous solid-phase fullerene-containing structures, with more powerful optical pump by means the light-emitting diode matrix and with a continuous flow of molecular oxygen through porous structure of the substrate is presented. Results of researches of the efficiency of singlet oxygen production are given for a wide range of the variation of operating conditions of the system.

Vibration states of micro- and nanocarbon: structural aspects

Bekhterev A.N.

Magnitogorsk State University, 455000, Magnitogorsk, Russia
e-mail: alexbehterev@yandex.ru

Carbon in a condensed state is polymorphic, which is determined by the possibility of the realization of different types of hybridization for valence electron orbitals: carbine (sp^1-), graphite (sp^2-), and diamond (sp^3-). In the indicated carbon systems, the physical properties vary from typically metallic to dielectric ones. Atoms in structural motives of GC and PC are in various hybridization states: sp^n- ($1 \le n \le 3$).

Phonon's structure of amorphous and crystal carbons is investigated in detail in Raman spectra. However, not all vibration states in view of an alternative selection rule are active in Raman spectra. Research of vibration states in IR-spectra of the condensed carbon is complicated by intensive not selective absorption of free carriers of a charge. The phonon spectrum in a series of nanocrystalline glassy carbon (GC) and microcrystalline pyrolytic carbon (PC) with the monotonously changing perfection degree of crystal structure is investigated in this work. Thermal processing of samples in the inert environment in the region of temperatures 1300–3000°C has allowed to change the sizes of fragments of coherent dispersion in a range 2, 5–800 nm. The natural surface of samples was investigated at a corner of reflection 20° on IFS-88 (Bruker) spectrometer in wide spectral area: 5000-400 cm^{-1} with the accuracy of 2 cm^{-1} and in a regime of accumulation up to hundred scans.

According to the theoretical-group analysis of fragments of crystal structure in IR- and Raman spectra of GC and PC should possess the optical activity intraplane and in plane vibrations of carbon atoms of graphite (D_{6h}^4) or fullerenes (I_h) mesh frame structures [1]. Selective absorption bands of vibration states E_{1u}, A_{2g}, T_{1u} in the aria of 1600-1300 cm^{-1} and A_{2u} - in the aria 900-800 cm^{-1} are registered in experimental IR-Fourier reflection spectra of GC and PC samples. Intensity and position of absorption bands considerably changed with the growth of temperature of samples processing and correlated with results of the structural researches, results of Raman and ATR (attenuated total reflection) spectra on the given objects [2].

[1] Carbon molecules and materials./Ed. by R. Setton, P. Bernier, S. Lefrant. - L.- N.Y.: Taylor and Francis. - 2002, 489 p.

[2] Bekhterev A. N. Vibration states in solid state carbon and nanocarbon. - Magnitogorsk: MaSU, 2007.

Phase transition in amorphous fullerites C_{70}

Agafonov S.S.*, Borisova P.A, Glazkov V.P., Somenkov V.A.

"Kurchatov Institute" , Moscow , Russia
**e-mail: agaph_isssph.rambler.ru*

It has been shown that at high-temperature annealing of amorphous fullerites, produced by mechano-activation treatment of crystal C_{60}, takes place polyamorphous phase transition from an amorphous molecular phase in amorphous atomic phase [1]. In this work we have tried to find out temperature evolution of pure amorphous C_{70}. After long time milling of C_{70} on the places of Bragg's reflexes, characteristic for initial crystalline fullerites we can observe diffuse gallo, typical for amorphous phases Areas of the coherent dispersion, estimated on gallo widths is about 3-5 nm.

After high-temperature (1300-1500 K) annealing we can observe diffraction picture, that corresponds to amorphous atomic phase, like in the case of C_{60}. Differential thermal analysis gives one sharp signal of thermal emission at 950°C, when the polyamorphous transition from molecular (fullerenelike) phases in atomic (probably diamondlike) phase takes place. At the same time comparison of gallo positions with reflexes of diamond and graphene ((h k 0) graphite peaks)shows that in the measured range of the transferred impulses all these positions are close, so it is impossible to make the conclusion, whether the high-temperature amorphous phase is diamondlike or graphenelike. However the transition between stable amorphous fullerites to amorphous graphites occurs through intermediate diamondlike (metastable) or graphenelike (quasitwo-dimensional) phase.

At high-temperature interaction of this phase to detonation diamond nanopowder there is a disappearance of a reflex of detonation diamond which, apparently, is dissolved in a high-temperature amorphous phase.

[1] S.S. Agafonov, V.P. Glazkov, I.F. Kokin, V.A. Somenkov, *Solid State Phys.* **52**(6), (2010).

Monodispersed nanodiamond powder obtained by laser synthesis

Zousman B., Levinson O.*

Ray Techniques Ltd, 91391, Jerusalem, Israel
**e-mail: olga.levinson@nanodiamond.co.il*

Innovative scalable technology of laser synthesis for producing ultrananocrystalline nanodiamond (ND) was developed by Ray Techniques Ltd, Israeli company located at the campus of the Hebrew University of Jerusalem.

ND is usually obtained by detonating TNT and RDX mixture in metal chambers, with subsequent separation and purification. ND is widely used in a wide range of application, among them fine polishing, galvanic and electroless coatings, and manufacturing of various nano-composites. In recent years ND has rapidly entered fields like electronics, energy and biotechnology. However, advanced applications of ND are currently limited since detonation ND does not meet the modern requirements for homogeneity due to the difference in the synthesis conditions inside a detonation chamber and the inconstancy of explosive raw materials. The second problem is insufficient purity, present of metals and graphite in the ND powder.

RayTechniques' novel technology of ND laser synthesis enables to obtain monodispersed ND (RayND) from pure carbon materials. RayND, compared with detonation ND, has a better diamond structure, is more homogeneous (both geometrically and chemically) and pure. The environment-friendly and non-hazardous manufacturing process does not require additional expenses for safety, security and environment protection.

Integrated investigation of electrical surface properties of detonation nanodiamond agglomerates in aqueous KCl solutions

Zhukov.N.*, Gareeva F.R.

St. Petersburg State University, 198504, St. Petersburg, Russia
**e-mail: zhuk@AZ1038.spb.edu*

An integrated investigation of the electrical surface properties of the microporous agglomerates of detonation nanodiamond (DND) in aqueous KCl solutions was carried out using various experimental techniques. The adsorption isotherms of potential determining ions Γ_{H^+,OH^-} (pH) and the pH dependences of the surface charge density σ_0 (pH) = F ($\Gamma_{H^+} - \Gamma_{OH^-}$) of agglomerates preliminary purified from the electrolyte admixtures by dialysis are obtained in a pH range of 4.0 - 10.5 by acid-base titration of DND hydrosols containing c = 0.0001- 0.1 M KCl (Fig. 1). The titration data and obtained FTIR spectrum argue in favor of chemical nonuniformity (heterogeneity) of a DND surface containing mainly two types of the ionizable surface functional groups: amphoteric hydroxylic –COH and acidic carboxylic –COOH groups. The point of zero charge (pH_{PZC} value corresponding to σ_0 = 0) is independent of the KCl concentration and equal to 9.5.

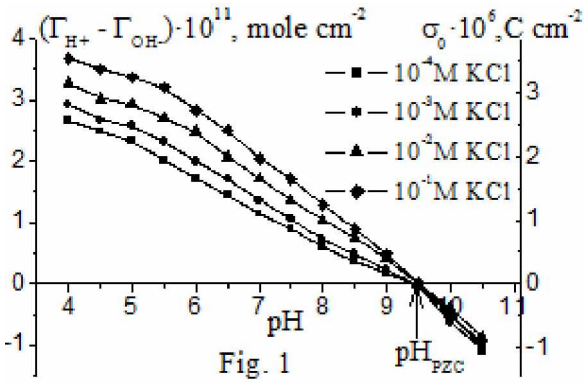

Fig. 1

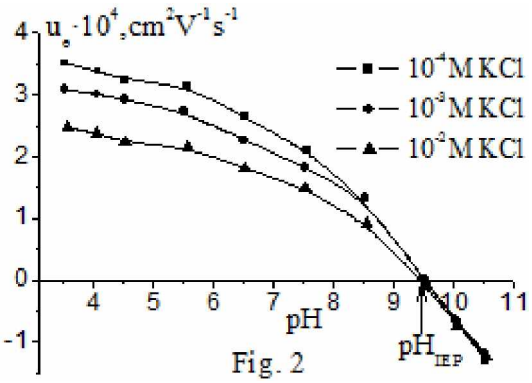

Fig. 2

The electrophoretic mobility u_e of the investigated agglomerates of DND as a function of pH = 3.5 - 10.5 and c = 0.0001 - 0.01 M KCl was measured by laser Doppler electrophoresis method (Fig. 2). The isoelectric point (pH_{IEP} value corresponding to u_e = 0) is equal to pH_{PZC} = 9.5. The conductivity of diluted DND hydrosols versus pH, c and DND volume fraction p = 0 – 0.001 was measured and conductivities K_p of microporous agglomerates impregnated with electrolyte solutions were determinated. It is shown that the magnitude of K_p is important for calculation of the correct ζ-potential values from the experimental u_e.

Interaction dynamics of the nanodiamond with living cells in culture

Yakovlev R.Yu.*[1], Alieva I.B.[2], Leonidov N.B.[1], Rakita D.R.[1], Agafonov V.N.[3], Uzbekov R.E.[2,3,4]

[1]*Pavlov Ryazan State Medical University, 390026, Russia*
[2]*Belozersky Institute of Physico-Chemical Biology Moscow State University, 119991, Moscow, Russia*
[3]*Rabelais Universitŭ, 37200, Tours, France*
[4]*Faculty of Bioengineering and Bioinformatics Moscow State University, 119991,Moscow, Russia*
**e-mail: yarules@yandex.ru*

Cells of four cell lines (HeLa, SPEV, human endotheliocytes and lymphoblasts MOLT-4) were cultivated in cell culture medium with water suspension of nanodiamonds (ND) for 15 min, 2, 8 and 24 hours. Three different suspension types were tested: pristine ND, ND modified with anxiolytic and ND modified with antibiotic (ND-A). After fixation cells were embedded in Epon resin by standard methods and ultra-thin sections (75 nm) were then observed in transmission electron microscope (TEM) JEM 1011 (Jeol).

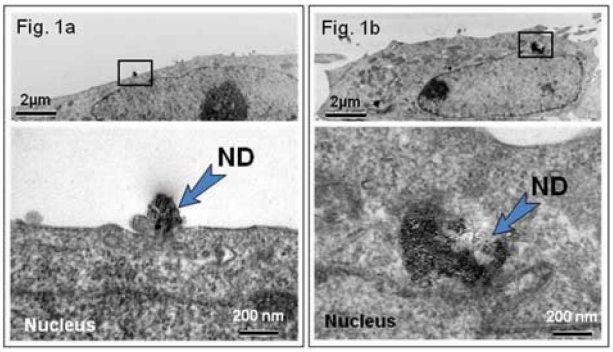

Figure 1. TEM images of HeLa cell cultivated 15 min with ND (**a**) or ND-A (**b**). Upper photos presented total cell view, down photos - magnified selected regions with ND.

Ultrastructural study showed that within 15 minutes of incubation ND aggregates were connected with cell membranes (Fig.1a). In TEM ND particles were clearly visible against the background of cellular structures without any additional staining. They represented very contrasting nanocrystals measuring about 5 nm. Cell membranes interacted with ND conjugates and formed intussusceptions, which gradually deepened leading to penetration of ND into the cell. 3D analysis on serial ultrathin sections revealed that part of the ND-A is found inside cells within 15 min of incubation. These conjugates were observed within the cytoplasm not surrounded by any membrane. It was also discovered that ND conjugates interacted with the outer nuclear membrane (Fig.1b). Our results demonstrated that the penetration of ND-A was more active than of pristine ND.

Development and investigation of drug delivery system based on the detonation nanodiamonds

Yakovlev R.Yu.*[1], Badun G.A.[2], Selezenev N.G.[1], Yakusheva E.N.[1], Leonidov N.B.[1]

[1]*Pavlov Ryazan State Medical University, 390026, Ryazan, Russia*
[2]*Lomonosov Moscow State University, 119991, Moscow, Russia*
**e-mail: yarules@yandex.ru*

The method of covalent binding of drugs with detonation nanodiamonds (NDs) was developed. It was shown that such basic methods of NDs modification as oxidation, reduction, halogenation and amination significantly influenced on their properties: dispersion, chemical composition and the density of grafted molecules. It should be mentioned that the derivatives produced by oxidation in gaseous and in liquid phases possess different properties. Variation of NDs reduction conditions let us simultaneously solve not only the problems of purification, disintegration and unification (lesser heterogeneity) of their surfaces but also gives us the possibilities to directionally change their chemical composition.

On this basis the modified NDs with tritium label and X-ray contrast substance were synthesized as well as systems of antibiotic and central neuromediator delivery. The physical and chemical properties of these substances were studied by different methods of electron microscopy (TEM, HRTEM, SEM, confocal), spectroscopy (IR, Raman, XPS, ICP-MS), XRD, DSC, DLS, radiometric analysis, etc. The particles of modified NDs were found to have of disturbed carbon shells up to 1 nm and can consist also chemisorbed molecules. The methods to estimate the number of grafted drug molecules to the NDs' surface were developed. The diffusion through the synthetic and natural (inverted rat's intestine) membranes of original and modified NDs of different dispersion was studied with/without ultrasonic treatment. Biodistribution of modified NDs was studied with rats and rabbits using different insertion ways. To this end X-ray computer tomography, mass-spectrometry and tritium tracer method were used. This work is a part of our preclinical trial of the drug delivery systems on the basis of detonation NDs created by us for the first time.

Structural investigations of carbon nanostructures produced by hydrodynamical cavitation technique

Voropaev S.*, Galimov E.M.

GEOKHI Vernadsky Institute, 119991, Moscow, Russia
**e-mail: svoropaev@rambler.ru*

Originally an idea of diamonds production by hydrodynamical cavitation was presented by academician E M Galimov [1]. He supposed the possibility of nature diamonds formation at fast magma flowing in kimberlitic pipes during bubbles collapse. Experimental setup to reproduce the high pressure and temperature reaction centers by means of the cavitation following the above idea was created. A few crystalline nanocarbon forms were successfully recovered after treatment of benzene (C_6H_6) [2].

From the general point of view, the physics by cavitational bubbles collapsing and by shock-compression is very similar [3]. But, the environment conditions, especially theirs that appropriate for the rapid cooling, are important as well. For example, the higher the cooling capacity, the larger the detonation nanodiamonds yield, which can reach 90%. Various measurements, including X-ray diffraction and high-resolution TEM revealed that the size of the diamond grains in the soot is distributed around 5 nm. The purpose of this study is to investigate a new rapid cooling technique under shock compression during hydrodynamical cavitation and to clarify carbon behavior under special range of P-T conditions. A special nanodiamond particles were found in the samples recovered from the benzene after treatment at the proper experimental setup. The results of characterization for the produced nanocarbon forms by means of the transmission electron microscope (TEM) and Raman spectroscopy are reported.

[1] Galimov E.M., *Nature* **243,** 389 (1973).
[2] Galimov E., Kudin A., Skorobogatskiy V., Aronin A., *Dok. Acad. of Sciences* **395,** 187 (2004).
[3] Dnestrovskiy A., Voropaev S., Ponomareva E., *Doklady Physics* **56,** 78 (2011).

Formation, distraction and drying of the "secondary structure" in detonation nanodiamonds

Volkov D.S.[1], Avramenko N.V.[1], Belyaeva L.A.[1], Davydov V.A.[2], Proskurnin M.A.[1], Korobov M.V.[1]

[1]*Department of Chemisry, Moscow State University, 119899, Moscow, Russia*
[2]*Institute of High-Pressure Physics of RAS, 142190 Troitsk, Moscow District, Russia*
**e-mail: dmsvolkov@gmail.com*

Disintegrated detonation nanodiamonds (DDND), though originally divided into individual diamond crystals (d = 5.2 nm) in the water dispersion, forms stable porous network ("secondary structure") as aqueous gel and dried powder [1].

In present study we attempted to follow formation and distraction of such a network by means of differential scanning calorimetry (DSC). The fingerprint of a network is a DSC peak corresponding to the melting of nano-sized water confined into the pores.

The network was not found in the original crude DND material. It appeared after an extensive acidic treatment of the samples at elevated temperature. Increasing the time of the treatment led to the diminishing of the size of voids filled with water. The minimum size (~6 nm) was close to the size of primary DND particles (d~5 nm). The smaller was the diameter of the voids in the "secondary structure", the smaller was the size of DND clusters in water dispersion made from the same material by ultrasonication.

The "secondary structure" disappeared in the DNDD samples subjected to high temperature – high pressure treatment (10 kbar, 870 K). Further increase of the temperature led to graphitisation of DDND. X-ray and SEM confirmed formation of a graphite phase.

Isothermal drying of aqueous gels DDND and DDN at temperatures 303–353 K was studied by means of thermogravimetry (TG) and DSC. The liquid was quantitatively removed from the samples. Two evaporation rates were observed for DDND at each temperature. The first corresponded to the evaporation of bulk water while the second – to nano-sized water. The amount of nano-sized water was 0.5 g per gram of ND. Parameters of the "secondary structure" account for the distinctive features of drying isotherms.

[1] Korobov M.V., Batuk M.M., Avramenko N.V., Ivanova N.I., Rozhkova N.N., Ōsawa E., *Diamond & Related Materials* **19**, 665 (2010).

Cluster models in small-angle scattering analysis of detonation nanodiamonds

Tomchuk O.V.*[1,2], Avdeev M.V.[1], Aksenov V.L. [3,1], Bulavin L.A.[2]

[1]*Joint Institute for Nuclear Research, Dubna, Moscow reg., Russia*
[2]*Taras Shevchenko Kyiv National University, Kyiv, Ukraine*
[3]*Russian Research Center "Kurchatov Institute", Moscow, Russia*
**e-mail: tomchuk@jinr.ru*

Various forms of detonation nanodiamond (DND) are characterized by cluster organization, which is well reflected in small-angle X-ray and neutron scattering [1-3]. The corresponding regions of the power-law type in the scattering intensity can be treated in the frame of the unified exponential/power-law approach [3], which allows us to follow changes in the fractal parameters of nanodiamond clusters under different conditions. Several models imitating the growth of fractal clusters are probed to understand the appearance of specific features in the scattering. Two- and three-dimensional cases for deterministic and stochastic fractals composed of nanoparticles with a finite size are considered. Both monodisperse and polydisperse basic structural units are used. It is shown that the Schmidt equation [4] for the small-angle scattering from mass fractals should be modified when applying to real systems.

[1] A.E. Aleksenskii, M.V. Baidakova, A.Ya. Vul', V.I. Siklitskii, *Phys. Solid State* **41**, 668 (1999).
[2] M.V. Avdeev, V.L. Aksenov, L. Rosta, *Diam. Relat. Mater.* **16**, 2050 (2007).
[3] M.V. Avdeev, N.N. Rozhkova, V.L. Aksenov, V.M. Garamus, R. Willumeit, E. Osawa, *J. Phys. Chem. C* **113**, 9473 (2009).
[4] G. Beaucage, *J. Appl. Cryst.* **29**, 134 (1996).
[5] P.W. Schmidt, *J. Appl. Cryst.* **29**, 414 (1991).

Manufacturing of seeding suspensions based on crushed nanodiamond for CVD diamond films

Stepanenko E.V.*[1], Levashov E.A.[1], Ralchenko V.G.[2], Patsera E.I.[1]

[1]*National University of Science and Technology "MISIS", 119049, Moscow, Russia*
[2]*A.M. Prokhorov General Physics Institute RAS, 119991, Moscow, Russia*
**e-mail: ev_azarova@mail.ru*

Growth of diamond films on a foreign substrate using a CVD process typically requires surface treatment in order to achieve a high nucleation density. One of the most widely used approaches is seeding of the substrate with diamond particles through the use of a slurry of diamond particles with grain size from nanometers to microns dispersed in an appropriate solvent (alcohol, acetone, etc.) accompanied by ultrasonic agitation [1]. Slurries of nanodiamond provide the highest nucleation density.

In this work we employed narrow distributed diamond powder MD20 with the average grain size 20 nm produced by a technique of crushing after static conversion from graphite ("Tomei Diamond Inc., Ltd", Japan) for preparing the diamond slurries. MD20 powder was dispersed in an ultrasonic horn-type ultrasound sonicator UZDN-2T with an output power of 400 W. Water and isopropyl alcohol were used as a solvent. Diamond suspensions were sonicated with the frequencies of 22 and 44 kHz and processing time from 5 to 60 minutes. The suspension of MD20 with isopropyl alcohol were compared to disaggregated detonation nanodiamond with average grain size 4 nm in a water solvent (supplied by Ioffe Physical-Technical Institute of Russian Academy of Science). Si wafers were seeded by sonication in a nanodiamond suspension. After 30 min of sonication, the substrates were removed and rinsed with water or isopropyl alcohol.

Particle size distributions in suspensions were measured by photon correlation spectroscopy (PCS) using a Beckman–Coulter N5 submicron particle size analyzer. Seeded Si substrates were observed with scanning electron microscopy.

As a result the relatively stable suspension of MD20 diamond powder in isopropyl alcohol with average particle size 20 nm has been obtained. Nucleating density on Si substrate was 10^9 cm^{-2}. In the case of water suspension the cleaning of Si surface is required as an additional step for liquid spreading and uniform particles distribution on the surface.

[1] Shenderova O., Hens S., McGuire G., *Diamond and Related Materials* **19**(2-3), 260 (2010).

Polycrystalline diamond fibres prepared by high temperature shock compression of the multi-walled carbon nanotube

Britun V.F., Kurdyumov A.V., Solonin Yu.M.*, Yarosh V.V.

Frantsevich Institute for the Problems of Materials Science of the NAS of Ukraine
03680, Krzhyzhanovsky, 3, Kyiv-142, Ukraine
e-mail: Solonin@ipms.kiev.ua

The high temperature shock compression (HTSC) method based on detonation treatment of the powder mixtures consisting of a substance investigated and some additives which possess higher compressibility and lower specific heat [1]. Such additives can be, for example, alkaline-haloid salts. Owing such properties mentioned additives provide the intensive heating of a basic substance during compression and sharp cooling during unloading, preventing thus reverse transformation.

In this work polycrystalline diamond fibers of 150-200 nm diameter have been produced by HTSC method [2]. The initial product was the multi-walled carbon nanotubes (fig. 1,2) A pressure of the process was estimated as 30 GPa and the temperature as 3500 K.

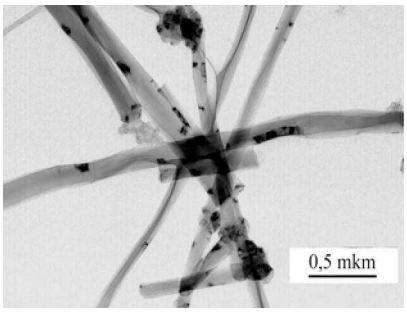

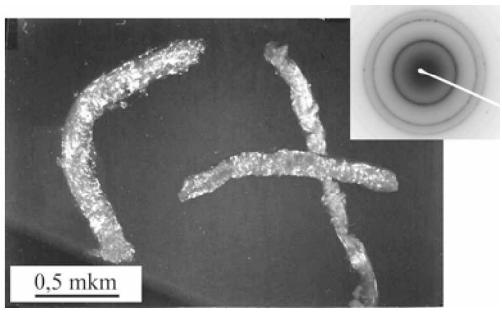

Figure 1. The multi-walled carbon nanotubes **Figure 2.** The polycrystalline diamond fibers

The study of the transformation products with the X-ray and electron microscopy methods revealed that the treated fibers consist of fine diamond particles with size about 10 nm and arbitrary orientation.

The preservation of the multi-walled carbon nanotubes morphology after their transformation into diamond caused by presence of the KCl additive softening the action of shock waves, especially when the additive melts at high temperature.

[1] Britun V.F., Kurdyumov A., Borimchuk N.I. et al., *Diam.Rel. Mater.* **16**(2), 267 (2007).
[2] V.F.Britun, A.V.Kurdyumov, Yu.M.Solonin, V.V.Yarosh, *Report of the National Academy of Science of Ukraine* 11, 86-90 (2009).

ODMR studies of fluorescent nitrogen-vacancy defects fabricated by sintering of detonation nanodiamonds

Soltamov V.A., Soltamova A.A.*, Bhoodoo C., Babunts R.A., Shakhov F.M., Kidalov S.V., Vul' A.Ya., Baranov P.G.

Ioffe Institute, 194021, St.Petersburg, Russia
**e-mail: alex.soltamova@hotmail.com*

Nitrogen-vacancy (NV) centres in diamond are one of the most prominent objects for applications in new generation of supersensitive magnetometers, biosensors which demand very bright and photostable fluorescence from high-density nitrogen-vacancy ensembles located in diamond core of nanoparticles. Fluorescence brightness strongly depends on the concentration of NV centres and the diamond quality. Although NV centres have effectively been generated in diamond by irradiation and following high temperature annealing they have not been observed in high concentrations in non-irradiated diamonds. Enormously high concentrations of NV centres going as high as 1% (10000 ppm) can be produced directly by high-pressure high-temperature sintering of detonation nanodiamonds (NV-diamond) without any post or prior irradiation of the samples.

Intensive fluorescence spectra with quite well distinguished zero-phonon line related to negatively charged NV centres even at the room temperature were observed. Anisotropic optically detected magnetic resonance (ODMR) and electron paramagnetic resonance (EPR) signals of NV centres and isolated nitrogen (N) have been detected in single arrays showing that sintering leads to self-organization of nanodiamond particles in oriented micron-size arrays which include high concentrations of NV and N centres.

In zero-field ODMR of NV centers which observed right up to room temperature the side band satellites observed which arise from triplet-doublet magnetic dipolar interactions of NV and N centers. Micron size single arrays of NV-diamond could be used as a very sensitive device for measuring of weak magnetic fields in micron scale.

This work has been supported by the Ministry of Education and Science of the Russian Federation under Contracts Nos. 14.740.11.0048, 02.740.11.0108; the Programs of RAS: Spin-Dependent Effects in Solids and Spintronics; Support of Innovations and Elaborations; Basic Researches of Nanotechnologies and Nanomaterials and by the RFBR under Grants Nos. 09-02-01409 and 09-02-00730.

[1] I.V. Ilyin, A.A. Soltamova, P.G. Baranov, A.Ya.Vul', S.V. Kidalov, F.M. Shakhov, G.V. Mamin, S.B. Orlinskii, N.I. Silkin, M.Kh. Salakhov, *Fullerenes, Nanotubes, and Carbon Nanostructures* **19**, 44 (2011)

[2] A.A. Soltamova, I.V. Il'in, F.M. Shakhov, S.V. Kidalov, A.Ya. Vul', B.V. Yavkin, G.V. Mamin, S.B. Orlinskii, P.G. Baranov, *JETP Letters* **92**, 102 (2010).

Effect of water adsorption on electrical conductivity and permittivity of diamond nanopowders

Sokolina G.A., Denisov S.A.*, Kiseleva O.A., Spitsyn B.V.

Frumkin Institute of Physical Chemistry and Electrochemistry RAS, 119991, Moscow, Russia
**e-mail: saldenisov@gmail.com*

Nanodiamond (ND) powders in vacuum are good insulators with conductivity (G) of the order of 10^{-12} Ohm^{-1} cm^{-1} or less and the magnitude of the dielectric constant ε of a few units. Due to the large specific surface area of powders and high conductivity of water comparing to the diamond it should be expected increase of G and ε in the system ND-adsorbed water.

Frequency dependence of the conductance G (f) and capacitance C (f) for dry and wet powders in the frequency range 1 Hz<f<1.6 MHz were measured. The data were obtained using two-electrode cell placed in vacuum set.

The water's isotherms were determined by weighing the samples after exposing them at various pressures of water vapor in region 0.5<P <15 Torr.

The detonation diamond powder with specific surface area 300 m^2/g UDD-SP (SPA "Sinta", Minsk) were studied. Dependence of G (f, p) and ε (f, p) were obtained for the initial hydrophilic powders with oxygen containing groups on the diamond surface and the hydrophobic surface with chlorine groups.

Dependences of G(f, p) are interpreted in the basis of percolation theory. In this theory percolation threshold is determined, when the non-conductive matrix becomes conductive. Our experiments show G increase starting from p/p_s=0.2 for hydrophilic and 0.40 for hydrophobic (p_s-saturated water vapor pressure). It can be explained by merging of water clusters [1]. Near the percolation threshold G(f) shows power-law dependence of frequency ($G \sim f^s$; *s*-is a function of pressure).

The theory [2] predicts the existence of non-trivial polarization processes leading to the effect of giant dielectric polarization for water bearing porous dielectrics at 1Hz<f<10^5 Hz. This theory takes into account the surface contribution to the polarization. It was shown in our experiments, that indeed in the low-frequency ε increases to 10^4-10^6. Significant polarization becomes possible after formation of polylayer of water. The various physical and chemical processes under the action of electric fields, explaining the phenomenon of giant polarization at interfaces, are discussed (the restructuring of electric double layers, surface migration and diffusion of charges).

The obtained information can be useful both for estimation of the properties and possible practical application of ND powders.

[1] P.S. Vartepetian, A.M. Voloshuk, *Uspehi Khimii* **64**(11), 1055 (1995) (In Russian).
[2] T.L. Chelidze, Y. Guergen, Geophys., *J. Int.* **137**, 1 (1999).

Problems of stability of disaggregated nanodiamond hydrosols

Aleksenskii A.E.[1], Shvidchenko A.V.*[1,2]

[1]*Ioffe Institute, 194021, St.Petersburg, Russia*
[2]*Academical Physical Technological University, 195220, St.Petersburg, Russia*
**e-mail: alexshvidchenko@mail.ru*

The recently obtained Disaggregated Detonation Nanodiamond (DDND) is a very perspective material for using in many areas. In this concern the investigations of it stability, especially in biological environment, are actual.

The two types of DDND (particle size 5 nm) were investigated in this work. The DDND hydrosols were prepared accordingly to [1-2]. The values of ζ-potential in these hydrosols were –45 and +45 mV respectively.

We investigated the ζ-potential and size values of DDND hydrosols in dependence of pH value. We have found that the both type of hydrosols were stable in a wide range of pH at low values of ionic strength.

The both types of hydrosol completely coagulates if pH<2. We have demonstrated the possibility of restoring of deagglomerated state of the DDND with negative ζ-potential after recovery of pH. The restoring of the positive charged DDND occurred being impossible.

We observed that increase of the ionic strength gives drop of the aggregative stability of DDND is even if the pH value is constant. The limit of coagulation stability of DDND is about 0.05 mol/l. We found that in isotonic solution (NaCl 0.9%) the DDND coagulates. Negatively charged DDND could be restored into deagglomerated state by washing although positively charged DDND couldn't be restored. The addition of multivalent metals into DDND hydrosol causes it partial coagulation, proportional by quantity of added metal.

The mixing of oppositely charged DDND hydrosols gives their coagulation.

Thus we found the potential instability of DDND in simulated biological environment. We have demonstrated that the DDND stability in bio-environment and in cell cultures is important, but still unsolved problem.

Presented work is supported by RFBR (grants 08-08-00983-a, 09-02-92477-MHKC_a).

[1] Aleksenskiy A.E., Eydelman E.D., Vul' A.Ya., *Nanoscience and Nanotechnology Letters* **3**, 68 (2011).

[2] Williams O.A., Hees J., Dieker Ch., Jager W., Kirste L., Nebel Ch.E., *ACS Nano* **4**(8) 4224 (2010).

Fluorinated nanodiamond and soot in tribological applications

Shenderova O.A.*[1], Ivanov M.G.[2], Deev L.E.[3], Ivanov D.M.[2]

[1]*International Technology Center, 27615, Raleigh, USA*
[2]*Ural Federal University, 620002,Yekaterinburg, Russia*
[3]*«RSC « Applied Chemistry», 614034, Perm, Russia*
**e-mail: oshenderova@itc-inc.org*

Different types of additives, including nanoparticles, are used with lubricants in order to reduce friction and wear as well as to increase the load carrying capacity of the lubricants. Detonation soot (a mixture of nanodiamond particles with different forms of sp^2-bonded carbon) has been used in commercial Class I oils for more than 2 decades and well purified nanodiamond (ND) particles demonstrated recently impressive antifriction and antiwear properties in polyalphaolefin (PAO) oils [1, 2]. Colloidal stability of nanoadditives in an industrial oil is the paramount requirement for their tribological applications. ND particles can be modified to enhance the stability of their dispersions in a suitable carrier or liquid, and provide chemical compatibility for oil. Particularly, fluorine-modified NDs demonstrate enhanced colloidal stability in oils. The introduction of fluorine-containing constituents result in enhanced lubricity and chemical stability under extreme conditions.

In the current work, treatment of detonation ND (DND) and detonation soot (F-DND and F-soot) in the flow of F_2 and SF_4 was performed, resulting in up to 8 at.% of fluorine in the DND composition. Mixtures for tribological tests were prepared using PAO-6 as the base oil. Fluorinated DND and soot were dispersed in PAO using fluorine-containing dispersant. Combinations of fluorinated DND with fluorine-containing dispersant in PAO with hexagonal boron nitride h-BN particles were also prepared for a comparison. Testing has been performed on these formulations using ring-on-ring (friction coefficient) and four ball tests (extreme pressure (EP) failure load and diameter of wear spot).

Fluorine-containing NDs and soot demonstrated superior tribological properties as compared to the pristine non-functionalized particles and h-BN additive used alone.

[1] M.G. Ivanov, S.V. Pavlyshko, D.M. Ivanov, I. Petrov, G. McGuire, O. Shenderova, *Mater. Res. Soc. Symp. Proc.* **1203**, 1203-J17-16 (2010).

[2] M.G. Ivanov, S.V. Pavlyshko, D.M. Ivanov, I. Petrov, O. Shenderova, *JVST. B* **28**(4), 869 (2010).

Self-organization of detonation nanodiamonds after treatment by high-energy methods

Shalimova A.S.*, Gasanov Z.D., Novikova K.O.

SiberianFederal University, 660074, Krasnoyarsk, Russia
**e-mail: asya_sx@mail.ru*

The use of achievements of nanotechnology in the real production is impossible without the development of processes for the production of nanomaterials in sufficient quantities. A successful example of such technology is the synthesis of detonation nanodiamonds (DND) with a particle size of 4 nm. Diamonds have a unique combination of high chemical, thermal and radiation resistance, the highest hardness and wearresistance among the known substances, low coefficient of thermal expansion and etc. [1].

In this paper, three effective methods of exposure to water suspension of nanodiamonds are considered: ultrasound (device UZDN-1 with the working frequency of 22 kHz and 44 kHz), cavitation (a rotating wedge with a frequency of 10-20 000 r/min) and laser radiation (femtosecond laser Tsunami, the wavelength of 800 nm, capacity 840-860 Mw). Time of exposure ranged from a few seconds to several minutes. Control of the size distribution was carried out by the "CPS Disc Centrifuge Model DC 24000".

After carrying out of experiments, in which intensity and exposure time each method are varied, the comparative analysis was made. This analysis showed that the most efficient and productive method of disintegration is the cavitation. The size of the primary diamond crystal is 4-5 nm.

After carrying out of works on the disintegration of nanodiamond agglomerates in water suspension by means of laser radiation it was found that the laser radiation promotes not only the destruction of aggregates, but also stimulates the formation of regular structures.

Laser treatment, in contrast to the other methods, leads to the growth of three-dimensional structures resembling the form of "baskets" from the primary DNA. The analysis of the AFM images shown, that at the deposition on a substrate of concentrated suspensions are formed aggregates (clusters) of a large number of nanodiamond particles, whose size is in the range from 20 up to 270 nm.

The further researches are conducted to specify the mechanism of the observed phenomena and the influence of external factors on the process of stimulation and self- organization processes control of DNA and properties of these structures.

[1] Lyamkin A.I., Petrov E.A., Ershov A.P., Sakovich G.V., Staver A.M., Titov V.M., *Dokl. Acad. Sci. USSR* **302**(3), 611 (1988) (in Russian).

Magnetic studies of nanodiamond – copper composites synthesized at high pressure and high temperature

Shakhov F.M[1]*, Osipov V.Yu.[1], Kidalov S.V.[1], Takai K.[2], Enoki T.[2], Vul' A.Ya.[1]

[1]*Ioffe Physical-Technical Institute, 194021, Saint-Petersburg, Russia;*
[2]*Tokyo Institute of Technology, 1528551, Tokyo, Japan;*
**e-mail: fedor.shakhov@mail.ioffe.ru*

Some widely used electrical and heat conductors such as copper and silver are the materials with low wear resistance and the enforcement of their abrasion resistance is the task which may be successfully solved by using the detonation nanodiamonds (DND). A series of copper composites with the inclusions of 0 wt.% DND was prepared at HPHT conditions (P~7 GPa, T=1100-1900°C, t=60 s).

The composites were studied by means of magnetic susceptibility (MS) method in the temperature range 2-300 K. The MS of all the samples follows well to the Curie-Weiss low in the temperature range below 100 K. The Curie-Weiss term in the MS is related with the presence of paramagnetic spins (S=1/2) or unpaired free radicals locating in the DND particles and not in the host copper matrix. Recently we found that these paramagnetic spins (S=1/2) are originated from the own point-like defects of diamond lattice which are located within thin (~1.5 nm) undersurface layer of DND particles with mean size ~5 nm [1]. The concentration of localized spins in a diamond phase of synthesized composites is about $5.4\text{-}6.0\times10^{19}$ g^{-1}, which is a little bit lower than that one in pristine DND in the powder form ($\sim6.3\times10^{19}$ g^{-1}). The increasing the temperature of HPHT synthesis from 1100°C to 1700°C does not practically affect on the concentration of unpaired radicals in DND phase although the subtle reducing of this value with raising the synthesis temperature is clearly seen. These results mean that during rapid HPHT synthesis of Cu/DND composites DND particles inside the matrix do not subjected to the intensive graphitization process and their crystalline cores are well conserved and unconventionally stable in a melted copper. Such stability can be easy understood taking in mind the facts that copper does not create compounds with external carbon atoms of DND and own defects of DND are not so movable at short time of HPHT synthesis. From the other hand the obtained results mean that own paramagnetic radicals of DND particles can serve as an unconventionally stable spin markers for some special tasks related with identification of objects with inclusions of detonation nanodiamonds.

This study was supported by the RFBR grant 09-08-01200-a and by the Ministry of Education and Science of the Russian Federation contract 16.740.11.0216.

[1] A.I. Shames, V.Yu. Osipov, A.E. Aleksenskiy, E. Ōsawa, A.Ya. Vul'. *Diamond Relat. Mater.* **20** (2011) 318.

High thermal conductivity diamond-copper composites

Shakhov F.M.[1], Kidalov S.V.[1]*, AbyzovA.M.[2]

[1]*Ioffe Physical-Technical Institute, 194021, Saint-Petersburg, Russia*
[2]*Saint-Petersburg State Institute of Technology, 190013, Saint-Petersburg, Russia*
**e-mail: kidalov@mail.ioffe.ru*

A composite material with high thermal conductivity of 600-900 W/(m K), as well as a process for fabricating a composite material is developed [1].

Diamond-copper composites are obtained from monodisperse fillers having the following characteristics:
- thermal conductivity is up to 800-900 W/(m*K) for diamond particles of 200-400 mkm size;
- diamond volume fraction ~62 %;
- composite density ~5,5 g/cm^3;
- coefficient of thermal expansion 5 ppm/K at 20°C and 8 ppm/K at 200°C;
- longitudinal speed of sound ~9 km/s;
- Young modulus ~300 GPa;
- specific electrical resistivity 5-10 mkΩ cm.

For comparison, the thermal conductivity of copper is 390 W/(m K). In regard to their characteristics the obtained materials do not inferior to or superior the diamond-metal composites fabricated by all other known means (pressure-assisted infiltration of copper alloys containing carbide-forming additives; sintering with copper or infiltration at high pressures more than 1 GPa).

The diamond-copper composite material is made by a method of capillary (spontaneous) infiltration of copper melt in a bed of diamond particles with preliminary applied coating of carbide-forming metal. The coating thickness is about 100-300 nm. Raw materials are available (powders of synthetic diamond and copper, alloys are not used). The infiltration is carried during short time (several minutes) and the process has almost no restrictions as to the form and sizes of product items. The products can be manufactured in final or close to the final form and can have cavities, ledges and through apertures in them. The product material can be easily jointed to other constructive elements by means of soldering.

The proposed composite material can be used in heat exchangers, heat sinks, heat spreaders for semiconductor and vacuum electronic devices, in high-heat-flux systems, for example, in synchrotron radiation sources, elementary particles accelerators and nuclear fusion reactors, etc.

This study was supported by the RFBR grant 09-08-01200-a and by the Ministry of Education and Science of the Russian Federation contract 16.740.11.0216.

[1] A.M. Abyzov, S.V. Kidalov, F.M. Shakhov. *J. Mater. Sci.* **46**, 1424 (2011).

Investigation of nanostructured particles obtained from sintered nanodiamonds

Vitiaz D.A.[1], Senyut V.T.*[2], Markova L.V.[3]

[1]*Presidium of the National Academy of Sciences of Belarus, 220072, Minsk, Belarus*
[2]*The Joint Institute of Mechanical Engineering of NAS of Belarus, 22072, Minsk, Belarus*
[3]*The Powder Metallurgy Institute of NAS of Belarus, 220600, Minsk, Belarus*
**e-mail: vsenyut@tut.by*

Research of the phase transformations occurring in nanodiamond cluster under the influence of high-temperature annealing in various atmospheres have shown, that the sequence of structural transformations takes place: nanodiamond - onion-like form of carbon - nanographite. It is essential, that if at annealing in inert atmosphere the relation sp^2/sp^3 - hybridized carbon grows, that is the share of a graphite phase increases, on the contrary, at annealing in hydrogen atmosphere there is an interval of temperatures in which the share of sp^3 - hybridized carbon grows [1]. In hydrogen atmosphere in some interval of temperatures transition from the onion-like form of carbon in diamond can be observed.

Therefore for increase in the output of a diamond phase and improvement of sintering quality it is expedient to carry out preliminary modifying of initial nanodiamond's powders before compaction.

Object of research in this work were both nanodiamonds and diamond-containing mixture of detonation synthesis manufactured by Joint-Stock company "Sinta" (Minsk) after annealing in various conditions (hydrocarbonateous, reducing atmospheres, vacuum) and sintering at pressures of 1-3 GPa in the temperature range of 1200-2000°C. The purpose of the work is to research the influence of annealing, temperature and pressure on structure and phase composition of the particles obtained both from nanodiamond and detonation diamond-containing mixture.

The carried out research of phase structure of milled compacts, obtained after various modes of annealing and sintering of nanodiamonds and diamond-containing mixture, has shown, that the basic phase for samples, sintered under pressure after annealing in reducing atmosphere is graphite with various degree of perfection. Research of phase structure of the powders subjected to the vacuum thermal treatment, has shown, that the basic crystal phase is diamond, instead of graphite, as by other modes of sintering. The content of a diamond phase over 50 % is revealed in the samples obtained after annealing in vacuum, hydrocarbonateous atmosphere and sintering under pressure.

[1] Vul A.Ya. Detonation nanodiamonds. Structure, phase transition and applications // VIII Int. Conf. "Hydrogen Materials Science and Chemistry of carbon Nanomaterials". Sudak, Ukraine.-Kiev.-P. 506. (2003).

Nucleation of CVD diamond particles and films on heat-treated polymers PHC and PNHC

Sedov V.S.*[1], Ralchenko V.G.[1], Sizov A.I.[2], Zvukova T.M.[2], Khomich A.A[1], Konov V.I.[1]

[1]*A.M. Prokhorov General Physics Institute RAS, 119991, Moscow, Russia*
[2]*Moscow State University, Chemical Department, 119991, Moscow, Russia*
**e-mail: sedovvadim@yandex.ru*

Formation of nucleation centers (seeding) on the substrate is a necessary step for CVD diamond growth, detonation nanodiamond particles commonly used now for this purpose. Here we report on alternative approach for the seeding that is based on heat treatment of a specific polymer layer, rich in sp^3 bonds, to produce nanodiamond particles (along with other carbonaceous species) [1,2], which serve further for diamond film nucleation.

Two types of polymers, poly(hydrocarbine) (PHC) and poly-(naphthylhydrocarbine) (PNHC), used as precursors, were spun-off on silicon substrates, and annealed at temperatures up to 700°C for 2 hours in Ar atmosphere to form diamond nuclei. Then the diamond films were deposited in a microwave plasma CVD system UPSA-100 (2.45 GHz) in the H_2/CH_4 gas mixtures for time intervals from 1 minute to 2 hours. Either isolated CVD diamond particles or continuous films were grown depending on deposition conditions.

Analysis of the samples before and after CVD process was performed with SEM and Raman spectroscopy (488 nm wavelength excitation). While only sp2-bonded carbon could be revealed in the annealed polymer products, diamond structure (with narrow Raman peak at 1333 cm^{-1}) was definitely was detected in the films just after first minutes of CVD process, confirming the presence of diamond nucleation sites with submicrometer dimensions in the polymer. The results of selective etching of graphite-like component from the polymers by oxidation and hydrogen plasma treatment to enrich the nucleation layer with diamond phase will also be reported. We believe that the use of the polymer precursors for seeding is especially helpful in case of porous substrates, e.g. zeolites, opals or nanoporous semiconductors.

The work was supported by RFBR grant No. 10-03-00943.

[1] Bianconi P.A., Joray S.J., Aldrich B.L., Sumranjit J., Duffy D.D., Long D.P., Lazorcik J.L., Raboin L., Keams J.K., Smulligan S.L., Babyak J.M., *J. Am. Chem. Soc.* **126**, 3191 (2004).

Catalytic activity of nanodiamonds in redox process

Rozhkova N.N.[1]*, Gorlenko L.E.[2], Yemelyanova G.I.[2], Ōsawa E[3]., Lunin V.V.[2]

[1]*Institute of Geology, Karelian Research Centre, RAS, 185910 Petrozavodsk, Russia*
[2]*Department of Chemistry, Moscow State University, 119991 Moscow, Russia*
[3]*NanoCarbon Research Institute, Asama Research Extension Centre, Shinshu University, 3-15-1 Tokita, Ueda, Nagano 386-8567, Japan*
**e-mail: rozhkova@krc.karelia.ru*

Detonation ultradisperse diamonds (UDD) are already offered on the market, but its properties and chemical composition vary with production conditions and degree of purification. The presence of catalytically active metals in UDD suggests that they could be regarded as ready-made nanostructured metallic catalysts on carbon carriers. Its catalytic activity in reaction of ozone decomposition was studied on UDD offered by various manufacturers: UDD-1 - Gansu Goldstone Nano-Material Co., Ltd., China; UDD-2 NanoCarbon Research Institute Ltd., Japan; UDD-3 Real-Dzerzhinsk, Russia; UDD-4 Tekhnolog FSUP SKTB, Russia. All of them, except UDD-1, are similar in elemental composition (carbon content 78.4 to 87.5%), and their H/C values 0.022-0.027, typical of a diamond phase (sp^3). Similar adsorptive characteristics are shown by UDD-2 and UDD-3. The average pore volume is 0.5-0.6 cm^3/g. The average pore radius is 3.4-3.8 nm. UDD-4 has a wider pore size distribution spectrum, and its volume and average radius are 2.5 times as large. The micropore radii, 3.4±0.1 nm, calculated from the Dubinin-Radushkevich equation, are characteristically identical [1].

The specific surface and volume of pores are observed to change slightly during ozonation, whereas the average radius of micropores remains constant and does not depend on the method of synthesis and the UDD purification details.

A high catalytic activity and stability of UDD in a low temperature ozone decomposition reaction could be extended to other redox processes. The catalytic activity depends on metal impurities content and particle size: it decreases by two orders of magnitude if the average particle size is > 200 nm.

The work was supported by Basic Research Program, RAS, Earth Sciences Section-5

[1] Rozhkova, N.N., Gorlenko, L.E., Emelyanova, G.I. Jankowska A., Korobov M.V., Lunin V.V., Osawa E., *Pure Appl. Chem.* **81**(11), 2093 (2009).

Use of mechanical alloying for production of MMC with nanodiamond reinforcements

Popov V.A.[1]*, Chernov B.B.[2], Nugmanov A.M.[2], Shchetinina G.P.[2]

[1]*MISIS, 119049, Moscow, Russia*
[2]*Adm. G.I. Nevelskoy Maritime State University, 690059 Vladivostok, Russia*
**e-mail: popov58r@inbox.ru*

MMC were produced by mechanical alloying of the components to obtain composite granules followed by their consolidation into a compact material. Commercially pure copper and nickel, as well as aluminium alloys, were used for the matrix. The content of the ND fraction was varied from 5 up to 40 vol.%. Mechanical alloying was performed in planetary mills with balls and quasicylindrical milling bodies as process tools.

The composite materials with an increased concentration of nanodiamond reinforcing particles feature an increased air oxidation after a small treatment time. This effect is found for all matrix materials studied, i.e., for aluminium, nickel, and copper. The emergence of cuprous oxide in granules with ND content greater than 20% is confirmed by the X-ray diffraction method. However, increased oxidation is observed only for clusters of crushed, separate, and partially matrix-bound ND particles. After a prolonged treatment in a planetary mill, which leads to an even distribution of nanoparticles in the matrix and to the absence of free particles on the surface of granules, the effect is much smaller or almost absent. Conditions are determined for the effect of the treatment regimes on the uniform distribution of reinforcing ND particles in the copper matrix for different milling tools.

It is known that copper oxides, especially copper(I) oxide, are the most efficient materials for protection from biofouling. That is why formation of copper oxides (including the large volume fraction of copper(I) oxide) on the surface of the copper matrix composites with large ND volume fraction suggests them to be suitable for biofouling protection systems of marine facilities. This material can be used in the form of granules after mechanical alloying, as a component of paints, lacquers, and polymer coatings; as a component of bulky composite materials (e.g., additives to concretes); and, after compaction, for articles operated in water but carrying no large loads. Three specimens were kept for 100 days in marine water during the summer season to determine the efficiency of using the developed material in biofouling protection systems of marine falicities: (1) the control specimen without protection; (2) a plate from chlorinated polyvinyl chloride resin CPVC+40% copper(I) oxide composite coated with standard antifouling paint; and (3) a specimen from the developed Cu+25%ND composite. The study shows the absence of biofouling on specimens 2 and 3; on the control specimen, the biofouling is 0.52 g/cm^2 per year.

An investigation of nanodiamond and carbon onion structures by UNR-TEM methods

Popov V.A.[1]*, Egorov A.V.[2], Savilov S.V.[2], Lunin V.V.[2], Khodos I.I.[3]

[1]*MISIS, 119049, Moscow, Russia*
[2]*M.V.Lomonosov MSU, 119991, Moscow, Russia*
[3]*IMT RAS, 142432, Chernogolovka, Russia*
**e-mail: popov58@inbox.ru*

Transformation processes in a isolated diamond nanoparticles under vacuum annealing were studied by combination of UHR-TEM method and nanodiffraction. Initially, part of diamonds were combined in agglomerates, consist of several blocks, others – were monocrystalline. It should be noted the latter predominated in initial detonation synthesis diamond particles. Still, a significant part of particles contained various defects of crystalline structure: twins with {111} twining plane; large-angle boundaries both with various twins and in between blocks, etc. Only the reflexes corresponded to one crystalline zone existed on the nanodiffraction patterns of the monocrystalline initial particles. After the annealing at 1000°C, three types of nanoparticles were observed on the surface of agglomerates: (1) diamond nanoparticles shaped similar to the initial state; (2) totally transformed onion-like carbon nanoparticles (carbon onions); and (3) unidentified owing to a poor contrast nanoparticles. It should be noted that on the surface of nanodiamond particles after small annealing many investigators observed layers often called as graphite-like. However, nanodiffraction patterns of such particles show that these layers should be assigned to the amorphous state, because reflexes corresponding to the crystalline phase do not appear. The nanodiffraction pattern of carbon onion consists of broadened rings, corresponded to graphite. No individual reflexes, which implies the complete transformation of the nanoparticles, were observed. Nanodiffraction patterns of unidentified nanoparticles were represented by many individual reflexes that fill with some density the diffraction rings corresponding to diamond. This fact allows to suggest that the monocrystalline structure breaks down into numerous fragments of extremely small size. That is why the crystal lattice does not resolve and the shape of the nanoparticle resembles an amorphous state. In the literature, such a state is often called “amorphous diamond”. In the transformation process, this state might be intermediate. In further transformation, the amount of amorphous diamond fraction goes down, while a graphite-like component increases. Thus, the diamond structure undergo the transformed into a graphite-like. The process is violent, and it is extremely difficult to observe nanoparticles simultaneously containing the graphite-like and diamond structures. Still, on large-size nanoparticles it is sometimes possible to register the residual part of the diamond constituent.

Treatment of detonation diamonds by metalcontained plasma of high frequency arc discharge and their properties

Kolonenko A.L.[1,2], Osipova I.V.[1], Vnukova N.G.[1,2], Tomashevich Ye.V.[3], Chiganov A.S.[2], Churilov G.N.*[1,2]

[1]*L.V. Kirensky Institute of Physics SB RAS, 660036, Krasnoyarsk, Russia*
[2]*Krasnoyarsk state pedagogical university, 660049, Krasnoyarsk, Russia*
[3]*Institute of Chemistry and Chemical Technology SB RAS, 660049, Krasnoyarsk, Russia*
**e-mail: Churilov@iph.krasn.ru*

Detonation diamonds have stable cover usually. This cover contained carbon and prevented from their using.

In this work the results of ultradispersed diamonds investigation after plasma treatment were presented. For arc plasma generation we developed the setup on the base of fourstreams high frequency plasmatron placed on the leakproof cell. Four plasma streams formed plasma cone. Ultradispersed diamond fed into plasma along the cone axis with the flow of inert gas. Initial ultradispersed diamond passed into metal cover diamond with 100% conversion.

Investigations by X-ray powder diffraction (see Fig.), XPS and Raman spectroscopy have shown that ultradispersed diamonds covered by thin layer of copper and its oxides. The presence of copper oxides connected with insufficient purity of using gases. Also we plan to present the investigation results of ultradispersed diamonds covered by palladium and nickel.

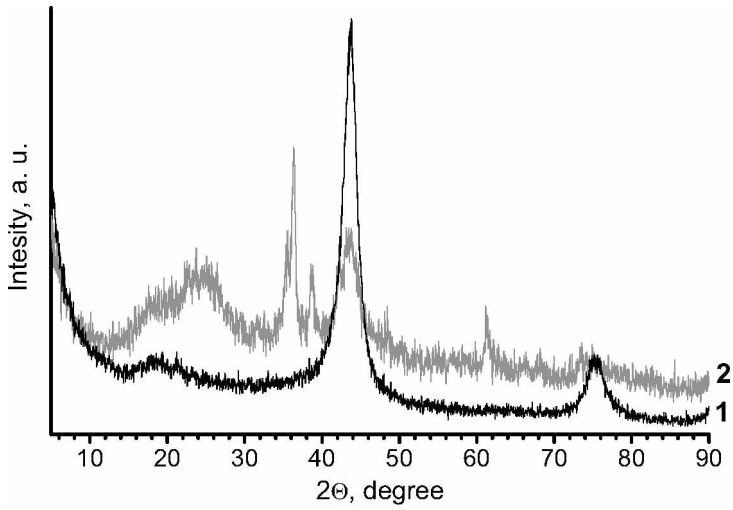

X-ray powder diffraction patterns of (1) initial ultradispersed diamonds before and (2) after treatment of plasma contained copper.

Synthesis and electronic structure of surface of CVD diamond films

Okotrub A.V.*, Polyakov O.V., Asanov I.P., Bulusheva L.G.

Nikolaev Institute of Inorganic Chemistry SB RAS, 6303090, Novosibirsk, Russia
**e-mail: spectrum@niic.nsc.ru*

The surface structure of diamond nanoparticles and films arouse an active interest, since just the chemical functionalizing of diamond surface exerts influence upon physicochemical and electric properties of diamond material. The synthesis of diamond films was performed employing AX5250 microwave plasma reactor (5kW power, Seki Technotron, Japan). The growth rate was amounting to about 10 μm/h and acetone vapor was used as a reactant source of carbon. For monitoring the process of diamond film growth, substrate temperature was measured and plasma optical emission spectra were registered.

The best quality films have been obtained on polished silicon surface after preliminary sputtering the suspension of nanodiamonds using an aerographic spray method. The films obtained were characterized by the methods of Raman spectroscopy, IR absorption spectroscopy, etc. It was revealed that varying the substrate temperature and the composition of the gas phase provides changing in the orientation of crystallites at the film surfaces as well as in the structure of surface layer.

CK-edge absorption spectra of diamond films have been measured at the Russian-German beamline of synchrotron radiation source BESSY-2. Simultaneously, measurements were performed within the framework of X-ray absorption spectroscopy with the use of internal photocurrent and Auger electron emission techniques. Thus, it could be possible to observe the difference between electronic structures of the surface layer 1 nm thick as well as that at the depth up to 100 nm. The features surface spectra indicate an increase in the contents of C-H of bonds and somewhat increase in sp^2 carbon fraction. The measurements of photoelectron valence band and C1s XPS spectra of the same samples allowed us to reveal the correlation between an increase in sp^3 C-H bonds and sp^2 carbon content. Comparing the spectra corresponding to different ratio between surface atoms existing in different electronic states, we have revealed the features of spectra related to precisely these conditions. Cluster approximation quantum-chemical calculations have been performed in order to interpret the spectra measured.

Nanodiamond influence on a microstructure of galvanic nickel coatings

Mordvinova L.E.*[1], Chiganova G.A.[1,2]

[1]*Siberian Federal University, 660074, Krasnoyarsk, Russia*
[2]*Krasnoyarsk Scientific Center RAS SB, 660036, Krasnoyarsk, Russia*
**e-mail: mellody86@yandex.ru*

Detonation synthesis nanodiamonds are common additives for metal-diamond galvanic coatings. Introduction of nanodiamonds in the electrolyte allows to obtain coatings with more fine-grained structure, which improves their quality. Surface modification of nanodiamonds with multivalent metal salts leads to additional increase of their application effectiveness in galvanic technologies.

Galvanic nickel coatings are widely used. Layers of galvanic nickel coatings to increase lifespan and improve the quality of stamping and pressing tools, parts of friction etc.

On photomicrographs (scanning electron microscope Hitachi TM-1000), we obtained samples of nickel coatings, coatings with nanodiamond and with modified nanodiamonds (modifier nickel chloride) was established reducing number-average radius of nickel coating grains from 0.83 to 0.74 micrometers with introduction of nanodiamonds, nanodiamonds surface modification leads to its reduction up to 0.66 micrometers.

On a powder diffractometer Bruker D8 Advance X-ray investigation of coating samples was carried out. Analysis of the diffraction patterns of all samples showed that intense reflection (200) is the most for the nickel coatings and coatings with nanodiamonds, reflection (111) for coatings with modified nanodiamonds. Experimental and literature data allows to suggest that as a result of the introduction of modified nanodiamonds in the coating is implemented high content of solid solution in the nickel matrix, as compared with unmodified nanodiamonds.

The lattice parameter, calculated by extrapolating of dependence of a from $\cos^2\theta/\sin\theta$ to $\theta = 90°$, was 0.35023, 0.35111 and 0.35136 nm, respectively, for nickel coatings, coatings with nanodiamonds and with the modified nanodiamonds. Calculated by the Debye-Scherrer for coherent scattering region also have the lowest value for the coating with the modified nanodiamonds (for (111) reflection is 14.5 ± 0.7 nm).

Coating with the modified nanodiamonds are also characterized by increase in microstrain lattice. Collection of X-ray structural analysis data about the effect of nanodiamond surface modification on the microstructure of obtained coatings allows to explain increase of nickel coatings microhardness with modified nanodiamonds.

Calculation of the electron effective mass in a nanodiamond-metal composite

Meylakhs A.P.[1,2], Eidelman E.D.[*1,3]

[1]*Ioffe Institute, 194021, St. Petersburg, Russia;*[2]*SPbSPU, 195251, St. Petersburg, Russia*
[3]*Saint-Petersburg Chemical-Pharmaceutical Academy, 197376, St. Petersburg, Russia*
**e-mail: eidelman@mail.ioffe.ru*

Under investigation is a material in which the diamond nanoparticles are immersed in the metal. The effective mass of electron m of such materials is essentially depends on sizes and mutual location of the differently conducting regions. In order to understand in workmanlike manner the available regularities, it is solved the problem with a periodic structure. Diamond nanoparticles will be considered to be the same size d and immersed in the metal at the same distances L. Nanoparticles make up a cubic lattice.

Calculation is made by the well known kp-method. Diamond nanoparticles influence on m is introduced by the local electron-phonon interaction potential in form of Gaussian function with maximum value U0~0,1eV [1]. The Schrödinger equation with corresponding potential is solved by means of the Fourier transformation, which gives the system of linear equations. So received Wave functions, received in that way, are used for calculation of effective mass [2].

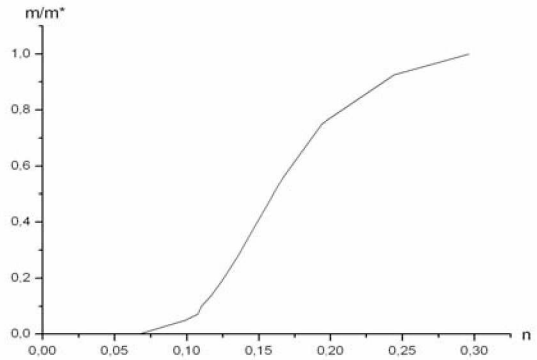

The dependence of inverse effective mass on the concentration is shown on the diagram. This diagram shows that in the area of applicability of the theory effective electron mass increases with increasing concentration of diamond nanoparticles and therefore, for example, the electrical conduction of the nanodiamond-metal composite is changed non monotonically. Experimental detection of this effect would confirm the correctness of the choice of such a potential of electron-phonon interaction. Of course, in a real sample effect will be less expressed because of the disorder.

Authors are grateful to Reich K.V. for discussion and Vul A.Y. for attention to this paper. This paper is made under support of RFBR (grant 09-08-01200-a and grant 11-02-01029-a).

[1] Reich KV, Eidelman ED. *Physics of the Solid State* **53**(9), (in press) (2011).
[2] Anselm A. Introduction to Semiconductor Theory (Translated from Russian by MM Samokhvalov), *Englewood Clifs*, N.Y. 2008 (Ch.4).

Diamond and nanodiamond new obtaining method in its metastable region: autoepitaxial growth from liquid carbon

Lysenko I.Yu.[1], Basharin A.Yu.*[1], Spitsyn B.V.[2]

[1]*Joint Institute for High Temperatures RAS, 125412, Moscow, Russia*
[2]*Frumkin Institute of Physical Chemistry and Electrochemistry, 199911, Moscow, Russia*
**e-mail: ayb@iht.mpei.ac.ru*

The possibility of diamond and nanodiamond epitaxial growth on the diamond substrate from the liquid carbon in the isobaric gas-static conditions with 30 MPa pressure has been experimentally demonstrated for the first time. Liquid carbon was obtained as the result of the laser melting of the microdisperse graphite islands held by the adhesive on the substrate - the edge of natural diamond crystal. The diamond original surface was formed by pyramidal growth hillocks, with steps oriented along the edges of the octahedron (111), as well as the tetrahedral cavities – trigons. Trigons are known to be strictly oriented in the direction opposite to the octahedron edge and are formed as the result of the peculiar growth discordance. Remelted island surface is the well known cobble structure [1] consisting of graphite densely packed hexagonal crystals and strikingly different from the flaky structure of the islands before melting. In the solidified carbon from the contact area of the liquid carbon and the substrate transparent crystal particles and films were detected, protruding above the original diamond.

The surface of the particles also had the form of "cobble" due to the different types of instabilities in the growth process, but the "cobbles" was the flattened octahedral-faceted crystals having the characteristic lateral dimension of about 100 nm and thickness 100-200 nm. Raman spectrum of the particles contains diamond narrow line 1332 cm^{-1}, as well as graphite lines: *D*-line (1349 cm^{-1}) and shifted to the 1589 cm^{-1} *G*-line with intensity ratio $k = I_D/I_G \approx 0.8$. The *G*-line shift and the value of *k*, however, correspond to the strongly disordered nanographite with crystallite size ~ 5 nm [2]. Therefore, the particles are characterized by the line 1332 cm^{-1} and have the diamond structure. Orientation of the particles on the diamond substrate surface was similar to the trigon orientation, that indicates the autoepitaxial growth character.

The transparent films have a thickness of 10-20 nm. Nanodiamond structure was identified by the Raman line 1320 cm^{-1} and *G*-line shift to the 1576 cm^{-1}.

[1] Kawasaki M, Onuma K., Sunagawa I., *J. Crystal Growth* **285**, 188 (2003).
[2] Ferrari A.C., Robertson J., *Phys. Rev. B,* **61**, 14095 (2000).

Electronic and elastic properties of diamond films with nanometer thickness

Sorokin P.V.*[1], Chernozatonskii L.A.[2], Avramov P.V.[3], Kvashnin A.G.[1,4]

[1]*Technological Institute for Superhard and Novel Carbon Materials, 142190 Troitsk, Moscow region, Russia*
[2]*Emanuel Institute of Biochemical Physics, Russian Academy of Sciences, Moscow, 119334, Russia*
[3]*Advanced Science Research Center, Japan Atomic Energy Agency, Tokai, Ibaraki319-1195, Japan*
[4]*Moscow Institute of Physics and Technology (State University), Dolgoprudny, Moscow region, 141700, Russia*
**e-mail: PBSorokin@gmail.com*

The graphene as two-dimensional material has attracted attention from the scientific community long before experimental fabrication. The first theoretical study of graphene is dated 1946, when the remarkable band structure of "Dirac cones" has been studied. First experimental observation of free standing graphene in 2004 [1] initiated the comprehensive study of this material.

Hydrogenation of graphene enlarges its potential application in nanoelectronics. Regular adsorption of hydrogen atoms changes graphene electronic structure and opens the band gap depending upon the distance between hydrogen regions. Total hydrogenation of graphene changes the nature of electronic states due to changing of sp^2 hybridization of C-C bonds to sp^3 one and opens the dielectric band gap. Such two-dimensional insulator was called as graphane. Graphane is an offspring of graphene along with graphene nanoribbons and carbon nanotubes. The other type of carbon bonding opens a new way for developing of two-dimensional carbon based materials.

Graphane is the first member in a series of sp^3 bonded diamond films with nanometer thickness (or diamanes) consist of a number of adjusted $\langle 111 \rangle$ oriented layers which display unique physical properties. The consequent study of graphene, graphane and proposed diamanes can be considered as bottom-up nanotechnological approach opposite to ordinary top-down paradigm. The main goal of this work is to study diamane physical properties. We consider diamanes with different thickness; we investigate their stability and compare them with known data for sp^3-hybridized hydrocarbon clusters. We study the elastic properties of the structures and obtain phonon dispersion, wave velocities and elastic constants. Finally we discuss possible ways to synthesize the structures.

[1] K.S. Novoselov, D. Jiang, F. Schedin, T.J. Booth, V.V. Khotkevich, S,V, Morozov, A.K. Geim, *Proc. Natl. Acad. Sci. USA* **102**, 10451 (2005).

Effect of detonation nanodiamond surface chemistry on its catalytic properties

Kulakova I.I.*, Tveritinova E.A., Zitnev Yu.N., Lunin V.V.

Lomonosov Moscow State University, Chemical Department 119991, Moscow, Russia
**e-mail : kulakova@petrol.chem.msu.ru*

Carbon materials used in catalysis, have usually graphite structure. Most often they are used as the supports of the active phase. Many researchers believe that the structure features formed by sp^2-carbon atoms contributes to the manifestation of their own catalytic activity. Indeed, in recent years the catalytic activity of various forms of nanocarbon (eg carbon nanotubes) has been identified and it has been found that the expression of the catalytic properties of such nanocarbon is due to the presence of certain functional groups on its surface [1].

Diamond materials with different structure, were not practically used in the catalysis before the appearance of detonation nanodiamond (ND). Data of the catalytic activity of the latter is extremely scarce. Chemical state of ND surface, as well as other carbonaceous materials, is determined by the conditions of their pre-treatment (modification) [2].

The aim of this study is to determine whether ND it has the catalytic activity and how the gas-phase pre-processing conditions will affect it. We chose a model reaction – the conversion of alcohols – to test of ND catalytic activity. The study was performed by the set of physicochemical methods: the pulse mikrocatalytic method, electron microscopy, optical (IR) and electron spectroscopy, elemental analysis.

We obtained data of ND catalytic activity in C_2-C_3 alcohols conversion, the products ratio through the dehydrogenation and dehydration as well as the effect on these parameters of pre-treatment conditions of ND and of alcohol nature (see, for example, the Figure at 330°C).

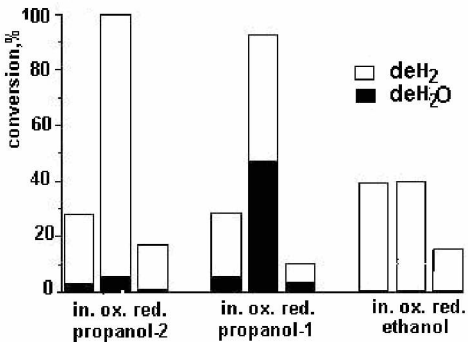

Thus, it was found that ND shows a significant catalytic activity and selectivity in conversion of alcohols. At the same air treatment (400°C, 5 h) increases its activity, whereas the hydrogen treatment (800°C, 5 h) reduces it.

[1] Figueiredo J.L., Pereira M.F.R., *Catalysis Today* **150**, 2 (2010).
[2] KulakovaI.I, Korol'kov V.V., Yakovlev R.Yu., Lisichkin G.V., *Nanotechnologies in Russia* **5**, 474 (2010).

The effect of filler surface chemistry on the tribology properties of nanodiamond/polytetrafluroethylene composites

Koscheev A.P.*, Tereshenkov A.V., Petrovskaya A.V, Chukov N.A., Sadovskaya N.V., Perov A.A., Khatipov S.A.

Karpov Institute of Physical Chemistry, 105064, Moscow, Russia
**e-mail: koscheev@nifhi.ru*

Detonation nanodiamond (DND) is very attractive nanoscale filler of polymers. The commercially available DND have quite different surface chemistry depending on the details of synthesis technology. The question of how the DND surface chemistry can affect the properties of polymer composites remains open.

We have studied the tribological behavior of polytetrafluoroethylene (PTFE) filled with DND of different types both in as received and chemically modified forms. The DND surface chemistry was characterized by IR-spectroscopy and thermodesoption mass spectrometry. DND(1-5%)/PTFE composites were prepared by mechanical mixing, compressing molding and sintering at 380°C. The composites samples were characterized by differential scanning calorimetry, scanning electron microscopy and wear/friction tests.

Experimental results showed that the wear rate reduction, caused by DND filler, depends strongly on the oxidation state of nanodiamond surface. The oxygenated groups at DND surface were found to influence the crystallinity of polymer matrix as well. These results indicate that DND particles in PTFE composites play not only the role of "mechanical" impurities but they also could interact chemically with PTFE matrix usually considered as "chemically inert". This suggestion was confirmed by the observed differences in mass spectrometric compositions of volatiles released during sintering of PTFE filled with DND of different surface chemistry (see Figure).

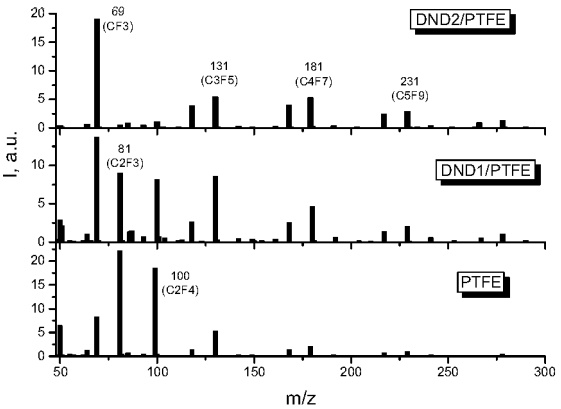

The obtained results give for the first time the evidences of: 1) the chemical interaction of DND filler with PTFE matrix during sintering procedure; 2) the dependence of this interaction on surface chemistry of DND; and 3) the influence of this interaction on the properties of DND/PTFE composites.

The authors acknowledge the support from the Russian Federal Agency for Science and Innovations (State Contract No. 02.523.12.3024).

Graphite diamond composites formed by a controlled oxidation of detonation blend

Korolev K.*[1], Makarov I.[1], Sustchev V.[1], Malygin A.[2], Marchukov V.[1]

[1]*FGUP «SCTB «Technolog», 192076, St. Petersburg, Russia*
[2]*SPbSTI (TU), 190013, St. Petersburg, Russia*
**e-mail: marvalal@mail.ru*

The most of publications describing research of detonation nanodiamonds (DND) are devoted either to pristine detonation blend (DB) or to the high purity DND. The latter is notable for the lack of graphite-like structural systems included.

However the intermediate products contained both the diamond-like fragments and the graphite-like ones may be the subject-matter, too. But, to meet such a challenge it is necessary to create convenient obtaining methods of the products with replicable features.

Special research of oxidation DB in water solutions of dilute nitric acid (5-50% weight) has been undertaken to that end. The amount of nitric acid used was not sufficient for the complete destructive oxidation of the «graphitic» component. The oxidizing process has been carried out in an autoclave at the temperature 150-250°C to achieve the maximal efficacy. Oxidation could be stopped at any desirable stage.

In this way specimens with various ratios of diamond and graphitic structures were produced and tested. The results obtained let us to analyze the behavior of nanodiamond products as a function of the oxidation extent (OE). It is remarkable to see substantial extremuma of a number of character properties depended on the OE. The properties are the ones to be of practical interest and their extreme values have a significant difference from that of the same properties of initial DB and high purity DND.

The authors explain these facts by particular principles of a functional group formation on «graphitic» areas of the nanoparticles. There are all reasons for selection of partial oxidized intermediate products as a particular class of graphite-diamond nanocomposite materials (GDNM). The pilot plant for the production of DND and GDNM has already been created in SCTB «Technolog», St. Petersburg.

Experimental study of electric discharge treatment of nanodiamond particles in flow liquid

Medvedev D.*, Petyev V., Potapkin B., Sapunov D., Prikhodko K., Domantovsky A., Korobtsev S.

Russian Research Center "Kurchatov Institute", 123182, Moscow, Russia
**e-mail: dmit.medvedev@gmail.com*

Nanodiamonds as well as their suspensions have been widely used for several decades in machinery as lubricants, additives to oil and galvanic electrolytes. But nowdays carbon nanodiamonds are believed to have even more profound practical applications in biology and other industries[1]. In present article electric discharge treatment of nanodiamond particles has been studied.

In liquid phase pulsed electric discharge in water flow in Venturi tube was used for nanodiamonds treatment and functionalization [2].

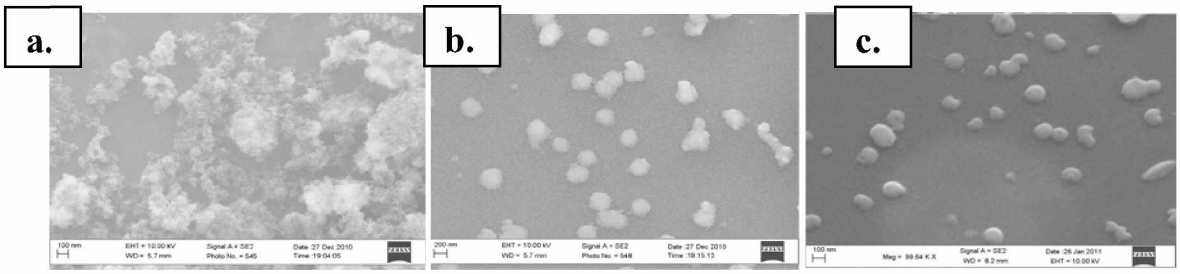

Nanodiamand powder structure modification after treatment in suspension in water by pulse electric discharge in water flow.
a. Before treatment- diamond crystals are completely covered by nondiamond carbon;
b. Initial treatment - diamond crystals conglomerates are separated from nondiamond carbon;
c. Final treatment - diamond primary crystals are completely escaped from conglomerates;

Ordered self-organizing cubic superlattice formed by diamond nanocrystals escaped and functionalized by electric discharge treatment have been observed. The effect of reversible stretching of cubic superlattice formed by diamond nanoparticles by Van der Waals forces caused by electric charging have been observed.

[1] K.B. Holt, *Philosophical Transactions of the Royal Society A* **365**, 2845 (2007).
[2] D. Medvedev, V. Petyaev, D. Sapunov, B. Potapkin, S. Korobtsev, Experimental study of electric discharge treatment of nanodiamond particles in liquid and gas phases, ISPlasma 2011, Nagoya , Japan, p. 211

Effect of detonation nanodiamond dopant on phase composition and strength of Portland cement materials

Korobkova A.I.*[1,2], Shilova O.A. [1], Frank-Kamenetskya O.V.[2]

[1]*Institute of Silicate Chemistry of RAS, 199034, St.Petersburg, Russia*
[2] *St.Petersburg State University, 199034, St.Petersburg, Russia*
**e-mail: korobulya@mail.ru*

Anhydrous Portland cement is essentially made of a synthetic rock, referred to as "clinker", which contains at least four major phases. Alite and belite are two calcium silicates, Ca_3SiO_5 (C_3S) and Ca_2SiO_4 (C_2S), respectively, with a few percent of impurities. Two calcium aluminate phases are also observed: $Ca_3Al_2O_6$ (C_3A) and $Ca_4(Al,Fe)_4O_{10}$ (C_4AF).

In the paper, the results of researching synthesized Portland cement materials based on the clinker from Suhologsky work doped detonation nanodiamond (DND) are presented.

As is known, there are a large number of active functional groups on the surface of DND, which additives are suggested to affect significantly on the features of cement materials properties. Also there was shown the addition of the DND in an amount of 0.1 wt.% increases the strength of cement materials [2].

There were two series of syntheses new materials doped DND (0; 0.1; 0.2; 0.5; 1 – 9 wt. %), distinguished by the absence ($1^{st.}$ series) or presence (2nd series) gypsum $CaSO_4*2H_2O$ addition in the amount of 5 wt. %. Phase composition was determined by X-Ray method (STOE STADI P powder diffractometer, transmission geometry, $Cuk_{\alpha 1}$=1.54056, 2θ=5-55°, $\Delta 2\theta$=0.02°, exposition 100 sec.) Besides, to identify features of DND particles distribution in hydrated samples light and scanning electron microscopy (Leica Microsystem CMS CmBh and Quanta 200 3D, respectively) were used. SEM research was carried out in reflected electrons (high vacuum, U=15-20kV, analyst S.J. Yanson).

Maximum strength of researching samples in $1^{st.}$ series of experiments is achieved at 0.1-0.5 and 4-5 wt.% DNA content with a large concentrations of calcium carbonates and portlandite $Ca(OH)_2$, which is a measure of hydration degree [2]. At higher contents of DND material becomes brittle and disintegrates. Gypsum addition alters the rate of hydration: there are a gradual increase of portlandite and calcium carbonates. Maximum strength in 2nd series is observed at 0.1 wt.% DND. The destruction of the material in investigative range isn't observed.

In general, the results had shown the addition of DND significantly affected on the phase composition and strength characteristics of Portland cement materials that is explained by the features of their hydration.

[1] Boikova A.I. et al, Alitinform: Cement. Concrete. Dry mixtures **8**(1) 37 (2009).
[2] Reichel W., Canrad D. Beton: in 2 B. B. 1. Eigenschaften Projektierung Prüfung.VEB Verlag für Bauwesen, Berlin, 1976.

Tailoring the electronic properties of CVD nanocrystalline diamond films by *in situ* nitrogen incorporation for selective electrochemical detection of neurotransmitters

Raina S.[1], Kang W.P.[2], Davidson J.L.[2], Huang J.H.[3]

[1]*Interdisciplinary Program in Materials Science,* [2]*Department of Electrical Engineering and Computer Science, Vanderbilt University, Nashville, TN, USA;* [3]*Dept. of Materials Science and Engineering, National Tsing Hua University, Taiwan*

CVD nanocrystalline diamond films are promising materials for field emission devices, microelectrodes, and NEMS applications due to the material properties such as chemically inert, mechanically hard, and biocompatible. We have reported on nanodiamond film for field emission devices [1] and chemical sensing [2]. In this work, we tailor the electronic properties of nanodiamond films by *in situ* nitrogen incorporation for selective electrochemical sensing of neurotransmitters.

Different nitrogen contents of nanodiamond films were grown in a microwave plasma enhanced CVD machine using $H_2/CH_4/N_2$ gases, keeping the H_2/CH_4 ratio (9:1) constant and increasing the N_2 flow rate for 15sccm, 30sccm, 60sccm and 90sccm labeled as film S0, S1, S2, and S3. SEM study shows complete and conformal nanodiamond coverage for all films with surface morphology changes from a distinct 'ridge'-like to a more 'cauliflower'-like nano-structures as the N_2 flow rates increased. XPS C1s spectra indicated presence of carbon-nitrogen bonding in addition to the sp^3 and sp^2 hybridized carbon-carbon bonds. The peaks fit at 284.6eV and 285.4eV, contributed by sp^2 C-C and sp^3 C-C hybrized bonds. The sp^3 peak intensity decreases (while the sp^2 increases) with increased N_2 flow rate. The peaks locate at 286.5eV and 287.5eV correspond to C-N and C_3N_4, respectively, and both of these peaks consistently increase in intensity with increased N_2 flow rate.

Cyclic voltammograms were used for characterizing the electrochemical and bio-sensing properties. The background scan at 100mV/s in 0.1M PBS at physiologic pH 7.4 revealed a working potential window of ~3.0 V for all the films. However, films S0 and S1 show distinctly different and better sensitivity for detection of dopamine as compared to S2 and S3. Films S0 and S1 showed very well defined redox peaks detectable due to dopamine/o-quinone redox reactions. Films S2 and S3 were also able to detect presence of dopamine but with poor peak definition and wide peak-peak separation, exhibiting sluggish reaction kinetics and the peak definition was completely lost at 1mM DA and at scan rates greater than 50mV/s. The findings demonstrate that a controlled amount of nitrogen incorporation in naodiamond film (S0 and S1) is vital to maintain superior bio-sensing behavior, however, higher N_2 inclusion (S2 and S3) degrades the sensing response due to change in surface morphology and increase in CN and C_3N_4 bonds.

In this work, we have successfully tailored the electronic properties of CVD nanodiamond films for selective detection of dopamine, serotonin, epinephrine, and acetylcholine independently, as well as in the presence of ascorbic acid and uric acid, without any surface modification, hence real-time detection with long-term stability and reliability.

[1] K. Subramanian, W.P. Kang, J.L. Davidson, *IEEE Electron Device Letters* **29**, 1259 (2008).

[2] S. Raina, W.P. Kang, J.L. Davidson, *Diam. and Rel. Mat.* **17**, 896 (2008).

Investigation on the microstructure and properties of composite nickel coatings with nanodiamond

Kaleicheva J.[1], Karaguiozova Z.*[2], Lyubchenko E.[3], Kandeva M.[1], Stavrev S.[2], Mishev V.[1]

[1]*Technical University of Sofia, 1000, Sofia, Bulgaria*
[2]*Space Research and Solar- Terrestrial Institute, Bulgarian Academy of Sciences, 1000, Sofia, Bulgaria*
[3]*National Technical University "Kharkov Polytechnical Institute", 61002, Kharkov, Ukraine*
**e-mail: zkaraguiozova@yahoo.com*

The work in this study is focused on investigation of composite nickel coatings. The coatings are deposited on ductile cast iron samples by electroless method EFTTOM NICKEL with addition of strengthened nanodiamond particles (2-4 nm) [1,2]. The ductile cast iron is of different composition. The samples are prepared by casting and austempering. The microstructure, microhardness and wear resistance of the coatings are investigated. The thickness of the coatings is also determined (8-10μm). Metallographic analyses, electronic microscopic analysis (SEM), microhardness measurements by Knoop Method, wear resistance tests are carried out. The coatings without heat treatment as well coatings with heat treatment at 290°C, 6 h are tested. Twice increase in microhardness value and improvement of the coating's properties of heat treated coatings is determined.

[1] Gavrilov, G. Electroless Nickel, Sofia, Bulgaria (1976).
[2] Karaguiozova, Z., Stavrev, S., Formation of nickel layer-covers on nanodiamond powder, Paper presented at the 8th International Workshop, Nanoscience & Nanotechnology, November 2006, Sofia, Bulgaria (2006).

Nanodiamond-based nanolubricant

Ivanov M.G.[1]*, Shenderova O.[2], Ivanov D.M.[1], Pavlyshko S.V.[3], Petrov I.[4], McGuire G.[2]

[1]*Ural Federal University, Yekaterinburg, Russia*
[2]*International Technology Center, Raleigh, USA*
[3]*Institute of Engineering, Science Ural Branch RAS, Yekaterinburg, Russia*
[4]*SKN, Snezinsk, Russia*
**e-mail: mig@mail.ustu.ru*

Recently, certain nanomaterials in powder and colloidal forms have emerged as potential anti-friction and wear additives to a variety of base lubricants. Highly purified detonation nanodiamonds (DND) with small aggregate sizes are a relatively new nanomaterial additive [1, 2]. In the current work, we report results of the comparative analysis of the colloidal stability and tribological performance of DND-based additives as well as other commercial additives based on detonation soot, boron nitride and PTFE particles, oil soluble molybdenum compounds and their combinations in PAO-6 and mineral engine oil 15W40 (API CF/CC).

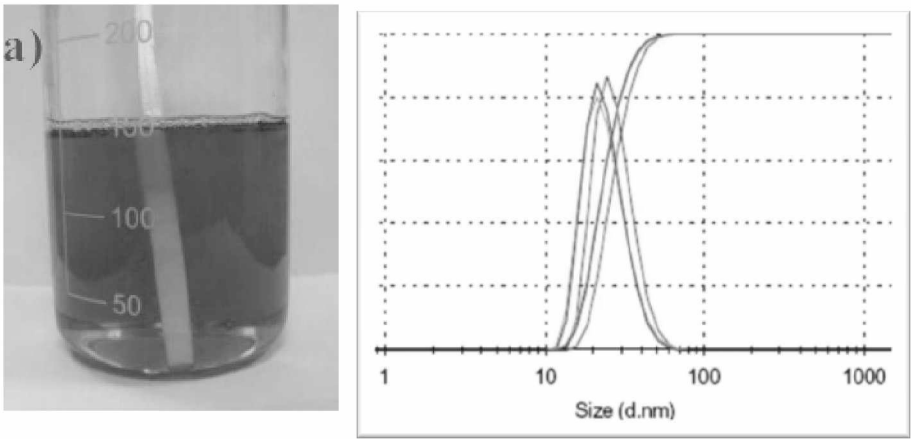

Figure 1. Photographs of colloidal suspension of 0.1% 10nm DND (10nm when dispersed in DI water) in PAO-6 oil (a) and volumetric size distribution of DND shown in PAO-6 oil (from [2]).

Testing has been performed on these formulations using ring-on-ring (friction coefficient) and four ball tests (extreme pressure (EP) failure load and diameter of wear spot). Effects of different parameters of the formulations on their tribological properties will be discussed.

[1] M.G. Ivanov, S.V. Pavlyshko, D.M. Ivanov, I. Petrov, G. McGuire, and O. Shenderova, *Mater. Res. Soc. Symp. Proc.* **1203**, 1203-J17-16 (2010).

[2] M.G. Ivanov, S.V. Pavlyshko, D.M. Ivanov, I. Petrov, and O. Shenderova, *JVST. B* **28**(4), 869 (2010).

Aerosol spraying of detonation nanodiamond for seeding and growth of transparent B-doped CVD nanodiamond films

Grudinkin S.A.*, Feoktistov N.A., Aleksenskii A.E., Vul' A.Ya., Golubev V.G.

Ioffe Physical-Technical Institute RAS, 194021, St.-Petersburg, Russia
**e-mail: grudink@gvg.ioffe.ru*

Transparent in ultraviolet (UV) region nanodiamond (ND) conducting films are necessary for creation of UV photoconverters and electroluminescent structures. In UV region it is necessary to be particularly attentive to receiving of smooth ND films to decrease the loss connected with light scattering by devices interfaces. For growth of smooth transparent diamond films you should create on the substrate a high density of diamond nucleation centers ($>10^{10}$ cm^{-2}). At present time the using of detonation nanodiamonds (DND) as nucleation centers for diamond films growth by the CVD deposition method is more widespread.

In this paper we report about development of new method of aerosol spraying of DND on silicon and quartz substrates with diameters less than 100 mm and receiving on them boron-doped ND films with surface roughness not exceeding 15 nm by the MWPECVD method. We investigated the change of transparency and conductivity of obtained films depending on boron concentration and on methane content in the methane-hydrogen gas.

During aerosol spraying we used a DND water suspension with average size of DND particle agglomerates about 40 nm, received by the additional treatment of industrial DND powder produced by SCTB «Technolog» (St.-Petersburg). We used diborane as a doping impurity in the MWPECVD process.

It is shown that by modifying of the DND deposition time and weight concentration in suspension over the range 0.001–1% you can change the DND agglomerates form and quantity per unit area of substrate surface from 10^8 to 10^{11} cm^{-2}. The optimization of MWPECVD conditions and the deposition of the DND nucleation layer with more amount of nucleation centers of diamond phase per unit area (10^{10}-10^{11} cm^{-2}) allowed us to receive a transparent in UV – visible region (T~50% at λ=300 nm) conducting (σ = 1–5 Ω^{-1} cm^{-1}) ND films on quartz substrates. The high content of diamond phase in these films was confirmed by the Raman spectroscopy method.

Synthesis, structure and magnetic properties of composite powders UDD/Ni-P and UDD/Co-P

Goncharova O.A.*[1], Chekanova L.A.[2], Iskhakov R.S.[2]

[1]*Siberian State Technological University, 660049, Krasnoyarsk, Russia*
[2]*L.V. Kirensky Institute of Physics SB, RAS, 660036, Krasnoyarsk, Russia*
**e-mail: log85@mail.ru*

A significant interest to composite powders is caused both by expectations to realize in compacted products a high level of physical and chemical properties (and consequently performance characteristics) and by structural features of this state, problems of it's technological realization. In resent years chemical methods have been developed for obtaining nanostructural composite powders widely used for catalysts, sorbates, medical filters, magnetic media production, drug targeting [1, 2].

Ultradispersed diamond (UDD) powders were obtained by explosive method. Coatings of Co-P or Ni-P alloy on UDD powders were prepared by a chemical deposition method from water solutions of Co or Ni salt. Sodium hypophosphite (NaH_2PO_2) was used as a reducing agent.

The structure and phase composition of the composite powders were studied by the X-ray diffraction method using CuKα radiation. The morphology of the particles was studied by scanning electron microscopy (see Figure 1). Magnetization versus field measurements were carried out by means of a vibrating sample magnetometer in external fields up to 14.5 kOe. Ferromagnetic resonance properties were measured using conventional spectrometer with working frequency 9.2 GHz.

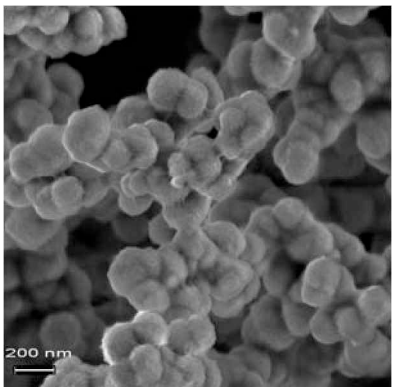

Figure 1. Scanning electron microscopy micrograph of composite powder UDD/Ni-P

[1] Han M., Ou Y., Deng L., *J. Magn. Magn. Matter.* **321**, 1125 (2009).
[2] Wu M., Zhangb Y.D., Huib S., Xiao T.D., Ge Sh., Hines W.A., Budnick J.I.б *J. Magn. Magn. Matter.* **268**, 20 (2004).

Quantum-chemical simulation of interaction of hydrogen atoms with diamond nanoclasters

Filicheva Yu.A.[1], Lvova N.A.*[1], Anan'ina O.Yu.[2]

[1]*Technological Institute for Superhard and Novel Carbon Materials, 142190, Troitsk, Moscow region, Russia*
[2]*Zaporizhzhya National University, 69600, Zaporizhzhya, Ukraine*
**e-mail: nlvova@ntcstm.troitsk.ru*

Hydrogen is one of the most important adsorbate which interacts with a diamond surface. Unique physical properties of the hydrogenated C(100) surface makes this material perspective for creation of nano- and microelectronic devices [1, 2]. Vacancies are the important surface defects influencing electric and optical properties. At formation of defect the process of the surface reconstruction, local regibridization of the electronic states, formation or break of bonds between superficial atoms may essentially influence energy characteristics and strongly complicate available models of hydrogen adsorption and desorption [3].

In this work using MNDO semiempirical method (Modified Neglect of Differential Overlap) and MOPAC program package calculations were carried out. Investigations of vacancy defect configurations on C(100)-2×1 surface at different hydrogen coverage are presented. Diamond nanoclasters $C_{63}H_{59}$ and $C_{126}H_{91}$ were used for C(100)-2×1 surface simulation. The potential primary adsorption centres of vacancy defect area and energy characteristics of adsorption - activation energy of chemisorption and C-H bond energy in mono- and dyhidride states have been defined. The analysis of molecular orbital compositions were carried out. Possible mechanisms of hydrogen desorption from mono- and dyhidride states in the defect are offered. The possibility of existence of two states of vacancy defect on a clean C(100)-2×1 surface with different geometry, electronic properties and energy of formation is discussed. It was found, that the activation barriers for hydrogen desorption from C(100) diamond surface containing the vacancy defect make values E_D =1,2÷4,3 eV, depending on the defect state and degree of surface hydrogenation.

However, full saturation by hydrogen of any of defect state leads to a uniform state in which carbon atoms occupy positions close to C(100)-1×1 surface.

[1] Ristein J., *Surface Science* **600**, 3677 (2006).
[2] Tachiki M., Kaibara Yu, Sumikawa Yu, Shigeno M., Kanazawa H., Banno T., Song K.S., Umesawa H., Kawarada H. *Surface Science* **581**, 207 (2005).
[3] Liu F.B., Wang J.D.,, Chen D.R., Liu B., *Solid State Phenomena* **121**, 1119 (2007).

Electrochemical silver-diamond coatings

Burkat G.K.[1], Dolmatov V.Yu.[1*], Myllymäki V.[2]

[1]*FGUP «Special design-engineering bureau «Technolog», 192076 Saint-Petersburg, Russia*
[2]*Carbodeon Ltd. Oy, Bulevardi 2 A, 00120 Helsinki, Finland*
**e-mail: DiamondCentre@mail.ru*

Main demerits of silver electrochemical coatings are low wear-resistance and high porosity.

The use of detonation nanodiamonds (DND) at deposition of silver coating from toxic cyanic electrolyte has been known [1]. In work [2] possibility of deposition of silver coating from ferricyanic and dicyanargentate electrolytes in the presence of DND has been described. At that, microhardness increased by 20-80% and wear-resistance had a 1.5-2.0-fold increase.

The present work is devoted to investigation of an influence of diamond-containing additives such as: DND modified with ammonia treatment at 230°C, initial diamond-containing blend (DB) and partly oxidized DB [3] on quality of the silver coatings obtained from low-toxic dicyanargentate- thiocyanate electrolyte with the following composition, g/l: Ag (calculating on a metal) – 25, K2CO3 – 25-30, KCNS – 150. Temperature – 20°C, current density – from 0.5 to 0.9 A/dm2, pH=10-11.

Kinetic studies showed that insertion of the additives into the electrolyte does not change known mechanism of deposition of silver, cathode process rate is limited by diffusion. The use of additives increases both electrolyte electroconductivity and throwing power. Specific electrical resistance of coatings does not practically increase.

In the presence of nanodiamond additives microhardness increases by 30-40% as compared with pure silver coatings (from 80 to 115 kg/mm2). As well microhardness rises as the current density is increased from 0.5 to 0.9 A/dm2. Nanodiamond additives appreciably decrease porosity of silver coatings (from 65 to 2-5 pores/cm2). At addition of 1 g/l DND or 1.5 g/l oxidized DB into electrolyte the porosity reduction is observed to be maximum (to 2 pores/cm2 at current density of 0.9 A/dm2). Wear-resistance of silver-diamond coatings increases ~5 times at 1 g/l DND or 1.5 g/l oxidized DB.

[1] USSR Inventor's Certificate No 1668490, C 25D 3/46, prior. 10.05.1989, *Bull.of Inventions*, **29**, 123 (1991)

[2] Patent application of Russia No 96104061, C 25D 3/46, prior. 16.03.1995, *Bull.of Inventions*, **12**(1), 67 (1998)

[3] Patent of Russia No 2046094, prior. 26.07.1995, *Bull.of Inventions*, **29**, c.189 (1995)

Chemical state of carbon atoms on nanodiamond surface: growth mechanism of detonation nanodiamond

Dementjev A.*, Maslakov K.

NRC "Kurchatov Institute", 123182, Moscow, Russia
**e-mail: demcarbon @yandex.ru*

Identification of intermediate and final products of a chemical reaction is a key factor in understanding its mechanism. In nanodiamonds the only possible practical way of studying the chemical reactions of carbon atoms is the after synthesis analysis. As a result the identification of different possible chemical states of carbon atoms (such as graphite, diamond, carbon nanotubes, fullerenes, onion-like and adventitious carbon) is required. X-ray photoelectron spectroscopy (XPS) (including electron energy loss at C1s and valence band spectra) and N(E) CKVV Auger spectroscopy are eminently suitable techniques for such an identification since they provide chemical information from the top 2–10 monolayers.

Nanodiamond samples were produced by ALIT (Kiev), SCINTA (Minsk) and Diamond Centre (Saint-Petersburg) and studied before and after chemical cleaning by XPS and Auger spectroscopy.

It was found that the chemical state of carbon atoms is the same before and after chemical cleaning and it can be described as carbon atoms being sp^3-bonded inside nanodiamond particles and having a new unique chemical state on the surfaces. The latter differs significantly from sp^2- and sp^3-bonded carbon and can be figured as the valence band near the Fermi level being occupied by three electrons.

We propose the following mechanism of nanodiamond growth:

1. Formation of CO_2, CO, N_2, NO_X-molecules and C-atoms in the gas phase as a result of the detonation;
2. Recombination of C atoms and NO_X-molecules with the formation of nanodiamond nuclei with the unique chemical state of carbon atoms on its surfaces;
3. Interaction of C atoms and NO_X-molecules with the surface of nanodiamond nuclei which leads to the growth of nanodiamond particles with the formation of sp^3-bonded carbon atoms inside particles but without changing of the chemical state of carbon atoms on their surfaces. The process lasts until no carbon atoms are available for further growth.

These results are contradictive to the generally accepted conception of chemical state of carbon atoms on the nanodiamond surface. The reason of such a contradiction is that XANES and EELS results which are widely used can't provide reliable information on the chemical state of carbon atoms on the surface of nanodiamond particles.

About creation of technology of "pure" synthesis of detonation nanodiamonds

Danilenko V.V.

Joint Stock Company "ALIT", Kiev, 03067, Ukraine
e-mail: vvdan@list.ru

Physical bases of nanodiamonds synthesis [1].

1. From comparison of the phase diagramme for nanocarbon with pressure and temperature of a detonation for alloys TNT/RDX follows that these parametres are in area of liquid sp3 nanocarbon ($p > 16.5$ GPa, above a line of threefold points) where nanodrops are formed and then crystallised at cooling by extending detonation products (DP) at $p < 16.5$ GPa, i.e. synthesis goes under the scheme gas - liquid - crystal. The temperature grows in a zone of chemical reaction of a detonation wave, therefore here carbon crystallisation is basically impossible.

2. Influence of the scale factor (weight of a charge and a cover) affects two competing processes – amorphization and crystallisation, and also nanoparticles interaction with formation of strong units. Depending on time these units transform from fractal structures to porous and non porous abrasive polycrystals. The great speed of interaction is caused by microturbulence in DP and small distances between nanodrops. Fast nanoparticles cooling in areas of liquid sp3 nanocarbon and nanodiamonds freezes growth of nanodrops and their crystallisation. Thus the volume of amorphous nanocarbon increases.

The ND output and their quality is also influenced by the form of a charge and its microstructure.

Manufacture condition for ND [2]. A potential market capacity of ND is really great. Nevertheless, the ND market is not created. The reasons are: small volume of detonation nanodiamonds (ND) is necessary for creation of optimum technology, high cost and low unstable ND quality.

Features of new technology of "pure" ND synthesis [2].

1. Explosions of charges in weight of 20 kg in the automated chamber with laser initiation of charges and protection of walls of the chamber against fast-flying ND particles. As a result ND doesn't have non carbon impurity, and the cost price of ND decreases in 4-5 times in comparison with use of charges in weight of 1 kg (for production 24 t/year).

2. The absence of metal impurity allows to refuse acid clearing, having replaced it with cheaper gas-phase oxidation of not diamond carbon. Such replacement reduces the cost price of ND even in ~ 3 times.

[1] V.V. Danilenko. EXPLOSION: physics, engineering, technology. M. Energoatomizdat, 2010, 784 p., chapter 16.

[2] V.V. Danilenko. *Superhard Materials* № 5, 15 (2010).

Synthesis of nanodiamond reinforced dental composite resins and their mechanical properties

Chu Y.Q.[1], Tong Y.[1*], Wang X.Z.[2], Zhang T.L.[1], Huang F.L.[1]

[1]*School of Mechatronical Engineering, Beijing Institute of Technology, Beijing, China*
[2]*Faculty of Prosthodontics, School of Stomatology, Beijing University, Beijing, China*
**e-mail: tongyi@bit.edu.cn*

To measure mechanical properties of dental composites reinforced by nanodiamond, three groups of independently synthesized dental composites were prepared with different diameter detonation nanodiamond (DND) clusters. DND cluster (100nm, 220nm and 500nm) were modified with γ-MPS, then added to matrix which was a mixture of Bis-GMA, TEGDMA, glass powder, CQ and DMAEMA, with DND content up to 0.25%. Flexural strength, elastic modulus and hardness were characterized for each material, using standard specification tests designed for the materials.

Mechanical properties of R-100 (resin with 100nm DND) were significantly lower than the other two groups, while R-220 and R-500 presented relatively higher values except at 0.25% content. Along with the increase of the content of diamond, flexural strength of all the three groups increased at first then reduced. Elastic modulus and hardness showed strong correlations with flexural strength except for elastic modulus of R-220, which had a higher value than that of R-500 at 0.25% content.

[1] V.V. Danilenko. Synthesis and sintering of diamonds by explosion. E'nergoatomizdat, Moscow, 2003
[2] Urmimala Maitra, K. Eswar Prasad, U. Ramamurty, C.N.R Rao, *Solid State Communications* **149**, 1693 (2009).
[3] Hu X.G., Gu X.Y., Tong Y., *New Chemical Materials* **34**(2), 60 (2006).
[4] Chu Y.Q., Tong Y., Wang X.Z., Wang Q., *International Journal of Stomatology* **38**(1), 27 (2011).

The nucleation and growth of nanocrystalline diamond films in millimeter-wave CVD reactor

Chernov V.V.[1], Vikharev A.L.*[1], Gorbachev A.M.[1], Kozlov A.V.[1], Vul' A.Ya.[2], Aleksenskii A.E.[2]

[1]*Institute of Applied Physics RAS, Nizhny Novgorod, Russia*
[2]*Ioffe Physical-Technical Institute RAS, St. Petersburg, Russia*
**e-mail: val@appl.sci-nnov.ru*

Nanocrystalline diamond films grown by CVD technique possess a number of unique properties. This makes it possible to use them in thermal management, electromechanical, microelectronic, optical, biological and many other scientific and industrial applications [1]. Due to these reasons the interest for the investigation and application of nanocrystalline diamond films has grown considerably in recent years.

An important role in deposition of uniform smooth nanocrystalline diamond films is played by the prior preparation of the substrate, the choice of the diamond nuclei and the method of its seeding on the substrate. In our experiments the diamond nuclei were particles of detonation nanodiamond [2] seeded on the substrate from suspension. The diamond powder from the suspension was deposited on the substrate by using the spin coating process. This method ensures the same uniform and high-density deposition of the diamond powder on the substrate as in the case of the ultrasonic bath, while the consumption of the nanopowder is lower.

Nano-diamonds of two types were prepared for the experiments on deposition of nanocrystalline diamond films, namely, those having the average sizes of nanoparticles 4 nm and 40 nm, correspondingly. Seeded by the spin coating silicon substrates having a diameter of up to 100 mm and nucleation density ranging from 10^{10} to 10^{12} cm^{-2} were put into the chamber of millimeter-wave CVD reactor [3] filled with the $Ar–H_2–CH_4$ mixture. As a result uniform smooth nanocrystalline diamond films with thicknesses of several hundreds of nanometers were obtained. Properties of the nanocrystalline diamond films were compared for two types of used seeding suspension.

[1] O.A. Williams, M. Nesladek, M. Daenen, S. Michaelson, A. Hoffman, E. Osawa, K. Haenen, R.B. Jackman, *Diam. Relat. Mater.* **17**, 1080 (2008).

[2] A.Ya. Vul', A.E. Aleksenskiy, A.T. Dydaikyn Detonation nanodiamonds: technology, properties, and applications. In the book «Encyclopedia of systems of life support» Nanoscience and nanotechnology, pp. 832-857 (2009).

[3] A.L. Vikharev, A.M. Gorbachev, A.V. Kozlov, D.B. Radishev, A.B. Muchnikov, *Diam. Relat. Mater.* **17**, 1055 (2008).

Effect of physical-chemical treatments on the aggregative properties of nanodiamond of detonation synthesis

Bogatyreva G.*, Marinich M.A., Ilnitskaya G.

ISM – V.Bakul Institute of Superhard Materials, National Academy of Sciences of Ukraine, 04074, Kiev, Ukraine

**e-mail: bogatyreva@ism.kiev.ua*

Results of studies of kinetics of aggregation of nanodiamond powders depending on the time, temperature and pH of medium (solution) are considered in this report.

It has been ascertained that the rate of aggregation of freshly-mixed suspension is so great that during 10 sec the near 90% (mass) of nanodiamond are aggregated. As temperature increases the aggregation rate increases as well. The rate of aggregation depends on the pH of solution. Alkalization of solution results in the reduction of aggregation rate due to the dissociation of the oxygen-containing compounds of surface layer.

Theoretical explanation of mechanism of aggregation has been proposed. Aggregation process has same phases: 1) adsorption of oxygen-containing groups from solution, 2) generation of functional cover, 3) adjustment of equilibrium between solution and functional cover, 4) agglomeration due to Van der Waals forces (bonding), 5) agglomeration due to covalent (chemical) bonds.

Effect of low-temperature cooling (freezing) of nanodiamond suspension (water) on the physical-chemical and physical-mechanical properties of nanodiamond was studied. It has been ascertained – for the first time – as a result of freezing the displacement of oxygen-containing groups from surface of nanodiamond is progressed. Agglomerates grow up– by 25 times – and physical-mechanical characteristics of it's is improved, apparently, due to the forming of double bonds (C=C) between surface atoms of distinct particles of nanodiamond.

Effect of proportion of carbon of sp^2 and sp^3 hybridization in nanodiamond on the aggregation of the powder was studied. As portion of non-diamond carbon in nanodiamond increases the average diameter of particles increases as well, i.e. agglomeration takes place.

Effect of thermochemical and electrochemical reconstruction of nanodiamond surface on the chemical composition and aggregation of the powder was studied. Thermochemical reconstruction of surface results in the downsizing of average diameter more than by 2 times.

Graphite remelting as a new method to obtain metastable carbon phases

Basharin A.Yu.

Joint Institute for High Temperatures RAS, 125412, Moscow, Russia
e-mail: ayb@iht.mpei.ac.ru

Advances in the investigations of carbon are associated with the search of new methods of its formation. Nowadays the opportunities of graphite remelting at gas-static conditions are investigated insufficiently. The versatility of mechanisms and crystallization products of liquid carbon (*LC*) from remelted graphite described in [1-4] showed this method to be promising to obtain metastable carbon phases (*MCF)*. The thermodynamics shows an opportunity of getting a *MCF* with the Gibbs potential G_M beyond the limits of stability of this phase on the carbon phase diagram resulted in by the homogeneous nucleation (*HN*) in strongly supercooled *LC*.

Experiments on local graphite melting by a laser pulse at isobaric conditions in the helium atmosphere at pressures 10-100 MPa allowed to find the conditions at which the *HN* takes place in a melt. It is cleared up that the wave properties of the laser radiation and correct choosing of the original HOPG sample orientation towards the laser beam direction have a leading role for this process. We succeeded in obtaining at *HN* the admixture of carbon components *sp* (carbine), sp^2 (graphite) и sp^3 (diamond) and C8 phase [2], which is a carbon alloy, according to [5]. The formation of this alloy is likely to obey the Ostwald rule of stages, according to which the transition from *MCF* to the stable phase (graphite) occurs via a number of intermediate stages with the potentials $G_1 > G_2 > G_3 ... > G_g$.

The diamond is also obtained as separate phase by the heterogeneous crystallization of *LC* on the diamond substrate. In the field of diamond surface forces there have been obtained transparent diamond microcrystals and nano-diamond white-colored films [4]. The influence of extremely high thermal conductivity of the substrate made of the natural diamond crystal on the process of autoepitaxy has been discussed. There had been also discussed an agglomeration of liquid carbon thin films caused by its instability on the surfaces of graphite and diamond and opportunities of using non-graphite liquid phase precursors.

[1] Basharin A.Yu., Brykin M.V., Marin M.Yu., Pakhomov I.S., Sitnikov S.F., *Teplofis. Vys. Temp.* **42**, 64 (2004).
[2] Basharin A.Yu., Dozhdikov V.S, Dubinchuk V.T., Kirillin A.V., Lysenko I.Yu., Turchaninov M.A., *Pis'ma Zh. Tekh. Fiz.* **35**, 84 (2009).
[3] Basharin A.Yu., Dozhdikov V.S, Kirillin A.V., Turchaninov M.A., Fokin L.R., *Pis'ma Zh. Tekh. Fiz.* **36**, 39 (2010).
[4] See this issue.
[5] Yasuda E., Inagaki M., Kaneco K., Endo M., Oya A., Tanabe Y. Carbon Alloys: Novel Concept to Develop Carbon Science and Technology, Elsevier, Tokyo (2003).

Carbon phase diagram and the liquid carbon properties: the new results

Basharin A.Yu.*, Lysenko I.Yu., Turchaninov M.A.

Joint Institute for High Temperatures RAS, 125412, Moscow, Russia
**e-mail: ayb@iht.mpei.ac.ru*

Carbon phase diagram is a basis for the graphite – diamond phase transition analysis. It defines these phase coexistence line parameters with carbon melt and vapor, as well as parameters of both carbon triple points. The results of the carbon phase diagram investigation and some properties of liquid carbon obtained recently by the authors are presented in this report.

Contact angle of graphite basal plane wetting by the liquid carbon 40 ± 10° was measured for the first time [1]. Thermodynamic estimation of the diamond melting temperature 4160±50 K at the pressure 12 MPa was made. [2] The analytical curve (fig. 1) separating metastable diamond from supercooled liquid carbon coexisting region was plotted down to the 12 MPa [3] using Simon's two-parameter equation:

$$p = p_0 + a\left[\left(\frac{T}{T^*_{dm}}\right)^c - 1\right]$$

where $a = 0.41$ GPa and $c = 18.42$ determined empirical parameters. The data for pressure range 10 MPa – 5 GPa were obtained for the first time, and for pressure range 5 – 12 GPa are in a good agreement with Bundy's data [4].

Minimal values of temperature 4750±100 K [1] and pressure 10.7±0.1 MPa at which graphite can be melted (carbon triple point graphite–liquid–vapor) were measured by us, and also are in a good agreement with the data from [4].

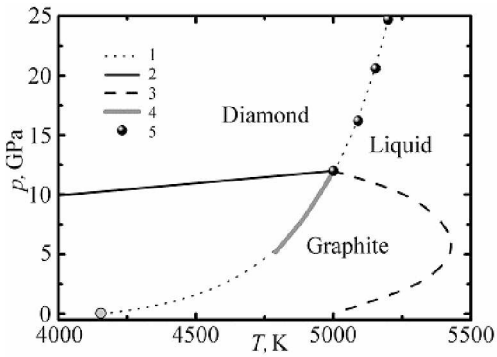

Figure 1. Carbon phase diagram. *1* – diamond melting curve (present work calculated data); ○ – metastable diamond melting point (12 MPa, 4160 K); coexistence curves according to Bundy et al. [4]: *2* – diamond - graphite, *3* – graphite - liquid carbon, *4* – metastable diamond - liquid carbon; *5* – data from [4], used for our calculation

[1] Basharin A.Yu., Brykin M.V., Marin M.Yu., Pakhomov I.S., Sitnikov S.F., *Teplofis. Vys. Temp.* **42**, 64 (2004).

[2] Basharin A.Yu., Dozhdikov V.S, Kirillin A.V., Turchaninov M.A., Fokin L.R., *Pis'ma Zh. Tekh. Fiz.* **36**, 39 (2010).

[3] Turchaninov M.A., Avtoref. Dissert. (2010)

[4] Bundy F.P., Bassett W.A., Weathers M.S., Hemley R.J., Mao H.K., Goncharov A.F., *Carbon* **34**, 141 (1996).

Comparative study of some commercial detonation nanodiamonds

Avramenko N.V.*[1], Kalachev A.[2], Korobov M.V.[1], Belyaeva L.A.[1], Semenyuk P.I.[3]

[1]*Department of Chemistry, Moscow State University, 119991, Moscow, Russia* [2]*PlasmaChem GMbH, Rudower Chaussee 29, 12489-Berlin, Germany*
[3]*Department of Bioengineering and Bioinformatics, 119991, Moscow State University, Moscow, Russia*
**e-mail:natali@td.chem.msu.ru*

Comparative systematic study of physical/chemical properties of series of commercial detonation nanodiamonds (DND) has been performed. In addition to conventional set of methods (HTEM, DLS, IR, x-ray) differential scanning calorimetry (DSC) was used to reveal dispersibility of DND in water.

The study was mainly focused on the materials, made by PlasmaChem GMbH. Single Digit ND (SDND) material produced by acidic/temperature treatment of crude DND [1] demonstrated unique properties both in DLS and DSC. The material easily forms stable in time almost mono-sized water dispersion. The DLS averaged diameter of DND species in the dispersion (~5-8 nm) was close to the size of primary DND particles (d~5nm).

Peak of melting of nanosized water (PMNW) [2] occurred in DSC traces of SDND at 263-264 K. This is the lowest temperature of PMNW measured for DND materials so far. One may assume that SDND as aqueous gel and dry powder is a completely disaggregated material consists of non-bonded primary particles.

For all the materials studied (SDND, WND, GO1, Nano-Pure GO1, made by PlasmaChem GMbH) the correlation was found between DLS and DSC data. The lower is the temperature of PMNW in the DSC trace; the smaller is the DLS diameter of DND aggregate in the dispersion. One may predict possible size of aggregate in the dispersion from the DSC traces of the material prior to making of the dispersion. Reproducibility of DSC traces is better than those of the DLS data.

The results obtained were compared with the data for other commercial DND.

[1] Fedutik Yu, Antipov A, Maltseva E, Kalachev A, Gubarevich T. Proceedings of 3rd International Symposium «Detonation Nanodiamonds: Technology, Properties and Applications» St.Petersburg; Russia; 2008 p.65 – 72

[2] Korobov M.V., Batuk M.M., Avramenko N.V., Ivanova N.I., Rozhkova N.N., Ōsawa E., *Diamond & Related Materials* **19**, 665 (2010).

Influence of local Coulomb potential on transport through carbon nanotubes

Zhukov A.[1*], Finkelstein G.[2]

[1]*Institute of Solid State Physic, 142432, Chernogolovka, Russia*
[2]*Duke University, 27708, Durham, North Carolina, USA*
**e-mail: azhukov@issp.ac.ru*

In this paper, we present the results of helium temperature transport measurements through carbon nanotubes using an AFM conductive tip as a mobile gate for creation of a local distributive Coulomb potential.

Shifting of the conductance peaks positions for the first hole states is observed and explained qualitatively in framework of particle in 1-D box model for semiconducting nanotubes.

Stability of the fourfold degeneracy of the energy states in a metallic nanotube to external Coulomb potential and coupling to the contacts is demonstrated (see Fig. 1). These observations are in agreement with previous theoretical calculations where no influence of local Coulomb potential and the opacity of potential barriers on degenerate states has been found [1]. Thus, we can conclude that destruction of the fourfold degeneration only comes from defects and imperfections of the metallic nanotube itself.

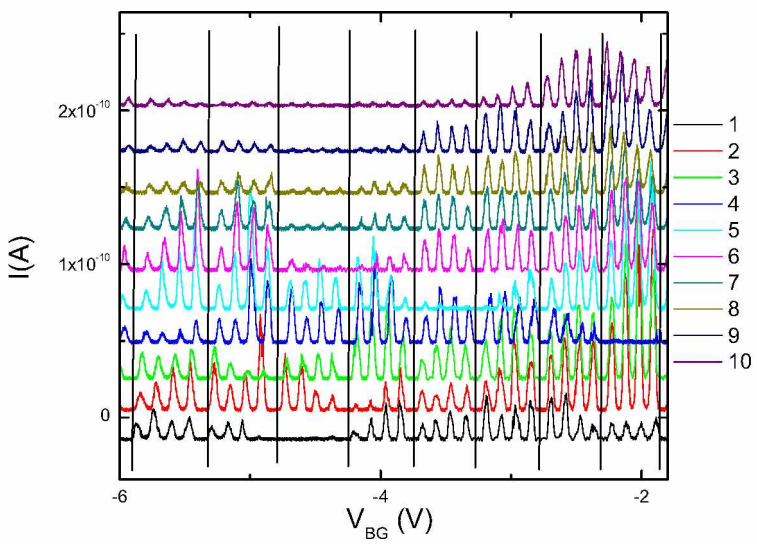

Figure. Conductivity of the CNT of high quality vs back gate voltage for different AFM tip positions. The value of tip voltage is of ~ 8 V.

[1] San-Huang Ke, H.U. Baranger, W. Yang, *Phys. Rev. Lett.* **91**, 116803 (2003).

Growth of vertically oriented nanotubes on clusters, made by nanoimprint lithography

Zaytsev A.A.[1], Simunin M.M.*[1], Egorkin V.I.[1], Solovyeva N.A.[1], Nikiforov D.N[1]

[1]*Moscow Institute of Electronic Technology, 124498, Zelenograd, Russia*
**e-mail: Michanel@mail.ru*

It's well known today, that properties and structure of catalytic particles determine key features of nanotubes growth and their properties. Catalytic particles engineering hereby determine further formation of carbon nanotube based nanostructures and this is why it is actual scientific problem. Nanoimprint lithography is a promising method of creation structured catalytic particles about 50 nm over [1].

100 nm thick PMMA layer was spun onto silicon substrate. Nanoimprint stamp and substrate were heated up to 180°C and then stamp was pressed into polymer. After releasing, substrate was cooled and polymer layer was etched in O_2 plasma. If time of etching is 35 seconds the remaining thickness of polymer is 40 nm. 6 nm of nickel was deposited by thermal evaporation and lift-off in warm dimethyl formamide. Finally there are Ni islands on the substrate with diameter of 50 nm.

CNT synthesis performed with CVDomna unit by catalytic pyrolysis of ethanol. Temperature of process is 600°C and ethanol vapour pressure is 10 kPa. Heated clusters tend to minimize their surface energy and relax to spherical form. When ethanol vapours get into the chamber, they decompose into carbon monoxide. Catalytic particles adsorb this monoxide. Disproportionation of CO molecules takes place on their surface. Products of this reaction are CO_2 and carbon dissolving in catalytic particles. Carbon nanotubes grow from these particles and according to existing models nanotube diameter must be determined by radius of curvature of catalytic cluster. Our results are in full accordance with this fact. Diameter of our nanotubes is about 30 nm (see Fig.), what corresponds with dimension of sphere, whose volume equal to the volume of cluster.

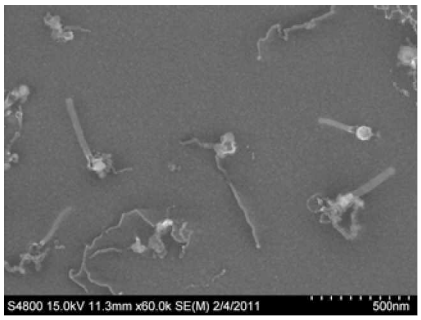

Figure: vertically oriented carbon nanotubes.

[1] S. Zankovych, T. Hoffmann, J. Seekamp, J.-U. Bruch, C.M. Sotomayor Torres, *Nanotechnology* **12**, 91 (2001).

Ethanol pyrolytic synthesis of carbon nanotubes using a novel Ni/(NiO+Y_2O_3) catalyst

Zaramenskikh K.S.[1], ZharikovE.V.[1], Faikov P.P.[1], Kovalenko A.N.[1], McRae E.[2], Devaux X.[3], Iskhakova L.D.[4]

[1]*D. Mendeleyev University of Chem. Techn. of Russia, Moscow, 125047, Russia*
[2]*Institut Jean Lamour UMR CNRS 7198, Nancy Université, Faculté des Sciences et Techniques, B.P. 70239, 54506 Vandoeuvre-lés-Nancy Cedex, France*
[3]*Institut Jean Lamour UMR CNRS 7198, Nancy Université, Ecole des Mines, CS14234, 54042, Nancy, France*
[4]*Fiber Optics Research Center of the Russian Academy of Sciences, Moscow, Russia*
**e-mail: zharikov@rctu.ru*

When carbon nanotubes (CNTs) are producing using the chemical vapor deposition method, the process of nanoscale catalyst particle (CP) formation plays an important role. The CPs can be efficiently obtained using a sol-gel technique allowing the obtaintion of a catalyst material with high specific area, containing previously fabricated metal nanoparticles with the desired size.

The prospects of using sol-gel technology for the manufacturing of the catalyst is rendered feasible by the possibility of preparing a material containing metal nanoparticles of predetermined and uniform size that subsequently determines the homogeneity of the CNTs fabricated.

The catalyst was synthesized by a modified sol-gel technique from $Ni(NO_3)_2$ and $Y(NO_3)_3$ using polyvinyl alcohol. The resulting material consisted of agglomerates of platelets (about 10 nm $\times$ 2 μ $\times$ 2 μ) which were nanostructured and contained the mixture NiO+Y_2O_3 (weight ratio ~ 4/1) with Ni inclusions in the form of nanoparticles (>3 nm in diameter).

Before synthesis, the catalyst was pre-treated by ultrasound in ethanol, then deposited on a quartz substrate, dried and placed in the reactor. Carbon nanostructures were synthesized by ethanol pyrolysis under both atmospheric and reduced (0.2 atm) pressure. The experimental temperature was varied from 600°C to 800°C. The carbon deposit was analyzed using scanning and transmission electron microscopy and X-ray diffraction.

All fabricated samples contained few-walled CNTs (mostly 10-20 nm in diameter) and carbon nanofibres. The specific microstructure of the new catalyst and optimized thermodynamic conditions of synthesis led to a high yield of CNTs with a low content of non-crystalline carbon.

The influence of both catalyst microstructure and synthesis parameters on the structure and morphology of the carbon deposit will be presented. The X-ray diffraction analysis of the deposit from different temperature zones of the pyrolysis furnace was carried out. The probable mechanism of formation of carbon nanotubes and nanofibres on the catalyst will be proposed.

Investigation of carbon nanotube activity to heavy organic molecules

Zaporotskova N.P., Zaporotskova I.V.*, Ermakova T.A.

Volgograd State University, 400062, Volgograd, Russia
**e-mail: irinaz@rbcmail.ru*

The high specific surface area of carbon nanotubes, which in several times exceeds the surface area of the best contemporary sorbents [1, 2], opens up the possibility of their using in filters and other equipment of chemical technology. Nanotubes can adsorb impurities on the outer and the inner surface. This allows to produce the selective adsorption. The effectiveness of nanotubes with respect to organic molecules is in ten times greater than the activity of graphite adsorbents, which are most popular means of treatment in this time. So proposed to use carbon nanotubes for purification of liquids, such as alcohol-based liquids, from the side (and / or toxic) products. These products include heavy organic alcohols.

In this work have been made the quantum-chemical researches of the adsorption interaction of carbon nanotubes with heavy organic molecules (in particular the isopropyl alcohol: n-propanol and i-propanol) using methods of MNDO, MNDO/PM3, DFT and program packages of MNDO92, HyperChem, Gamess. Energy curves of interaction processes are built and main geometric parameters of adsorption complexes and energy characteristics of the process are defined. It has been theoretically proved the carbon nanotube activity to heavy organic molecules.

Cleaning of the alcohol-based liquids by the extra small quantity of carbon nanomaterials was made. To prove the purification of water-alcohol solutions from the heavy organic alcohols have been used methods such as IR-spectroscopy, titrimetry, chromatography. We have proved, that the cleaning the water-ethanol mixtures of nanotubes contributes to a decrease in their content of heavy alcohols and other impurity substances.

This research was supported by Russian Federal Target Program "Scientists and pedagogical workers of innovation's Russia", 2009-2013 (Grant No. P328).

[1] A.V. Eletskii, *Physics-Uspekhi* (*Advances in Physical Sciences*) **174**, 1191 (2004).
[2] I.V. Zaporotskova, Carbon and noncarbon nanomaterials and composite structures based on them: structure and electronic properties. Volgograd Russia, 2009, 490 p.

Synthesis of high quality single-wall carbon nanotubes by CCVD method

Zaglyadova S.V.*[1], Maslov I.A.[1], Don A.K.[1], Kuptsov A.K.[1], Zhigalina V.G.[2]

[1]*United Research and Development Centre, 119333, Moscow, Russia*
[2]*A.V.Shubnikov Institute of Crystallography, RAS, 119333, Moscow, Russia*
**e-mail: ZaglyadovaSV@yrd.ru*

YRD-Centre Ltd carries out research work in the field of development of a highly capacity synthesis SWCNTs by a catalytic chemical vapour deposition (CCVD) methods with use floating catalyst

This work is dedicated to optimization of technological parameters of synthesis with use such quality analysis methods of SWCNTs as: TEM, SEM, and Raman spectroscopy.

All experiments were spent on vertical type set-up with use of the flow reactor, power system of a reaction mix and carrier gases, and collection systems of the carbon material on reactor outlet. As a carbon precursors used a methanol, ethanol, n-propanol, isopropyl alcohol, and hexane; catalyst precursor – ferrocene $(\eta^5\text{-}C_5H_5)_2Fe$; activator of growth SWCNTs – thiophene C_4H_4S; carrier gas – hydrogen, argon. The reaction time was varied from 0.1 to 3 hr at temperature 850-1200°C. All experiments was led to formation of black fibrous material consist of SWCNTs and metal particles. The best results were reached for the reaction mixes based on ethanol. Characterization of synthesis products with TEM, SEM and Raman spectroscopy showed that it is dominated by SWCNTs with relatively narrow size distribution and missing amorphous carbon. The absence of amorphous carbon in the product makes final purification much easier.

It is necessary to note that high quality SWCNTs was achieved by combination of such technological parameters as: composition and flow rate of feed-stock and carrier gas, methods of reaction mix input in synthesis zone, and synthesis temperature.

A p-electron conjugation in fullerenes and carbon nanotubes

Tomilin O.B.*, Muryumin E.E., Rodionova E.V.

Ogarev Mordovian State University, 430005, Saransk, Russia
**e-mail: tomilinob@mail.ru*

Properties of fullerenes and nanotubes are considerably determinel by conjugated p-electron system. If the p_Z-AO axes coincide with a perpendiculars to a core plane in a hydrocarbon conjugated molecules then in fullerenes and nanotubes the p_Z-AO axes coincide with a normals to spherical and cylindrical surfaces, respectively. Therefore π– and σ–electron systems are not orthogonal in these molecules. This fact bears witness about a distinction of π - conjugation in a plane molecules from ρ-conjugation [1] in fullerenes and nanotubes.

For an investigation of ρ-conjugation peculiarities we made calculations of the two groups of molecules with ab initio Hartry-Fock method in 3-21G basis set: 1) cis- and trans-polyenes and 2) polyacenes and polyphenes. In every group was examined the following location of carbon atoms: a) open on a plane (linear), b) cycled on a cylindrical surface (cyclic), c) cycled on an one-side Mobius surface (mobius). A double C-C bond number n is equal n=6-16 in the first group, a hexagon number m – m=6-16 in the second group.

As distinctive characteristics of p-electron conjugation the value of the band gap is used. The carried out calculations show:

1) The value ΔE for all types of cis-polyenes decreases monotonously asymptotically with an increase of n (n is even for a security of a chosen structure), for all types of cis-polyenes there is $\Delta E_{lin} < \Delta E_{mob} < \Delta E_{cyc}$.

2) The value ΔE for linear trans-polyenes decreases monotonously asymptotically with an increase of n, ΔE_{cyc} oscillates asymptotically with an increase of n, what a maxima of amplitude reaches when n is odd, ΔE_{mob} oscillates also asymptotically with an increase of n though oscillations have enough rather a complicated character.

3) The value ΔE for linear polyphenes decreases monotonously asymptotically with an increase of m (m is even for a security of a chosen structure), for cyclic and mobius polyphenes ΔE increases monotto asymptotically with an increase of m. Fof all types of polyphenes there is $\Delta E_{cyc} < \Delta E_{lin} < \Delta E_{mob}$.

4) The value ΔE for linear polyacenes decreases m monotonously asymptotically with an increase of m, ΔE_{cyc} oscillates asymptotically with an increase of m, maxima of amplitude are reached when n is odd, ΔE_{mob} also oscillates asymptotically with an increase of m though oscillations have rather a complicated character.

Thus, ρ-conjugation of carbon atoms situated on non-linear surfaces has a peculiarities distinguishing from π-conjugation of a plane hydrocarbon molecules.

[1] D.A. Bochvar, E.G. Galpern, *Dokl. Akad. Nauk SSSR* **209**, 610 (1973).

The regularities of p-electron conjugation in carbon nanotubes

Tomilin O.B.*, Muryumin E.E., Rodionova E.V.

Ogarev Mordovian State University, 430005, Saransk, Russia
**e-mail: tomilinob@mail.ru*

The axes of p_z-atomic orbitals coincide with normals to cylindrical surface consisting of carbon atoms. Thus the conjugation of p-electrons differs from conjugation of π-electrons in plane conjugated hydrocarbon molecules and singles out in special ρ-electron conjugation type [1]. Calculations of molecules modeling single walled carbon nanotubes (SWNT) (n,0) for n=6-9 were carried out for research of specific features of p-electron conjugation. The length of molecules was 12 hexagons placed on graphen surface along cylindrical axis of SWNT. The end carbon atoms were saturated with hydrogen atoms. Ab initio Hatree-Fock calculations were carried out in 3-21G basis set. The cylindrical stripes were selected in central part of molecules. The trans-carbon cycled chains were placed in those stripes. The number of chains m in cylindrical stripe ranged within 1-6 for each molecule. Electronic structure and band gap ΔE of molecules were calculated for optimized geometry conditions. Received results are presented in fig. 1.

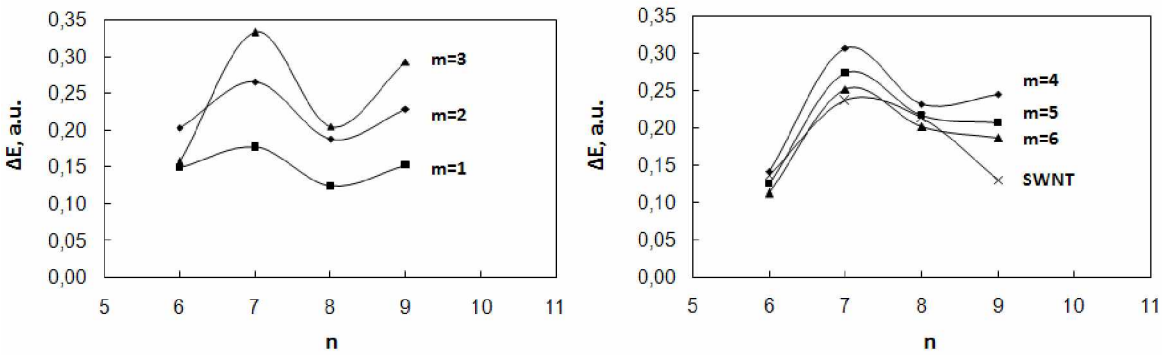

Figure 1: Dependence ΔE on index chirality n and number of trans-carbon chains m.

As follows from fig. 1 the band gap has oscillating behavior for trans-carbon chains for m=1-4. The maxima of amplitude agree with odd chirality index n. At the same time the oscillations for model molecule SWNT have minima in n = 3k. With further increase of m the character of band gap oscillations changes to SWNT oscillations. Thus, the p-electron conjugation corresponds to the combination of conjugation of p-electrons in cross-section SWNT and π-electron conjugation of cis-carbon chains placed on graphen surface in parallel with cylindrical axis of SWNT.

[1] D.A. Bochvar, E.G. Galpern, *Dokl. Akad. Nauk SSSR* **209**, 610 (1973).

Infrared spectroscopic investigation on non-covalently functionalized single walled carbon nanotubes

Tóháti H.-M.[1]*, Németh[1] K., Kamarás K.[1], Ben-Valid S.[2], Zeng A.[2], Reiss L.[2], Yitzchaik S.[2], Pietraszkiewicz M.[3], Pietraszkiewicz O.[3], Maggini L.[4], Bonifazi D.[4]

[1]*Research Institute for Solid State Physics and Optics, Hungarian Academy of Sciences, 1121 Budapest, Hungary*
[2]*Institute of Chemistry and the Center of Nanoscience and Nanotechnology, The Hebrew University of Jerusalem, 91904 Jerusalem, Israel*
[3]*Institute of Physical Chemistry, Polish Academy of Sciences, 01224 Warsaw, Poland*
[4]*Department of Chemistry, University of Namur, 5000 Namur, Belgium*
**e-mail: tohati@szfki.hu*

Hybrid materials formed by adsorption of organic molecules on the surface of carbon nanotubes form an important class of nanotube chemistry. This importance originates in the possibility of combining special (optical, electric or dispersive) properties of the added molecules with the mechanical stability of carbon nanotubes (CNTs). Functionalization of CNTs by polymers or aromatic systems is not only relevant from the functional groups' point of view, but the easier applicability of host nanostructure also plays an essential role.

The key to all applications is a method to study the qualitative properties of interaction (strength, bond type, etc.) between nanotubes and the associated species. We use infrared (IR) transmission and attenuated total reflection (ATR) spectroscopy to understand how these compounds are adsorbed or attached to the surface of the nanotube. Aromatic systems tend to adsorb by π-π stacking, which causes surface-attenuated infrared absorption (SAIRA) and thus peculiar vibrations of the added molecules can be investigated through the interaction of the evanescent field on the surface of the nanotube with the vibrations of the adsorbed species. We have studied these effects on pyrene-based systems and on luminescent rare-earth complexes.

Hydrogen sorption process modeling on the periodic structures formed by carbon nanotubes

Slepicheva M.[1], Chernyshev Y.[1], Basteev A.[1], Bazyma L.*[1], Ugryumov M.[1]

[1]*National Aerospace University, 61070, Kharkov, Ukraine*
**e-mail: bazima@htsc.kipt.kharkov.ua*

The process of molecular hydrogen physical sorption on the surfaces of carbon nanotubes (CNT) which are forming the spatial pattern is interesting from mathematical point of view and numerical simulation of above process has scientific interest as well [1]. The cell of computational region (see Fig.) in which three or mutually orthogonal CNT without intersection are replaced was considering for simplification.

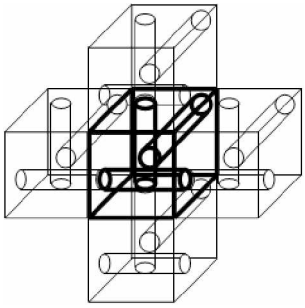

Cells periodic structure.

The molecular hydrogen as the model particles are sited in the cells. All involved in consideration model particles have rectangle-shape potential that gives us the opportunity to use the event-driven simulation method [2]. The hypothesis about periodical conditions on the region borders was assumed and it physically means that infinitely long CNT are closely interwoven one with another [3]. The model particles are supplied from selected facet of cells system. The percentage of sorbet hydrogen molecules at high temperatures was calculated taking into account single sorption layer only. The reducing of system temperature after initial filling and with primary adsorption layers formation has been proposed with the aim to suppress the re-adsorption process.

The results of numerical investigations of defects-vacancies influence in the CNT structure on the sorption capability at different thermo dynamical conditions were obtained on the base of proposed method.

[1] B. Assfour, S. Leoni, G. Seifert and I. Baburin A., Advanced Materials, DOI: 10.1002/adma.201003669, (2011).

[2] A. Basteev, L. Bazyma, M. Ugryumov, Y. Chernishov, M. Slepicheva, 2010 MRS Fall Meeting, Boston, 29 November – 3 December, USA, MRSF10-1284-C10-08 (2011).

[3] M. Slepicheva, Proceedings of the International Scientific Conference of Students and Young Scientists, Kyiv: Bukrek, 294 (2011).

Fabrication and characterization of hybrid solar cells based on semiconducting single-walled carbon nanotubes

Shoji M.[1], Ito T.[2], Ogata H.*[1,2]

[1]*Graduate School of Engineering, Hosei University, 3-7-2, kajino-cho, koganei-shi, Tokyo 184-8584, Japan*
[2]*Department of Chemical Science and Technology, Hosei University, 3-7-2, kajino-cho, koganei-shi, Tokyo 184-8584, Japan*
**e-mail: hogata@hosei.ac.jp*

Recently, hybrid solar cells used single-walled carbon nanotubes (SWNTs) and the organic materials [1], and the hybrid solar cells based on semiconducting SWNTs (s-SWNT)/Si heterojunctions [2] was reported. In the former case, the SWNTs were used as a conducting component on the organic solar cells, in the latter case, the SWNTs were employed as charge separator, transporter, and light absorber component on the s-SWNT/Si heterojunction hybrid solar cells. However, these hybrid solar cells used the SWNTs were indicated low conversion efficiency (~1.7%).

In this study, we fabricated the s-SWNT/organic hybrid solar cells. S-SWNT/N-type Si heterojunction hybrid solar cells and TTF or TMTSF@SWNT/P-type Si heterojunction hybrid solar cells were also fabricated. The s-SWNTs were prepared by separation of metal and semiconducting SWNTs using agarose gel method [3]. The structure of the s-SWNTs/organic hybrid solar cells were ITO-coated glass /PEDOT-PSS/s-SWNTs/PCBM/Al. PEDOT-PSS and PCBM layer was fabricated using spin-coating, and Al layer was prepared by vapor deposition. We were compared drop-cast with spray method for preparing of the s-SWNTs layer. Both the *J-V* curve and the impedance measurement both dark and under illumination up to simulated air mass 1.5 global(AM1.5G)conditions were carried out in an inert gas atmosphere glovebox.

The detail results will be presented in the conference.

[1] Jianxin Geng and Tingying Zeng, *Journal of Chemical Society* **128,** 16827 (2006).
[2] P.L. Ong, W.B. Eluer and I.A. Levitsky, *Nanothechnology* **21**, 105203 (2010).
[3] T. Tanaka, Y. Urabe, D. Nishide and H. Kataura, *Applied Physics Express* **2**, 125002 (2009)
[4] T. Takenobu, T. Takano, M. Shiraishi, Y. Murakami, M. Ata, H. Kataura, Y. Achiba and Y. Iwasa, *Nature Materials* **2**, 683 (2003).

Electronic structure of carbon nanotubes in benzene solution

Shamina E.N.*[1], Lebedev N.G.[2]

[1]*Volgograd State Medical University, 400131, Volgograd, Russia*
[2]*Volgograd State University, 400062, Volgograd, Russia*
**e-mail: shamina.alena@gmail.com*

In this work the single-walled nanotubes (n, n) type (n = 5, 6) are considered. As the geometrical models of nanotubes the clusters (fragments) containing n six-member cycles (hexagons) on a tube perimeter and 8 - 10 elementary cells along an axis of a tube are chosen. The boundary broken off chemical bonds became isolated atoms of hydrogen. The calculations of an electronic structure of the structures are carried out within the frameworks of the simple molecular cluster model [1] with the use of quantum-chemical semi-empirical schemes MNDO [1].

Studied three variants of the orientation of benzene molecules on the surface of carbon nanotubes: I) over a center of the hexagon (the plane of the molecule perpendicular the plane of the hexagon); II) over the center of the hexagon (the molecular plane parallel the plane of the hexagon); III) plane of the benzene molecule parallel the nanotube. In each of the three cases the molecule was located in the center of the cluster to reduce the influence of boundary conditions.

The analysis of quantum-chemical calculation results has shown that the the highest occupied molecular orbital energy (E_{HOMO}) increases with the tube diameter growth and the lowest unoccupied molecular orbital energy (E_{LUMO}) decreases. Change of E_{HOMO} and E_{LUMO} sizes testifies the change of nanotube properties caused by adsorption, namely the increase in reactionary ability of the given systems. I.e. the tubes of a particle adsorbed on a surface increase affinity carbon nanotubes to other particles.

The analysis of the length of the adsorption of chemical bonds has shown that in cases (I) and (III) between the benzene molecule and the atoms of carbon nanotubes form only hydrogen bonds. And in case (II) formed covalent chemical bond type 6 +6 between the carbon atoms of the molecule and the tube. The latter case seems unlikely, since the formation of both 6 bonds need only possible mutual orientation of the particles, the steric factor which in solution is very low compared to other options.

The analysis of results has shown that due to the adsorption of the benzene molecule the band gap of the nanotube increases slightly. This indirectly leads to a slight change in the physical properties of carbon nanotubes, in particular, the conductivity and transparency. This effect can be used to develop chemical sensors [2], aimed at registering considered in the particles, and the creation of optically active medium based on carbon nanotubes solutions in benzene.

[1] Stepanov N.F. Quantum mechanic and quantum chemistry. Moscow: MSU, 2001. 519 p.
[2] Aggins B. Chemical and biological sensor controls. Moscow: Technosphere. 2005, 336 p.

Composite material with the carbon nanostructures for the applications in optical power limiting

Belousova I.M.[1,2], Kislyakov I.M.[1,2], Videnichev D.A.*[1,2], Ryzhov A.A.[1,2], Volynkin V.M.[3]

[1]*SIC Vavilov State Optical Institute, St. Petersburg, 199034, Russia*
[2]*St. Petersburg State University of ITMO, St. Petersburg, 197101, Russia*
[3]*FSUE NITIOM A-RSC "Vavilov GOI", St.Petersburg, Russia*
**e-mail: vid-dmitry@yandex.ru*

It is well known that suspensions of the different carbon nanoparticles such as carbon black [1], nanotubes [2], multi-shell fullerene-like particles [3] and other show the abilities for the optical power limiting. The phenomenon in such suspensions derives from the light-induced scattering. However, bleaching of the suspension under the radiation of the laser pulse constrains their use as an effective limiter in the rate repetition mode of the laser radiation [4]. We experimentally showed the possibility of the composing of the carbon nanotubes suspension on the organic polymer base which limits the laser impulses coming in with the rate up to 10 Hz. This composite material with carbon nanotubes possesses good optical quality, is transparent in optical spectrum (about 70%) and does not have any coloration. Moreover it showed long-term stability and can act in the wide range of the temperature. So the limiter with this composite material can be used in the observation devices for the protection of the eyes and detectors.

[1] Kamjou Mansour, M.J. Soileau, E.W. Van Stryland, *J. Opt. Soc. Am. B* **9**, 1100 (1992).
[2] Rahman S., Mirza S., Sarkar A., Rayfield G.W., *J Nanosci. Nanotechnol.* **10**(8), 4805 (2010).
[3] O.B. Danilov, I.M. Belousova, A.A. Mak, V.P. Belousov, A.S. Grenishin, V.M. Kiselev, A.V. Kris'ko, T.D. Murav'eva, A.N. Ponomarev, E. N. Sosnov, *SPIE Proc.* 5777, 277 (2005).
[4] Belousova I.M., Belousov V.P., Mironova N.G., Murav'eva T.D., Scobelev A.G., Yur'ev M.S., Videnichev D.A., *Proceedings of SPIE* **6455**, 64551D1 (2007).

Carbon clusters as an example for self-organization

Prikhodko A.[1]*, Konkov O.[2]

[1]*St.Petersburg State Polytechnical University, 195251 St.Petersburg, Russia*
[2]*Ioffe Physical-Technical Institute RAS, 194021 St.Petersburg, Russia*
**e-mail: aleks@tuexph.stu.neva.ru*

According to the main principles of self-organized criticality (SOC) concept [1], there is a number of giant dissipative dynamical systems which are able to accumulate small external perturbations. Mathematical criterion of self-organization is a power-law behavior of avalanche size probability density. Several systems have been shown to exhibit SOC in terms of finite-size scaling as well as power law avalanches, such as pile of rice, magnetic vortices in superconductors [2] etc. The aim of this work is to show that carbon clusters such as nanotubes and graphite powder can serve as convenient objects for experimental investigations of SOC. Self-organized criticality can be experimentally observed as a power-law resistivity behavior. The samples investigated were in the form of carbon nanotubes (CNTs) with 20–70 nm diameter and up to 150 nm length and in the form of graphite powder of grains with 3-5 μm diameter. We need to measure the slope of the heap (φ_c) for «avalanches» of CNTs and single grains of the powder. We present here the experimental study results of the evolving sandpile resistivity dynamics. The samples were formed on an inclined plane with fixed angle (φ_c) with electrodes as described in [3]. Each sample was formed by periodically adding material portions (n) of the same volume (~10^{-5} cm^3). The φ_c value is 55° for CNT, and 35° for graphite. We present a detailed study of the static voltage-current characteristics which vary from ohmic (U_{min}) to breakdown (U_{max}) on above mentioned samples (U=0-20V). The typical I–V curves with an S-type instability region are obtained. At voltages close to the critical one, the detailed shape of the I–V curve is typical of multi-walled CNTs [4]. Typical dependencies of CNTresistance R by the number of material portions n are shown at the Fig. The power-law behavior of R(n) typical for SOC is observed. Dependency of line slope (B) by voltage (see Fig.) can be an evidence of inter-nanotube circuits influence to the critical state formation. Line slopes of graphite powder are: B=-1.27 (U_{min}), B=-0.45 (U_{max}). The experimentally observed curves are attributed to CNTs and graphite powders for angles $0 \le \varphi \le \varphi_c$ and voltages $0 \le U \le U_{max}$.

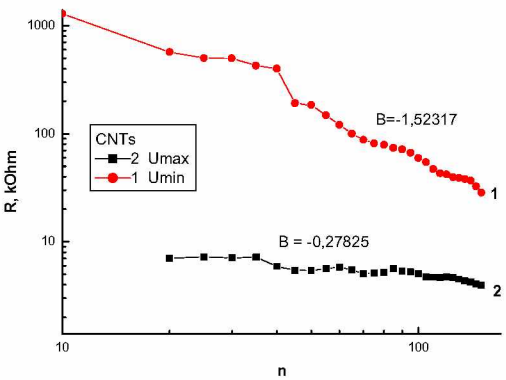

Figure. The resistance R of CNTs at U_{min} (1) and U_{max} (2) as a function of n. Best fit line slope-B.

[1] P. Bak, C. Tang, K. Wiesenfeld, *Phys. Rev. Lett.* **59**, 381 (1987).
[2] S.L. Ginzburg, N.E. Savitskaya, *Phys. Rev. E* **66**, 026128 (2002).
[3] G.A. Held, et al., *Phys. Rev. Lett.* **65**, 1120 (1990).
[4] A. Prikhodko, O. Konkov, E. Terukov, A. Filippov, *Fullerenes, Nanotubes, and Carbon Nanostructures* **19**, 1 (2010).

Propagating of a light bullet through the beam of CNT with a metallic inhomogeneity lattice

Popov A.S.[1]*, Belonenko M.B.[2], Lebedev N.G.[1]

[1]*Volgograd State University, 400062, Volgograd, Russia*
[2]*Volgograd Institute of Business, 400048, Volgograd, Russia*
**e-mail: A.Popov.VolSU@gmail.com*

Creation of powerful lasers and the unique accuracy of optical measurements have led recently to a considerable progress in the study of nonlinear phenomena observed in a wide range of substances with very different physical properties [1, 2]. The subject of inquiry should be a substance with pronounced nonlinear properties, and, on the other hand, it should be extensively used in applications. Carbon nanotubes (CNTs) are unique macromolecular systems [3], so they are increasingly attracting the attention of the researchers in the last decade. Their rather small nanometer diameters and relatively large micrometer lengths make them a novel system for the use in nano- and microelectronics. The study of optical solitons in carbon nanotubes is one of the promising fields of modern research.

In the construction of the model of electromagnetic field propagation in a 2D array of carbon nanotubes we assume that the electromagnetic field strength vector $\mathbf{E}(x, y, t)$ is directed along the tube axis z, while the electromagnetic wave moves in the transverse direction. Here we consider the ideal case, when carbon nanotubes have a zigzag structure, and are situated at equal distances (0.34 nm) from each other.

We used the simplest model to determine the current in the region occupied by the metal wire, namely we supposed that the Ohm's law is satisfied in the area occupied by the wire: $\boldsymbol{j} = \sigma \boldsymbol{E} = -\sigma \partial \boldsymbol{A}/c\partial t$, where σ is the complex conductivity, which generally depends on the applied field frequency.

The results of numerical simulation show that periodic partition of the maximum does not occur and there is no exciting of inner vibrational modes of light bullets in contrast to the system considered in [4].

The light bullet decays rapidly for a sufficiently large number of layers. However, when a number of layers in the lattice are small (in the direction of the light bullet) the bullet propagation is stable, but its duration is reduced. This fact can be used to create a ultrashort light pulses.

This work is supported by The Education Ministry of Russian Federation (project No. NK-16 (3)).

[1] A. Jeltikov M. *UFN* **177**, 737 (2007).
[2] Maksimenko S. A., Slepyan G. Ya. In: Handbook of nanotechnology. Nanometer structure: theory, modeling, and simulation. SPIE Press, Bellingham. 2004.
[3] P. Harris Carbon Nanotubes and Related Structures, Cambridge University Press, 2001.
[4] M. Belonenko, A.Popov, N. Lebedev, *JTP Letters* **37**, 51 (2011).

Oldest natural carbon micro-and nanotubes on the Earth

Ponomarchuk V.A.[1,2]*, Titov A.T.[1], Semenova D.V.[1]

[1]*Sobolev Institute of Geology and Mineralogy SB RAS, 630090, Novosibirsk, Russia*
[2]*Novosibirsk State University, 630090, Novosibirsk, Russia*
**e-mail: ponomar@igm.nsc.ru*

Synthesising and isolating new forms of carbon allotropes (fullerenes, nanotubes, graphene) has been the focus of much scientific and industrial research during the last three decades in different countries. In magmatic and metamorphic rocks the main form of carbon allotropes is graphite that usually observed in the form of lamellar crystals of hexagonal syngony.

However, the study of graphite mineralization in intrusive rocks have established submicroscopic carbon of different morphologies in the forms of singlewalled and multiwalled micro- and nanotubes, foam-like and wool-like spongy aggregates, onion-like carbon particles and graphene. The combination of all of these forms in a single aggregate is an intriguing challenge to the existing models of the formation of carbon nanostructured materials.

Study of multiple scan-frames allowed to distinguish different morphological forms of carbon nanostructured materials: 1) Cylindrical tubes consisted of three complex zones: a) the inner hollow tubes (diameter less than 100 microns (μm)); b) intermediate foam-like layer (10-20 μm); c) outer zone consisting of a "forest" of microtubes (diameter - 1-5 μm) and nanotubes (diameter 100nm). 2) Planar carbon structures, characterized by zonal morphologies: a) plane of nanometer thickness; b) intermediate foam and wool-like layer (20 μm); c) microtubes and nanotubes emerged from the intermediate layer (diameter less than 5 μm, length - 100-150 μm). 3) Large onion-like fullerens (diameter ~5 μm).

Carbon isotope composition analyses of different carbon morphologies have shown the variability of the $\delta^{13}C$ values in range from -12.5 to -14.6‰ (VPDB).

The available data on the morphology of nanostructured materials and their combination in single aggregate, as well as isotopic data allow to reconstruct the processes of formation of carbon nanomaterials in the natural environment that is of interest for specialists in nanotechnology.

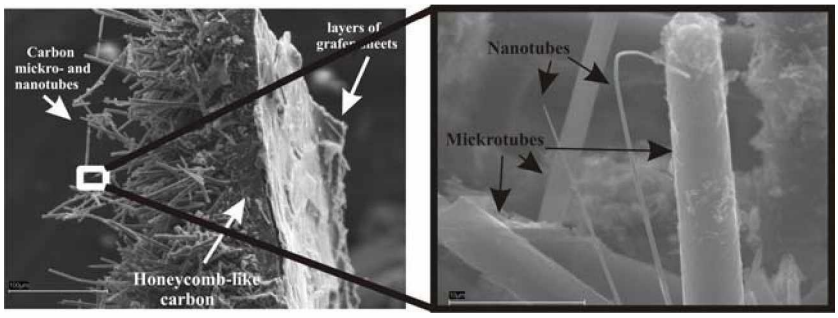

Figure. The fragment of the carbon aggregate (the scale: figure - 100 μк, inset – 10 μк).

Adsorption of methylene blue onto chemical modificated carbon nanotubes

Pełech R.[1*], Pełech I.[2]

[1]*Institute of Chemical Organic Technology, West Pomeranian University of Technology, Szczecin, Pulaskiego 10, 70-322 Szczecin, Poland*
[2]*Institute of Chemical Technology and Environmental Engineering, West Pomeranian University of Technology, Szczecin, Pulaskiego 10, 70-322 Szczecin, Poland*
**e-mail: robert.pelech@zut.edu.pl*

Carbon nanotubes possess splendid potential applications in energy storage, environmental remediation and medical delivery due to their unusual one-dimensional hollow nanostructures and unique chemical and physical characteristics. The strong adsorption affinity of carbon nanotubes towards organic contaminants, such as dioxins, trihalomethanes, aromatic organic chemicals, antibiotics and organic pesticides was approved. In order to improve carbon nanotubes properties, pristine CNTs are oxidized in nitric acid or hydrogen peroxide.

In this work the studies of sorption properties of modified carbon nanotubes are presented. The pristine carbon nanotubes were produced by a chemical vapor deposition method using iron-cobalt catalyst and subsequent modified using chlorine gas at 150°C under atmosphere pressure. When the process was ended, the sample was degasified under vacuum in the same temperature like temperature of chlorination process. Next the material was washed with acetone, filtered and dried at 120°C under vacuum. Additionally the carbon material after chlorination process was boiled using 1M NaOH for 1h. After that the sample was neutralized using 0.1 M HCl and washed with distilled water up to pH≅7. At the end the sample was dried under vacuum at 120°C.

Both carbon nanotubes after chlorination and oxidation using sodium hydroxide were studied in the process of methylene blue (MB) adsorption from aqueous solution. Adsorption process was conducted in the batch agitator containing 500cm^3 of solution of MB. The initial concentration of MB was fixed to 10mg/dm^3, the mixing velocity - 300 rpm, the weight of carbon material - 200mg.

It was found that on the raw material adsorption process practically didn't proceed. The material is characterized by very poor wettability and its dispersion in the aqueous solution wasn't observed. Carbon nanotubes after modification processes possessed very good wettability with water and formed a homogeneous suspension. In this case reduction of MB concentration at 25°C amounted about 45%.

Microwave-assisted acid digestion method for purification of carbon nanotubes

Pełech I.*[1], Narkiewicz U.[1], Owodziń K.[1], Borowiak-Paleń E.[1]

[1]*Institute of Chemical and Environmental Engineering, West Pomeranian University of Technology, Pułaskiego 10, 70-310 Szczecin, Poland*
**e-mail: ipelech@zut.edu.pl*

Carbon nanotubes can be produced at a large scale using chemical vapor deposition method. The CVD method involves catalyst-assisted decomposition of hydrocarbons. The best results are obtained with iron, nickel and cobalt catalysts supported on various carriers. While the strong points of the CVD method are connected with its low production costs, the method's weak point is the quality of the obtained product – i.e. the presence of defects, amorphous carbon and metal particles. To purify CNTs from carbon impurities, chemical oxidation including gas phase oxidation using air or steam or by liquid phase oxidation using potassium permanganate, hydrogen peroxide or nitric acid is applied. The separation of carbon nanotubes from catalyst traces is most often carried out using acid reflux method in the presence hydrofluoric, hydrochloric, sulfuric or nitric acid.

The present work deals with the synthesis of multi walled carbon nanotubes by chemical vapor deposition using ethylene as a carbon source and nanocrystalline iron with an addition of a small amount (2-3 wt.%) of CaO and Al_2O_3 as the catalyst To the purification microwave-assisted acid digestion method was applied. Carbon materials directly after synthesis or additionally treated under air atmosphere was immersed in the Teflon vessel filled with nitric or hydrochloric acid. Then the whole was placed in the reactor heated with microwaves. Experiments were conducted under pressure in the range form 10 to 30 at. Reaction time from 5 to 60 minutes was changed.

To characterize CNTs different methods were employed. The phase composition of the samples was studied using X-ray diffraction method. Transmission electron microscopy was used to determine the type of carbon nanotubes obtained and to verify their structures. To determine metal quantity in the samples thermogravimetric analysis was applied.

CNT/ PMMA electromagnetic coating: effect of carbon nanotube diameter

Paddubskaya A.G.[1], Kuzhir P.P.*[1], Kuznetsov V.L.[2,3,4], Mazov I.N.[2,3], Moseenkov S.I.[2,3], Ishchenko A.V.[2,3], Romanenko A.I.[3,5], Anikeeva O.B.[3,5], Buryakov T.I.[3,5]

[1]*Research Institute for Nuclear Problems of Belarusian State University, 220030, Minsk, Belarus*
[2]*Boreskov Institute of Catalysis SB RAS, 630090, Novosibirsk, Russia*
[3]*Novosibirsk State University, 630090, Novosibirsk, Russia*
[4]*Novosibirsk State Technical University,630092, Novosibirsk, Russia*
[5]*Nikolaev Institute of Inorganic Chemistry, 630090, Novosibirsk, Russia*
**e-mail: polina.kuzhir@gmail.com*

In the present communication we focus on the comparative study of the electromagnetic response properties provided by polymethylmetacrylate (PMMA) filled with well purified CVD multi-walled carbon nanotubes of two different mean diameters (9nm and 12-14nm). The effect of smaller diameter together with higher electromagnetic shielding effectiveness has been observed experimentally in Ka-band and interpreted theoretically. Geometry and polarizability of individual filler constituents – the constitutive parameters of nanocarbon assemblies – is addressed here to be pointed out as controllable factors for producing effective electromagnetic coating.

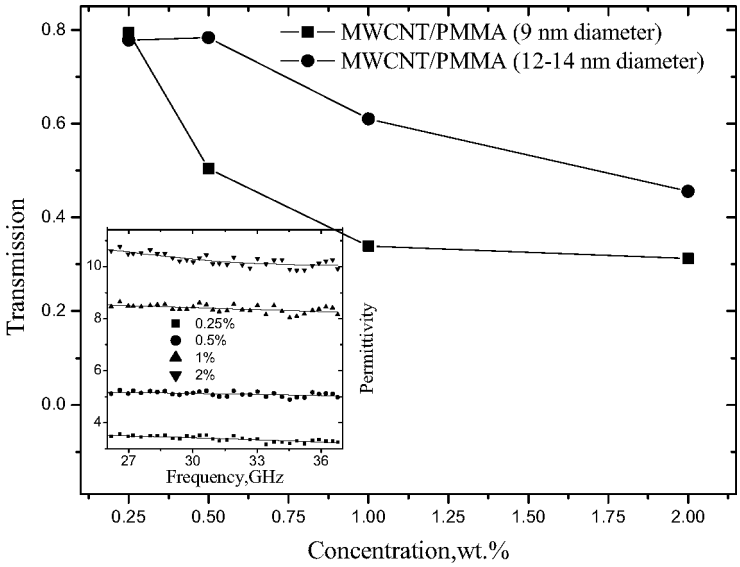

Figure: MWCNT/PMMA EM transmittance versus concentration of MWCNT. The inset figures: frequency dependence of real parts of the permittivity in Ka-band for MWCNT (9 nm diameter)/PMMA samples.

The work was partially supported by the ISTC project B-1708, and the EU FP7 project FP7-266529 BY-NanoERA.

Comparative study of NVM elements based on single-walled carbon nanotubes and silicon nanocrystals

Orlov O.M., Matyushkin I.V., Krasnikov G.Ya.

Mikron JSC, 124460, Zelenograd, Moscow, Russia
**e-mail: oorlov@sitronics.com*

Discrete storage nodes type of NVM (nonvolatile memory) devices have a high potential to improve its properties on the contrary to conventional floating gate memory; due to the absence of adjacent nodes interference further technological scaling becomes reachable. Based on Si nanocrystals (nc-Si) NVM is of considerable interest last decade [1]. One of expected applications of single-walled carbon nanotubes (SWCNTs) is NVM by using it instead of nc–Si as charge storage nodes within, e.g. SiO_2, wide-band dielectric ambient.

There are advantages [2]: 1) compatibility with a standard CMOS process (high thermal stability 1500°C); 2) supplying of a profitable CNT work function (4.8 eV) by via diameter control, chemical doping, and O_2 desorption. SSWCNTs on the SiO_2 surface can be form by various CNT growth methods [3]. The performance of two SWCNT NVM device subtypes was discussed earlier [4]: with embedded into SiO_2 vertically standing SWCNTs and horizontally lying SWCNTs. By extrapolation it was shown that after 10 years at room temperature levels of 60% and 15% stored charges are preserved for S- and L-subtypes respectively. S-subtype shows [4] better program/erase switch and enhanced retention time compared to L-subtype due to high coupling ratio (that relates with increased effective surface of control electrode) and the defect immunity based on the isolated distribution SWCNTs.

Evaluation of SONOS structure retention time gives about 100 years at room temperature condition [5]. Here we estimate the charge retention time for nc–Si NVM as 10–20 years at the 67%-level. The further improving technology and design of NVM based on SSWCNT with high coupling ratio will develop competitive devices compared to devices on nc–Si.

[1] M. Cooks. Semiconductor Today. Comp. & Adv. Silicon, 3 (2008), 45, No.5
[2] P. G. Collins, K. Bradley, M. Ishigami, and A. Zettl, Science 287, 1801, 2006.
[3] X. J. Huang, S. W. Ryu, H. S. Im, and Y. K. Choi, Langmuir 23, 991, 2007.
[4] Seong-Wan Ryu, Xing-Jiu Huang, and Yang-Kyu Choi J. Apl. Phys. Let., 91, 063110, 2007
[5] O. Orlov, N. Shelepin, F. Meyer, U. Paschen, H. Vogt. X International Conference on Nanostructured Materials NANO 2010, ROMA, Italy, Abstract book, p.78 (2010)

Solubility of functionalized carbon nanofibers in different aqueous media

Nguyen H.V., Luu S.T., Fadeeva E.V., Rakov E.G.

Mendeleev University of ChemicalTtechnology of Russia, 125047, Moscow, Russia

Carbon nanofibers (CNF) represents a variety of filamentous carbon nanomaterial and inherently are similar to multi-walled carbon nanotubes. Interaction with concentrated HNO_3 or mixture with concentrated H_2SO_4 leads to oxidation of CNFs, formation of surface carboxyl, hydroxyl, carbonyl and other oxygen-containing functional groups. The functionalization allows to form stable dispersion of CNFs in different solvents.

In our work we used functionalized CNFs with a solubility (concentration in aqueous dispersion) from 1.9 to 8.7 g L^{-1} at pH = 6–7. To measure the solubility at different pH value (in a range from –1 to 12) HCl or NaOH were added to the dispersions.

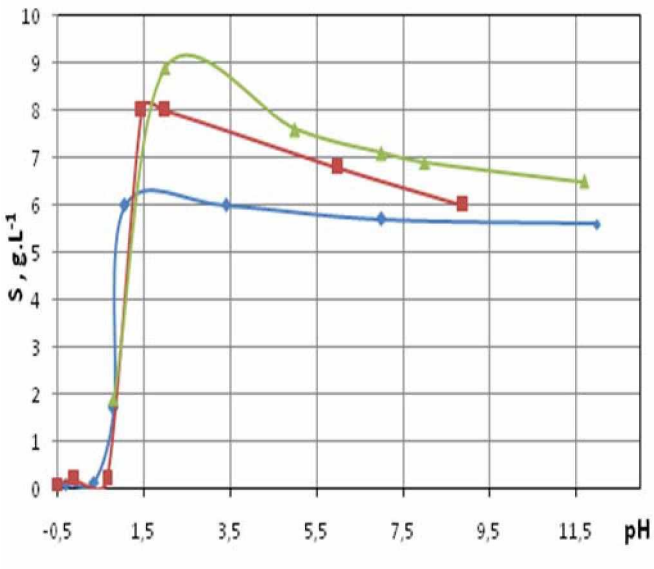

As it is shown on the presented graph, sharp change of solubility at pH = 1.0 is evident for all studied samples. The difference in solubility is due to the formation of hydrogen bonds between carboxyl groups, which are formed at pH < 1. Bonding of the adjacent CNFs leads to aggregation, constitutive growth of mean molecular mass and precipitation of the formed particles. In the area of pH > 1 deprotonation of carboxyl group and decomposition of the aggregates are evident.

The deprotonation can proceed not only at pH > 1. Addition of aqueous solutions of some salts to deposit of carboxylated CNFs also causes decomposition of the aggregates and solubilization of CNFs even at pH < 1. The mechanism of this process is connected to substitution of protons by metals due to ion exchange sorption. Such behavior was registered for $ZrOCl_2$ and $ZrOSO_4$, but was not observed for Ni and Cu salts.

Synthesis of end-cap precursor molecules for the controlled growth of single-walled carbon nanotubes

Mueller A.[1], Amsharov K.[1], Jansen M.*[1]

[1]*Max Planck Institute for Solid State Research,70569 Stuttgart, Germany*
**e-mail: M.Jansen@fkf.mpg.de*

Despite considerable advance in growth methods for single-walled carbon nanotubes (SWCNTs) it is still not possible to rationally control their diameters and chiralities.

According to recent theoretical and experimental work, growth of SWCNTs starts by nucleation of an end-cap fragment on the catalyst particle followed by subsequent growth through incorporation of carbon atoms.[1, 2] Considering this growth mechanism of CNTs, it appears prospective to avoid the usual nucleation step of CNTs leading to the formation of an end-cap with accidental geometry by introducing a predefined end-cap molecule, the structure of which can be fully controlled. Subsequent growth will lead to the desired SWCNT species as determined by the end-cap geometry.

Several precursor molecules for different SWCNT species, including armchair, zigzag or chiral type have been prepared.[3] Such polyaromatic hydrocarbons can then be condensed to the corresponding bucky bowls by catalyzed cyclodehydrogenation on a metal surface. [4]

The synthesized precursors were used for the growth scenario shown in the scheme below and their influence on the carbon nanotube growth was investigated.

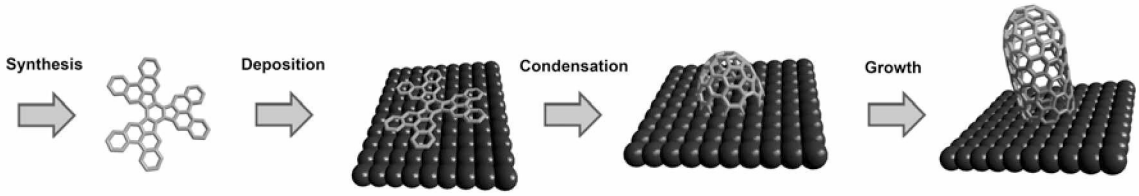

General scheme for the cyclodehydrogenation of the SWCNT end-cap precursor molecules and the subsequent growth of the CNT.

[1] Y. Ohta, Y. Okamoto, S. Irle, K. Morokuma, *J. Phys. Chem. C* **113**, 159-169 (2009).
[2] S. Hofmann, R. Sharma, C. Ducati, G. Du, C. Mattevi, C. Cepek, M. Cantoro, S. Pisana, A. Parvez, F. Cervantes-Sodi, A. C. Ferrari, R. Dunin-Borkowski, S. Lizzit, L. Petaccia, A. Goldoni, J. Robertson, *Nano Lett.* **7**, 602-608 (2007).
[3] A. Mueller, K. Amsharov, M. Jansen, *Tet. Lett.* **51**, 3221-3225 (2010).
[4] K.Yu. Amsharov, N. Abdurakhmanova, S. Stepanow, S. Rauschenbach, M. Jansen, K. Kern, *Angew. Chem. Int. Ed.* **49** , 9392 (2010).

Comparative study of reflectance properties of nanodiamonds, onion-like carbon and multiwalled carbon nanotubes

Moseenkov S.I.[1,3]*, Kuznetsov V.L.[1,3], Elumeeva K.V.[1,3], Larina T.V.[1], Anufrienko V.F.[1], Romanenko A.I.[2,3], Anikeeva O.B.[2,3]

[1]*Boreskov Institute of catalysis, 630090, Novosibirsk, Russia*
[2]*Nikolaev Institute of Inorganic Chemistry, 630090, Novosibirsk, Russia*
[3]*Novosibirsk State University, 630090, Novosibirsk, Russia*
**e-mail: moseenkov@catalysis.ru*

Carbon nanomaterials are promising candidates for potential broadband limiting applications and extremely low reflectance coatings, particularly in the infrared, visible and UV spectral regions. In this paper we have performed comparative study of diffuse reflectance of nanodiamond (ND), sp^2/sp^3 composites and onion-like carbon (OLC) and multiwalled carbon nanotubes (MWNTs) in visible and UV regions.

ND, sp^2/sp^3 composites and onion-like carbon (OLC) produced via high temperature annealing of the same set of NDs allow us to vary sp^2/sp^3 carbon ration, size of primary particle agglomerates and concentration of defects while MWNT set provides possibility to vary NT diameters and length, order/disorder degree (via high temperature MWNTs annealing).

The diffuse reflectance of carbon nanomaterials depends mainly on electronic configuration, defect concentration, size of graphene-like ordered fragments and agglomerates in nanocarbons along with their morphology. Thus the increase of nanographene shells size in the interval of 1-200 nm on ND particle (produced after elimination of surface functional groups) results in the increase of the absorbance accompanied with red shift (because of the π band's optical transition). The increase of number and size of fullerene-like shells demonstrates significant increase of absorbance (decrease of reflectance) which correlates with increase of density states at the Fermi level calculated from temperature dependence of conductivity of NDs annealed at different temperatures.

Thin MWNTs (d~10 nm) demonstrate higher absorbance than that of thick MWNTs (~20 nm). This phenomenon may be described taking into account significant difference between numbers of individual nanotubes of each type incorporated in the same volume of sample surface layers while conductivity of thinner MWNTs is lower than that of thick NTs.

Decrease of defect number in nanocarbon materials, annealed at temperature higher then Debye temperature results in the increase EMI reflectance.

Stone–Wales defect generation in carbon nanotube being fractured

Moliver S.S.

State University Ulyanovsk, 432970, Ulyanovsk, Russia
e-mail: moliver@sv.uven.ru

Quantum-chemistry modelling of small-radii nanotubes, was fulfilled in frame of INDO parametrization, the same one had been applied previously to other condensed states of carbon. These total-electron calculations of the supercell models reveal some properties of the Stone–Wales defect (SW), i.e. a topo-chemical turning of a C–C bond, providing 5-7-7-5 cycling within graphene net. It was found, that rolling of the plane graphene into (8,0) nanotube decreases SW defect formation energy by 0.6 eV. The electronic spectrum obtains resonant levels when SW defect appears in the tube. Under the fracture-type loading (see figure below) of the tube, SW position at the compressed side has an advantage over stretched-bond side. Critical value of the zigzag (8,0) tube fracture was found to be 1.7 degree (this angle is marked on figure below): it is a ductility barrier, at which SW defect generation reduces the total energy [1].

Recently it was proved by many-electron calculations, that SW defects and their complexes may be generated in carbon nanotubes under tensile strain [2-3]. To compare our semi-empirical calculations with *ab initio* level [3], one should note the similarity of the above mentioned difference of SW defect formation energy in graphene and nanotubes.

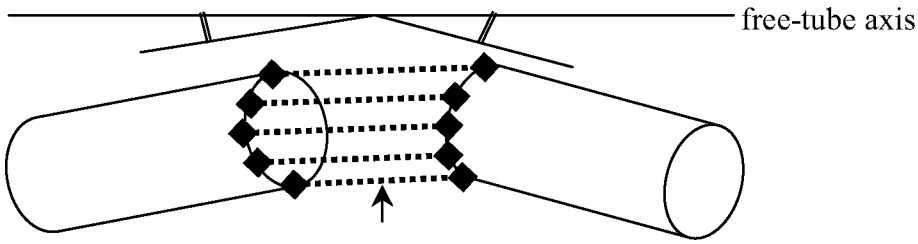

Supercell model of (8,0) tube of 192 atoms is divided on 2 cylinders, whose axes make a fracture. 5 of 3 C–C bonds between undistorted half-tubes are shown by dashed lines.

Grant-in-aid 08-03-97000 of Russian foundation for basic research is acknowledged.

[1] Moliver S.S., Zimagullov R.R., Semenov A.L. *Tech.Phys.Lett.* **37**, in print (2011).
[2] Orlikowski D., Buongiorno Nardelli M., Bernholc J., Roland C. *Phys.Rev.Lett.* **83**, 4132 (1999); *Phys.Rev.B.* **61**, 14194 (2000).
[3] Zhao Q., Buongiorno Nardelli M., Bernholc J. *Phys.Rev.B.* **65**, 144105 (2002).

Dielectric properties of the nano composites on the base of crosslinked poly(ε-caprolactone)

Meriakri V.V.*[1], Chmutin I.A.[1], Ryvkina N.V.1, Zhou S.[2]

[1]*Kotel'nikov Institute of Radioengineering and Electronics RAS (Fryazino branch), 141190, Fryazino Moscow Region, Russia*
[2]*Southwest Jiaotang University, Chengdu, 610031, P. R. China*
**e-mail: meriakri@ms.ire.rssi.ru*

Till now the dielectric parameters of nano composites based on crosslinked poly(ε caprolactone) (cPCL) remain poorly investigated in enough wide frequency range.

In the present work a research of the complex dielectric permittivity of cPCL composites with nano particles of multiwall carbon nano tubes (MWNT), nano Fe_3O_4 and Fe_3O_4 absorbed MWNT is carried out at wide ranges of frequencies $f = 10^{-1}$–2×10^{6} Hz and in the millimeter wave range (f = 80-100 GHz). On different frequencies the different equipment was used, and different measurement techniques of parameters of materials were applied.

At low frequencies up to 10 kHz we used laboratory equipment, at frequencies from 10 kHz to 2 MHz device BDS-40 (Novocontrol) was used.

In the millimeter range Scalar Network Analyzer working in the frequency band 78–118 GHz was applied. The complex parameters of a material, such as real n and imaginary k parts of the refraction index, real $\varepsilon' = n^2 - k^2$ and imaginary $\varepsilon'' = 2nk$ parts of dielectric permittivity in the millimeter range were calculated from the measured quantities of transmission and reflection coefficients of plane- parallel samples.

Sample cPCL changes ε' from 13 at frequency 10^{-1} Hz to 7 at frequency 10 Hz and does not changes up to 2 MHz. Nano composites have much more ε', from 48 to 19 at frequency 10^{-1} to 13-8 more than 10 Hz. $\varepsilon''$of cPCL changes from 40 at frequency 10^{-1} Hz to 0.03, has minimum at 200 kHz, and then increases up to 0.08 at 2 MHz. Nano composites have ε'' = 115-40 at frequency 10^{-1} Hz and then decreases up to ′ approximately 0.1 at frequency 2 MHz.

In the frequency band 90–100 GHz sample of cPCL has ε' 2.9 and ε''= 0.03. Nano composites have ε' = 3.0- 3.4 and ε'' = 0.045 -0.27.

[1] B.M. Garin , I.A. Chmutin, V.V. Meriakri, B.A. Murmuzhev, E.E. Chigryai, M.P. Parkhomenko, V.S. Solosin, S.V. von Gratowsky, N.A. Fedoseev, Chen Wang, Jingsong Zhu, International Kharkov Symposium on Physics and Engineering of Microwave, Millimeter and Submillimeter Waves, Proceedings, paper W 10, Kharkov, Ukraine, June 31-26, 2010, IEEE Catalog Number: CFP10780-CDR, ISBN: 978-1-4244-7898-9.

Anizotropic reinforcement of polymeric composites properties by electromagnetic orientations of carbon nanotubes

Latypov Z.Z.

Institute for Analytical Instrumentation RAS, 198103, St. Petersburg, Russia
e-mail: Latypov_ Zeidel@yandex.ru

We consider methods of nanoparticles orientations in polymer matrix by various electromagnetic fields to produce composites with desirable properties of individual nanotubes as bulk properties. Analytical expressions are obtained for the purposeful choice of a method with taking into account properties of particles and field strengths. At present the following methods of particle orientation are under consideration by affecting them with 1) the external electric field, 2) the external magnetic field, 3) the nonuniform electric field of dielectrophoretic phenomena. Each method orients the particles according to their properties, which makes it possible to create desirable composites. The conditions for particle orientation with polarizability α and the magnetic moment p_b are: **1.** $E \geq \sqrt{4kT \ln|tg\theta| / \varepsilon_0 \alpha} / \theta$, where E is the electric field with strength, ε_0 is the electric constant, θ is the angle for the nanoparticle with respect to $\vec{E}$, T is the temperature of liquid polymer precursor; **2.** $B = (8\pi r^3 \eta / p_m t)\{\ln|tg\theta/2| - \ln|tg\theta_0/2|\}$, where B is magnetic field intensity, t is time of alignment, η is fluid matrix viscosity, r is radius of sphere equal particle volume, θ_0 and θ are initial and final angles between vectors $p_ь$ and B. Comparison of the considered methods allow us to conclude: 1) For using the electrostatic field the polarizability of particles must be not lower than $\alpha \approx 10^4$ nm^3; 2) For using the magnetic field the particles must have sufficiently high magnetic moments. This method allows to obtain films of relatively large size which are often in demand: 3) In using DEP it is difficult to obtain films larger than 1cm^2 in area. 4) Analytical formulas for fields intensities E and B helps to choose the method.

Alignment of single-wall carbon nanotubes along preferred axis in suspensions and polymeric films

Kuznetsov K.M.*[1,2], Arutyunyan N.R.[1], Chernov A.I.[1], Obraztsova E.D.[1]

[1]*A.M. Prokhorov General Physics Institute RAS,119991, Moscow, Russia*
[2]*Moscow State Institute of Radio-engineering Electronics and Automation, 119454, Moscow, Russia*
**e-mail: zrezop@mail.ru*

Physical properties of single-walled carbon nanotubes (SWNTs) have an anisotropic character due to their unique geometrical structure. In order to observe and to investigate an anisotropic character of SWNT ensemble it is necessary to form a massif of nanotubes oriented along some preferential direction [3].

The ordering of SWNTs along some preferred axis could be achieved using the self-assembly process of nanotubes in suspensions [1]. The substrate was placed into an enriched suspension of SWNTs. SWNTs precipitated on the substrate during the evaporation of the liquid, keeping horizontal orientation along the line of meniscus. SWNTs ordering may be also reached by the mechanical stretching of different polymeric films with nanotubes implemented [2].

It was discovered that the width of the angular distribution of nanotubes in the structures described above was equal to 7 degrees. The polarization dependence of the main Raman modes was investigated for semiconducting and metallic SWNTs. The laser wavelength was $\lambda = 647$ nm. The behavior of these modes varied depending on the relative orientation of the sample and the polarization of the incident radiation. That can be explained by the different mode symmetry.

The work was supported by the federal target program "Scientific and academic and teaching staff of innovative Russia" for 2009–2013, contract П1286, and the Russian President grant МК-2164.2011.2.

[1] Engel M., Small J.P., Steiner M., Freitag M., Green A., Hersam M., Avouris P., *ASC Nano* **2**(12), 2445 (2008).
[2] Ichida M., Mizuno S., Kataura H., Achiba Y., Nakamura A., *Appl. Phys. A* **78**, 1117 (2004).
[3] N.R. Arutyunyan, A.I. Chernov, E.D. Obraztsova, *Phys. Stat. Solidi b* **247**, 2814 (2010).

Impedance of single-wall carbon nanotubes fibers

Ksenevich V.K.*[1], Gorbachuk N.I.[1], Poklonski N.A.[1], Samuilov V.A.[1 2], Kozlov M.E.[3], Wieck A.D.[4]

[1]*Belarus State University, 220030, Minsk, Belarus*
[2]*State University of New York at Stony Brook, N.Y. 11794-2275, USA*
[3]*The Nano Tech Institute, University of Texas at Dallas, TX 75083-0688, USA*
[4]*Bochum Ruhr-University, 44780, Bochum, Germany*
**e-mail: ksenevich@bsu.by*

Understanding of charge transport mechanisms in carbon nanotubes arrays is a crucial task for their possible application as a humidity-, gas- and biosensors and as interconnects in integrated circuits. Therefore electrical transport in carbon nanotubes arrays of different morphology has been studied intensively during last decades.

Highly non-linear DC electrical properties of the single-wall carbon nanotubes (SWCNT) fibers were earlier observed [1]. In order to clarify the physical nature of nonlinearity and to determine the role of contact barriers between individual nanotubes in fibers impedance measurements of SWCNT fibers were carried out in the frequency range of $100-10^6$ Hz at temperatures $4.2<T<300$ K and in the range of applied bias voltage 0-5 V. It was found (see Fig.1) that in the low frequency range ($f<1$ kHz) at the bias voltage $U_b > 2$ V sign of the imaginary part of impedance was changed from negative to positive, in-dicating the existence of the crossover from capacitive reactance to inductive one.

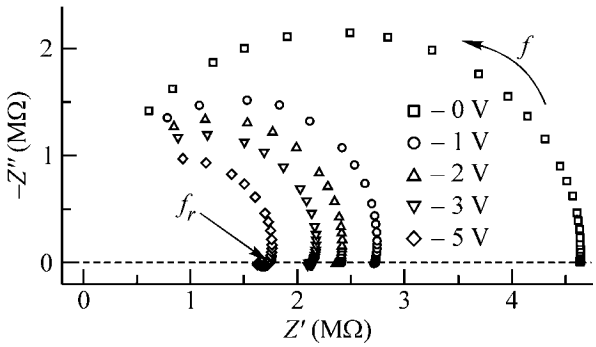

Figure. Impedance diagram of SWCNT fiber measured at T=4.2 K with different applied DC bias voltage.

This crossover is induced by the decreasing of height of the energy barriers between nanotubes at the rising of U_b. As a result decrease of the fiber's impedance is accompanied by the rising of the role of kinetic inductance of nanotubes, which is predicted to be much larger than magnetic inductance [2].

[1] V.K. Ksenevich, V.B. Odzaev, Z. Martunas, D. Seliuta, G. Valusis, J. Galibert, A.A. Melnikov, A.D. Wieck, D. Novitski, M.E. Kozlov, and V.A. Samuilov, *J. Appl. Phys.* **104**, 073724 (2008).

[2] P.J. Burke, IEEE Trans. *Nanotechnol.* **2**, 55 (2003).

Investigation of the interaction between some polymers and carbon nanotubes

Zaporotskova I.V.*, Krutoyarov A.A., Krutoyarova N.V., Perevalova E.V., Boroznin S.V.

Volgograd State University, 400062, Volgograd, Russia
**e-mail: irinaz@rbcmail.ru*

Carbon nanotubes are ideal reinforcing materials, including for polymeric materials, because they have unique properties. Carbon nanotubes in polymer matrices have a great influence on the electrical conductivity, viscosity and other transport properties, being a hybrid of nano-scale fillers and additives [1].

A theoretical study of the interaction between the nanotubes and monomer units of several common polymers has been done. The mechanisms of these processes and their main characteristics have been identified. The possibility of joining of the monomer unit of ethylene (CH2=CH2) and propylene (CH3-CH=CH2) to the external surface of single-walled carbon (6, 6)-nanotube *have been* investigated. The research was carried out by applying the Molecular Cluster model (MC) and semi-empirical quantum-chemical MNDO scheme [2].

The process of adsorption for both cases was simulated by step-by-step approach (with a step of 0.1 Å) of monomer molecules of polyethylene or polypropylene to the carbon nanotube surface. The geometry of system was optimized on each step. The calculations have allowed to model energy curves of these processes. The research showed the most probable mechanisms of these processes and their basic characteristics. The calculated values of the adsorption energy suggested the strength of the resulting hybrid polymer material.

It was proved, that the hybrid polymer nanostructures are stable. The values of intermolecular interaction energy have been carried out. This research suggests that the reinforcement of polymer polyethylene and polypropylene matrices with carbon nanotubes is possible and efficient. This fact cans ensure the creation of new polymer nanocomposite materials with new physical and chemical properties.

This work was suggested with Federal Target Program “Scientifical and pedagogical Staff of Innovative Russia” 2009-2013 (grant No.P328).

[1] Dyachkov P.N., Carbon nanotubes: Structure, properties and applications .- Moscow. - 2005. –196 P.

[2] Zaporotskova I.V., Carbon and noncarbon nanomaterials and composite structures on its base: the structure and electronic properties. - Volgograd: VolSU, - Volgograd, 2009.– 490.P.

About the mechanism of field emission of carbon nanostructures

Kosakovskii G.G.*, Kosakovskaya Z.Ya., Orlov A.N., Smolovich A.M.

Institute of Radioengineering and Electronics RAS,Mokhovaya 11-7, Moscow, 125009, Russia
**e-mail: german_kos@mail.ru*

The mechanism of field emission from nanodimensional cathodes doesn't understand [1]. The carbon nanotubes were most studied among carbon cathodes. The majority of researchers treat the field emission characteristics of carbon nanotubes cathodes by Fauler-Nordgeim model accepting it as the pointed cathode with metal conductivity and very big strengthening factor of electric field intensity [2]. It is known that the carbon nanotube and graphite is not metal. They are semimetal with energy gap width Eg =0 and two type of charge carrier, which together take part in field emission. The articles where authors observed the deviations of I-V characteristics from Fauler-Nordgeim law for carbon nanodimensional cathodes are known. For example, data of emission current CNT cathode appreciably above their value which have been calculated by Fauler-Nordgeim equation [3].

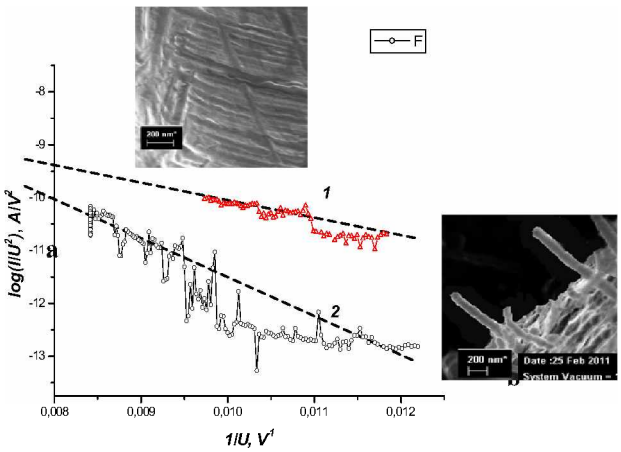

Fig.1. The I-V characteristic in the Fauler-Nordgeim coordinates for the graphite nanoplates and CNT cathodes . On inserts SEM image of their structures

In this work the field emission mechanism from various carbon nanostructures was studied. Graphite nanoplates (Fig. 1a), carbon multi walled nanotube (Fig. 1b) and normal aligned nanotube film were deposited on a nickel wire. The aspect ratio approximately was 80 and 600 for graphite nanoplates and carbon nanotube cathodes respectively. The I-U characteristics of all carbon cathodes have been measured in cell of electron microscope Carl Zeiss NEON-40. It is noted, the I-V characteristic in the Fauler-Nordgeim coordinates isn't linear for all cathodes. (Fig.1). The strengthening factor of electric field intensity near at the cathode top was calculated for both types cathodes. It finds the wide disagreement of strengthening factors with their aspect ratio. Consequently the Fauler-Nordgeim model for carbon nanostructure is not valid.

[1] Stetsenko B.V., *JPT* **81**(4), 152 (2011).
[2] Eletskii A., *UFN* **172**(4), 402 (2002).
[3] Stetsenko B.V., Shchurenko A.I., *Plasma Physics* 136 (2009).
[4] Sveningsson M., Morjan R.-E. et. al., *Appl. Phys.A* **73**, 409 (2001).

Toroidal modification of carbon nanotubes

Kondrashov V.A.*, Nevolin V.K.

Moscow Institute of Electronic Technology, 124498, Zelenograd, Russia
**e-mail: kondrashovva@mail.ru*

At the moment, carbon nanotubes (CNTs) are widely known and widespread material that is used in various industries such as construction, engineering, electronics, space technologies. For their realization are used different nanotubes, multiwall and singlewall, of different length and diameter. In this paper we explore another type of carbon nanotubes, rolled into a torus shaped ring. Such nanotubes may possess unique electrical and magnetic properties, such as weakly damped ring currents which generate significant diamagnetism.

Three approaches of CNTs modification are considered: ultrasonic treatment, exposure to magnetic fields and modification by spark. All these options imply that the change will occur with carbon nanotubes which have already prepared in another process. Research of the material, obtained by these methods, is carried out by atomic-force and high-resolution scanning electron microscopy.

Ultrasonic treatment of carbon nanotubes is an oxidizing environment. Since the cavitation bubbles appear on the inhomogeneities in the bulk of liquid, the bubbles will be formed near the CNTs, which lead to their flexion, by the impact of capillary forces on CNTs due to collapsing bubble. The size of obtained CNT torus was 500-1000 nm in diameter and 10 nm thickness.

In fact the impact of the magnetic field is the same way as the first modification. Carbon nanotubes are in an oxidizing environment and are subjected to ultrasonic treatment and the impact of external rotating magnetic field. There are some publications about the application of a magnetic field for separation of carbon nanotubes, so we can suggest that CNTs will rotate in the field, as a rotor induction motor does. The size was 500 nm in diameter and 5 nm thickness.

There is the third of methods of CNTs modification. When spark discharge is going through the carbon containing gas and catalyst particles (Fe, Ni, Co), carbon nanotubes are growing. Such catalyst particles will rotate in an electromagnetic field of the discharge, thus the growth of ring shaped nanotubes will start. The size of the CNT torus was 200 nm in diameter and 12 nm thickness.

There is the possibility to combine these methods to increase the quantity of the material. Thus it is proposed to produce a spark discharge (28 kV, 190 Hz) in a carbon-containing dielectric liquid (2-propanol) with a solution of carbon nanotubes. Due to discharge it will be observed the effect of cavitation which is mixing of CNTs in solution. The discharge will evaporate and ionize a liquid, releasing free carbon which will create a reducing environment. Due to the discharge CNT will be activated for twisting by the spark field and/or external magnetic field, which will lead to the folding and stitching the ends of carbon nanotubes by free carbon. Expected size will near 80 nm in diameter and 3 nm.

Thus, we have developed three approaches to obtain toroidal carbon nanotubes and have shown how to combine these methods at one process.

Investigation of the effect of bending on the polymerization of fullerenes inside carbon nanotubes

Glukhova O.[1]*, Kirillova I.[2], Kolesnikova A.[2]

[1]*Department of Physics, Saratov State University, 410012, Saratov, Russia*
[2]*Institute of Nanostructures and Biosystems, Saratov State University, 410012, Saratov, Russia*
**e-mail: glukhovaoe@info.sgu.ru*

The aim of this work is to investigate theoretically the influence of peapod bending on the process of C_{60} fullerenes polymerization with the help of the model that effectively combines molecular and quantum techniques and is well recommended to study the mechanical properties of carbon nanostructures [1-3].

The process of peapod bending formed from nanotube (10,10) with the length of 0.244 nm, filled with twenty-seven C_{60}. C_{60} is distanced from the tube walls at a distance equal to 0.338 nm. Fullerenes are on the tube axis at the distance between their centers equal to 0.815 nm. The polymerization of fullerenes and partial connection with the walls of the tube were observed at the bending of 270 degrees.

It was established that at such a bending:

1. The atomic structure of peapod is not destroyed.
2. The nanotubes surface of smaller radius is becomes wave-like and in some places of trough is connected with the fullerenes.
3. The fullerenes come to the distance of 0.14 nm between the atoms of the cell and are polymerized.
4. The hybrid compound of the nanotube, which was formed, retains the atomic structure unchanged even when there is no external load.

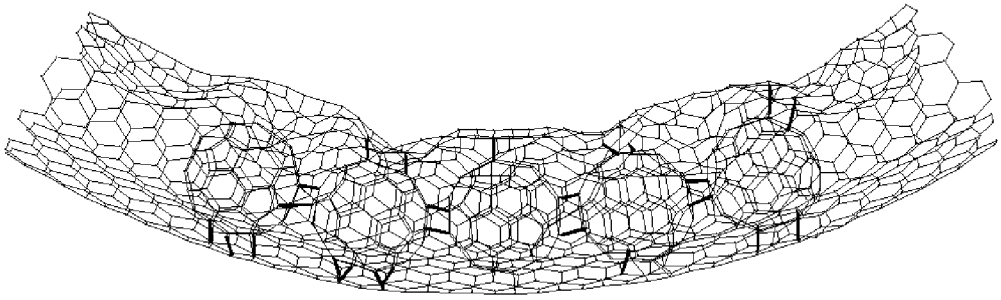

Figure. Fragment of peapod at bending of 270 degrees. The thick lines show the connections formed during the polymerization of fullerenes with neighboring fullerenes and a nanotube.

[1] O.E. Glukhova, I.N. Saliy, R.Y. Zhnichkov, I.A. Khvatov, A.S. Kolesnikova, M.M. Slepchenkov. *Journal of Physics: Conference series*, **248**, 012004 (2010).

[2] O.E. Glukhova, I.V. Kirillova, I.N. Saliy, A.S. Kolesnikova, M.M. Slepchenkov. *Proc. of SPIE* **7910**, 79101 (2011)

Theoretical study of CNTs functionalized by fluorine and chlorine

Khavrel P.A.*, Ioffe I.N., Chernukhina A.A., Skokan E.V., Sidorov L.N.

M.V. Lomonosov Moscow State University, Chemistry Department, 119991, Moscow, Russia
**e-mail: khavrel@thermo.chem.msu.ru*

Functionalization of carbon nanotubes (CNTs) via chemical attachment of atoms, molecules or molecular groups has attracted much attention, as it offers a prospective approach towards modification of the electronic, chemical, optical and mechanic properties of CNTs. Besides, CNTs can be used as starting material for bulk synthesis of graphene nanoribbons (GNRs), another promising system for nanoelectronics, by means of axial unzipping [1]. To date, studies of polyfunctionalized CNTs are mostly limited to the theoretical realm, which is due to the complexity of experimentally obtainable mixtures. Unfortunately, most of the said theoretical studies consider addition motives that are not supported by any kinetic or thermodynamic arguments.

The present quantum chemical study follows the sequential functionalization approach based on energetic criteria, as suggested by the authors of [2]. It is aimed at determining the most preferable arrangement of fluorine and chlorine atoms chemisorbed on a CNT's backbone. The choice of fluorine as fuctionalizing addend is motivated by high stability of carbon-fluorine bonds, which makes fluorinated CNTs a reliable test case for future experimental verification of the theoretical results. Chlorine addends are more interesting with regard to unzipping CNTs into GNRs analogously to the theoretical suggestions made in [3] for hydrogenated CNTs. Chlorine addends may be even more efficient as promotors of unzipping due to lower C-Cl bond energy, which facilitates the necessary sigmatropic rearrangements. Model systems considered in this work are based on the (6,6) and (12,0) CNTs. Quantum chemical calculations were performed at the DFT level of theory using the PRIRODA package (PBE exchange correlation functional, TZ2P basis set) [4].

[1] D.V. Kosynkin, A.L. Higginbotham, A.Sinitskii, J.R. Lomeda, A.Dimiev, B.K. Price and J.M. Tour, *Nature* **458**, 872 (2009).
[2] S.M. Avdoshenko, I.N. Ioffe and L.N. Sidorov, *ACSNano* **4**, 6260 (2010).
[3] S. Berber and D. Tomanek, *Phys.Rev. B* **80**, 075427-1 (2009).
[4] D.N. Laikov, *Chem. Phys. Lett.* **281**, 151 (1997).

Influence of stretch ratio on the dielectric response of polymer composite, consisting multiwall carbon nanotubes

Kanygin M.A.[1*], Bychanok D.S.[2], Okotrub A.V.[1]

[1]*Nikolaev Institute of Inorganic Chemistry SB RAS, 630090, Novosibirsk, Russia*
[2]*Research Institute for Nuclear Problems Belarusian State University, 220030, Minsk, Belarus*
**e-mail: mkanygin@gmail.com*

Composite materials based on the organic polymers with carbon nanotubes (CNT) are the object of many scientific investigations according to promising of their application during creation of novel broadband absorbing and reflecting electromagnetic wave materials [1]. Insertion of nanotubes in the composition of composite material allows producing materials, which have variable dielectric and magnetic properties. Materials with such properties can be demanded during creation of electromagnetic shields with definite absorption coefficients [2].

Influences of stretch ratio on the dielectric properties of obtained composite materials are propose in the present work. Composite materials were produced using CNT, which were produced by chemical vapor deposition method. Concentrations of nanotubes in the samples were varied from 0.1% to 2%. Polystyrene was used as a matrix of composite material. Obtained samples were mechanicaly stretched up to 30%. For comparison with experimental results polystyrene sample without nanotubes were espoused under the same conditions. The homogeneous of derived composite materials were investigated by optical microscopy methods. The dielectric response of samples was measured by double-electrode method. Investigation of stretch influence on the value of dielectric permittivity show that rick of composite material lead to decrease of dielectric permittivity of which is a result of orientation changes of nanotubes in the samples. It was detected that dielectric permittivity proportional decrease in comparison with stretch ratio.

[1] P. Saini, V. Choudhary, B.P. Singh, R.B. Mathur, S.K. Dhawan, *Materials Chemistry and Physics* **113**(2-3), 919 (2009).

[2] M.C. Paiva, B. Zhou, K.A.S. Fernando, Y. Lin, J.M. Kennedy, Y.-P. Sun, *Carbon* **42**, 2849 (2004).

The research on adsorption of methane on carbon nanotube surface

Ivanchenko G.S.*, Nevzorova Yu.V., Mikhaylov A.V.

Volgograd State University, 400062, Volgograd, Russia
**e-mail: genaivanchenko@yandex.ru*

High sensitivity of electronic properties to the presence of molecules, sorbed on a surface, as well as the record size of a specific surface area (1300 m_2/g), promoting such adsorption make carbon nanotubes (NT) a perspective basis for the creation of subminiature biochemical sensors [1]. The major part of natural gas is up to 98 % composed of methane (CH_4). Thus, in order to create such a device it is necessary to research the influence of adsorption of methane molecule on the surface of carbon nanotubes on their electronic properties.

The result of the conducted research was the calculation of key parameters of the process of methane atom adsorption on the carbon nanotubes surfaces of various types [2]. It has been shown that adsorption can be performed in four different ways: physical adsorption of methane molecules; adsorption of hydrogen atom on NT and formation of CH_3 radical; adsorption with decomposition into H and CH_3; 2H and CH_2. In all cases there appears a change of the width of the forbidden zone of nanotubes, and all the states are steady.

As a result, it is possible to say that the methane molecule will be adsorbed onto a surface of carbon NT of small diameter. Therefore, it is rational to use the tubes of the diameter of no more than 20 nm for the creation of a gas sensors on the basis of carbon NT. The values of bond energies and top filled and bottom vacant orbitals, the values of the forbidden zones of various carbon nanotubes with the adsorbed methane molecule have been received.

The work was held during the Federal Aimed Program “The Scientific and Scientific-Pedagogical personnel of the innovative Russia”, 2009-2013 (the State contract № P892).

[1] Eletski A.V. *UFN* **174**(11), 1191-1231 (2004).
[2] Lebedev N.G. Metodi kvantovoy himii dlya issledovaniya elektronnogo stroeniya molekul i kristallov. Chast. 1 Metod Hartri – Foka / N.G. Lebedev. – Volgograd. VolSU. - 2010. – P. - 116.

Electrical conductivity of composite nanomaterial with carbon nanotubes

Ichkitidze L.P.*, Podgaetsky V.M., Selishchev S.V.

Moscow Institute of Electronic Technology, 124498 Moscow, Russia
**e-mail: leo852@inbox.ru*

Conducted are the experimental studies of the electrical conductivity σ of thick layers (thickness 10-80 μm) from composite nanomaterial (CNM), consisting of a gel for medical purposes based on carboxymethylcellulose (CMC) and multiwall carbon nanotubes (MWCNT) by "Taunit". Also studied is the dependence of σ of CNM from the intensity of infrared laser radiation (λ=970 nm).

In the 4% aqueous solution of CMC at t = 20 °C the value of σ is negligible ~ 0.5 S/m, its temperature dependence is positive with value $\alpha \sim 0.0024$ K^{-1} in the range t = (20-70)°C. After adding into the solution of CMC the MWCNTs with $c \leq 0.5$ wt. % the obtained suspension was carefully stirred, then put onto a strip of cotton cloth and exposed to laser irradiation.

In the dried layers of CMC+MWCNT the value of $\sigma \approx 1.5$ kS/m, $\alpha \sim 0.004$ K^{-1}, the percolation threshold corresponded to $c \sim 0.1$ wt.%. In the control samples, consisting of CMC and carbon black K-354 with $c \sim 0.5$ wt.% and prepared identically to CMC+MWCNT, obtained values of $\sigma \sim 0.06$ S/m and $\alpha \sim 0.004$ K^{-1}, and the percolation threshold was not observed.

Laser irradiation of the samples resulted in an increase of their relative conductivity $\sigma_w = (1-\sigma_T/\sigma)/W$, where σ is the conductivity before irradiation, σ_T – the conductivity after irradiation, W – the irradiation power density in [W/cm^2]. In layers of CMC+carbon black observed were higher values of σ_w = 25-35 %·cm^2/W, while for layers of CMC+MWCNT the value of σ_w = 3-5 %·cm^2/W. Photosensitivity of the studied samples is apparently due to the·bolometric effect.

High specific electrical conductivity, low percolation threshold, photosensitivity and biocompatibility allow us to consider the studied conducting composite nanomaterial as promising for biomedical and other applications.

Composite nanomaterial based on protein and multiwall carbon nanotubes

Ichkitidze L.P.*[1], Selishchev S.V.[1], Ryndina T.S.[1], Tabulina L.V.[2], Shulitski B.G.[2], Galperin V.A.[3], Shaman Yu.P.[3]

[1]*Moscow Institute of Electronic Technology, 124498 Moscow, Russia*
[2]*Belarusian State University of Informatics and Radioelectronics, Belarus, Minsk*
[3]*SRC SMC "Technological centre", 124498 Moscow, Russia*
**e-mail: leo852@inbox.ru*

The optical and mechanical properties of bulk composite nanomaterials (BCNM) based on bovine serum albumin (BSA) and multiwall carbon nanotubes (MWNT) are investigated.

For the synthesis of MWCNT used was bimetallic catalyst Fe-Mo/MgO. Synthesis of MWNT at 900°C took place in a stream of Ar and CH_4 for 40 minutes. After synthesis the material was subjected to multi-step chemical processing, which resulted in sticking of the functional groups to MWCNTs (func.), enabling the formation of stable aqueous suspensions. Proportion of MWCNTs in the final material after treatment was 95±1 wt. %.

In 25% aqueous solution of BSA were added the MWCNTs, MWCNT (func.) in the interval (0.004-0.1) wt.%, while for the control samples added was black K-354 in the same proportions. Suspensions of BSA+MWCNT, BSA+MWNT (func.), BSA+black were obtained after mechanical and ultrasonic stirring and decanting.

There were established the following absorption coefficients at a wavelength of 970 nm: for BSA solution – 0.004 mm^{-1}, for a suspension of MWCNT (func.) – 0.06 mm^{-1}, of BSA+black – 0.4 mm^{-1}, of BSA+MWCNT – 0.17 mm^{-1}, of BSA+MWNT (func.) – 1.1 mm^{-1}. Higher absorption coefficient in suspensions of BSA+MWCNT (func.) were caused by many factors, perhaps including their high uniformity and the increase in defectiveness of MWCNT (func.) during functionalization.

Solutions and suspensions were exposed to the laser radiation at wavelength of 970 nm in different modes (pulse, continuous) while varying levels of power and exposure time. The hardness of the samples was measured by Vickers.

The studies have shown that the maximum hardness (220-320 MPa) BCNM is 3-5 times higher than that of the dried BSA and BSA+black and is at the level of hardness of human bone tissue (~ 500 MPa).

Semi-analytical theory of exciton fine structure in carbon nanotubes

Goupalov S.V.*[1,2]

[1]*Jackson State University, Jackson, MS 39217, USA*
[2]*Ioffe Institute, 194021, St.Petersburg, Russia*
**e-mail: serguei.goupalov@jsums.edu, goupalov@coherent.ioffe.ru*

Optical properties of single-walled carbon nanotubes (CNTs) are dominated by the excitonic effects. The high spin and subband (valley) degeneracy of the electron-hole pair ground state in the absence of the Coulomb interaction leads to a fine structure of excitonic levels when this interaction is taken into account.

It has been realized that both the long-range and the short-range parts of the Coulomb interaction are essential for a description of the exciton fine structure in CNTs. It has long been believed [1,2] that the best way to account for the short-range part of the Coulomb interaction in CNTs within the tight-binding method is to replace the Coulomb potential by the phenomenological Ohno potential of the form $V(r) = \frac{U}{\sqrt{\left(\frac{rU}{e^2}\right)^2 + 1}}$, where U is the energy cost to place two electrons on a single site.

We present an alternative approach whereby the matrix elements of the Coulomb potential are expanded into a series over CNT's one-dimensional reciprocal lattice vectors, $g_n = 2\pi n/|\boldsymbol{T}|$, where $\boldsymbol{T}$ is the CNT translational vector [3]. We show that, in order to make a non-vanishing contribution to this expansion, the reciprocal lattice vector g_n must satisfy the condition $|n| < N/M$, where N and M are the chirality-specific integers relating the chiral, $\boldsymbol{C}_h$, symmetry, $\boldsymbol{R}$, and translational, $\boldsymbol{T}$, vectors of the CNT by $N\boldsymbol{R} = \boldsymbol{C}_h + M\boldsymbol{T}$ [2] (N has meaning of the number of hexagons within the CNT unit cell).

We obtain analytical expressions for the Coulomb matrix elements which provide an insight into exciton physics which cannot be gained using a formalism based upon the phenomenological Ohno potential [1,2]. The calculated splittings between the dark and bright exciton states are in good agreement with the results of recent measurements [4,5].

[1] V. Perebeinos, J. Tersoff, P. Avouris, *Phys. Rev. Lett.* **92**, 257402 (2004).
[2] J. Jiang, R. Saito, Ge.G. Samsonidze, A. Jorio, S.G. Chou, G. Dresselhaus, M.S. Dresselhaus, *Phys. Rev. B* **75**, 035407 (2007).
[3] R. Saito, G. Dresselhaus, M.S. Dresselhaus, *Physical Properties of Carbon Nanotubes* (Imperial College Press, London, 1998).
[4] I.B. Mortimer, R.J. Nicholas, *Phys. Rev. Lett.* **98**, 027404 (2007).
[5] A. Srivastava, H. Htoon, V.I. Klimov, J. Kono, *Phys. Rev. Lett.* **101,** 087402 (2008).

Implications of time-reversal symmetry for band structure and optical properties of carbon nanotubes

Goupalov S.V.*[1,2]

[1]*Jackson State University, Jackson, MS 39217, USA*
[2]*Ioffe Institute, 194021, St.Petersburg, Russia*
**e-mail: serguei.goupalov@jsums.edu, goupalov@coherent.ioffe.ru*

When single-particle electron states in single-walled carbon nanotubes (CNTs) are characterized by two-dimensional wave vectors with the components K_1 and K_2 along the CNT circumference and cylindrical axis, respectively, then two such vectors symmetric about a ***M***-point in the reciprocal space of graphene are shown to be related by the time-reversal operation. We show that to each CNT there correspond five relevant ***M***-points with the following coordinates [1]: $K_1^{(1)} = N/2R$, $K_2^{(1)} = 0$; $K_1^{(2)} = M/2R$, $K_2^{(2)} = -\pi/T$, $K_1^{(3)} = (2N-M)/2R$, $K_2^{(3)} = \pi/T$, $K_1^{(4)} = (M+N)/2R$, $K_2^{(4)} = -\pi/T$, and $K_1^{(5)} = (N-M)/2R$, $K_2^{(5)} = \pi/T$, where *N* and *M* are the integers relating the chiral, $\boldsymbol{C}_h$, symmetry, ***R***, and translational, ***T***, vectors of the CNT by $N\boldsymbol{R}=\boldsymbol{C}_h + M\boldsymbol{T}$ [2], $T=|\boldsymbol{T}|$, and *R* is the CNT radius. We show that the states at the edges of the one-dimensional Brillouin zone which are symmetric about the ***M***-points with $K_2 = \pm\pi/T$ are degenerate due to the time-reversal symmetry.

We also discuss implications of the time-reversal symmetry for optical properties of CNTs [3].

In addition to the ***M***-points, we obtain explicit expressions for the coordinates of the ***K***-points in the reciprocal space of graphene relevant to a given CNT. If for a (n,m) CNT, $(n-m)$ is not a multiple of $3d$, where d is the greatest common divisor of n and m, then the coordinates of the relevant ***K***-points (corresponding to the ***K*** and ***K'*** valleys, respectively) are $K_1 = N/3R$, $K_2 = 0$ and $K_1 = 2N/3R$, $K_2 = 0$. This case includes all semiconductor CNTs and some metal ones. In particular, all the zigzag CNTs ($m = 0$) belong to this case. For the armchair nanotubes $(n = m)$ one has $K_1 = n/R$, $K_2 = \pm 2\pi/3T$. For the rest of the metal CNTs the choice is to be made between the two cases: (i) $K_1 = (N-M)/3R$, $K_2 = 2\pi/3T$ and $K_1 = (2N+M)/3R$, $K_2 = -2\pi/3T$ and (ii) $K_1 = (N+M)/3R$, $K_2 = -2\pi/3T$ and $K_1 = (2N-M)/3R$, $K_2 = 2\pi/3T$. (Which case realizes for a particular chirality turns out to be a more subtle question.) Knowing the coordinates of the relevant ***K***-points greatly simplifies comparison of CNT descriptions within the zone-folding and effective-mass approaches.

[1] S.V. Goupalov, *JETP Letters* **92**, 507 (2010).
[2] R. Saito, G. Dresselhaus, M.S. Dresselhaus, *Physical Properties of Carbon Nanotubes* (Imperial College Press, London, 1998).
[3] S.V. Goupalov, A. Zarifi, T.G. Pedersen, *Phys. Rev. B* **81**, 153402 (2010).

Laser-produced plasma of carbon nanotubes

Fronya A.A.*[1], Chernodub M.L.[1], Osipov M.V.[1], Puzyrev V.N.[1], Starodub A.N.[1], Zaramenskikh K.S. [2], Zharikov E.V.[2]

[1]*P.N. LebedevPhysical Institute, 119991, Moscow, Russia*
[2]*D. Mendeleyev University of Chem. Techn. of Russia, 9, Miusskaya sq., 125047, Moscow, Russia*
**e-mail: nastya708@yandex.ru*

Interaction of laser radiation with nano- and microstructured materials is intensively developing direction of investigations. Such studies are conducted to find optimum parameters and configurations of targets for inertial cornfinement fusion [1], as well as the development of radiation sources with specified characteristics in different spectral ranges, such as X-ray [2]. Carbon nanotubes as a promising type of nanostructured materials are of interest for laser-matter interaction.

Experimental studies of X-ray characteristics of the laser-produced plasma of carbon nanotubes are presented. Multi-walled carbon nanotubes (diameter ~ 30nm) were fabricated by catalytic pyrolysis of benzene using ferrocene as a precatalyst [3]. Nanotubes deposited onto the quartz substrate have been used as the targets. The experiments have been carried out using the powerful laser installation "Kanal-2" [4]. The target has been irradiated by nanosecond IR laser pulse (λ = 1,06 μm) with controllable function of mutual coherence. The power flux density of the laser radiation on a target was ~10^{13} W/cm^2.

The spatial, temporal and energy characteristics of X-ray plasma radiation have been investigated by means of pinhole-camera, Schwarzschild objective, and time resolution detector. Radiation of plasma was registered in soft X-ray (180-200Å) and hard X-ray ($\lambda \leq$ 9 Å).

The work is partly supported by the Russian Foundation for Basic Researches, grant # 10-02-00113.

[1] Borisenko N.G., Merkul'ev Yu.A., and Gromov A.I. *Journal of the Moscow Physical Society* **4**,247 (1994).
[2] Bagchi S., Kiran P., Yang K., Rao A.M., Bhuyan M.K., Krishnamurthy M., Kumar G.R. *Phys. Plasmas* **18**, 014502 (2011).
[3] X. Devaux, S.Yu. Tsareva, A.N. Kovalenko, E.V. Zharikov, E. McRae. *Carbon* **47**, 1244 (2009).
[4] S.I. Fedotov, L.P. Feoktistov, M.V. Osipov, A.N Starodub. *Journal of Russian Laser Research* **25**, 1 (2004).

Polyaniline coated aligned carbon nanotubes for electrochemical supercapacitors

Fedorovskaya E.O.*, Okotrub A.V., Bulusheva L.G.

Nikolaev Institute of Inorganic Chemistry, SB RAS, 630090, Novosibirsk, Russia
**e-mail: fedorovskaya-eo@yandex.ru*

Electrochemical capacitors, known as supercapacitors, have attracted great interest as promising energy storage devices due to their high power energy density and long cycle performance than conventional dielectric capacitors. Among various conducting polymer, polyaniline has emerged as the one of the most promising class of active materials for electrochemical capacitor, due to its high capacitive characteristics, easy processing and environmental friendliness. Carbon nanotubes commonly possess large specific surface area, remarkable chemical inertness and physical stability. Formation of three-dimensional conducting network from aligned nanotubes coated with a layer of polyaniline, involved in the Faraday processes, seems to be promising for obtaining of high-capacitance supercapacitors. Direct contact of carbon nanotubes with conductive substrate provides fast charge/discharge and high stability of capacitor. Arrays of vertically aligned carbon nanotubes have been grown on silicon substrates using an aerosol-assistant catalytic chemical vapour deposition (CCVD) method. The carbon nanotubes were synthesized from toluene. Ferrocene was used as a catalyst source and its concentration in a solution was equal to 2 wt.%. The substrate was gradually heated to 800°C in an argon flow and injection of the ferrocene–toluene solution was performed for 30 or 60 min. Deposition of polyaniline was carried out in two ways. The chemical polycondensation of aniline occurred under an influence of an oxidant in an acidic environment. In our experiments we used potassium dichromate. The electrochemical deposition of polyaniline was performed during the carbon nanotube electrode cycling in a solution of aniline in sulfuric acid in a three-electrode cell. Synthesis time was 500-4000 seconds, the potential range was [-300, 700] mV. A study of the electronic structure of the carbon nanotubes and composites was carried out by X-ray photoelectron spectroscopy and X-ray absorption spectroscopy (NEXAFS) near the K-edges of carbon and nitrogen. The length and defectness of CNTs were determined by Raman spectroscopy and scanning electron microscopy. The electrochemical measurements were carried out on a potentiostat Elins P-30S working in potentiodynamic mode. Electrochemical measurements showed that the capacity of carbon nanotube electrode increases with the polyaniline coating formation. Furthermore, specific capacity for the composites based on the aligned carbon nanotube arrays is higher than that for the composites from random nanotubes.

The work was financially supported by the Russian Foundation for Basis Research (grant No. 10-03-91163).

The investigation of photoactive J-aggregates of cyanine dyes – carbon nanotubes composite for the application in high-efficiency photoelectric converters

Fedorov I.V.*, Kireev D.M., Bobrinetskiy I.I., Nevolin V.K.

Moscow Institute of Electronic Technology (Technical University), 124498 Moscow, Russia
**e-mail: farewell_iv@mail.ru*

For the time being one of the promising courses for the science and industry is the development of photoactive devices on the basis of organic materials. For instance, OLED technology enables us to transfer the energy of electricity into radiation by means of using specific polymer luminophor for the goal of enhancing efficiency and durability of the device. However, despite the overall success in that field, there are still many difficulties to confront, e.g. issues with the increase of efficiency should be paid significant attention.

Thus, for solving that problem we suggest to implement the idea of merging two different approaches – the first one is to use cyanine dye J-aggregate composite as a new luminophor material, owing to its outstanding quantum yield properties, and the other – the usage of carbon nanotubes (CNT) as a superior conductive medium for sufficient energy transfer. This method also provides us with the ability of conducting two opposite processes, the transition of light energy into electricity and vice-versa.

The process description: a glass substrate or a silicon chip with pre-deposited contacts is coated with the film of carbon nanotubes (by drop-coating or electrophoresis). In the next stage this layer is coated with the J-aggregates of cyanine dyes (by spin-coating or cross-dielectrophoresis). The aim of CNT arrays is to make good electrical contact and junction with J-aggregates. The final stage is the testing of spectrophotometric and photoelectric properties of the device.

The results are fascinating: conductivity of the structure increased dramatically (in 2-3 orders) when exposed to light (see Figure). Briefly, the structure could be used as an optical sensor and as an excitation-sensitive matrix.

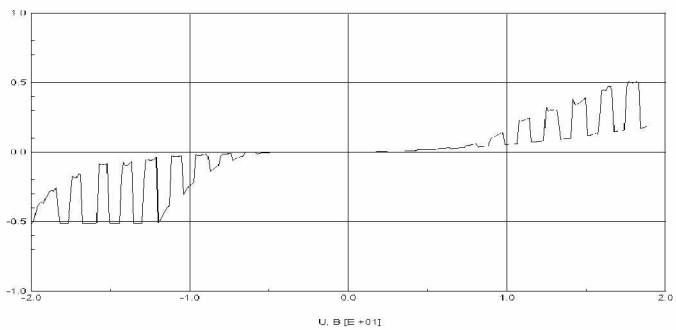

Figure. Dependence of the output current on the light excitation during the measurement. As the measurement takes some time, periodic light exposition results in the shown way.

Degradation of a CNT-based field emission cathode due to ion sputtering

Bocharov G.S.[1], Eletskii A.V.[2]*

[1]*Moscow Power Engineering Institute (Technical University), Moscow, Russia*
[2]*Russian Research Center "Kurchatov Institute", 123182 Kurchatov Sq. Moscow, Russia*
**e-mail: eletskii@imp.kiae.ru*

The rate of degradation of carbon nanotubes (CNT) comprising a field emission cathode is calculated. The sputtering of CNT material by incident ions formed through the electron impact ionization of the residual gas molecules is considered as the degradation mechanism. It has been found the abrupt dependence of the degradation rate on the applied voltage which is caused by a sharp character of the Fowler-Nordheim dependence.

The rate of degradation of a CNT was calculated using the following expression

$$\frac{dm_c}{dt} = \frac{M_c I N_M}{e} \int_{r_o}^{R} \sigma_{ion}[E_e(x)] Y[E_i(x)] dx = \frac{M_c I N_M}{e} J(U), \qquad (1)$$

where M_c is the mass of the carbon atom; the axis x coincides with the direction of the electrical field so that the point $x = 0$ corresponds to the nanotube's tip; $N_e(x)$ is the electron number density; I is the emission current; $v_e(x)$ is the electron velocity; $E_e(x)$ is the electron energy that is determined by the distribution of the electrical potential $U(x)$ along the electrical field; $E_i(x)$ is the kinetic energy of an ion formed in the x and reached the emitter surface in the point $x = 0$; N_m is the number density of the residual gas molecules subjected to the electron impact ionization; $\sigma_{ion}[E_e(x)]$ is the electron impact ionization cross section for the residual gas molecules; $S(x)$ is the cross section of the cone where the electron beam is found; $Y[E_i(x)]$ is the ion sputtering coefficient. The applied voltage and the emission current are inter-connected through the Fowler-Nordheim equation with taking into account the electrical field amplification factor for a CNT of specific geometry. The results of calculation are shown on Figure.

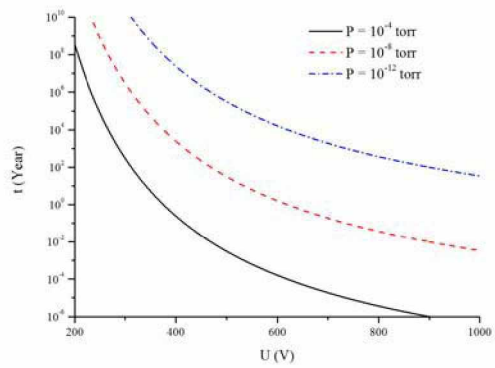

Figure. Dependences of the lifetime of a nanotube defined as $t = M_i / dm/dt$ on the applied voltage calculated for a CNT of $d = 10$ nm in diameter and $L = 1$ μm in height on the basis of Eq. (1) at various residual gas (air) pressures. The inter-electrode distance $H = 100$ μm, the electron work function for a nanotube $\varphi = 5$ eV.

Potential magnetic properties of carbon nanotube fragments (n, 0) with asymmetrical edges

Chernukhina A.A., Ermilov A.Yu.*

Lomonosov Moscow State University, 119991, Moscow, Russia
**e-mail: Sanchik-U@yandex.ru*

Since the very discovery carbon nanotubes attracted interest of scientists thanks to the vast perspectives of their application. According to the concrete ways of rolling up, these structures unexpectedly display a wide variety of properties, including magnetic [1].

The principal aim of this work was to investigate magnetic properties of single-walled carbon nanotube fragments with zigzag-shaped edges (n, 0). In order to compare results of this work and of the main article [2] and to observe regularity of properties, it was suggested to examine finite carbon nanotubes (8, 0) with fragments as long as q = 3, 4, 5. With reference to the main article of comparison a structure with the dehydrogenated zigzag edge (DHZE) at one end and the mono-hydrogenated zigzag edge (MHZE) at the other end was created.

For the electronic structure calculation, we used the same B3LYP functional, basis set 6-31G* as in the article [3]. All the theoretical calculations were performed with PC GAMESS [4]. All the structures were optimized.

Two main schemes of spin coupling were calculated. High-spin scheme (ferromagnetic properties) resulted much lower on the energetic scale than the low--spin variant. Low-spin model correlates with antiferromagnetic properties; in the literature this type of solutions is called the Broken-Symmetry. Furthermore, the energetic differences between the investigated spin states were analyzed.

The results obtained in this work contrast sharply with [2], where LSDA functional was used. An assumption was allowed that such calculation procedure may depend on the type of the exchange-correlation functional. True results can not be yielded using functionals not advanced enough.

Nano-scaled magnetic materials based on suggested structures are extremely promising.

This work was supported by RFBR (grant № 10-03-00665).

[1] Dyachkov, P.N. Carbon nanotubes: structure, properties, applications. Binom. Laboratoriya Znaniy: Moscow, 2006; P. 4.
[2] Higuchi Y., Kusakabe K., Suzuki K., Tsuneyuki S., Yamauchi J., Akagi K., Yoshimoto Y., *J. Phys.:Condens. Matter*. **16**, 5689 (2004).
[3] Chen Z., Jiang D., Lu X., Bettinger H.F., Dai S., Schleyer P.R., Houk K.N., *Org. Lett.* **9**, 5449 (2007).
[4] Granovsky A.A., Firefly version 7.1.G
[5] http://classic.chem.msu.su/gran/gamess/index.html.

Model of anisotropy of deformed polymer carbon nanotube based composites in Ka-band (26-37 GHz)

Bychanok D.S.*[1], Shuba M.V.[1], Maksimenko S.A.[1], Kanygin M.A.[2], Okotrub A.V.[2]

[1]*Research Institute for Nuclear Problems of Belarusian State University, 220030, Minsk, Belarus*
[2]*Nikolaev Institute of Inorganic Chemistry SB RAS, 630090, Novosibirsk, Russia*
**e-mail: dzmitrybychanok@ya.ru*

Theoretical model of the deformation influence on electromagnetic response of carbon nanotube (CNT) based polymer composites is presented. Anisotropy of dielectric permittivity was observed and theoretically modeled in frequency range 26-37 GHz (Ka-band).

Extremely high aspect ratio and cylindrical structure of CNT causes anisotropy of their mechanical and electromagnetic properties. For instance, polarizability of isolated CNT in axial direction is much greater than polarizability in perpendicular direction. Therefore in the case, when CNT are oriented in composite, we can observe the anisotropy of electromagnetic properties. Stretching deformation was used for orientation of CNT in polymer matrix (PMMA). In this case electromagnetic response of composite depends on direction of electric-field vector of scattered electromagnetic wave. The change of nanotube orientation during stretch deformation of composite was simulated. The distribution function of carbon nanotubes in deformed composite material was analytically derived and used for calculation of complex dielectric permittivity tensor of composite material (see Fig.).

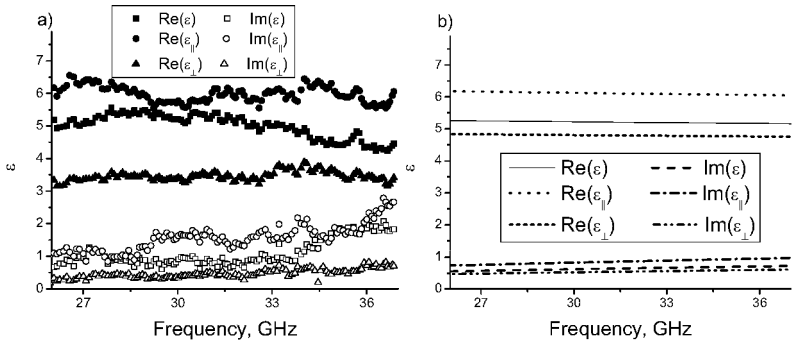

Figure: (a)Experimental data of dielectric permittivity of deformed CNT/PMMA composite. (b) Calculated permittivity of deformed CNT/PMMA composite (ε - permittivity of not deformed composite, $\varepsilon\perp=\varepsilon_x=\varepsilon_z$, $\varepsilon_{||}=\varepsilon_y$ – diagonal components of dielectric permittivity tensor of deformed along y-axis composite).

This research was partially supported by the RFBR Project No. 10-03-90901-mob-sng-st, the BRFBR Projects No. F10R-002 and No. F10CO-020, EU FP7 under Project FP7-266529 BY-NanoERA, and ISTC Project No. B-1708.

Carbon nanotube fabrication inside nano-channel porous materials

Butko V.Y.[1,2]*, Fokin A.V.[1], Nevedomsky V.N.[1], Sisoeva A.A.[1], Kumzerov Y.A.[1]

[1]*Ioffe Physical Technical Institute RAS, 26 Polytechnichesaya st., St. Petersburg 194021, Russia*

[2]*St. Petersburg Academic University, Nanotechnology Research and Education Centre, RAS, Khlopin street 8/3, St. Petersburg, 195220, Russia*

**e-mail: vladimirybutko@gmail.com*

Carbon nanostructural materials have received increased attention in the last several years because they offer the promise of bulk processing of flexible, electronic devices at low cost. Among the most important carbon nanostructural systems are carbon nanotubes. The interest stems in part from the room temperature charge carrier mobility that is much higher compare to silicon, unique thermal and mechanical properties of the nanotubes, and their possible transistor applications. One of the most important current limitations to nanotube technology is an ability to control their geometrical parameters that are also determining their electronic properties. Among the techniques that have been used for these purposes is a pyrolysis of organic materials inside nanoporous substances. We have developed a new modification of this method to fabricate carbon nanotubes and other graphene related compound in the restricted geometry. Our obtained TEM images demonstrate that this new technique allows growing crystalline carbon nanotubes and nanofibers with the length least up to 10 μm that is much longer compare to other nanoporous fabrication methods. The simplicity of our method, the observed transport properties, and TEM structural results suggest that this technique can successfully be used for a device fabrication. Interpretations of the obtained experimental results and device applications including Field Effect Transistors will also be discussed.

We are grateful to A.Y. Egorov and A.V. Babichev for help. This work was supported by the Russian Foundation for the Basic Research under project № 10-02-00853-a, by the St. Petersburg Scientific Center of the RAS, and under the Collaborative European Project EU-RU.NET.

The creation of biocompatible transparent CNT-electrodes

Bobrinetskiy I.I., Kireev D.M.*, Seleznev A.S., Morozov R.A.

Moscow Institute of Electronic Technology, 124498 Moscow, Russia
**e-mail: kirdmitry@gmail.com*

Carbon nanotubes still show a big perspective in purpose of creation biocompatible composites. Bovine serum albumin (BSA) is very common protein which can be used as biocompatible surfactant for hydrophobic carbon nanotubes.

Also, the creation of transparent conductive electrodes is a very promising field of work. For example, by CNT-BSA composite creation we can solve a problem of biocompatibility of the CNT films and consequently it allows to create a quite new devices.

At this work CNT-BSA water solution was used as a source of refined CNT coated with albumin. The method of solution preparation: a distilled water mixes up with BSA (2mg/1ml) and single-walled carbon nanotubes (1mg/1ml) followed by ultrasonication (duration is about 10 hours).

There are a lot of methods (dip-coating, drop-coating, spin-coating, etc.) of transparent and conductive films creation from carbon nanotubes arrays. But there are some difficulties in achieving of desired results. The cause is that the more density of CNT arrays, the more conductivity, but the less transparency.

At this work suggest a drop-coating method. The method description: on a glass or other optically-transparent and non-conductive substrate drops a solution followed by short-time (5-10 min) lamp heating until the drop dries out. Next, the film (see Fig.) is tested on transparency and conductivity.

To conclude, the work presents the results of the tests. The main problem is that the films are non-uniform. The close to a side, the more transparent film and less percolated (R=1-3 MOhm at 92-95% transparency and R=20-50 kOhm at 85% transparency), and consequently, the more concentrated close to center (R=100-200 kOhm at 92-95% transparency and R=10-15 kOhm at 85% transparency).

Furthermore, the results show us that our methodology could be very promising in purpose of creation brand-new, differently works biocompatible devices (like smart-clothes or pluggable displays, etc.).

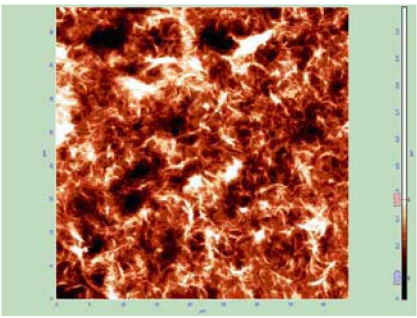

Figure: AFM image of the CNT-BSA film on a glass substrate.

The macropores investigation in carbon nanotubes agglomerates

Bessonova A.V., Bobrinetskiy I.I., Nevolin V.K.*, Simunin M.M.

Moscow Institute of Electronic Technology (Technical University), 124498, Moscow, Russia
**e-mail: vkn@nanotube.ru*

The scanning electron microscopy (SEM) is the basic method of carbon nanotubes (CNT) geometrical sizes definition. However this method doesn't allow to investigate macroscopical quantities of CNTs and is labor-consuming. There is a method based on nitrogen adsorption at 77 K to define a specific surface area and porosity of CNTs, and there is a certain dependence between these characteristics and the CNTs geometrical sizes. Revealing of this dependence is the purpose of this work.

In this work we investigated sorption properties of various types multi-walled carbon nanotubes (MWNT), produced by method of chemical vapour deposition and method of catalytic pyrolysis of ethanol. The specific surface area and porosity of MWNT samples were defined by nitrogen sorption at 77 K.

It was shown that experimental dependence of MWNT specific surface area on their average diameter can be approximated as inversely proportional [1]. The given approximation is chosen from calculation of CNT specific surface area as relations of the CNT surface area to its weight.

The method of calculation of agglomerates pore volume in CNT as a difference of limiting filling of all pores and filling of internal CNT cavities is offered. The method is based on distinction of limiting pore filling and fillings of CNT channels, and this distinction decreases with growth of CNT diameter. CNT with smaller diameter are inclined to formation of agglomerates the agglomerates pore volume increases with reduction of CNT diameter [2].

It was shown that at constant pressure of ethanol vapour with increase in temperature of CNTs synthesis reduction of a specific surface both specific pore volume and increase in the average pore size of CNTs is observed. It is related to increase of CNT average diameter with growth temperature. At constant growth temperature the increase in a specific surface and reduction of CNT pore volume with increase of pressure of ethanol vapour is observed.

In the work dependences of a specific surface, specific pore volume from average CNT diameter have been investigated. Selection of the models is spent, allowing to find dependence of specific pore volume on the CNT sizes.

[1] K.A. Williams, P.C. Eklund, *Chemical Physics Letters* **320**, 352-358 (2000).
[2] Hou P., Xu S., Ying Z., Yang Q., Liu C., Cheng H., *Carbon* **41**, 2471-2476 (2003). Abstract information.

The quantum chemical research of the dependence of SWCN's dipole moment

Belolipetskii A.A.*, Lebedev N.G.

Volgograd State University, 400062, Volgograd, Russia
**e-mail: alexbelster@gmail.com*

It is interesting to investigate the possibility of using carbon nanotubes [1] as some electronic gauges. The main feature of carbon nanotube which can be used in the gauges is dipole moment. We have considered the fragments of single-wall polarized carbon nanotubes (n, n) and (n, 0) types (n = 3, 4). The unsaturated cluster boundary chemical bonds have been completed by some atoms (or groups of atoms) on the both sides. The length of tubes has been varied. The electronic structure and energetic properties of nanotubes were calculated by applying the semi-empirical methods of quantum chemistry [2].

The results of the calculation have shown that the dependence of the dipole moment from the length of nanotubes has a nonlinear character and dipole moment value is depending on the boundary atom types. The values of the dipole moment of carbon nanotubes oscillate and these oscillations are different for each of the tube's types. But the oscillations are less pronounced with increasing the diameter of (n, n) type of nanotubes and the curves become smoother. For (n, 0) type of nanotubes such dependence is not observed.

The work is supported by Russian foundation of basic research (project 08-02-00663) and by Education Ministry of Russian Federation (project NK-16(3)).

[1] Harris P. Carbon nanotubes and related structures. New materials of the XXI century. - M: the Technosphere, 2003.
[2] Stepanov N.F. Quantum mechanics and quantum chemistry. - M: Mir, 2001.

The features of the low temperature behavior of heat capacity and thermal expansion of bundles of single-walled carbon nanotubes

Bagatskii M.I.*, Dolbin A.V., Sumarokov V.V., Barabashko M.C.

B.Verkin Institute for Low Temperature Physics & Engineering NASU, Kharkov 61103, Ukraine
**e-mail: bagatskii@ilt.kharkov.ua*

The heat capacity of bundles of single-walled carbon nanotubes (SWNTs) has been investigated in a temperature interval of 2-120K using a compact adiabatic calorimeter [1]. A cylindrical sample (0.71602 g) was prepared from a SWNT powder (Cheap Tubes, USA).

The temperature dependence of the heat capacity $C(T)$ of the measured SWNT bundles has breaks near 36 K and 100 K. In the temperature intervals 2-34 K, 40-78 K, 86-100 K and 110-120 K the curve is described by different power functions with the exponents varying from 2 to 1. At T=65-80 K the curve $C(T)$ has a deflection.

The coefficient of the radial thermal expansion $\alpha_R(T)$ of SWNT bundles has been investigated at T=2-120 K [2]. The measurements were made using a dilatometer with the sensitivity $2\cdot10^{-9}$cm. A cylindrical sample 7 mm high and 10 mm in diameter was prepared by compacting of a SWNT powder, which oriented the tubes in the bundles perpendicular to the sample axis. The sign of $\alpha_R(T)$ was observed to change below T=5.5 K. The heat capacity and the thermal expansion [2] were measured on samples obtained by the same preparation technique.

The temperature dependences of heat capacity and the coefficient of radial thermal expansion $\alpha_R(T)$ have features near T=36 K.

The Gruneisen coefficient ($\gamma= \alpha_r(T)\cdot V/(\chi\cdot C_v(T))$) was estimated for the SWNT bundles oriented perpendicular to the sample axis. It is found that γ is weakly dependent on temperature above 37 K.

The origin of the features observed is discussed.

[1] M.I. Bagatskii, V.V. Sumarokov, A.V. Dolbin, CC2010: 8th Conference on Cryocrystals and Quantum Crystals CC-2010 (Chernogolovka, Russia, July 26-31, 2010).

[2] A.V. Dolbin, V.B. Esel'son, V.G. Gavrilko, V.G. Manzhelii, N.A. Vinnikov, S.N. Popov, and B. Sundqvist, *Fiz. Nizk. Temp.* **34**, 860 (2008) [*Low Temp. Phys.* **34**, 678 (2008)].

Transparent SWNT and MWNT mixture films

Blank V.D., Alshevskiy Yu.L., Batov D.V.*, Kazennov N.V., Tatyanin E.V., Ivanov L.A.

Technological Institute for Superhard and Novel Carbon Materials (FSI TISNCM), 142190, 7a Centralnaya street, Troitsk, Russia
**e-mail: batov@tisnum.ru*

In most cases by synthesis of single and double walled carbon nanotubes, the bundles are formed. There need a special treatment to separation them into individual nanotubes.

We found the experimental conditions permitting to grow the films of individual nanotubes situated in substrate plane. The thickness of the film depend on sputtered layers and process time.

We synthesized thin films consisted of long carbon nanotubes and others nanostructures in HF CVD reactor using various gas mixtures and temperature up to 1100°C. This method allows to grow carbon films of different thickness.

TEM investigations and Raman spectroscopy investigations shown that the films consist of single- and double walled carbon nanotubes with several quantity of thin multiwalled nanotubes and small quantity of disordered graphite (peak D at 1345 cm^{-1}). Rough estimate of nanotubes diameter by radial breathing mode frequency (empirical formula from [1]) says that diameter of multiwalled nanotubes is approx 10-20 nm and the one of single- and double walled carbon nanotubes 0.8-0.9 nm

[1] J. Kurti, V. Zolyomi, M. Kertesz, and G. Sun. *New Journal of Physics* **5**, 125 (2003).

Investigation of properties of carbon nanotube-cadmium sulfide nanoparticle hybrids

Algaer Yu.A. [1,2]*, Okotrub A.V.[1]

[1]*Institute of Inorganic Chemistry, 630090, Novosibirsk, Russia*
[2]*Novosibirsk State University, 630090, Novosibirsk, Russia*
**e-mail: yalgaer@gmail.com*

At present the development of hybrid nanosystems combining the properties of one-dimentional carbon nanotubes (CNTs) and quantum dots from semiconducting materials attracts considerable interest. Interaction of semiconducting nanoparticles with light is expected to have result in the electron photocurrent through CNT and localization of the hole on nanoparticle. This effect can be used for creating a new type of photovoltaic devices. Here, we present a preparation and investigation of hybrid materials from CNT and CdS nanoparticles.

CdS nanoparticles have been grown on the surface of aligned multi-walled CNTs from an aqueous solution of $CdCl_2$, $(NH_2)_2CS$ (Thio), and NH_3. Scanning electron microscopy has showed that size of the nanoparticles varied from 5 to 100 nm. The synthesis conditions has preserved an alignment of CNTs in the array and uniformly decorated the CNTs with CdS nanoparticles. Continuous CdS/CNT interface indicated that nucleation and growth of the nanoparticles has taken place directly on the nanotube surface. XPS evidenced that the formed CdS particles have had the oxidized outer layer that is probably related to the reactions occuring in basic solution in the process of the nanoparticle growth.

Electroluminescence properties of CdS nanoparicles deposited at the CNT tips have been measured in the conditions of field electron emission from the CNT array. ITO glass has been used as an anode and image has been taken with a photocamera. Images exhibited a set of luminous points corresponding to individual CdS nanoparticles, which have been deposited on the CNT tips. The points have been of green and red coloure and different colouring could be related to the different size of the nanoparticles.

Solitons in a system of a coupled bilayer graphene waveguides

Yanyushkina N.N.[1]*, Belonenko M.B.[2], Lebedev N.G.[1]

[1]*Volgograd State University, 400062, Volgograd, Russia*
[2]*Volgograd Institute of Business, 400048, Volgograd, Russia*
**e-mail: yana_nn@inbox.ru*

We consider a propagation of ultra-short optical pulses, which can be represented as discrete solitons in the bilayer graphene waveguides. The effective equation, which has the form of an analog of the classical sine-Gordon equation was obtained. And the effects associated with changing of the width of initial momentum and of the Coulomb energy were investigated.

The unique properties of graphene and bilayer graphene [1-2], largely related to the periodical dispersion law, and also works on ultrashort optical pulses amplification in nanotubes and graphene [3] give additional incentive to study the problem of the propagation of electromagnetic pulses through a system consisting of several bilayer graphene sheets.

Studying the dynamics of the momentum carried in the nine parallel bilayer graphene planes. The dependence of electric field on waveguide number is presented in Figure. The dependences suggest a significant effect of the pulse width β on the energy distribution between the waveguides.

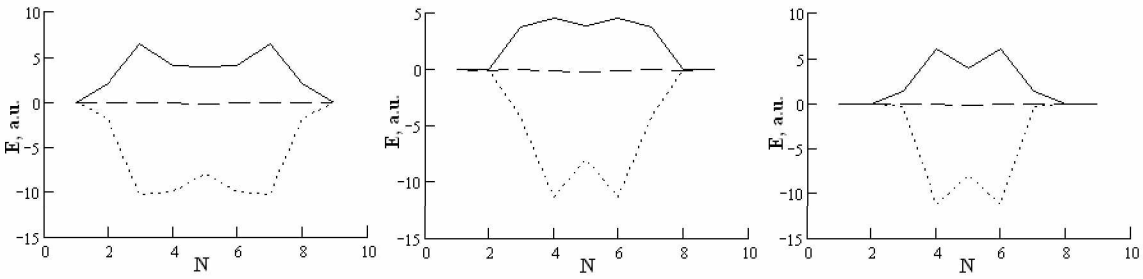

Figure. Dependence of the electric field on the waveguide number. All magnitudes are in the non-dimensionless units. For the solid curve the time is t=130, for the dotted curve t=200, for the dashed curve t=250: a) β=1; b) β=2; c) β=3.

This work was supported by the Federal Target Program "Scientific and pedagogical manpower" for 2010-2013 (project № NK-16(3)) and by the Grant for younger scientists of VolSU №3-2011-MU/VolSU.

[1] K.S. Novoselov, A.K. Geim, S.V. Morozov, D. Jiang, Y. Zhang, S.V. Dubonos, I.V. Grigorieva, A.A. Firsov. *Science* **306**, 666 (2004).
[2] K.S. Novoselov, A.K. Geim, S.V. Morozov, D. Jiang, M.I. Katsnelson, I.V. Grigorieva, A.A. Firsov. *Nature* **438**, 197 (2005).
[3] N.N. Yanyushkina, M.B. Belonenko, N.G. Lebedev. *Opt. and Spec.* **108**, 618 (2010).

Reversible chemical reactions on adsorbed graphene

Vinogradov N.[1,2]*, Ng M.L.[1,2], Simonov K.[3], Mårtensson N.[1,2], Preobrajenski A.B.[1]

[1]*MAX-lab, Lund University, 22100 Lund, Sweden*
[2]*Department of Physics, Uppsala University, 75121 Uppsala, Sweden*
[3]*V.A. Fock Institute of Physics, St. Petersburg State University, 198504 St. Petersburg, Russia*
**e-mail: nikolay.vinogradov@maxlab.lu.se*

A robust thin film platform is a fundamental requirement for chemical sensing implying that the system must be chemically, physically and thermally stable. In addition, chemical reactions taking place on the sensors must result in detectable property changes and these reactions have to be reversible. Calculations [1] have shown that the band structure (gap size) of carbon nanotubes changes specifically upon interaction with chemical functional groups (-CH, -C-O, -C-OH and –C=O). Experimental studies [2] have proven that there is a profound conductance change when graphene oxide is reduced.

It has been demonstrated recently that a monolayer of graphite (MG or graphene) adsorbed on transition metal (TM) such as Ir and Pt is more susceptible for chemical reaction with atomic H and the adsorption process is reversible upon soft annealing, i.e. the perfect MG surface can be recovered [3]. However, not all chemical processes on such systems are perfectly reversible by thermal treatment due to the formation of strong chemical bonds between carbon atoms and an adsorbate. For example thermal breakdown of -C-O-C- and –C=O functional groups which form upon atomic oxygen adsorption on graphene can rip off carbon atoms and cause defects in the MG layer [4]. Here we report on our x-ray spectroscopic studies confirming that MG adsorbed on Ir(111) can be reduced and oxidized at room temperature repeatedly and with high degree of reversibility by atomic H and O, respectively (RT).

[1] H. Park, J. Zhao, J.P. Lu, *Nanotechnology* **16**, 635 (2005).
[2] J.T. Robinson, F.K. Perkins, E.S. Snow, Z. Wei, P.E. Sheehan, *Nano Letters* **8**(10), 3137 (2008).
[3] M.L. Ng, R. Balog, L. Hornekær, A.B. Preobrajenski, N.A. Vinogradov, N. Mårtensson, K. Schulte, *JPCC* **114**, 18559 (2010).
[4] N. Vinogradov, K. Schulte, M. L. Ng, A. Mikkelsen, E. Lundgren, N. Mårtensson, A.B. Preobrajenski, *submitted to* JPCC 2011.

Transport coefficients of bilayer graphene

Sudorgin S.A.*[1], Belonenko M.B.[2], Lebedev N.G.[1]

[1]*Volgograd State University, 400062, Volgograd, Russia*
[2]*Volgograd Institute of Business, 400048, Volgograd, Russia*
**e-mail: sergsud@mail.ru*

Currently, scientists are paying great attention to the study of a new carbon material – graphene [1-2]. Determination of its transport properties and their dependence on external fields is one of the most pressing problems in the physics of low dimensional nanostructures.

In this paper, the semiclassical approximation of the relaxation time to obtain an expression for the current density and transport coefficients of two-layer graphene in the presence of an external electric field. Double-layer graphene consists of two graphite layers with a hexagonal structure. Between two layers of graphene attached electrostatic potential. The electronic structure of such a system is usually considered in the π-electrons in the nearet framework of tight-binding model for neighbors.

The dispersion relation for bilayer graphene is chosen in the form [3]. From the periodicity of the dispersion that can be represented as a Fourier series. In the semiclassical approximation of the electron distribution function is found from the Boltzmann equation in the τ-approximation. We can assume that the relaxation time experimentally established that in graphene even at temperatures of about 40 K, the relaxation time constant and does not depend on temperature.

Obtained by the method of theoretical calculation of transport coefficients of electrons of semiconducting single-walled carbon nanotubes in an electric field in the relaxation time approximation. Obtained analytically and numerically analyzed the expression for the diffusion of electrons and nonlinear electronic conductivity. Found nonlinear dependence of these factors on the field. When the diameter of CNTs these ratios are also increasing. It is shown that for strong fields, these ratios tend to saturation.

This work was supported by the Federal Target Program "Scientific and pedagogical manpower" for 2010-2013 (project № NK-16(3)).

[1] K.S. Novoselov, A.K. Geim, S.V. Morozov, D. Jiang, Y. Zhang, S.V. Dubonos, I.V. Grigorieva, A.A. Firsov, *Science* **306**, 666 (2004).
[2] K.S. Novoselov, A.K. Geim, S.V. Morozov, D. Jiang, M.I. Katsnelson, I.V. Grigorieva, A.A. Firsov, *Nature* **438**, 197 (2005).
[3] N.N. Yanyushkina, M.B. Belonenko, N.G. Lebedev, *Phys. Scr.* **83**, 015603 (2011).

Research of the nanopour creation mechanism at the thin-filmed systems of the different nature

Zaporotskova I.V., Stepanova A.U.*

Volgograd State University, 400062, Volgograd, Russia
**e-mail: austepanova@volsu.ru*

Recently one of the most perspective direction of the nanoelectronic becomes a creation of ordered arrays of the nanocrystals at the porous of the thin films different nature, which have novel physical properties. It is due to their develop surface and quantum dimensional effect.The most famous materials for preparation thin-filmed systems are graphene films, films of $\gamma - Al_2O_3$ and films of silicon oxide. But there is no theoretical research of these objects till present time.

That's why in our paper we report about calculations of the vacancy creation mechanism at the graphene layer and at the surface of aluminum oxide $\gamma - Al_2O_3$ to prove the possibility of the nanopour creation mechanism in these thin-filmed systems.

As a geometric model of thin film graphene film and film of $\gamma - Al_2O_3$ were used. The research was carried out by applying the Molecular Cluster model (MC) and semi empirical quantum-chemical MNDO scheme. Graphene film cluster consiSt of 60 carbon atoms. As a basic model for $\gamma - Al_2O_3$ layer building crystal lattice of spinel, in which Mg atoms were changed on Al atoms, was used [1].The process of the vacancy creation at the surface of graphene and $\gamma - Al_2O_3$ films has been modeled by step-by-step removal (minimal step 0.1 A) of carbon and aluminum atom from the surface of the film respectively till their full break-off. Geometry of the system was optimized on the each step. The analysis of energy curves of these processes show that there are two extremum on it: minimum and maximum. Minimum of the energy corresponds to stable state of the thin-filmed system. In that state carbon or aluminum atom is located near to the film surface. Maximum of the energy corresponds to activation energy of the vacancy defect. This fact caused the creation of different topological structures near the place where the vacancy located. This defect might be called nanopour.

The theoretical findings were experimentally confirmed by growing the porous aluminum oxide by electrochemical method. Analysis of the oxide surface's topology showed that there are periodically arranged pore diameter of 26 nm in it.

So, we have proved the possibility of nanopour's creating on the surface of filmed systems, which can become a place, where arrays of nanocrystals of different metals can be further formed.

This work was suggested with Federal Target Programm "Scientifical and pedagogical Staff of Innovative Russia" 2009-2013 (grant No.P328).

[1] Litinskij A.O., Gohbere P. Ja, Shatkovskaja D.B., Bolotin A.B., Litinskaja N.N., Popov G.P. *TEC* 19(4) 486 (1983).

Nanoroads and quantum dots on fluorinated graphene

Ribas M.A.[1], Singh A.K.[2], Sorokin P.B.[*3], Yakobson B.I.[1]

[1]*Rice University, 77005, Houston, Texas, USA*
[2]*Materials Research Centre Indian Institute of Science 560012, Bangalore, India*
[3]*Technological Institute for Superhard and Novel Carbon Materials, 142190 Troitsk, Moscow region, Russian Federation*
**e-mail: PBSorokin@gmail.com*

After the first experimental evidence of graphene research on its properties and applications has continued to grow with unprecedented pace. However, a lot remains to be done to fully incorporate graphene's unique properties into electronic devices. The quick advances on fabrication methods have now made it possible to produce graphene in larger scale. The major hurdle for its application in electronic devices is the lack of a consistent method to open the zero gap of graphene in a controlled fashion.

A recently proposed alternative [1] to open the zero-gap is to use a fully hydrogenated graphene (also known as graphane) as a matrix where graphene nanoroads or dots are patterned. The biggest advantage over the nanoribbons is that both semiconducting and metallic elements can be patterned on the same graphene sheet. The nanoroads and quantum dots can be patterned on any insulating functionalized graphene, e.g., graphane. Here we explore the functionalization of graphene by fluorine which was released experimentally quite recently [2].

Using *ab initio* methods we investigate the fluorination of graphene and find that a complete CF phase can be formed without any nucleation barrier. The fluorinated graphene is an insulator and turns out to be a perfect host for patterning nanoroads and quantum dots of graphene. Depending upon the edge orientation and width the electronic and magnetic properties of the nanoroads can be tuned. The energy gap between the highest occupied and lowest unoccupied molecular orbitals (HOMO-LUMO) of quantum dots are size dependent and show a typical confinement of Dirac fermions. Furthermore, we study the effect of different coverages of F on graphene on their band gaps, and show their suitability to host quantum dots of graphene with unique electronic properties.

[1] A.K. Singh, B.I. Yakobson, *Nano Lett.* **9**, 1540 (2009); L.A. Chernozatonskii, P.B. Sorokin and J. Brüning. *Applied Physics Letters* **91**, 183103 (2007)

[2] R.R. Nair, W. Ren, R. Jalil, I. Riaz, V.G. Kravets, L. Britnell, P. Blake, F. Schedin, A.S. Mayorov, S. Yuan, M.I. Katsnelson, H.M. Cheng, W. Strupinski, L.G. Bulusheva, A.V. Okotrub, I.V. Grigorieva, A.N. Grigorenko, K.S. Novoselov, A.K. Geim, *Small* **6**, 2877 (2010); S.H. Cheng, K. Zou, F. Okino, H.R. Gutierrez, A. Gupta, N. Shen, P.C. Eklund, J.O. Sofo, J. Zhu, *Phys. Rev. B* **81**, 205435 (2010); J.T. Robinson, J.S. Burgess, C. Junkermeier, S.C. Badescu, T.L. Reinecke, F.K. Perkins, M.K. Zalalutdniov, J.W. Baldwin, J.C. Culbertson, P.E. Sheehan, E.S. Snow, *Nano Lett.* **10**, 3001 (2010).

Electron-hole cooper pairing in graphene bilayer

Lozovik Yu.E.*, Sokolik A.A.

Institute of Spectroscopy RAS, 142190, Troitsk, Moscow Region, Russia
**e-mail: lozovik@isan.troitsk.ru*

Monoatomic thickness of graphene [1] allows fabrication of bilayer structures with nanometer-scale separation between graphene layers [2, 3]. The gate electrodes can independently dope these two layers and create equal concentrations of electrons and holes in them. In these conditions, spatially separated electrons and holes can form Cooper pairs due to their Coulomb attraction [4–6].

The theory of this pairing is presented with taking into account peculiarities of electron dynamics in graphene described by the Dirac equation for massless fermions. At strong coupling, the pairing is multi-band [7, 8]. The factors leading to enlargement or reduction of gap and critical temperature are considered (static and dynamical screening of electron-hole interaction, self-consistent weakening of the screening and others). The critical temperature at achievable experimental conditions is estimated.

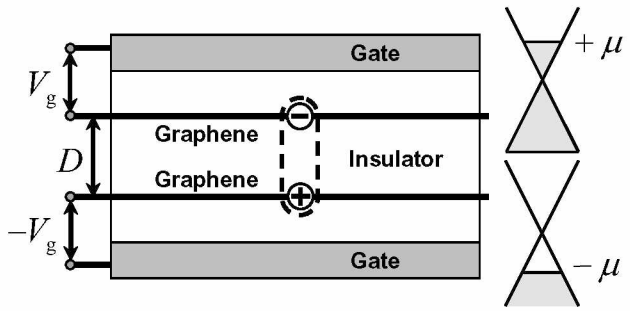

Schematic of graphene bilayer. Independent doping of two layers by gate voltages V_g and $-V_g$ allows to achieve equal concentrations of electrons and holes with chemical potentials μ and $-\mu$.

[1] K.S. Novoselov, A.K. Geim, S.V. Morozov, D. Jiang, M.I. Katsnelson, I.V. Grigorieva, S.V. Dubonos, A.A. Firsov, *Nature* **438**, 197 (2005).
[2] H. Schmidt, T. Lüdtke, P. Barthold, E. McCann, V.I. Falko, R.J. Haug, *Appl. Phys. Lett.* **93**, 172108 (2008).
[3] H. Schmidt, T. Lüdtke, P. Barthold, R.J. Haug, *Phys. Rev. B* **81**, 121403(R) (2010).
[4] Yu.E. Lozovik, A.A. Sokolik, *JETP Lett.* **87**, 55 (2008).
[5] H. Min, R. Bistritzer, J.-J. Su, A.H. MacDonald, *Phys. Rev. B* **78**, 121401(R) (2008).
[6] C.-H. Zhang, Y.N. Joglekar, *Phys. Rev. B* **77**, 233405 (2008).
[7] Yu.E. Lozovik, S.P. Merkulova, A.A. Sokolik, *Phys-Usp.* **178**, 757 (2008).
[8] Yu.E. Lozovik, S.L. Ogarkov, A.A. Sokolik, *Phil. Trans. Roy. Soc. A* **368**, 5417 (2010).

Low temperature thermal-CVD of methane

Smovzh D.V.[1]*, Koverznev M.P.[1], Nerushev O.A.[2]

[1]*Institut of Thermophysics SB RAS, 630090, Novosibirsk, Russia*
[2]*School of Chemistry the University of Edinburgh, EH9 3JJ, Edinburgh, Scotland*
**e-mail: smovzh@itp.nsc.ru*

Catalytic Vapour Decomposition (CVD) process is widely used for carbon nanostructures growth (CNT, Fullerenes, Graphene and etc.). The type of feedstock gas and temperature of synthesis are main parameters influencing efficiency of CVD. One possible way for decreasing synthesis temperature is use complex mixture of feedstock gases that have different decomposition temperature. Authors in [1] have shown that addition of acetylene or ethylene in methane leads to methane decomposition at low temperature about 500°C. Explanations of this temperature decrease are coadsorbtion of methane and acetylene/ethylene on surface of catalytic particles or phase transitions in catalytic particles due to exothermic reaction of acetylene/ethylene decomposition.

Experiments were carried out at thermal-CVD setup in conditions appropriate for CNT growth. A carbon containing gas mixture ($Ar/H_2+CH_4+C_2H_2/C_2H_4$) was supplied to quarts tube reactor after pre-warming with neutral gas flow. Iron catalySt was delivered to reactor hot zone by bubbling controllable portion of buffer gas flow through liquid iron pentacarbonyl at 0°C. Gas composition at the end of reactor was in situ controlled by gas analyzer RGA 200. Structures formed in reactor volume were collected at Teflon filter. Analysis of carbon soot was performed using TEM and SEM technique.

We observed that addition of small amount of acetylene/ethylene decrease temperature of decomposition methane however amount of decomposed methane equal to addition concentration. Therefore the most probable mechanism is formation of aromatics on surface of catalytic particles. Carbon soot collected from filter consists of CNT, onion like nanoparticles and amorphous carbon.

[1] Weizhong Qian,Tao Tian, Chenyi Guo, Qian Wen, Kuangjie Li, Hongbo Zhang, Haibo Shi, Dezheng Wang, Yi Liu, Qiang Zhang, Yongxiong Zhang, Fei Wei, Zhanwen Wang, Xiaodong Li, Yongdan Li. *J. Phys. Chem. C* **112**, 7588 (2008).

Investigation of graphene films grown on SiC substrate subjected to original pre-growth treatment

Shnitov V.V.*[1], Lebedev S .P.[1], Lebedev A.A.[1], Mikoushkin V.M.[1], Nikonov S.Yu.[1],Yakimova R.[2], Vilkov O.Yu.[3,4] Nelyubov A.V.[3,4]

[1]*Ioffe Institute, 194021, St. Petersburg, Russia*
[2]*Linkoping University, S-581 83, Linkoping, Sweden*
[3]*Institute of Physics,St. Petersburg State University, St. Petersburg, Russia*
[4]*Technische Universität Dresden, D-01062, Dresden, Germany*
**e-mail: v.shnitov@mail.ioffe.ru*

At present time only the epitaxial growth technology based on high temperature annealing of SiC substrates has a real potential for mass production of wafer-scaled and high quality graphene films [1]. Despite the quickly increasing number of publications developing fundamental and applied aspects of this technology, it is still far from being accomplished. In this work we demonstrate that our original technique of substrate pre-growth treatment may promote considerable progress in this field. To this effect we investigated graphene films grown on a high quality commercial 6H-SiC (0001) substrates which were preliminary subjected to pre-growth treatment, that is, were annealed for 30 minutes in a high-vacuum chamber in a quasi-closed growth cell at a temperature about 1300°C. Then, the substrate was again annealed for 30 minutes, but at an ambient argon pressure of 1 atm. and at temperature 2000°C [2].

Properties of the film thus grown were studied by atomic force microscopy (AFM), low energy electron diffraction (LEED), x-ray photoelectron spectroscopy (XPS), and near edge x-ray absorption fine structure (NEXAFS) spectroscopy. AFM study showed that substrate surface consists of flat and wide (~1 μm) terraces covered with sufficiently large and continuous graphene domains. Numerous LEED patterns (see example in the figure) obtained from different points of the sample demonstrate concurrent presence of a well-ordered graphite (1×1) pattern and $(6\sqrt{3}\times6\sqrt{3})R30$ pattern inherent to the underlying buffer layer [1] and, thereby, evidence mainly bilayer character of the grown film. XPS and NEXAFS data obtained on synchrotron BESSY II (Berlin) allowed us to specify a chemical composition and electron structure of grown graphene film and confirmed its high quality and mostly bilayer nature.

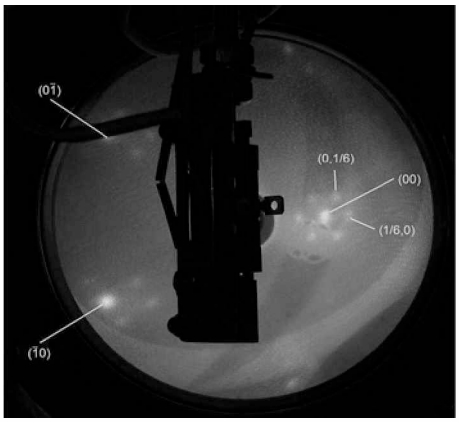

LEED pattern of graphene film grown on SiC substrate subjected to pre-growth treatment.

The research was supported by the Russian-German Laboratory at BESSY II, by the FASR contract 02.740.11.0108 and by the program "Quantum physics of condensed matter" of the Russian Academy of Sciences.

[1] Hass J., de Heer W.A., Conrad E.H. *Phys. J. Phys.:Condens Matter.* **20,** 323202 (2008).
[2] Virojanadara C., Yakimova R., Zakharov A.A., Johansson L.I., *J. Phys. D: Appl. Phys.* **43**, 374010 (2010).

The hexagon molecular motive as main factor for the failure of chemically modified graphene

Shaymardanova L.Kh.*, Sheka E.F., Popova N.A.

Peoples' Friendship University of Russia, 117198 Moscow, Russia
**e-mail: landy.nur@gmail.com*

Recently the response of a nanographene sheet to external stresses has been considered in terms of a mechanochemical reaction [1-3]. As shown, a high stiffness of the graphene body is connected with that of the benzenoid unit. The anisotropy of the unit mechanical behavior in combination with different packing of the units either normally or parallel to the body C-C bond chains forms the ground for the structure-sensitive mechanism of the mechanical behavior of the object that drastically depends on the deformation modes. The mechanical behavior of graphene under *zg* and *ach* deformation modes is similar to that of a tricotage when either the sheet rupture has both commenced and completed by the rupture of a single stitch row (*ach* mode) or the rupture of one stitch is 'tugging at thread' the other stitches that are replaced by still elongated one-atom chain of carbon atoms (*zg* mode). For the first time, the approach makes allowance for tracing deformation-stimulated change in the chemical reactivity of both nanographene sheet as a whole and its individual atoms in terms of total and partial numbers of effectively unpaired electrons.

The current paper presents a comparative study of mechanical properties of a set of molecules involving hexametyl (HXM) and hexamethylene (HXMe) benzene, HXM cyclohexane, HXM hexafluoro cyclohexane, and HXM cyclobornitrid (HXM B_3N_3) that constitute the main hexagon patterns of pristine and chemically modified graphene as well as its bornitrid analogue under uniaxial tension. HXM and HXMe framing of the molecules makes the molecule hexagon motive alike to that of the related graphenium bodies. Cyclohexanes in both cases correspond to chair-like conformers.

As follows from the study, both the Young moduli and their gradual lowering when going from HXM benzene to HXM hexafluoro cyclohexane and HXM cyclobornitrid are well consistent with experimental data related to graphene and both graphane $(CH)_n$, graphene fluoride $(CF)_n$ as well as to bornitrid analogue $(B_3N_3)_n$ thus confirming the hexagon pattern responsibility for both mechanical characteristics of graphenium bodies and mechanical anisotropy of their properties.

[1] E.F. Sheka, N.A. Popova, V.A. Popova, E.A. Nikitina, L.Kh. Shaymardanova. arXiv:1005.0796 [cond- mat_mess-hall], 2010.

[2] E.F. Sheka, N.A. Popova, V.A. Popova, E.A. Nikitina, L.Kh. Shaymardanova. *J. Exp. Theor. Phys.* **139**(4) (2011).

[3] E.F. Sheka, N.A. Popova, V.A. Popova, E.A. Nikitina, L.Kh. Shaymardanova. *J. Mol. Mod.* DOI: 10.1007/s00894-010-0816-3, 2011.

Curvature-induced optical transitions in graphene

Sedelnikova O.V.*, Bulusheva L.G., Okotrub A.V.

Nikolaev Institute of Inorganic Chemistry, Siberian Branch of Russian Academy of Science, 630090, Novosibirsk, Russia
**e-mail: o.sedelnikova@gmail.com*

Graphene is a two-dimensional hexagonal crystal with an atomic thickness and its isolation has opened new frontiers for the researches. Recent observations showed that suspended graphene sheets are not perfectly flat showing corrugations that have been detected from electron microscopy and diffraction. Besides the intrinsic corrugation, the structure of graphene supported on substrate was found to be dedicated by the substrate roughness. Establishment of relationship between properties and geometrical configuration of graphene may add to the design of electronic and optical graphene-based devices.

We have performed ab initio calculations using plane-wave self-consistent field formalism to investigate the electronic and optical properties of rippled graphene. Armchair-edged graphene models were constructed using a cylindrical arrangement of carbon atoms. Dielectric function calculation was performed in the framework of the random-phase approximation.

We found that corrugation of graphene results in appearance of additional peaks in the imaginary components of the dielectric function and shift of main resonances typical for flat graphene for certain light polarization. Analysis of interband transitions demonstrated a contribution of electron transitions being forbidden for the flat graphene ($\pi \to \sigma^*$ and $\sigma \to \pi^*$ transitions for $E \perp c$ and $\pi \to \pi^*$ and $\sigma \to \sigma^*$ transitions for $E \| c$) in the in-plane and out-of-plane components of dielectric function of rippled graphene. Thereby, we conclude that positions and shape of peaks in optical absorption spectra are very sensitive to the geometry of rippled models. Stressing the graphene mechanically or placing the layer on an artificial substrate one could control the graphene rippling constructing a material with optical properties adjusted for a certain application. Particularly, bending of graphene can tune optical transparency window of the material.

On the calculation of the charge transfer due to atom adsorption on graphene

Sabirova G.I.,[1,2] Davydov S.Yu.*[1,2]

[1]*Saint Petersburg Electrotechnical University, 197376, St.Petersburg, Russia*
[2]*Ioffe Institute, 194021, St.Petersburg, Russia*
**e-mail: sergei_davydov@mail.ru*

In the recent years, increasing attention has been focused on the adsorptive properties of the carbon nanostructures. As to graphene, any atom interacting with monolayer carbon sheet is in fact adsorbed on it. Moreover, under some conditions adsorption leads not only to the doping of graphene but can manifests itself as the energy gap opening. The most part of the theoretical studies in the field are based on the density-functional formalism. Here we present the model approach to the problem.

Recently we have proposed simple model for the graphene density of states (DOS) [1], which permits us to obtain an analytical expression for the adatom's local DOS. With this in hand we have calculated the corresponding occupation numbers for the adatom's states taking part in the charge-transfer processes. This scenario has been applied to the alkali metals [1], atomic hydrogen [2], and the halogens. It was found that hydrogen and alkali metals act as donors, while halogens appear themselves as acceptors. Furthermore, their charges are: 1) 0.2 – 0.4 for hydrogen, 2) increase from 0.8 to about of 1 in the row of Li → Cs, 3) change around − 0.5 for the halogens.

Furthermore, we have studied the effect of the carbon orbitals hybridization type on the adatom's occupation number and demonstrated that this effect is not crucial for the charge transfer value. The role of the adsorption bond length and graphene work function has been also analyzed.

[1] S.Yu. Davydov, G.I. Sabirova. *Phys. Solid State* **53**, (2011).
[2] S.Yu. Davydov, G.I. Sabirova. *Tech. Phys. Lett.* **36**, 1154 (2010).

Catalytic activity of nanodiamonds in redox process

Rozhkova N.N.[1]*, Gorlenko L.E.[2], Yemelyanova G.I.[2], Ōsawa E.[3], Lunin V.V.[2]

[1]*Institute of Geology, Karelian Research Centre, RAS, 185910 Petrozavodsk, Russia*
[2]*Department of Chemistry, Moscow State University, 119991 Moscow, Russia*
[3]*NanoCarbon Research Institute, Asama Research Extension Centre, Shinshu University, 3-15-1 Tokita, Ueda, Nagano 386-8567, Japan*
**e-mail: rozhkova@krc.karelia.ru*

Detonation ultradisperse diamonds (UDD) are already offered on the market, but its properties and chemical composition vary with production conditions and degree of purification. The presence of catalytically active metals in UDD suggests that they could be regarded as ready-made nanostructured metallic catalysts on carbon carriers. Its catalytic activity in reaction of ozone decomposition was studied on UDD offered by various manufacturers: UDD-1 - Gansu Goldstone Nano-Material Co., Ltd., China; UDD-2 NanoCarbon Research Institute Ltd., Japan; UDD-3 Real-Dzerzhinsk, Russia; UDD-4 Tekhnolog FSUP SKTB, Russia. All of them, except UDD-1, are similar in elemental composition (carbon content 78.4 to 87.5%), and their H/C values 0.022-0.027, typical of a diamond phase (sp^3). Similar adsorptive characteristics are shown by UDD-2 and UDD-3. The average pore volume is 0.5-0.6 cm^3/g. The average pore radius is 3.4-3.8 nm. UDD-4 has a wider pore size distribution spectrum, and its volume and average radius are 2.5 times as large. The micropore radii, 3.4±0.1 nm, calculated from the Dubinin-Radushkevich equation, are characteristically identical [1].

The specific surface and volume of pores are observed to change slightly during ozonation, whereas the average radius of micropores remains constant and does not depend on the method of synthesis and the UDD purification details.

A high catalytic activity and stability of UDD in a low temperature ozone decomposition reaction could be extended to other redox processes. The catalytic activity depends on metal impurities content and particle size: it decreases by two orders of magnitude if the average particle size is > 200 nm.

The work was supported by Basic Research Program, RAS, Earth Sciences Section-5.

[1] Rozhkova, N.N., Gorlenko, L.E., Emelyanova, G.I. Jankowska A., Korobov M.V., Lunin V.V., Osawa E. *Pure Appl. Chem.* **81**(11), 2093 (2009).

Effect of chemical modification on tricotage-like deformation of graphene

Popova N.A., Sheka E.F.

Peoples' Friendship University of Russia, 117198 Moscow, Russia
**e-mail: nad.3785@mail.ru*

The response of a nanographene sheet to external stresses can be successfully considered in terms of mechanochemical reaction [1-3]. The quantum chemical realization of the approach is based on the coordinate-of-reaction concept for introducing a mechanochemical internal coordinate (MIC) that specifies a deformational mode. The related force of response is calculated as the energy gradient along the MIC, while the atomic configuration is optimized over all of the other coordinates under the MIC constant-pitch elongation. The approach has been applied first to the benzene molecule and (5, 5) nanographene [1-3]. In the current study the response to uniaxial tension has been considered concerning hexamethyl cyclohexane (HMCH) molecule and (5, 5) nanographane sheet.

The quantum-mechanochemical-reaction-coordinate approach has disclosed atomically matched peculiarities that accompany the deformation-failure-rupture process occurred in the bodies. A high stiffness of both graphene and graphane bodies is provided by the related hexagon units. The two units are characterized by anisotropy in the microscopic behavior under elongation along a MIC when the MIC is oriented either along (*zg*) or normally (*ach*) to the C-C bonds chain. The unit feature in combination with different configuration of the units packing with respect to the body C-C bond chains forms the ground for the structure-sensitive mechanical behavior that is drastically different for *zg* and *ach* deformation modes. The *zg* deformation mode is particularly manifested with the formation of one-atom chains. Hydrogenation of graphene drastically influences both behavior and numerical characteristics of the body making tricotage-like pattern of the graphane failure less pronounced.

[1] E.F. Sheka, N.A. Popova, V.A. Popova, E.A. Nikitina, L.Kh. Shaymardanova. arXiv:1005.0796 [cond- mat_mess-hall], 2010.

[2] E.F. Sheka, N.A. Popova, V.A. Popova, E.A. Nikitina, L.Kh. Shaymardanova. *J. Exp. Theor. Phys.* 139(4) (2011).

[3] E.F. Sheka, N.A. Popova, V.A. Popova, E.A. Nikitina, L.Kh.Shaymardanova. *J. Mol. Mod.* DOI: 10.1007/s00894-010-0816-3, 2011.

Stepwise hydrogenation and fluorination of graphene towards graphane and fluoride

Popova N.A.*, Sheka E.F.

Peoples' Friendship University of Russia, 117198 Moscow, Russia
**e-mail: nad.3785@mail.ru*

A great efficacy of molecular quantum chemistry applied to basic graphene problems has been recently demonstrated by the authors when studying the formation of peculiar composites between carbon nanotubes and graphene [1] as well as considering tensile deformation and fracture of a graphene sheet in due course of a mechanochemical reaction [2]. The optimistic results obtained in the studies make it possible to shift attention from the solid state problems and consider chemical modification of graphene as a multistep addition reaction applied to the pristine molecule. The paper concerns the reactions that involve atomic addends such as hydrogen and fluorine. To proceed we have to answer the following questions: 1) what is a characteristic image of the addend atom attachment to the substrate; 2) which carbon atom (or atoms) is the first target subjected to the attachment and how carbon atoms are selected for the next steps of the adsorption; 3) is there any connection between the sequential adsorption pattern and cyclohexane-like conformers? First results obtained on this way are presented in the current paper. The calculations were performed within the framework of unrestricted broken symmetry Hartree-Fock approach by using semiempirical AM1 technique implemented in CLUSTER-Z1 codes.

Our study has convincingly shown that similarly to fullerenes and carbon nanotubes [3], the formation of polyhydride and polyfluoride graphene can be considered in the framework of stepwise computational synthesis, each subsequent step of which is controlled by the distribution of atomic chemical susceptibility in terms of partial numbers of effectively unpaired electrons on atom, N_{DA}, of preceding derivative over the substrate atoms. The high-rank N_{DA} values definitely distinguish the atoms that should serve as targets for the next chemical attack. The performed investigations have shown that there is a direct connection between the state of graphene substrate and the conformer pattern of the polyderivatives formed so that chair-like regular structures can be obtained only under particular conditions.

[1] E.F. Sheka, L.A. Chernozatonskii. *J. Theor. Compt. Nanosci.* **7**, 1814, 2010.
[2] E.F. Sheka, N.A. Popova, V.A. Popova, E.A. Nikitina, L.Kh. Shaymardanova. *J. Exp. Theor. Phys.* **139**(4), (2011).
[3] E.F. Sheka. Fullerenes: Nanochemistry, Nanomagnetism, Nanomedicine, Nanophotonics. CRC Press, Taylor&Francis group: Boca Raton 2011.

Features of the electronic structure of graphene on top of different substrates

Popova A.*[1], Shikin A.M.[1], Rybkin A.G.[1], Marchenko D.[2], Vilkov O.[1], Varykhalov A.[2], Rader O.[2]

[1]*St.-Petersburg State University, 198504 St. Petersburg, Russia*
[2]*BESSY II, Helmholtz Zentrum Berlin, D-12489, Berlin, Germany*
**e-mail: popova.anna@bk.ru*

Investigation of the graphene monolayer have attracted considerable intereSt in recent years due to its unusual electronic structure (linear "photon-like" dispersion of electron states near the Fermi level in the region of the K-point of the Brillouin zone) and related to this its unique transport properties. So far the only feasible route toward large-scale production of graphene is epitaxial growth on a substrate. The presence of the substrate will, however, influence the electronic properties of the graphene layer. The main aim of our work was investigation of principal features of electronic properties which appear as the result of the interaction of the graphene layer with different substrates.

In the present work the electronic structure of such systems as 1ML graphene on top of Ni(111), SiC(0001), Cu/Ni(111) and Au/Ni(111) was studied [1]. All this data was compared with each other and with electronic structure of bulk monocrystalline graphite. Systems were investigated by angle-resolved photoelectron spectroscopy (ARPES) with the application of synchrotron radiation.

The analysis of dispersion relations of graphene on top of intercalated Au and Cu layers shows that hybridization of d states of Au and Cu with π states of graphene takes place. This hybridization leads to modification of dispersion relations in the region of crossing of these states. Gaps of dispersion relations and the bonding and the antibonding (d - π)-states above and below the gap are formed. For graphene formed on top of Ni(111), covalent interaction of π states with d states of Ni substrate is stronger. It leads to the shift of π-states about 2 eV in comparison with those of bulk graphite [2]. Unoccupied π^*-states are located above Fermi level and only bonding π-states are occupied, therefore the interaction of graphene with Ni(111) substrate is very strong.

In some systems besides covalent interaction ionic bond is existed, i.e. charge transfer from atoms of metal to graphene monolayer takes place. For instance, for systems MG/Cu/Ni(111) and MG/SiC(0001) there are partial occupation of unoccupied earlier π^*-states at Fermi level near the K point of the surface Brillouin zone of graphene.

[1] A. Varykhalov et al., *Phys. Rev. Lett.* **101**, 157601 (2008).
[2] Th. Seyller et al., *Surf. Sci.* **600**, 3906 (2006).

The study of exchange indirect interaction in the impurity bigraphene

Pak A.V.*[1], Lebedev N.G.[1], Belonenko M.B.[2]

[1]*Volgograd State University, 400062, Volgograd, Russia*
[2]*Volgograd Institute of Business, 400048, Volgograd, Russia*
**e-mail: pak.anastasia@gmail.com*

Recently the big attention of researchers is concentrated on calculations of electronic, magnetic, conductive changes and other properties of graphene, caused by introduction of single atomic impurity on its surface [1]. It is known, that strong updating of electronic or magnetic properties is possible at impurity introduction.

Therefore research of the collective effects connected with interaction of the impurity with a crystal lattice of graphene, i.e. RKKY (Ruderman-Kittel-Kasuya-Yosida) interaction [2-3] is very interesting.

In the given work in the framework of s-d model features of RKKY-interaction in double-layer impurity graphene have been calculated. Atomic hydrogen was considered as an impurity. Calculations have shown that on small distances antiferromagnetic ordering of the impurity spins is preferable, and with distance increasing the ordering becomes ferromagnetic.

The increase of electric field intensity leads to the strongly oscillating dependence of indirect interaction of the impurity spins on the distance between impurities that can be connected with resonant transitions of the electrons between the split levels.

The feature of the RKKY-interaction of adsorbed atoms on the surface of double-layer graphene, made in this paper is that it considered the exchange interaction on the basis of the total (including short-wave part) electron spectrum of the crystal lattice.

This work is supported by The Education Ministry of Russian Federation (project No. NK-16 (3)).

[1] A. Lugo-Solis, I. Vasiliev, *Phys. Rev. B* **76**, 235431 (2007).
[2] M.I. Katsnelson, *Phys. Rev. B* **74**, 201401 (R) (2006).
[3] A.M. Black-Schaffer, *Phys. Rev. B* **82**, 073409 (2010).

The conductivity two-layer graphene nanoribbons in external electric field

Nevzorova J.V.*[1], Lebedev N.G.[1], Ivanchenko G.S.[1]

[1]*Volgograd State University, 400062, Volgograd, Russia*
**e-mail: nevzorkina@yandex.ru*

A nanostructure and nanoclusters of the system very interesting with standpoint of their using in is nano- and optoelectronics but studies of the fundamental nature have brought about arising the new direction - a physicists nanostructures. The Special place in these study occupy nanostructure on base of carbon.

Graphene is interesting not only from the viewpoint of possible applications, but also from a fundamental point of view - because of their unique electronic properties. Model band structure of graphene has served as a launching pad for studying the properties of graphite, but in multilayer stacks, in particular in the bilayer, the interaction between the layers is significantly distorts the properties of graphene [1].

In this paper, a theoretical study of the influence of an external electric field applied as perpendicular to the graphene layers, and along them, the temperature dependence of conductivity bilayer graphene nanoribbons.

The band structure of the system by the method of molecular orbitals as linear combination of atomic orbitals (MO LCAO) using the Huckel approximation.

To simulate the electronic structure of bilayer graphene, we used a model Huckel-Habbard. In this model, the Hamiltonian system takes the following form [2]:

$$\begin{aligned}\hat{H} = &-\sum_{j\Delta\sigma} t_{\Delta}^{a}\left(a_{j\sigma}^{+}a_{j+\Delta\sigma} + a_{j+\Delta\sigma}^{+}a_{j\sigma}\right) - \mu^{a}\sum_{j\Delta\sigma} a_{j\sigma}^{+}a_{j\sigma} + U\sum_{j} a_{j\sigma}^{+}a_{j\sigma}a_{j-\sigma}^{+}a_{j-\sigma} \\ &-\sum_{j\Delta\sigma} t_{\Delta}^{c}\left(c_{j\sigma}^{+}c_{j+\Delta\sigma} + c_{j+\Delta\sigma}^{+}c_{j\sigma}\right) - \mu^{c}\sum_{j\Delta\sigma} c_{j\sigma}^{+}c_{j\sigma} + U\sum_{j} c_{j\sigma}^{+}c_{j\sigma}c_{j-\sigma}^{+}c_{j-\sigma} - \\ &-\sum_{j\xi\sigma} t_{\xi}^{ac}\left(a_{j\sigma}^{+}c_{j+\xi\sigma} + c_{j+\xi\sigma}^{+}a_{j\sigma}\right) + e\varphi\sum_{j\Delta\sigma} c_{j\sigma}^{+}c_{j\sigma}\end{aligned} \quad (1)$$

It takes into account the energy of electronic transitions, the Coulomb interaction between electrons, as well as the interaction of electrons with an external electric field.

Were built by different temperature dependence of the conductivity of the external field applied perpendicular to the layers of graphene and along them.

The results of calculations for showed that at low electric fields at low temperatures (around 40 K) is the deflection of the temperature dependence of conductivity observed phase transition "conductor-semiconductor interface. With further increase of the electric field phase transition disappears.

This work is supported by The Education Ministry of Russian Federation (project No. NK-16 (3)).

[1] L. Chernozatonskii, E. Sheka, A. Artukh, *JETP Letters* **89**, 412 (2009).
[2] G. Ivanchenko, N. Lebedev, *FTT* **49**, 183 (2007).

Some aspects of the graphene-graphane problem

Nechaev Yu.S.

G.V. Kurdjumov Institute of Metals Science and Physics; I.P. Bardin Institute for Ferrous Metallurgy, 105005 Moscow, Russia
e-mail: yuri1939@inbox.ru

Some discussion basic and technological (methodological) aspects, or "open questions", on the graphene/graphane problem [1, 2] have been considered.

It has been shown [3-7] the following:

1. It is expedient to consider graphane (CH) not as a hydrocarbon, but as a carbohydride (the graphene hydride).
2. Graphane can have not only the diamond-like structure, but the graphite-like one, as well.
3. The graphane-like (carbohydride-like) regions can have place in carbonaceous multilayer nanomaterials.
4. The intercalated ("megabar") hydrogen, with the density up to ~0.7 g/cm^3, can be formed (at the expense of the hydrogen association energy) between graphene (graphane) layers in some carbonaceous nanomaterials, under the definite conditions (regimes) of their hydrogenation.
5. It can satisfy the most of the DOE requirements to technologies of the on-board hydrogen storage in fuel-cell-powered vehicles.

[1] D.C. Elias, R.R. Nair, T.M.G. Mohiuddin, S.V. Morozov, P. Blake, M.P. Halsall, A.C. Ferrari, D.W. Boukhvalov, M.I. Katsnelson, A.K. Geim, K.S. Novoselov. *Science* **323**, 610 (2009).
[2] J.O. Sofo, A.S. Chaudhari, G.D. Barber. *Phys. Rev. B* **75**, 153401-1 (2007)
[3] Yu.S. Nechaev. *Physics-Uspekhi*, **49**(6), 581 (2006).
[4] Yu.S. Nechaev. *J. Nano Res.* **12**, 1 (2010).
[5] Yu.S. Nechaev, O.K. Alexeeva, and A. Oechsner. *J. Nanosci. Nanotechnology*, **9**(6), 3949 (2009).
[6] Yu.S. Nechaev. Int. Sc. J. *Alternative Energy & Ecology* **10**, 50 (2010).
[7] Yu.S. Nechaev. *Int. Sc. J. Astronautics* **1**, 52 (2010).

Chemical restoration of few layer exfoliated graphite oxide studied by photoelectron spectroscopy

Mikoushkin V.M.*[1], Shnitov V.V.[1], Nikonov S.Yu.[1], Dideykin A.T.[1], Vyalikh D.V.[3], Vilkov O.Yu.[2,3]

[1]*Ioffe Institute, 194021 St.-Petersburg, Russia*
[2]*Institute of Physics, St.-Petersburg State University, St.-Petersburg, Russia*
[3] *Technische Universität Dresden, D-01062 Dresden, Germany*
**e-mail: V.Mikoushkin@mail.ioffe.ru*

Among technological approaches to fabrication of graphene, the exfoliation of thermally expanded graphite oxide (GO) is considered to be one of the most promising [1]. Deoxidation of GO is the most critical stage of the technology since the residual oxygen crucially affects the electronic structure and physical properties of graphene sheet. The aim of the research was to study transformation of chemical bonds and electronic structure of few layer GO films in the course of their deoxidation by annealing in hydrogen. A set of GO films deposited on SiO_2/Si substrate and treated at different temperatures were studied by means of x-ray photoelectron spectroscopy (XPS) using synchrotron radiation and the station of the Russian-German beam-line at BESSY II (Berlin). C1s XPS spectra of few layer GO films represented at Fig.1 show that different carbon oxide groups disappear when the temperature increases. At T=800°C the binding energy E_b of C1s core electron practically coincides with that of highly oriented pyrolytic graphite (HOPG). The residual high energy shoulder in the spectrum measured at T=800°C corresponds to some contribution of C-H bonds. To characterize physical properties, the valence band (VB) spectra of the same samples were studied as well. They show rather wide band gap for GO, which disappear in the film treated at T = 800°C: the VB edge practically merges with the Fermi level indicating occurrence of metallic conductivity. Thus, it has been shown that chemical restoration of thermally expanded graphite oxide in hydrogen is an effective way of fabrication of few layer graphene films.

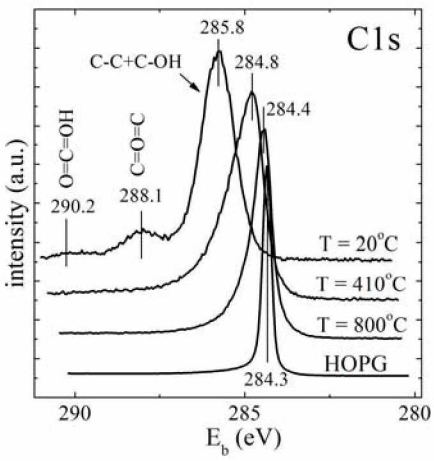

Figure. 1. C1s XPS spectra of few layer GO films and HOPG measured at the photon energy hν =450 eV.

The research was supported by the Russian-German Laboratory at BESSY II, by the FASR contract 02.740.11.0108 and by the program "Quantum physics of condensed matter" of the Russian Academy of Sciences.

[1] K.A. Mkhoyan, A.W. Contryman, J.S. Derek at al., *Nanoletters* **9**(3), 1058 (2009).

Nonlinear electromagnetic waves in a graphene ribbon system under the deformation gauge fields

Lyapkosova O.S.*[1], Lebedev N.G.[1], Belonenko M.B.[2]

[1]*Volgograd State University, 400062, Volgograd, Russia*
[2]*Volgograd Business Institute, 400010, Volgograd, Russia*
**e-mail: lyapkosovaolga@mail.ru*

As it is known from the literature [1], one of the main purposes of modern optics is the design of all-optical devices in which light can be controlled by light. The object of investigation should be a material with pronounced nonlinear properties, on the one hand, and a material important from the viewpoint of practical applications, on the other hand. One of the promising directions in this area is the investigation of the propagation of ultra short light pulses in carbon nanomaterials (nanotubes, graphene). In view of all the aforementioned factors and circumstances, the study of nonlinear dynamic processes in carbon nanotubes is an important problem from both the theoretical and practical stand points.

In constructing the model of propagation of an ultrashort optical pulse in a parallel graphene ribbon system, we assume that the electric field strength vector $\mathbf{E}(x, t)$ is parallel to the ribbons and the electromagnetic wave propagates in the transverse direction to ribbon planes. For simplicity and definiteness, it is assumed that the ribbons are ideal, have a armchair conformation, and are equally spaced at 0.34 nm. The interaction between carbon nanoribbons is disregarded.

The electromagnetic field of the pulse is classically described in terms of the Maxwell equations. The evolution of an ensemble of Fermi particles is described by the Boltzman kinetic equation in the relaxation-time approximation. We obtain the effective equation for the vector potential. The equations under investigation were numerically solved according to the cross type finite difference scheme [2]. The time and coordinate steps were determined from the standard conditions of stability. The steps of the finite difference scheme were sequentially decreased by a factor of two until the solution changed in the eighth significant figure.

We have considered the gauge fields which arise in defect-free graphene ribbons due to smooth elastic deformations. We investigate the evolution of ultra short light pulses of a graphene ribbons system. The existence of stable nonlinear electromagnetic waves is confirmed by the results of numerical calculations. The influence of a electric field magnitude on the wave propagation is analyzed. As result we observed effect of electrical pulse rectification.

The work is supported by Education Ministry of Russian Federation (project NK-16(3)).

[1] H. Gibbs, Optical Bistability: Controlling Light with Light (Academic, New York, 1985; Mir, Moscow, 1988).
[2] N.S. Bakhvalov, Numerical Methods: Analysis, Algebra, and Ordinary Differential Equations (Nauka, Moscow, 1975; Mir, Moscow, 1977).

The CVD formation of multi-graphene clusters in CNT growth system CVDomna

Bobrinetskiy I.I., Levin D.D., Nevolin V.K., Simunin M.M.

[1]*Moscow Institute of Electronic Technology, 124498, Zelenograd, Moscow, Russia*
e-mail: vkn@nanotube.ru

Practical realization of nanostructures based on graphene in electronics and optoelectronics has raised the question of obtaining high-quality graphene samples of large area. One of the promising method of monolayers graphite formation (graphene) and other electrically conductive layered materials is the chemical vapor deposition (CVD) that allows to produce large area graphene monolayers [1].

We suggeSt the methodic of graphene growth based on the ethanol pyrolysis from the gas phase.

The investigation of growth methods were carried out on carbon nanotubes growth system CVDomna, which allows to grow carbon nanotubes by ethanol. Unlike the devices of a similar type, CVDomna can synthesize a variety of carbon nanomaterials on different surfaces with a dimensions up to 3 inches. Usage the gas mixture of ethanol requires the control of the reaction, because simultaneously with the process of growth occurs the material oxidation.

The dissolution process of reactivity from carbon monoxide in a metal catalySt (in this work Ni film of 200 nm thickness) occurs before the complete dissolution of the liberated carbon in the bulk of the catalyst

Thus, the saturation of carbon-film catalySt and the formation of solid solution of metal-carbon bonds. When the critical carbon content is reached the reaction chamber cooling leads to faster release of carbon, as well as to stop the growth of graphene monolayers. Consequently, the higher the temperature of the reaction, the more carbon will react withthe catalyst, and the sooner we will cool the reaction chamber, the less carbon is formed on the film surface of the catalyst

The thickness of multi-graphene clusters been grown using this technology, was investigated by scanning probe microscopy. Studies have shown that a thin film multi-graphene formed by the reaction on the catalyst surface. Cooling rate, which determines the surface morphology is also affect quality of the material. In one case, we obtain a homogeneous film, otherwise there is a formation of graphene islands.

These results show that need further study the mechanism of action at the substrate-catalystand its influence on the growth of carbon nanomaterials.

[1] Yasumitsu M., Keiichi K., Kazunori O., Ryo K., Masamichi Y., Hisanori S., *Applied Physics Letters* 96 (2010).

Transport properties of multi-graphene films grown on semi-insulating SiC

Lebedev S.P.*[1], Strel'chuk A.M.[1], Shamshur D.V.[1], Agrinskaya N.V.[1], Lebedev A.A.[1]

[1]*Ioffe Physical-Technical Institute RAS, St.-Petersburg 194021, Russia*
**e-mail: lebedev.sergey@mail.ioffe.ru*

High-quality monolayer graphene has been obtained in small tens of microns areas by exfoliation of highly ordered pyrolytic graphite. However, this exfoliation process cannot form the basis for a large scale manufacturing process. To become a viable technology, wafer-scale graphene muSt be grown on a substrate while preserving the electronic properties of an isolated graphene sheet. A potential platform is epitaxial graphene on SiC(0001).

For our investigations we used multi-graphene films grown on semi-insulating 6H-SiC on-axis wafers with polished $C(000\bar{1})$-face. Graphene was formed by sublimation of Si from wafer surface. The wafers were annealed in a high-vacuum chamber (residual pressure of ~10^{-6} Torr) in the temperature range of 1400-1500°C. Quality of multi-graphene films was examined by Atomic force microscopy (AFM) and Raman spectroscopy.

On the beSt samples Hall-Bar structures with 6 ohmic contacts for transport properties investigation was formed. The electro-physical measurements were done on graphene area with small sizes. To get small size graphene area (10×120 mkm) photolithography and argon beam etching was used.

Volt-ampere and Hall-effect measurements were done in the temperature range of 1.4-300K. It was founded, that at $T \leq 40$ samples conductivity decrease with decreasing temperature varies logarithmically, which is typical for two dimensional metals (regime of weak localization). Hall-effect measured by 4.2K and 1.4K gave the carrier concentration $n \approx 5 \times 10^{12} cm^{-2}$.

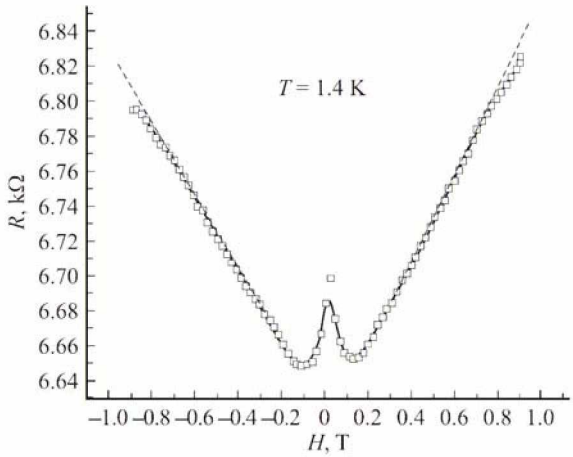

Figure. 1 Magnetoresistance of multi-graphene film on SiC (Temperature – 1.4K)

On the Figure 1 low temperature measurement of multi-graphene film magnetoresistance is shown. At low magnetic fields negative magnetoresistance appears which is also connected with weak localization.

Thus, low temperature features of charge carriers transport properties confirm presents of two dimensional holes gas in investigated samples.

This study was in part supported by Program of the Presidium of the Russian Academy of Sciences "Quantum physics of condensed matter" and FANI Contract N 02.740.11.0108.

Aharonov-Bohm effect on nanoholes in thin graphite and graphene

Latyshev Yu.I.*[1], Orlov A.P.[1], Monceau P.[2], Escoffier W.[3]

[1]*Kotelnikov Institute of Radio-Engineering and Electronics, 125009, Moscow, Russia*
[2]*Neel Institute, 38042, Grenoble, France,*
[3]*National Laboratory of High Magnetic Fields, 31400, Toulouse, France*
**e-mail: yurilatyshev@yahoo.com*

We studied magnetoresistance of thin graphite single crystals containing nanoholes produced by irradiation with heavy ions or by etching with focused ion beam. The diameter of nanoholes was correspondingly 24nm and 35nm. Crystal thickness has been varied from 50nm down to 1nm using soft beam-plasma etching. For samples of both types we found pronounced field periodic oscillations of magnetoresistance with periodicity corresponding to flux quantum hc/e per nanohole area independently of sample thickness [1, 2]. This kind of periodicity is expected for Dirac fermions [3]. The fact that effect does not depend on sample thickness indicates that effect is very likely related with the surface layer of graphite which is often represents as a graphene layer lying on graphite substrate [4, 5].

Normally, Aharonov-Bohm effect is observed in ring geometry samples. This geometry lets fix the quantized orbits between inner and outer boundary of the ring. In our experiment Aharonov-Bohm type effect was observed on non-ring geometry and as shown is determined by the orbits located close to the hole. We consider that the restricted orbits near the hole can exiSt due to the edge states located near graphene boundary. Otherwise, the averaging contribution of all possible orbits around hole would smear out interference effect. Existence of the edge states in graphene has been recently predicted theoretically [6]. Our observations of Aharonov-Bohm effect on nanoholes (antidots) strongly support the existence of the edge states in graphene.

The work was supported by the state contract No 16.740.11.0146 and by the Russian Academy of Sciences (programs “Strongly Correlated Electrons in Solids and Structures” and “Physics of New Materials and Structures”).

[1] Yu.I. Latyshev, A.Yu. Latyshev, A.P. Orlov, A.A. Schekin, V.A. Bykov,C. van der Beek, M. Konczykowski, I. Monnet, *JETP Lett.* **90,** 480 (2009).

[2] Yu.I. Latyshev, A.P. Orlov, E.G. Shustin, N.V. Isaev, W.Escoffier,P. Monceau, C.J. van der Beek, M. Konczykowski, I. Monnet, *Journ. of Physics: Conf. Series* **248**, 012001 (2010).

[3] S. Russo, J.B. Oostinga, D. Wehenkel, H.B. Heershe, S.S. Sobhhani, L.M.K Vandersypen, A. Morpurgo, *Phys. Rev., B* **77,** 085413 (2008).

[4] G. Li, A. Luican, E.Y. Andrei, *Phys. Rev. Lett.* **102**, 176804 (2009).

[5] P. Nuegebauer,M. Orlita, C. Faugeras,A.-L. Barra, M. Potemski, *Phys. Rev. Lett.* **103**, 136403 (2009).

[6] V.A. Volkov, I.V. Zagorodnev, *Journal of Physics: Conf. Series* **193**, 012113 (2009).

Quantum dots based on graphane and graphane ribbons: structure and properties

Chernozatonskii L.A., Kvashnin D.G.*, Eliseev A.I.

Emanuel Institute of Biochemical Physics RAS, 119334, Moscow, Russia
**e-mail: cvashnini@gmail.com*

The emergence of graphene as a stable pure two-dimensional system [1] has been one of the most important events in electronic condensed matter physics over the laSt years. One of many interesting properties of graphene is the Dirac type of electronic band structure and the drastic changes of the conductivity of graphene-based structures with electron confinement. Thus, two possibilities for the realization of this effect have been realized: carbon nanotubes and graphene ribbons (GNR).

The GNRs are very interesting graphene successors. They have attracted much attention because of their properties and their potential for applications. In recent years GNRs have been experimentally obtained and theoretically investigated in details.

The total hydrogenation of graphene opens the dielectric gap in electronic band structure. The interface between hydrogenated and pure graphene shows the interesting quantum properties e.g. the confined graphene region in graphane shows the behavior of electronic structure like in quantum dots.

In this work the theoretical study of atomic structure and electronic properties of a quantum dots on graphane and graphane nanoribbons was carried out. The accurate theoretical approaches tight binding (TB) method and DFT were used for the description of the electronic properties of structures under study. The semiempirical tight binding scheme was chosen because it gives a good qualitative description along with high speed of calculation whereas DFT approach was used for verification of TB scheme. Using DFT method the quantum dots based on zigzag graphane roads and graphane nanoribbons with removed hydrogen atoms were investigated. The stability of the structures was analyzed and electronic properties (HOMO and LUMO levels) of the structures as well as dependence of the band gap upon the geometry of quantum dots were obtained.

[1] K.S. Novoselov, D. Jiang, F. Schedin, T.J. Booth, V.V. Khotkevich, S,V, Morozov, A.K. Geim, *Proc. Natl. Acad. Sci. USA* **102**, 10451 (2005).

Graphene from graphite: the "wet" approach

Kozhemyakina N.V.[1], Hirsch A.*[1]

[1]*University of Erlangen-Nuremberg, Department of Chemistry and Pharmacy and Institute of Advanced Materials and Processes, Henkestr. 42, 91054, Erlangen, Germany*
**e-mail: andreas.hirsch@chemie.uni-erlangen.de*

Graphene, being the youngest extensively studied carbon allotrope, offers unprecedented physical properties for high-performance applications in the field of molecular electronics. From the known graphene production methods, i.e. the "top-down" exfoliation of graphite (mechanical in the solid state or chemical in solution) and the "bottom-up" direct synthesis of extended polyaromatic hydrocarbons, the "wet" chemical approach offers the most promising opportunities for macroscale graphene production, with fineSt tuning of the conditions and, consequently, properties of the material obtained.

Our work is aimed at finding best systems (type of graphite and solvent or surfactant) for graphene solution production, and learning about the nature of the interactions which facilitate and enhance graphene exfoliation.

For the first time, electronic communication involving π-π interactions between graphene and a perylene derivative has been proved to occur in an organic solvent [1] (N-methylpyrrolidone), previously this phenomenon reported for probes deposited on substrates in the solid state only [2]. By a set of titration experiments, the relative quantum yield of the fluorescent dye was shown to decrease to 65% on interacting with graphene. Several complementary characterization methods were used: UV/Vis absorption, fluorescence and Raman spectroscopy, optical (white light and fluorescence) microscopy, and high resolution TEM.

In addition, an overview of different grades of graphite will be presented, regarding their easiness of dispersion and exfoliation in a few solvents (aqueous and organic) by stirring (no ultrasonication). The relation between "carbon uptake" into the solvent and "exfoliation" will be discussed, and whether these two parameters vary simbate. A number of graphite grades characteristics (origin and type of production or post-treatment, grain size, surface area, spectroscopic data, etc.) will be correlated with physical and thermodynamical solvent properties. Problems arising during characterizing graphite/graphene dispersions by common colloidal chemistry techniques will be addressed in the light of the non-equilibrium nature of graphene solutions and dispersions.

[1] N.V. Kozhemyakina, J.M. Englert, G. Yang, E. Spiecker, C.D. Schmidt, F. Hauke, A. Hirsch, *Adv. Mater.* **22**, 5483 (2010).

[2] L. Xie, X. Ling, Y. Fang, J. Zhang, Z. Liu, *J. Am. Chem. Soc.* **131**, 9890 (2009).

Graphene on a subwavelength metallic grating: anomalous optical properties

Kotov O.V.[1,2], Lozovik Yu.E.[1,2]* , Medvedev V.V.[1,2]

[1]*Moscow Institute of Physics and Technology, 141700, Dolgoprudny, Moscow Region, Russia*
[2]*Institute of Spectroscopy, Russian Academy of Sciences, 142190, Troitsk, Moscow Region, Russia*
**e-mail: lozovik@isan.troitsk.ru*

We study the electromagnetic response of a composite structure consisting of monolayer graphene [1] on the metallic grating with narrow subwavelength slits. The spectral response of the grating without and with graphene on it was theoretically obtained in the scattering matrix formalism [2]. For this purpose we have developed S-matrix method for graphene. By examining the grating transmission spectrum without and with graphene we found extraordinary sensitivity of grating to the presence of graphene manifested as the anomalous transmission of light on the wavelength corresponding to the transmission dip for grating. We attribute this effect to the enhancement of the field in the slits in the immediate vicinity of the surface of the grating. The effect was studied for various geometrical parameters of the grating and different carrier densities in graphene.

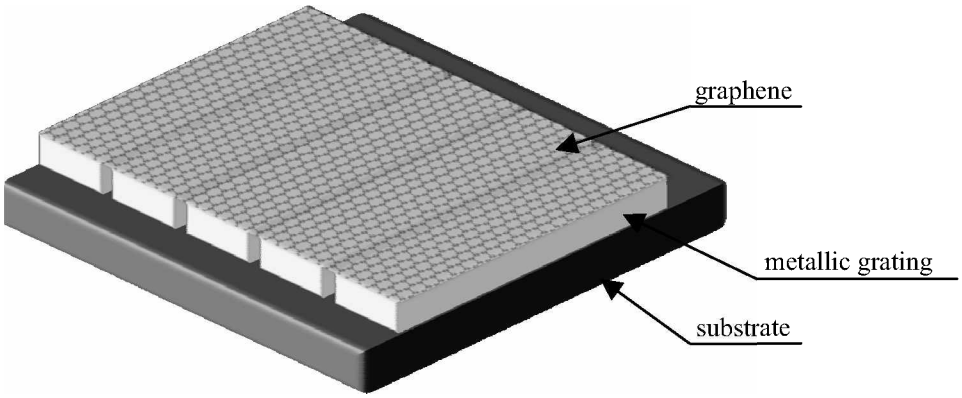

Schematic of graphene on a subwavelength metallic grating.

[1] K.S. Novoselov, A.K. Geim, S.V. Morozov, D. Jiang, M.I. Katsnelson, I.V. Grigorieva, S.V. Dubonos, A.A. Firsov, *Nature* **438**, 197 (2005).
[2] S.G. Tikhodeev, A.L. Yablonskii, E.A. Muljarov, N.A. Gippius, T. Ishihara, *Phys. Rev. B* **66**, 045102 (2002).

Phonon spectrum of graphene bilayer and monolayer graphene

Ivanchenko G.S.*, Nevzorova Ju.V., Kolesnikov D.V. Khimicheva A.A.

Volgograd State University, 400062, Volgograd, Russia
e-mail: genaivanchenko@yandex.ru

In this work numerical calculation of the phonon spectrum of double carbon nanoribbons is hold. The phonon spectrum was calculated by methods of classical mechanics in the framework of the Hamilton. The mutual arrangement of layers of graphene corresponds ABAB packing. Hamiltonian system is written in the harmonic approximation, taking into account the nearest-neighbor interactions. The quantum-chemical semi-empirical MNDO method is used to calculate the coupling constants in the framework of a molecular cluster.

The homogeneous system of linear algebraic equations for the amplitudes of the oscillations was obtained by writing the equations of motion of atoms and substituting the solution in the form of plane waves. From this we obtain the dispersion equation for the phonon spectrum of double graphene layer [1]. The boundary conditions for the two types of carbon nanoribbons "arm-chair" and "zig-zag" are used in solving the dispersion equation. The varying the width of the tapes is also carried out.

The results of the calculations shows that the phonon spectrum of double-wall carbon nanoribbons has a doublet character, that in turn is associated with the interaction of layers with each other. The effect of the configuration relative position of layers of double-wall carbon nanoribbons on the phonon spectrum is also studied. Because of the weak interaction of atoms at different layers, changes in the phonon spectrum were several orders of magnitude smaller compared with the values of characteristic frequencies. Thus we can say that the phonon spectrum calculated in the harmonic approximation, and the neareSt neighbor approximation with sufficient accuracy remains unchanged at a bias layers.

The gap is present between the acoustic and optical vibration modes in contraSt to graphene in the phonon spectrum of graphene nanoribbons of any type and width. Features of the vibration spectrum of graphene may serve as an indicator to identify this structure.

The calculated phonon spectra allow us to determine the Debye temperature for the bilayer graphene and graphene 1832 to 6052 K, as well as sound velocity 22390 m / s and 50,334 m / s, respectively.

The work was held during the Federal Aimed Program “The Scientific and Scientific-Pedagogical personnel of the innovative Russia”, 2009-2013 (the State contract № P892).

[1] G.S. Ivanchenko, N.G. Lebedev, *Solid State Physics* **48**(12), 2354 (2006).

Substrate-induced magnetism in epitaxial single layer graphene

Ilyasov V.*, Meshi B., Ryzhkin A., Ershov I., Ilyasov A.

Don State Technical University, 344000 Rostov-on-Don, Russia
**e-mail: viily@mail.ru*

Of particular intereSt is the magnetism of the single layer graphene (SLG). As we know published experimental data on a ferromagnetism of materials based on graphene in the paper [1] only are presented. The authors [1] suppose that the ferromagnetism at the room temperature is caused by defects of graphene. We have studied the band structure as well as magnetic properties in the ferromagnetic heterointerface SLG/MnO(001) using *ab initio* calculations.

We have modeled the SLG/MnO(001) ultra-thin film by a slab using a supercell approach with periodic boundary conditions. The slab included four-six layers containing 33 - 153 atoms in the supercell and each slab was separated from the other by a vacuum region. The band structure calculations were performed using the self-consistent plane-wave pseudopotential method within the framework of DFT. On the basis of the atomic effective charge concept estimations of the value Q_{eff} have been performed. The estimations analysis permits to calculate a charge transfer to the bond Mn – O that amounts ~ 0.50*e*. It is possible to suppose that an additional charge transfer from the manganese atoms to the carbon atom exists and amounts ~ 0.04 e.

Our estimations of the magnetic moment value at carbon atoms have shown that the total magnetic moment of the graphene islet formed by 28 atoms amounts $0.28\mu_B$. The analysis shows that the little magnetic moment at carbon atom amounts: ~ 0 μ_B (14%); 0,01 μ_B (58%); 0,02 μ_B (21%) and 0,03 μ_B (7%). Due to the band structure analysis of the system SLG/MnO(001) above we have drawn a conclusion of the C*2p*-Mn*3d*-hybridization formation of free and filled states. As a result of the *pd*-hybridization an orbital energy of free electron *2p*-states of carbon in graphene lowers that reduces to these states admixture to valent *3d*-states of manganese in the ultrathin layer MnO(001) and to Fermi surface topology change. This circumstance may be responsible for the "flickering" magnetism formation in graphene of the system SLG/MnO(001). Noteworthy that in graphene the magnetism revealed in the present paper is induced by the substrate MnO(001) as the *pd*-hybridization result.

Several laSt carbon atoms ("zigzag" type) of the graphene islet turn out to be nonmagnetic and within the bounds of the authors' concept [2] one can suppose that these atoms have a sp^3-configuration as well as take part in a bond formation with the substrate.

Therefore the obtained data on the magnetism nature in the ferromagnetic heterointerface SLG/MnO(001) can be considered as the possible base for implementations in spintronics devices.

[1] Y. Wang, Yu. Huang, Y. Song. *Nano Lett.* **9**, 220 (2009).
[2] A. Ramasubramaniam, N.V. Medhekar, V.B. Shenov. *Nanotechnology* **20**, 275705 (2009).

Spin-polarized quantum pumping in zigzag graphene nanoribbons

Grichuk E.*[1], Manykin E.[2]

[1]*National Research Nuclear University "MEPhI", 115409, Moscow, Russia*
[2]*National Research Centre "Kurchatov Institute", 123182, Moscow, Russia*
**e-mail: evgeny.sg@gmail.com*

The experimental discovery of graphene in 2004 has initiated intense experimental and theoretical research of this material [1]. Due to its attractive properties, such as electric field controlled conductivity, long spin lifetimes, large spin diffusion lengths and two-dimensional nature, graphene is considered as a good candidate for applications in electronics and spintronics.

Infinite graphene is non-magentic, but some of its derivative nanostructures, such as nanoislands, nanoribbons and defective graphene sheets, demonstrate magnetism. Specifically, zigzag nanoribbons are predicted to have antiferromagnetic structure at low doping with up-spins and down-spins being localized at opposite edges of a ribbon [2]. This fact paves the way for generating spin-polarized currents in graphene by breaking the symmetry between the edges [3].

We use a simple tight-binding approximation and a constant magnetization model [3] to numerically demonstrate that the quantum pump effect [4] in zigzag nanoribbons can be used to generate spin currents and pure spin currents (finite spin current with vanishing total electric current) provided the symmetry between up-spins and down-spins is broken. We propose two such mechanisms: a defect localized at one of the edges and a transverse electric field.

The considered effect may be utilized in graphene based spintronics devices as a method of controlled generation of spin-polarized currents.

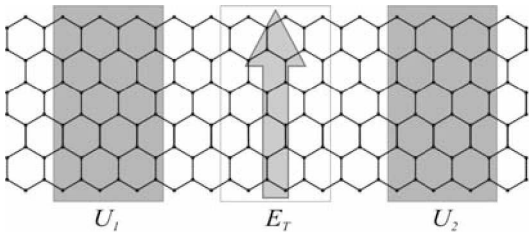

Schematic of a zigzag nanoribbon based quantum pump device. Pumping is achieved by a cyclic variation of gate voltages U_1 and U_2. The symmetry between up-spins and down-spins is broken by a transverse electric field E_T (or by a defect – not shown).

[1] A.H. Castro Neto, F. Guinea, N.M. R. Peres, K.S. Novoselov, A.K. Geim, *Rev. Mod. Phys.* **81**, 109 (2009).
[2] M. Fujita, K. Wakabayashi, K. Nakada and K. Kusakabe, *J. Phys. Soc. Jpn.* **65**, 1920 (1996).
[3] M. Wimmer, I. Adagideli, S. Berber, D. Tománek, K. Richter, *Phys. Rev. Lett.* **100**, 177207 (2008).
[4] P. Brouwer, *Phys. Rev. B.* **58**, R10135 (1998).

μSR study of hydrogen interactions with defective graphene

Gaboardi M.[1], Riccò M.[1]*, Pontiroli D.[1], Mazzani M.[1], Aramini M.[1], Choucair M.[2], Stride J.A.[2], Yazyev O.V.[3]

[1]*Dip. di Fisica, Università di Parma, Via G.Usberti 7/a, 43100 Parma, Italy*
[2]*School of Chemistry, University of New South Wales, Sydney 2052, Australia*
[3]*Department of Physics, University of California and Lawrence Berkeley National Laboratory, Berkeley, CA 94720, USA*
** e-mail: Mauro.Ricco@fis.unipr.it*

Macroscopic quantities of graphene, prepared by different chemical methods [1], have been investigated by Muon Spin Rotation. The implanted muons capture an electron and form muonium (Mu), an isotope of hydrogen with similar chemical behaviour. In all the investigated samples a clear oscillation in the time dependence of the muon polarization is observed, while it is missing in graphite, where juSt a slow Korringa-like depolarization is observed [2]. A zero field precession signal is usually the fingerprint of long range magnetism, but in this case the observation that: 1- the treatment of samples with molecular hydrogen at moderately high temperatures (800°C) induces a relevant increase of the precession signal amplitude, and 2- the signal disappears if the treatment is made with deuterium, indicates that origin of this precession is the dipolar interaction of the muon with the H nucleus [3]. The analysis of the muon spin precession under the hypothesis of the formation of a Mu-H entangled state suggests an inter-nuclear distance of 1.75 Å, fully compatible with a CHMu group. This witnesses an exceptional capture efficiency of mono-hydrogenated defects of graphene for atomic hydrogen (muonium in our case), to form an highly stable di-hydrogenated defect whose structure is shown in Figure 1. The exceptional stability of this moiety is confirmed by the persistence of the precession signal up to 900°C.

Acknowledgments: ISIS Lab. for provision of beam time and S.Giblin and I. McKenzie for support during the μSR experiments.

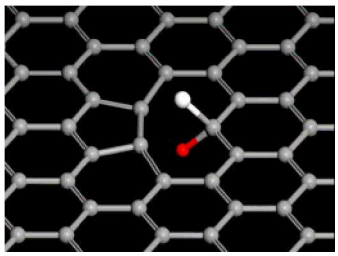

Figure 1. CHMu defect formed by the Muonium capture by an hydrogenated carbon vacancy.

[1] S. Park, R.S. Ruoff, *Nature Nanotechnology* **4**, 217 (2009).
[2] S.F.J. Cox, *Reports on Progress in Physics* **72**, 116501 (2009).
[3] T. Lancaster, S.J. Blundell, et al., *Physical Review Letters* **99**, 267601 (2007).

Kinetics of graphene hydrogenation: XPS study

Fedorov A.V.[1*], Haberer D.[2], Liu X.[3], Treske U.[2], Grobosch M.[2], Vilkov O.Yu.[1], Grueneis A.[2], Usachov D.U.[1], Adamchuk V.K.[1]

[1]*St. Petersburg State University, 198504, St. Petersburg, Russia*
[2]*IFW Dresden,P.O. Box 270116, D-01171, Dresden, Germany*
[3]*University of Vienna,1090 Wien , Vienna, Austria*
**e-mail: a_v_fyodorov_spb@inbox.ru*

Recently graphene has been discussed as a material with higheSt potential for post-silicon electronics [1]. The main requirement for graphene to have applications in electronics is existence of a phase transition from semimetal to semiconductor or insulator. The most promising route for the realization of this transformation is through chemical functionalization, such as hydrogenation.

The totally hydrogenated graphene is well known as the "graphane". Electronically, graphene is the zero-gap semiconductor and graphane is an insulator with an energy gap of 3.5 eV [2] which makes it an attractive material for optoelectronics in the UV range. For graphane theory predicts electron localization[3], a peculiar midgap state [4], strong excitation effects[5] and high-Tc superconductivity in hole-doped graphane [6].

In this work kinetic properties of the graphene hydrogenation were studied by means of X-Ray photoelectron spectroscopy (XPS) approach with high energy resolution, achieved by using the synchrotron radiation source. Graphene was prepared using chemical vapor deposition technique (CVD) on the Ni(111) thin film. Gold intercalation approach was used to obtaine quasi-freestanding graphene and to reduce Ni influence on the hydrogen adsorption process.

Stability of the intermediate states of the hydrogenation process was observed, which allowed using "step by step" technique for investigation of kinetic process. By performing long hydrogenation cycle it was shown with XPS that only 25% of carbon atoms can be bonded with hydrogen. The results of quantitative XPS data analysis were treated in the frameworks of the Langmuir adsorption theory to obtained kinetics constants. Low adsorption probability - only 3.5% and high reflection (85.5%) and stimulated hydrogen desorption (11%) probabilities were demonstrated.

[1] Geim A.K., Novoselov K.S., *Nature Mat.* **6**,183(2007).
[2] Richard B., Bjarke J., Louis N., Mie A., Emile R., Marco B., Mattia F., Erik L., Alessandro B., Silvano L., Zeljko S., Flemming B., Bjørk H., Thomas G. Pedersen, Philip H., Liv Hornekær *Nature Mat.* **9**, 315(2010).
[3] Skrypnyk Y. *Phys.Rev.B* **70**, 212201(2004).
[4] Duplock E.J., Scheffler M., Lindan P.J.D. *Phys.Rev.Lett.* **92**, 225502 (2004).
[5] Cudazzo P., Attaccalite C., Tokatly I.V., Rubio A. *Phys.Rev.Lett.* 104, 226804(2010).
[6] Savini G., Ferrari A.C., Giustino F. *Phys.Rev.Lett.* 105, 037002.(2010).

Vacancies influence on elastic properties of graphene and their migration rate under deformation

Fedorov A.S.*[1], Fedorov D.A.[1], Eliseeva N.S.[2], Kuzubov A.A.[2]

[1]*Kirensky Institute of Physics, 660036, Krasnoyarsk, Russia*
[2]*Siberian Federal University, 660041, Krasnoyarsk, Russia*
**e-mail: alex99@iph.krasn.ru*

Formation and properties of defects, first of all – single vacancies inside sp2 form of carbon (graphite, graphene and carbon nanotubes (CNT)) have been investigated in many works, both experimental and theoretical [1,2,3]. This intereSt is explained by determinative role of such defects during utilization of graphite inside nuclear reactors, junction of CNT under irradiation etc. At that majority of works was deal with electronic, geometrical and magnetic structure of the defects. Investigations of dynamics of vacancies and their influence on elastic properties of sp2 form of carbon, especially under deformations practically absent. So, in this work influence of the vacancies on elastic properties of graphene and their migration rate under deformations are investigated by DFT calculations with help of VASP [4] package.

At that nearly linear negative dependence of graphene Young moduli on vacancies concentration has been detected, see Fig.1. One can see the Young modulus values can be decreased at ~20% when a distance between nearest vacancies is ~12Å. Also potential barrier values for single vacancies jumps between neareSt positions are calculated for different deformations. Using transition state theory the dependence of vacancies migration rate on applied deformation is calculated for different temperatures. It is shown this rate can be changed on ~10 orders of magnitude by using deformation of 5% only.

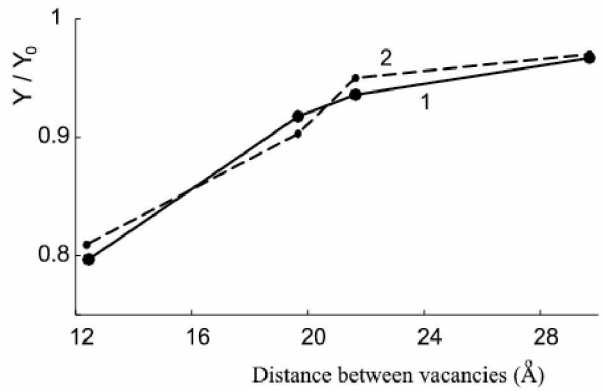

Figure 1. Dependence of ratio of defective graphene Young moduli to moduli of defect-free graphene on distance between neareSt vacancies. Curve 1 correspond on deformation along X axis, 2- along Y axis.

[1] J.R. Hahn, H. Kang, *Phys. Rev. B* **60**, 6007 (1999).
[2] A.J. Lu, B.C Pan, *Phys. Rev. Lett.* **92**, 105504 (2004).
[3] M. Sammalkorpi, A. Krasheninnikov, A. Kuronen, K. Nordlund, K Kaski, *Phys. Rev. B* **70**, 245416 (2004).
[4] G. Kresse, J. Furthmöller, *Phys. Rev. B* **54**, 11169 (1996).

Ab initio study of surface states at the graphene/Al_2O_3(0001) interface

Ershov I.

Don State Technical University, 344000 Rostov-on-Don, Russia
e-mail: thijd@mail.ru

It is well known that for a practical usage, graphene should be fixed on a solid substrate. There are number of various methods for deposition of graphene on a substrate, including mechanical exfoliation of graphite, growth from SiC surfaces via Si sublimation, epitaxial growth, chemical methods, and others. Traditionally SiO_2 substrates have been used for investigations of graphene properties. However, there are number of reasons for studying graphene on a larger variety of substrates like CaF_2, TiO_2 and Al_2O_3 [1, 2]. Of particular intereSt are such effects as bonding, doping, electron and hole mobility and magnetic properties, which strongly depends on the type of substrate and its orientation.

In the present work the properties of the graphene/Al_2O_3(0001) interface were investigated within the framework of density functional theory (DFT) using ab initio pseudopotential method. We have modeled the system in the tri-periodic slab approximation. The slab consists of 20 inequivalent atomic layers including the passivating hydrogen layer. The periodicity of the slab allowed us to calculate band structure in the interface which helped to estimate the degree of interaction between graphene and the substrate. The analysis of the chosen one-electron Kohn-Sham orbitals in the vicinity of Fermi level allowed us to identify the positions and character of surface states of the substrate in the interface. The total energy of the system was calculated in order to estimate the binding energy of graphene with the surface.

The relaxation of the substrate surface atoms and graphene show that the distance between graphene and the topmost substrate layer amounts 3.2 Å. The latter is in good agreement with the lateSt experiments [1, 2]. The band structure analysis indicates that the band of the substrate surface states turned out splitted in the presence of graphene. The shift of the surface states curves in the valence band could be indicative of the change of work function in the system.

[1] S. Akcoltekin, M. El Kharrazi, B. Kohler, A. Lorke, M. Schleberger, *Nanotechnology* **20**, 155601 (2009).

[2] T. Tsukamoto, T. Ogino. *Jap. Applied Physics Express* **2**, 075502 (2009).

Electron-hole pairing with finite value of Cooper pair momentum in graphene bilayer

Efimkin D.K.[1], Lozovik Yu.E.*[1,2]

[1]*Institute of Spectroscopy RAS, 142190, Troitsk, Moscow region, Russia*
[2]*Moscow Institute of Physics and Technology, 141700, Moscow, Russia*
**e-mail: lozovik@isan.troitsk.ru*

Electron-hole (e-h) pairing caused by Coulomb interaction in the system [1,2,3] of independently gated graphene layers is considered. We investigate influence of Fermi lines mismatch caused by density imbalance of electrons and holes and triangle distortion of their spectrum on e-h pairing.

Dependence of critical temperature and corresponding Cooper pair momentum on mismatch of Fermi lines of e and h is calculated. We predict appearance of the state with finite value of Cooper pair momentum - Larkin-Ovchinnikov-Fulde-Ferrell-like (LOFF) state [4,5] - at mismatch of the Fermi lines above the critical value.

Dependence of critical temperature and corresponding Cooper pair momentum on intensity of triangle distortion of quasiparticle spectrum is obtained. We show that triangle distortion contrary to the e-h densities mismatch does not lead to stabilization of LOFF-like state.

Internal Josephson effect in LOFF-like state caused by interlayer tunneling is considered. We suggeSt new experimental method to probe nonuniform distribution of order parameter of the system in LOFF state. We show that spatial structure of the order parameter in LOFF state can be reconstructed from the dependence of tunnel current between the layers from value and direction of magnetic field parallel to the layers.

[1] Yu.E. Lozovik, V.I. Yudson, *JETP Lett.* **22**, 274 (1975).
[2] Yu.E. Lozovik, A.A. Sokolik, *JETP Lett.* **87**, 55 (2007).
[3] D.K. Efimkin, V.A. Kulbachinskii, Yu.E. Lozovik, *JETP Lett.* **93**, 238 (2011).
[4] P. Fulde, R.A. Ferrell, *Phys. Rev.* **135**, A550 (1964).
[5] A.I. Larkin, Y.N. Ovchinnikov, *Sov. Phys. JETP* **20**, 762 (1965).

Graphene elastic moduli in the Keating model

Davydov S.Yu.

Ioffe Institute, 194021, St.Petersburg, Russia
e-mail: sergei_davydov@mail.ru

Now it is generally accepted that the single-layer graphene (SLG) has the most outstanding elastic properties. Hence, the growing intereSt in the problem of the graphene elasticity is not surprising. There are a number of different methods permit one to calculate the elastic moduli for the SLG. Here we demonstrate that the use of well known Keating model permits one to find the analytical expressions for the second- and third-order elastic constants [1,2], which are the direct characteristics of the harmonic and unharmonic sample response to the external mechanical perturbation.

We begin with the expansion of the SLG potential energy in the series using the Keating parameter $(\vec{R}_{0i}\vec{R}_{0j} - \vec{r}_{0i}\vec{r}_{oj})$, where $\vec{R}_{0i}$ $_{00}(\vec{r}_{0i})$ is the radius-vector from the reference atom 0 to the deformed (undeformed) position of the nearest-neighbor atom i = 1, 2, 3. Now we take into account only the harmonic central and noncentral terms, which are proportional to $\alpha(\vec{R}_{0i}^2 - \vec{r}_{0i}^2)^2$ and $\beta(\vec{R}_{0i}\vec{R}_{0j} - \vec{r}_{0i}\vec{r}_{oj})^2$ correspondingly, and the anharmonic central term $\propto \gamma(\vec{R}_{0i}^2 - \vec{r}_{0i}^2)^3$. Thus, we arrive at the three force-constant model.

Using the standard procedure, we find two second-order elastic constants: $c_{11} = (A+B)/(3)^{1/2}$, $c_{12} = (A-B)/(3)^{1/2}$, where $A = 4\alpha + \beta$, $B = 18\alpha\beta/A$. For and three third-order elastic constants we get: $c_{111} = C[(1.5-\zeta)^3 + 4\zeta^3]$, $c_{222} = C[(0.5+\zeta)^3 + 4(1-\zeta)^3]$, $c_{112} = C[(1.5-\zeta)^2(0.5+\zeta) + 4\zeta^2(1-\zeta)]$, where the Kleinman internal displacement parameter $\zeta = (2\alpha - \beta)/A$ and $C = 16\gamma/(3)^{1/2}$.

It is worthy to note here that graphene is isotropic only in the harmonic approximation, while the anharmonicity introduces some difference in its response to the deformation along the zigzag and armchair directions. This effect has been also analyzed by the consideration of the hydrostatic pressure effect on the second-order elastic constants.

[1] S.Yu. Davydov, *Phys. Solid State* **52**, 810 (2010).
[2] S.Yu. Davydov, *Phys. Solid State* **53**, 665 (2011).

Epitaxial graphene on metals: charge-transfer effect

Davydov S.Yu.

Ioffe Institute, 194021, St.Petersburg, Russia
e-mail: sergei_davydov@mail.ru

To use the unique properties of the single-layer graphene (SLG) in nanoelectronics one has to have appropriate metal contacts and corresponding substrate to include SLG in the device configuration. Hence the problem of the SLG – metal interface arises. On of the main point in this problem is the electron-hole symmetry braking which originates from the charge transfer across metal- SLG interface. Here we consider this effect within the frame of the model used earlier for the description of the epitaxial SLG on the silicon carbide substrate [1].

We begin with the Anderson model for substrate which we cover by the carbon adatoms arranged them to form the SLG structure. Then we find corresponding Green function and the epitaxial SLG (ESLG) density of states (DOS). This DOS permits us to calculate the occupation number for the carbon adatoms. It is this characteristic which accounts for charge-transfer effect. Underline, that the well-known small k approximation for the electron dispersion has been used to obtain the analytical expressions for the ESLG DOS and occupation numbers.

We have analyzed the number of metal components of the SLG-metal interfaces, such as: Ru, Al, Ni, Cu, Ag, Au, Pd, and Pt. It is shown that the electrons transfer from metals to the SLG. Rough estimations of the charge transfer values are fulfilled.

[1] S.Yu. Davydov. *Fizika i Tekhnika Poluprovodnikov* **45**, 629 (2011). (In Russian).

Evaluation of adsorption properties of graphene

Davydov V.Ya., Kalashnikova E.V.

Department of Chemistry, M.V.Lomonosov Moscow State University, 119992 Moscow, Russia
e-mail: VYaDavydov@phys.chem.msu.ru

Graphene as one of the carbon allotropes prepared in 2004 [1] is of grate interests owing to its electronic and structural properties.

At the same time graphene can be powerful adsorbent with uniform very large specific surface area 2630 m^2/g [2]. At present there are no methods of preparation of graphene in large quantities for the investigation of adsorption properties of graphene sheets. Although it is possible to produce large quantities of graphene by reduction of graphene oxides but graphene prepared by such method has chemical and physical defects.

Adsorption properties of graphene can be evaluated from numerous data on investigation adsorption properties of graphitized carbon black with uniform surface by chromatographic methods e.g. [3].

In [4] the potential energy functions for interactions between a carbon atom and monolayer graphite sheet, between a carbon atom and a semi-infinite graphite crystal were computed. From this data it is possible to assume that energy interaction of molecules with monolayer graphite sheet is about 90% of energy interaction with a semi-infinite graphite crystal. So from the data on adsorption properties of graphite (graphitized carbon black) it is possible to evaluate the heats of adsorption and adsorption equilibrium constant (Henry constant) of different organic compounds at small coverage on graphene sheets.

The contributions of different functional groups to the heats of adsorption and Henry constants were evaluated from the calculated data on heats of adsorption at small coverage and retention volumes (adsorption equilibrium constant) of organic compounds with different functional groups on graphene.

It is possible to calculate the thermodynamic characteristics of adsorption for great numbers of organic compounds on graphene by using these contributions.

[1] Novoselov K.S., Geim A.K., Morozov S.V., Jiang D., Zhang V., Dubonos S.V., Grigorieva I.V., Firsov A.A., *Science* **306**(5696), 666 (2004).
[2] Setoyama N., Suzuki T., Koneko K., *Carbon* **36**(10), 1459 (1998).
[3] Kalashnikiva E.V., Kiselev A.V., Makagon A.M., Shcherbakova, *Chromatographia* **8**(8), 399 (1975).
[4] Girifalco L.A., Lad R.A., *J. Chem. Phys.* **25**(4), 693 (1956).

Electron transport and thermoelectric power in CVD grown centimeter size graphene

Babichev A.V.[1,2], Gasumyants V.E.[3], Butko V.Y.*[1,2]

[1]*Ioffe Physical Technical Institute RAS, 26 Polytechnichesaya street, St. Petersburg 194021, Russia*

[2]*St. Petersburg Academic University, Nanotechnology Research and Education Centre, RAS, Khlopin street 8/3, St. Petersburg, 195220, Russia*

[3]*St. Petersburg State Polytechnical University, 29 Polytechnichesaya street, St. Petersburg 195251, Russia*

**e-mail: vladimirybutko@gmail.com*

In the paSt few years graphene has emerged as one of the most promising materials for future electronics. Graphene prepared even with extremely crude techniques has shown a wide range of remarkable properties that suggeSt it could become the natural successor to silicon. One of the most important current limitations to graphene technology is an ability to produce large size graphene samples in clean and reproducible ways. Recently developed CVD graphene preparation techniques are currently considered among the most practically applicable. We study here CVD grown 4 layer graphene samples up to 1 cm by 1 cm in size. Room temperature electrical resistivity of ~4 10^{-5} Ohm*cm and weakly semiconducting type of the temperature dependence from room temperature down 77 K have been observed. We have also made thermopower measurements to obtain additional information on electronic band structure. Room temperature hole transport Seebeck coefficient of ~ 12 μV/K has been obtained. A typical for metallic system temperature dependence of the measured thermopower has been observed. Interpretations of the obtained experimental results and device applications including Field Effect Transistors will also be discussed.

We are grateful to Y.A.Kumzerov, A.Y. Egorov, I.P. Soshnikov, E.V.Nikitina, M.M. Kulagina, and E. Polyakova for help. This work was supported by the Russian Foundation for the Basic Research under project № 10-02-00853-a, by the St. Petersburg Scientific Center of the RAS, and under the Collaborative European Project EU-RU.NET.

Structure, potential energy surfaces and electronic states of graphene- and multigraphene-based 2D extended complex nanocomposites

Avramov P.[*1,2,3], Sakai S.[1], Kuzubov A.[2], Entani S.[1], Matsumoto Y.[1], Naramoto H.[1]

[1]*Advanced Science Research Center, Japan Atomic Energy Agency, 2-4 Shirakata Shirane, Tokai-mura, Naka-gun, Ibaraki-ken 319-1195, Japan*
[2]*Siberian Federal University, 79 Svobodny, Krasnoyarsk 660041, Russia*
[3]*L.V. Kirensky Institute of Physics, SB RAS, Krasnoyarsk 660036, Russia*
**e-mail: paul@iph.krasn.ru*

The atomic and electronic structure and potential energy surfaces of 2D extended graphene- and multilayer graphene-based nanocomposites were studied using sophisticated *ab initio* Long-Corrected DFT (LC-DFT) technique. It was found that LC-DFT scheme coupled with periodic boundary conditions (PBC) allows one to calculate atomic structure of weakly bound multilayer graphenes and graphite with high accuracy. Using PBC and cluster approximations the potential energy surfaces (PES) of migration on and penetration through the carbon lattice of a set of adatoms (carbon, oxygen, nickel) were studied and a number of special points on PESes were found. It was found that LC-DFT scheme predicts the potential energy barriers of adatom migration on graphene surface with high accuracy.

Atomic and electronic structure and spin states of 2D extended complex graphene/Ni, bigraphene/Ni and trigraphene/Ni nanocomposites in all possible coordinations were studied using PBC DFT technique. It was found that eclipsed graphene/Ni coordination is energetically preferable (see Figure). The bi- and trigraphenes display AB and ABA stacking sequences coupled with small changes of interlayer distances in comparison with parent weakly bound multigraphenes. The spin states of graphene/Ni, bigraphene/Ni and trigraphene/Ni nanocomposites are determined by Ni substrates.

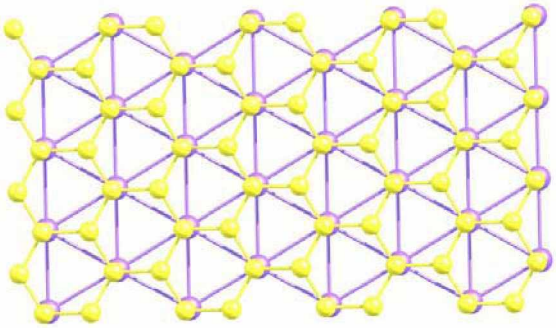

Atomic structure of 2D extended Graphene/Ni nanocomposite in eclipsed configuration.

Facile synthesis of graphene nanoribbons with adjustable width at surfaces

Abdurakhmanova N.*[1], Amsharov N.[1], Amsharov K.[1], Stepanow S.[1], Jansen M.[1], Kern K.[1,2]

[1]*Max Planck Institute for Solid State Research, D-70569 Stuttgart, Germany*
[2]*Institut de Physique de la Matière Condensée, Ecole Polytechnique Fédérale de Lausanne, CH-1015 Lausanne, Switzerland*
**e-mail: nasiba.a@fkf.mpg.de*

Graphene Nanoribbons (GNRs) have been predicted to show interesting electronic properties that depend largely on their width and edge structure. Despite the many curious theoretical investigations demonstrating the particular properties of GNRs [1], the experimental verification is still challenging because the production of GNRs of well-defined width and edge structure are still limited. Recently the possibility to grow narrow nanoribbons from poly-aromatic hydrocarbon precursors has been demonstrated at surfaces [2].

Here, we present the synthesis of armchair nanoribbons at surfaces with adjustable width using specially designed precursor molecules with an unusual coupling scheme. The class of precursors allows for the facile modification of the edge structure with heteroatoms.

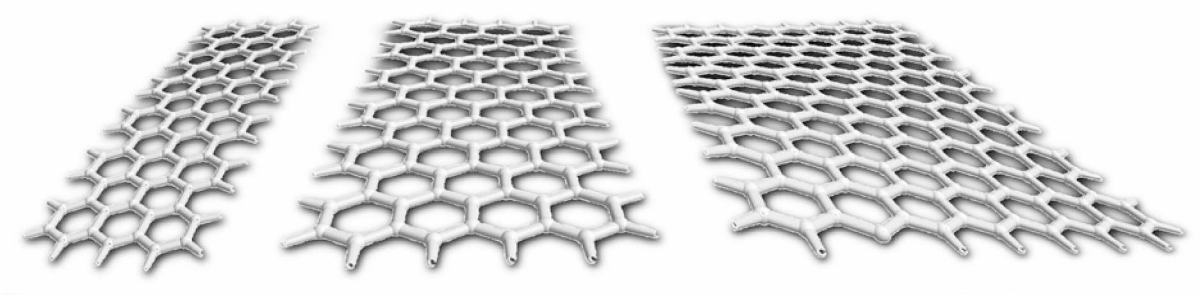

[1] Li Yang et. Al., *Phys. Rev. Lett.* **99**, 186801 (2007).
[2] J. Cai et. Al., *Nature* **466**, 470 (2010).

Funding graphene research in the European Research Area

Sadowski M.L.

European Commission, DG Research and Innovation

The European Union and its Member States will be confronted in the coming decades with growing challenges: the new industrial and trade situations, pressure on supplies and energy security, climate change, technological revolutions, increased ageing of the population, internal migrations and the availability of critical raw materials, to mention only a few.

Materials research has an essential role in supporting development of competitive and sustainable economic growth in Europe: the globalisations of the markets and the increasing complex needs of society demand improved industrial processes and products with better service performance, quality, reliability, durability, specific functionalities and end-of-life destiny.

The European Commission promotes research in materials science and engineering. The EU 7th Framework Programme for Research and Technological Development (FP7) is currently supporting research actions to overcome scientific, technological and related bottlenecks, provoking or facilitating new ideas that can give Europe a competitive advantage internationally in the forthcoming years.

One of the very important materials to have appeared on the scene in recent years is graphene; this talk concerns the funding of graphene-related research projects under FP7, as well as associated European programmes – the current state of play and outlooks for the future

.

Conformational changes and chemistry of single-layer graphene oxide

Whitby R.L.D.*[1], Korobeinyk A.[1], Gun'ko V.M.[1,2], Busquets R.[1], Cundy A.B.[1,2], Laszlo K.[3], Skubiszewska-Zięba J.[4], Leboda R.[4], Tombacz E.[5], Toth I.[5], Kovacs K.[5], Mikhalovsky S.V.[1]

[1]*Nanoscience & Nanotechnology Group, Faculty of Science and Engineering, University of Brighton, Lewes Road, Brighton, BN2 4GJ, United Kingdom*
[2]*Institute of Surface Chemistry, 17 General Naumov Street, 03164 Kiev, Ukraine*
[3]*BudapeSt. University of Technology and Economics, H-1521 Budapest, Hungary*
[4]*Maria Curie-Skłodowska University, 20031 Lublin, Poland*
[5]*Department of Physical Chemistry and Material Science, University of Szeged, H-6720 Szeged, Hungary*
**e-mail: r.whitby@brighton.ac.uk*

Single-layer graphenes (SLG) possess thermal and electronic conductive properties superior to those for carbon nanotubes [1], but in order to release their potential, chemical modification will often be necessary to tailor (or integrate) graphenes for a particular end purpose [2]. The type and distribution of acidic groups on SLG and oxygenated forms (SLGO) has been inferred from NMR, XPS and micro-Raman analyses, which include carboxylic, alcohol, hydroxyl / phenolic, lactone, ester, epoxy and ketones [3]. However, a conventional method of detecting the type of acidic groups on carbons through acid-base (Boehm) titrations offers both quantitative and qualitative analysis [4]. Moreover, this route can be utilized to monitor the depletion (or increase) in the number of functional groups, which directly correlates to their chemical reactivity [5,6].

When considering the chemical reactivity of SLGO, the type and conditions of the desired process can lead to degradation of the sheet structure and/or conformational changes that affect its overall reactivity. Nonetheless, elucidation of the controlling mechanisms can be exploited to develop the structure of SLGO-composites on the macroscale, promising useful applications in the field of nanomaterial capture for waste clean-up, slow drug release, material storage, etc. A number of covalent reactions have been considered and, currently, diisocyanate functionalisation proffers a useful intermediate for conducting covalent modification without dramatically altering the underlying graphene.

[1] Novoselov K.S., Geim A.K., Morozov S.V., Jiang D., Zhang Y., Dubonos S.V., et al. *Science* **306**, 666 (2004)
[2] Park S., Dikin D.A., Nguyen S.T., Ruoff R.S., J. Phys. Chem. C, 113, 15801 (2009).
[3] Yang D., Velamakanni A., Bozoklu G., Park S., Stoller M., Piner R.D., Stankovich S., Jung I., Field D.A., Ventrice C.A., Ruoff R.S., *Carbon* **47**, 145 (2009)
[4] Boehm H.P., *Carbon* **40**, 145 (2002)
[5] Wang Z., Shirley M.D., Meikle S.T., Whitby R.L.D., Mikhalovsky S.V., *Carbon* **47**, 73 (2009)
[6] Wang Z., Korobeinyk A., Whitby R.L.D., Meikle S.T., Mikhalovsky S.V., Aquah S.F.A., Kroto H.W., *Carbon* **48**, 916 (2010)

Growth and electrochemical properties of carbon nanosheets via microwave plasma enhanced chemical vapor deposition

Wang Z.P. *[1,2], Shoji M.[2], Ogata H.[1,2]

[1]*Institution for Sustainability Research and Education, Hosei University, 2-17-1, fujimi, chiyoda-ku,102-8160, Tokyo, Japan*

[2]*Department of Chemical Science and Technology, Faculty of Bioscience and Applied Chemical & Graduate School of Engineering, Hosei University, 3-7-2, kajino-cho, koganei, 184-8584, Tokyo, Japan*

**e-mail: wangzhipeng11@gmail.com*

Since the successful fabrication by Geim and his coworkers in 2004 [1], single-layer sheet of graphene is "rising-star" materials and has attracted a great attention because of its promising properties and potential applications. Certainly, multilayered graphene nanostructures are equally interesting and worthy of investigation in the fields of electronic devices, supercapacitprs, solar cells, sensors and so on. Carbon nanosheets (CNSs, also named as carbon nanowalls, nanoflakes, petal-like films and so on), one of the multilayered graphene nanostructures, have been reported by many groups employing various synthetic methods such as arc discharge-based techniques, radio frequency sputtering, plasma enhanced chemical vapor deposition (PECVD) and other chemical processes. Among those methods, PECVD is regarded as promising means for CNS growth due to its feasibility and potentiality for large-area production with high quality, high growth rate and/or atomically thin. Here, we report a facile growth of CNSs by microwave PECVD (MPECVD) without any catalySt at relatively low temperatures (less than 500 ^{o}C). Significantly, as-grown CNSs mainly consiSt of from 2 to 7 layers of graphene in large quantity. Detailed results including electrochemical properties will be presented in the conference.

[1] K.S. Novoselov, A.K. Geim, S.V. Morozov, D. Jiang, Y. Zhang, S.V. Dubonos, I.V. Grigorieva, A.A. Firsov, *Science* **306**, 666 (2004).

A Monte Carlo study of C_{70} molecular motion in C_{70}@SWCNT peapods

Verberck B.*[1,2], Cambedouzou J.[2], Vliegenthart G.A.[3], Gompper G.[3,4], Launois P.[2]

[1]*Departement Fysica, Universiteit Antwerpen, Groenenborgerlaan 171, B-2020 Antwerpen, Belgium*
[2]*Laboratoire de Physique des Solides, UMR CNRS 8502, Université Paris-Sud 11, F-91405 Orsay, France*
[3]*Institute for Advanced Simulation, Forschungszentrum Jülich, D-52425 Jülich, Germany*
[4]*Theoretical Soft Matter and Biophysics, Institut für Festkörperforschung, Forschungszentrum Jülich, D-52425 Jülich, Germany*
**e-mail: bart.verberck@ua.ac.be*

Since their discovery more than a decade ago, fullerene nanopeapods — single-walled carbon nanotubes (SWCNTs) filled with fullerenes — have been the subject of extensive experimental and theoretical research, and have paved the way for a new direction in the field of one-dimensionally confined systems. C_{60}@SWCNT peapods were discovered first [1], but various other fullerenes have been inserted in nanotubes as well, e.g. C_{70} [2]. We present Monte Carlo simulations of chains of C_{70} molecules in a SWCNT. For various tube radii R (6.5 Å $\leq R \leq$ 7.5 Å), we analyze rotational and translational motion of the C_{70} molecules as a function of temperature. We not only reproduce the experimentally well-established lying and standing molecular orientations for small and large tube radii [2], respectively, but we also observe a variety of molecular motions, including orientational flipping of lying molecules and the migration of molecules resulting in a continual rearrangement of the C_{70} molecules in clusters of varying lengths. An analysis of the pair correlation functions reveals a transition from a linear harmonic chain to a hard-sphere liquid with increasing temperature, making C_{70}-peapods tunable physical realizations of two well-known one-dimensional model systems [3]. Our results are in agreement with recent X-ray diffraction experiments [4] and are relevant for possible applications using the dependence of a nanopeapod's electronic properties on the molecules' orientations [5].

[1] B.W. Smith, M. Monthioux, and D.E. Luzzi, *Nature* **396**, 323 (1998).
[2] H. Kataura, Y. Maniwa, T. Kodama, K. Kikuchi, H. Hirahara, and K. Suenaga, Synth. Met. **121**, 1195 (2001); K. Hirahara, S. Bandow, K. Suenaga, H. Kato, T. Okazaki, and H. Shinohara, *Phys. Rev. B* **64**, 115420 (2001).
[3] B. Verberck, J. Cambedouzou, G.A. Vliegenthart, G. Gompper, and P. Launois, *Carbon* **49**, 2007 (2011).
[4] P. Launois, M. Chorro, B. Verberck, P.-A. Albouy, S. Rouzière, D. Colson, A. Forget, L. Noé, H. Kataura, M. Monthioux, and J. Cambedouzou, *Carbon* **48**, 89 (2010).
[5] S. Okubo, T. Okazaki, K. Hirose-Takai, K. Suenaga, S. Okada, and S. Bandow, *J. Am. Chem. Soc.* **132**, 15252 (2010).

Nitrogen-doped graphene: synthesis and properties

Usachov D. [1], Fedorov A.V.[1], Vilkov O.Yu.[1], Vyalikh D.V.[1,2], Adamchuk V.K.[1]

[1]*St. Petersburg State University, 198504, St. Petersburg, Russia*
[2]*Institute of Solid State Physics, Dresden University of Technology, D-01062 Dresden, Germany*
**e-mail: usatchevd@bk.ru*

Graphene is considered as one of the moSt perspective materials for different nanoelectronic devices. Due to aspiration for controlling its electronic properties, a variety of possible functionalized forms of graphene attracts particular attention [1, 2]. The moSt obvious route in this direction is graphene doping by different types of atoms. Simulations show than graphene doping opens a possibility to construct tunable electronic devices through control of the dispersions and electron-phonon coupling [3]. One of the possibilities for graphene doping is incorporation of nitrogen atoms into the graphene lattice [2, 4].

This work is dedicated to exploration of the possibility of CVD-grown graphene electronic structure tuning by nitrogen doping. A combined study by means of core-level (XPS) and angle-resolved (ARPES) photoelectron spectroscopy as well as scanning tunneling microscopy (STM) is presented.

In order to study the process of N-doped graphene synthesis, a real-time photoemission study was carried out during chemical vapor deposition (CVD) procedure. It provided comprehensive information on the mechanism of N-graphene growth. It is shown that N-doped graphene with nitrogen concentration of 0.5-2% can be synthesized by means of CVD on a nickel surface. Spatial distribution of N atoms in graphene film is discussed in view of XPS and STM results.

In order to explore the bandstructure at the Fermi level, graphene was transformed into a quasi-freestanding state using gold intercalation technique. It is shown that N atoms, incorporated into graphene lattice, act as electron donors, transforming graphene into n-type semiconductor. This results in a shift of a Dirac cone towards higher binding energies, observed with ARPES.

[1] J. T. Robinson et al., *Nano Lett.* **10**, 3001 (2010).
[2] Y. Wang et al., *ACS Nano* **4**, 1790 (2010).
[3] C. Attaccalite et al., *Nano Lett.* **10**, 1172 (2011).
[4] J.C. Meyer et al., *Nature Mat.* **10**, 209 (2011).

Engineering nanodiamond-PANI nanocomposites: structural features and mutual arrangements

Terranova M.L.*[1], Orlanducci S.[1], Tamburri E.[1], Guglielmotti V.[1], Sordi D.[1], Toschi F.[1], Matassa R.[2], Passeri D.[2], Rossi M.[2]

[1]*Dept. of Chemical Science and Technology-MINASlab, University of Rome Tor Vergata, 00133, Roma, Italy*
[2]*Dept. of Fundamental and Appl. Sciences for Engineering and CNIS, University Sapienza, 00162, Roma, Italy*
**e-mail: terranova@roma2.infn.it*

Innovative composites formed by detonation nanodiamond (DND) inserted in Polyaniline (PANI) matrices have been prepared and investigated. PANI is one of the moSt interesting conducting polymers, with striking electronic and optical properties, widely used as matrix for the preparation of nanocomposites. However the use of detonation nanodiamond as gueSt component of PANI-based nanocomposites was never been proposed up to now. As a general rule, the fillers are viewed as agents able to modify some functional properties of the matrix, and a variety of nanocomposites based on DND are presently designed and manufactured for a variety of applications. In such a context, this research was aimed at the investigation of the mutual lay-out of DND and conducting polymers, and of the architectures obtained by coupling them. Several preliminary and stimulating results were obtained from deep investigations carried out by using FE-SEM, TEM, TED, XRD and micro-Raman. FirSt of all, it has been evidenced that the DND dispersions did not modify substantially the structural features of the polymer. Nevertheless, the arrangement of the polymer segments and the spatial distribution of DND appear to be reciprocally influenced. These effects seem to be correlated to the increase of the thermal stability and reduction of the T-induced decomposition of the PANI backbone, as detected by TGA and DGT measurements. From the structural point of view, the moSt intriguing result has been the discover that the DND crystallites embedded in the PANI matrix show an unexpected preferential self-orientation probably driven by the tendency of PANI chains to a self-organization in elongated architectures. For embedded DND crystallites a slight modification of interplanar distances has been also detected

From the functional point of view an important consequence of the DND insertion is the speed-up of the polymerization process, demonstrating a high catalytic activity on the chemical oxidative polymerization of the momomer. Electrochemical tests also indicate that DND/PANI materials act as efficient catalytic mediator for some processes of electron transfer.

Overall these DND-PANI materials are not only promising for challenging technological applications but also important for the controlled growth of polymeric units, for the fabrication of nanoarchitectures and for understanding the mechanisms of crystallites alignment/orientation triggered by foreign structures.

Structural study of graphite oxide hydration: effects of temperature and pressure

Talyzin A.

Department of Physics, Umeå University, Umeå, 901 87 Sweden
e-mail: alexandr.talyzin@physics.umu.se

Hydration of graphite oxide by excess of water was studied in the temperature interval 295-230K using synchrotron X-ray diffraction [1]. Expansion of hydrated graphite oxide structure due to insertion of additional water occurs upon cooling down from ambient temperature to the point of water media freezing as evidenced from continuous shift of (001) reflection which corresponds to interlayer distance of graphite oxide structure. Structural breathing is found around the freezing point of H_2O and connected to insertion/expulsion of water to/from interlayer space. Cooling down below the point of water medium solidification results in stepwise contraction of graphite oxide interlayer distance by ~25% due to partial withdrawal of water from the hydrated structure. Heating back from 230K to ambient temperature results in graphite oxide structure expansion due absorption of water from medium, thus making a reversible cycle. Structural breathing of graphite oxide was also studied at high pressure conditions using excess of basic or acidic water media. The lattice spacing of graphite oxide in excess of NaOH solution increases by 85% at 1.6 GPa. In contrast, structure expansion of graphite oxide immersed in liquid water with added HCl is significantly less pronounced compared to compression in pure water. The point of media solidification correlated with sharp decrease of graphite oxide layers separation due to partial withdrawal of water from the structure [2].

The effect of structure breathing is important for chemical treatments performed with graphite oxide in solution, e.g. graphite oxide functionalization and conversion into graphene-related materials

[1] A.V. Talyzin, S.M. Luzan, T. Szabó, D. Chernyshev, V. Dmitriev, *Carbon*, Available online (2011).

[2] A.V. Talyzin, B. Sundqvist, T. Szabo, V. Dmitriev, *J. Phys. Chem. Lett.* 2, 309 (2011).

Evaporation of detonation nanodiamonds

Šiller L.*[1], Astuti Y.[1], Butenko Y.V.[1,2], Brieva A.C.[1], Coxon PR.[1], Alves L.[1], van Papendrecht G.[2], Bangert U.[3], Gass M.[4], Mendis BG.[5]

[1]*Newcastle University, NE1 7RU, UK;*
[2]*European Space Agency, Noordwijk 2201 AZ, Netherlands*
[3]*University of Manchester, M1 7HS, Manchester, UK*
[4]*SuperSTEM, STFC Daresbury Laboratory, WA4 4AD, UK*
[5]*Durham University, Durham, DH1 3LE, UK*
**e-mail: Lidija.Siller@ncl.ac.uk*

Diamond nanoparticles have drawn significant attention from a wide range of researchers for use in a variety of applications including, plating, lubricating oils, polishing, and biomedical devices.[1] The optical properties of the nitrogen-vacancy colour centre,[2] which can undergo strong spin-sensitive optical transitions under ambient conditions, makes them attractive for example for quantum optics[3] and biolabelling.[4] Until now one of the main approaches for producing large quantities of sub 10 nm nanodiamonds has been a top-down approach involving milling luminescent high pressure high temperature (HPHT) microdiamonds into 7 nm particles and forming water dispersible colloidal quasi-spherical nanodiamonds.[5]

An alternative approach for producing nanodiamonds is by direct treatment of detonation nanodiamond powder. The typical worldwide output by this approach is several tonnes each year. However, a major drawback of this method is that the individual particles agglomerate into clusters ranging from hundreds of nanometres to several micrometres in diameter owing to strong interparticle bonding and the presence of soot-like structures surrounding the nanodiamond crystals.[6] Since the nature of this material has the potential to limit the range of viable nanodiamond applications, many groups have investigated routes towards separating persistent nanodiamond agglomerates.

In this work we report a method for the complete separation of detonation nanodiamond agglomerates yielding well-dispersed nanodiamond particles passivated with surface alkyl groups in solution and powder form. Powder of isolated diamond nanoparticle than can be re-suspended, deposited on any substrate and then evaporated. This evaporation processing route could open a way to nanodiamond size-selection and hence new applications.

[1] Vereschagin, A.L. *Detonation Nanodiamonds;* Altai State Technical University, Barnaul: Russia, 2001.
[2] Vlasov, I. I.; Barnard, A. S.; Ralchenko, Lebedev, O.I.; Kanzyuba, M.V.; Saveliev, A.V.; Konov, V.I., Goovaerts, E. *Adv. Mater.* **21**, 808 (2009).
[3] Kurtsiefer, C.; Mayer, S.; Zarda, P.; Weinfurter, H. *Phys. Rev. Lett.* **85**, 290 (2000).
[4] Smith, B. R.; Inglis, D. W.; Sandnes, B.; Rebeau J.R.; Zvyagin A.V.; Gruber D.; Noble C.J.; Vogel V.R.; Osawa, E.; Plakhotnik T., *Small* 5, 1649 (2009).
[5] Boudou, J. P.; Curmi, P. A.; Jelezko, F.; Wrachtrup, J. ; Aubert P. ; Sennour, M., Balasubramanian, G. ; Reuter, R. ; Thorel A. ; Gaffet, E. ; *Nanotechnology* **20**, 235602 (2009).
[6] Kruger, A.; Kataoka, F.; Ozawa, M. ; Fujino, T.; Suzuki, Y.; Aleksenskii A.E.; Vul', A.Y.; Osawa, E; *Carbon* **43**, 1722 (2005).

Carbon dots decorated nanodiamond

Shenderova O.A.* [1], Hens S.[1], Turner S.[2], Van Tendeloo G.[2], Vlasov I.[3]

[1]*International Technology Center, 27615, Raleigh, USA*
[2]*EMAT, University of Antwerp, 2020 Antwerp, Belgium*
[3]*General Physics Institute, Russian Academy of Sciences, 119991 Moscow, Russia*
**e-mail: oshenderova@itc-inc.org*

Although nanodiamonds produced by detonation synthesis (detonation nanodiamond (DND)) from carbon-containing explosives, have a low level of intrinsic photoluminescence (PL), for typical DND samples it is too weak to be useful for many applications. However, DNDs are inexpensive to produce in large quantities, so it would be advantageous to produce enhanced PL properties in DNDs. There are numerous approaches for synthesis of so called carbon dots, the luminescent graphite or amorphous carbon particles juSt a few nanometers in size. In the current work, we report how carbon dots decorated DND (Fig.1) can be produced from detonation soot demonstrating surprisingly strong photoluminescence of different colors depending on the conditions of treatment and the type of soot treated.

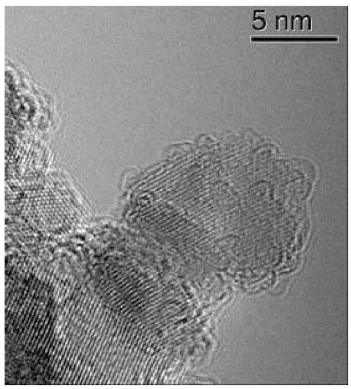

Figure 1. HRTEM of photoluminescent carbon dots decorated nanodiamond.

The PL spectra demonstrated a factor of more than 20 times enhancement of red luminescence in these samples as compared to typical DND from detonation synthesis. Mechanisms of formation of these hybrid structures will be discussed.

[1] M.G. Ivanov, S.V. Pavlyshko, D.M. Ivanov, I. Petrov, G. McGuire, O. Shenderova, *Mater. Res. Soc. Symp. Proc.* **1203**, 1203-J17-16 (2010).

[2] M.G. Ivanov, S.V. Pavlyshko, D.M. Ivanov, I. Petrov, O. Shenderova, *JVST. B* **28**(4), 869 (2010).

Graphene in view of atomic-molecular approach

Sheka E.F.

Peoples' Friendship University of Russia, 117198 Moscow, Russia
e-mail: sheka@icp.ac.ru

Atom-molecular approach suggested in the paper concentrates attention on characteristics of graphene that follow from peculiarities of its atomic electronic structure, main of which is effective unpairing of odd electrons. The feature makes graphene stand in one row with fullerenes and carbon nanotubes, which opens large facilities of application of a number of conceptually original and practically efficient approaches developed for and checked over the latter to the graphene case [1]. This concerns the following fundamental properties of graphene

1. Chemical activity and chemical modification;
2. Magnetic behavior;
3. Mechanical strength and failure;

sp^2 Nanocarbons become partially radicalized when the length of their C-C bonds exceeds a limit value of 1.395Å, under which two odd electrons related to the bond are covalently coupled forming a classic pair of π electrons but over which the two electrons become effectively unpaired, the more, the bigger length of the bond. In the case of benzenoid-based structures, the number of the unpaired electrons constitutes ~0.6 *e* per the unit which is typical for fullerenes, carbon nanotubes, and graphene. All together the unpaired electrons of total number N_D quantitatively determine the molecule chemical susceptibility while their fractions on each atom N_{DA} quantify the atomic chemical susceptibility. Both quantities lay the foundation of the computational synthesis of both one-step and multi-step derivatives governed by strictly defined algorithm.

Weakening the interaction between odd electrons exhibited by their effective unpairing promotes the magnetic behavior of the molecule, once existing in the singlet ground state. The weakening increases with the molecule size thus providing quite a low values for the magnetic coupling constant *J* that becomes sufficient for a noticeable van Fleck's admixture of high spin states to the singlet one [2]. When the molecule size exceeds the electron mean free path, quantization of electron properties strongly increases the constant *J*, which removes high-spin contribution from the singlet state making it non-magnetic.

The molecular approach based on mechanochemical reaction is suitable for describing deformation and failure of graphene as well as exhibiting a peculiar tricotage-like behavior of the graphene molecule under uniaxial tension [3] as well as the effect of chemical modification.

[1] E.F.Sheka. *Fullerenes: Nanochemistry, Nanomagnetism, Nanomedicine, Nanophotonics*. CRC Press, Taylor&Francis group: Boca Raton 2011, pp. 328.
[2] E.F.Sheka and L.A.Chernozatonskii. *J. Exp. Theor. Phys.* **111**, 222, 2010.
[3] E.F.Sheka, N.A.Popova, V.A.Popova, E.A.Nikitina, L.Kh.Shaymardanova. *J. Mol. Mod.* DOI:10.1007/s00894-010-0816-3, 2011.

High density nanodiamond monolayer obtained by an electrophoretic process

Schmidlin L.[1*], Pichot V.[1], Josset S.[1], Comet M.[1], Spitzer D.[1]

[1]*NS3E « Nanomatériaux pour les Systèmes Sous Sollicitations Extrêmes » UMR CNRS-ISL n° 3208, French-German Research Institute of Saint-Louis, 5 rue du général Cassagnou 68301 Saint-Louis, France*
**e-mail: loic.schmidlin@isl.eu*

Electrophoretic deposition is an efficient method to deposit colloidal particles on an electrode by using an electrical field. This technique has already been used for the deposition of nanoparticles [1] or nanodiamonds [2] and was here applied to detonation ultra-nanocrystalline diamonds (D-UNCD). To obtain ultrathin D-UNCD deposit, the use of suspension containing individual nanodiamonds is crucial.

The D-UNCD used in this study were synthesized and purified at the ISL [3]. The D-UNCD particles surface is mainly covered by carboxylic groups [4] resulting in a negative surface charge when suspended in water. A mechanical treatment was applied to the D-UNCD to obtain suspension containing separated nanodiamonds with an average size of 3-5 nm. An electrical field was applied to this colloidal suspension to deposit the D-UNCD on a Highly Oriented Pyrolitic Graphite electrode. The obtained deposits were characterised by Atomic Force Microscopy (AFM). The deposits topography is 5 nm, corresponding to a monolayer deposition of D-UNCD (Figure 1). The deposits density obtained with this technique is estimated to be over 10^{12} particles/cm^2. Due to the proximity of the nanodiamonds particles, an AFM tip with a radius of 2 nm wasn't able to discern them. To our knowledge such a density has never been obtained before.

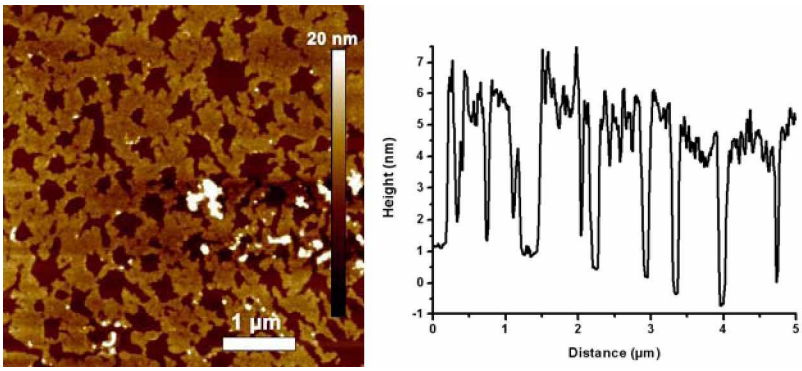

Figure 1. AFM image of an electrophoretic deposit of a D-UNCD monolayer

[1] Giersig M., Mulvaney P., *Journal of Physical Chemistry* **97**, 6334 (1993).
[2] Affoune A.M., Prasad B.L.V., Sato H., Enoki T., *Langmuir* **17**, 547 (2001).
[3] Pichot V., Comet M., Fousson E., Baras C., Senger A., Le Normand F., Spitzer. D., *Diamond and Related Materials* **17**, 13 (2008).
[4] Schmidlin L., Pichot V. Comet M., Rabu P., Spitzer D, *Diamond and Related Materials* (submitted).

Inelastic neutron investigations of AC_{60} compounds with $A=Li_4$, Mg_2 and C_8H_8

Rols S.[1], Pontiroli D.[2], Ricco M.[2], Mazzani M.[2], Launois P.[1,3], Bousige C.[3], Pekker S.[4]

[1]*Institut Laue Langevin, Grenoble, France*
[2]*University of Parma, Parma, Italy*
[3]*Laboratoire de Physique des Solides, Orsay, France*
[4]*Research Institute for Solid State Physics and Optics, Budapest, Hungary*

The research on the so called fulleride compounds (fullerene based material) has been extensively conducted for almoSt two decades now. One has to find the reason for this longevity in the exciting electronic and transport properties of these materials, ranging from high Tc superconductivity to molecular magnetism. It provides also almoSt perfect molecular models of novel organization, and the recent advances in synthesis resulted in the discovery of new phases of upmoSt interest In this presentation we will focus on the dynamics of two of these novel form of fullerides, investigated by inelastic neutron scattering:

1) Li_4C_{60} is a stacking of polymeric fullerenes linked by covalent [2+2] double bridges in one directions and one single covalent bond in the perpendicular direction. It is a ionic conductor with a very large conductivity allowed by the partial filling of the large octahedral voids found in the structure. This compound is isostructural to the Mg_2C_{60} system which is found to be the moSt resilient fulleride of its family at high temperatures: while moSt of the polymeric fullerides transform to monomer above 600 K, Mg_2C_{60} is observed to be stable up to 1000°C. We will discuss these peculiarities in parallel to their structure and dynamics.

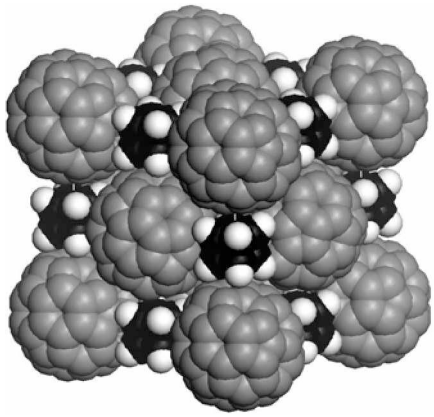

Figure1. The fullerene-cubane "rotor stator" molecular system: at ambient conditions, the fullerene molecule is a rotor-rotating freely around its center-while the stator cubane acts as static bearings.

2) The laSt system that will be discussed concerns the rotor-stator co-molecular crystal, which is composed of cubane molecules inserted in between C_{60} at the octahedral sites in the FCC lattice. It is found that this peculiar arrangement of these highly symmetric molecules provides this system with a specific dynamics where the C_{60} perform faSt rotation while the cubane molecules remains orientationally fixed.

Site-selective spectroscopy of electronic states of fullerene derivatives

Razbirin B.S.[1], Sheka E.F.[2], Nelson D.K.*[1], Starukhin A.N.[1], Degunov M.Yu.[1], Shukov I.V.[1]

[1]*Ioffe Institute, 194021, St. Petersburg, Russia*
[2]*Peoples' Friendship University, 117923, Moscow, Russia*
**e-mail: d.nelson@mail.ioffe.ru*

Knowledge of the detailed electronic structure of fullerene derivatives is very essential for understanding their molecular structure, photophysical and chemical properties. Optical spectroscopy is a powerful method of obtaining information about electronic and vibronic states of molecules. However, absorption and luminescence spectra of fullerenes and their derivatives in condensed state are usually inhomogeneously broadened even at low temperatures, which prevents from using all the variety of spectroscopic techniques for their characterization.

Traditionally, one attempts to overcome the inhomogeneous broadening by using crystalline Shpolskii's matrices which provide fine-structured optical spectra. However, in the case of fullerenes and their derivatives, this measure is successful for a very limited number of species [1–3] while a predominant majority of the spectra remain broad. This forces to look for another way to solve the problem. Quite suitable has turned out the site-selective laser spectroscopy, firSt application of which to fullerene C_{60} derivatives is presented in the paper.

A structuring of purely electronic transition (0-0) bands was observed under monochromatic excitation by laser beam within the region of vibronic bands. The substitution of the broad 0-0 emission band by a multiplet of narrow lines is explained by a combine action of several reasons among which there are 1) a weak electron-phonon interaction that provides the intense narrow zero-phonon lines accompanied with relatively weak phonon sidebands for all electronic and vibronic transitions; 2) the absence of the electron excitation transfer over different impurity centers; and 3) the electron-vibrational resonance in the excited state. The vibrational analysis of the fine-structured luminescence spectra revealed under the site selective excitation made possible to determine the frequencies of a number of intramolecular vibrations in the excited state of species under study.

The study was financially supported by the Presidium of the RAS (Program "Quantum physics of condensed matter").

[1] B.S. Razbirin, A.N. Starukhin, A.V. Chugreev, Yu.S. Grushko, S.N. Kolesnik, *JETP Lett.* **60**, 451 (1994).

[2] B.S. Razbirin, A.N. Starukhin, D.K. Nelson, E.F. Sheka, M. Prato, *Int. J. Quantum Chem.* **107**, 2787 (2007).

[3] B.S. Razbirin, E.F. Sheka, A.N. Starukhin, D.K. Nelson, M.Yu. Degunov, P.A. Troshin, R.N. Lyubovskaya, *Phys. Solid State* **51**, 1315 (2009).

SAXS measurement and dynamics of condensed carbon growth at detonation of condensed high explosives

Pruuel E.R., Ten K.A., Titov V.M.

Lavrentyev Institute of Hydrodynamics SB RAS, 630090, Novosibirsk, Russia

When using small-angle X-ray scattering (SAXS), a diffraction signal from a sample in the small-angle region is detected. This method is widely applied to static analysis of nano-dispersion structures. At SAXS measurements with the application of the highly-periodic synchrotron radiation from the VEPP-3 accelerator facility (with an exposure of 1 ns and periodicity of 250 ns), the evolution of the angular distribution of signal in the process of detonation of high explosives is recorded. A numerical simulation shows that the SAXS signal amplitude is equal to

$$E(q,R) = i_0 \cdot n \cdot \frac{1}{q^3}\left[Sin(qR) - (qR)\cdot Cos(qR)\right],$$

where

$$I_0(q,R) = i_0 \cdot \left[E(q,R)\right]^2 = i_0 \cdot ((R^3 n))^2 \cdot P(q)$$

is the amplitude of the scattered synchrotron radiation, i0 is the scattering by electrons in a 1-cm3 volume of the sample (carbon nanoparticles), n is the sample density, R is the radius of the sample, $\vec{q} = \vec{k} - \vec{k}_0$ - is the scattering vector, and P(q) is the form factor. The angular distribution of SAXS is determined by the form factor P(q), analyzing which one can determine the sizes of the arising particles of condensed carbon and changes in these sizes with time after the passage of the detonation wave.

In the experiments, we recorded the dynamics of the angular distribution of the small-angle scattering of synchrotron radiation, as well as the integrated SAXS signal. We investigated pressed charges of the following mixtures: 50/50 TNT/RDX, TATB (triaminotrinitrobenzene, $C_6H_6N_6O_6$), and BTF (benzo-tris(1,2,5-oxadiazolile oxide), $C_6N_6O_6$). The charges were 20 mm in diameter. Nanoparticles of d ~ 1.5-2 nm are recorded at the detonation front. Then the particle size increases and by the time t ~ 3 μs it reaches d ≈ 4 nm in TATB; in TG 50/50 the particle size d ≈ 6 nm; while in the BTF explosion products, particles with d ≈ 70 nm are detected.

Nanocarbon modified epoxy resin and microwaves

Pliushch A.[1], Kuzhir P.*[1], Maksimenko S.A., Coderoni L.[2], MicciullaF.[2], Sacco I.[2], Rinaldi G.[3], Bellucci S.[2]

[1]*Institute for Nuclear Problems, 220050, Minsk, Belarus,*
[2]*Frascati National Laboratory, 00044, Rome (Frascati), Italy*
[3]*University of Rome "Sapienza", 00133, Rome, Italy*
**e-mail: polina.kuzhir@gmail.com*

The study is focused on electromagnetic (EM) response properties of Modified Bisphenol A Epoxy Resin, widely used in aerospace applications, as paint and structural glue, enriched with a low concentration of laboratory-made arc-discharge carbon nanotubes (CNT) and commercially available CVD-made single-walled and multi-walled carbon nanotubes. The EM attenuation and reflection in X-band (8–12 GHz), Ka-band (26–37 GHz) and W-band (78–118 GHz) provided by fabricated samples were measured as a function of the functional filler content (0.25-1.5 wt.%). The constitutive parameters of nanocarbon based composites in microwave frequencies has been theoretically modeled by means of nanoelectromagnetics and reconstructed from the experimental data. The EM effectiveness has been found to be strongly dependent on the nanocarbon percentage, type and synthesis conditions.

The work was partially supported by the ISTC project B-1708, the EU FP7 project FP7-266529 BY-NanoERA and the Italian Ministry PRIN 2008 research program Development and Electromagnetic Characterization of Nano Structured Carbon Based Polymer CompositEs (DENSE).

Nitrogen doping of detonation nanodiamonds

Pichot V.[1]*, Stephan O.[2], Comet M.[1], Mory J.[1], Fousson E.[1], March K.[2], Spitzer D.[1]

[1]*NS3E « Nanomatériaux pour les Systèmes Sous Sollicitations Extrêmes » UMR CNRS-ISL n° 3208, French-German Research Institute of Saint-Louis, 5 rue du général Cassagnou 68301 Saint-Louis, France*
[2]*Laboratoire de Physique des Solides (UMR CNRS 8502), bât. 510, Université Paris Sud, 91405 Orsay, France*
**e-mail: vincent.pichot@isl.eu*

The presence of nitrogen/vacancies inside nanodiamond particles is of great importance to confer them luminescent properties which open a wide field of applications in biology and in quantum physics. Bradac et al. has reported an intermittency luminescence in 5 nm detonation nanodiamonds [1]. Varying nitrogen content inside detonation nanodiamonds should be very helpful to obtain stable photoluminescence properties.

Ultra-nanocystalline nanodiamonds are synthesized at the ISL by detonation using a high explosive mixture composed of trinitrotoluene (TNT) and hexogen (RDX) (70/30). The detonation of the charge leads to a powder containing nanodiamond crystallites ($\Phi \sim 5$ nm) [2]. The content of the nitrogen present inside these as-synthesized nanoparticles was determined by Electron Energy-Loss Spectroscopy (EELS) and is about 3 wt.%. EELS is a very useful tool for determining the location and the quantity of nitrogen within individual nanodiamonds [3, 4]. The doping nitrogen comes from the explosive molecules which contain a lot of nitrogen atoms. A study on the nitrogen doping of detonation nanodiamonds was carried out.

The experimental results demonstrate that the nitrogen content strongly depends on the precursors used in the explosive charge composition. We have demonstrated that with the incorporation of a nitrogen rich compound, it is possible to increase the nitrogen content by a factor two or three. Such high nitrogen contents have never been reported in detonation nanodiamonds. A careful study of the nitrogen spectroscopic signature revealed that it is present inside the nanodiamond core in a sp^3 hybridization configuration [4].

[1] Bradac C., Gaebel T., Naidoo1 N., Sellars M. J., Twamley J., Brown L.J., Barnard A.S., Plakhotnik T., Zvyagin A.V., Rabeau J.R., *Nature Nanotechnology* **5**, 345 (2010).

[2] Pichot V., Comet M., Fousson E., Baras C., Senger A., Le Normand F., Spitzer. D., *Diamond and Related Materials* **17**, 13 (2008).

[3] Turner S., Lebedev O.I., Shenderova O., Vlasov I.I., Verbeeck J., Van Tendeloo G., *Advanced Functional Materials* **19**, 2116 (2009).

[4] Pichot V., Stephan O., Comet M., Mory J., Fousson E., March K., Spitzer D., *Journal of Physical Chemistry C* **114**(22), 10082 (2010).

Diamond nanoparticles with functionalized surface –a NMR study

Panich A.M.

Department of Physics, Ben-Gurion University of the Negev, Be'er Sheva 84105, Israel
e-mail: pan@bgu.ac.il

Nanodiamond (ND) particle consists of a mechanically stable and chemically inert diamond core and a chemically active surface. On-purpose functionalization of the ND surface with targeted species allows preparation of NDs with specified chemical, physical and electronic properties. Here we review our recent NMR studies of structure, chemical bonding and properties of fluorinated (F-ND), hydroxylated (OH-ND) NDs and those with surface decorated by transition metal ions (Cu-ND and Co-ND).

In F-ND, we obtained formation of different fluorocarbon groups on the nanodiamond surface, which substitute for hydrocarbon and hydroxyl groups. Our data provide detailed information about the structure and bonding in both diamond core and surface of the F-ND particle. The NMR data are supported by EPR, XPS and Raman findings. F-ND sample has a significant number of paramagnetic defects located mainly near the diamond surface, resulting in faSt ^{19}F and ^{13}C nuclear spin-lattice relaxation.

NMR studies of Cu-ND and Co-ND exhibit that chemical modification results in appearance of paramagnetic Cu^{2+} and Co^{2+} complexes at the ND surface. This conclusion comes from the increase in the ^{1}H and ^{13}C nuclear spin-lattice relaxation rates of the surface hydrocarbon and hydroxyl groups and of the diamond core carbons obtained in the experiment, revealing appearance of paramagnetic Cu^{2+} and Co^{2+} complexes at the ND surface and their interaction with the hydrogen and carbon nuclear spins. Subsequent annealing of the modified samples up to 900°C results in an inverse process, i.e., a reduction of the relaxation rate, indicating that these complexes are destroyed, and metal ions join each other forming copper and cobalt nanoclusters.

OH-ND reveals complex spectra consisting of several components coming from the diamond core, surface CH_x and C-OH groups and adsorbed moisture.

Polymer-nanodiamond composites

Ozerin A.N.[1], Ozerin A.N.*[1], Alkhanishvili G.G.[1], Kurkin T.S.[1], Kechek'yan A.S.[1], Gritsenko O.T.[1], Ozerina L.A.[1], Sustchev V.G.[2], Dolmatov V.Yu.[2]

[1]*Enikolopov Institute of Synthetic Polymeric Materials, 117393, Moscow, Russia*
[2]*JSC "Diamond Centre", 193177, St.-Petersburg, Russia*
**e-mail: ozerin@ispm.ru*

Polymer-based filled with particles composite materials are widely used in the modern industry and technologies, including nanotechnologies, thanks to their light processing into final products.

Among other species, the promising components for the polymer nanocomposites are nanodiamond (or inexpensive in production nanodiamond soot) prepared by the detonation synthesis (ND and NDS) [1]. ND and NDS can be used as effective modifying agents providing improved mechanical or tribological characteristics of the filled polymer systems.

The objective of this study was to examine the structure and properties of the new type of polymer/ND(S) composites and to investigate the possibility of the nanocomposite morphology, structure and properties regulation under controllable loading of the nanoparticles into polymeric matrix.

Poly(vinyl alcohol) as well as commercially produced polybutadiene/polystyrene thermoplastic elastomer DST-30®, poly(propylene), poly(amide) and epoxy resin were used as matrix polymers for nanocomposites. The ND and NDS were supplied by JSC "Diamond Center", St. Petersburg, Russia. SAXS, WAXS, DLS, DSC, SEM, TEM, mechanical and tribological testing were used for samples characterization.

For the oriented fibers based on poly(vinyl alcohol) impregnated with ND(S), the maximum increase in the longitudinal elastic modulus over nonmodified fibers (from 30 GPa up to 45 GPa) and in the energy stored by oriented fiber modified with NDS upon breaking (from 3 up to 6 J/g) was obtained at a small (1% by volume) NDS content, which is technologically attractive [2]. For thermoplastic elastomer/NDS composites, the addition of NDS had a significant influence on the mechanical properties of the modified polymeric matrix [3].

Finally, some problems of current importance and unresolved tasks are considered in connection with a global task of polymer nanocomposites design.

This work was supported by the RFBR and the Research Program P-21 of the Presidium of RAS.

[1] Dolmatov, V. Yu. *Russian Chem. Rev.* **76**, 339 (2007); *Nanotechnologies in Russia* **4**, (9–10), 556 (2009).

[2] Kurkin, T. S.; Ozerin, A. N.; Kechek'yan, A. S.; Gritsenko, O. T.; Ozerina, L. A.; Alkhanishvili, G. G.; Sushchev, V. G.; Dolmatov. V. Yu. *Nanotechnologies in Russia* **5**, (5–6), 340 (2010).

[3] Ozerin, A.N.; Kurkin, T.S.; Alkhanishvili, G.G.; Kechek'yan, A.S.; Gritsenko, O.T.; Perov, N.S.; Ozerina, L.A.; Beshenko, M.A.; Dolmatov, V.Yu. *Nanotechnologies in Russia*, **4**(7–8), 480 (2009).

Electronic properties of fluorinated graphite and graphene

Okotrub A.V.*[1], Bulusheva L.G.[1], Makarova T.L.[2], Yudanov N.F.[1], Chehova G.N.[1], Asanov I.P.[1], Gusel'nikov A.V.[1]

[1]*Nikolaev Institute of Inorganic Chemistry SB RAS, 6303090, Novosibirsk, Russia*
[2]*Ioffe Institute, 194021, St.-Petersburg, Russia*
**e-mail: spectrum@niic.nsc.ru*

Depending on synthesis method graphite fluorides CF_x ($x \leq 1$) with different composition can be obtained. In the stoichiometric compounds, CF and C_2F, fluorine atoms form covalent bonds with each carbon atom or with half of carbon atoms of a graphene layer. The large interlayer spacing (more than 0.6 nm) allows preparing intercalates with various molecules. Depending on synthesis method graphite fluorides CF_x ($x \leq 1$) with different composition can be obtained. The large interlayer spacing (more than 0.6 nm) allows preparing intercalates with various molecules.

Graphite fluoride with a composition close to C_2F has been synthesized by fluorination of highly oriented pyrolytic and natural graphite using a BrF_3 at room temperature. Electronic structure of graphite fluoride was probed using near edge x-ray absorption fine structure (NEXAFS) spectroscopy. The spectra measured near the C K- and F K-edges showed retention of delocalized π^*-system in graphite fluoride C_2F. The probable distribution of fluorine atoms on the graphite surface was determined from quantum-chemical modeling of the NEXAFS spectra. The fluorine atoms were found to be easy detached from the C_2F surface under electron beam irradiation in a high vacuum or with a hydrazine vapor treatment. Resulting restoration of graphene π-system produces channels for electron transport. Surface electric conductivity of C_2F sample was found to appear after ~1 min exposure to hydrazine vapor and increase after additional ~40 sec treatment. The dependence of sample resistance on the exposure time is fitted by a triple exponential function exhibiting complex character of the reduction process. Investigation of sensor properties of the reduced C_2F surface to NH_3, NO_2, and Cl_2 was carried out by home-made gas sensing detection system at room temperature. Calculations revealed that NH_3 or NO_2 molecule is readily adsorbed on the reduced surface with a charge transfer from the molecule to the carbon layer or verse versa.

The changes in C_2F_x stoichiometry are shown to have a decisive effect on magnetic properties of produced complexes. The spin concentration decreases with the increase of fluorine content in fluorocarbon matrix. All samples have groups of correlated spins; at the temperatures 1.75–5 K nonlinear magnetization is observed, indicating a high-spin state. Application of the Langevin formula shows that the clusters consiSt of 10–20 interacting spins.

Fabrication, characterization and properties of $C_{60}(OH)_x$ nanocrystals by a reprecipitation method

Ogata H.*[1,2], Baba K.[1]

[1]*Graduate School of Engineering, Hosei University, 3-7-2, kajino-cho, koganei, Tokyo 184-8584, Japan*
[2]*Research Center for Micro-Nano Technology, Hosei University, 3-11-15, Midori-cho, Koganei, Tokyo 184-0003, Japan*
**e-mail: hogata@hosei.ac.jp*

Recently, various kinds of fullerene nanocrystals were reported to be easily grown by the precipitation methods[1-3]. Much interests are concentrated on these methods as the useful techniques for applications of fullerene materials. Polyhydroxylated fullerenes ($C_{60}(OH)_x$:fullerenol) are promising materials for use in the field of life science and so on because of their water-solubility. In this study, we report the fabrication of $C_{60}(OH)_x$ nanocrystals by a reprecipitation method. The structural and morphological characterization of these crystals was performed by SEM and TEM.

Figure 1 shows the SEM image of $C_{60}(OH)_{20}$ (average composition) nanocrystals by using pyridine (good solvent) and *m*-xylene(poor solvent). Nano-crystals with truncated octahedral surface morphology were observed. In this presentation, the detailed relation between morphology and distribution of particle size of the nanocrystals and solvating media will be presented. The electronic properties of these nanocrystals will be also presented.

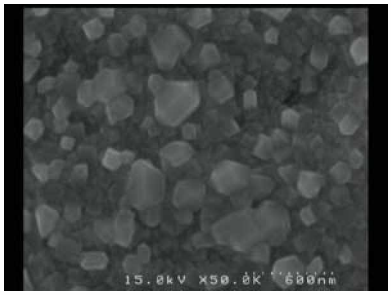

Figure 1. SEM image of $C_{60}(OH)_{20}$ nanocrystals by the reprecipitation method using pyridine (good solvent) and *m*-xylene(poor solvent).

[1] H. Kasai, et al., *Jpn. J. Appl. Phys.* **31**, L1132 (1992).
[2] K. Miyazawa, et al., *Journal of Materials Research* **17**, 83 (2002).
[3] Akito M. et al., *Jpn. J. Appl. Phys.* **48**, 050206 (2009).
[4] L. Y. Chiang et al., *J. Org. Chem.* **59**, 3960 (1994).
[5] K. Kokubo et al. *ACSNano* **2**, 327 (2008).

Ordering of hydroxylated fullerenes in aqueous solutions

Nikolaev I.V.*[1], Torok Gy.[2], Lebedev V.T.[1], Grushko Yu.S.[1], Melenevskaya E.Yu.[3], Sedov V.P.[1], Shilin V.A.[1]

[1]*Petersburg Nuclear Physics Institute, 188300, Gatchina St.Petersburg, Russia*
[2]*Research Institute for Solid State Physics and Optics, POB-49, Budapest, Hungary*
[3]*Institute of Macromolecular Compounds, 199004, St.Petersburg, Russia*
**e-mail: kriwna2010@mail.ru*

Water-soluble derivatives of fullerenes $C_{60}(OH)_X$ have been studied in aqueous solutions (25°C, pH = 5-8, addition of sodium citrate or phosphate) to examine molecular self-organization via van-der-Waals forces and hydrogen bonds by small-angle neutron scattering. There were used the solutions of $C_{60}(OH)_X$ (X ~ 20, concentration C_F = 0.5 mg/ml in H_2O, pH=5), the systems containing also sodium citrate (c = 2.8 mg/ml, pH = 6; c = 10 mg/ml, pH = 7). Salt addition caused a stronger clustering and the increase of scattering cross sections

$$dy/dЩ = y(q) = y_o/[1+ (R_C q)^2]^{D/2}, \qquad (1)$$

at momentum transfers q = 0.08-4.4 nm^{-1}. Here y_o is forward cross section, R_C ~ 16-25 nm is the size of cluster. The exponent D =4 indicates globular clusters. The system with the amount of sodium phosphate c = 0.6 mg/ml has demonstrated the scattering described by the function (1), but at the content of sodium phosphate c = 4.4 mg/ml the scattering became stronger by 2 orders in magnitude

$$y(q) = y_o/[1+(R_C q)^2]^{D/2}+y_G \exp[-(R_G q)^2/3]. \qquad (2)$$

The 1st component does not differ from the function (1), the 2nd one depends on forward cross section y_G and the gyration radius R_G of large structures. The parameters of functions (1), (2) for solutions with different salts are displayed in Fig. The association of fullerenes in aqueous solutions can be varied using additives to regulate the interactions of fullerenes. The evaluation of peculiarities of fullerenes association is important for medical applications: contraSt agents for Nuclear Magnetic Tomography Diagnostics, carriers of medicine etc.

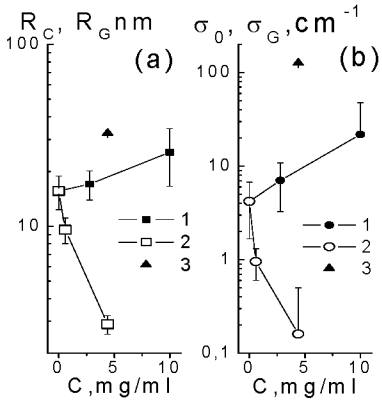

Parameters of scattering functions (1) and (2): forward cross sections (a) and radii (b). Notations: 1 – data for solutions with sodium citrate; 2 and 3 – data for solutions with sodium phosphate (parameters of the 1St and the 2nd components of scattering function (2).

Nanodiamond-containing polymers for structural and biological applications

Neitzel I., Gogotsi Y.*, Mochalin V.

Drexel University, 19104, Philadelphia, PA, USA
**e-mail: gogotsi@drexel.edu*

Due to their favorable strength to weight ratio, polymer composite materials find numerous applications in construction, transportation, biomedical, sports industry and other areas. A nanocomposite is a composite material in which at leaSt one of the components has at leaSt one spatial dimension smaller than 100 nm. At these small length scales, the specific surface area becomes large and polymer-filler interactions become increasingly important, since polymer properties change in the vicinity of the surface. The resulting third phase, called interphase, plays an important role in the overall properties of the nanocomposite since its volume fraction becomes significant at the nanoscale.

The small 5 nm diameter of detonation nanodiamond (ND) particles in combination with their rich surface chemistry [1] makes ND an optimal candidate for polymer reinforcement. Furthermore, ND can be used to engineer multifunctional composites due to its various properties. In the case of an epoxy matrix [2], ultimate mechanical reinforcement has been achieved by using high loadings of ND powder. Also, the effect of functionalized (aminated) ND on the epoxy stoichiometry and the resulting mechanical properties has been investigated and resulted in new insights in engineering nanocomposites. To reinforce a thermoplastic and biodegradable poly(L-lactic) acid (PLLA) polymer, ND's surface chemistry has been tailored to match this hydrophobic polymer, resulting in improved mechanical properties, along with biocompatibility and blue fluorescence [3]. Several complementary mechanical characterization techniques have been used to understand the reinforcing mechanisms of ND. Results of compression and fracture toughness measurements have been compared with depth-sensing indentation data. This research gives new insights in the reinforcing mechanisms of ND in polymer matrices.

[1] Osswald S., Yushin G., Mochalin V., Kucheyev S., Gogotsi Y., *JACS* **128**, 11635 (2006).
[2] Neitzel I., Mochalin V., Palmese G., Gogotsi Y., *Composites Science and Technology,* in press, (2011).
[3] Zhang Q., Mochalin V., Neitzel I., et al., *Biomaterials* **32**, 87 (2011).

Longer carbon nanotubes by controlled catalytic growth in the presence of water vapor

Karaeva A.R.[1,2], Khaskov M.A.[1,2], Mitberg E.B.[1,2], Kulnitskiy B.A.[1], Perezhogin I.A.[1], Ivanov L.A.[1], Denisov V.N.[1], Kirichenko A.N.[1], Mordkovich V.Z.*[1,2]

[1]*Technological Institute for Superhard and Novel Carbon Materials, 142190 Troitsk, Russia*
[2]*INFRA Technologies, 125993 Moscow, Russia*
**e-mail: mordkovich@tisnum.ru*

The growth of longer carbon nanotubes (CNT) for construction nanomaterials is one of the major challenges of CNT research [1]. It has been demonstrated that long contact time is a powerful tool and obvious precondition for longer CNT [2]. However it is well known since 1970s that longer contact time may lead to stronger radial growth [3]. The competition between axial and radial growth at longer contact time usually results in the production of microfibers other than CNT. The introduction of oxygen-containing compounds may be used as a means of controlling CNT structure and/or suppressing radial growth.

The purpose of the present work was to study possibilities of water vapor control over growth of longer CNT from ethylene-based feedstock. SEM, TEM and Raman spectroscopy were used for the resulting deposit characterization. The synthesis was carried out at the temperature of up to 1150°C. H_2 was used as a carrier gas at the flow rate of 600 ml/min. The reactor allowed contact time up to 1 min.

It was found that H_2O/C ratio in the range from 0.5/1 to 2.0/1 influences both yield and the structure of CNT. It is shown that the yield of centimeter-long CNT can be maximized at an optimum H_2O/C ratio.

A mechanism for the water-assisted growth of CNT is proposed and discussed.

[1] Mordkovich V. Z., Karaeva A. R., Zaglyadova S. V., Maslov I. A., Don A. K., Mitberg E. B., and Kharitonov D. N., *Mat. Res. Soc. Symp. Proc.* **1142**, 5 (2009).

[2] Hofmann M., Synthesis and Fluid Interaction of Ultra-long Carbon Nanotubes. Massachusets Institute of Technology, Thesis. 50 p. (2008).

[3] Endo M., Oberlin A., and Koyama T., *Jpn J. Appl. Phys.* **16**, 1519 (1977).

Diamond nanoparticles: purification, deagglomeration and functionalization

Pentecost A., Neitzel I., Mochalin V.*, Gogotsi Y.

A.J. Drexel Nanotechnology Institute and Department of Materials Science and Engineering, Drexel University, 19104, Philadelphia, U.S.A.
**e-mail: vadym@coe.drexel.edu*

Diamond nanoparticles (nanodiamond, ND) have outstanding mechanical, optical, thermal, and electrical properties in combination with biocompatibility, low toxicity, and tuneable, highly stable surface structure and chemistry. The unique feature of ND as compared to carbon nanotubes, graphene, and other carbon nanomaterials with sp^2 bonding is that its surface chemistry can be fully controlled without compromising the structure and useful properties of the material. However, ND has not been used to its full potential because of as yet unsatisfactory control of the particle size, surface chemistry and interior structure, as well as particle agglomeration. Our ability to address these issues will lead to breakthroughs in using ND in biomedical and other applications.

A set of techniques was developed for de-agglomeration, purification and surface modification aimed at large scale production of high quality ND with precisely controlled characteristics for advanced composites and biomedical applications. Dry milling of ND with sodium chloride, sugar, and other inexpensive, non-toxic, non-contaminating media allows for reduction of ND agglomerates from micron-size down to 10-15 nm (2-3 single ND particles). Controlled oxidation of ND in air followed by treatment with diluted aqueous acids yields high purity ND with 95-97 % wt. sp^3 carbon and sub-ppm levels of heavy metals. It also results in changes of surface chemistry, uniformly converting different functional groups present on the surface of non-purified ND into carboxylic groups. In this way various grades of ND from different manufacturers are brought to the same standardized stage. Further functionalization of this material can be done in numerous ways using gas annealing or wet chemistry techniques based on the chemistry of carboxylic groups, yielding ND powders finely tuned for specific purposes.

Applications of de-agglomerated, purified, and functionalized ND including reinforcement of polymers, biodegradable tissue engineering scaffolds, drug delivery systems, and biomedical imaging will be discussed.

Open-shell fullerene derivates: low temperature ESR spectroscopy and quantum chemical (DFT) calculations

Misochko E.Ya.[1], Akimov A.V.[1], Tyurin D.A.[2]

[1]*Institute of Problems of Chemical Physics of the Russian Academy of Sciences, 142432 Chernogolovka, Moscow Region, Russia*
[2]*Lomonosov Moscow State University, Department of Chemistry, 119899, Moscow, Russia*
**e-mail: misochko@icp.ac.ru*

Here we report how ESR and matrix-isolation techniques supported by quantum-chemical computations can be used for molecular modeling of novel open-shell species, such as paramagnetic fullerene derivates. In this study, free radicals $^{\bullet}C_{60}F$ and $^{\bullet}C_{70}F$ and paramagnetic endometallofullerene $Y@C_{82}$ molecules were isolated in sold argon matrices at cryogenic temperatures. High resolution anisotropic EPR spectra of the isolated molecules at temperature 5 K have been obtained for the first time. [1]

Both of hyperfine coupling constants characterizing Fermi contact interaction and electron-nuclear-magnetic-dipole interaction have been derived from the ESR spectra recorded. We have used these parameters for testing the validity of various computational methods (PBE, PBE1, and B3LYP) to predict an electronic structure of such type species. Based on the comparison of the measured hyperfine constants with those estimated by the quantum chemical calculation, the electron spin distribution and reactivity of the radical $^{\bullet}C_{60}F$, various regioisomers of $^{\bullet}C_{70}F$, and endometallofullerenes $M@C_{82}$ (M = Sc, Y, La) are discussed.

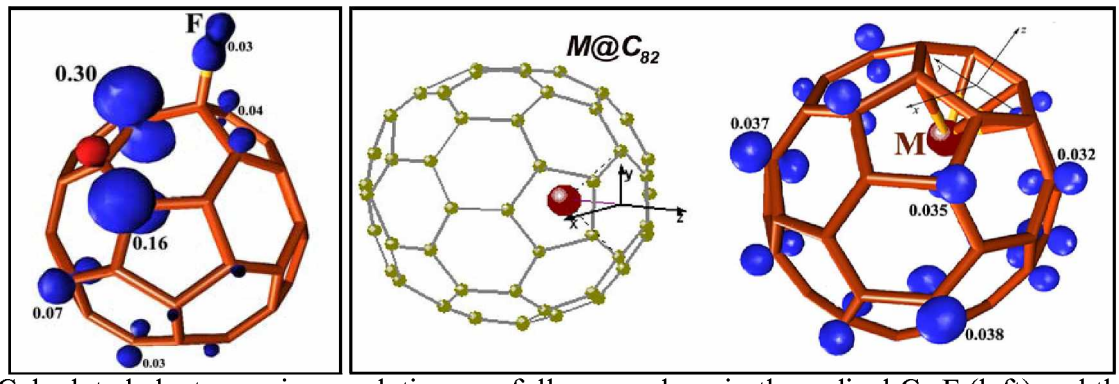

Calculated electron spin populations on fullerene sphere in the radical $C_{60}F$ (left) and the endometallofullerene $Y@C_{82}$ (right).

Relativistic and solvatation effects in a series of encaged 3B group metal atoms in the molecules $M@C_{82}$ are discussed based on the results of these calculations and available experimental data.

[1] Misochko E.Ya., Akimov A.V. et all., *Phys. Chem. Chem. Phys.* **12**, 8863, (2010).

Structural and physical properties of MWNT/polyolefine composites

Mazov I.N.*[1], Kuznetsov V.L.[1,2], Romanenko A.I.[2,3], Anikeeva O.B.[3], Suslyaev V.I.[4], Zhuravlev V.A.[4]

[1]*Boreskov Institute of Catalysis, 630090, Novosibirsk, Russia*
[2]*Novosibirsk State University, 630090, Novosibirsk, Russia*
[3]*Nikolaev Institute of Inorganic Chemistry, 630090, Novosibirsk, Russia*
[4]*National Research Tomsk State University, 634050, Tomsk, Russia*
**e-mail: mazov@catalysis.ru*

In the present work we have investigated structural and physical properties of polymer composites, comprising multiwalled carbon nanotubes (MWNTs) in polyolefine (polyethylene (PE) and polypropylene (PP)) matrix.

Carbon nanotubes with average outer diameter 8-10 nm were prepared by decomposition of ethylene over metallic catalySt and incorporated in polymer matrix using so-called coagulation technique. Composites with MWNT loading 0.5-20 wt.% were synthesized and investigated using various physical-chemical methods.

MWNT state in the polymer matrix was investigated by means of electron microscopy both for powder samples and hot-pressed composite films. It was shown that the surface of MWNTs is wetted by the polymer (Fig. 1) thus resulting in good interaction between filler and the matrix.

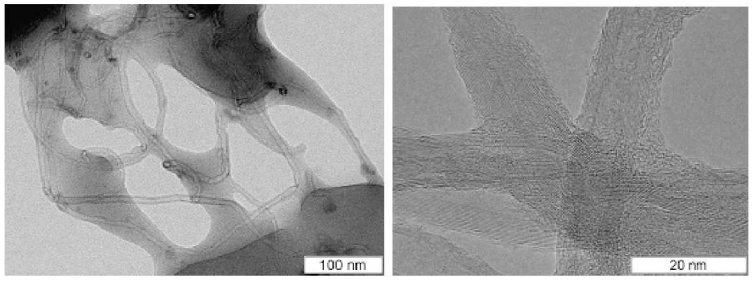

Figure 1. TEM images of MWNT-polypropylene composite (8 wt. %) showing good wetting of MWNT surface with polymer.

Thermal, electrical and electromagnetic properties of composites were also investigated, showing improvement with growing MWNT loading. Electromagnetic response properties of MWNT/PP and MWNT/PE composites were studied in broad frequency range, showing high shielding efficiency due to both reflection and absorption of EM radiation.

Thus MWNT-polyolefine composite materials are perspective for design of durable EM-shielding coatings for wide application range.

CVD facility for formation of carbon nanomaterials on a space station board

Malinovskaya O.S.[1,2]*, Rizakhanov R.N.[1], Polyanskiy M.N.[1], Tsvetkova E.V.[1]

[1]*Federal State Unitary Enterprise "Keldysh Research Center", Moscow, Russia*
[2]*National Research Nuclear University MEPhI, Moscow, Russia*
**e-mail: nanocentre@kerc.msk.ru*

A facility for formation of carbon nanotubes, diamond-like coatings and other carbon nanostructures by chemical vapor deposition [1] carrying out on a space station board is presented.

Unique solutions for thermal protection, optimal weight and size without explosive gases and dangerous materials offer an opportunity to use the facility for the formation of carbon nanostructures under complex conditions: large temperature and pressure drops, microgravity and cosmic radiation. This facility consist of a quartz chamber for the CVD-process, a bulb with evaporating liquid and a substrates holder fixed inside the chamber (see Fig.). Varying gas environment, temperature and pressure inside the chamber and using various types of substrates leads to formation various types of nanomaterials.

To analyse of materials were used auger-spectroscopy, scanning and transmission electron microscopy and x-ray microanalysis.

In particular, at the temperature ~ 800ºC and pressure less than 10 Torr on steel substrates carbon nanotubes coating within the range 10-100 nm in diameter and up to 100 microns in length is formed. It's necessary to mention that increasing time of process results in increasing maximum length of nanotubes. At the temperature 950-1000ºC and pressures over 20 Torr continuous diamond-like coating with crystal dimensions from several nanometers to 10 microns is formed.

There are prerequisites that nanostructures would be defectless and growing processes more productive due to microgravity and high vacuum on the space station board.

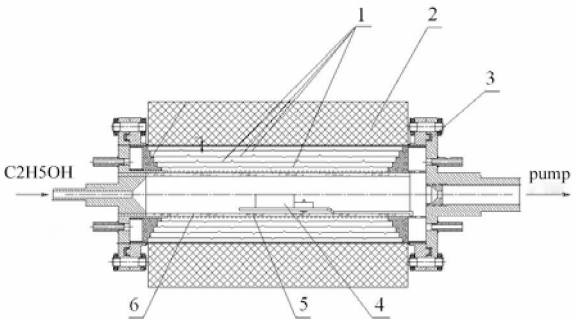

Facility for formation carbon nanomaterials on a space station board.

[1] X. Wang, Q. Li, J. Xie, Z. Jin, J. Wang, Y. Li, K. Jiang, S. Fan, *Nano Letters* **9**, 3137 (2009).

Two-dimensional magnetism of fluorinated graphite

Makarova T.L.[1,2]*, Shames A.I., Zagainova V.S., Okotrub A.V., Chekhova G.N., Pinakov D.V., Yudanov N.F., Bulusheva L.G.

[1]*Umeå University, 90187, Umeå, Sweden*
[2]*Ioffe Institute, 194021, St.Petersburg, Russia*
[3]*Department of Physics, Ben-Gurion University of the Negev, Be'er-Sheva 84105, Israel*
[4]*Nikolaev Institute of Inorganic Chemistry, SB RAS, 630090, Novosibirsk, Russia*
**e-mail: tatiana.makarova@physics.umu.se*

A series of layered inclusion compounds based on fluorinated graphite C_2F_x ($x \leq 1$) was obtained by a room temperature synthesis. Electronic and magnetic properties of graphene sheet can be delicately tuned by the fluorination degree and the nature of the inclusion compound in the layered fluorographene compounds. Magnetic phase transitions have been observed using both magnetic susceptibility measurements and electron spin resonance. The changes in C_2F_x stoichiometry are shown to have a decisive effect on magnetic properties of produced complexes. The spin concentration decreases with the increase of fluorine content in fluorocarbon matrix.

As prepared fluorinated samples have groups of correlated spins; at the temperatures 1.75–5 K nonlinear magnetization is observed, indicating a high-spin state. Application of the Langevin formula shows that the clusters consiSt of 10–20 interacting spins.

The outer layers of graphite fluoride can be reduced by water present in the atmosphere, and graphene layers are formed. New magnetic features appear: large orbital diamagnetism, the difference between the measurements in field cooled and zero field cooled regimes, and characteristic kinks at the zero field cooled curves reveal the temperature at which magnetic moments become blocked. However, superparamagnetic description is not applicable to this system. The temperature dependence of the magnetization M(T) above a transition temperature takes the form $M(T) = M_0 [1- AT \ln(\beta T)]$, typical for two-dimensional systems. ESR line below the transition point splits into the in-plane and out-of-plane contributions. The semifluorinated graphite provides a unique opportunity to study the magnetism of two-dimensional system without metallic impurities

Template-assisted fabrication and study of 2D and 3D ordered porous nanodiamond films

Kurdyukov D.A.*, Feoktistov N.A., Medvedev A.V., Nashchekin A.V., Aleksenskii A.E., Vul' A.Ya., Golubev V.G.

Ioffe Physical-Technical Institute, 194021, St.Petersburg, Russia
**e-mail: kurd@gvg.ioffe.ru*

Two-dimensional (2D) and three-dimensional (3D) porous nanodiamond (ND) films are known to be unique versatile materials for applications in sensing, photonic crystal devices, fuel cells, energy harvesting, chromatography, and biomedicine due to their superior physical, chemical, and mechanical properties. We hereby, describe a novel method of nanocasting fabrication of 2D and 3D ordered porous ND films.

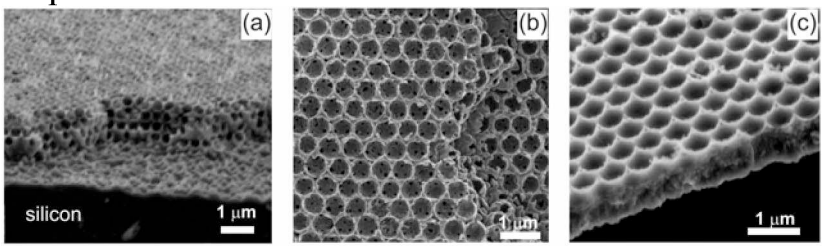

Figure 1: SEM images. (a) Cross section and (b) surface of 3D porous opal-based nanodiamond film. (c) Surface of free-standing 2D ND film.

We used self-assembled silica fcc colloidal crystal films (opals) as templates for the fabrication of the nanostructured diamond films. First, we synthesized highly ordered opal films on Si substrates from 500 nm diameter amorphous SiO_2 spheres. Then we filled the interstitial space within an opal film with detonation nanodiamond (DND) particles, using a specially designed evaporation-driven infiltration technique. This technique allowed us to uniformly fill the porous of opal film with DND to the given depth variable by controlling the parameters inside the evaporation chamber. Further growth of ND inside the opal pores was performed by MPCVD technique. DND particles, previously seeded inside the pores, provide a densely arranged nucleation centres for CVD diamond growth. Using a set of opal films filled with DND to different depths we could control the level of infiltration of opal with CVD nanodiamond. To fabricate porous ND the silica template was subsequently etched away in HF aqueous solution.

The finally made samples were either connected to the Si substrate (Fig. 1a,b) or free-standing (Fig. 1c) 2D and 3D ordered porous ND films of various thicknesses. The morphology of fabricated films replicated the pore structure of opal template. Raman spectra of the samples confirmed nanocrystalline structure of diamond in the synthesized films. Comprehensive studies of luminescent defects were carried out.

Technology and main products of single-walled carbon nanotubes produced by arc discharge process

Krestinin A.V.*, Zvereva G.I., Kislov M.B.

Institute of Problems of Chemical Physics RAS (IPCP RAS), Chernogolovka, 142432, Russia
**e-mail: kresti@icp.ac.ru*

IPCP RAS has developed technology and equipment to produce single-walled carbon nanotubes (SWCNTs) based on the arc discharge process as a result of accomplished R&D contract entitled "Technology and equipment for production of high quality single-walled and multi-walled carbon nanotubes". A technological setup has been designed to produce up to 50 g/shift of raw-SWCNTs (as-produced condensed arc discharge products) with nanotube content of 15-25wt.%, and up to 5-10 g/shift SWCNT-products of different degree of purification including SWCNT-powder with 90 wt.% of nanotubes and SWCNT-colloidal solution with 98 wt.% of nanotubes in dispersed phase.

The main characteristics of production technology are the following:

- a specially designed arc reactor (supported by RF patent) allows one to work in semiautomatic conditions. Design solution of the reactor allows the yield of condensation products to be increased to ~ 30% of evaporated carbon and percentage of nanotubes in raw SWCNT material up to 20-25 wt.%;
- a combination of chemical and physical methods of purification is used to attain both high percentage of nanotube recovery from raw SWCNT material and high quality of the final product;
- special methods of material treatment are involved to retain high dispersion of nanotube in the desired product.

Comparison of developed technology with existing one reveals the following advantages of the former:

1) 10 times higher capacity for one technological setup in production of high-quality desired product;

2) developed technology allows the treatment of "lean" raw SWCNT material, which make it possible to scale up arc discharge production technology provided that such scale-up is inevitably associated with raw SWCNTs quality lowering.

Advantages of technology of SWCNT synthesis and purification are pronounced in coSt of final products. Calculated net costs of proposed products should be 2-3 times lower than those existing in the market.

The liSt of products which are either produced or at the final stage of preparation is presented and discussed. Some properties, which are important in commercial application of SWCNTs, are listed along with measurement techniques for SWCNT product certification. A market niche for arc discharge synthesized SWCNTs is discussed.

Comparative study of fullerene-cubane rotor-stator systems

Kováts É.[1], Bortel G.[1], Pekker S.[1]

[1]*Research Institute for Solid State Physics and Optics, Budapest, Hungary*
**e-mail: kovatse@szfki.hu*

Fullerenes form a large variety of high symmetry cocrystals with cubane molecules [1]. The basic material, $C_{60}C_8H_8$ has a face centered cubic crystal structure at ambient condition, with significantly expanded lattice, related to the parent fullerene structure. This cocrystal consists of separated sublattices of rotating and static components. The moSt important structural characteristics is the significant shape and size recognition of the constituent molecules. The unusual structure gives rise to a complex dynamics, called rotor-stator feature, that is different from both the orientationally ordered and the plastic crystals. A series of related materials has been prepared by similar cocrystallization of higher fullerenes and 1,4-disubstituted cubanes [2]. The different size and symmetry of the components slightly modified the rotor-stator properties.

Here we present the formation and crystal structure of the recently synthethized members of the fullerene-cubane cocrystals and discuss the effect of the molecular geometry on the crystal structure and the rotor-stator dynamics. We compare the moSt important characteristics of these cocrystals with those of the host-gueSt type derivatives of fullerenes.

[1] Pekker, S., Kováts, É., Oszlányi, G., Bényei, G., Klupp, G., Bortel, G., Jalsovszky, I., Jakab, E., Borondics, F., Kamarás, K., Bokor, M., Kriza, G., Tompa, K., Faigel, G., *Nature Materials* **4**(10), 764 (2005).

[2] Pekker, S.; Kováts, É.; Oszlányi, G.; Bényei, G.; Klupp, G.; Bortel, G.; Jalsovszky, I.; Jakab, E.; Borondics, F.; Kamarás, K.; Faigel, G., *Phys. Stat. Sol. (B)* **243**, 3032 (2006).

Detonation nanodiamonds as revealed by differential scanning calorimetry

Korobov M.V.*[1], Avramenko N.V.[1], Batuk M.M[1], Osawa E [2]

[1]*Department of Chemisry, Moscow State University, 119899, Moscow, Russia*
[2]*NanoCarbon Research Institute, AREC, Faculty of Textile Science and Engineering, Shinshu University, 3-15-1 Tokita, Ueda 386-8567, Japan*
**e-mail:mkorobov49@gmail.com*

Detonation nanodiamonds (DND) is a useful nanomaterial with many potential applications in material science, biology and medicine. Various forms of DND (dry powders or flakes, aqueous gels, dispersions) were carefully studied and characterized by different experimental methods. The moSt valuable characteristics are size and structure of the primary particles (x-ray, HRTEM, NMR and etc), chemical identity of the surface groups (IR), size of the clusters in the dispersions (DLS, SANS).

In present study we introduce additional analytical tool to gain some insight into the properties of DND, namely, differential scanning calorimetry (DSC). The original idea was to determine the size of the liquid nanoparticles confined in DND samples using Gibbs-Thomson equation. DSC fills the gap in the understanding of state of DND gels and dry powders. It has a unique sensitivity towards disintegration process in DND. Chemically bonded aggregated samples can be easily distinguished from the dry powders/gels consisted of non-bonded primary particles (d~5nm). This is hardly possible with any other method. There is a strong correlation between DSC and DLS data. One may estimate possible size of the ND cluster in dispersion based on the preliminary DSC trace of DND gel or powder, e.g. *prior to preparation of dispersion.*

It was demonstrated that disintegrated DND forms a "secondary structure", consisted of primary particles and a system of voids of certain reproducible size (d~8 nm) and volume. This reproducible "structure" was observed in dry powders, gels and indirectly in large porous clusters (d ~ 50 nm) dispersed in water. Similar structures were found earlier in dry carbon nanohorns and C_{60} aqueous gels.

With DSC it was possible to follow the steps of formation and collapse of a "secondary structure". The former was observed in chemical disintegration of crude DND samples and the latter after high pressure treatment (~10 kbar, 900 K) of originally disintegrated samples. The attempts were made to detect the "secondary structure" in DND by means of HRTEM, STEM, AFM and etc.

The DSC data for DND samples of different origin are presented. Typical traces of aggregated, disintegrated and modified DND are given. The results were discussed along with data of other experimental methods (DLS, adsorption, HRTEM and etc.)

This work was supported by the RFBR grant 09-03-00004 and by the grant for Leading Scientific Schools in Russia.

Exfoliation of single- and multi-layer graphenes from the surface of polyacrylonitrile-based copolymer under thermal treatment

Korobeinyk A.V.*, Whitby R.L.D., Salvage J., Mikhalovsky S.V.

School of Pharmacy and Biomolecular Sciences, University of Brighton, Lewes Road, Brighton, BN2 4GJ, United Kingdom
**e-mail: A.Korobeinyk@brighton.ac.uk*

Single-layer graphenes (SLGs) are sheets of sp^2-hybridized carbon atoms [1], which have several advantages compared to other carbon materials. For example, the calculated conductivity of single-layer graphene (assuming thickness of 0.34 nm [2]) is six orders of magnitude higher than the conductivity of amorphous carbon [3]. SLGs are also demonstrated to be superior in thermal conductivity [4], elastic response to deformations [5] and high mechanical strength [6]. Although the pristine graphenes are hydrophobic the chemical modification [7] of pre-oxidized single-layer graphenes provides ample opportunities for incorporating such a material into a range of possible applications.

Nonetheless, single-layer graphenes are expensive and therefore efforts have been focussed on cheaper manufacturing solutions. In this study, we demonstrate that under heating to 850°C of a polyacrylonitrile-based copolymer, the sample undergoes subtle contraction due to mass loss, which also manifests itself in the exfoliation of its outer layers. Transmission Electron Microscopy, Selected Area Electron Diffraction and Atomic Force Microscopy reveal the presence of single- and multi-layered graphenes [8].

[1] Geim A.K., Novoselov K.S., *Nat Mater.* **6**(3),183 (2007).
[2] Eda G., Fanchini G., Chhowalla M. *Nat Nano.***3**(5),270 (2008).
[3] Ziegler K. Robust, *Physical Review Letters* **97**(26), 266802 (2006).
[4] Balandin A.A., Ghosh S., Bao W., Calizo I., Teweldebrhan D., Miao F., et al., *Nano Letters* **8**(3), 902 (2008).
[5] Zakharchenko K.V., Katsnelson M.I., Fasolino A., *Physical Review Letters* **102**(4), 046808 (2009).
[6] Wang G., Shen X., Wang B., Yao J., Park J., *Carbon* **47**(5), 1359 (2009).
[7] Whitby R.L.D., Korobeinyk A., Glevatska K.V., *Carbon* **49**(2), 722 (2010).
[8] Korobeinyk A., Whitby R.L.D., Salvage J., Mikhalovsky S.V., submitted 2011.

Structure and electronic properties of single-walled carbon nanotubes intercalated by transition metal halogenides

Kharlamova M.V.*[1], Eliseev A.A.[1], Yashina L.V.[1,2], Lukashin A.V.[1], Tretyakov Yu.D.[1]

[1]*Moscow State University, 119991, Moscow, Russia*
[2]*GIREDMET OJSC, 119017, Moscow, Russia*
**e-mail: mv.kharlamova@gmail.com*

Single-walled carbon nanotubes (SWCNTs) are studied intensively during laSt decade due to their unusual electronic, chemical and structural properties accompanied by extraordinary mechanical behavior with all these features being strongly dependent on the diameter and conformation of tube. Currently, the researchers are focused on finding tools to govern the electron structure of nanostructures designed on the basis of single-walled carbon nanotubes (SWCNT) [1]. One of the approaches is given by filling the internal channels of nanotubes with inorganic one-dimensional nanocrystals. In some cases, this approach makes it possible to get the material with well-defined electron structure and properties even without separating of SWCNTs on their size and chirality [2].

The aims of our study were the controllable growth of 1D nanocrystals (AgHal, CuHal and $MHal_2$, where Hal=Cl, Br, I and M=Mn, Fe, Co, Ni, Zn) in channels of single-walled carbon nanotubes with inner diameter 1-1.4 nm and investigation of structure and electronic properties of these nanostructures. The synthetic strategy was based on the impregnation of pre-opened SWCNTs by molten salts in vacuum.

The atomic structure of Ag and Cu halides within SWCNTs was found to correspond to distorted two-layer *hcp* of halide atoms arranged laterally with respect to the SWCNT and metal atoms located in incomplete octahedral positions. EXAFS data revealed the metal atoms coordination with nanotube walls in nanocomposites, and it was also proved by HAADF HRTEM imaging. According to work function measurements, Fermi level downshift of SWCNTs was observed for all composites. XPS data exposes an acceptor behavior of metal halides accompanied by partial charge increase on halogen atoms while no noticeable alteration of charge was observed on metal atoms. Raman spectroscopy performed under an electrochemical charging enabled the direct determination of charge transfer efficiency for selective-chirality metallic SWCNTs intercalated by metal halogenides.

[1] Tans S.J., Verschueren A.R.M., Dekker C., *Nature* **393**, 49 (1998).
[2] Dresselhaus M.S., Dresselhaus G., Saito R., *Carbon* **33**, 883 (1995).

Effects of concentrated sunlight on efficiency and stability of fullerene-polymer solar cells

Katz E.A.,[*1,2] Manor A.,[1] Tromholt T.,[3] Krebs F.C.[3]

[1]*Dept. of Solar Energy and Environmental Physics, Jacob Blaustein Institutes for Desert Research, Ben-Gurion University of the Negev, Sede Boker 84990, Israel*
[2]*Ilze Kats Institute for Nanoscale Science and Technology, Ben-Gurion University of the Negev, Beer-Sheva 84105, Israel*
[3]*Risø National Laboratory for Sustainable Energy, Technical University of Denmark, Frederiksborgvej 399, DK-4000 Roskilde, Denmark*
**e-mail: keugene @bgu.ac.il*

After reviewing state-of-the-art in two seemingly discontiguous areas of photovoltaic (PV) research - PV conversion of concentrated sunlight and organic photovoltaics (OPV) based conjugated polymer / fullerene bulk hetero-junction solar cells - we address the following questions:

(1) can organic cells be part of the concentrator PV?

(2) can concentrated sunlight be useful for investigation of OPV cells and, in particular, for accelerated studies of light induced mechanisms in the OPV degradation?

Answering to the firSt question, we suggeSt that in addition to power generation at 1 sun (1 sun = 100 mW/cm^2), stable OPV device can also be used for power generation with low-coSt stationary concentrators of sunlight working in the low concentration regime (1 sun < C < 10 suns). To check this hypothesis the effects of sunlight concentration on the PV performance and stability of OPV devices were investigated. In particular, we report our experimental results [1] for the exploitation of concentrated sunlight for such a study using an outdoor/indoor teSt facility [2-3] based on the fiber-optic/mini-dish concentrator.

Addressing the second question, we demonstrate that our experimental approach can be used for accelerated tests of light induced degradation mechanisms in the OPV devices [1, 4] and materials [5].

[1] T. Tromholt, E.A. Katz, B. Hirsch, A. Vossier, F.C. Krebs. *Appl. Phys. Lett.* **96**, 073501 (2010).

[2] J.M. Gordon, E.A. Katz, D. Feuermann and M. Huleihil. *Appl. Phys. Lett.* **84**, 3642 (2004).

[3] E.A. Katz, J.M. Gordon, W. Tassew and D. Feuermann. *J. Appl. Phys.* **100**, 044514 (2006).

[4] T. Tromholt, A. Manor, E.A. Katz and F.C. Krebs. *Nanotechnology* (2011), in press.

[5] T. Tromholt, M. Manceau, M. Helgesen, J.E. Carlé and F.C. Krebs. *Solar Energy Materials and Solar Cells*, 2011 (in press).

Synthesis and supercapacitor performance of arrayed MWCNT-MnO_2 nanocomposites

Sie Y.C., Huang J.H.*, Chen Y.S.

Department of Materials Science and Engineering, National Tsing Hua University, Hsinchu 300, Taiwan
**e-mail: jihhuang@mx.nthu.edu.tw*

Hybrid nanocomposites containing CNTs and transition metal oxides have been considered potential electrode materials for supercapacitors. This work reports the fabrication and supercapacitor performance of arrayed MWCNT-MnO_2 nanocomposites. MWCNTs were grown directly on Si substrates by microwave plasma-enhanced chemical vapor deposition. MnO_2 was electrodeposited on MWCNTs from an aqueous solution containing 0.1 M $MnSO_4$ and 1 M Na_2SO_4. The depositions were carried out in a potential window of 0 to 1 V for 30, 50, and 70 scan cycles at scan rates of 20–200 mV/s. Prior to electro deposition, a 6 M HNO_3 solution was used to purify and activate the MWCNTs. The effects of the electro-deposition condition on the morphology and capacitance of the as-fabricated MWCNT-MnO_2 nanocomposites were investigated.

We found that MnO_2 could be uniformly coated on the sidewalls of MWCNTs at scan rates of 100 and 150 mV/s, which enhances the effective surface area for ion transportation at the MnO_2-MWCNT interface. The optimum electro-deposition condition is found to be a scan rate of 100 mV/s and scan cycle of 30. The resulting nanocomposite fabricated under this condition achieved a high specific capacitance of 649 F/g at 20 mV/s. The decay in specific capacitance based on this maximum value after a 1080-cycle teSt is only 4%, revealing the excellent stability of the product. This work demonstrates that arrayed MWCNT-MnO_2 nanocomposite is a potential cost-effective and clean supercapacitor material.

Synthesis carbon-encaspsulated metal nanoparticles by a detonation method

Hao Y.[1], Pengwan C.*[1]

[1]*State Key Laboratory of Explosive Science and Technology, Beijing Institute of Technology, 100081 ,Beijing, PR China*
** e-mail: pwchen@bit.edu.cn*

Nanosized metal/carbon-composite systems are considerable concern because of their possibility for magnetic materials[1], catalysts[2], electrode in batteries[3], against oxidization and further agglomeration to form bigger crystallites[4] and so on.

Uniform carbon-encapsulated metal-based nanoparticles with a well-constructed core–shell structure(see Fig.1) were produced by detonation decomposition of explosive mixture precursors containing metal ion components in a vacuum detonations vessel, which is characterized by a self-heating, extremely faSt process and cost-efficient. The C/metal-ion ratio of origin materials was a key factor which determines the formations of carbon - encapsulated metal or metal carbide nanoparticles. The different sizes of the nanocrystal core and the thickness of the carbon shell were yielded by adjusting the component materials of the explosive precursors during the course of these detonation reactions.

HRSEM,HRTEM,XRD, DTA/TG were used to studied composition and morphology of nanoparticles. The magnetic properties of encapsulates were also measured. Results showed that the diameters of nanoparticles are 10-50 nm, metal/ metal carbide cores and graphitic/amorphous shells are formed in these nanoparticles. The carbon shells could protect effectively the cores againSt the attack of either strong acid or strong base solution. The thickness of the carbon shells are 3-10nm with 10-30 layers. The interlamellar spacing, which is approximately equal to the distance between graphite layers, is about 0.34 nm. The nanoparticles showed the properties of superparamagnetism.

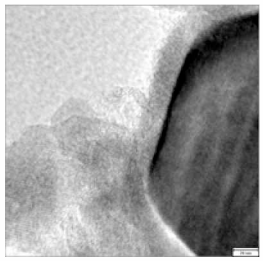

Figure.1. HR TEM images of nanoparticle.

[1] Michal B., Andrzej H., Hubert L., Stanislaw C., Woiciech K. *Diamond & Related Materials* **16**(2), 225 (2007).
[2] Herdt A., Kim B., Taton T. *Bioconjugate Chem.* **18**(1), 183 (2007).
[3] Nam J., Thaxton C., Mirkin C. *Science* **301**(5641), 1884 (2003).
[4] Lu A., Li E., Matoussevitch N., Spliethoff B., Bonnemann H., Schuth F. *Chem. Commun.* 1, 98 (2005).

Growth of ultrananocrystalline diamond films on non-silicon substrates using electrophoresis-deposited nano-diamond as nucleation layer

Cheng H.-F.[1], Tai N.-H.*[2], Chang T.-H.[2], Chen H.-C.[3], Lin I-N.[3]

[1]*Department of Physics, National Taiwan Normal University, Taipei, Taiwan 116, R. O. C.*
[2]*Department of Materials Science and Engineering, National Tsing-Hua University, Hsin-Chu, Taiwan 300, R. O. C.*
[3]*Department of Physics, Tamkang University, Tamsui, Taiwan 251, R. O. C.*
**e-mail: nhtai@mx.nthu.edu.tw*

Ultrananocrystalline diamond (UNCD) films possess many marvelous physical and chemical properties and several of them actually exceed those of conventional microcrystalline diamond (MCD) films. The UNCD films possess good potential for device applications. However, efficient nucleation technique is required to grow uniform UNCD films in large area on these substrates. In this work, we will firSt report the utilization of nano-diamond layer electrophoresis-deposited on Si (for only 30 s) as nucleation layer for growing UNCD and MCD films on Si-substrate. The films obtained possess better good electron field emission as those grown from a nucleation layer on Si substrate, which was obtained through ultrasonication in diamond/methanol solution (for 45 min), viz. high efficiency on nucleating the UNCD film has been observed. In this work, we will demonstrate the novel nucleation technique to solve the difficulty in growing the diamond films on non-silicon substrates such as stainless steel.

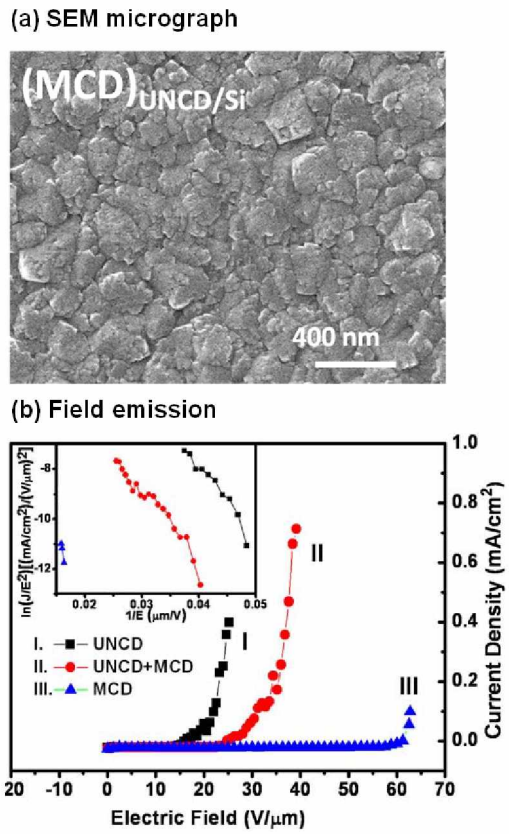

Figure 1 (a) The SEM micrograph of $(MCD)_{UNCD/Si}$ diamond films and (b) EFE properties of UNCD, MCD, $(MCD)_{UNCD/Si}$ diamond films

[1] A.M. Affoune, B.L. V. Prasad, H. Sato, T. Enoki, *Langmuir* **17**, 547 (2001).
[2] C.S. Wang, H.C. Chen, H.F. Cheng, I.N. Lin, *J. Appl. Phys.* **105**, 124311 (2009).

Interplay between intrinsic and contact phenomena in carbon nanotube devices: from exponential magnetoresistance to chemical sensing

Fedorov G.*[1], Yang Y.[2], Barabra P.[2], Jiménez D.[3], Smirnov D.[4], Roche S.[5]

[1]*NRC "Kurchatov Institute", 123182, Moscow, Russia*
[2]*Georgetown University, 20057, Washington, DC, USA*
[3]*Universitat Autònoma de Barcelona, 08193 Barcelona, Spain*
[4]*National High Magnetic Field Laboratory, Tallahassee, 32310, USA*
[5]*CIN2, ICN, CSIC, Barcelona, E-08193 Bellaterra, Spain*
**e-mail: gefedorov@mail.ru*

Back in 1993 Ajiki and Ando predicted linear dependence of the band gap of a carbon nanotubes (CNT) on a magnetic field parallel to the CNT axes [1]. This effect arises from modulation of the Aharonov-Bohm phase of the electronic wave functions and peculiar topology of the graphene's Fermi surface. In our previous work [2] we employed this effect to study relationship between the band structure of a CNT and transport properties of a CNT-based device. Our experimental results were successfully interpreted within a compact phenomenological model describing charge transport in CNT-based field-effect transistors (CNFETs) [3]. Here we present this model and its implementation to analysis of chemical sensitivity of CNT-based FET devices.

We have studied transport characteristics of CNFETs of different configuration as a function of the concentration of ammonia and nitrogen dioxide in the surrounding atmosphere. Interpretation of experimental results is based on the assumption that adsorption of gas molecules on the CNT surface changes parameters of its band profile, i.e. the Schottky barrier height and the CNT doping level. It is shown that within this approach, we get at a good qualitative description of our experimental data, as well as previously published data obtained by other research groups. We conclude that the presented model for Schottky-barrier nanotube-based transistors can be successfully implemented to simulate the response of CNT-based chemical sensors.

[1] H. Ajiki, T. Ando, *J. Phys. Soc. Jpn.* **62**, 1255 (1993).
[2] G. Fedorov, A. Tselev, D. Jimenez, S. Latil, N.G. Kalugin, P. Barbara, D. Smirnov, S. Roche, *Nano Lett.* **7**, 960 (2007).
[3] D. Jiménez, X. Cartoixà, E. Miranda, J. Suñé, F.A. Chaves, S. Roche, *Nanotechnology* **18**, 025201 (2007).

Carbon nanotubes reinforced alumina composites fabricated by vacuum sintering

Faikov P.P.*[1], Zharikov E.V.[1], Zaramenskikh K.S.[1], Popova N.A.[1], Iskhakova L.D.[2], Gerke M.N.[3], Kutrovskaya S.V.[3], Nogtev D.S.[3]

[1]*D. Mendeleev University of Chemical Technology of Russia, 125047, Moscow, Russia*
[2]*Fiber Optics Research Center of the Russian Academy of Sciences, 119333, Moscow, Russia*
[3]*Vladimir State University, 600026, Vladimir, Russia*
**e-mail: faikov_p@inbox.ru*

Due to high chemical resistance and perfect mechanical properties carbon nanotubes (CNT) are a promising material for production of composite materials with improved properties. Between the composites based on ceramic matrix the reinforcing of alumina seems to be the moSt promising since this type of ceramics initially possesses a number of attractive properties and it is widely used as a constructional material. The significant increase of fracture toughness and flexure strength after CNT insertion into alumina matrix was demonstrated nowadays only for materials, produced by hot-pressing and spark plasma sintering techniques [1-2].

The present work is devoted to the development of alumina – CNT composite preparation technology using vacuum sintering for the ceramics densification as well as to investigation of CNT concentration and sintering parameters influence on the microstructure of fabricated material.

The initial batch Al_2O_3 (0.25-0.5%MgO) was prepared by solid-phase synthesis at 1100°C. Multi-walled CNT were produced using chemical vapor deposition technique by benzene and ferrocene pyrolysis [3] and then purified by acid treatment.

Various combinations of inserted CNT concentration (up to 2%vol.) and regimes of vacuum sintering for composite samples preparation were used. The samples were heated at residual pressure 10-4 mm Hg up to the temperature 1700-1730°C.

The microstructure of fabricated samples, CNT distribution, mean size of matrix grains, type and value of closed porosity was investigated using optical (POLAM P-211), scanning electron (Jeol JSM-5910LV, QUANTA 3D 200) and atomic-force (Ntegra Aura) microscopy. Fracture toughness and micro-hardness were evaluated according to the indentation results.

In conclusion, the novel composite ceramic material based on alumina reinforced by multiwall carbon nanotubes is developed. The regimes of vacuum sintering and initial batch treatment are developed; the ceramic matrix composition, the CNT concentration, and other technological parameters are optimized. The uniform distribution of CNT in ceramic matrix is achieved. The developed composite possesses the framed network structure of CNT distribution and demonstrates the enhance of fracture toughness in 1.5 - 2 times.

[1] Johann Cho, Aldo R. Boccaccini, Milo S. P. Shaffer, *J. Mater. Sci.* **44**, 1934 (2009).
[2] N. Ueda, T. Yamakami, T. Yamaguchi, K. Kitajima, Y. Usui, K. Aoki, T. Nakanishi, F. Miyaji, M. Endo, N. Saito and S. Taruta, *Journal of the Ceramic Society of Japan* **118** (9), 847 (2010).
[3] X. Devaux, S.Yu. Tsareva, A.N. Kovalenko, E.V. Zharikov, E. McRae, *Carbon* **47**, 1244 (2009).

Growth and characterization of one-dimensional semiconductor nanocrystals within single-walled carbon nanotube channels

Eliseev A.A.[1], Kharlamova M.V.*[1], Yashina L.V.[1,2], Lukashin A.V.[1], Tretyakov Yu.D.[1]

[1]*Moscow State University, 119991, Moscow, Russia*
[2]*GIREDMET OJSC, 119017, Moscow, Russia*
**e-mail: mv.kharlamova@gmail.com*

One-dimensional (1D) crystals of compound semiconductors with a diameter of 3-5 atoms currently attract attention due to their unique properties, in particular size-dependent quantum effects like van Hove singularities etc. [1]. From the fundamental perspective, it is also of importance to understand the interplay between the electronic and atomic structure of the 1D-crystals and the relationship between the structural parameters of a 1D-crystal and the bulk. Unfortunately, in practice it is difficult to prepare and study 1D-crystals in its free state. Within the last decade it has been proposed to use single-walled carbon nanotubes (SWCNTs) as a template for growing 1D-crystals since these nanotubes are known to be chemically inert towards moSt inorganic substances; under certain conditions, it is also possible to avoid a charge transfer between the crystal and the nanotube wall [2].

The aims of this work were the synthesis of SnTe 1D crystals in channels of SWCNTs with inner diameter 1-1.4 nm and characterization of the atomic structure and the crystal-template interactions for SnTe@SWCNT nanocomposite. The synthetic strategy was based on the impregnation of pre-opened single-walled carbon nanotubes by molten salt in vacuum.

TEM measurements in combination with DFT calculations clearly show that the atomic structure of the 1D SnTe crystals corresponds to $(SnTe)_{5n}$ with a significant bond lengths relaxation (contraction) along the SWCNT axis in comparison to the bulk structure. The effective charges of both the Sn and Te atoms are lower than in the bulk of SnTe. X-ray photoemission and Raman spectroscopy data show no noticeable interaction between the 1D SnTe crystal and the SWCNTs, except for a minor influence of the intercalated crystal on metallic SWCNTs. From this observation we conclude that the reported relaxation effects for the bond lengths are inherent to the 1D SnTe crystal. This also suggests that SnTe@SWCNT is a well-suited model system to study the physics of non-interacting 1D-crystals.

[1] Garcia de Abajo F. J., Cordon J., Corso M., Shiller F., Ortega J.E., *Nanoscale* **2**, 717 (2010).

[2] Sloan J., Wright D.M., Woo H.-G., Bailey S., Brown G., York A.P.E., Coleman K.S., Hutchison J.L., Green M.L., *Chem. Commun.* **23**, 699 (1999).

Nanotructures based on H-(or F-) atom functionalized graphene elements for electronic and optic nano engineering

Chernozatonskii L.A.*[1], Artyukhov V.I.[1,2], Biro L.[3], Mark G.[3], Sorokin P.B.[1], Kvashnin A.G.[1], Kvashnin D.G.[1], Yakobson B.I.[2]

[1]*Institute of Biochemical Physics, RAS, Moscow, 119334, Russia*
[2]*Rice University, Houston, Texas 77251, USA*
[3]*Research Institute for Technical Physics and Materials Science MTA, HAS, H-1525 Budapest, Hungary*
**e-mail: cherno@sky.chph.ras.ru*

This report is review of experimental data and modeling (based on author papers) of main graphene nanostructures coved H (or F) prepared by special ways.

It is known hydrogenation (as well as fluorization) of graphene changes ith electronic properties due to changing of sp2 hybridization of C-atoms to sp3 one. Presence of the C-H regions can open the dielectric gap and organizes semimetal-like (M) or semiconductor (S) electronic waveguide paths (graphene nanopaths - GNPs) on this graphene sheet [1,2] and also organize graphene quantum dots (GQD) on graphane (or diamane - diamond-like nano thin films and nanribbons) matrix [3,4]. We consider next main structures: 1) semiconductor superlattices of periodically changed graphane and graphene paths (or graphane piaces divided semimetal-like and semiconductor GNP); 2) arrays of individual graphene quantum dots (GQDs) on graphane matrix, and GQDs formed on graphene nanoribbons - GNRs; 3) modeling of mechanisms of formation of considered structures.

The electronic and mechanic properties of proposed structures studied by using *ab initio* (DFT) and molecular dynamics methods and compared them with the same properties of graphene-graphane (or graphene fluoride) structures. Possible ways of fabrication of nanoelectronic and nanooptics elements have been discussed.

[1] L.A. Chernozatonskii, P.B. Sorokin, J. Bruening, *Appl. Phys. Lett.* **91**,1831 (2007).
[2] A.K.Singh, B.I.Yakobson, *Nano Letters* **9**, 1540 (2009).
[3] V.I. Artyukhov, L.A. Chernozatonskii, *J. Phys. Chem. A* **114**, 5389 (2010).
[4] L. Chernozatonskii, P. Sorokin, A. Kuzubov, P. Avramov, A. Kvashnin, D. Kvashnin, B. Yakobson, *J. Phys. Chem. C* **115**, 132 (2011).

Translational dynamics of 1D fullerenes chains encapsulated inside single-walled carbon nanotubes

Bousige C.[1,2,*], Rols S.[1], Kataura H.[3], Launois P.[2]

[1]*Institut Laue Langevin, F-38042 Grenoble, France*
[2]*Laboratoire de Physique du Solide, F-91405 Orsay, France*
[3]*National Institute of Advanced Industrial Science and Technology, Tsukuba, Ibaraki 305-8562, Japan*
**e-mail: bousige@ill.fr*

In addition to their numerous interesting physical properties, single-walled carbon nanotubes offer an inner cavity available to host molecules. It provides scientists with an exceptional molecular model system to study one-dimensional physics and confinement. This is particularly true when the inner molecules size is comparable to the tubes' diameters, as is the case with C_{60} fullerenes – such compound being called fullerene "peapods". In this communication, we propose to review some recent inelastic neutron scattering measurements that highlight the exotic behaviour of this system due to their low dimensionality: the rotational dynamics of the encapsulated fullerenes [1], and their translational one. The latter has recently been observed thanks to the synthesis of a large amount of peapods under the form of buckypapers – in which the tubes are mainly oriented along the buckypaper's plane. Using the time of flight spectrometer IN5 at the ILL, we showed that the translational motion of the confined fullerenes is characterized by an additional signal in the configuration where the scattering vector corresponding to the reciprocal parameter of the 1D chain is set parallel to the paper's plane. This signal has a quasielastic-like part due to the density of states of the longitudinal 1D phonons, whose analytical formula has been calculated, allowing extracting the sound velocity within the 1D fullerenes chains. Contrary to what is expected in the usual model of 1D liquid with infinite chains, this signal also features an elastic part due to the additional correlations induced by the confinement of the chains inside the nanotubes -- and of the finite size of the fullerenes chains. The good comprehension of this two-part signal and its evolution with temperature allow shedding light on the different forces at stake in this system, as well as probing fine structure parameters.

[1] S. Rols, J. Cambedouzou, M. Chorro, H. Schober, V. Agafonov, P. Launois, V. Davydov, A. Rakhmanina, H. Kataura, J.-L. Sauvajol, *Phys. Rev. Lett.* **101**, 065507 (2008).

Diamond-tungsten carbide nanocomposite based on detonation synthesized diamond nanopowder

Novikov N.V., Bochechka A.A.*, Nazarchuk S.N., Gavrilova V.S., Romanko L.A.

V.Bakul Institute for Superhard Materials, 04074, Kyiv, Ukraine
**e-mail: obochechka@gmail.com*

The diamond-tungsten carbide nanocomposite was developed by HP-HT sintering of detonation synthesized diamond nanopowder – ultradispersed diamond (UDD) with nanoparticles of substance tungsten containing. The mixture was prepared by chemical method [1].

Composite samples were sintered from the mixture of UDD nanopowder with a nanopowder of tungsten trioxide. Before sintering, the mixture in a hydrogen atmosphere was heat treated. According to X-ray analysis, the composite includes tungsten carbide WC and tungsten oxide WO_3. Tungsten carbide was formed both the direct interaction of diamond with tungsten, and as a result of reactions in the W–C–O system [2].

Nanoparticles of tungsten carbide formed in voids between the diamond nanoparticles are chemically bonded with them. This improves the physico-mechanical properties of the composite. The composite has the structure, where the tungsten carbide and diamond grains are regularly placed and are uniform in size (Figure).

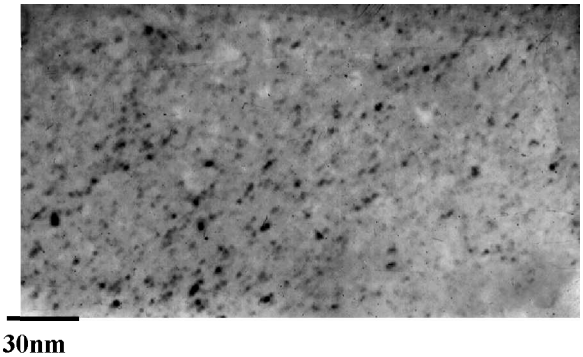

Figure. Typical SEM image of the structure of diamond–tungsten carbide nanocomposite.

Optimal sintering parameters and composition of the composite were determined. The composite combines high hardness (H_V = 25 GPa) and fracture toughness (K_{IC} = 6.6 MPa·m$^{1/2}$).

[1] Novikov M.V., Bochechka O.O., Nazarchuk S.M., Gavrilova V.S., Oleinik G.S., Romanko L.O., Sveshnikov I.A., Zabolotnyi S.D., Patent of Ukraine 50931, 2010, Byull. 12

[2] S.N. Nazarchuk, A.A. Bochechka, V.S. Gavrilova, L.A. Romanko, N.N. Beljavina, L.I. Alexandrova, V.N. Tkach, E.F. Kuzmenko, S.D. Zabolotnyi, *J. Superhard Materials* **1,** 3 (2011).

Solvatochromism and cluster formation in solutions of fullerene C_{60}

Avdeev M.V.*[1], Aksenov V.L.[2,1], Kyzyma O.A.[1,3], Kyrey T.O.[1,3], Bulavin L.A.[3]

[1]*Joint Institute for Nuclear Research, Dubna, Moscow reg., Russia*
[2]*Russian Research Center "Kurchatov Institute", Moscow, Russia*
[3]*Taras Shevchenko Kyiv National University, Kyiv, Ukraine*
**e-mail: avd@nf.jinr.ru*

The relation of solvatochromism with the appearance, growth and reorganization of fullerene clusters in C_{60} solutions under different conditions has been actively discussed in the last decade (e.g., see review [1]). The present report summarizes the results on this question basing on the data of a number of methods including various types of spectroscopy, dynamic light scattering, extraction, small-angle neutron scattering, mass spectrometry, and others. For the most part, it concerns rather polar solvents (with dielectric constant ε above 10) such as pyridine with $\varepsilon = 12.5$ or N-methyl-2-pyrrolidone (NMP) with $\varepsilon = 32.2$, where the so-called temporal solvatochromism (time evolution of UV-Vis spectrum) is accompanied by the formation of large (characteristic size of more than 100 nm) but stable (years) fullerene clusters. Along with sharp changes in the absorption characteristics after a new solvent (polar or non-polar) is added to such a solution, some cluster reorganization is observed as well. It is difficult, however, to establish a direct relationship between two effects. The reason is a significant influence of the solvent-solute interaction resulting in specific donor-acceptor complexes. As it has been recently shown [2,3], in addition to the dependence on fullerene concentration [4], the complex formation changes in time, thus contributing to the temporal solvatochromism. Such complexes can be responsible for the long-term cluster stabilization. They also increase the solvation rate of highly polar solvents (e.g. water with $\varepsilon = 80$, where C_{60} is totally insoluble) with respect to fullerene, which causes partial cluster dissolution on addition of these solvents to fullerene solutions. So, the processes reflected in the discussed solvatochromic effects are a significant part of somewhat a transition from the molecular to colloidal states of fullerene in polar solvents, the origin of which is still to be clarified.

[1] Avdeev M.V., Tropin T.V., Aksenov V.L., *Rus. J. Phys. Chem. A.* **84**(8), 1273 (2010).
[2] Kyzyma O.A., Korobov M.V., Avdeev M.V., Garamus V.M., Snegir S.V., Petrenko V.I., Aksenov V.L., Bulavin L.A., *Chem. Phys. Lett.* **493**, 103 (2010).
[3] Kyzyma O.A., Korobov M.V., Avdeev M.V., Garamus V.M., Petrenko V.I., Aksenov V.L., Bulavin L.A., *Fullerenes, Nanotubes and Carbon Nanostructures* **18**, 458 (2010).
[4] Yevlampieva N.P., Biryulin Yu.F., Melenevskaja E.Yu., et al. *Coll. Surf. A* **209**, 167 (2002).

Surface modifications of nanodiamonds for higher surface reactivity

Arnault J.C. *[1], Petit T.[1], H. Girard A.[1], Gesset C.[1]

[1]*CEA, LIST, Diamond Sensors Laboratory, F-91191 Gif sur Yvette, France*
**e-mail: jean-charles.arnault@cea.fr*

Nanodiamonds (NDs) constitute excellent candidates for biomarkers, combining the ability to covalently graft biomolecules on their surface with the presence of stable coloured N-V centers. However, their surface chemistry presents a wide variety of oxidized groups as well as amorphous carbon. An initial surface treatment is thus required to ensure high grafting yield and reproducibility. Different strategies were previously reported in the literature [1-5].

We investigated two different ways to homogenize NDs surface terminations: hydrogenation and surface graphitisation. Our original approach combines *in situ* and *ex situ* experiments. First, surface modifications of NDs are monitored by electron spectroscopies without air exposure to better understand the involved mechanisms. Second, suitable conditions are used for *ex situ* treatment to modify larger quantities of NDs, usable for chemistry. Efficient surface hydrogenation of NDs using MPCVD will be first presented [6]. The MPCVD reactor is connected to a UHV system equipped with XPS and AES. Kinetics of oxygen removal were followed by surface analysis of hydrogen treated NDs. Their enhanced surface reactivity was then confirmed using photochemical reaction with alkenes and a spontaneous coupling of aryldiazonium salts. These results strongly suggest similar electronic surface properties between bulk and nanodiamond materials.

Surface graphitisation of NDs is also a promising way for chemistry. Prato reaction was recently reported on such modified surfaces [7]. Our *in situ* study of NDs using UHV annealing will be presented. The effects of the annealing parameters on the graphitization kinetics will be discussed. The best conditions were then used in an *ex situ* furnace allowing the preparation of stable colloid suspension of graphitised NDs characterised using DLS and Zeta potential measurements.

[1] A. Krueger, J. Stegk, Y. Liang, L. Lu and G. Jarre, *Langmuir* **24**, 4200 (2008).
[2] S. Osswald, G. Yushin, V. Mochalin, S.O. Kucheyev, Y. Gogotsi, *J. of the American Chem. Soc.* **128**, 11635 (2006).
[3] K.B. Holt, C. Ziegler, D.J. Caruana, J. Zang, E.J. Millan-Barrios, J.Hu, J.S. Foord, *Phys. Chem. Chem. Phys.* **10**, 303 (2008).
[4] Y. Liu, Z. Gu, J. L. Margrave, V.N. Khabashesku, *Chem. of Materials* **16**, 3924 (2004).
[5] Q.S. Yu, Y.J. Kim, H.B. Ma, *Appl. Phys. Lett.* **88**, 231503 (2006).
[6] H.A. Girard, J.C. Arnault, S. Perruchas, S. Saada, T. Gacoin, J.P. Boilot, P. Bergonzo, *Diam. and Relat. Mater.* **19**, 1117 (2010).
[7] D. Lang, A. Krueger, *Diam. Relat. Mater.* **20**, 101 (2011).

Novel graphene based hybrid material with tunable electronic properties

Antonova I.V.* [1], Kotin I.A.[1,2], Soots R.A.[1], Volodin V.A.[1,3], Prinz V.Ya.[1]

[1]*A.V.Rzhanov Institute of Semiconductor Physics SB RAS, 630090, Novosibirsk, Russia*
[2]*Novosibirsk State Technical University, Novosibirsk, 630092, Russia*
[3]*Center of Science and Education, Novosibirsk State University, Novosibirsk, 630090, Russia*
**e-mail: antonova@isp.nsc.ru*

Chemical functionalization of graphene (or a few-layered graphene) is an advanced approach for creation of complementary materials with wide spectrum of electronic properties. This method is used for a band gap opening and a managing with carrier concentration, type and mobility. The band gap has a central role in modern device physics and technology and governs the operation of semiconductor devices. A tunable band gap would be highly desirable because it would allow great flexibility in design and devices optimization. In present study we have used intercalation of N-methylpyrrolidone (NMP, C_5H_9NO) into a few-layered graphene with the aim to create a new graphene-based material with variable properties in controllable manner. Such approach as intercalation provides a pure and two-side functionalization of graphene. A choose of intercalation agent is based on well-known property of the NMP to penetrate between every graphene layers. As a result, we have created a new hybrid material with variable properties.

Fabrication process of our hybrid structures includes the follows steps: (1) an electrostatic exfoliation of the few-layered graphene film with thickness about d ~ 2–5 nm and transfer it on the 300 nm SiO_2/Si substrate; (2) an intercalation of the NMP into graphene flakes; (3) annealing of the intercalated structures at temperature in the range of 125–250°C was the final operation which creates the hybrid structures.

Tunable electronic properties with strong and non-monotonic dependence on the fabrication temperature were revealed for this hybrid material. Opening of the band gap, wide variation of resistivity (up to 10^7 times), relatively high mobility and sp^2 or sp^3 hybridization of carbon atoms are attributed to our hybrid material. Hybrid structures created in temperature ranges of T < 200°C and T > 200°C were found to demonstrate different properties. The first type of hybrid structures created at the temperatures lower 200°C have high resistivity (~ 10^2–10^6 Ohm.cm), p-type conductivity, a strong temperature dependence of resistivity in the range of 77–300 K, and the band gap ~ 3 - 3.5 eV (for structures created at temperature of 150°C). We have presumed for these structures that bonds between NMP and graphene are formed through oxygen atoms. The second type of hybrid structures corresponded to T > 200°C is distinguished by appearance of the sp^3 hybridization of carbon atoms typically observed in the case of graphane formation. In our case this process can be caused by NMP polycondensation with releasing of hydrogen atoms. The band gap (~ 3.5 - 4.0 eV) is revealed for structures created at 250°C.

Nanocarbons-induced hardening of ultrathin polysiloxane block copolymer films

Ankudinov A.V.*[1,2], Voznyakovskii A.P.[3], Nyapshaev I.A.[1]

[1] *Ioffe Institute, 194021, St.Petersburg, Russia*
[2] *National Research University ITMO, 197101, St.Petersburg, Russia*
[2] *Scientific Research Institute for Synthetic Rubber,198021,St.Petersburg, Russia*
**e-mail: Alexander.Ankudinov@mail.ioffe.ru*

Ultrathin films of polysiloxane block copolymers and their composites with modifying addition of C_{60} were studied by atomic force microscopy (AFM). Independently on the concentration of additives, nanometre scale surface patterns were revealed in the relief of the films. These patterns were associated with the spatial distribution of rigid block domains at the block copolymer surface. Reliable quantitative data of the mechanical parameters of the films were obtained in indentation tests using specially manufactured spherical AFM probes of calibrated submicron radius of curvature. The measured parameters correlated with standard physical and mechanical testing parameters for thick films. It was found that the addition of C_{60} at the level of 0.01% significantly improved the elasticity of the block copolymer surface layers. This concentration may introduce a few fullerene molecules into each nanodomain of rigid blocks. The results on modification of polysiloxane block copolymers by nanodiamond particles will be also considered.

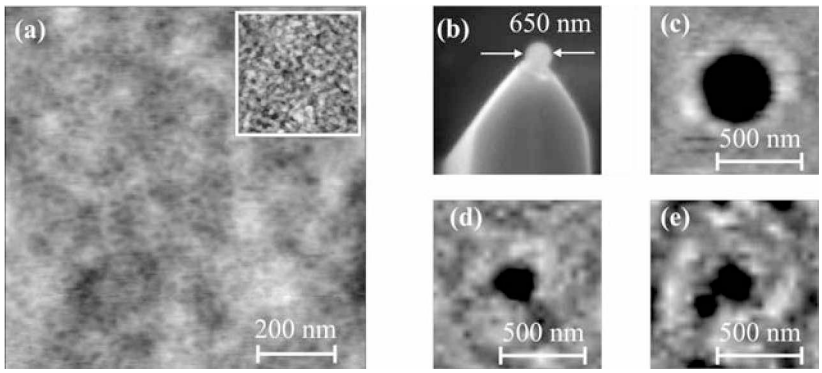

Figure.1. High resolution tapping mode AFM image of block copolymer surface topography measured with a standard sharp probe (averaged tapping force is 150 pN), (a). In the upper right corner of the image (a) a fragment of the TEM micrographs of the block copolymer is inserted. SEM image of the special AFM probe, (b). Tapping mode AFM images of the surface areas of different block copolymer films measured after indentation tests with a maximum force (strain): 265 nN (99 nm), (c); 560 nN (42 nm), (d); 570 nN (32 nm), (e). Films description: (c) block copolymer without curing agent, (d) with curing agent, (a) and (e) with curing agent and with addition of 0.01 weighting % of C_{60}. Gray scale of AFM images: (a) 2.7 nm, (c) 20 nm, (d) 9 nm, (e) 4 nm. AFM image (a) and TEM insert have the same scale bar.

Deagglomeration of detonation nanodiamonds. Problem and its decision

Aleksenskii A.E.*, Baidakova M.V., Brunkov P.N., Dideykin A.T., Shalnev I.V., Veinger A.I., Vul' A.Ya.

Ioffe Institute, 194021, St.Petersburg, Russia
**e-mail: blin@mail.ioffe.ru*

It is well known that a commercial powder of detonation nanodiamonds (DND) and their aqueous suspensions consist of 100-200 nm agglomerates of 4 - 5 nm crystalline diamond grains [1]. We have recently submitted a method for production of stable mono-disperse hydrosol of 4 nm isolated DND particles [2]. The method includes deep purification of initial industrial DND with ESR control of residual metal impurity, annealing of the purified DND in air, ultrasonic dispergation in water and centrifugation. We have also confirmed effect of DND deagglomeration after annealing in hydrogen atmosphere suggested last year in [3], however we revealed that zeta potential was negative in that case.

In all cases the annealing of nanodiamond and the chemical treatment of surface were needed for the deagglomeration. The size distribution of DND particles with maximum around 4 nm confirmed by DLS method as well as AFM of DND particles deposited from suspension on silicon substrate.

We have experimentally verified our idea suggested in [2] that penetration of water into nanopores of DND agglomerate during centrifugation generates a sizable capillary pressure and this pressure results in DND deagglomeration, however our attempt to get the deagglomeration of DND in water under high pressure did not confirm the idea.

Here we proposed two new possible explanations of deagglomeration of nanodiamonds. The first hypothesis is destruction of bonding chemical groups on the surface of the nanodiamond grains at the annealing. The second one is the destruction of interparticle bonds in agglomerates due to accumulation of defects at interfaces of grains. In the second case we believe that concentration of defects at the interfaces increases due to migration of defects from core to surface during the annealing.

The study was supported by the Russian Ministry of Education and Science and Programs of the Russian Academy of Sciences.

[1] M. Baidakova, A. Vul'. *Journal Phys. D: Appl. Phys.* **40**, 6300 (2007).
[2] A.E. Aleksenskii, E.D. Eydelman, A.Ya. Vul, *Nanoscience and Nanotechnology Letters* **3**, 68 (2011).
[3] O.A. Williams, J. Hees, C. Dieker, W. Jager, L. Kirste, C.E. Nebel, *ACS Nano* **4**(8) 4224 (2010).

Edge effect on electronic properties in nanoscale graphene systems

Wakabayashi K.[1,2]

[1] *WPI-MANA, NIMS, 305-0044, Tsukuba, Japan*
[2] *PRESTO, JST, Japan*
e-mail: WAKABAYASHI.Katsunori@nims.go.jp

The discovery of graphene and successive fabrication of graphene devices [1,2] have triggered intensive and diverse research on carbon related systems. The honeycomb crystal structure of single layer graphene consists of two nonequivalent sublattices and results in a unique band structure for the itinerant p-electrons near the Fermi energy which behave as massless Dirac fermion. In graphene, the presence of edges can have strong implications for the spectrum of the p-electrons. In graphene nanoribbons with zigzag edges, localized states appear at the edge with energies close to the Fermi level.[3] In contrast, edge states are absent for ribbons with armchair edges. Recent experiments have succeeded to synthesize graphene nanoribbons using lithography techniques[4], chemical techniques.[5,6]

In my talk, we focus on edge and geometry effects of the electronic properties of graphene nanoribbons. The electronic states of graphene nanoribbons crucially depend on the edge orientation and boundary condition.[3,7] (1) In zigzag nanoribbons, for disorder without inter-valley scattering a single perfectly conducting channel emerges associated with such a chiral mode due to edge states, i.e. the absence of the localization.[8-10] (2) In armchair nanoribbons, the single-channel transport subjected to long-ranged impurities is nearly perfectly conducting, where the backward scattering matrix elements in the lowest order vanish as a manifestation of the existence of Berry phase.[11-12] (3) Nano-graphene junctions are shown to have the zero-conductance anti-resonances associated with the edge states. The relation between the condition of the resonances and geometry is discussed.[13] (4) Finally, we will discuss the effect of edge chemical modification on magnetic properties of nanographene systems[14], and the hole doping effect on zigzag edge magnetic states.[15]

[1] K.S. Novoselov, A.K. Geim, S.V. Morozov, et.al., *Nature* **438**, 197 (2005).
[2] Y. Zhang, Y.-W.Tan, H.L.Stormer, and P.Kim, *Nautre* **438**, 201 (2005).
[3] M. Fujita, K. Wakabayashi, et.al, *J. Phys. Soc. Jpn.* **65**, 1920 (1996).
[4] M.Y. Han, B. Oezyilmaz, Y. Zhang, and P. Kim, *Phys. Rev. Lett.* **98**, 206805 (2007).
[5] X. Li, X. Wang, L. Zhang, S. Lee, H. Dai, Science **31**, (2008) 122.
[6] J. Cai, P. Ruffieux, R. Jaafar, M. Bieri, et.al., *Nature* **466**, 470 (2010).
[7] K. Wakabayashi, et.al., *Sci. Technol. Adv. Mat.* **11**, 054504 (2010).
[8] K. Wakabayashi, et.al., *Phys. Rev. Lett.* **99**, 036601 (2007).
[9] K. Wakabayashi, et.al., CARBON **47** (2009) 124
[10] K. Wakabayashi, New J. Phys. **11** (2009) 095016.
[11] M. Yamamoto, Y. Takane, and K. Wakabayashi, Phys. Rev. B**79** (2009) 125421.
[12] K. Sasaki, K. Wakabayashi, T. Enoki, New J. Phys. **12** (2010) 083023.
[13] M. Yamamoto and K. Wakabayashi, Appl. Phys. Lett. **95** (2009) 082109.
[14] K. Wakabayashi, S. Okada et.al., J. Phys. Soc. Jpn. **79** (2010) 034706
[15] S. Dutta and K. Wakabayashi, in preparation.

Nitrogen in nanodiamonds of dynamic synthesis

Vlasov I.I.*[1], Shenderova O.A.[2], Turner S.[3], Shiryaev A.A.[4], Orlinskii S.B.[5], Sildos I.[6]

[1]*General Physics Institute RAS, 119991 Moscow, Russia*
[2]*International Technology Centre, 27617 Raleigh, NC, USA*
[3]*EMAT, University of Antwerp, 2020 Antwerp, Belgium*
[4]*Institute of Physical Chemistry and Electrochemistry RAS, Moscow 119991, Russia*
[5]*Federal Center of Shared Facilities of the Kazan State University, 420008 Kazan, Russia*
[6]*Institute of Physics, University of Tartu, 51014 Tartu, Estonia*
**e-mail: vlasov@nsc.gpi.ru*

Development of efficient production methods of nanodiamond (ND) particles containing substitutional nitrogen and nitrogen-vacancy (NV) complexes remains an important goal in the nanodiamond community. We report on systematic studies of the microstructure, concentration, and spatial distribution of nitrogen-related defects in different classes of dynamically synthesized nanodiamonds with primary particle sizes ranging from 5 to 50 nm using high-resolution transmission electron microscopy, spatially resolved electron energy loss spectroscopy, confocal Raman and photoluminescence spectroscopy, and pulsed electron paramagnetic resonance spectroscopy. The highest concentration of atomic nitrogen in a diamond core (3-5 at.%) was found for ND produced from explosive. The highest concentration of nitrogen paramagnetic centers (1.2 ppm) was detected in ND synthesized from a mixture of graphite and explosive. Well-pronounced narrow-band photoluminescence at 575 nm and 637 nm wavelengths related to NV centers was observed in primary ND particles of different origin with sizes larger than 20-30 nm. Perspectives and ways to control nitrogen state and content in dynamically synthesized NDs is discussed.

This work was supported by Ministry of Education and Science of Russia under the Contract no. P925.

Structures and cage transformations of higher fullerenes

Troyanov S.I.

Moscow State University, Department of Chemistry, 119991, Moscow, Russia
e-mail: stroyano@thermo.chem.msu.ru

Since the discovery of fullerenes, rapid development of their chemistry was mostly restricted to C_{60} and C_{70}. The chemistry of higher fullerenes of more than 70 carbon atoms remains largely unexplored due to much lower abundance and difficulties in isolation thereof. Moreover, these complications grow more severe with molecular size due to increasing isomeric complexity even under the restrictions of the Isolated Pentagon Rule (IPR). Separation of higher fullerenes is usually achieved by chromatographic methods (HPLC) augmented by ^{13}C NMR characterization, which is, however, not fully reliable in some cases. An efficient alternative is constituted by chemical derivatization of higher fullerenes followed by separation and direct structural characterization of the derivatives thus obtained, as illustrated by several examples within the C_{76} - C_{96} range [1].

Reactions of mixtures of higher fullerenes with CF_3I or C_2F_5I followed by HPLC separation of the resulting perfluoroalkylated derivatives and their X-ray diffraction study enabled determination of cage connectivity in C_{76}, C_{78} (two isomers), C_{82}, C_{84} (six isomers), C_{86}, C_{88}, C_{92}, C_{94}, and C_{96}. Further, chlorination with inorganic chlorides ($SbCl_5$, VCl_4, etc.) afforded isolation and crystallographic characterization of chlorinated derivatives of C_{76}, C_{78}, and C_{90} [2].

An entirely new phenomenon, chlorination-promoted skeletal transformations, has been discovered in several higher fullerenes including C_{76}, C_{82}, C_{86}, and C_{88}. Chlorination of IPR D_2-C_{76} fullerene with $SbCl_5$ is accompanied by a 7-step Stone-Wales skeletal rearrangement to non-IPR $^{\#18917}C_{76}Cl_{24}$ containing five pairs of fused pentagons in the carbon cage [3]. Chlorination of C_{86} (isomer 16) accompanied by the loss of a C_2 unit resulted in $C_{84}Cl_{32}$ with a non-classical heptagon-containing cage [4]. Also, very recent results on skeletal rearrangements in C_{82} and C_{88} will be presented. The driving forces and possible pathways of the skeletal rearrangements will be discussed in more detail.

This work was supported by the Russian Foundation for Basic Research (09-03-00433, 09-03-01131, and 09-03-91337).

[1] N.B. Tamm, L.N. Sidorov, S.I. Troyanov, *Moscow Univ. Chem. Bull.* **64**, 327 (2009).
[2] E. Kemnitz, S. I. Troyanov, *Angew. Chem. Int. Ed.* **48**, 2584 (2009).
[3] I.N. Ioffe, A.A. Goryunkov, N.B. Tamm, L.N. Sidorov, E. Kemnitz, S.I. Troyanov, *Angew. Chem. Int. Ed.* **48**, 5904 (2009).
[4] I.N. Ioffe, C. Chen, S. Yang, L.N. Sidorov, E. Kemnitz, S.I. Troyanov, *Angew. Chem. Int. Ed.* **49**, 4784 (2010).

Recent progress in dispersed detonation nanodiamond

Ōsawa E.

NanoCarbon Research Institute, AREC, Faculty of Textile Science and Engineering, Shinshu University, 386-8567, Ueda, Japan
e-mail: osawaeiji@aol.com

Manufacture of Dispersed Primary Particles

Attrition milling of the conglomerated detonation nanodiamond powder with spherical 30μm ZrO_2 beads still remains as the only viable method for the mass-production of its 5-nm primary particles. We find that combination of the mill with a 400W/24KHz powerful supersonic processor in series within circular disintegration process produces significant improvements. Re-optimization of operation conditions by *experimental design* led to overall reduction of milling time by 25%, and contamination with zirconia to 0.02 wt% (*S. Sasaki*).

Agglutination Structure and Mechanism

Abberation-corrected TEM and complementary computer simulations provide further confirmation on the mechanism of electrostatic and anisotropic self-assembly between crystal facets of the adjacent primary particles. While the strongest calculated interfacial interactions, $(111)^-/(111)^0$, could be observed and characterized, another predicted strong interaction, $(100)^+/(111)^0$, could not be found at all despite intensive search. The failure suggests that the latter interaction must have been dissociated by charging during TEM observation (*L.-Y. Chang, A. S. Barnard*). This conclusion leads to a possibility of partial non-milling disintegration of agglutinates by polarization, which later has been confirmed.

Nanospacer Lubrication, an Application Unique to the Dispersed Single-Nano Diamond Particles

Following our discovery of remarkably small friction coefficient of 0.01 for 1% 5nm-diamond aqueous colloidal solution as lubricant liquid in 2008, we found more dilute colloidal solutions of the same in water and in ethylene glycol showing similar lubricating behavior. The surprising results can be explained by invoking Bowden's fusion mechanism of lubrication at very early stages of true contacts between the asperities of interacting surfaces, very small rolling resistance of quasi-spherical and dispersed diamond particles, and high number density of single-nano colloidal solution. This is the first hint of promising and disposable spacer lubrication that will eventually be capable of replacing traditional but ineffective and environmentally hazardous lubricating oil (*S. Mori*).

Detonation Synthesis of Luminescent Nanodiamond

In view of the importance of intensely fluorescent nanodiamond in the emerging optically detected NMR technique in cell biology, detonation experiments of TNT-hexogen are being carried out in the presence of various elements X to produce versatile X-V color centers (X=Si, Ni *etc*) in the core of diamond crystals. Progress will be reported (*Y. Harada, P. Yan*).

One-dimensional molecular nano-structures inside single-walled carbon nanotubes

Okazaki T.

Nanotube Research Center, National Institute of Advanced Industrial Science and Technology (AIST), 305-8565, Tsukuba, Japan
e-mail: toshi.okazaki@aist.go.jp

One of the most interesting features of molecular materials is the fact that their physical properties change with the molecular arrangement as well as the properties of the molecule itself. Self-organization is an efficient pathway through which organic molecules assemble to form well-ordered nanometre-scale objects that are hardly synthesized by conventional chemical reactions. In these systems, two or more molecules are held together and assembled by means of intermolecular (noncovalent) bonding such as ion-dipole or dipole-dipole interactions, hydrogen bonding, hydrophobic interactions, or π–π stacking.

Single-walled carbon nanotubes (SWCNTs) can offer a suitable interior space for accommodating molecules. The nanostructures produced by incorporating such molecules into SWCNTs are expected to exhibit several superior features. For example, because the diameter of SWCNTs can be adjusted to the size of the molecules, well-ordered molecular arrangements beyond a micro-metre long can be easily produced. The synthesized molecular arrangements are also expected to be strong and flexible against mechanical strain because the nanotube templates sustain the structure. Furthermore, the synthesized nanostructures are isolated from active molecules by the tube wall, which leads to the superior durability of the encapsulated molecules.

In this conferenece, we will report several characteristic nanostructures formed inside SWCNTs. For example, planner π-conjugated molecules, coronenes form nano-scale columns in a way that differs from 3D solid coronenes, resulting in electronic and optical properties peculiar to the 1D structure (Fig. 1) [1]. The basic properties of the produced 1D molecular crystal will be discussed in detail.

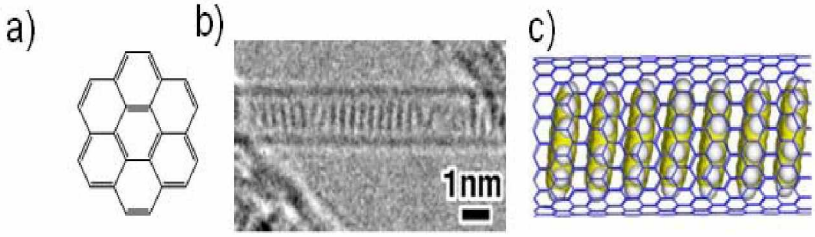

Figure 1. (a) Molecular structure of coronene. (b) HRTEM images of coronenes encapsulating SWCNTs. (c) Schematic illustration of coronenes encapsulating SWCNTs.

[1] T. Okazaki, Y. Iizumi, S. Okubo, H. Kataura, Z. Liu, K. Suenaga, Y. Tahara, M. Yudasaka, S. Okada, S. Iijima, *Angew. Chem. Int. Ed.*, in press.

From neutral complexes to ionic compounds of fullerenes with magnetic transitions and metallic conductivity

Konarev D.V.*[1], Lyubovskaya R.N.[1], Khasanov S.S.[2]

[1]*Institute of Problems of Chemical Physics RAS, 142432, Chernogolovka, Russia*
[2]*Institute of Solid State Physics RAS, 142432, Chernogolovka, Russia*
**e-mail: konarev@icp.ac.ru*

Fullerenes are π-acceptors with spherical shape of the molecule, high symmetry and polarizability, and unusual band structure. Donor-acceptor complexes can be precursors in the design of new materials possessing metallic conductivity, superconductivity and ferromagnetism as well as showing magnetic transitions. Here we present different approaches to the synthesis of fullerene compounds, discuss their structures and properties.

Only neutral complexes of fullerenes can be obtained with relatively weak organic and organometallic donors such as saturated amines, metalloporphyrins and metal dithiocarbamates. Though they do not show dark conductivity, photoinduced charge transfer and relatively high photoconductivity are possible in some of them.

For preparation of ionic complexes we used direct fullerene reduction by strong donors or cationic metathesis reaction. These methods can be varied by the multi-component approach which allows one to introduce different neutral organic and organometallic compounds (D_2) into the ionic complexes to form the $(D_1^+)\cdot(\text{Fullerene}^{\bullet-})\cdot(D_2)$ complexes which show a wide variety of crystal structures and properties.

The preparation of various ionic complexes showed that fullerene radical anions have strong tendency to dimerize to form diamagnetic singly bonded $(C_{60}^-)_2$ and $(C_{70}^-)_2$ dimers [1]. Their formation is accompanied by phase transitions in the 120-320 K range and results in the reversible transition of the compound from paramagnetic to diamagnetic state. Fullerene radical anions can also coordinate to cobalt(II) porphyrins and form diamagnetic σ-bonded $(\text{Co}^{\text{II}}\text{porphyrin}\cdot C_{60}^-)$ structures.

In the absence of dimerization and close contacts between fullerenes, compounds can demonstrate high conductivity and magnetic interaction of spins. The layered complex $(\text{MDABCO}^+)\cdot(C_{60}^{\bullet-})\cdot\text{TPC}$ (MDABCO^+ is the cation of *N*-methyldiazabicyclooctane; TPC is triptycene) obtained by us is an unique pure organic quasi-two dimensional metal with unusual properties. The coexistence of metallic layers with nonmetallic layers having antiferromagnetic interaction of spins is observed in the 200-360 K range, whereas nonmetallic layers transfer to the metallic state below 200 K due to the ordering of $C_{60}^{\bullet-}$ [2]. In the series of C_{60} salts with *d*- metal cations: $(C_{60}^{\bullet-})_2\cdot\{(M^{2+})\cdot(\text{DMF})_x\}$ (M = Co, Fe, Ni and Cd; x = 2.4 – 4) high conductivity (0.4-12 $S\cdot cm^{-1}$) coexists with antiferromagnetic interaction of spins localized on the metal cations [3]. The preparation of the complexes with partial charge transfer possessing metallic conductivity is also discussed.

[1] D.V. Konarev, S.S. Khasanov, G.R. Mukhamadieva, L.V. Zorina, A. Otsuka, H. Yamochi, R.N. Lyubovskaya, *Inorg. Chem.* **49**, 3881 (2010).
[2] D.V. Konarev, S.S. Khasanov, A. Otsuka, M. Maesato, G. Saito, R.N. Lyubovskaya, *Angew. Chem.* **49**, 4829 (2010).
[3] D.V. Konarev, R.N. Lyubovskaya, *Russ. Chem. Bull.*, **57**, 1944-1954 (2008).

Nanocarbon field emission devices and their applications

Kang W. P.*, Gosh N., Xu S. H., LeQuan C., Davidson J. L.

Electrical Engineering & Computer Science, Vanderbilt University, Nashville, TN, USA
**e-mail: wkang@vuse.vanderbilt.edu*

The attractive material properties of carbon-derived materials, such as low electron affinity of diamond or the high aspect ratio of carbon nanotubes (CNT), coupled with practical chemical vapor deposition (CVD) processing of deposited nanocrystalline diamond and CNT on a variety of substrates prompts interest in their use as cold cathodes. In this work, various configurations of nanocarbon-derived vacuum electronic devices are examined. The material properties, device structure and fabrication process, and the electrical performance of these devices are presented.

Nanocarbon-derived vacuum field emission devices, specifically, nitrogen-incorporated nanodiamond field emission triodes, transistors and integrated CNT amplifiers are new configurations for robust micro- and nanoelectronic devices. These novel micro/nanostructures provide an alternative and efficient means of accomplishing electronics that are impervious to temperature and radiation. For example, nitrogen-incorporated nanocrystalline diamond has been lithographically micropatterned to utilize the material as an electron field emitter. Arrays of laterally arranged nanodiamond emitters constitute the cathode in a versatile diode configuration with small interelectrode separation. Sub-micron emission gap lateral field emission diodes derived from nanocarbon, specifically nanodiamond, provide an alternative means of accomplishing electronics that operate at very low power. Electron beam lithography (EBL) approach for realizing the nano gap structure of the CVD diamond lateral diode is presented. In three-terminal configuration, we have realized distinct triode and transistor devices. Also, field emission integrated amplifiers based on self-align gated CNT arrays with low turn-on voltage and negligible gate leakage current and high performance differential amplifier characteristics have been achieved. The ruggedness of these devices has been demonstrated by their operation at high temperatures (400°C) and radiation hardness to > 20Mrad(SiO_2) and total fluence of 4.4×10^{13} neutrons/cm^2. The frontier research in nanocarbon-derived field emission micro- and nanoelectronic devices will be discussed.

Functionalization of synthetic carbon allotropes

Hirsch A.*

Department of Chemistry and Pharmacy, University of Erlangen-Nuremberg, Henkestrasse 42, 91054 Erlangen, Germany
**e-mail: andreas.hirsch@chemie.uni-erlangen.de*

Chemical functionalization of new C-allotropes is of fundamental interest and opens the door to unprecedented materials applications. In principle, the physical and chemical properties of fullerenes, carbon nanotubes (CNTs) and graphene are related to each other, although their levels of development vary considerably. In order to efficiently explore the reactivity of the less developed CNTs and especially that of graphene it is our goal to provide a unifying approach for the chemistry of all three new carbon allotropes. The fullerenes present the first family of synthetic carbon allotropes. Since their availability in macroscopic quantities numerous investigations with respect to their physical characterization and chemical functionalization have been carried out. CNTs - the second new family of C-allotropes - exhibit at least the same potential for unprecedented applications. Their chemistry, however, is much less developed. Although many protocols for covalent and non-covalent CNT functionalization have been published there are still many fundamental problems to be solved. This includes *inter alia* the highly selective functionalization of metallic- or semiconducting SWNTs, the high throughput isolation of SWNTs with single helicity, the development of general concepts allowing for tunable doping of individualized tubes with single helicity or least defined transport characteristics (metallic – semiconductive). Finally, the youngest representative in the list of new C-allotropes is graphene and the exploration of its chemistry has just begun to start. So far only investigation on the functionalization of defect rich graphene oxide (GO) but not intact graphene itself have been published. Compared to the various flavours of CNTs (broad variation of helicities, single walled, multi walled) graphene is a much more uniform material. This will facilitate the development of its chemistry considerably. We will present a series of new results of covalent and non-covalent functionalizations of fullerenes, carbon nanotubes and graphene.

The role of zigzag and armchair edges in the electronic structure of nanographene

Enoki T.

Chemistry Department, Tokyo Institute of Technology, Ookayama, Meguro-ku, Tokyo, 152-8551, Japan
e-mail: tenoki@chem.titech.ac.jp

The electronic structure of graphene is described in terms of massless Dirac fermion with two Dirac cones (K and K') in the Brillouin zone, giving unconventional features of zero-gap semiconductor. When a graphene sheet is cut, the created edges affect seriously the electronic structure depending on the edge shape (zigzag and armchair edges) as observed with the electron wave interference and the creation of non-bonding π-state (edge state). We investigated the edge-inherent electronic features by STM/STS observations and Raman spectra. Graphene nanostructures were fabricated using graphene oxide with an AFM tip.

STM/STS observations demonstrate that edge states are created in zigzag edges in spite of the absence of such state in armchair edges. In addition, zigzag edges tend to be short and defective whereas armchair edge is long and continuous in general. These findings suggeSt that zigzag edge is less stable in comparison with armchair edge, consistent with Clar's aromatic sextet rule.

The electron wave scattering takes place differently between zigzag and armchair edges, showing different superlattice patterns in STM lattice images. In the vicinity of an armchair edge, a hexagonal pattern was observed together with a fine structure of three-fold symmetry at the individual superlattice spots. At a zigzag edge, the electron wave is subjected to the K-K intravalley scattering without interference, whereas the K-K' intervallery scattering with interference takes place in the scattering event at an armchair edge. The appearance of the hexagonal superlattice is a consequence of electron wave interference. The three-fold symmetric fine structure is understood as the antibonding coupling between the adjacent spots in the hexagonal superlattice.

The Raman G-band shows the edge-shape dependence same to that observed in the STM superlattices. The intervalley scattering at an armchair edge gives specific dependence of the G-band intensity on the polarization direction of the incident laser beam as expressed by $\cos^2\Theta$ (Θ; the angle between the polarization and the armchair edge direction). A nanographene ribbon of 8 nm$\times$>1 μm prepared by heat-treatment of graphite step edges shows this angular dependence, being demonstrated to consiSt of pure armchair edges.

Single sheet graphene oxide was found to form a two dimensional regular arrangement of linear wrincles of oxidized lines running along the zigzag direction with an interline spacing of ca.10 nm. This suggests that zigzag edged nanographene ribbons with a width of ca.5 nm are created between the oxidized lines. Nanofabrication by an AFM tip can allow us to create a nanostructure of graphene sheet intentionally.

Exotic transport properties of monolayer and bilayer graphene

Ando T.

Department of Physics, Tokyo Institute of Technolocy
2-12-1 Ookayama, Meguro-ku, Tokyo 152-8551.Japan
e-mail: ando@phys.titech.ac.jp

Graphene, fabricated recently, has been attracting much attention since the observation of transport properties including the half-integer quantum Hall effect. The electron motion in graphene is governed by Weyl's equation for a neutrino or the Dirac equation with vanishing reSt mass characterized by a velocity which is about 1/300 of the light velocity. The pseudo-spin wave function exhibits a sign change due to Berry's phase when the wave vector is rotated around the origin and therefore has a topological singularity there. This singularity is the origin of the peculiar behavior in transport properties of graphene, such as the minimum conductivity in the absence of a magnetic field, the half-integer quantum Hall effect, the dynamical conductivity, and antilocalization behavior. A very singular diamagnetic response is another example.

There have been various theoretical and experimental investigations on dominant scattering mechanisms, including effects of charged impurities and environmental dielectric screening effect, resonance scattering effects due to strong and short-range scatterers, etc. A recent theoretical study showed that the minimum conductivity is sensitive to effective potential range of dominant scatterers in agreement with experiments. The appearance of effective vector potential due lattice distortion was recently demonstrated in deformed graphene.

Inter-layer interaction in bilayer graphene destroys the linear dispersion into an approximate parabolic dispersion with a trigonal warping. Electronic states of multi-layer graphene depend critically on the number of layers. This becomes clear if we consider only the major coupling terms and neglect other small parameters considered in bulk graphite. In fact, for odd-layer graphene, the Hamiltonian can be decomposed into those of bilayers with different interlayer coupling and that of a monolayer graphene, while for even-layer graphene, the Hamiltonian can be decomposed into those of bilayers only. This decomposition is quite useful for understanding main features of electronic states in multi-layer graphene. A perpendicular electric field or asymmetry between two layers opens up an energy gap in bilayer graphene. Interfaces between monolayer and bilayer graphenes were shown to exhibit peculiar dependence on incident angle, giving rise to valley polarization of transmitted electron, and characteristic Landau-level structure.